Scattering Amplitudes in Four- and Six-Dimensional Gauge Theories

D I S S E R T A T I O N

zur Erlangung des akademischen Grades

d o c t o r r e r u m n a t u r a l i u m
(Dr. rer. nat.)
im Fach Physik

eingereicht an der
Mathematisch-Naturwissenschaftlichen Fakultät I
der Humboldt-Universität zu Berlin

von

Dipl.-Phys. Theodor Schuster

Präsident der Humboldt-Universität zu Berlin:
Prof. Dr. Jan-Hendrik Olbertz

Dekan der Mathematisch-Naturwissenschaftlichen Fakultät I:
Prof. Stefan Hecht, Ph.D.

Gutachter:
1. Prof. Dr. Jan Plefka
2. Prof. Dr. Matthias Staudacher
3. James Drummond, Ph.D.

Tag der mündlichen Prüfung: 11. Juli 2014

To my parents

Abstract

We study scattering amplitudes in quantum chromodynamics (QCD), $\mathcal{N} = 4$ super Yang-Mills (SYM) theory and the six-dimensional $\mathcal{N} = (1, 1)$ SYM theory, focusing on the symmetries of and relations between the tree-level scattering amplitudes in these three gauge theories.

We derive the tree-level superconformal and dual superconformal symmetries of $\mathcal{N} = 4$ SYM theory in non-chiral superspace using the non-chiral BCFW recursion to prove the latter. Similarly we give a complete derivation of the symmetries of the tree-level superamplitudes of $\mathcal{N} = (1, 1)$ SYM theory in six dimensions, again using the BCFW recursion to prove their dual conformal symmetry and thereby correcting some minor mistakes in the proof previously known in the literature.

We provide the means necessary for efficient next to leading order QCD calculations by deriving the tree level and one-loop color decomposition of an arbitrary QCD amplitude into primitive amplitudes. This generalizes the known analytic results for amplitudes of arbitrary multiplicity with up to one quark anti-quark pair and provides an alternative to the Feynman diagram based algorithm for the determination of the decomposition into primitive amplitudes. Furthermore, we derive general fermion flip and reversion identities, spanning the null space among the primitive amplitudes. An accompanying, public `Mathematica` package `QCDcolor` contains implementations of the color decompositions as well as the flip and reversion identities.

Based on the obtained color decomposition of QCD tree amplitudes and the fermion flip identities we prove that every color ordered tree amplitude of massless QCD can be written as a linear combination of gluon-gluino amplitudes of $\mathcal{N} = 4$ SYM theory. The proof includes a general construction of these linear combinations. For all color ordered QCD amplitudes with up to four quark-anti-quark pairs and an arbitrary number of gluons, we determine representations containing a minimal number of gluon-gluino amplitudes. Furthermore, we derive analytical formulae for all gluon-gluino amplitudes relevant for QCD by projecting the previously-found expressions for the superamplitudes of $\mathcal{N} = 4$ SYM onto the relevant components. The obtained analytical formulae are implemented in the public `Mathematica` package `GGT`, and in turn yield all QCD tree amplitudes as well as the cut constructable part of all QCD loop amplitudes.

We compare the numerical efficiency of evaluating these closed analytic formulae for color ordered QCD tree amplitudes to a numerically efficient implementation of the Berends-Giele recursion. We compare calculation times for tree amplitudes with parton numbers ranging from 4 to 25 with no, one, two and three external quark lines. It turns out that the analytical results are generally faster in the case of MHV and NMHV amplitudes. Starting with the NNMHV amplitudes the Berends-Giele recursion becomes more efficient. In addition to the runtime we also compare the numerical accuracy, finding that the analytical formulae are on average more accurate than the off-shell recursion relations though both are well suited for complicated phenomenological applications. In both cases we observe a reduction in the average accuracy when phase space configurations close to singular regions are evaluated. We believe that the above findings provide valuable information to select the right method for phenomenological applications.

As a first step of trying to expand our results to massive QCD amplitudes, we investigate massive tree amplitudes on the coulomb branch of $\mathcal{N} = 4$ SYM

theory, which in turn can be obtained by dimensionally reducing the massless tree amplitudes of the six-dimensional $\mathcal{N} = (1, 1)$ SYM theory. We exploit this correspondence to derive the symmetries of massive tree amplitudes in $\mathcal{N} = 4$ SYM theory. Furthermore, we investigate the tree amplitudes of $\mathcal{N} = (1, 1)$ SYM theory and explain how analytical formulae can be obtained from a numerical implementation of the supersymmetric BCFW recursion relation. We derive compact, manifest dual conformal covariant representations of the five- and six-point superamplitudes as well as arbitrary multiplicity formulae valid for large classes of component amplitudes with two consecutive massive legs. In the literature it has been claimed that all superamplitudes of $\mathcal{N} = (1, 1)$ SYM theory can be easily obtained by uplifting massless tree amplitudes of $\mathcal{N} = 4$ SYM theory. We confirm the uplift for multiplicities up to eight by performing numerical checks but prove that uplifting $\mathcal{N} = 4$ SYM amplitudes is non-trivial for multiplicities larger than five.

Finally we study an alternative to dimensional regularization of planar scattering amplitudes in $\mathcal{N} = 4$ SYM theory by going to the Coulomb branch of the theory. The infrared divergences are regulated by masses obtained from a Higgs mechanism, allowing us to work in four dimensions. The corresponding string theory set-up suggests that the amplitudes have an exact dual conformal symmetry. The latter acts on the kinematical variables of the amplitudes as well as on the Higgs masses in an effectively five dimensional space. We confirm this expectation by an explicit calculation in the gauge theory. A consequence of this exact dual conformal symmetry is a significantly reduced set of scalar basis integrals that are allowed to appear in an amplitude. We argue that the study of exponentiation of amplitudes is simpler in the Higgsed theory because evanescent terms in the mass regulator can be consistently dropped. We illustrate this by showing the exponentiation of a four-point amplitude to two loops. Finally, we also analytically compute the small mass expansion of a two-loop master integral with an internal mass.

Zusammenfassung

Wir untersuchen die Streuamplituden der Quantenchromodynamik (QCD), $\mathcal{N} = 4$ Super-Yang-Mills-Theorie (SYM-Theorie) und der sechsdimensionalen $\mathcal{N} = (1, 1)$ SYM-Theorie, mit einem Fokus auf die Symmetrien und Relationen zwischen den Streuamplituden dieser Eichtheorien auf dem Baum-Niveau.

Wir bestimmen die superkonforme und duale superkonforme Symmetrie, welche die $\mathcal{N} = 4$ SYM-Theorie im nichtchiralen Superraum auf dem Baum-Niveau besitzt. Hierbei verwenden wir die nicht-chirale BCFW-Rekursion um die duale superkonforme Symmetrie zu beweisen. Gleichermaßen werden die Symmetrien der Baum-Niveau-Superamplituden der $\mathcal{N} = (1, 1)$ SYM-Theorie in sechs Dimensionen vollständig bestimmt. Wieder wird die BCFW-Rekursion verwendet um die duale konforme Symmetrie zu beweisen, was zur Korrektur geringfügiger Fehler des bisherigen in der Literatur vorhandenen Beweises führt.

Durch die Bestimmung der Baum-Niveau- und Ein-Schleifen-Farbzerlegung beliebiger QCD-Amplituden in primitive Amplituden stellen wir die notwendigen Mittel für QCD-Rechnungen in nächst führender Ordnung bereit. Dies verallgemeinert die bekannten Resultate für Amplituden mit maximal einem Quark–Anti-Quark–Paar und stellt eine Alternative zu dem auf Feynman-Diagrammen basierenden Algorithmus zur Bestimmung der Zerlegung in primitive Amplituden dar. Darüber hinaus werden allgemeine Fermion-Flip- und Umkehr-Identitäten hergeleitet, welche den Nullraum unter den primitiven Amplituden aufspannen. Ein begleitendes, öffentliches `Mathematica` Paket `QCDcolor` beinhaltet Implementierungen der Farbzerlegungen und der Flip- und Umkehr-Identitäten.

Basierend auf der Farbzerlegung der QCD-Baum-Niveau-Amplituden und den Fermion-Flip-Identitäten beweisen wir, dass alle farbgeordneten Baum-Niveau-Amplituden der masselosen QCD als Linearkombination von Gluon-Gluino-Amplituden der $\mathcal{N} = 4$ SYM-Theorie geschrieben werden können. Dabei beinhaltet der Beweis eine allgemeine Konstruktion dieser Linearkombination. Für alle farbgeordneten QCD-Amplituden mit bis zu vier Quark–Anti-Quark-Paaren bestimmen wir Darstellungen mit einer minimalen Anzahl an Gluon-Gluino-Amplituden. Darüber hinaus bestimmen wir analytische Formeln für alle für die QCD relevanten Gluon-Gluino-Amplituden, indem wir zuvor bekannte Ausdrücke für die Superamplituden der $\mathcal{N} = 4$ SYM-Theorie auf die relevanten Komponenten projizieren. Die erhaltenen analytischen Formeln wurden in dem öffentlichen `Mathematica` Paket `GGT` implementiert und liefern wiederum alle QCD-Amplituden auf Baum-Niveau sowie den durch Unitaritätsschnitte bestimmten Teil aller Schleifen-Amplituden der QCD.

Wir vergleichen die Effizienz der numerischen Auswertung der analytischen Formeln für farbgeordnete QCD-Baum-Niveau-Amplituden mit einer effizienten numerischen Implementierung der Berends-Giele-Rekursion. Dabei vergleichen wir die Rechenzeit für Baum-Niveau-Amplituden mit einer Anzahl von Partonen von vier bis 25 mit keiner, einer, zwei und drei externen Quark-Linien. Es zeigt sich, dass die analytischen Formeln generell schneller sind für MHV- und NMHV-Amplituden. Beginnend mit den NNMHV-Amplituden ist die Berends-Giele-Rekursion effizienter. Zusätzlich zur Laufzeit vergleichen wir auch die numerische Genauigkeit, wobei die analytischen Formeln im Mittel genauer sind als die Off-Shell-Rekursion, beide Methoden jedoch gut geeignet sind für komplizierte phenomänologische Anwendungen. In beiden Fällen beobachten wir eine Reduktion der mittleren Genauigkeit, wenn Phasenraumpunkte in der Nähe singulärer Bereiche ausgewertet werden. Unsere Untersuchungen liefern wertvolle

Informationen für die Auswahl der richtigen Methode für phenomänologische Anwendungen.

Als ersten Schritt zu einer Erweiterung unserer Resultate auf massive QCD-Amplituden untersuchen wir massive Amplituden auf dem Coulomb-Zweig der $\mathcal{N} = 4$ SYM-Theorie. Diese können durch eine dimensionale Reduktion der masselosen Baum-Niveau-Amplituden der sechsdimensionalen $\mathcal{N} = (1, 1)$ SYM-Theory erhalten werden. Wir nutzen diese Korrespondenz, um die Symmetrien der massiven Baum-Niveau-Amplituden der $\mathcal{N} = 4$ SYM-Theory herzuleiten. Darüber hinaus untersuchen wir die Baum-Niveau-Superamplituden der $\mathcal{N} = (1, 1)$ SYM-Theory und erklären, wie es möglich ist analytische Formeln mit Hilfe einer numerischen Implementierung der BCFW-Rekursion zu erhalten und nutzen diese Methode um kompakte, manifest dual konform kovariante Darstellungen der Fünf- und Sechs-Punkt-Superamplitude sowie Formeln für große Klassen von Amplituden beliebiger Multiplizität mit zwei benachbarten massiven Beinen zu bestimmen. In der Literatur wurde behauptet, dass man die Superamplituden der $\mathcal{N} = (1, 1)$ SYM- Theory durch Upliften masseloser Baum-Niveau-Amplituden der $\mathcal{N} = 4$ SYM-Theory erhalten kann. Dies bestätigen wir durch numerische Tests bis zu einer Multiplizität von acht, beweisen jedoch, dass das Upliften von $\mathcal{N} = 4$ SYM-Amplituden nicht-trivial ist für Multiplizitäten größer als fünf.

Schließlich untersuchen wir eine Alternative zur dimensionalen Regularisierung der planaren Streuamplituden in der $\mathcal{N} = 4$ SYM-Theorie durch einen Übergang zum Coulomb-Zweig der Theorie. Die Infrarotdivergenzen werden durch Massen regularisiert, die durch einen Higgs-Mechanismus erhalten wurden, was ein Rechnen in vier Dimensionen erlaubt. Die Regularisierung ist motiviert durch die korrespondierende Stringtheorie-Beschreibung, die auf eine exakte duale konforme Symmetrie der Streuamplituden hindeutet. Jene wirkt sowohl auf die kinematischen Variablen der Amplituden als auch auf die Higgs-Massen in einem effektiv fünfdimensionalen Raum. Eine Konsequenz der exakten dualen konformen Symmetrie ist eine signifikante Reduktion der möglichen skalaren Basis-Integrale, die in einer Amplitude auftreten können. Wir argumentieren, dass das Exponentieren von Amplituden mit Hilfe des Higgs-Regulators einfacher zu untersuchen ist, da infinitesimale Terme in der massiven Regularisierung konsistent weggelassen werden können. Dies illustrieren wir durch eine Demonstration des Zwei-Schleifen-Exponentierens der Vier-Punkt-Amplitude. Abschliessend berechnen wir die Entwicklung nach kleinen Massen eines allgemeinen Zwei-Schleifen-Integrals mit einer internen Masse.

Publications

The results presented in this thesis have been or are going to be published in the papers [1–5]. The manuscripts of [1–4] have been freely used for writing this thesis, i. e. several text passages of this thesis have been taken from [1–4] without or with only minor modifications.

chapters 2 and 3

- L. J. Dixon, J. M. Henn, J. Plefka, and T. Schuster, "All tree-level amplitudes in massless QCD", *JHEP* **1101** (2011) 035, `arXiv:1010.3991 [hep-ph]`.
- T. Schuster, "Color ordering in QCD", *Submitted to Phys.Rev.D*, `arXiv:1311.6296 [hep-ph]`.

chapter 4

- S. Badger, B. Biedermann, L. Hackl, J. Plefka, T. Schuster, *et al.*, "Comparing efficient computation methods for massless QCD tree amplitudes: Closed analytic formulas versus Berends-Giele recursion", *Phys.Rev.* **D87** (2013) no. 3, 034011, `arXiv:1206.2381 [hep-ph]`.

chapter 5 and part of chapter 1

- J. Plefka, T. Schuster, and V. Verschinin, "From Six to Four and More", *In preparation for submission to JHEP*.

chapter 6

- L. F. Alday, J. M. Henn, J. Plefka, and T. Schuster, "Scattering into the fifth dimension of $\mathcal{N} = 4$ super Yang-Mills", *JHEP* **1001** (2010) 077, `arXiv:0908.0684 [hep-th]`.

Outline

This Thesis is organized as follows. Each chapter starts out with a short summary of its content. If not covered by the general introductory chapter 1, some further introduction only relevant to its particular topic may be given.

In chapter 1 we give a brief motivation for the consideration of scattering amplitudes in gauge theories. The spinor helicity formalism is reviewed and the three gauge theories of interest, QCD, $\mathcal{N} = 4$ SYM theory and $\mathcal{N} = (1,1)$ SYM theory are introduced, with a focus on their symmetries at tree level. Finally the BCFW recursion and its supersymmetric generalizations are reviewed. Apart from sections 1.5.1, 1.6.1 and 1.6.2 no new results are contained in this introductory chapter.

In chapter 2 we review the concept of color decomposition in gauge theories. We derive the general color decomposition of QCD tree and one-loop amplitudes as well as all identities among the primitive amplitudes.

In chapter 3 we investigate the relations between QCD and $\mathcal{N} = 4$ SYM theory. We prove that all tree-level amplitudes of massless QCD can be obtained from linear combinations of tree amplitudes of $\mathcal{N} = 4$ SYM theory. General analytical formulae are derived for all gluon-gluino amplitudes of $\mathcal{N} = 4$ SYM theory that are relevant for QCD.

In chapter 4 we test the numerical efficiency and accuracy of the analytical formulae for QCD amplitudes obtained in chapter 3 against an efficient implementation of the Berends-Giele recursion.

In chapter 5 we turn our attention to the massive tree-level amplitudes on the Coulomb branch of $\mathcal{N} = 4$ SYM theory. We derive their symmetries and investigate the massless six-dimensional superamplitudes of $\mathcal{N} = (1,1)$ SYM theory. A general method to determine analytical formulae from a numerical implementation of the BCFW recursion is developed and successfully applied to determine manifest dual conformal covariant representations of the five- and six-point superamplitudes of $\mathcal{N} = (1,1)$ SYM theory. We propose a little group decomposition of the six-dimensional superamplitudes and derive arbitrary multiplicity formulae for large classes of amplitudes with two consecutive massive legs. Furthermore we investigate the potential uplift of massless non-chiral superamplitudes of $\mathcal{N} = 4$ SYM theory to six-dimensional superamplitudes of $\mathcal{N} = (1,1)$ SYM theory.

Finally, in chapter 6, we investigate a dual conformal covariant alternative to the dimensional regularization of the infrared divergences of $\mathcal{N} = 4$ SYM theory at loop level. We investigate the corresponding string picture as well as the realization of the massive regulator on the field theory side of the AdS/CFT correspondence. We test the dual conformal symmetry of the regulated amplitudes at the one-loop four-point level and demonstrate the exponentiation of the four-point amplitude to two loops.

The various appendices A to G supply additional details to the considerations in chapters 1 to 6.

Contents

1

Introduction

In this chapter we motivate the investigation of scattering amplitudes in gauge invariant quantum field theories. Furthermore, we briefly review the four- and six-dimensional spinor helicity formalism and introduce the three theories of interest, which are the theory of strong interactions called quantum chromodynamics (QCD), the maximally supersymmetric $\mathcal{N} = 4$ super Yang-Mills theory ($\mathcal{N} = 4$ SYM) and the $\mathcal{N} = (1, 1)$ super Yang-Mills theory in six dimensions. Finally we present the BCFW on-shell recursion and its supersymmetric generalizations for the theories of interest.

1.1. Scattering Amplitudes in Gauge Theories

Gauge theories form the basis of our theoretical understanding of the electro-weak and strong forces. The central objects of gauge theories are the scattering amplitudes. At a phenomenological level, they are critical to the prediction of cross sections at high-energy colliders for processes within and beyond the Standard Model.

A precise theoretical understanding of the Standard Model contributions to the multiple jet events observed at the Large Hadron Collider (LHC) is crucial for the discrimination of new physics as well as for precision measurements of Standard Model parameters. Since the scattering processes observed at the LHC are dominated by strong interactions, perturbative QCD is of major interest.

Tree amplitudes can be used to predict cross sections at leading order (LO) in the perturbative expansion in the strong coupling α_s of QCD. Such results are already available numerically for a wide variety of processes. Programs such as MadGraph [6, 7], CompHEP [8], and AMEGIC++ [9] are based on fast numerical evaluation of Feynman diagrams. Other methods include the Berends-Giele recursion relations [10], as implemented for example in COMIX [11], and the related ALPHA [12,13] and HELAC [14,15] algorithms based on Dyson-Schwinger equations, as well as O'Mega/WHIZARD [16,17]. The computation time required in these latter methods scales quite well with the number of legs.

Calculating high multiplicity next to leading order (NLO) QCD scattering amplitudes, the technique of color decomposition [18–22] has become an essential tool. Color decomposition provides a systematic way to treat the color degrees of freedom in a scattering process by separating them from the kinematical parts, called partial amplitudes. Since the color structures appearing in a certain amplitude are straightforward to identify, the non-trivial part of the color decomposition of an amplitude is to express the partial amplitudes in terms of gauge invariant, color ordered objects called primitive amplitudes. Besides the obvious computational advantages, such decompositions into primitive amplitudes open up the possibility to relate different gauge theories. On the level of primitive amplitudes the differences between gauge theories reduce to the helicities and flavors of the matter fields and the pure matter interactions present in the theories. Since the interactions with the gauge field are universal, as they are induced by the covariant derivative, a surprisingly large number primitive tree amplitudes are equivalent between differing gauge theories. Decompositions of QCD amplitudes into primitive amplitudes are known for all one-loop amplitudes with up to one quark–anti-quark pair [20, 22]. To obtain decompositions for amplitudes with more than one quark line a diagram based algorithm has been developed in references [23–26] which involves performing the color decomposition of a sufficiently large set of Feynman diagrams for quarks transforming in the fundamental as well as for quarks in the adjoint representation of the gauge group. The resulting linear equations can be solved for the partial amplitudes, leading to the desired decomposition into primitive amplitudes. If the algorithm incorporates the Furry relations between different diagrams, as has been done in [26], it delivers all diagram based identities among the primitive amplitudes as well. The fixed ordering of the external legs results in a simpler analytical structure of the primitive amplitudes. The development of powerful non-diagrammatic methods for their computation, such as the Berends-Giele off-shell recursion [10] or the BCFW on-shell recursion relation [27, 28] at tree level and the generalized unitarity technique, which constructs loop amplitudes by sewing together

tree amplitudes [21, 29, 30] (see [31] for a review), has been key to the recent progress in calculating NLO QCD corrections. State-of-the-art are the recent computations of NLO QCD corrections to the four [32, 33], and five jet production [34].

The properties of scattering amplitudes have long provided numerous clues to hidden symmetries and dynamical structures in gauge theory. It was recognized early on that tree amplitudes in gauge theory are effectively supersymmetric [35, 36], so that they obey supersymmetric S-matrix Ward identities [37, 38]. Soon thereafter, Parke and Taylor [39] discovered a remarkably simple formula for the maximally-helicity-violating (MHV) amplitudes for n-gluon scattering, which was proven by Berends and Giele [10], and soon generalized to $\mathcal{N} = 4$ super Yang-Mills theory (SYM) by Nair [40].

After Witten reformulated gauge theory in terms of a topological string propagating in twistor space [41], there was a huge resurgence of interest in uncovering new properties of scattering amplitudes and developing new methods for their efficient computation. Among other developments, Britto, Cachazo, Feng and Witten proved a new type of recursion relation [27, 28] for gauge theory. In contrast to the earlier Berends-Giele off-shell recursion relations [10], the BCFW relation uses only on-shell lower-point amplitudes, evaluated at complex, shifted momenta. A particular solution to this recursion relation was found for an arbitrary number of gluons in the split-helicity configuration $(-\cdots-+\cdots+)$ [42].

The BCFW recursion relation was then recast as a super-recursion relation for the tree amplitudes of $\mathcal{N} = 4$ SYM theory, which involves shifts of Grassmann parameters as well as momenta [43, 44]. A related construction is given in ref. [45]. The super-recursion relation of ref. [43] was solved for arbitrary external states by J. Drummond, J. Henn [46]. Tree-level super-amplitudes have a dual superconformal symmetry [44, 47]. This has been the guiding principle to find the solution to the BCFW recursion [46], which is written in terms of dual superconformal invariants, that are a straightforward generalization of those that first appeared in next-to-MHV (NMHV) superamplitudes [47, 48]. This dual superconformal invariance of tree-level amplitudes is a hallmark of the integrability of the planar sector of $\mathcal{N} = 4$ SYM, as it closes with the standard superconformal symmetry into an infinite-dimensional symmetry of Yangian type [49] (a recent review is ref. [50]).

While the massless tree amplitudes of $\mathcal{N} = 4$ SYM are very well studied, not so much is known about the massive amplitudes on the coulomb branch of the theory. The massive amplitudes of $\mathcal{N} = 4$ SYM are the simplest massive amplitudes in four dimensions. Indeed very compact arbitrary multiplicity formulae for particular subclasses of coulomb branch amplitudes have been obtained by N. Craig, H. Elvang, M. Kiermaier, T. Slatyer in reference [51]. Massive amplitudes on the coulomb branch of $\mathcal{N} = 4$ SYM theory can be obtained by a dimensional reduction of the six-dimensional amplitudes of $\mathcal{N} = (1, 1)$ SYM theory, thereby providing an alternative way to study the massive four-dimensional amplitudes. Recently, Tristan Dennen and Yu-tin Huang [52] were able to prove the dual conformal symmetry of the superamplitudes of $\mathcal{N} = (1, 1)$ SYM theory, which in principle should carry over to the massive four-dimensional superamplitudes. With regard to the importance of the dual conformal symmetry for the determination of all massless tree-level superamplitudes of $\mathcal{N} = 4$ SYM theory [46] this is a very promising result.

1.2. Spinor Helicity Formalism

Calculating scattering amplitudes of massless particles, the spinor helicity formalism has become a powerful tool in obtaining compact expressions for tree-level and one-loop amplitudes. Its basic idea is to use a set of commuting spinor variables instead of the parton momenta $\{p_i\}$. These spinors trivialize the on-shell conditions for the momenta

$$(p_i)^2 = 0\,. \tag{1.1}$$

In what follows we will briefly review the spinor helicity formalism in four and six dimensions. Additional details and conventions can be found in appendix A.

1.2.1. Four Dimensions

The starting point of the spinor helicity formalism in four dimensions, see e. g. [53] for a review, is to express all momenta by (2×2) matrices

$$p_{\alpha\dot\alpha} = \sigma^\mu_{\alpha\dot\alpha}\, p_\mu\,, \quad p^{\dot\alpha\alpha} = \bar\sigma^{\mu\,\dot\alpha\alpha}\, p_\mu, \quad \text{or inversely} \quad p_\mu = \tfrac{1}{2} p_{\alpha\dot\alpha}\bar\sigma^{\dot\alpha\alpha}_\mu = \tfrac{1}{2} p^{\dot\alpha\alpha}\sigma_{\mu\,\alpha\dot\alpha}\,, \tag{1.2}$$

where we take $\sigma^\mu = (\mathbf{1}, \vec\sigma)$ and $\bar\sigma^\mu = (\mathbf{1}, -\vec\sigma)$ with $\vec\sigma$ being the Pauli matrices. Raising and lowering of the α and $\dot\alpha$ indices may be conveniently defined by left multiplication with the antisymmetric ϵ symbol for which we choose the following conventions

$$\epsilon_{12} = \epsilon_{\dot1\dot2} = -\epsilon^{12} = -\epsilon^{\dot1\dot2} = 1\,, \qquad \epsilon_{\alpha\beta}\epsilon^{\beta\gamma} = \delta^\gamma_\alpha \qquad \epsilon_{\dot\alpha\dot\beta}\epsilon^{\dot\beta\dot\gamma} = \delta^{\dot\gamma}_{\dot\alpha}\,. \tag{1.3}$$

Besides being related by $p_{\alpha\dot\alpha} = \epsilon_{\alpha\beta}\epsilon_{\dot\alpha\dot\beta}p^{\dot\beta\beta} = p_{\dot\alpha\alpha}$, these matrices satisfy $p^2 = \det(p_{\alpha\dot\alpha}) = \det(p^{\alpha\dot\alpha})$, $p_{\alpha\dot\alpha}p^{\dot\alpha\beta} = p^2\delta^\beta_\alpha$ and $p^{\dot\alpha\alpha}p_{\alpha\dot\beta} = p^2\delta^{\dot\beta}_{\dot\alpha}$. Hence, the matrices $p^{\dot\alpha\alpha}$ and $p_{\alpha\dot\alpha}$ have rank one for massless momenta, implying the existence of chiral spinors λ_α and anti-chiral spinors $\tilde\lambda^{\dot\alpha}$ solving the massless Weyl equations

$$p_{\alpha\dot\alpha}\tilde\lambda^{\dot\alpha} = 0\,, \qquad p^{\dot\alpha\alpha}\lambda_\alpha = 0\,. \tag{1.4}$$

These spinors can be normalized such that

$$p_{\alpha\dot\alpha} = \lambda_\alpha\, \tilde\lambda_{\dot\alpha}\,. \tag{1.5}$$

For complex momenta the spinors λ and $\tilde\lambda$ are independent. However, for real momenta we have the reality condition $p^*_{\alpha\dot\beta} = p_{\dot\alpha\beta}$, implying $\tilde\lambda_{\dot\alpha} = c\,\lambda^*_\alpha$ for some $c \in \mathbb{R}$. Hence, the spinors can be normalized such that

$$\lambda_{\dot\alpha} = \pm\,\lambda^*_\alpha\,. \tag{1.6}$$

An explicit representation is

$$|\lambda\rangle := \lambda_\alpha = \tfrac{\sqrt{p_0+p_3}}{p_1-ip_2}\begin{pmatrix} p_1 - ip_2 \\ p_0 - p_3 \end{pmatrix}, \qquad |\tilde\lambda] := \tilde\lambda^{\dot\alpha} = \tfrac{\sqrt{p_0+p_3}}{p_1+ip_2}\begin{pmatrix} -p_0 + p_3 \\ p_1 + ip_2 \end{pmatrix}, \tag{1.7}$$

with $\lambda_{\dot\alpha} = \mathrm{sign}(p_0 + p_3)\,\lambda^*_\alpha$.

Obviously, eq. (1.5) is invariant under the $SO(2)$ little group transformations

$$\lambda_\alpha \to z\lambda_\alpha\,, \qquad \tilde\lambda_{\dot\alpha} \to z^{-1}\tilde\lambda_{\dot\alpha} \qquad \text{with} \qquad |z| = 1\,. \tag{1.8}$$

Labeling the external particles by i, each parton momentum is invariant under its own little group transformation $\lambda_i \to z_i\,\lambda_i$. The simplest Lorentz invariant and little group covariant objects that can be built out of the chiral and anti-chiral spinors are the anti symmetric spinor products

$$\langle i\,j\rangle = \langle \lambda_i\,\lambda_j\rangle = \lambda_i{}^{\alpha}\lambda_{j\alpha}\,, \qquad\qquad [i\,j] = [\tilde\lambda_i\,\tilde\lambda_j] = \tilde\lambda_{i\dot\alpha}\tilde\lambda_j^{\dot\alpha} \tag{1.9}$$

The little group invariant scalar products of massless momenta are then given by a product of two spinor brackets

$$2p_ip_j = p_{i\,\alpha\dot\alpha}p_j^{\dot\alpha\alpha} = \langle i\,j\rangle[j\,i]\,. \tag{1.10}$$

Together with the reality condition this implies that the spinor products are, up to a phase and a numerical factor of $\sqrt{2}$, the square roots of scalar products

$$|\langle i\,j\rangle| = \sqrt{|2p_ip_j|} = |[j\,i]|\,. \tag{1.11}$$

Hence, the spinor products are well suited to capture the collinear behavior of massless gauge theory amplitudes and in general lead to improved numerical stability. Due to the two-dimensional nature of the spinors they obey the non-linear Schouten identity

$$\langle i\,j\rangle\lambda_k + \langle j\,k\rangle\lambda_i + \langle k\,i\rangle\lambda_j = 0\,, \qquad [i\,j]\tilde\lambda_k + [j\,k]\tilde\lambda_i + [k\,i]\tilde\lambda_j = 0\,, \tag{1.12}$$

making simplifications of spinor expressions non-straightforward.

The remaining part of the spinor helicity formalism involves the treatment of the polarization vectors of the gluons. Each external gluon has a certain helicity $h_i = \pm 1$ and a momentum specified by the spinors λ_i and $\tilde\lambda_i$. Given this data the associated polarization vectors are

$$\left(\varepsilon_i^+\right)^{\dot\alpha\alpha} = \sqrt{2}\frac{\tilde\lambda_i^{\dot\alpha}\,\mu_i^{\alpha}}{\langle\lambda_i\,\mu_i\rangle}\,, \qquad \left(\varepsilon_i^-\right)^{\dot\alpha\alpha} = \sqrt{2}\frac{\tilde\mu_i^{\dot\alpha}\,\lambda_i^{\alpha}}{[\tilde\mu_i\,\tilde\lambda_i]}\,, \qquad \left(\varepsilon_i^\pm\right)^{\mu} = \tfrac{1}{2}\sigma^{\mu}_{\alpha\dot\alpha}\left(\varepsilon_i^\pm\right)^{\dot\alpha\alpha}\,, \tag{1.13}$$

where $(q_i)_{\alpha\dot\alpha} = \mu_i^{\alpha}\tilde\mu_i^{\dot\alpha}$ are auxiliary light-like momenta reflecting the freedom of on-shell gauge transformations. It is straightforward to verify that the polarization vectors fulfill

$$\varepsilon_i^\pm\cdot p_i = 0\,, \quad \varepsilon_i^\pm\cdot q_i = 0\,, \quad \varepsilon_i^\pm\cdot\varepsilon_i^\pm = 0\,, \quad \varepsilon_i^\pm\cdot\varepsilon_i^\mp = -1\,, \quad (\varepsilon_i^+)^*_\mu = (\varepsilon_i^-)_\mu\,, \tag{1.14}$$

as well as the completeness relation

$$\sum_{h=\pm}(\varepsilon_i^h)_\mu(\varepsilon_i^h)^*_\nu = -\eta_{\mu\nu} + \frac{p_{i\,\mu}q_{i\,\nu} + p_{i\,\nu}q_{i\,\mu}}{p_i\cdot q_i}\,. \tag{1.15}$$

A summary of all our conventions for four dimensional spinors can be found in appendix A.

1.2.2. Six Dimensions

Similar to four dimensions, the six-dimensional spinor-helicity formalism [54] provides a solution to the on-shell condition $p^2 = 0$ for massless momenta by expressing them in terms of spinors. As a first step one uses the six-dimensional Pauli matrices Σ^μ and

$\widetilde{\Sigma}^\mu$ to represent a six-dimensional vector by an antisymmetric 4×4 matrix

$$p_{AB} = p_\mu \Sigma^\mu_{AB}\,, \quad p^{AB} = p_\mu \widetilde{\Sigma}^{\mu\,AB}\,, \quad \text{or inversely} \quad p^\mu = \tfrac{1}{4}\, p_{AB}\widetilde{\Sigma}^{\mu\,BA} = \tfrac{1}{4}\, p^{AB}\Sigma^\mu_{BA}\,. \tag{1.16}$$

Besides being related by $p_{AB} = \frac{1}{2}\,\epsilon_{ABCD}\,p^{CD}$, these matrices satisfy $p_{AB}p^{BC} = \delta^C_A p^2$ and $\det(p^{AB}) = \det(p_{AB}) = (p^2)^2$. Hence, for massless momenta, p_{AB} and p^{AB} have rank 2 and therefore the chiral and anti-chiral part of the Dirac equation

$$p_{AB}\lambda^{B\,a} = 0\,, \qquad\qquad p^{AB}\tilde{\lambda}_{B\,\dot{a}} = 0 \tag{1.17}$$

have two independent solutions, labeled by their little group indices $a = 1, 2$ and $\dot{a} = \dot{1}, \dot{2}$ respectively. Raising and lowering of the $SU(2)\times SU(2)$ little group indices may be conveniently defined by contraction with the antisymmetric tensors ϵ_{ab} and $\epsilon^{\dot{a}\dot{b}}$

$$\lambda^A{}_a = \epsilon_{ab}\lambda^{A\,b}\,, \qquad\qquad \tilde{\lambda}_A{}^{\dot{a}} = \epsilon^{\dot{a}\dot{b}}\tilde{\lambda}_{A\,\dot{b}}\,. \tag{1.18}$$

Due to $p_{AB}\,p^{BC} = 0$ the chiral and anti-chiral spinors are orthogonal $\lambda^{A\,a}\tilde{\lambda}_{A\,\dot{b}} = 0$ and can be normalized such that a massless six-dimensional vector is given by

$$p_{AB} = \tilde{\lambda}_{A\,\dot{a}}\tilde{\lambda}_B{}^{\dot{a}} \qquad \text{or} \qquad p^{AB} = \lambda^{A\,a}\lambda^B{}_a\,. \tag{1.19}$$

An explicit representation of the chiral and anti-chiral spinors is given by

$$\lambda^{A\,a} = \begin{pmatrix} 0 & \sqrt{p_0+p_3} \\ \frac{-p_5+ip_4}{\sqrt{p_0+p_3}} & \frac{p_1+ip_2}{\sqrt{p_0+p_3}} \\ \frac{-p1+ip_2}{\sqrt{p_0+p_3}} & \frac{-p_5-ip_4}{\sqrt{p_0+p_3}} \\ \sqrt{p_0+p_3} & 0 \end{pmatrix}, \qquad \tilde{\lambda}_{A\,\dot{a}} = \begin{pmatrix} 0 & \sqrt{p_0-p_3} \\ \frac{p_5+ip_4}{\sqrt{p_0-p_3}} & \frac{-p_1+ip_2}{\sqrt{p_0-p_3}} \\ \frac{p_1+ip_2}{\sqrt{p_0-p_3}} & \frac{p_5-ip_4}{\sqrt{p_0-p_3}} \\ \sqrt{p_0-p_3} & 0 \end{pmatrix}. \tag{1.20}$$

As a consequence of the properties of the six-dimensional Pauli matrices, the spinors are subject to the constraint

$$\lambda^{A\,a}\lambda^B_a = \tfrac{1}{2}\epsilon^{ABCD}\tilde{\lambda}_{C\,\dot{a}}\tilde{\lambda}^{\dot{a}}_D\,. \tag{1.21}$$

It is convenient to introduce the bra-ket notation

$$\lambda^a_i = |p^a_i\rangle = |i^a\rangle\,, \qquad\qquad \tilde{\lambda}_{i\,\dot{a}} = |p_{i\,\dot{a}}] = |i_{\dot{a}}] \tag{1.22}$$

By fully contracting all $SU(4)$ Lorentz indices it is possible to construct little group covariant and Lorentz invariant objects. The simplest Lorentz invariants are the products of chiral and anti-chiral spinors

$$\langle i^a|j_{\dot{a}}] = [j_{\dot{a}}|i^a\rangle = \lambda_i^{A\,a}\tilde{\lambda}_{j\,A\,\dot{a}} \tag{1.23}$$

These little group covariant spinor products are related to the little group invariant scalar products by

$$2p_i\cdot p_j = \tfrac{1}{2}p_i^{AB}p_{j\,BA} = \det\left(\langle i|j]\right)\,. \tag{1.24}$$

The spinor products are 2×2 matrices whose inverse is

$$(\langle i^a | j_{\dot{b}}])^{-1} = -\frac{[j^{\dot{b}} | i_a\rangle}{2 p_i \cdot p_j} \tag{1.25}$$

Each set of four linear independent spinors labeled by i, j, k, l can be contracted with the antisymmetric tensor, to give the Lorentz invariant four brackets

$$\langle i^a j^b k^c l^d \rangle = \epsilon_{ABCD} \lambda_i^{A\,a} \lambda_j^{B\,b} \lambda_k^{C\,c} \lambda_l^{D\,d} = \det(\lambda_i^a \lambda_j^b \lambda_k^c \lambda_l^d)\,, \tag{1.26}$$

$$[i_{\dot{a}} j_{\dot{b}} k_{\dot{c}} l_{\dot{d}}] = \epsilon^{ABCD} \tilde{\lambda}_{i\,A\,\dot{a}} \tilde{\lambda}_{j\,B\,\dot{b}} \tilde{\lambda}_{k\,C\,\dot{c}} \tilde{\lambda}_{l\,D\,\dot{d}} = \det(\tilde{\lambda}_{i\,\dot{a}} \tilde{\lambda}_{j\,\dot{b}} \tilde{\lambda}_{k\,\dot{c}} \tilde{\lambda}_{l\,\dot{d}})\,. \tag{1.27}$$

The four brackets are related to the spinor products by

$$\langle I_1 I_2 I_3 I_4 \rangle [J_1 J_2 J_3 J_4] = \det(\langle I_i | J_j])\,, \tag{1.28}$$

where $I_k = (i_k)^{a_k}$, $J_k = (j_k)_{\dot{a}_k}$ are some multi indices labeling the spinors. Finally, it is convenient to define the following Lorentz invariant objects

$$\langle i^a | k_1 k_2 \cdots k_{2m+1} | j^b \rangle = \lambda_i^{A_1\,a} (k_1)_{A_1 A_2} (k_2)^{A_2 A_3} \ldots (k_{2m+1})_{A_{2m+1} A_{2m+2}} \lambda_j^{A_{2m+2}\,b}\,, \tag{1.29}$$

$$\langle i^a | k_1 k_2 \cdots k_{2m} | j_{\dot{b}}] = \lambda_i^{A_1\,a} (k_1)_{A_1 A_2} (k_2)^{A_2 A_3} \ldots (k_{2m})^{A_{2m} A_{2m+1}} \tilde{\lambda}_{j\,A_{2m+1}\,\dot{b}}\,, \tag{1.30}$$

$$[i_{\dot{a}} | k_1 k_2 \cdots k_{2m+1} | j_{\dot{b}}] = \tilde{\lambda}_{i\,A_1\,\dot{a}} (k_1)^{A_1 A_2} (k_2)_{A_2 A_3} \ldots (k_{2m+1})^{A_{2m+1} A_{2m+2}} \tilde{\lambda}_{j\,A_{2m+2}\,\dot{b}}\,. \tag{1.31}$$

Similar to the four dimensional case, the polarization vectors of the gluons can be expressed in terms of spinors by introducing some light-like reference momentum q with $q \cdot p \neq 0$, where p denotes the gluon momentum. The four polarization states are labeled by $SO(4) \simeq SU(2) \times SU(2)$ little group indices and can be defined as

$$\varepsilon^{\mu}_{a\dot{a}} = \frac{1}{\sqrt{2}} \langle p_a | \Sigma^{\mu} | q_b \rangle (\langle q_b | p^{\dot{a}}])^{-1} = \frac{1}{\sqrt{2}} [p_{\dot{a}} | \widetilde{\Sigma}^{\mu} | q_{\dot{b}}] (\langle p^a | q_{\dot{b}}])^{-1}\,. \tag{1.32}$$

It is straightforward to verify the properties

$$\varepsilon_{a\dot{a}} \cdot p = 0\,, \qquad \varepsilon_{a\dot{p}} \cdot q = 0\,, \qquad \varepsilon_{a\dot{a}} \cdot \varepsilon_{b\dot{b}} = -\epsilon_{ab} \epsilon_{\dot{a}\dot{b}}\,, \tag{1.33}$$

as well as the completeness relation

$$\varepsilon^{\mu}_{a\dot{a}} \varepsilon^{\nu\,a\dot{a}} = -\eta^{\mu\nu} + \frac{p^{\mu} q^{\nu} + p^{\nu} q^{\mu}}{p \cdot q}\,. \tag{1.34}$$

1.3. QCD and Gauge Theory Basics

Gauge theories are quantum field theories with a local invariance under some Lie-group G. All matter fields transform under different representations of G. In what follows we will stick to $G = SU(N)$ and the matter fields we will be dealing with transform in either the fundamental, anti-fundamental or adjoint representation, i. e.

$$\psi_i \to U_{ij} \psi_j \qquad \bar{\psi}_i \to U^*_{ij} \bar{\psi}_j \qquad \psi_{ij} \to U_{ik} \psi_{kl} U^{-1}_{lj} \tag{1.35}$$

for some local group element $U(x) \in SU(N)$. The invariance under these transformations and the requirement of renormalizability severely constrain the Lagrangian. In

fact, all interactions with the gauge field A_μ are induced by the covariant derivative

$$D_\mu = \partial_\mu - igA_\mu \,. \tag{1.36}$$

The gauge field takes values in the Lie algebra. With the help traceless Hermitean generators T^a of the $su(N)$ Lie algebra

$$[T^a, T^b] = if^{abc}T^c \tag{1.37}$$

normalized by

$$\mathrm{Tr}(T^a T^b) = \delta^{ab} \,, \tag{1.38}$$

the gauge field can be represented by the $N^2 - 1$ real fields $A^a_\mu = \mathrm{Tr}(A_\mu T^a)$

$$A_\mu = A^a_\mu T^a \,, \tag{1.39}$$

which we will call gluons. The self interactions of gluons are governed by the Yang-Mills Lagrangian

$$\mathcal{L}_{\mathrm{YM}} = -\tfrac{1}{4}\,\mathrm{Tr}\,(F_{\mu\nu}F^{\mu\nu}) \tag{1.40}$$

with the the field strength tensor being defined as

$$F_{\mu\nu} = \frac{i}{g}[D_\mu, D_\nu] = \partial_\mu A_\nu - \partial_\nu A_\mu - ig[A_\mu, A_\nu] \,. \tag{1.41}$$

Quantum chromodynamics (QCD) is the theory of strong interaction of quarks and gluons. Here we will only be concerned with the high energy limit of QCD, neglecting all quark masses. The Lagrangian of massless QCD

$$\mathcal{L}_{\mathrm{QCD}} = -\tfrac{1}{4}\,\mathrm{Tr}\,(F_{\mu\nu}F^{\mu\nu}) + i\bar{q}^I\gamma^\mu D_\mu q_I \,, \tag{1.42}$$

besides the gauge field A_μ contains n_f quarks q_I and their anti-quarks $\bar{q}^I$transforming in the fundamental and anti-fundamental representation of the gauge group $SU(N)$. Throughout the following we will keep the number of quark flavors n_f as well as the number of colors N as free parameters. The reader may specialize to $n_f = 6$ and $N = 3$ at any point.

Besides the local $SU(N)$ gauge symmetry, QCD has an obvious global $SU(n_f)$ flavor symmetry of the quarks. Similar to all massless gauge theories in four dimensions, QCD tree-level amplitudes are conformal invariant. Conformal symmetry is an extension of the Poincaré symmetry

$$\begin{aligned}
p^{\dot\alpha\alpha} &= \sum_i \lambda_i^\alpha \tilde\lambda_i^{\dot\alpha} && \text{translations} \\
m_{\alpha\beta} &= \sum_i \lambda_{i(\alpha}\partial_{i\beta)} && \\
\overline{m}_{\dot\alpha\dot\beta} &= \sum_i \tilde\lambda_{i(\dot\alpha}\partial_{i\dot\beta)} && \text{Lorentz rotations}
\end{aligned} \tag{1.43}$$

by

$$d = \tfrac{1}{2}\sum_i \left(\lambda_i^\alpha\partial_{i\alpha} + \tilde\lambda_i^{\dot\alpha}\partial_{i\dot\alpha} + 2\right) \qquad \text{dilatations} \tag{1.44}$$

and

$$k_{\alpha\dot\alpha} = \sum_i \partial_{i\alpha}\partial_{i\dot\alpha} \qquad \text{special conformal transformations} \quad (1.45)$$

The conformal generators $\{p^{\dot\alpha\alpha}, m_{\alpha\beta}, \overline{m}_{\dot\alpha\dot\beta}, d, k_{\alpha\dot\alpha}\}$ fulfill the conformal algebra $su(2,2)$ which is part of the superconformal algebra $u(2,2|4)$ presented in appendix C. At loop level the conformal symmetry of QCD is broken by the UV divergences which lead to a non-vanishing β-function and thus a renormalization of the gauge coupling. For a review of applications of conformal symmetry in QCD we refer to reference [55].

1.4. $\mathcal{N} = 4$ Super Yang Mills

The maximally supersymmetric Yang-Mills theory in four dimensions is special as it is the most symmetric version of a four dimensional gauge theory and possesses a host of interesting features: It has a powerful quantum superconformal symmetry due to its vanishing β-function, thus leaving the massless $SU(N)$ gauge theory controlled by only two tunable parameters, the number of colors N and the coupling constant g. Furthermore, highly nontrivial evidence has been accumulated in favor of the AdS/CFT conjecture, claiming an exact duality to the maximally supersymmetric superstring theory on an $AdS_5 \times S^5$ space-time background [56–58]. In the planar 't Hooft limit of the $\mathcal{N} = 4$ SYM model, where the interactions in the dual string theory are absent, the gauge/string duality system displays fascinating integrable structures. Prominently, the spectrum of anomalous dimensions of local operators is governed by an integrable model [59–61], providing formulae valid to high loop orders or even at finite 't Hooft coupling $\lambda = g^2 N$, see [62–67] for reviews.

The action of $\mathcal{N} = 4$ super Yang-Mills theory [68, 69]

$$S_{\mathcal{N}=4} = \int d^4x \ \mathrm{Tr}\Big(-\tfrac{1}{4} F_{\mu\nu}^2 + \tfrac{1}{4} D_\mu \Phi_{AB} D^\mu \Phi^{AB} + \tfrac{g^2}{8} [\Phi_{AB}, \Phi_{CD}][\Phi^{AB}, \Phi^{CD}] + i\, \bar\psi^A_{\dot\alpha} D^\mu \bar\sigma_\mu^{\dot\alpha\alpha} \psi_{A\,\alpha} \\ - \tfrac{g}{\sqrt{2}} \psi^\alpha_A [\Phi^{AB}, \psi_{B\,\alpha}] - \tfrac{g}{\sqrt{2}} \bar\psi^A_{\dot\alpha} [\Phi_{AB}, \bar\psi^{B\,\dot\alpha}] \Big) \quad (1.46)$$

is uniquely fixed by maximal supersymmetry up to the coupling constant g and the rank N of the $SU(N)$ gauge group. Equation (1.46) can be obtained by dimensional reduction of $\mathcal{N} = 1$ super Yang-Mills theory in ten dimensions. A detailed derivation can be found in appendix B. The field content of the theory is

$$\text{bosons:} \quad A^a_\mu\,, \qquad \Phi^a_{AB} \qquad\qquad \text{fermions:} \quad \psi^a_{\alpha A}\,, \qquad \overline{\psi}^{a\dot\alpha A} \quad (1.47)$$

with $a \in \{1, \ldots, N^2 - 1\}$ being adjoint indices of the $SU(N)$ gauge group, α, $\dot\alpha \in \{1, 2\}$ are $SL(2,C) \times SL(2,C)$ Lorentz indices and $A \in \{1, \ldots, 4\}$ are $SU(4)$ indices to the R-symmetry. The antisymmetric scalars $\Phi^a_{AB} = \frac{1}{2}\epsilon_{ABCD}\Phi^{a\,CD} = (\Phi^{a\,AB})^*$ are related to the six real scalars by the six-dimensional euclidean Pauli matrices $\Phi^a_{AB} = \frac{1}{\sqrt{2}}\Sigma^I_{AB}\Phi^a_I$ and $\Phi^{a\,AB} = \frac{1}{\sqrt{2}}\bar\Sigma^{I\,AB}\Phi^a_I$. We emphasize that the six-dimensional euclidean Pauli matrices, introduced in appendix B, should not be confused with the six-dimensional Pauli matrices of the spinor helicity formalism, section 1.2.2.

1.4.1. Superspaces and Superamplitudes

Dealing with scattering amplitudes of supersymmetric gauge theories is most conveniently done using appropriate on-shell superspaces. Most common for treating $\mathcal{N}=4$ super Yang-Mills theory are [40, 41, 70]

$$\text{chiral superspace:} \quad \{\lambda_i, \tilde{\lambda}_i, \eta_i^A\}\,, \qquad \text{anti-chiral superspace:} \quad \{\lambda_i, \tilde{\lambda}_i, \tilde{\eta}_{i\,A}\}\,. \tag{1.48}$$

The Grassmann variables η_i^A ($\tilde{\eta}_{iA}$) transform in the fundamental (anti-fundamental) representation of $SU(4)$ and can be assigned the helicities

$$h_i \eta_i^A = \tfrac{1}{2}\eta_i^A\,, \qquad\qquad h_i \tilde{\eta}_{iA} = -\tfrac{1}{2}\tilde{\eta}_{iA}\,, \tag{1.49}$$

with h_i denoting the helicity operator acting on leg i. With their help it is possible to decode the sixteen on-shell states

$$\text{gluons: } G_\pm \quad \text{scalars: } \phi_{AB} = \tfrac{1}{2}\epsilon_{ABCD}\phi^{CD} \quad \text{gluinos: } \psi_A \quad \text{anti-gluinos: } \overline{\psi}^A \tag{1.50}$$

into a chiral or an anti-chiral superfield $\Phi(\eta)$, $\overline{\Phi}(\tilde{\eta})$, defined by

$$\Phi(\eta) = G_+ + \eta^A\psi_A + \frac{1}{2!}\eta^A\eta^B\phi_{AB} + \frac{1}{3!}\eta^A\eta^B\eta^C\epsilon_{ABCD}\overline{\psi}^D + \frac{1}{4!}\eta^A\eta^B\eta^C\eta^D\epsilon_{ABCD}G_-\,, \tag{1.51}$$

$$\overline{\Phi}(\tilde{\eta}) = G_- + \tilde{\eta}_A\overline{\psi}^A - \frac{1}{2!}\tilde{\eta}_A\tilde{\eta}_B\phi^{AB} + \frac{1}{3!}\tilde{\eta}_A\tilde{\eta}_B\tilde{\eta}_C\epsilon^{ABCD}\psi_D + \frac{1}{4!}\tilde{\eta}_A\tilde{\eta}_B\tilde{\eta}_C\tilde{\eta}_D\epsilon^{ABCD}G_+\,. \tag{1.52}$$

As a consequence of eq. (1.49) the super fields carry the helicities

$$h_i\Phi_i(\eta) = \Phi_i(\eta)\,, \qquad\qquad h_i\overline{\Phi}_i(\tilde{\eta}) = -\overline{\Phi}_i(\tilde{\eta})\,. \tag{1.53}$$

The chiral and anti-chiral superfield are related by a Grassmann Fourier transformation

$$\overline{\Phi}(\tilde{\eta}) = \int d^4\eta\, e^{\eta^A\tilde{\eta}_A}\,\Phi(\eta)\,, \qquad\qquad \Phi(\eta) = \int d^4\tilde{\eta}\, e^{-\eta^A\tilde{\eta}_A}\,\overline{\Phi}(\tilde{\eta})\,. \tag{1.54}$$

Chiral and anti-chiral color ordered superamplitudes $\mathcal{A}_n$ can be defined as functions of the respective superfields

$$\mathcal{A}_n = \mathcal{A}_n(\Phi_1, \Phi_2, \ldots, \Phi_n)\,, \qquad\qquad \overline{\mathcal{A}}_n = \overline{\mathcal{A}}_n(\overline{\Phi}_1, \overline{\Phi}_2, \ldots, \overline{\Phi}_n)\,. \tag{1.55}$$

Due to eq. (1.54) both superamplitudes are related by a Grassmann Fourier transformation

$$\mathcal{A}_n(\Phi_1, \Phi_2, \ldots, \Phi_n) = \prod_i \int d_i^4\tilde{\eta}\; e^{-\sum_j \eta_j^A\tilde{\eta}_{j\,A}}\;\overline{\mathcal{A}}_n(\overline{\Phi}_1, \overline{\Phi}_2, \ldots, \overline{\Phi}_n) \tag{1.56}$$

The superamplitudes are inhomogeneous polynomials in the Grassmann odd variables η_i^A, $\tilde{\eta}_{i\,A}$, whose coefficients are given by the color ordered component amplitudes. A particular component amplitude can be extracted by projecting upon the relevant term in the η_i expansion of the super-amplitude via

$$G_i^+ \to \eta_i^A = 0\,, \qquad G_i^- \to \int d^4\eta_i\,, \qquad\qquad \phi_{i\,AB} \to \int d\eta_i^B d\eta_i^A\,, \tag{1.57}$$

$$\psi_{i,A} \to \int d\eta_i^A \,, \qquad \bar{\psi}_i^A \to -\int d^4\eta_i \, \eta_i^A \,, \tag{1.58}$$

and similar in anti-chiral superspace. By construction the chiral and anti-chiral superamplitudes have a manifest $SU(4)_R$ symmetry. The only $SU(4)_R$ invariants are contractions with the epsilon tensor

$$\eta_i^A \eta_j^B \eta_k^C \eta_l^D \epsilon_{ABCD} \,, \qquad \text{or} \qquad \tilde{\eta}_{i\,A} \tilde{\eta}_{j\,B} \tilde{\eta}_{k\,C} \tilde{\eta}_{l\,D} \epsilon^{ABCD} \,. \tag{1.59}$$

Consequently the appearing powers of the Grassmann variables within the superamplitudes need to be multiples of four. As a consequence of supersymmetry the superamplitudes are proportional to the supermomentum conserving delta function

$$\delta^{(8)}(q^{\alpha A}) := \prod_{\alpha=1}^{2} \prod_{A=1}^{4} q^{\alpha\, A} \qquad \text{or} \qquad \delta^{(8)}(\tilde{q}_A^{\dot{\alpha}}) := \prod_{\dot{\alpha}=1}^{2} \prod_{A=1}^{4} \tilde{q}_A^{\dot{\alpha}} \,, \tag{1.60}$$

with the chiral $q^{\alpha A} = \sum_i \lambda_i^\alpha \eta_i^A$ or anti-chiral conserved supermomentum $\tilde{q}_A^{\dot{\alpha}} = \sum_i \tilde{\lambda}_i^{\dot{\alpha}} \tilde{\eta}_{i\,A}$. Since the Grassmann variables carry helicity, eq. (1.49), their powers keep track of the amount of helicity violation present in the component amplitudes. Hence, decomposing the superamplitudes into homogeneous polynomials is equivalent to categorizing the component amplitudes according to their degree of helicity violation

$$\mathcal{A}_n(\Phi_1, \Phi_2, \ldots, \Phi_n) = \mathcal{A}_n^{\text{MHV}} + \mathcal{A}_n^{\text{NMHV}} + \mathcal{A}_n^{\text{N}^2\text{MHV}} + \cdots + \mathcal{A}_n^{N^{(n-4)}\text{MHV}} \,, \tag{1.61}$$

$$\overline{\mathcal{A}}_n(\overline{\Phi}_1, \overline{\Phi}_2, \ldots, \overline{\Phi}_n) = \overline{\mathcal{A}}_n^{\overline{\text{MHV}}} + \overline{\mathcal{A}}_n^{N\overline{\text{MHV}}} + \overline{\mathcal{A}}_n^{N^2\overline{\text{MHV}}} + \cdots + \overline{\mathcal{A}}_n^{N^{(n-4)}\overline{\text{MHV}}} \,, \tag{1.62}$$

with

$$\mathcal{A}_n^{\text{N}^p\text{MHV}} = \mathcal{O}(\eta^{4(p+2)}) \,, \qquad \overline{\mathcal{A}}_n^{N^p\overline{\text{MHV}}} = \mathcal{O}(\tilde{\eta}^{4(p+2)}) \,. \tag{1.63}$$

The highest amount of helicity violation is present in the maximally helicity violating (MHV) superamplitude or in the $\overline{\text{MHV}}$ superamplitude in anti-chiral superspace. In general, $\mathcal{A}_n^{\text{N}^p\text{MHV}}$ and $\overline{\mathcal{A}}_n^{N^p\overline{\text{MHV}}}$ are the (Next to)^p MHV and the (Next to)^p $\overline{\text{MHV}}$ superamplitudes . The complexity of the amplitudes is increasing with the degree p of helicity violation, the simplest being the MHV superamplitude in chiral superspace [40]

$$\mathcal{A}_n^{\text{MHV}} = i \frac{\delta^{(4)}(\sum_i p_i^{\alpha\dot{\alpha}}) \delta^{(8)}(\sum_i q_i^{\alpha A})}{\langle 12\rangle \langle 23\rangle \ldots \langle n1\rangle} \,, \tag{1.64}$$

and the $\overline{\text{MHV}}$ superamplitude in anti-chiral superspace

$$\mathcal{A}_n^{\overline{\text{MHV}}} = i(-1)^n \frac{\delta^{(4)}(\sum_i p_i^{\alpha\dot{\alpha}}) \delta^{(8)}(\sum_i \tilde{q}_{iA}^{\dot{\alpha}})}{[12]\,[23] \ldots [n1]} \,, \tag{1.65}$$

which are supersymmetric versions of the well known Parke-Taylor formula [39]. The increasingly complicated formulae for the amplitudes $\mathcal{A}_n^{\text{N}^p\text{MHV}}$ have been obtained in reference [46], and are presented in section 3.7. Plugging the MHV decomposition, eq. (1.61), into eq. (1.56) we obtain the relation

$$\mathcal{A}_n^{\text{N}^p\text{MHV}} = \prod_i \int d_i^4\tilde{\eta}\; e^{-\sum_j \eta_j^A \tilde{\eta}_{jA}} \overline{\mathcal{A}}_n^{N^{n-4-p}\overline{\text{MHV}}} \,, \tag{1.66}$$

simply stating that $\mathcal{A}_n^{\mathrm{N}^p\mathrm{MHV}}$ and $\overline{\mathcal{A}}_n^{N^{n-4-p}\overline{\mathrm{MHV}}}$ contain the same component amplitudes. Depending on whether $p < n-4-p$ or $p > n-4-p$ it is therefore more convenient to use the chiral or the anti-chiral description of the amplitudes, e. g. the $\mathrm{N}^{n-4}\mathrm{MHV} = \overline{\mathrm{MHV}}$ amplitudes are complicated in chiral superspace whereas they are trivial in anti-chiral superspace. Hence the most complicated amplitudes appearing in an n point chiral or anti-chiral superamplitude are the helicity amplitudes of degree $p = \lfloor \frac{n}{2} \rfloor - 2$, called minimal helicity violating (minHV) amplitudes .

Non-Chiral Superspace

Besides the well studied chiral and anti-chiral superspaces there is as well the non-chiral superspace

$$\{\lambda_i, \tilde{\lambda}_i, \eta_i^m, \tilde{\eta}_{i\,m'}\}\,. \tag{1.67}$$

Here the $SU(4)$ indices of the fields get split into two $SU(2)$ indices m and m' according to

$$\psi_A = \{\psi_m, \psi_{m'}\}\,, \qquad \bar{\psi}^A = \{\bar{\psi}^m, \bar{\psi}^{m'}\}\,, \qquad \phi_{AB} = \{\phi_{mn}, \phi_{m'n}, \phi_{mn'}, \phi_{m'n'}\}\,. \tag{1.68}$$

If raising and lowering of the $SU(2)$ indices are defined by left multiplication with $\epsilon = i\sigma_2$ and ϵ^{-1}, the non-chiral superfield reads

$$\begin{aligned}\Upsilon = \tfrac{1}{2}\phi^{m'}{}_{m'} + \eta^m\overline{\psi}_m + \tilde{\eta}_{m'}\psi^{m'} + \eta^m\tilde{\eta}_{m'}\phi_m{}^{m'} + \eta^2 G_- + \tilde{\eta}^2 G_+ \\ + \eta^2\tilde{\eta}_{m'}\overline{\psi}^{m'} + \tilde{\eta}^2\eta^m\psi_m + \tfrac{1}{2}\tilde{\eta}^2\eta^2\phi^m{}_m\,,\end{aligned} \tag{1.69}$$

with the abbreviations $\eta^2 = \frac{1}{2}\eta^m\eta_m$, $\tilde{\eta}^2 = \frac{1}{2}\tilde{\eta}_{m'}\tilde{\eta}^{m'}$. The non-chiral superfield is a scalar and has zero helicity. In contrast to the chiral superamplitudes, which have a manifest $SU(4)$ symmetry with respect to the Grassmann variables η_i^A, the non-chiral superamplitudes are invariant under $SU(2,2)$ transformations of $\{\eta_i^m, \tilde{\eta}_i^{m'}\}$. By construction only the subgroup $SU(2) \times SU(2)$ of $SU(2,2)$ is a manifest symmetry. With the convention $m \in \{1,4\}$, $m' \in \{2,3\}$ the non-chiral superfield is related to the chiral and anti-chiral superfield by the half Grassmann Fourier transformations

$$\Upsilon = \int d\eta^3 d\eta^2\; e^{\eta^2\tilde{\eta}_2 + \eta^3\tilde{\eta}_3}\Phi = \int d\tilde{\eta}_1 d\tilde{\eta}_4\; e^{-\eta^1\tilde{\eta}_1 - \eta^4\tilde{\eta}_4}\overline{\Phi}\,. \tag{1.70}$$

As a consequence of supersymmetry, the superamplitudes are proportional to the supermomentum conserving delta functions

$$\delta^{(4)}(q^{\alpha m}) := \prod_{\alpha=1}^{2}\prod_{m=1}^{2} q^{\alpha\,m} \qquad \text{and} \qquad \delta^{(4)}(\tilde{q}^{\dot{\alpha}}_{m'}) := \prod_{\dot{\alpha}=1}^{2}\prod_{m'=1}^{2} \tilde{q}^{\dot{\alpha}}_{m'}\,, \tag{1.71}$$

with the conserved supermomenta $q^m_\alpha = \sum_i \eta_i^m \lambda_{i\,\alpha}$ and $\tilde{q}^{m'}_{\dot{\alpha}} = \sum_i \tilde{\eta}_i^{m'}\tilde{\lambda}_{i\,\dot{\alpha}}$. Since we additionally have $h_i\Upsilon_i = 0$, the non-chiral superamplitudes have the general form

$$\mathcal{A}_n(\Upsilon_1, \ldots, \Upsilon_n) = \delta^4(\sum_i q^m_{i\,\alpha})\delta^4(\sum_i \tilde{q}^{m'}_{i\,\dot{\alpha}}) f_n(\{p_i, q_i, \tilde{q}_i\})\,. \tag{1.72}$$

Analyzing the half Fourier transform (1.70) relating the superfields we see that the non-chiral superamplitudes are homogeneous polynomials in the variables q_i and $\tilde{q}_i$ of degree $2n$ and the MHV decomposition (1.61) of the chiral superamplitudes translates

to a MHV decomposition of the non-chiral superamplitudes

$$f_n = f_n^{\text{MHV}} + f_n^{\text{NMHV}} + \cdots + f_n^{\overline{\text{MHV}}}\,, \tag{1.73}$$

where the N^{p}MHV sector corresponds to a fixed degree in the variables q_i and $\tilde{q}_i$

$$f_n^{\text{N}^p\text{MHV}} = \mathcal{O}(q^{2p}\tilde{q}^{2n-8-2p})\,. \tag{1.74}$$

This reflects the chiral nature of $\mathcal{N} = 4$ SYM theory.

Each of the three superspaces presented above has an associated dual superspace. In general, dual superspaces naturally arise when studying dual conformal properties of color ordered scattering amplitudes. Part of the spinor variables get replaced by the region momenta x_i, which are related to the ordinary momenta of the external legs by

$$x_i - x_{i+1} = p_i \tag{1.75}$$

and a new set of dual fermionic variables θ_i or $\tilde{\theta}_i$ is introduced, related to the fermionic momenta by

$$\theta_i - \theta_{i+1} = q_i\,, \qquad\qquad \tilde{\theta}_i - \tilde{\theta}_{i+1} = \tilde{q}_i\,. \tag{1.76}$$

Obviously, the amplitudes will depend on differences of dual variables $x_{ij} = x_i - x_j$, $\theta_{ij} = \theta_i - \theta_j$ and $\tilde{\theta}_{ij} = \tilde{\theta}_i - \tilde{\theta}_{i+1}$, as the dual variables are only defined up to an overall shift. With the identifications $x_1 = x_{n+1}$, $\theta_1 = \theta_{n+1}$, and $\tilde{\theta}_1 = \tilde{\theta}_{n+1}$, the dual variables trivialize the momentum and supermomentum conservation. The dual chiral superspace is given by

$$\{\lambda_i^\alpha, x_i^{\dot{\alpha}\alpha}, \theta_i^{A\,\alpha}\} \tag{1.77}$$

with the constraints

$$x_{i\,i+1}^{\dot{\alpha}\alpha}\lambda_{i\,\alpha} = 0\,, \qquad\qquad \theta_{i\,i+1}^{A\,\alpha}\lambda_{i\,\alpha} = 0\,. \tag{1.78}$$

Analogously, the dual anti-chiral superspace is given by

$$\{\tilde{\lambda}_i^{\dot{\alpha}}, x_i^{\dot{\alpha}\alpha}, \tilde{\theta}_{i\,A}^{\dot{\alpha}}\} \tag{1.79}$$

with the constraints

$$(x_{i\,i+1})_{\alpha\dot{\alpha}}\tilde{\lambda}_i^{\dot{\alpha}} = 0\,, \qquad\qquad (\tilde{\theta}_{i\,i+1})_A^{\dot{\alpha}}\tilde{\lambda}_{i\,\dot{\alpha}} = 0\,. \tag{1.80}$$

In the case of the dual non-chiral superspace it is possible to completely eliminate all spinor variables and express the superamplitudes solely with the dual variables

$$\{x_i^{\dot{\alpha}\alpha}, \theta_i^{m\,\alpha}, \tilde{\theta}_i^{m'\,\dot{\alpha}}, y_i^{nn'}\} \tag{1.81}$$

which are subject to the constraints

$$x_{i\,i+1}^{\dot{\alpha}\alpha}\theta_{i\,i+1\,\alpha}^{m} = 0\,, \qquad (x_{i\,i+1})_{\alpha\dot{\alpha}}\tilde{\theta}_{i\,i+1}^{m'\,\dot{\alpha}} = 0\,, \qquad x_{i\,i+1}^{\dot{\alpha}\alpha}y_{i\,i+1}^{mm'} = \theta_{i\,i+1}^{m\,\alpha}\tilde{\theta}_{i\,i+1}^{m'\,\dot{\alpha}}\,. \tag{1.82}$$

Note that $x_{i\,i+1}^2 = 0$ is a consequence of eq. (1.82). In fact the Grassmann even dual variables $y_i^{mm'}$ are not independent as they can be expressed by $\{x_i^{\dot{\alpha}\alpha}, \theta_i^{m\,\alpha}, \tilde{\theta}_i^{m'\,\dot{\alpha}}\}$. Hence, the amplitudes will not depend on them. However, the variables $y_i^{mm'}$ are

necessary for the construction of the dual non-chiral superconformal symmetry algebra presented in section 1.4.2 and appendix C.2 .

A further possibility is to study superamplitudes using the full superspaces obtained by adding the dual variables to the chiral, anti-chiral and non-chiral superspaces. The full chiral superspace is given by

$$\{\lambda_i^\alpha, \tilde{\lambda}_i^{\dot{\alpha}}, x_i^{\dot{\alpha}\alpha}, \eta_i^A, \theta_i^{A\,\alpha}\} \tag{1.83}$$

with the constraints

$$x_{i\,i+1}^{\dot{\alpha}\alpha} = \lambda_i^\alpha \tilde{\lambda}_i^{\dot{\alpha}}\,, \qquad\qquad \theta_{i\,i+1}^{A\,\alpha} = \lambda_i^\alpha \eta_i^A\,. \tag{1.84}$$

Analogously, the full anti-chiral superspace has the variables

$$\{\lambda_i^\alpha, \tilde{\lambda}_i^{\dot{\alpha}}, x_i^{\dot{\alpha}\alpha}, \tilde{\eta}_{i\,A}, \tilde{\theta}_{i\,A}^{\dot{\alpha}}\} \tag{1.85}$$

subject to the constraints

$$x_{i\,i+1}^{\dot{\alpha}\alpha} = \lambda_i^\alpha \tilde{\lambda}_i^{\dot{\alpha}}\,, \qquad\qquad (\tilde{\theta}_{i\,i+1})_A^{\dot{\alpha}} = \tilde{\lambda}_i^{\dot{\alpha}} \tilde{\eta}_{i\,A}\,. \tag{1.86}$$

Finally, the full non-chiral superspace is given by

$$\{\lambda_i^\alpha, \tilde{\lambda}_i^{\dot{\alpha}}, x_i^{\dot{\alpha}\alpha}, \eta_i^m, \tilde{\eta}_i^{m'}, \theta_i^{m\,\alpha}, \tilde{\theta}_i^{m'\,\dot{\alpha}}, y_i^{nn'}\} \tag{1.87}$$

with the constraints

$$x_{i\,i+1}^{\dot{\alpha}\alpha} = \lambda_i^\alpha \tilde{\lambda}_i^{\dot{\alpha}}\,, \qquad \theta_{i\,i+1}^{m\,\alpha} = \lambda_i^\alpha \eta_i^m\,, \qquad \tilde{\theta}_{i\,i+1}^{m'\,\dot{\alpha}} = \tilde{\lambda}_i^{\dot{\alpha}} \tilde{\eta}_i^{m'} \qquad y_{i\,i+1}^{mm'} = \eta_i^m \tilde{\eta}_i^{m'}\,. \tag{1.88}$$

1.4.2. Symmetries

This section contains a brief recap of the symmetries of the tree-level superamplitudes of $\mathcal{N} = 4$ SYM theory. For further details we refer to references [41, 47, 49, 50, 71] and appendix C.

Superconformal Symmetry of Chiral Superamplitudes

In addition to the invariance under the conformal algebra $su(2,2)$ with generators $\{p^{\dot{\alpha}\alpha}, m_{\alpha\beta}, \overline{m}_{\dot{\alpha}\dot{\beta}}, d, k_{\alpha\dot{\alpha}}\}$, introduced in section 1.3, the tree level superamplitudes are invariant under the supersymmetry generators

$$q^{\alpha A} = \sum_i \lambda_i^\alpha \eta_i^A\,, \qquad \overline{q}_A^{\dot{\alpha}} = \sum_i \tilde{\lambda}_i^{\dot{\alpha}} \partial_{iA} \qquad \text{with} \qquad \partial_{iA} = \frac{\partial}{\partial \eta_i^A} \tag{1.89}$$

and by construction invariant under the generators

$$r^A{}_B = \sum_i \left(\eta_i^A \partial_{iB} - \tfrac{1}{4} \delta_B^A \eta_i^C \partial_{iC} \right) \tag{1.90}$$

of the $SU(4)_R$ symmetry. This promotes the $su(2,2)$ conformal algebra to the superconformal algebra $u(2,2|4)$. The superconformal generators

$$s_{\alpha A} = \sum_i \partial_{i\alpha}\partial_{iA}\,, \qquad\qquad \overline{s}^A_{\dot\alpha} = \sum_i \eta_i^A \partial_{i\dot\alpha}\,, \tag{1.91}$$

follow from the commutators

$$\left[k_{\alpha\dot\alpha}, \overline{q}^{\dot\beta}_A\right] = \delta^{\dot\beta}_{\dot\alpha} s_{\alpha A}\,, \qquad\qquad \left[k_{\alpha\dot\alpha}, q^{\beta A}\right] = \delta^{\beta}_{\alpha} \overline{s}^A_{\dot\alpha}\,. \tag{1.92}$$

and the central charge is given by the helicity

$$c = \tfrac{1}{2}\sum_i \left(-\lambda_i^\alpha \partial_{i\alpha} + \tilde\lambda_i^{\dot\alpha}\partial_{i\dot\alpha} - \eta_i^A \partial_{iA} - 2\right). \tag{1.93}$$

Each generator $\boldsymbol{j}$ gets assigned a hypercharge hyp($\boldsymbol{j}$) determined by its commutator

$$[b, \boldsymbol{j}] = hyp(\boldsymbol{j})\boldsymbol{j} \tag{1.94}$$

with the hypercharge generator

$$b = \tfrac{1}{2}\sum_i \eta_i^A \partial_{iA}\,. \tag{1.95}$$

A summary of the $u(2,2|4)$ algebra can be found in appendix C.1.

Dual Superconformal Symmetry of Chiral Superamplitudes

Besides the superconformal symmetry, the tree-level chiral superamplitudes of $\mathcal{N} = 4$ SYM have a dual superconformal symmetry. Hints for a dual conformal symmetry first appeared in [72], and then independently in [73]. Since then, it has been developed [74–76] and, importantly, it was discovered that it extends to a dual superconformal symmetry [44, 46, 47].

The dual conformal symmetry can be understood through the string theory description of scattering amplitudes at strong coupling [73, 77], which identifies the scattering amplitude calculation with a Wilson loop computation in a T-dual AdS space. Quite remarkably the scattering amplitude/Wilson loop relation extends all the way down to weak coupling [74, 75, 78], for reviews see [79–81]. Dual conformal symmetry is then interpreted as the usual conformal symmetry of the dual Wilson loop. Furthermore, the dual superconformal symmetry of [47] can also be seen from the string theory perspective, through a novel fermionic T-duality [82, 83].

In the remainder of this section we will give a brief introduction to the dual superconformal symmetry, based on [44, 47, 50, 84]. The starting point is the full chiral superspace $\{\lambda_i^\alpha, \tilde\lambda_i^{\dot\alpha}, x_i^{\dot\alpha\alpha}, \eta^A, \theta_i^{A\,\alpha}\}$ introduced in eq. (1.83) and the invariance of the chiral superamplitudes under the dual super Poincaré generators

$$\{P_{\alpha\dot\alpha}, M_{\alpha\beta}, \overline{M}_{\dot\alpha\dot\beta}, Q_{\alpha A}, \overline{Q}^A_{\dot\alpha}\}\,, \tag{1.96}$$

where $M_{\alpha\beta}$, $\overline{M}_{\dot\alpha\dot\beta}$ are the ordinary Lorentz generators in full chiral superspace and the dual momentum $P_{\alpha\dot\alpha}$ and dual supermomentum $Q_{\alpha A}$ are simply the generators of

translations with respect to the dual variables x, and θ

$$P_{\alpha\dot{\alpha}} = \sum_i \partial_{i\alpha\dot{\alpha}}\,, \qquad\qquad Q_{\alpha A} = \sum_i \partial_{i\alpha A}\,, \tag{1.97}$$

where we used the abbreviations $\partial_{i\alpha\dot{\alpha}} = \frac{\partial}{\partial x_i^{\dot{\alpha}\alpha}} = \frac{1}{2}\sigma^\mu_{\alpha\dot{\alpha}}\frac{\partial}{\partial x_i^\mu}$, $\partial_{i\alpha A} = \frac{\partial}{\partial\theta_i^{\alpha A}}$. The dual superconformal generator $\overline{Q}^A_{\dot{\alpha}}$ is equal to the action of the superconformal generator $\overline{s}^A_{\dot{\alpha}}$ in full chiral superspace. Hence, we have

$$\overline{Q}^A_{\dot{\alpha}} = \sum_i \left(\theta_i^{\alpha A}\partial_{i\alpha\dot{\alpha}} + \eta^A\partial_{\dot{\alpha}}\right)\,. \tag{1.98}$$

It is a well known fact that the superconformal group can be obtained by adding the discrete transformation of conformal inversion I to the super Poincaré group. The superconformal generators $K_{\alpha\dot{\alpha}}$, S^A_α, $\overline{S}^{\dot{\alpha}}_A$ are then given by

$$K_{\alpha\dot{\beta}} = IP_{\beta\dot{\alpha}}I\,, \qquad\qquad S^A_\alpha = I\overline{Q}^A_{\dot{\alpha}}I\,, \qquad\qquad \overline{S}^{\dot{\alpha}}_A = IQ^\alpha_A I\,, \tag{1.99}$$

and their commutators and anti-commutators immediately follow from the dual super Poincaré algebra and the fact that the inversion is an involution, i. e. $I^2 = \mathbb{1}$. Using the supersymmetric BCFW recursion, described in section 1.6.1, it is possible to show that the tree-level chiral superamplitudes transform covariantly under inversions [44]

$$I\left[\mathcal{A}_n\right] = x_1^2x_2^2\ldots x_n^2\,\mathcal{A}_n \tag{1.100}$$

if the coordinates of full chiral superspace invert as [47]

$$\begin{aligned}
I\left[x_i^{\dot{\alpha}\beta}\right] &= -\frac{x_i^{\dot{\beta}\alpha}}{x_i^2} = -(x_i^{-1})^{\dot{\beta}\alpha}\,, \quad I\left[x_{i\,j}^{\dot{\alpha}\beta}\right] = \left(x_i^{-1}x_{ij}x_j^{-1}\right)^{\dot{\beta}\alpha}\,,\\
I\left[\lambda_i^\alpha\right] &= (x_i^{-1})^{\dot{\alpha}\beta}\lambda_{i\,\beta}\,, \qquad\qquad I[\tilde{\lambda}_i^{\dot{\alpha}}] = \tilde{\lambda}_{i\,\dot{\beta}}(x_{i+1}^{-1})^{\dot{\beta}\alpha}\,,\\
I[\theta_i^{\alpha A}] &= (x_i^{-1})^{\dot{\alpha}\beta}\theta^A_{i\,\beta}\,, \qquad\qquad I[\eta_i^A] = \frac{x_i^2}{x_{i+1}^2}\left(\eta_i^A - \langle\theta_i^A|x_i^{-1}|\tilde{\lambda}_i]\right)\,.
\end{aligned} \tag{1.101}$$

The inversion rules of the Levi-Civita tensors,

$$I[\epsilon_{\alpha\beta}] = \epsilon_{\dot{\alpha}\dot{\beta}}\,, \qquad\qquad I[\epsilon_{\dot{\alpha}\dot{\beta}}] = \epsilon_{\alpha\beta} \tag{1.102}$$

can be deduced from $I^2[\lambda_i^\alpha] = \lambda_i^\alpha$, and $I^2[\tilde{\lambda}_i^{\dot{\alpha}}] = \tilde{\lambda}_i^{\dot{\alpha}}$ since the inversion is an involution. Note that the inversion defined in eqs. (1.101) and (1.102) is compatible with the constraints eq. (1.84) in full chiral superspace. The simplest purely bosonic dual conformal covariants are

$$I[\,x_{ij}^2\,] = \frac{x_{ij}^2}{x_i^2x_j^2}\,, \qquad I[\,\langle i\;i+1\rangle\,] = \frac{\langle i\;i+1\rangle}{x_i^2}\,, \qquad I[\,[i\,i+1]\,] = \frac{[i\,i+1]}{x_{i+2}^2}\,. \tag{1.103}$$

Together with the dual conformal invariance of the product of the momentum and supermomentum conserving delta functions

$$I\left[\,\delta^{(4)}(x_{1\,n+1})\delta^{(8)}(\theta_{1\,n+1})\,\right] = \delta^{(4)}(x_{1\,n+1})\delta^{(8)}(\theta_{1\,n+1}) \tag{1.104}$$

this immediately proves the dual conformal symmetry of the MHV superamplitude eq. (1.64).

With the help of the inversion rules eq. (1.101), it is straightforward to calculate the dual conformal boost generator from its definition eq. (1.99) by applying the chain rule

$$\begin{aligned} K_{\alpha\dot\beta} = \sum_i \sum_j \Bigg[& I\left[\frac{\partial I[x_j^{\gamma\dot\delta}]}{\partial x_i^{\dot\alpha\beta}}\right]\partial_{j\,\gamma\dot\delta} + I\left[\frac{\partial I[\theta_j^{\gamma\,A}]}{\partial x_i^{\dot\alpha\beta}}\right]\partial_{j\,\gamma\,A} \\ & + I\left[\frac{\partial I[\lambda_j^{\gamma}]}{\partial x_i^{\dot\alpha\beta}}\right]\partial_{j\,\gamma} + I\left[\frac{\partial I[\tilde\lambda_j^{\dot\gamma}]}{\partial x_i^{\dot\alpha\beta}}\right]\partial_{j\,\dot\gamma} + I\left[\frac{\partial I[\eta_j^{A}]}{\partial x_i^{\dot\alpha\beta}}\right]\partial_{j\,A}\Bigg]. \end{aligned} \tag{1.105}$$

Applying the Schouten identity (A.4) we obtain

$$\frac{\partial x_{i\delta\dot\gamma}^{-1}}{\partial x_i^{\dot\alpha\beta}} = \frac{\epsilon_{\beta\delta}\epsilon_{\dot\alpha\dot\gamma}}{x_i^2} - \frac{x_{i\,\delta\dot\gamma}x_{i\,\beta\dot\alpha}}{x_i^4} = -\,x_{i\beta\dot\gamma}^{-1}x_{i\delta\dot\alpha}^{-1}\,, \tag{1.106}$$

immediately leading to e. g.

$$I\left[\frac{\partial I[x_j^{\gamma\dot\delta}]}{\partial x_i^{\dot\alpha\beta}}\right] = \delta_{ij}\, x_{i\alpha}{}^{\dot\gamma}\, x_{i\dot\beta}{}^{\delta}\,. \tag{1.107}$$

The final result is

$$K^{\alpha\dot\alpha} = \sum_i (x_i^{\dot\beta\alpha}x_i^{\dot\alpha\beta}\partial_{i\beta\dot\beta} + x_i^{\dot\alpha\beta}\theta_i^{\alpha B}\partial_{i\beta B} + x_i^{\dot\alpha\beta}\lambda_i^{\alpha}\partial_{i\beta} + x_{i+1}^{\dot\beta\alpha}\tilde\lambda_i^{\dot\alpha}\partial_{i\dot\beta} + \tilde\lambda_i^{\dot\alpha}\theta_{i+1}^{\alpha B}\partial_{iB})\,. \tag{1.108}$$

Given the dual conformal boost generator, the dual superconformal generators S_α^A and $\overline{S}_A^{\dot\alpha}$ directly follow from the commutators $[K_{\alpha\dot\alpha}, Q_A^\beta] = \delta_\alpha^\beta \overline{S}_{\dot\alpha\,A}$ and $[K_{\alpha\dot\alpha}, \overline{Q}^{\dot\beta\,A}] = \delta_{\dot\alpha}^{\dot\beta} S_\alpha^A$

$$\begin{aligned} S_\alpha^A &= \sum_i (-\theta_{i\alpha}^B\theta_i^{\beta A}\partial_{i\beta B} + x_{i\alpha}{}^{\dot\beta}\theta_i^{\beta A}\partial_{i\beta\dot\beta} + \lambda_{i\alpha}\theta_i^{\gamma A}\partial_{i\gamma} + x_{i+1\alpha}{}^{\dot\beta}\eta_i^A\partial_{i\dot\beta} - \theta_{i+1\alpha}^B\eta_i^A\partial_{iB})\,, \\ \overline{S}_{\dot\alpha A} &= \sum_i (x_{i\dot\alpha}{}^{\beta}\partial_{i\beta A} + \tilde\lambda_{i\dot\alpha}\partial_{iA})\,. \end{aligned} \tag{1.109}$$

The action of $K_{\alpha\dot\alpha}$, S_α^A, $\overline{S}_A^{\dot\alpha}$ on the chiral superamplitude follows from eqs. (1.99) to (1.101)

$$K^{\dot\alpha\alpha}\mathcal{A}_n = -\sum_i x_i^{\dot\alpha\alpha}\mathcal{A}_n\,, \qquad S^{\alpha\,A}\mathcal{A}_n = -\sum_i \theta_i^{\alpha\,A}\mathcal{A}_n\,, \qquad \overline{S}_A^{\dot\alpha}\mathcal{A}_n = 0\,. \tag{1.110}$$

For a complete definition of all generators of the dual superconformal algebra we refer to appendix 6.3.6.

The most important consequence of dual superconformal invariance is that it constrains the functional form of the amplitudes and leads to compact analytical formulae if dual conformal invariance is made manifest. The idea is to factor out the MHV superamplitude, compare eq. (1.61),

$$\mathcal{A}_n = \mathcal{A}_n^{\mathrm{MHV}}\left(1 + \mathcal{P}^{\mathrm{NMHV}} + \cdots + \mathcal{P}^{\overline{\mathrm{MHV}}}\right)\,, \tag{1.111}$$

where the dual conformal invariant functions $\mathcal{P}^{\mathrm{N}^p\mathrm{MHV}}$ have Grassmann degree $4p$ and

helicity zero on every point $h_i \mathcal{P}^{\mathrm{N}^p\mathrm{MHV}} = 0$. It is straightforward to construct such dual conformal invariant functions. The dual conformal invariant building blocks naturally emerging from the supersymmetric BCFW recursion are

$$\frac{1}{x_{ab}^2} \frac{\langle a\, a-1\rangle\langle b\, b-1\rangle \delta^4(\langle \xi_I | x_{i_{2k+1}a} x_{ab} | \theta_{b\, i_{2k+1}}\rangle + \langle \xi_I | x_{i_{2k+1}b} x_{ba} | \theta_{a\, i_{2k+1}}\rangle)}{\langle \xi_I | x_{i_{2k+1}b} x_{ba} | a\rangle \, \langle \xi_I | x_{i_{2k+1}b} x_{b\, a-1} | a-1\rangle \, \langle \xi_I | x_{i_{2k+1}a} x_{ab} | b\rangle \, \langle \xi_I | x_{i_{2k+1}a} x_{a\, b-1} | b-1\rangle}\,, \tag{1.112}$$

with the abbreviation $\langle \xi_I | = \langle i_1 | x_{i_1\, i_2} x_{i_2\, i_3} \dots x_{i_{2k}\, i_{2k+1}}$, or the invariants obtained from the above by making either one or both of the replacements

$$\langle a-1| \to \langle a_1 | x_{a_1\, a_2} x_{a_2\, a_3} \dots x_{a_{2m}\, a}\,, \qquad \langle b| \to \langle b_1 | x_{b_1\, b_2} x_{b_2\, b_3} \dots x_{b_{2k}\, b}\,. \tag{1.113}$$

Some details about how these invariants make up the superamplitudes will be presented in sections 3.4 and 3.7.

Superconformal Symmetry of Non-Chiral Superamplitudes

We are now going to give a complete derivation of the symmetry generators of the non-chiral superamplitudes, which has not yet been done in full detail in the literature. Part of the results presented here can be found in reference [85].

Due to the half Fourier transformation connecting the non-chiral and the chiral superspace, the manifest $SU(4)$ symmetry with respect to η_i^A transforms into a $SU(2,2)$ symmetry with respect to $\{\eta_i^m, \tilde{\eta}_i^{m'}\}$. The conformal symmetry does not involve Grassmann variables, hence the tree-level non-chiral superamplitudes are invariant under the conformal algebra $su(2,2)$, with generators

$$\{p^{\dot{\alpha}\alpha}, m_{\alpha\beta}, \overline{m}_{\dot{\alpha}\dot{\beta}}, d, k_{\alpha\dot{\alpha}}\}\,, \tag{1.114}$$

introduced in section 1.3. As a consequence of the supersymmetry of the chiral and anti-chiral superamplitudes and eq. (1.70) relating the superfields, the non-chiral superamplitudes are invariant under the $(2,2)$-supersymmetry generators

$$q^{\alpha n} = \sum_i \lambda_i^\alpha \eta_i^n\,, \qquad\qquad \tilde{q}^{\dot{\alpha} n'} = \sum_i \tilde{\lambda}_i^{\dot{\alpha}} \tilde{\eta}_i^{n'} \tag{1.115}$$

and their conjugates

$$\overline{q}_n^{\dot{\alpha}} = \sum_i \tilde{\lambda}_i^{\dot{\alpha}} \partial_{in}\,, \quad \overline{\tilde{q}}_{n'}^{\alpha} = \sum_i \lambda_i^\alpha \partial_{in'}\,, \qquad \text{with} \qquad \partial_{in} = \frac{\partial}{\partial \eta_i^n}\,, \quad \partial_{in'} = \frac{\partial}{\partial \tilde{\eta}_i^{n'}}\,. \tag{1.116}$$

All other symmetry generators now follow from the non-chiral superconformal symmetry algebra listed in appendix C.2. Commuting the supersymmetry generators $q^{\alpha n}$, $\tilde{q}^{\dot{\alpha} n'}$, $\overline{q}_n^{\dot{\alpha}}$, $\overline{\tilde{q}}$ with the conformal boost generator $k_{\alpha\dot{\alpha}}$ yields the superconformal generators

$$\begin{aligned} s_{\alpha n} &= \sum_i \partial_{i\alpha} \partial_{in}\,, & \overline{s}_{\dot{\alpha}}^n &= \sum_i \eta_i^n \partial_{i\dot{\alpha}} \\ \tilde{s}_{\dot{\alpha} n'} &= \sum_i \partial_{in'} \partial_{i\dot{\alpha}}\,, & \overline{\tilde{s}}_{\alpha}^{n'} &= \sum_i \tilde{\eta}_i^{n'} \partial_{i\alpha}\,. \end{aligned} \tag{1.117}$$

The central charge c and the hypercharge b are given by:

$$c = \tfrac{1}{2}\sum_i \left(-\lambda_i^\alpha \partial_{i\alpha} + \tilde{\lambda}_i^{\dot\alpha}\partial_{i\dot\alpha} + \eta_i^n \partial_{in} - \tilde{\eta}_i^{n'}\partial_{in'}\right), \qquad b = \tfrac{1}{2}\sum_i \left(\eta_i^n \partial_{in} - \tilde{\eta}_i^{n'}\partial_{in'}\right). \tag{1.118}$$

As already stated at the beginning, the non-chiral superamplitudes have a $su(2,2)$ symmetry with respect to the Grassmann variables. Up to the constant in the dilatation $\not{d}$ and some sign ambiguities, the generators of this fermionic conformal symmetry $\{\not{p}^{nn'}, \not{m}_{nm}, \widetilde{\not{m}}_{n'm'}, \not{d}, \not{k}_{nn'}\}$ are related to the conformal generators $\{p^{\dot\alpha\alpha}, m_{\alpha\beta}, \overline{m}_{\dot\alpha\dot\beta}, d, k_{\alpha\dot\alpha}\}$ by the replacements $\lambda \leftrightarrow \eta$ and $\tilde\lambda \leftrightarrow \tilde\eta$

$$\begin{aligned} \not{p}^{nn'} &= \sum_i \eta_i^n \tilde{\eta}_i^{n'}, & \not{k}_{nn'} &= \sum_i \partial_{in}\partial_{in'}, \\ \not{m}_{nm} &= \sum_i \eta_{i(n}\partial_{im)}, & \widetilde{\not{m}}_{n'm'} &= \sum_i \tilde\eta_{i(n'}\partial_{im')}, \\ & & \not{d} &= \tfrac{1}{2}\sum_i \left(\eta_i^n\partial_{in} + \tilde{\eta}_i^{n'}\partial_{in'} - 2\right). \end{aligned} \tag{1.119}$$

Whereas the generators $\not{m}_{nm}$, $\widetilde{\not{m}}_{n'm'}$ and $\not{d}$ are obvious symmetries of the non-chiral superamplitudes, invariance under $\not{p}^{nn'}$ and $\not{k}_{nn'}$ is not manifest.

Dual Superconformal Symmetry of Non-Chiral Superamplitudes

By analogy to the chiral superamplitudes we expect the non-chiral superamplitudes to have a dual superconformal symmetry as well. The starting point is the dual non-chiral superspace $\{x_i^{\dot\alpha\alpha}, \theta_i^{m\,\alpha}, \tilde\theta_i^{m'\,\dot\alpha}, y_i^{mm'}\}$, introduced in eq. (1.81), and the invariance of the non-chiral superamplitudes under the dual super Poincaré symmetry

$$\{P_{\alpha\dot\alpha}, M_{\alpha\beta}, \overline{M}_{\dot\alpha\dot\beta}, Q_{\alpha m}, \overline{Q}_{\dot\alpha m}, \widetilde{Q}_{\dot\alpha m'}, \overline{\widetilde{Q}}_{\alpha m'}\} \tag{1.120}$$

where

$$\begin{aligned} M_{\alpha\beta} &= \sum_i \left(\theta^n_{i(\alpha}\partial_{i\beta)n} + x^{\dot\alpha}_{i(\alpha}\partial_{i\beta)\dot\alpha}\right) \\ \overline{M}_{\dot\alpha\dot\beta} &= \sum_i \left(\tilde\theta^{n'}_{i(\dot\alpha}\partial_{i\dot\beta)n'} + x^{\alpha}_{i(\dot\alpha}\partial_{i\dot\beta)\alpha}\right) \end{aligned} \tag{1.121}$$

are just the ordinary Lorentz generators $m_{\alpha\beta}$, $\overline{m}_{\dot\alpha\dot\beta}$ acting in dual non-chiral superspace. The dual momentum $P_{\alpha\dot\alpha}$ and the dual supermomenta $Q_{\alpha m}$, $\widetilde{Q}_{\dot\alpha m'}$ are the generators of translations with respect to the dual variables x and θ, $\tilde\theta$

$$P_{\alpha\dot\alpha} = \sum_i \partial_{i\alpha\dot\alpha}, \qquad Q_{\alpha n} = -\sum_i \partial_{i\alpha n}, \qquad \widetilde{Q}_{\dot\alpha n'} = -\sum_i \partial_{i\dot\alpha n'}, \tag{1.122}$$

where we used the abbreviations $\partial_{i\alpha n} = \frac{\partial}{\partial\theta_i^{\alpha n}}$, $\partial_{i\dot\alpha n'} = \frac{\partial}{\partial\tilde\theta_i^{\dot\alpha n'}}$. The trivial translation invariance in the dual y variable leads to the dual R-symmetry generator

$$\not{\mathcal{P}}_{mm'} = -\sum_i \partial_{imm'} \qquad \text{with} \qquad \partial_{imm'} = \frac{\partial}{\partial y_i^{mm'}}. \tag{1.123}$$

The conjugate dual supermomenta $\overline{Q}^n_{\dot\alpha}$, $\overline{\widetilde{Q}}^{n'}_{\alpha}$ are given by the action of the superconformal generators $\overline{s}^n_{\dot\alpha}$, $\overline{\widetilde{s}}^{n'}_{\alpha}$ in dual non-chiral superspace. Hence, we have

$$\overline{Q}^n_{\dot\alpha} = \sum_i (\theta_i^{\alpha n}\partial_{i\alpha\dot\alpha} + y_i^{nn'}\partial_{in'\dot\alpha})\,, \qquad \overline{\widetilde{Q}}^{n'}_{\alpha} = \sum_i (\tilde\theta_i^{\dot\alpha n'}\partial_{i\alpha\dot\alpha} - y_i^{nn'}\partial_{in\alpha})\,. \tag{1.124}$$

Similar to the chiral case, the non-chiral dual superconformal symmetry can be obtained by adding the discrete transformation of dual conformal inversion I to the super Poincaré group. The conformal generator $K_{\alpha\dot\alpha}$ and the superconformal generators $S_{\alpha m}$, $\widetilde{S}_{\dot\alpha m'}$, $\overline{S}_{\dot\alpha m}$, $\overline{\widetilde{S}}_{\alpha m}$ are then given by

$$\begin{aligned} K_{\alpha\dot\beta} &= I P_{\beta\dot\alpha} I \\ S_{\alpha m} = I\overline{Q}_{\dot\alpha m} I\,, &\qquad \overline{S}_{\dot\alpha m} = I Q_{\alpha m} I\,, \\ \widetilde{S}_{\dot\alpha m'} = I\overline{\widetilde{Q}}_{\alpha m'} I\,, &\qquad \overline{\widetilde{S}}_{\alpha m'} = I\widetilde{Q}_{\dot\alpha m'} I\,, \end{aligned} \tag{1.125}$$

and their commutators and anti-commutators immediately follow from the dual super Poincaré algebra and the fact that the inversion is an involution, i. e. $I^2 = \mathbb{1}$. As we are going to show in section 1.6.1, using the BCFW recursion, the tree-level non-chiral superamplitudes transform covariantly under inversions

$$I\left[\mathcal{A}_n\right] = x_1^2 x_2^2 \dots x_n^2\, \mathcal{A}_n \tag{1.126}$$

if the coordinates of full non-chiral superspace invert as, compare eq. (1.101),

$$\begin{aligned} I\left[x_i^{\dot\alpha\beta}\right] &= -(x_i^{-1})^{\dot\beta\alpha}\,, & I\left[y_i^{mm'}\right] &= y_i^{mm'} - \langle\theta_i^m|x_i^{-1}|\tilde\theta_i^{m'}]\,, \\ I[\theta_i^{\alpha m}] &= (x_i^{-1})^{\dot\alpha\beta}\theta^m_{i\,\beta}\,, & I[\tilde\theta_i^{\dot\alpha m'}] &= \tilde\theta^{m'}_{i\,\dot\beta}(x_i^{-1})^{\dot\beta\alpha}\,, \\ I\left[\lambda_i^\alpha\right] &= (x_i^{-1})^{\dot\alpha\beta}\lambda_{i\,\beta}\,, & I[\tilde\lambda_i^{\dot\alpha}] &= \tilde\lambda_{i\,\dot\beta}(x_{i+1}^{-1})^{\dot\beta\alpha}\,, \\ I[\eta_i^m] &= \frac{x_i^2}{x_{i+1}^2}\left(\eta_i^m - \langle\theta_i^m|x_i^{-1}|\tilde\lambda_i]\right)\,, & I[\tilde\eta_i^{m'}] &= \tilde\eta_i^{m'} - [\tilde\theta_i^{m'}|x_i^{-1}|\lambda_i]\,. \end{aligned} \tag{1.127}$$

The inversion rules of the Levi-Civita tensors are given in eq. (1.102). Note that the inversion defined in eq. (1.127) is compatible with the constraints eq. (1.88) in full non-chiral superspace. With the help of the inversion rules (1.127) and its definition (1.125), the action of the dual conformal boost generator in dual non-chiral superspace can be calculated by applying the chain rule, compare eq. (1.105),

$$K_{\alpha\dot\alpha} = \sum_i \left(x_{i\alpha}{}^{\dot\beta} x_{i\dot\alpha}{}^{\beta}\partial_{i\beta\dot\beta} + x_{i\dot\alpha}{}^{\beta}\theta^n_{i\alpha}\partial_{in\beta} + x_{i\alpha}{}^{\dot\beta}\tilde\theta^{n'}_{i\dot\alpha}\partial_{in'\dot\beta} + \theta^n_{i\alpha}\tilde\theta^{n'}_{i\dot\alpha}\partial_{inn'}\right)\,. \tag{1.128}$$

Note that it would be equally straightforward to obtain the action of $K_{\alpha\dot\alpha}$ in full non-chiral superspace from eqs. (1.125) and (1.127). All other generators of the dual non-chiral superconformal symmetry now follow from the algebra listed in eq. (C.29) of appendix C.2. Similar to the chiral case, part of the generators of the dual non-chiral superconformal algebra are directly given by the action of chiral generators in dual

non-chiral superspace

$$\begin{aligned} m_{\alpha\beta} &= M_{\alpha\beta}\,, \qquad \overline{m}_{\dot\alpha\dot\beta} = \overline{M}_{\dot\alpha\dot\beta}\,, \\ \mathfrak{m}_{nm} &= \mathcal{M}_{nm}\,, \quad \widetilde{\mathfrak{m}}_{n'm'} = \widetilde{\mathcal{M}}_{n'm'}\,, \\ \overline{s}^{n}_{\dot\alpha} &= \overline{Q}^{n}_{\dot\alpha}\,, \qquad \overline{\widetilde{s}}^{n'}_{\alpha} = \overline{\widetilde{Q}}^{n'}_{\alpha}\,, \\ \overline{q}^{n}_{\dot\alpha} &= -\overline{S}^{n}_{\dot\alpha}\,, \qquad \overline{\widetilde{q}}^{n'}_{\alpha} = -\overline{\widetilde{S}}^{n'}_{\alpha}\,, \\ d = -D + n\,, &\quad \mathfrak{d} = -\mathcal{D} - n\,, \quad b = -B\,. \end{aligned} \tag{1.129}$$

Non trivial are the dual superconformal generators

$$\begin{aligned} S^{\alpha n} &= \sum_i \left(-\theta_i^{\alpha m}\theta_i^{\beta n}\partial_{i\beta m} + x_i^{\alpha\dot\beta}\theta_i^{\beta n}\partial_{i\beta\dot\beta} - \theta_i^{\alpha m} y_i^{nm'}\partial_{imm'} + y_i^{nm'} x_i^{\alpha\dot\alpha}\partial_{i\dot\alpha m'}\right)\,, \\ \widetilde{S}^{\dot\alpha n'} &= \sum_i \left(-\tilde\theta_i^{\dot\alpha m'}\tilde\theta_i^{\dot\beta n'}\partial_{i\dot\beta m'} + x_i^{\dot\alpha\beta}\tilde\theta_i^{\dot\beta n'}\partial_{i\beta\dot\beta} - \tilde\theta_i^{\dot\alpha m'} y_i^{mn'}\partial_{imm'} - y_i^{mn'} x_i^{\dot\alpha\alpha}\partial_{i\alpha m}\right)\,. \end{aligned} \tag{1.130}$$

and the dual R-symmetry boost generator

$$\mathcal{K}^{nn'} = \sum_i \left(-y_i^{nm'} y_i^{mn'}\partial_{imm'} - \tilde\theta_i^{\dot\alpha n'} y_i^{nm'}\partial_{i\dot\alpha m'} - \theta_i^{\alpha n} y_i^{mn'}\partial_{i\alpha m} + \theta_i^{n\alpha}\tilde\theta^{n'\dot\alpha}\partial_{\alpha\dot\alpha}\right)\,, \tag{1.131}$$

Due to the covariance of the non-chiral superamplitudes under dual conformal inversions, eq. (1.126), some of the generators only act covariantly on the amplitude. From eqs. (1.125) and (1.126) and the algebra eq. (C.29) it follows

$$K^{\dot\alpha\alpha}\mathcal{A}_n = -\sum_i x_i^{\dot\alpha\alpha}\mathcal{A}_n\,, \qquad \mathcal{K}^{mm'}\mathcal{A}_n = -\sum_i y_i^{mm'}\mathcal{A}_n\,, \tag{1.132}$$

$$S^{\alpha m}\mathcal{A}_n = -\sum_i \theta_i^{\alpha m}\mathcal{A}_n\,, \qquad \widetilde{S}^{\dot\alpha m'}\mathcal{A}_n = -\sum_i \tilde\theta_i^{\dot\alpha m'}\mathcal{A}_n\,, \tag{1.133}$$

$$D\mathcal{A}_n = n\,\mathcal{A}_n\,, \qquad \mathcal{D}\mathcal{A}_n = -n\,\mathcal{A}_n\,. \tag{1.134}$$

For a complete list of the non-chiral superconformal algebra and its dual representation we refer to appendix C.2.

Yangian Symmetry of Superamplitudes

With regard to the two copies of the superconformal algebra present at tree level, it is natural to ask which algebraic structure the closure of both superconformal and dual superconformal generators gives rise to. In reference [49] it was shown by J. Drummond, J. Henn and J. Plefka that the tree level chiral superamplitudes have an infinite dimensional Yangian symmetry whose level zero generators $J_a^{[0]} = \sum_i J_{a\,i}^{[0]}$ with local densities $J_{a\,i}^{[0]}$ are given by the original superconformal generators

$$[J_a^{[0]}, J_b^{[0]}\} = f_{ab}{}^{c}\, J_c^{[0]}\,, \tag{1.135}$$

where $[\cdot,\cdot\}$ denotes the graded commutator and $f_{ab}{}^{c}$ are the structure constants of the superconformal algebra presented in appendix C.1. Invariance under the level one Yangian generators $J_a^{[1]}$ with the bi-local representation

$$J_a^{[1]} = f_a{}^{cb}\sum_{i<j} J_{b\,i}^{[0]} J_{c\,j}^{[0]} \tag{1.136}$$

then follows from the covariance under the non-trivial dual superconformal generators $K_{\alpha\dot{\alpha}}$, S^{α}_{A}. The level one generators obey the commutation relations

$$[J_a^{[1]}, J_b^{[0]}\} = f_{ab}{}^{c}\, J_c^{[1]} \tag{1.137}$$

as well as the Serre relation, for details we refer to [49].

Similar to the chiral superamplitudes the non-chiral superamplitudes have a Yangian symmetry as well, which has been investigated in [85]. The infinite dimensional Yangian symmetry of the tree-level superamplitudes is a manifestation of the expected integrability of the planar sector of $\mathcal{N} = 4$ SYM. In principle it should be possible to exploit the algebraic constraints, the Yangian invariance puts on the amplitudes, to determine the amplitudes efficiently. The fact that the Yangian symmetry is obscured by the manifest local and unitary Lagrangian formulation of $\mathcal{N} = 4$ SYM theory led to the development of promising alternative formulations [86–88], that enjoy a manifest Yangian symmetry but lack manifest locality and manifest unitarity.

1.5. Six-Dimensional $\mathcal{N} = (1,1)$ SYM Theory

In this section we are introducing the maximal supersymmetric $\mathcal{N} = (1,1)$ SYM theory in six dimensions based on references [52, 85, 89–93]. The $\mathcal{N} = (1,1)$ SYM theory can be obtained by dimensionally reducing the $\mathcal{N} = 1$ SYM theory in ten dimensions and the dimensional reduction of $\mathcal{N} = (1,1)$ SYM to four dimensions is given by $\mathcal{N} = 4$ SYM theory. Hence, without presenting its Lagrangian we can immediately write down its on-shell degrees of freedom:

$$\text{gluons:}\quad g^{a}{}_{\dot{a}} \quad \text{scalars:}\quad s, s', s'', s''' \quad \text{gluinos:}\quad \chi^{a}, \lambda^{a} \quad \text{anti-gluinos:}\quad \tilde{\chi}^{\dot{a}}, \tilde{\lambda}_{\dot{a}} \tag{1.138}$$

The amplitudes of $\mathcal{N} = (1,1)$ SYM theory are most conveniently studied using the six dimensional spinor helicity formalism introduced in section 1.2.2 and the non-chiral DHS on-shell superspace introduced by T. Dennen, Y.-t. Huang, and W. Siegel in [89]

$$\{\, \lambda_i^{A\,a}\,,\ \tilde{\lambda}_{i\,A\,\dot{a}}\,,\ \xi_{i\,a}\,,\ \tilde{\xi}_i^{\dot{a}}\,\}\,, \tag{1.139}$$

whose Grassmann variables ξ_a, $\tilde{\xi}^{\dot{a}}$ carry little group indices and can be used to encode all the on-shell degrees of freedom into the scalar superfield

$$\Omega \;=\; s + \chi^{a}\,\xi_a + s'\,\tfrac{1}{2}\xi^{a}\xi_a + \tilde{\chi}_{\dot{a}}\,\tilde{\xi}^{\dot{a}} + g^{a}{}_{\dot{b}}\,\xi_a\tilde{\xi}^{\dot{b}} + \tilde{\lambda}_{\dot{b}}\,\tilde{\xi}^{\dot{b}}\xi^2 + s''\,\tilde{\xi}^2 + \lambda^{a}\,\xi_a\tilde{\xi}^2 + s'''\,\xi^2\tilde{\xi}^2\,, \tag{1.140}$$

with the abbreviations $\tilde{\xi}^2 = \frac{1}{2}\tilde{\xi}_{\dot{a}}\tilde{\xi}^{\dot{a}}$, $\xi^2 = \frac{1}{2}\xi^{a}\xi_a$. Superamplitudes can now be defined as functions of the superfields

$$\mathcal{A}_n = \mathcal{A}_n(\Omega_1, \Omega_2, \ldots, \Omega_n)\,. \tag{1.141}$$

By construction these superamplitudes are invariant under the $SU(2) \times SU(2)$ little group but, as explained in [89], do not have the $SU(2)_R \times SU(2)_R$ symmetry of $\mathcal{N} = (1,1)$ SYM theory. As a consequence of the missing R-symmetry, the superamplitudes can not be decomposed according to the degree of R-symmetry violation as in four dimensions (1.61).

The non-chiral superamplitudes are homogeneous polynomials of degree $n+n$ in the Grassmann variables

$$\mathcal{A}_n(\{\,\lambda_i^{A\,a}\,,\,\tilde{\lambda}_{i\,A\,\dot{a}}\,,\,\alpha\xi_{i\,a}\,,\,\tilde{\alpha}\tilde{\xi}_i^{\dot{a}}\,\}) = \alpha^n\tilde{\alpha}^n\mathcal{A}_n(\{\,\lambda_i^{A\,a}\,,\,\tilde{\lambda}_{i\,A\,\dot{a}}\,,\,\xi_{i\,a}\,,\,\alpha\tilde{\xi}_i^{\dot{a}}\,\}) \tag{1.142}$$

The tree-level superamplitudes of $\mathcal{N} = (1,1)$ are known only up to five external legs [89].

We now review the known amplitudes starting with $n = 3$. The special three point kinematics require the introduction [54] of the bosonic spinor variables u_i^a, w_i^a, $\tilde{u}_{i\dot{a}}$ and $\tilde{w}_{i\dot{a}}$, defined in appendix A.2.1. With the definition

$$\boldsymbol{u}_i = u_i^a\xi_{ia}\,, \qquad \tilde{\boldsymbol{u}}_i = \tilde{u}_{i\dot{a}}\tilde{\xi}_i^{\dot{a}}\,, \qquad \boldsymbol{w}_i = w_i^a\xi_{ia}\,, \qquad \tilde{\boldsymbol{w}}_i = \tilde{w}_{i\dot{a}}\tilde{\xi}_i^{\dot{a}} \tag{1.143}$$

the three point amplitude reads

$$\mathcal{A}_3 = -i\delta^6(\sum_i p^{AB})\,(\boldsymbol{u}_1\boldsymbol{u}_2 + \boldsymbol{u}_2\boldsymbol{u}_3 + \boldsymbol{u}_3\boldsymbol{u}_1)\left(\sum_{i=1}^3 \boldsymbol{w}_i\right)(\tilde{\boldsymbol{u}}_1\tilde{\boldsymbol{u}}_2 + \tilde{\boldsymbol{u}}_2\tilde{\boldsymbol{u}}_3 + \tilde{\boldsymbol{u}}_3\tilde{\boldsymbol{u}}_1)\left(\sum_{i=1}^3 \tilde{\boldsymbol{w}}_i\right)\,, \tag{1.144}$$

and has a manifest cyclic symmetry, and symmetry under chiral conjugation. The four point amplitude has the nice and simple form

$$\mathcal{A}_4 = -\delta^6\,(p)\,\delta^4\left(q^A\right)\delta^4\,(\tilde{q}_A)\,\frac{i}{x_{13}^2x_{24}^2}\,. \tag{1.145}$$

with the conserved supermomenta being given by

$$q^A = \sum_i \lambda_i^{Aa}\xi_{ia}\,, \qquad \tilde{q}_A = \sum_i \tilde{\lambda}_{iA\dot{a}}\tilde{\xi}_i^{\dot{a}}\,, \tag{1.146}$$

and the Grassmann delta functions

$$\delta^4\left(q^A\right) = \tfrac{1}{4!}\epsilon_{ABCD}q^Aq^Bq^Cq^D\,, \qquad \delta^4\,(\tilde{q}_A) = \tfrac{1}{4!}\epsilon^{ABCD}\tilde{q}_A\tilde{q}_B\tilde{q}_C\tilde{q}_D\,. \tag{1.147}$$

The five point amplitude can be computed using the BCFW recursion, presented in section 1.6.2. The result, obtained in [90], has the form

$$\begin{aligned}\mathcal{A}_5 = -\delta^6\,(p)\,\delta^4\,(q)\,\delta^4\,(\tilde{q})\,\frac{i}{x_{13}^2x_{24}^2x_{35}^2x_{41}^2x_{52}^2}\Big(&\langle q_1|p_2p_3p_4p_5|\tilde{q}_1] + \text{cyclic permutations}\\ &+ \tfrac{1}{2}\langle q_1|p_2p_3p_4p_5 - p_2p_5p_4p_3|\tilde{q}_2] + \tfrac{1}{2}\langle q_3|p_4p_5p_1p_2 - p_4p_2p_1p_5|\tilde{q}_4] + \text{c.c.}\\ &+ \tfrac{1}{2}\langle q_4|p_5p_1p_2p_3 - p_5p_3p_2p_1|\tilde{q}_5] + \tfrac{1}{2}\langle q_3|p_5p_1p_2p_3 - p_5p_3p_2p_1|\tilde{q}_5] + \text{c.c.}\,\Big)\,.\end{aligned} \tag{1.148}$$

This representation of five-point superamplitude lacks any manifest non-trivial symmetry apart from supersymmetry and is much more complicated then the four point amplitude eq. (1.145). As the five point amplitude indicates, superamplitudes with more than three partons have the general form

$$\mathcal{A}_n = \delta^{(6)}\,(p)\,\delta^{(4)}\,(q)\,\delta^{(4)}\,(\tilde{q})\,f_n(\{p_i, q_i, \tilde{q}_i\})\,. \tag{1.149}$$

Judging from the increase in complexity going from $n = 4$ to $n = 5$, any straightforward application of the BCFW recursion, using eq. (1.148) as initial data, cannot be expected to yield reasonable results for amplitudes with more than five external legs. Obviously

new strategies are necessary to investigate higher point tree amplitudes of $\mathcal{N} = (1,1)$ SYM theory.

1.5.1. Symmetries

Though part of the symmetries of tree-level $\mathcal{N} = (1,1)$ SYM theory amplitudes appear in the literature, e. g. in [52, 93], a complete list of all generators and their algebra is missing. This section aims to close this gap.

We start with the symmetries of the tree level superamplitudes in DHS on-shell superspace $\{ \lambda_i^{A\,a}\,,\, \tilde{\lambda}_{i\,A\,\dot{a}}\,,\, \xi_{i\,a}\,,\, \tilde{\xi}_i^{\dot{a}} \}$. In contrast to its four-dimensional daughter theory, $\mathcal{N} = 4$ SYM theory, the six-dimensional $\mathcal{N} = (1,1)$ SYM theory has no conformal symmetry since the gauge coupling constant in six dimensions is not dimensionless. However, we have a super Poincaré symmetry

$$\{p_{AB}, m^A{}_B, q^A, \overline{q}_A, \widetilde{q}_A, \overline{\widetilde{q}}^A\}\,. \tag{1.150}$$

The super Poincaré algebra is given by the supersymmetry algebra

$$\left\{q^A, \overline{q}^B\right\} = p^{AB}\,, \qquad \left\{\widetilde{q}_A, \overline{\widetilde{q}}_B\right\} = p_{AB} \tag{1.151}$$

and the commutators involving the $m^A{}_B$ of the $SU(4)$ Lorentz symmetry

$$\begin{aligned}
[m^A{}_B, m^C{}_D] &= \delta^C_B m^A{}_D - \delta^A_D m^C{}_B\,, & [m^A{}_B, p_{CD}] &= \delta^A_{[C} p_{D]B} + \tfrac{1}{2}\delta^A_B p_{CD}\,,\\
[m^A{}_B, q^C] &= \delta^C_B q^A - \tfrac{1}{4}\delta^A_B q^C\,, & [m^A{}_B, \overline{q}^C] &= \delta^C_B \overline{q}^A - \tfrac{1}{4}\delta^A_B \overline{q}^C\,,\\
[m^A{}_B, \widetilde{q}_C] &= -\delta^A_C \widetilde{q}_B + \tfrac{1}{4}\delta^A_B \widetilde{q}_C\,, & [m^A{}_B, \overline{\widetilde{q}}_C] &= -\delta^A_C \overline{\widetilde{q}}_B + \tfrac{1}{4}\delta^A_B \overline{\widetilde{q}}_C
\end{aligned} \tag{1.152}$$

The translation symmetry is trivially given by momentum conservation

$$p_{AB} = \sum_i \tilde{\lambda}_{iA\dot{a}} \tilde{\lambda}^{\dot{a}}_{iB}\,, \tag{1.153}$$

and the representation of the $(1,1)$ supersymmetry generators and their conjugates is

$$\begin{aligned}
q^A &= \sum_i \lambda_i^{Aa} \xi_{ia}\,, & \widetilde{q}_A &= \sum_i \tilde{\lambda}_{iA\dot{a}} \tilde{\xi}_i^{\dot{a}}\,,\\
\overline{q}^A &= \sum_i \lambda_i^{Aa} \partial_{ia}\,, & \overline{\widetilde{q}}_A &= \sum_i \tilde{\lambda}_{iA\dot{a}} \partial_i^{\dot{a}}\,,
\end{aligned} \qquad \text{with} \quad \partial_{ia} = \frac{\partial}{\partial \xi_i^a}\,, \quad \partial_i^{\dot{a}} = \frac{\partial}{\partial \tilde{\xi}_{i\dot{a}}}\,. \tag{1.154}$$

The correct form of the $su(4)$ Lorentz generators

$$m^A{}_B = \sum_i \lambda_i^{Aa} \partial_{iBa} - \tilde{\lambda}_{iB\dot{a}} \partial_i^{A\dot{a}} - \tfrac{1}{4}\delta^A_B \lambda_i^{Ca} \partial_{iCa} + \tfrac{1}{4}\delta^A_B \tilde{\lambda}_{iC\dot{a}} \partial_i^{C\dot{a}}\,. \tag{1.155}$$

is a bit more involved since the chiral and anti-chiral spinors are subject to the constraints

$$\lambda_i^{A\,a} \lambda^B_{i\,a} = \tfrac{1}{2}\epsilon^{ABCD} \tilde{\lambda}_{iC\,\dot{a}} \tilde{\lambda}^{\dot{a}}_{iD}\,, \qquad \lambda_i^{A\,a} \tilde{\lambda}_{iA\,\dot{a}} = 0\,. \tag{1.156}$$

However, it is straightforward to show that the generators $m^A{}_B$ given above commute with these constraints.

Besides the super Poincaré symmetry there are a few additional trivial symmetries.

First of all, we have the dilatation symmetry whose generator

$$d = \tfrac{1}{2}\sum_i \Big[\lambda_i^{Aa}\partial_{iAa} + \tilde{\lambda}_{iA\dot{a}}\partial_i^{A\dot{a}}\Big] + n + 2 \tag{1.157}$$

simply measures the dimension of a generator $\mathbb{G}$

$$[d, \mathbb{G}] = \dim(\mathbb{G})\mathbb{G}\,. \tag{1.158}$$

The non-zero dimensions are

$$\dim(\,p\,) = 1 \qquad \dim(\,q\,) = \dim(\,\overline{q}\,) = \dim(\,\widetilde{q}\,) = \dim(\,\overline{\widetilde{q}}\,) = \tfrac{1}{2}\,. \tag{1.159}$$

As already mentioned before, the DHS superfield and consequently the superamplitudes are manifest symmetric under the $SO(4) \simeq SU(2) \times SU(2)$ little group, whose generators are given by

$$h_{ab} = \sum_i \lambda^A_{i(a}\partial_{iAb)} - \xi_{i(a}\partial_{ib)}\,, \qquad \tilde{h}_{\dot{a}\dot{b}} = \sum_i \tilde{\lambda}_{iA(\dot{a}}\partial^A_{i\dot{b})} - \tilde{\xi}_{i(\dot{a}}\partial_{i\dot{b})}\,. \tag{1.160}$$

Finally there are two fermionic charges

$$b = \sum_i \left(\xi_{ia}\partial_i^a - 1\right)\,, \qquad \tilde{b} = \sum_i \left(\tilde{\xi}_i^{\dot{a}}\partial_{i\dot{a}} - 1\right) \tag{1.161}$$

that correspond to a $U(1) \times U(1)$ subgroup of the $SU(2) \times SU(2)$ R-symmetry that we sacrificed for the manifest little group invariance. The action of the hyper charges on some generator $\mathbb{G}$ are given by

$$[b, \mathbb{G}] = \mathrm{ferm}(\mathbb{G})\mathbb{G}\,, \qquad [\tilde{b}, \mathbb{G}] = \widetilde{\mathrm{ferm}}(\mathbb{G})\mathbb{G}\,, \tag{1.162}$$

and the non-zero fermionic charges are

$$\mathrm{ferm}(\,q\,) = \widetilde{\mathrm{ferm}}\,(\,\widetilde{q}\,) = 1\,, \qquad \mathrm{ferm}(\,\overline{q}\,) = \widetilde{\mathrm{ferm}}\left(\,\overline{\widetilde{q}}\,\right) = -1\,. \tag{1.163}$$

Note that the constants in d, b, $\tilde{b}$ are not fixed by the algebra and have been chosen such that they annihilate the superamplitude.

All the symmetries presented up to this point exactly match the expectations. Fortunately, as has been shown by Tristan Dennen and Yu-tin Huang in reference [52], there is an additional non-trivial symmetry of the superamplitudes. Similar to $\mathcal{N} = 4$ SYM theory in four dimensions, the $\mathcal{N} = (1,1)$ SYM theory in six dimensions has a tree-level dual conformal symmetry. Due to the lack of a superconformal symmetry, the dual conformal symmetry does not promote to a full dual superconformal symmetry.

In analogy to four dimensions we extend the DHS on-shell superspace by dual variables to the full non-chiral superspace

$$\{\,\lambda_i^{A\,a}\,,\,\tilde{\lambda}_{i\,A\,\dot{a}}\,,\,\xi_{i\,a}\,,\,\tilde{\xi}_i^{\dot{a}}\,,\,x_i^{AB}, \theta_i^A, \tilde{\theta}_{i\,A}\}\,. \tag{1.164}$$

The variables are subject to the constraints

$$\begin{aligned} x^{AB}_{ii+1} &= \lambda_i^{Aa}\lambda^B_{ia}\,, & x_{ii+1\;AB} &= \tilde{\lambda}_{iA\dot{a}}\tilde{\lambda}^{\dot{a}}_{iB} \\ \theta^A_{ii+1} &= \lambda_i^{Aa}\xi_{ia}\,, & \tilde{\theta}_{ii+1\;A} &= \tilde{\lambda}_{iA\dot{a}}\tilde{\xi}_i^{\dot{a}} \end{aligned} \tag{1.165}$$

Similar to the non-chiral superamplitudes of $\mathcal{N}=4$ SYM theory, it is possible to express the superamplitudes of $\mathcal{N}=(1,1)$ SYM solely using the dual superspace variables $\{x,\theta,\tilde{\theta}\}$. The amplitudes only depend on differences of dual variables, resulting in translation symmetries with respect to each of the dual variables. Hence, we define the dual translation generator to be

$$P_{AB}=\sum_i \partial_{iAB}\,,\quad \text{with}\quad \partial_{iAB}=\frac{\partial}{\partial x_i^{AB}}=\tfrac{1}{2}\widetilde{\Sigma}^{\mu\,BA}\frac{\partial}{\partial x_i^{\mu}}\,, \tag{1.166}$$

and the dual supermomenta are

$$Q_A=\sum_i \partial_{iA}\,,\qquad \widetilde{Q}^A=\sum_i \partial_i^A\,,\qquad \text{with}\qquad \partial_{iA}=\frac{\partial}{\partial\theta_i^A}\qquad \partial_i^A=\frac{\partial}{\partial\tilde{\theta}_{iA}}\,. \tag{1.167}$$

Although it is easy to algebraically construct conjugates $\overline{Q}_A$, $\overline{\widetilde{Q}}^A$ to the dual supermomenta, these conjugates would imply the invariance under the superconformal generators $\overline{s}_A=\sum\xi_i^a\partial_{iAa}$ and $\overline{\widetilde{s}}^A=\sum\widetilde{\xi}_{i\dot{a}}\partial^{iA\dot{a}}$, which is not the case. We conclude that the amplitudes have an supersymmetry enhanced dual Poincaré symmetry

$$\{P_{AB},M^A_{\ B},Q_A,\widetilde{Q}^A\} \tag{1.168}$$

Though we do not have a full dual super Poincaré symmetry we have a dual conformal symmetry, which we are going to derive in what follows. First we recall that for $n>3$ the superamplitudes have the form

$$\mathcal{A}_n=\delta^{(6)}\left(p\right)\delta^{(4)}\left(q\right)\delta^{(4)}\left(\tilde{q}\right)f_n\,. \tag{1.169}$$

It is possible to define a dual conformal inversion I of the variables of the full superspace eq. (1.164) such that the function f_n inverts covariantly

$$I[f_n]=\left(\prod_i x_i^2\right)\,f_n\,. \tag{1.170}$$

In contrast to four dimensions the product of momentum and supermomentum conserving delta functions is not dual conformal invariant due to the mismatch of the degrees of momentum and supermomentum conserving delta functions

$$I[\delta^{(6)}(x_{1\,n+1})\delta^{(4)}(\theta_{1\,n+1})\delta^{(4)}(\tilde{\theta}_{1\,n+1})]=(x_1^2)^2\delta^{(6)}(x_{1\,n+1})\delta^{(4)}(\theta_{1\,n+1})\delta^{(4)}(\tilde{\theta}_{1\,n+1})\,. \tag{1.171}$$

The inversion leading to eq. (1.170) is defined as

$$I[x_i^{\mu}]=-(x_i^{-1})_{\mu}=-\frac{x_{i\,\mu}}{x_i^2}\,,\qquad I[x_i^{AB}]=(x_i^{-1})_{AB}\,, \tag{1.172}$$

$$I[\theta_i^A]=\theta_i^B(x_i^{-1})_{BA}\,,\qquad I[\tilde{\theta}_{i\,A}]=(x_i^{-1})^{AB}\tilde{\theta}_{i\,B} \tag{1.173}$$

$$I[\lambda_i^{Aa}]=\frac{x_{i\,AB}\lambda_{i\,a}^B}{\sqrt{x_i^2x_{i+1}^2}}\,,\qquad I[\tilde{\lambda}_{iA\dot{a}}]=\frac{x_i^{AB}\tilde{\lambda}_{iB}^{\dot{a}}}{\sqrt{x_i^2x_{i+1}^2}}\,, \tag{1.174}$$

$$I[\xi_{i\,a}]=\sqrt{\frac{x_i^2}{x_{i+1}^2}}\left(\xi_i^a+\langle\theta_i|x_i^{-1}|i^a\rangle\right)\,,\qquad I[\tilde{\xi}_i^{\dot{a}}]=-\sqrt{\frac{x_i^2}{x_{i+1}^2}}\left(\tilde{\xi}_{i\,\dot{a}}+[\tilde{\theta}_i|x_i^{-1}|i_{\dot{a}}]\right)\,, \tag{1.175}$$

$$I[u_{i\,a}] = \frac{\beta\, u_i^a}{\sqrt{x_{i+2}^2}}\,, \qquad\qquad I[\tilde{u}_{i\,\dot{a}}] = \frac{\tilde{u}_i^{\dot{a}}}{\beta\sqrt{x_{i+2}^2}}\,. \tag{1.176}$$

Equations (1.172) and the fact that the inversion needs to be an involution on the dual variables, i. e. $I^2 = \mathbb{1}$, imply the inversion rules of the sigma matrices

$$I[\Sigma^\mu_{AB}] = \widetilde{\Sigma}^{BA}_\mu\,, \qquad\qquad I[\widetilde{\Sigma}^{AB}_\mu] = \Sigma^\mu_{BA}\,. \tag{1.177}$$

Consistency between the inversions of x and the chiral and anti-chiral spinors requires the following inversion of the epsilon tensors of the little group

$$I[\epsilon_{ab}] = \epsilon^{ba}\,, \qquad\qquad I[\epsilon_{\dot{a}\dot{b}}] = \epsilon^{\dot{b}\dot{a}}\,. \tag{1.178}$$

Consequently, we have $I^2 = -\mathbb{1}$ on all variables carrying a little group index. Since the superamplitude is little group invariant this is no obstacle. We note that the inversion defined in eqs. (1.172) to (1.178) differs from the one presented in [52] by some signs which are necessary in order to yield the desired inversion of the amplitudes. The prove of eq. (1.170) is straightforward to carry out using the BCFW recursion and will be presented in section 1.6.2.

Similar to the four dimensional case we now define the generators

$$K^{AB} = I P_{AB} I\,, \qquad\qquad \overline{S}^A = I Q_A I\,, \qquad\qquad \overline{\widetilde{S}}_A = I \widetilde{Q}^A I\,. \tag{1.179}$$

From eq. (1.170) it immediately follows, that f_n is annihilated by the dual superconformal generators $\overline{S}^A$, $\overline{\widetilde{S}}_A$, but is covariant under dual conformal boosts

$$K^{AB}\, f_n = -\left(\sum_i x_i^{AB}\right) f_n\,. \tag{1.180}$$

From the inversion rules eqs. (1.172) to (1.178) and the defining equation (1.179) we can obtain the action of the dual conformal boost generator by applying the chain rule, compare the four-dimensional case eq. (1.105). Since on all variables carrying little group indices we have $I^2 = -\mathbb{1}$, the action of K^{AB} on a little group invariant object is given by

$$\begin{aligned} K^{AB} = \sum_i \sum_j \Bigg[& I\left[\frac{\partial I[x_j^{CD}]}{\partial x_{i\,AB}}\right] \partial_{j\,CD} + I\left[\frac{\partial I[\theta_j^C]}{\partial x_{i\,AB}}\right] \partial_{j\,C} + I\left[\frac{\partial I[\tilde{\theta}_{j\,D}]}{\partial x_{i\,AB}}\right] \partial_j^D \\ & - I\left[\frac{\partial I[\lambda_j^{Ca}]}{\partial x_{i\,AB}}\right] \partial_{j\,Ca} - I\left[\frac{\partial I[\tilde{\lambda}_{j\,E\dot{a}}]}{\partial x_{i\,AB}}\right] \partial_j^{E\dot{a}} \\ & - I\left[\frac{\partial I[\xi_{j\,a}]}{\partial x_{i\,AB}}\right] \partial_j^a - I\left[\frac{\partial I[\tilde{\xi}_j^{\dot{a}}]}{\partial x_{i\,AB}}\right] \partial_{j\,\dot{a}} \Bigg]\,. \end{aligned} \tag{1.181}$$

The coefficients of the derivatives are straightforward to obtain leading to

$$\begin{aligned} K^{AB} = \sum_i \Big[& x_i^{AC} x_i^{BD} \partial_{i\,CD} - \theta_i^{[A} x_i^{B]C} \partial_{iC} - \epsilon^{ABCD} \tilde{\theta}_{iC} x_{iDE} \partial_i^E \\ & - \tfrac{1}{2} \lambda_i^{[Aa} \left(x_i + x_{i+1}\right)^{B]C} \partial_{iCa} - \tfrac{1}{2} \epsilon^{ABCD} \tilde{\lambda}_{iC\dot{a}} \left(x_i + x_{i+1}\right)_{DE} \partial_i^{E\dot{a}} \\ & + \tfrac{1}{2} \left(\theta_i + \theta_{i+1}\right)^{[A} \lambda_{ia}^{B]} \partial_i^a + \tfrac{1}{2} \epsilon^{ABCD} (\tilde{\theta}_i + \tilde{\theta}_{i+1})_C \tilde{\lambda}_{iD}^{\dot{a}} \partial_{i\dot{a}} \Big] , \end{aligned} \tag{1.182}$$

In an analogue calculation or by calculating the commutators of K^{AB} with the dual supermomenta Q^A, $\tilde{Q}_A$ we obtain

$$\overline{S}^A = \sum_i x_i^{AB} \partial_{iB} - \lambda_{ia}^A \partial^a , \qquad \overline{\tilde{S}}_A = \sum_i x_{iAB} \partial_i^B - \tilde{\lambda}_{iA\dot{a}} \partial^{\dot{a}} . \tag{1.183}$$

Obviously the dual superconformal generators $\overline{S}^A$, $\overline{\tilde{S}}_A$ are related to the conformal generators $\overline{q}^A$, $\overline{\tilde{q}}_A$ by $\overline{S}^A = -\overline{q}^A$ and $\overline{\tilde{S}}_A = -\overline{\tilde{q}}_A$.

Adding dual conformal inversions promotes the enhanced Poincaré symmetry to an enhanced dual conformal symmetry

$$\{P_{AB}, M^A{}_B, D, K_{AB}, Q_A, \tilde{Q}^A, \overline{S}^A, \overline{\tilde{S}}_A\} . \tag{1.184}$$

The generators $M^A{}_B$ of the $SU(4)$ Lorentz symmetry act canonically on all generators carrying $SU(4)$ indices

$$\begin{aligned} [M^A{}_B, M^C{}_D] &= \delta_B^C M^A{}_D - \delta_D^A M^C{}_B , \\ [M^A{}_B, P_{CD}] &= \delta_{[C}^A P_{D]B} + \tfrac{1}{2} \delta_B^A P_{CD} , \qquad [M^A{}_B, K_{CD}] = \delta_{[C}^A K_{D]B} + \tfrac{1}{2} \delta_B^A K_{CD} , \\ [M^A{}_B, Q_C] &= -\delta_C^A Q_B + \tfrac{1}{4} \delta_B^A Q_C , \qquad [M^A{}_B, \overline{\tilde{S}}_C] = -\delta_C^A \overline{\tilde{S}}_B + \tfrac{1}{4} \delta_B^A \overline{\tilde{S}}_C , \\ [m^A{}_B, \tilde{Q}^C] &= \delta_B^C \tilde{Q}^A - \tfrac{1}{4} \delta_B^A \tilde{Q}^C , \qquad [M^A{}_B, \overline{S}^C] = \delta_B^C \overline{S}^A - \tfrac{1}{4} \delta_B^A \overline{S}^C . \end{aligned} \tag{1.185}$$

The remaining non-zero commutation relations are

$$\begin{aligned} [K^{AB}, Q_C] &= \delta_C^{[A} \overline{S}^{B]} , \qquad [K_{AB}, \tilde{Q}^C] = \delta_{[A}^C \overline{\tilde{S}}_{B]} , \\ [P^{AB}, \overline{\tilde{S}}_C] &= \delta_C^{[A} \tilde{Q}^{B]} , \qquad [P_{AB}, \overline{S}^C] = \delta_{[A}^C Q_{B]} , \\ [K_{AB}, P^{CD}] &= \delta_{[A}^{[C} M^{D]}_{\ \ B]} + \delta_{[A}^C \delta_{B]}^D D . \end{aligned} \tag{1.186}$$

The dual dilatation generator is given by

$$D = -\tfrac{1}{2} \sum_i \left(\lambda_{ia}^A \partial_{iA}^a + \tilde{\lambda}_{iA\dot{a}} \partial_i^{A\dot{a}} + \theta_i^A \partial_{iA} + \tilde{\theta}_{iA} \partial_i^A + x_i^{AB} \partial_{i\,AB} \right) \tag{1.187}$$

and, as a consequence of eqs. (1.180) and (1.186), acts covariantly

$$D\, f_n = n\, f_n . \tag{1.188}$$

The dual Lorentz generators $M^A{}_B$ are equal to the action of the on-shell Lorentz generators $m^A{}_B$ in the full superspace. Their representation can be obtained from the dual

conformal algebra eq. (1.186) and is given by

$$M^A{}_B = \sum_i \Big[x_i^{AC}\partial_{i\,BC} - \tfrac{1}{4}\delta^A_B x_i^{CD}\partial_{i\,CD} + \lambda_i^{Aa}\partial_{iBa} - \tfrac{1}{4}\delta^A_B\lambda_i^{Ca}\partial_{iCa} + \theta_i^A\partial_{iB} - \tfrac{1}{4}\delta^A_B\theta_i^C\partial_{iC} - \tilde{\lambda}_{iB}^{\dot{a}}\partial_i^{A\dot{a}} + \tfrac{1}{4}\delta^A_B\tilde{\lambda}_{iC}^{\dot{a}}\partial_i^{C\dot{a}} - \tilde{\theta}_{iB}\partial_i^A + \tfrac{1}{4}\delta^A_B\tilde{\theta}_{iC}\partial_i^C \Big] \tag{1.189}$$

Finally, we define the dual R-symmetry charges to be

$$B = \sum_i \left(\xi_{ia}\partial_i^a + \theta_i^{Aa}\partial_{iA}^a\right) - n + 4\,, \qquad \widetilde{B} = \sum_i \left(\tilde{\xi}_i^{\dot{a}}\partial_{i\dot{a}} + \tilde{\theta}_{iA\dot{a}}\partial_i^{A\dot{a}}\right) - n + 4\,. \tag{1.190}$$

The non-zero charges are $\mathrm{ferm}(Q) = \widetilde{\mathrm{ferm}}(\widetilde{Q}) = -\mathrm{ferm}(\overline{S}) = -\widetilde{\mathrm{ferm}}(\overline{\widetilde{S}}) = 1$, and the constants in the definitions of B and $\widetilde{B}$ have been fixed such that f_n gets annihilated.

1.5.2. Dimensional Reduction to Massless $\mathcal{N} = 4$ SYM

In this section we explain how the six dimensional tree-level superamplitudes can be mapped to non-chiral superamplitudes of massless $\mathcal{N} = 4$ SYM. Similar mappings can be found in references [85, 89, 90, 93].

In order to perform the dimensional reduction we restrict the six dimensional momenta to the preferred four dimensional subspace $p_4 = p_5 = 0$. Because of our special choice of six dimensional Pauli matrices, compare eq. (A.24), we can express the six dimensional spinors in terms of four dimensional ones

$$\lambda^{Aa} = \begin{pmatrix} 0 & \lambda_\alpha \\ \tilde{\lambda}^{\dot{\alpha}} & 0 \end{pmatrix}, \qquad \tilde{\lambda}_{A\dot{a}} = \begin{pmatrix} 0 & \lambda^\alpha \\ -\tilde{\lambda}_{\dot{\alpha}} & 0 \end{pmatrix}. \tag{1.191}$$

In the four dimensional subspace the contractions with the six-dimensional Pauli matrices read

$$p_{AB} = \begin{pmatrix} 0 & -p^\alpha{}_{\dot{\beta}} \\ p_{\dot{\alpha}}{}^\beta & 0 \end{pmatrix}, \qquad p^{AB} = \begin{pmatrix} 0 & -p_\alpha{}^{\dot{\beta}} \\ p^{\dot{\alpha}}{}_\beta & 0 \end{pmatrix}, \tag{1.192}$$

and the supermomenta are

$$q^A = \lambda^{Aa}\xi_a = \begin{pmatrix} \lambda_\alpha\xi_2 \\ \tilde{\lambda}^{\dot{\alpha}}\xi_1 \end{pmatrix}, \qquad \tilde{q}_A = \tilde{\lambda}_{A\dot{a}}\tilde{\xi}^{\dot{a}} = \begin{pmatrix} \lambda^\alpha\tilde{\xi}^{\dot{2}} & -\tilde{\lambda}_{\dot{\alpha}}\tilde{\xi}_{\dot{1}} \end{pmatrix}. \tag{1.193}$$

Obviously, both, ξ_a and $\tilde{\xi}^{\dot{a}}$ have to be mapped to η^A and $\tilde{\eta}_A$. Here we make the choice

$$\xi_a = \left(\tilde{\eta}_3, \eta^1\right), \qquad \tilde{\xi}^{\dot{a}} = \left(\tilde{\eta}_2, -\eta^4\right), \tag{1.194}$$

implying the maps of the supermomenta

$$q^A = \begin{pmatrix} q^1_\alpha \\ \tilde{q}_3^{\dot{\alpha}} \end{pmatrix}, \qquad \tilde{q}_A = \begin{pmatrix} -q^{\alpha\,4} & -\tilde{q}_{\dot{\alpha}\,2} \end{pmatrix}, \tag{1.195}$$

and supermomentum conserving delta functions

$$\delta^4\left(\sum_i q_i^A\right)\delta^4\left(\sum_i \tilde{q}_{iA}\right) = \delta^4\left(\sum_i q_{i\alpha}^m\right)\delta^4\left(\sum_i \tilde{q}_{im'}^{\dot{\alpha}}\right). \tag{1.196}$$

Applying the map of the Grassmann variables eq. (1.194) to the six dimensional superfield eq. (1.140) and comparing it with the four dimensional non-chiral superfield eq. (1.69) yields the following map of the six and four dimensional on-shell states

$$\begin{aligned}
&\text{scalars:} && s = \phi_{23}\,, \quad s' = \phi_{21}\,, \quad s'' = \phi_{43}\,, \quad s''' = \phi_{41}\,, \\
&\text{gluinos:} && \chi^a = \left(\overline{\psi}^4, -\psi_2\right)\,, \qquad \lambda^a = \left(\psi_4, -\overline{\psi}^2\right)\,, \\
& && \tilde{\chi}_{\dot{a}} = \left(-\psi_3, -\overline{\psi}^1\right)\,, \quad \tilde{\lambda}_{\dot{a}} = \left(-\psi_1, -\overline{\psi}^3\right)\,, \\
&\text{gluons:} && g^a{}_{\dot{a}} = \begin{pmatrix} G_+ & \phi_{42} \\ \phi_{31} & -G_- \end{pmatrix}\,.
\end{aligned} \tag{1.197}$$

With the help of eqs. (1.191), (1.192), (1.194) and (1.195) it is possible to perform the dimensional reduction of any six dimensional superamplitude.

For a detailed analysis of the connection between the massless amplitudes in six and four dimensions and an investigation of a potential uplift from four to six dimensions we refer to section 5.5.

1.6. BCFW On-Shell Recursion

The BCFW on-shell recursion [27, 28] is a valuable tool in calculating color ordered tree-level amplitudes in gauge theories, as it allows to recursively calculate an n point amplitude from lower point amplitudes. As a direct consequence, the knowledge of the three point amplitudes and the BCFW recursion relation are sufficient to obtain all color ordered tree amplitudes of a particular gauge theory. In what follows we will briefly outline the general form of the BCFW recursion, for some more details we refer to to the excellent review [31].

The basic idea is to analytically continue two external momenta by introducing light-like shifts proportional to the complex parameter z that neither spoil the on-shell condition of the two shifted momenta nor the overall momentum conservation. If the shift vector r has the properties

$$r^2 = 0\,, \qquad r \cdot p_1 = 0\,, \qquad r \cdot p_n = 0\,, \tag{1.198}$$

then the shift

$$p_1 \to p_{\hat{1}}(z) = p_1 + zr\,, \qquad p_n \to p_{\hat{n}}(z) = p_n - zr\,, \qquad A_n \to \widehat{A}_n(z)\,, \tag{1.199}$$

has the desired properties

$$p_{\hat{1}}^2 = p_{\hat{n}}^2 = 0 \qquad p_{\hat{1}} + p_{\hat{n}} = p_1 + p_n\,. \tag{1.200}$$

Using region momenta instead, the shifts in eq. (1.199) can be reproduced by the single shift

$$x_1 \to x_{\hat{1}} = x_1 + z\,r\,. \tag{1.201}$$

Color ordered tree amplitudes have simple analytic structure since they only have poles where sums of consecutive momenta go on-shell, i. e. $x_{i\,j}^2 = 0$. As a consequence $\widehat{A}_n(z)$

is an analytical function that has only the simple poles z_j solving the on-shell condition

$$x^2_{\hat{1}\,j+1} = (x_{1\,j+1} + z\,r)^2 = x^2_{1\,j+1} + 2z\,r\cdot x_{1\,j+1} = 0\,, \tag{1.202}$$

i. e. the poles are given by

$$z_j = -\frac{x^2_{1\,j+1}}{2r\cdot x_{1\,j+1}}\,. \tag{1.203}$$

If the analytically continued amplitude $\widehat{A}_n$ is vanishing as $|z|\to\infty$ it is a simple fact that the contour integral of $\frac{\widehat{A}_n}{z}$ over a circle at infinity is vanishing. By virtue of the residue theorem this allows to relate the physical amplitude to the residues of $\frac{\widehat{A}_n}{z}$ at the poles z_j

$$\frac{1}{2\pi i}\oint dz\frac{\widehat{A}_n}{z} = A_n + \sum_{j=2}^{n-2}\operatorname*{Res}_{z=z_j}\frac{\widehat{A}_n}{z} = 0\,. \tag{1.204}$$

Due to the general factorization properties of tree amplitudes, these residues are given by products of lower-point on-shell amplitudes multiplied by the residue

$$-\operatorname*{Res}_{z=z_j}\left(\frac{1}{z}\frac{i}{x^2_{\hat{1}\,j+1}}\right) = \frac{i}{x^2_{1\,j+1}}\,. \tag{1.205}$$

Introducing the abbreviations

$$\hat{P}_j = x_{\hat{1}\,j+1}\,, \qquad\qquad P_j = x_{1\,j+1}\,, \tag{1.206}$$

the final form of the BCFW on-shell recursion is

$$A_n = \sum_{j=2}^{n-2}\sum_h A_{j+1}(p_{\hat{1}}, p_2, \ldots, p_j, -\hat{P}_j^{(-h)})\frac{i}{P_j^2}A_{n-j+1}(\hat{P}_j^{(h)}, p_{j+1}, \ldots, p_{\hat{n}})\Big|_{z=z_j} \tag{1.207}$$

where the sum goes over all poles z_j and over all helicities of the intermediate states. Note that we assumed the vanishing of $\widehat{A}_n(z)$ for large z to derive the recursion relation which is not a general feature for all gauge theories and all possible shifts. For details we refer to [94] and [95].

In the following sections we will derive supersymmetric version of the BCFW recursion eq. (1.207) for the four-dimensional $\mathcal{N}=4$ SYM theory and the six-dimensional $\mathcal{N}=(1,1)$ SYM theory.

1.6.1. Supersymmetric BCFW for $\mathcal{N}=4$ SYM

As explained in section 1.1 there are three possible superspaces available for treating $\mathcal{N}=4$ SYM. The chiral and anti-chiral superspace, as well as the non-chiral superspace.

BCFW in Chiral and Anti-Chiral Superspace

Based on references [44, 46, 50, 96] and [84] we are now going to introduce the BCFW on-shell recursion in chiral and anti-chiral superspace. Besides the shifts of the bosonic momenta

$$p_1^{\alpha\dot{\alpha}} \to p_{\hat{1}}^{\alpha\dot{\alpha}} = \lambda_1^\alpha\tilde{\lambda}_1^{\dot{\alpha}} + z\,r^{\alpha\dot{\alpha}}\,, \qquad\qquad p_n^{\alpha\dot{\alpha}} \to p_{\hat{n}} = \lambda_n^\alpha\tilde{\lambda}_n^{\dot{\alpha}} - z\,r^{\alpha\dot{\alpha}}\,, \tag{1.208}$$

which are equivalent to the dual shift

$$x_1^{\alpha\dot{\alpha}} \to x_{\hat{1}}^{\dot{\alpha}\alpha} = x_1^{\dot{\alpha}\alpha} + z\, r^{\alpha\dot{\alpha}}\,, \tag{1.209}$$

it will be necessary to shift the fermionic momenta as well. Obviously the shift vector

$$r^{\dot{\alpha}\alpha} = \tilde{\lambda}_1^{\dot{\alpha}} \lambda_n^{\alpha} \tag{1.210}$$

has the desired properties listed in eq. (1.198). This shift can be interpreted as a shift of the spinors

$$\lambda_1 \to \lambda_{\hat{1}}(z) = \lambda_1 + z\lambda_n\,, \qquad \tilde{\lambda}_n \to \tilde{\lambda}_{\hat{n}}(z) = \tilde{\lambda}_n - z\tilde{\lambda}_1\,. \tag{1.211}$$

In order to not spoil the conservation of chiral super momenta, $\sum q_i = 0$, we need to introduce a shift of the Grassmann variable η_n

$$\eta_n \to \eta_{\hat{n}}(z) = \eta_n - z\eta_1\,, \tag{1.212}$$

leading to the shifted fermionic momenta

$$q_{\hat{1}}^{\alpha A} = \lambda_{\hat{1}}^{\alpha}\eta_1^A = q_1^{\alpha A} + z\lambda_n^{\alpha}\eta_1^A\,, \qquad q_n^{\alpha A} \to q_{\hat{n}}^{\alpha A} = \tilde{\lambda}_n\eta_{\hat{n}}^A = q_n^{\alpha A} - z\lambda_2^{\alpha}\eta_1^A\,, \tag{1.213}$$

or equivalently to the dual shift

$$\theta_{\hat{1}}^{\alpha A} = \theta_1^{\alpha A} + z\,\lambda_n^{\alpha}\eta_1^A\,. \tag{1.214}$$

In anti-chiral superspace the conservation of the fermionic momenta, $\sum \tilde{q}_i = 0$, requires the additional shift

$$\tilde{\eta}_1 \to \tilde{\eta}_{\hat{1}}(z) = \tilde{\eta}_1 + z\tilde{\eta}_n\,, \tag{1.215}$$

resulting in the shifted fermionic momenta

$$\tilde{q}_{\hat{1}\,A}^{\dot{\alpha}} = \tilde{q}_{1\,A}^{\dot{\alpha}} + z\tilde{\lambda}_1^{\dot{\alpha}}\tilde{\eta}_{n\,A}\,, \qquad \tilde{q}_{\hat{n}\,A}^{\dot{\alpha}} = \tilde{q}_{n\,A}^{\dot{\alpha}} - z\tilde{\lambda}_1^{\dot{\alpha}}\tilde{\eta}_{nA}\,. \tag{1.216}$$

or equivalently the dual shift

$$\tilde{\theta}_{\hat{1}\,A}^{\dot{\alpha}} = \tilde{\theta}_{1\,A}^{\dot{\alpha}} + z\tilde{\lambda}_1^{\dot{\alpha}}\tilde{\eta}_{n\,A}\,. \tag{1.217}$$

Similar to the non-supersymmetric case the shifted superamplitude has poles at

$$z_j = -\frac{x_{1\,j+1}^2}{\langle n|x_{1\,j+1}|1]}\,. \tag{1.218}$$

As discussed in [96], the shifted superamplitude vanishes for large z and the arguments presented within the derivation of the non-supersymmetric recursion directly carry over to the supersymmetric case. Hence, the residues of the shifted superamplitude at the poles z_j are given by a product of two lower point superamplitudes. The superfield formalism greatly simplifies the sum over all possible intermediate states, which is simply given by an integration over the Grassmann variables associated to the intermediate state. The Grassmann integration picks exactly those contributions where the intermediate legs in the left and the right superamplitudes have opposite helicity. The BCFW

recursion in chiral superspace reads

$$\mathcal{A}_n\left(\{\lambda_i,\tilde{\lambda}_i,\eta_i\}\right)=\sum_{j=2}^{n-2}\int d^4\eta_{\hat{P}_j}\mathcal{A}_{j+1}(p_{\hat{1}},\ldots,p_j,-\hat{P}_j)\frac{i}{P_j^2}\mathcal{A}_{n-j+1}(\hat{P}_j,p_{j+1},\ldots,p_{\hat{n}})\Big|_{z=z_j}, \tag{1.219}$$

and analogously in anti-chiral superspace

$$\mathcal{A}_n\left(\{\lambda_i,\tilde{\lambda}_i,\tilde{\eta}_i\}\right)=\sum_{j=2}^{n-2}\int d^4\tilde{\eta}_{\hat{P}_j}\mathcal{A}_{j+1}(p_{\hat{1}},\ldots,p_j,-\hat{P}_j)\frac{i}{P_j^2}\mathcal{A}_{n-j+1}(\hat{P}_j,p_{j+1},\ldots,p_{\hat{n}})\Big|_{z=z_j}. \tag{1.220}$$

The initial values for these recursions are the MHV and $\overline{\text{MHV}}$ three-point functions in chiral superspace

$$\mathcal{A}_3^{\text{MHV}}=i\frac{\delta^4(p)\delta^8(q)}{\langle 12\rangle\langle 23\rangle\langle 31\rangle}\,,\qquad \mathcal{A}_3^{\overline{\text{MHV}}}=-i\frac{\delta^4(p)\delta^4(\eta_1^A[23]+\eta_2^A[31]+\eta_3^A[12])}{[12][23][31]}\,, \tag{1.221}$$

and in anti-chiral superspace

$$\mathcal{A}_3^{\text{MHV}}=i\frac{\delta^4(p)\delta^4(\tilde{\eta}_{1A}\langle 23\rangle+\tilde{\eta}_{2A}\langle 31\rangle+\tilde{\eta}_{3A}\langle 12\rangle)}{\langle 12\rangle\langle 23\rangle\langle 31\rangle}\,,\quad \mathcal{A}_3^{\overline{\text{MHV}}}=-i\frac{\delta^4(p)\delta^8(\tilde{q})}{[12][23][31]} \tag{1.222}$$

The supersymmetric BCFW recursion relations eqs. (1.219) and (1.220) are a very elegant and practical way of writing down the BCFW recursion relations eq. (1.207) for all component amplitudes of $\mathcal{N}=4$ SYM at once. Indeed, Johannes Henn and James Drummond [46] were able to come up with a solution to the supersymmetric recursion relation , thereby providing analytical formulae for all superamplitudes of $\mathcal{N}=4$ SYM.

BCFW in Non-Chiral Superspace

As it has not been done in the literature before, we are going to present the BCFW recursion in the non-chiral super space $\{\lambda_i^\alpha,\tilde{\lambda}_i^{\dot{\alpha}},\eta_i^m,\tilde{\eta}_i^{m'}\}$, introduced in section 1.4.1. Additionally we will use the BCFW recursion to prove the covariance (1.126) of the non-chiral superamplitudes under the dual conformal inversions (1.127), as well as to calculate the four-, five- and six-point superamplitude.

Based on the previous section it is straightforward to write down a set of shifts preserving both bosonic and fermionic momentum conservation

$$\lambda_1\to\lambda_{\hat{1}}(z)=\lambda_1+z\lambda_n\,,\qquad \tilde{\lambda}_n\to\tilde{\lambda}_{\hat{n}}(z)=\tilde{\lambda}_n-z\tilde{\lambda}_1\,, \tag{1.223}$$

$$\eta_n\to\eta_{\hat{n}}(z)=\eta_n-z\eta_1\,,\qquad \tilde{\eta}_1\to\tilde{\eta}_{\hat{1}}(z)=\tilde{\eta}_1+z\tilde{\eta}_n\,, \tag{1.224}$$

leading to the same poles, eq. (1.218), of the shifted superamplitude. The corresponding dual shifts are

$$x_{\hat{1}}^{\dot{\alpha}\alpha}=x_1^{\dot{\alpha}\alpha}+z\,\tilde{\lambda}_1^{\dot{\alpha}}\lambda_n^\alpha\,,\qquad \tilde{\theta}_{\hat{1}}^{\dot{\alpha}\,m'}=\tilde{\theta}_1^{\dot{\alpha}\,m'}+z\tilde{\lambda}_1^{\dot{\alpha}}\tilde{\eta}_n^{m'}\,,\qquad \theta_{\hat{1}\,m}^\alpha=\theta_{1\,m}^\alpha+z\,\lambda_n^\alpha\eta_1^m\,. \tag{1.225}$$

According to the same arguments as in chiral and anti-chiral superspace, the BCFW

recursion in non-chiral superspace is given by

$$\mathcal{A}_n = \sum_{j=2}^{n-2} \int d^2\eta_{\hat{P}_j} \int d^2\tilde{\eta}_{\hat{P}_j} \mathcal{A}_{j+1}(p_{\hat{1}}, \ldots, p_j, -\hat{P}_j) \frac{-i}{P_j^2} \mathcal{A}_{n-j+1}(\hat{P}_j, p_{j+1}, \ldots, p_{\hat{n}}) \Big|_{z=z_j} , \tag{1.226}$$

with the explicit minus sign originating from the definition of the Grassmann integration measures $d^2\eta = \frac{1}{2} d\eta^m d\eta_m$, $d^2\tilde{\eta} = \frac{1}{2} d\tilde{\eta}_{m'} d\tilde{\eta}^{m'}$. The initial values for this recursion can be obtained by a half Fourier transform of the MHV and $\overline{\text{MHV}}$ three point amplitudes in chiral (1.221) or anti-chiral superspace (1.222), and are

$$\mathcal{A}_3^{\text{MHV}} = -i \frac{\delta^4(p)\delta^4(q)\delta^2(\tilde{\eta}_1\langle 23\rangle + \tilde{\eta}_2\langle 31\rangle + \tilde{\eta}_3\langle 12\rangle)}{\langle 12\rangle\langle 23\rangle\langle 31\rangle} , \tag{1.227}$$

$$\mathcal{A}_3^{\overline{\text{MHV}}} = i \frac{\delta^4(p)\delta^4(\tilde{q})\delta^2(\eta_1[23] + \eta_2[31] + \eta_3[12])}{[12][23][31]} , \tag{1.228}$$

where the two dimensional delta functions of objects χ_m, $\tilde{\chi}_{m'}$ carrying Grassmann indices have the definition $\delta^2(\chi_m) = \frac{1}{2}\chi_m\chi^m$, $\delta^2(\tilde{\chi}_{m'}) = \frac{1}{2}\tilde{\chi}^{m'}\chi_{m'}$ such that $\int d^2\eta\, \delta^2(\eta) = \int d^2\tilde{\eta}\, \delta^2(\tilde{\eta}) = 1$. We recall that the superamplitudes with $n > 3$ partons in non-chiral superspace have the form

$$\mathcal{A}_n = \delta^4(q)\delta^4(\tilde{q}) f_n(\{x_{ij}, \theta_{ij}, \tilde{\theta}_{ij}\}) \tag{1.229}$$

i. e. the only $\eta_{\hat{P}_j}$, $\tilde{\eta}_{\hat{P}_j}$ dependence of the integrand in the BCFW recursion eq. (1.226) originates from delta functions of the three point amplitudes and the delta functions of the fermionic momenta, making the Grassmann integrations straightforward. For the four point amplitude we obtain

$$\mathcal{A}_4 = -i\delta^4(q)\delta^4(\tilde{q}) \frac{1}{x_{13}^2 x_{24}^2} . \tag{1.230}$$

Introducing the definitions

$$|B_{ijk}\rangle = x_{ij}x_{jk}|\theta_{ki}\rangle + x_{ik}x_{kj}|\theta_{ji}\rangle , \qquad |\tilde{B}_{ijk}] = x_{ij}x_{jk}|\tilde{\theta}_{ki}] + x_{ik}x_{kj}|\tilde{\theta}_{ji}] \tag{1.231}$$

we present the results of the Grassmann integrations in eq. (1.226) for the three different cases $j = 2$, $2 < j < n-2$ and $j = n-2$. In the case $j = 2$ the left superamplitude has to be $\mathcal{A}_3^{\overline{\text{MHV}}}$ since $\mathcal{A}_3^{\text{MHV}}$ is ill defined in the three point kinematics of this case. We obtain

$$\begin{aligned} \mathcal{B}_2 &= \int d^2\eta_{\hat{P}_2} \int d^2\tilde{\eta}_{\hat{P}_2} \mathcal{A}_3^{\overline{\text{MHV}}}(p_{\hat{1}}, p_2, -\hat{P}_2) \frac{i}{P_2^2} \mathcal{A}_{n-1}(\hat{P}_2, p_3, \ldots, p_{\hat{n}}) \Big|_{z=z_2} \\ &= \frac{\delta^4(q)\delta^4(\tilde{q})[1\,2]\delta^2([P_2|\tilde{\theta}_{\hat{1}3}]) f_{n-1}(x_{\hat{1}}, x_3, \ldots, x_n)}{x_{2n}^2 x_{13}^2 [1\,P_2][2\,P_2]} \Big|_{z=z_2} . \end{aligned} \tag{1.232}$$

For practical applications it is convenient to rewrite $\mathcal{B}_2$ as

$$\mathcal{B}_2 = \frac{\delta^4(q)\delta^4(\tilde{q})\delta^2([1|\tilde{B}_{13n}]) f_{n-1}(x_{\hat{1}}, x_3, \ldots, x_n)\big|_{z=z_2}}{x_{2n}^2 x_{13}^2 [1|x_{13}|n\rangle [1\,n]} . \tag{1.233}$$

For $2 < j < n-2$ we have

$$\mathcal{B}_j = \int d^2\eta_{\hat{P}_j} \int d^2\tilde{\eta}_{\hat{P}_j} \mathcal{A}_{j+1}(p_{\hat{1}}, \ldots, p_j, -\hat{P}_j) \frac{i}{P_j^2} \mathcal{A}_{n-j+1}(\hat{P}_j, p_{j+1}, \ldots, p_{\hat{n}}) \Big|_{z=z_j} =$$
$$\frac{i\,\delta^4(q)\delta^4(\tilde{q})\delta^2([P_j|\tilde{\theta}_{\hat{1}j+1}])\delta^2(\langle P_j|\theta_{\hat{1}j+1}])f_{j+1}(x_{\hat{1}}, \ldots, x_{j+1})f_{n-j+1}(x_{\hat{1}}, x_{j+1}, \ldots, x_n)\big|_{z=z_j}}{x_{\hat{1}j+1}^2}\,. \tag{1.234}$$

For practical applications it is more convenient to use the following expression for $\mathcal{B}_j$

$$\frac{i\,\delta^4(q)\delta^4(\tilde{q})\delta^2([1|\tilde{B}_{1j+1n}])\delta^2(\langle 2|B_{21j+1}])f_{j+1}(x_{\hat{1}}, \ldots, x_{j+1})f_{n-j+1}(x_{\hat{1}}, x_{j+1}, \ldots, x_n)\big|_{z=z_j}}{x_{1j+1}^2\langle n|x_{1j+1}|1]^2[n\,1]^2\langle 1\;2\rangle^2}\,. \tag{1.235}$$

In the case $j = n-2$ the right superamplitude has to be $\mathcal{A}_3^{\text{MHV}}$ due to the special three point kinematics and the integration gives

$$\begin{aligned}\mathcal{B}_{n-2} &= \int d^2\eta_{\hat{P}_{n-2}} \int d^2\tilde{\eta}_{\hat{P}_{n-2}} \mathcal{A}_{n-1}(p_{\hat{1}}, \ldots, p_{n-2}, -\hat{P}_{n-2}) \frac{i}{P_{n-2}^2} \mathcal{A}_3^{\text{MHV}}(\hat{P}_{n-2}, p_{n-1}, p_{\hat{n}}) \Big|_{z=z_{n-2}} \\ &= \frac{\delta^4(q)\delta^4(\tilde{q})\langle n\;n-1\rangle\delta^2(\langle P_{n-2}|\theta_{\hat{1}n-1}])f_{n-1}(x_{\hat{1}}, x_2, \ldots, x_{n-1})\big|_{z=z_{n-2}}}{x_{1n-1}^2\langle P_{n-2}\;n-1\rangle\langle P_{n-2}\;n\rangle}\,,\end{aligned} \tag{1.236}$$

which may be rewritten as

$$\mathcal{B}_{n-2} = \frac{\delta^4(q)\delta^4(\tilde{q})\delta^2(\langle 2|B_{21n-1}])f_{n-1}(x_{\hat{1}}, x_2, \ldots, x_{n-1})\big|_{z=z_{n-2}}}{x_{1n-1}^2\langle n|x_{1n-1}|1]\langle 1\;2\rangle^2[1\,n]}\,. \tag{1.237}$$

Now the integrated non-chiral BCFW recursion relation reads

$$\mathcal{A}_n = \sum_{j=2}^{n-2} \mathcal{B}_j\,. \tag{1.238}$$

In this form it is straightforward to prove the dual conformal symmetry of the non-chiral superamplitudes. Applying the inversion rules eq. (1.127), we find

$$\begin{aligned} I\,(\,[j\,P_j]\,) &= \frac{[j\,P_j]}{x_{j+1}^2}\,, & I\,(\,[1\,P_j]\,) &= \frac{x_{\hat{1}}^2}{x_2^2 x_{j+1}^2}[1\,P_j]\,, \\ I\,(\,\langle j+1\,P_j\rangle\,) &= \frac{\langle j+1\,P_j\rangle}{x_{\hat{1}}^2}\,, & I\,(\,\langle n\,P_j\rangle\,) &= \frac{\langle n\,P_j\rangle}{x_n^2}\,, \\ I\left([P_j|\tilde{\theta}_{\hat{1}j+1}]\right) &= \frac{[P_j|\tilde{\theta}_{\hat{1}j+1}]}{x_{j+1}^2}\,, & I\left(\langle P_j|\theta_{\hat{1}j+1}\rangle\right) &= \frac{\langle P_j|\theta_{\hat{1}j+1}\rangle}{x_{\hat{1}}^2}\,. \end{aligned} \tag{1.239}$$

Hence, it follows from eqs. (1.232), (1.234) and (1.236) that

$$I[\mathcal{B}_j] = \left(\prod_i x_i^2\right)\mathcal{B}_j \tag{1.240}$$

which proves the covariance (1.126) of the non-chiral superamplitude under the dual conformal inversions (1.127).

In order to obtain reasonable representations of the non-chiral superamplitudes from the integrated BCFW recursion eq. (1.238) it remains to remove the hats from the the shifted dual point $\hat{1}$ by using identities like e. g.

$$x_{\hat{1}k}^2\Big|_{z=z_j} = -\frac{\langle n|x_{nj+1}x_{j+1k}x_{k1}|1]}{\langle n|x_{1\,j+1}|1]}\,, \tag{1.241}$$

or

$$\langle B_{kk+1\hat{1}}|\,\Big|_{z=z_j} = \frac{1}{\langle 1|x_{1k}|k]\langle n|x_{nj+1}|1]}\Big(\,\langle n|x_{nj+1}x_{j+12}x_{2k}|k]\langle B_{kk+11}| + x_{1j+1}^2\langle n|x_{nk}|k]\langle B_{kk+12}|\Big)\,. \tag{1.242}$$

After removing all hats the obtained expression may still contain spinors. However, these spinors can be removed by multiplying and dividing with the chiral conjugate spinor brackets. The final expression will only depend on $\{x_i,\,\theta_i,\,\tilde{\theta}_i\}$ and besides x_{ij}^2 it can be expressed by the dual conformal covariant objects

$$\begin{aligned}
\mathrm{Tr}(i_1\ldots i_{2k}) &:= \mathrm{Tr}(x_{i_1\,i_2}x_{i_2\,i_3}\,\ldots\,x_{i_{2k-1}\,i_{2k}}x_{i_{2k}\,i_1})\,, \qquad & x_{ij}^2 &= -\tfrac{1}{2}\,\mathrm{Tr}(i\,j)\,,\\
\langle B_{ijk}|i_1\,\ldots\,i_{2k+1}|B_{ijk}\rangle &:= \tfrac{1}{2}\langle (B_{ijk})^m|x_{i\,i_1}x_{i_1\,i_2}\ldots x_{i_{2k+1}\,i}|(B_{ijk})_m\rangle & &\\
[\tilde{B}_{ijk}|i_1\,\ldots\,i_{2k+1}|\tilde{B}_{ijk}] &:= \tfrac{1}{2}[(\tilde{B}_{ijk})_{m'}|x_{i\,i_1}x_{i_1\,i_2}\ldots x_{i_{2k+1}\,i}|(\tilde{B}_{ijk})^{m'}]\,, & &
\end{aligned} \tag{1.243}$$

where the prefactor of $\frac{1}{2}$ has been introduced for convenience. Carrying out the recursion step from four to five points we obtain

$$\mathcal{A}_5 = i\delta^4(q)\delta^4(\tilde{q})\frac{\langle B_{542}|\,1\,2\,3\,|B_{542}\rangle + [\tilde{B}_{542}|\,1\,2\,3\,|\tilde{B}_{542}]}{x_{13}^2x_{24}^4x_{25}^4x_{35}^2x_{41}^2} \tag{1.244}$$

and for the six-point amplitude we get

$$\begin{aligned}
\mathcal{A}_6 = i\delta^4(q)\delta^4(\tilde{q})\Big(&\frac{\langle B_{625}|\,4\,3\,2\,|B_{625}\rangle\langle B_{235}|\,6\,5\,1\,|B_{235}\rangle}{x_{13}^2x_{24}^2x_{35}^4x_{46}^2x_{51}^2x_{52}^4x_{62}^4\,\mathrm{Tr}(6235)} + \text{chiral conjugate}\\
&+\frac{[\tilde{B}_{136}|\,2\,3\,5\,|\tilde{B}_{136}]\langle B_{436}|\,5\,6\,1\,|B_{436}\rangle}{x_{13}^4x_{26}^2x_{35}^2x_{36}^2x_{46}^4x_{51}^2\,\mathrm{Tr}(2356)\,\mathrm{Tr}(3461)}\\
&-\frac{[\tilde{B}_{325}|\,4\,5\,1\,|\tilde{B}_{325}]\langle B_{215}|\,6\,5\,3\,|B_{215}\rangle}{x_{13}^2x_{15}^2x_{24}^2x_{25}^2x_{35}^4x_{51}^2x_{62}^2\,\mathrm{Tr}(1245)\,\mathrm{Tr}(2356)}\\
&-\frac{[\tilde{B}_{146}|\,2\,4\,5\,|\tilde{B}_{146}]\langle B_{214}|\,6\,4\,3\,|B_{214}\rangle}{x_{13}^2x_{14}^2x_{24}^4x_{46}^4x_{51}^2x_{62}^2\,\mathrm{Tr}(1245)\,\mathrm{Tr}(3461)}\Big)
\end{aligned} \tag{1.245}$$

Dual conformal invariance of these expressions is easy to verify by simply counting the inversion weights on each dual point.

In principle all non-chiral amplitudes could be obtained by a half Fourier transform of the known chiral or anti-chiral superamplitudes. However, it is in general nontrivial to carry out these integrations in a way that leads to a useful representation of the amplitude. One exception are the MHV and $\overline{\mathrm{MHV}}$ part of the non-chiral superamplitude, which can be obtained by either solving the BCFW recursion or by performing the half Fourier transform in the way described in [85]. The result we found and also

checked numerically is

$$\mathcal{A}_n^{\overline{\text{MHV}}} = \frac{i\delta^4(q)\delta^4(\tilde{q})}{\prod_{k=1}^n x_{kk+2}^2} \frac{\langle B_{n\,2\,n-1}|\, n{-}2\, n{-}3\, n{-}4\,|B_{n\,2\,n-1}\rangle}{x_{n-3n-1}^2 x_{n2}^2} \prod_{k=1}^{n-5} \frac{\langle B_{k+1\,k+2\,n-1}|\, n\, n{-}1\, k\,|B_{k+1\,k+2\,n-1}\rangle}{x_{n-1k+1}^2\, \mathrm{Tr}(n\, k{+}1\, k{+}2\, n{-}1)}, \tag{1.246}$$

and similar for the MHV part. Note that our result differs from the one presented in [85].

1.6.2. Supersymmetric BCFW for $\mathcal{N} = (1,1)$ SYM

The supersymmetric BCFW recursion of $\mathcal{N} = (1,1)$ SYM theory in six dimensions will play a central role when investigating massive amplitudes in chapter 5. It has been introduced in reference [89]. In what follows we will closely follow the detailed review presented in reference [90]. At the end of this section we will use the BCFW recursion relation to prove the dual conformal covariance, eq. (1.179), of the superamplitudes.

As a first step we introduce the shift vector

$$r^\mu = \frac{1}{2s_{1n}} X_{a\dot{a}} \langle 1^a | \Sigma^\mu p_n | 1^{\dot{a}}] \,, \tag{1.247}$$

that obviously has the desired properties $r \cdot p_1 = 0 = r \cdot p_n$. The requirement $r^2 = 0$, implies $0 = \epsilon^{ab}\epsilon^{\dot{a}\dot{b}} X_{a\dot{a}} X_{b\dot{b}} = 2\det(X)$. Hence $X_{a\dot{a}}$ is some arbitrary rank one matrix and has a bispinor representation $X_{a\dot{a}} = x_a \tilde{x}_{\dot{a}}$. Equation (1.247) implies

$$r^{AB} = X_{a\dot{a}} \frac{[A|p_n|1^{\dot{a}}]\langle 1^a|^B]}{s_{1n}} \,, \qquad r_{AB} = -X_{a\dot{a}} \frac{[A|1^{\dot{a}}]\langle 1^a|p_n|_B]}{s_{1n}} \,, \tag{1.248}$$

and the shifts of the momenta p_1 and p_n (1.199) can be reinterpreted as shifts of the chiral and anti-chiral spinors. The equations

$$\begin{aligned} p_{\hat{1}}^{AB} &= \lambda_{\hat{1}}^{A\,a} \lambda_{\hat{1}\,a}^B \,, & p_{\hat{n}}^{AB} &= \lambda_{\hat{n}}^{A\,a} \lambda_{\hat{n}\,a}^B \,, \\ p_{\hat{1}\,AB} &= \tilde{\lambda}_{\hat{1}\,A\,\dot{a}} \tilde{\lambda}_{\hat{1}\,B}^{\dot{a}} \,, & p_{\hat{n}\,AB} &= \tilde{\lambda}_{\hat{n}\,A\,\dot{a}} \tilde{\lambda}_{\hat{n}\,B}^{\dot{a}} \end{aligned} \tag{1.249}$$

have the simple solutions

$$\begin{aligned} \lambda_{\hat{1}}^{A\,a} &= s_{1n}^{-1} \langle 1^a | p_n\, p_{\hat{1}} |^A = \lambda_1^{A\,a} + \frac{z}{s_{1n}} \langle 1^a | p_n\, r |^A \,, \\ \lambda_{\hat{n}}^{A\,b} &= s_{1n}^{-1} \langle n^a | p_1\, p_{\hat{n}} |^A = \lambda_1^{A\,a} - \frac{z}{s_{1n}} \langle n^a | p_1\, r |^A \,, \\ \tilde{\lambda}_{\hat{1}A\dot{a}} &= s_{1n}^{-1} [1_{\dot{a}} | p_n\, p_{\hat{1}} |_A = \tilde{\lambda}_{1\,A\,\dot{a}} + \frac{z}{s_{1n}} [1_{\dot{a}} | p_n\, r |_A \,, \\ \tilde{\lambda}_{\hat{n}A\dot{b}} &= s_{1n}^{-1} [n_{\dot{a}} | p_1\, p_{\hat{n}} |_A = \tilde{\lambda}_{n\,A\,\dot{a}} - \frac{z}{s_{1n}} [n_{\dot{a}} | p_1\, r |_A \,. \end{aligned} \tag{1.250}$$

Or after inserting the definition (1.248) of the shift vector

$$\begin{aligned}\lambda_{\hat{1}}^{Aa} &= \lambda_1^{Aa} + \frac{z}{s_{1n}} X^{a\dot{a}}[1_{\dot{a}}|n_b\rangle \lambda_n^{A\,b}\,, \qquad \lambda_{\hat{n}}^{Ab} = \lambda_n^{Ab} - \frac{z}{s_{1n}} X_{a\dot{a}}[1^{\dot{a}}|n^b\rangle \lambda_1^{A\,a}\,,\\ \tilde{\lambda}_{\hat{1}A\dot{a}} &= \tilde{\lambda}_{1A\dot{a}} + \frac{z}{s_{1n}} X_{a\dot{a}}[n_{\dot{b}}|1^a\rangle \tilde{\lambda}_{nA}^{\dot{b}}\,, \quad \tilde{\lambda}_{\hat{n}A\dot{b}} = \tilde{\lambda}_{nA\dot{b}} + \frac{z}{s_{1n}} X_{a\dot{a}}[n_{\dot{b}}|1^a\rangle \tilde{\lambda}_{1A}^{\dot{a}}\,.\end{aligned} \tag{1.251}$$

Supermomentum conservation can only be maintained if the Grassmann variables of legs 1 and n are shifted as well

$$\begin{aligned}\xi_{\hat{1}a} &= \xi_{1a} + z X_{a\dot{a}}[1^{\dot{a}}|q_n\rangle / s_{1n}\,, \quad \xi_{\hat{n}b} = \xi_{nb} + z X_{a\dot{a}}[1^{\dot{a}}|n_b\rangle \xi_1^a / s_{1n}\,,\\ \tilde{\xi}_1^{\dot{a}} &= \tilde{\xi}_1^{\dot{a}} - z X^{a\dot{a}}[\tilde{q}_n|1_a\rangle / s_{1n}\,, \quad \tilde{\xi}_{\hat{n}}^{\dot{b}} = \tilde{\xi}_n^{\dot{b}} - z X_{a\dot{a}}[n^{\dot{b}}|1^a\rangle \tilde{\xi}_1^{\dot{a}} / s_{1n}\,,\end{aligned} \tag{1.252}$$

resulting in the following shifts of the supermomenta

$$\begin{aligned}q_{\hat{1}}^A &= [\tilde{\chi}|p_{\hat{1}}|^A = q_1^A + z\, s^A\,, \qquad q_{\hat{n}}^A = [\tilde{\chi}|p_{\hat{n}}|^A = q_n^A - z\, s^A\,,\\ \tilde{q}_{\hat{1}A} &= \langle \chi|p_{\hat{1}}|_A = \tilde{q}_{1A} + z\, \tilde{s}_A\,, \quad \tilde{q}_{\hat{n}A} = \langle \chi|p_{\hat{n}}|_A = \tilde{q}_{nA} - z\, \tilde{s}_A\,,\end{aligned} \tag{1.253}$$

with

$$\begin{aligned}\chi &= s_{1n}^{-1}([\tilde{q}_1|p_n| + [\tilde{q}_n|p_1|)\,, \quad \tilde{\chi} = s_{1n}^{-1}(\langle q_1|p_n| + \langle q_n|p_1|)\\ s &= [\tilde{\chi}|r|\,, \qquad\qquad \tilde{s} = \langle \chi|r|\,,\end{aligned} \tag{1.254}$$

or with the definition of r being inserted

$$\begin{aligned}s^A &= \frac{X_{a\dot{a}}}{s_{1n}^2}\left(\langle q_1|p_n|1^a\rangle [1^{\dot{a}}|p_n|^A + s_{1n}\langle q_n|1^{\dot{a}}] \lambda_1^{A\,a}\right)\,,\\ \tilde{s}_A &= \frac{X_{a\dot{a}}}{s_{1n}^2}\left(-[\tilde{q}_1|p_n|1^{\dot{a}}]\langle 1^a|p_n|_A - s_{1n}[\tilde{q}_n|1^{\dot{a}}\rangle \tilde{\lambda}_{1\,A}^{\dot{a}}\right)\,.\end{aligned} \tag{1.255}$$

The dual shifts are given by

$$x_{\hat{1}} = x_1 + z\, r \qquad\qquad \theta_{\hat{1}} = \theta_1 + z\, s \qquad\qquad \tilde{\theta}_{\hat{1}} = \tilde{\theta}_1 + z\, \tilde{s}\,. \tag{1.256}$$

Note that the Grassmann shift variables s^A and $\tilde{s}_A$ can alternatively be obtained by solving the equations

$$\langle \theta_{\hat{1}2}|x_{\hat{1}2}| = 0\,, \qquad \langle \theta_{n\hat{1}}|x_{n\hat{1}}| = 0\,, \qquad [\tilde{\theta}_{\hat{1}2}|x_{\hat{1}2}| = 0\,, \qquad [\tilde{\theta}_{n\hat{1}}|x_{n\hat{1}}| = 0\,. \tag{1.257}$$

The above set of supersymmetry preserving shifts leads to a shifted superamplitude whose residues at the poles eq. (1.203) are given by a product of two lower point superamplitudes. Similar to the supersymmetric BCFW recursions of $\mathcal{N} = 4$, the sum over intermediate states is realized by an integration with respect to the Grassmann variables of the intermediate leg. Using the abbreviations introduced in eq. (1.206) the BCFW recursion of $\mathcal{N} = (1,1)$ SYM theory in six dimensions reads

$$\mathcal{A}_n(p_1,\ldots,p_n) = \sum_{j=2}^{n-2} \int d^2\tilde{\xi}_{\hat{P}_j} \int d^2\xi_{\hat{P}_j} \mathcal{A}_{j+1}(\hat{p}_1,\ldots,p_j,-\hat{P}_j) \frac{-i}{P_j^2} \mathcal{A}_{n-j+1}(\hat{P}_j,p_{j+1},\ldots,p_{\hat{n}})\Big|_{z=z_j} \tag{1.258}$$

Similar to the non-chiral BCFW recursion in four dimensions, eq. (1.226), the explicit minus sign originates from the choice $d^2\xi = \frac{1}{2} d\xi^a d\xi_a$, $d^2\tilde{\xi} = \frac{1}{2} d\tilde{\xi}_{\dot{a}} d\tilde{\xi}^{\dot{a}}$ for the integration measure and can be fixed by projecting the four point function resulting from

the six-dimensional BCFW recursion eq. (1.258) to four dimensions and comparing it with eq. (1.230). The initial value for the recursion is the three-point superamplitude eq. (1.144). For applications of the BCFW recursion it is more convenient to use the following alternative representation of the three point amplitude

$$\mathcal{A}_3 = i\delta^6(p)(\boldsymbol{u}_1 - \boldsymbol{u}_2)(\tilde{\boldsymbol{u}}_1 - \tilde{\boldsymbol{u}}_2)\left(\boldsymbol{u}_3 - \tfrac{1}{2}(\boldsymbol{u}_1 + \boldsymbol{u}_2)\right)\left(\tilde{\boldsymbol{u}}_3 - \tfrac{1}{2}(\tilde{\boldsymbol{u}}_1 + \tilde{\boldsymbol{u}}_2)\right)\delta(\boldsymbol{w})\,\delta(\tilde{\boldsymbol{w}})\,. \tag{1.259}$$

As has been shown in [89], the BCFW recursion yields the four point function

$$\mathcal{A}_4 = -\delta^6(p)\,\delta^4(q)\,\delta^4(\tilde{q})\,\frac{i}{x_{13}^2 x_{24}^2}\,. \tag{1.260}$$

Note that the four-point amplitude is fixed up to a numerical factor by supersymmetry and dual conformal symmetry.

In the remainder of this section we will explicitly carry out the Grassmann integrations in the BCFW recursion eq. (1.258). First of all we recall that for $n \geq 4$ an n-point superamplitude has the form

$$\mathcal{A}_n = \delta^6(p)\delta^4(q)\,\delta^4(\tilde{q})\,f_n(\{x_i, \theta_i, \tilde{\theta}_i\}) \tag{1.261}$$

In order to consistently treat ingoing and outgoing particles we adopt the prescription

$$\lambda_{(-p)} = i\,\lambda_p\,, \quad \tilde{\lambda}_{(-p)} = i\,\tilde{\lambda}_p\,, \quad \xi_{(-p)} = i\,\xi_p\,, \quad \tilde{\xi}_{(-p)} = i\,\tilde{\xi}_p\,. \tag{1.262}$$

In principle there are the three different cases $j = 2$, $2 < j < n-2$ and $j = n-2$. Starting with the contribution $j = 2$ in eq. (1.258), we want to evaluate

$$\mathcal{B}_2 = \frac{-i}{x_{13}^2}\int d^2\xi_{\hat{P}} d^2\tilde{\xi}_{\hat{P}_2}\mathcal{A}_3\left(p_{\hat{1}}, p_2, -\hat{P}_2\right)\delta^4\left(q_{\hat{P}_2} + \theta_{3\hat{1}}\right)\delta^4\left(\tilde{q}_{\hat{P}_2} + \tilde{\theta}_{3\hat{1}}\right)f_{n-1}\left(x_{\hat{1}}, x_3, \ldots, x_n\right) \tag{1.263}$$

Taking the representation eq. (1.259) of $\mathcal{A}_3$, the only dependence on $\xi_{\hat{P}_2}, \tilde{\xi}_{\hat{P}_2}$ is contained in Grassmann delta functions, and the integration boils down to solving the linear equations

$$\boldsymbol{u}_K = \tfrac{1}{2}(\boldsymbol{u}_{\hat{1}} + \boldsymbol{u}_2)\,, \qquad \boldsymbol{w}_K = -\boldsymbol{w}_{\hat{1}} - \boldsymbol{w}_2\,, \tag{1.264}$$

$$\tilde{\boldsymbol{u}}_K = \tfrac{1}{2}(\tilde{\boldsymbol{u}}_{\hat{1}} + \tilde{\boldsymbol{u}}_2)\,, \qquad \tilde{\boldsymbol{w}}_K = -\tilde{\boldsymbol{w}}_{\hat{1}} - \tilde{\boldsymbol{w}}_2\,, \tag{1.265}$$

for $\xi_{\hat{P}_2}, \tilde{\xi}_{\hat{P}_2}$, with the abbreviation $K = -\hat{P}_2$. The solution is

$$\xi^a_{\hat{P}_2} = -\tfrac{i}{2}\left(\boldsymbol{u}_{\hat{1}} + \boldsymbol{u}_2\right)w_K^a - i\left(\boldsymbol{w}_{\hat{1}} + \boldsymbol{w}_2\right)u_K^a\,, \quad \tilde{\xi}^{\dot{a}}_{\hat{P}_2} = \tfrac{i}{2}\left(\tilde{\boldsymbol{u}}_{\hat{1}} + \tilde{\boldsymbol{u}}_2\right)\tilde{w}_K^{\dot{a}} + i\left(\tilde{\boldsymbol{w}}_{\hat{1}} + \tilde{\boldsymbol{w}}_2\right)\tilde{u}_K^{\dot{a}}\,. \tag{1.266}$$

Using eqs. (A.28) to (A.30) it is straightforward to show that on the support of $(\boldsymbol{u}_{\hat{1}} - \boldsymbol{u}_2)(\tilde{\boldsymbol{u}}_{\hat{1}} - \tilde{\boldsymbol{u}}_2)$ this implies

$$q_{\hat{P}_2} = q_{\hat{1}} + q_2\,, \qquad \tilde{q}_{\hat{P}_2} = \tilde{q}_{\hat{1}} + \tilde{q}_2\,, \tag{1.267}$$

and therefore

$$\mathcal{B}_2 = \delta^4(q)\,\delta^4(\tilde{q})\,\frac{-i}{x_{13}^2}f_{n-1}\left(x_{\hat{1}}, x_3, \ldots, x_n\right)\int d^2\xi_{\hat{P}_2}d^2\tilde{\xi}_{\hat{P}_2}\,\mathcal{A}_3\left(p_{\hat{1}}, p_2, -\hat{P}_2\right)\,. \tag{1.268}$$

The integration of the three-point amplitude has the solution

$$i\left(\boldsymbol{u}_{\hat{1}}-\boldsymbol{u}_2\right)\left(\tilde{\boldsymbol{u}}_{\hat{1}}-\tilde{\boldsymbol{u}}_2\right)=i\left(\frac{\langle q_2|k_2p_{\hat{1}}|\tilde{q}_2]}{2\,p_2\cdot k_2}-\langle q_{\hat{1}}|\tilde{q}_2]+\langle q_2|\tilde{q}_{\hat{1}}]-\frac{\langle q_{\hat{1}}|k_1p_2|\tilde{q}_{\hat{1}}]}{2\,p_{\hat{1}}\cdot k_1}\right), \tag{1.269}$$

where k_1 and k_2 are some arbitrary reference vectors and $u^aw_a=1=\tilde{u}^{\dot{a}}\tilde{w}_{\dot{a}}$ has been used. The final result is

$$\mathcal{B}_2=\delta^4\left(q\right)\delta^4\left(\tilde{q}\right)\frac{f_{n-1}\left(x_{\hat{1}},x_3,\ldots,x_n\right)}{x_{13}^2}\left(\frac{\langle q_2|k_2p_{\hat{1}}|\tilde{q}_2]}{2\,p_2\cdot k_2}-\langle q_{\hat{1}}|\tilde{q}_2]+\langle q_2|\tilde{q}_{\hat{1}}]-\frac{\langle q_{\hat{1}}|k_1p_2|\tilde{q}_{\hat{1}}]}{2\,p_{\hat{1}}\cdot k_1}\right), \tag{1.270}$$

evaluated at $z=z_2$. In the case $j=n-2$ we need to evaluate

$$\mathcal{B}_{n-2}=\frac{-i}{x_{1\,n-1}^2}\delta^4\left(q\right)\delta^4\left(\tilde{q}\right)f_{n-1}\left(x_{\hat{1}},\ldots,x_{n-1}\right)\int d^2\xi_{\hat{P}_{n-2}}d^2\tilde{\xi}_{\hat{P}_{n-2}}\mathcal{A}_3\left(p_{n-1},p_{\hat{n}},\hat{P}_{n-2}\right). \tag{1.271}$$

Here we already exploited that on the support of the three-point amplitude we have

$$\xi^a_{\hat{P}_{n-2}}=\tfrac{1}{2}\left(\boldsymbol{u}_{\hat{n}}+\boldsymbol{u}_{n-1}\right)w^a_{\hat{P}_{n-2}}+\left(\boldsymbol{w}_{\hat{n}}+\boldsymbol{w}_{n-1}\right)u^a_{\hat{P}_{n-2}}, \tag{1.272}$$

$$\tilde{\xi}^{\dot{a}}_{\hat{P}_{n-2}}=-\tfrac{1}{2}\left(\tilde{\boldsymbol{u}}_{\hat{n}}+\tilde{\boldsymbol{u}}_{n-1}\right)\tilde{w}^{\dot{a}}_{\hat{P}_{n-2}}-\left(\tilde{\boldsymbol{w}}_{\hat{n}}+\tilde{\boldsymbol{w}}_{n-1}\right)\tilde{u}^{\dot{a}}_{\hat{P}_{n-1}} \tag{1.273}$$

or more conveniently

$$q_{\hat{P}_{n-2}}=-q_{\hat{n}}-q_{n-1}\,,\qquad\qquad \tilde{q}_{\hat{P}_{n-2}}=-\tilde{q}_{\hat{n}}-q_{n-1}\,. \tag{1.274}$$

The remaining integral of the three-point amplitude in eq. (1.271) is given by

$$\begin{aligned}i\left(\boldsymbol{u}_{n-1}-\boldsymbol{u}_{\hat{n}}\right)\left(\tilde{\boldsymbol{u}}_{n-1}-\tilde{\boldsymbol{u}}_{\hat{n}}\right)=&\\ i\left(\frac{\langle q_{\hat{n}}|k_np_{n-1}|\tilde{q}_{\hat{n}}]}{2\,p_{\hat{n}}\cdot k_n}-\langle q_{n-1}|\tilde{q}_{\hat{n}}]+\langle q_{\hat{n}}|\tilde{q}_{n-1}]-\frac{\langle q_{n-1}|k_{n-1}p_{\hat{n}}|\tilde{q}_{n-1}]}{2\,p_{n-1}\cdot k_{n-1}}\right),&\end{aligned} \tag{1.275}$$

leading to

$$\begin{aligned}\mathcal{B}_{n-2}=\delta^4\left(q\right)\delta^4\left(\tilde{q}\right)\frac{f_{n-1}\left(x_{\hat{1}},\ldots,x_{n-1}\right)}{x_{1\,n-1}^2}\times&\\ \left(\frac{\langle q_{\hat{n}}|k_np_{n-1}|\tilde{q}_{\hat{n}}]}{2\,p_{\hat{n}}\cdot k_n}-\langle q_{n-1}|\tilde{q}_{\hat{n}}]+\langle q_{\hat{n}}|\tilde{q}_{n-1}]-\frac{\langle q_{n-1}|k_{n-1}p_{\hat{n}}|\tilde{q}_{n-1}]}{2\,p_{n-1}\cdot k_{n-1}}\right),&\end{aligned} \tag{1.276}$$

evaluated at $z=z_{n-2}$. Similar to the case $j=2$, arbitrary reference momenta k_n, k_{n-1} have been introduces in order to get rid of the u, $\tilde{u}$ variables. Finally there is the general case $2<j<n-2$ with no three-point amplitudes involved

$$\begin{aligned}\mathcal{B}_j=\frac{-i}{x_{1\,j+1}^2}\delta^4\left(q\right)\delta^4\left(\tilde{q}\right)f_{j+1}\left(x_{\hat{1}},\ldots,x_{j+1}\right)f_{n-j+1}\left(x_{\hat{1}},x_{j+1},\ldots,x_n\right)\times&\\ \int d^2\xi_{\hat{P}_j}d^2\tilde{\xi}_{\hat{P}_j}\delta^4\left(q_{\hat{P}_j}+\theta_{j+1\,\hat{1}}\right)\delta^4\left(\tilde{q}_{\hat{P}_j}+\theta_{j+1\,\hat{1}}\right)&\end{aligned} \tag{1.277}$$

To carry out the integration we want to rewrite the fermionic delta functions. Due to

the algebra eq. (A.12) of the six-dimensional Pauli matrices, we have the identity

$$\delta_C^A = s_{ij}^{-1}(p_i^{AB} p_{j\,BC} + p_i^{AB} p_{j\,BC})\,, \tag{1.278}$$

which implies

$$\begin{aligned} q_i^A + q_j^A + Q^A &= (\xi_{i\,a} + s_{ij}^{-1}\langle i_a|p_j|Q\rangle)\lambda_i^{A\,a} + (\xi_{j\,a} + s_{ij}^{-1}\langle j_a|p_i|Q\rangle)\lambda_j^{A\,a}\,, \\ \tilde{q}_{i\,A} + \tilde{q}_{j\,A} + \tilde{Q}_A &= (\tilde{\xi}_i^{\dot{a}} + s_{ij}^{-1}[i^{\dot{a}}|p_j|\tilde{Q}])\tilde{\lambda}_{i\,A\,\dot{a}} + (\tilde{\xi}_j^{\dot{a}} + s_{ij}^{-1}[j^{\dot{a}}|p_i|\tilde{Q}])\tilde{\lambda}_{j\,A\,\dot{a}}\,. \end{aligned} \tag{1.279}$$

Consequently the fermionic delta functions can be rewritten as follows

$$\begin{aligned} \delta^4(q_i + q_j + Q) &= -s_{ij}\delta^2(\xi_{i\,a} + s_{ij}^{-1}\langle i_a|p_j|Q\rangle)\delta^2(\xi_{j\,a} + s_{ij}^{-1}\langle j_a|p_i|Q\rangle)\,, \\ \delta^4(\tilde{q}_i + \tilde{q}_j + \tilde{Q}) &= -s_{ij}\delta^2(\tilde{\xi}_i^{\dot{a}} + s_{ij}^{-1}[i^{\dot{a}}|p_j|\tilde{Q}])\delta^2(\tilde{\xi}_j^{\dot{a}} + s_{ij}^{-1}[j^{\dot{a}}|p_i|\tilde{Q}])\,. \end{aligned} \tag{1.280}$$

The two-dimensional Grassmann delta functions are defined as $\delta^2(\chi_a) = \frac{1}{2}\chi_a\chi^a$ and $\delta^2(\tilde{\chi}^{\dot{a}}) = \frac{1}{2}\tilde{\chi}^{\dot{a}}\tilde{\chi}_{\dot{a}}$ such that $\int d^2\xi\,\delta^2(\xi_a) = 1 = \int d^2\tilde{\xi}\,\delta^2(\tilde{\xi}^{\dot{a}})$. This allows us to easily carry out the Grassmann integrations

$$\begin{aligned} \int d^2\xi_{\hat{P}_j}\,\delta^4\left(q_{\hat{P}_j} + \theta_{j+1\,\hat{1}}\right) &= -s^{-1}_{\hat{P}_j\,\hat{n}}\delta^2(\langle\hat{n}_a|\hat{P}_j|\theta_{j+1\,\hat{1}}\rangle) \\ &= -\tfrac{1}{2}s^{-1}_{\hat{P}_j\,\hat{n}}\langle\hat{n}_a|\hat{P}_j|\theta_{j+1\,\hat{1}}\rangle\langle\hat{n}^a|\hat{P}_j|\theta_{j+1\,\hat{1}}\rangle \\ &= -\tfrac{1}{2}s^{-1}_{\hat{P}_j\,\hat{n}}\langle\theta_{j+1\,\hat{1}}|\hat{P}_j p_{\hat{n}}\hat{P}_j|\theta_{j+1\,\hat{1}}\rangle \\ &= -\tfrac{1}{2}\langle\theta_{j+1\,\hat{1}}|x_{\hat{1}\,j+1}|\theta_{j+1\,\hat{1}}\rangle\,, \end{aligned} \tag{1.281}$$

and similarly for the anti-chiral integration

$$\int d^2\tilde{\xi}_{\hat{P}_j}\delta^4\left(\tilde{q}_{\hat{P}_j} + \theta_{j+1\,\hat{1}}\right) = -\tfrac{1}{2}[\tilde{\theta}_{j+1\,\hat{1}}|x_{\hat{1}\,j+1}|\tilde{\theta}_{j+1\,\hat{1}}]\,. \tag{1.282}$$

The full contribution is

$$\begin{aligned} \mathcal{B}_j = -i\,\delta^4(q)\,\delta^4(\tilde{q})\,f_{j+1}(x_{\hat{1}},\ldots,x_{j+1})\,f_{n-j+1}(x_{\hat{1}},x_{j+1},\ldots,x_n)\,\frac{1}{x_{\hat{1}\,j+1}^2}\times \\ \tfrac{1}{4}\langle\theta_{j+1\,\hat{1}}|x_{\hat{1}\,j+1}|\theta_{j+1\,\hat{1}}\rangle[\tilde{\theta}_{j+1\,\hat{1}}|x_{\hat{1}\,j+1}|\tilde{\theta}_{j+1\,\hat{1}}]\,, \end{aligned} \tag{1.283}$$

evaluated at $z = z_j$. Hence, given all lower point amplitudes, the n-point super amplitude is simply given by

$$\mathcal{A}_n = \sum_{j=2}^{n-2}\mathcal{B}_j\,. \tag{1.284}$$

This expression is straightforward to implement numerically. Unfortunately, it is ill suited to directly obtain reasonable analytical expressions for higher point amplitudes because of the auxiliary variable $X_{a\dot{a}} = x_a\tilde{x}_{\dot{a}}$ contained in the shift eq. (1.247). In contrast to four dimensions the shift vector is not fixed by requiring $r^2 = 0$, $r\cdot p_1 = 0 = r\cdot p_n$. This ambiguity is reflected by the presence of $X_{a\dot{a}}$ in the definition of the shift vector. Obviously the amplitudes are independent of the shift vector, i. e. independent of $X_{a\dot{a}}$. In principle it should be possible to remove the shift vector from the right hand side of eq. (1.284) without inserting its definition eq. (1.248), only using its general properties eq. (1.198). Unfortunately, even in the easiest case of the five point

superamplitude this is very hard to achieve. As long as it is not understood how to obtain $f_n(\{x_i, \theta_i, \tilde{\theta}_i\})$ from the output of the BCFW recursion, eq. (1.284) will be limited to numerical applications.

Indeed, in chapter 5 we will extensively use a `Mathematica` implementation of the integrated BCFW recursion (1.284). Independence of $X_{a\dot{a}}$ and the arbitrary reference momenta entering $\mathcal{B}_2$ and $\mathcal{B}_{n-2}$ provides a nontrivial check of the numerical results obtained from the implementation. In fact, taking the four point amplitude (1.260) as initial data, independence of the six-point component amplitudes on $X_{a\dot{a}}$ requires the explicit minus sign appearing in the BCFW recursion relation eq. (1.258).

Proof of Dual Conformal Symmetry

With the help of the BCFW recursion and the inversion rules (1.172) to (1.178) it is straightforward to inductively prove the dual conformal covariant inversion of the superamplitudes by showing that each term $\mathcal{B}_i$ in the integrated BCFW recursion eq. (1.284) inverts as

$$I[\mathcal{B}_j] = \left(\prod_i x_i^2\right) \mathcal{B}_j \,. \tag{1.285}$$

Since the BCFW diagrams involving three-point amplitudes $\mathcal{B}_2$, $\mathcal{B}_{n-2}$ are related by cyclic relabeling of the indices, we only need to consider one of them as well as the general diagram $\mathcal{B}_j$ without three-point functions.

We start out with $\mathcal{B}_2$, eq. (1.269), and investigate the inversion of $(\boldsymbol{u}_{\hat{1}} - \boldsymbol{u}_2)\,(\tilde{\boldsymbol{u}}_{\hat{1}} - \tilde{\boldsymbol{u}}_2)$. Simply plugging in the inversion rules yields

$$I[\tilde{\boldsymbol{u}}_2 - \tilde{\boldsymbol{u}}_{\hat{1}}] = \beta^{-1}\sqrt{\frac{x_2^2}{x_{\hat{1}}^2 x_3^2}}\tilde{\boldsymbol{u}}_2 - \beta^{-1}\sqrt{\frac{x_{\hat{1}}^2}{x_2^2 x_3^2}}\tilde{\boldsymbol{u}}_{\hat{1}} + \frac{\beta^{-1}}{\sqrt{x_{\hat{1}}^2 x_2^2 x_3^2}}\left(\tilde{u}_{\hat{1}}^{\dot{a}}[\tilde{\theta}_{\hat{1}}|x_{\hat{1}}|\hat{1}_{\dot{a}}] - \tilde{u}_2^{\dot{a}}[\tilde{\theta}_2|x_2|2_{\dot{a}}]\right) \tag{1.286}$$

Using $\tilde{u}_2^{\dot{a}}[2_{\dot{a}}| = \tilde{u}_{\hat{1}}^{\dot{a}}[\hat{1}_{\dot{a}}|$ and $x_2|\hat{1}_{\dot{a}}] = x_{\hat{1}}|\hat{1}_{\dot{a}}] = \frac{1}{2}(x_{\hat{1}} + x_2)|\hat{1}_{\dot{a}}]$ the inhomogeneous term can be rewritten

$$\begin{aligned}\left(\tilde{u}_{\hat{1}}^{\dot{a}}[\tilde{\theta}_{\hat{1}}|x_{\hat{1}}|\hat{1}_{\dot{a}}] - \tilde{u}_2^{\dot{a}}[\tilde{\theta}_2|x_2|2_{\dot{a}}]\right) &= \tfrac{1}{2}\,\tilde{u}_{\hat{1}}^{\dot{a}}\,\tilde{\xi}_{\hat{1}}^{\dot{b}}\,[1_{\dot{b}}|x_{\hat{1}} + x_2|1_{\dot{a}}] = \tfrac{1}{4}\,\tilde{\boldsymbol{u}}_{\hat{1}}\;\mathrm{Tr}\,[\,(x_{\hat{1}} + x_2)(x_{\hat{1}} - x_2)\,] \\ &= \tilde{\boldsymbol{u}}_{\hat{1}}(x_{\hat{1}}^2 - x_2^2)\end{aligned} \tag{1.287}$$

and leads to the result

$$I[\tilde{\boldsymbol{u}}_2 - \tilde{\boldsymbol{u}}_{\hat{1}}] = \beta^{-1}\sqrt{\frac{x_2^2}{x_{\hat{1}}^2 x_3^2}}\,(\tilde{\boldsymbol{u}}_2 - \tilde{\boldsymbol{u}}_{\hat{1}}) \,. \tag{1.288}$$

Similarly we find

$$\begin{aligned}I[\boldsymbol{u}_2 - \boldsymbol{u}_{\hat{1}}] &= \beta\sqrt{\frac{x_2^2}{x_{\hat{1}}^2 x_3^2}}\boldsymbol{u}_2 - \beta\sqrt{\frac{x_{\hat{1}}^2}{x_2^2 x_3^2}}\boldsymbol{u}_{\hat{1}} + \frac{\beta}{\sqrt{x_{\hat{1}}^2 x_2^2 x_3^2}}\left(u_{\hat{1}\,a}\langle\theta_{\hat{1}}|x_{\hat{1}}|\hat{1}^a\rangle - u_{2\,a}\langle\theta_2|x_2|2^a\rangle\right) \\ &= \beta\sqrt{\frac{x_2^2}{x_{\hat{1}}^2 x_3^2}}\,(\boldsymbol{u}_2 - \boldsymbol{u}_{\hat{1}}) \,,\end{aligned} \tag{1.289}$$

which together with

$$I\left[\frac{f_{n-1}\left(x_{\hat{1}},x_3,\ldots,x_n\right)}{x_{13}^2}\right]=\frac{x_{\hat{1}}^2x_3^2}{x_2^2}\left(\prod_{i=1}^n x_i^2\right)\ \frac{f_{n-1}\left(x_{\hat{1}},x_3,\ldots,x_n\right)}{x_{13}^2}\,, \tag{1.290}$$

proves the desired inversion of $\mathcal{B}_2$. What remains is to check the inversion of $\mathcal{B}_j$ given in eq. (1.283). Again inserting the inversion rules we obtain

$$\begin{aligned} I\Big[\,\langle\theta_{j+1\,\hat{1}}|x_{\hat{1}\,j+1}|\theta_{j+1\,\hat{1}}\rangle\,\Big] &= \Big(\langle\theta_{j+1}|x_{j+1}^{-1}-\langle\theta_{\hat{1}}|x_{\hat{1}}^{-1}\Big)\ x_{\hat{1}}^{-1}x_{\hat{1}\,j+1}x_{j+1}^{-1}\ \Big(x_{j+1}^{-1}|\theta_{j+1}\rangle-x_{\hat{1}}^{-1}|\theta_{\hat{1}}\rangle\Big)\\ &=\frac{1}{x_{\hat{1}}^2x_{j+1}^2}\,\langle\theta_{j+1\,\hat{1}}|x_{\hat{1}\,j+1}|\theta_{j+1\,\hat{1}}\rangle\,, \end{aligned} \tag{1.291}$$

where we have used $x_{\hat{1}\,j+1}^2=0$. The inversion of $[\tilde{\theta}_{j+1\,\hat{1}}|x_{\hat{1}\,j+1}|\tilde{\theta}_{j+1\,\hat{1}}]$ can be obtained by chiral conjugation[1] of (1.291) and together with

$$\begin{aligned} I\left[\frac{f_{j+1}\left(x_{\hat{1}},\ldots,x_{j+1}\right)f_{n-j+1}\left(x_{\hat{1}},x_{j+1},\ldots,x_n\right)}{x_{1\,j+1}^2}\right]=&\\ x_{\hat{1}}^4\,x_{j+1}^4\left(\prod_{i=1}^n x_i^2\right)\ \frac{f_{j+1}\left(x_{\hat{1}},\ldots,x_{j+1}\right)f_{n-j+1}\left(x_{\hat{1}},x_{j+1},\ldots,x_n\right)}{x_{1\,j+1}^2}& \end{aligned} \tag{1.292}$$

this concludes the proof of the dual conformal symmetry of the tree superamplitudes.

[1] The relative minus sign in the inversion of θ, $\tilde{\theta}$ drops out.

2

Color Decomposition in Gauge Theories

Color decomposition is an essential tool in calculating scattering amplitudes in gauge theories. It provides a systematic way to treat the color degrees of freedom in a scattering process by separating them from the kinematical part. Since the color structures appearing in a certain amplitude are straight forward to identify, the nontrivial part of the color decomposition of an amplitude is expressing the partial amplitudes in terms of primitive amplitudes. We derive the tree level and one-loop color decomposition of an arbitrary quark gluon amplitude in QCD. This generalizes the known analytic results for amplitudes of arbitrary multiplicity with up to one quark anti-quark pair [20, 22] and provides an alternative to the Feynman diagram based algorithm for the determination of the partial amplitudes in terms of primitive amplitudes [23–26]. Furthermore, we derive general fermion flip and reversion identities spanning the null space among the primitive amplitudes.

2.1. The General Idea of Color Decompositions

Within a brute force diagrammatic calculation of a gauge theory scattering amplitude the gauge dependence of the individual Feynman diagrams leads to gauge redundancies. As a consequence a diagrammatic calculation is ill suited to obtain compact analytical expressions for the scattering amplitudes, which are gauge independent. One possibility to reduce the complexity within an amplitude calculation is to decompose the amplitudes into gauge independent pieces that allow for a non-diagrammatic calculation. This can be accomplished by factoring the amplitudes into color structures $C_{n,k}$, depending solely on the gauge group and the representations of the gauge group the partons are transforming in, and the gauge independent partial amplitudes $P_{n,k}$ only depending on the flavors f_i, helicities h_i and momenta p_i of the scattered particles. To be more precise, at each loop order a scattering amplitude of some gauge theory can be written as

$$\mathcal{A}_n^{L\text{-loop}}(\{p_i, f_i, h_i, r_i\}) = g^{n+2(L-1)} \sum_k C_{n,k}^{L\text{-loop}}(\{r_i\}, N) P_{n,k}^{L\text{-loop}}(\{p_i, f_i, h_i\}) \,, \tag{2.1}$$

where $\{r_i\}$ are the gauge group indices of the partons. Hence, the calculation of a scattering amplitude boils down to the determination of the partial amplitudes. Depending on the gauge theory and particular color structure under consideration the partial amplitudes can have additional symmetries which they inherit from the color structures. Note that we adopt the convention to include all powers of N and $\frac{-1}{N}$ as well as additional free parameters such as e. g. the number of fermion flavors n_f into the color structures, resulting in partial amplitudes independent of these parameters.

Of particular interest are the partial amplitudes appearing in the large N limit of a $U(N)$ or $SU(N)$ gauge theory with only adjoint particles. The color decomposition of such a theory reads

$$\mathcal{A}_n^{L\text{-loop}}(\{p_i, h_i, f_i, a_i\}) = g^{n+2(L-1)} N^L \left(\sum_{\sigma \in S_n/Z_n} \mathrm{Tr}(T^{a_{\sigma(1)}} \dots T^{a_{\sigma(n)}}) \, A_n^{L\text{-loop}}(\sigma) + \mathcal{O}(\tfrac{1}{N}) \right), \tag{2.2}$$

and the leading color partial amplitudes $A_n^{L\text{-loop}}$ are called color ordered amplitudes. The color ordered amplitudes are specified by a particular ordering of the external legs. As will become clear in section 2.1.1, color ordered amplitudes can be calculated applying the color ordered Feynman rules of fig. 2.1 to all planar diagrams with the particular ordering of the external legs. The fixed ordering of the external particles leads to a simpler analytic structure, i. e. tree level color ordered amplitudes only receive poles when sums of successive momenta go on-shell. Color ordered amplitudes are subject to a large number of identities, both at tree and at loop level. A detailed investigation of their symmetries can be found in section 2.3. However, the most striking feature of the color ordered amplitudes is that they can be calculated in a non-diagrammatic way using on-shell methods, that is the BCFW recursion [27, 28] at tree level and generalized unitarity at loop level [21, 29, 30]. By modifying all particles to transform in the adjoint representation of the gauge group we can properly associate color ordered amplitudes to every gauge theory, e. g. the color ordered QCD amplitudes are the leading color partial amplitudes in a modified gauge theory where the quarks transform in the adjoint representation.

Given the simplicity of the color ordered amplitudes it is convenient to try to decom-

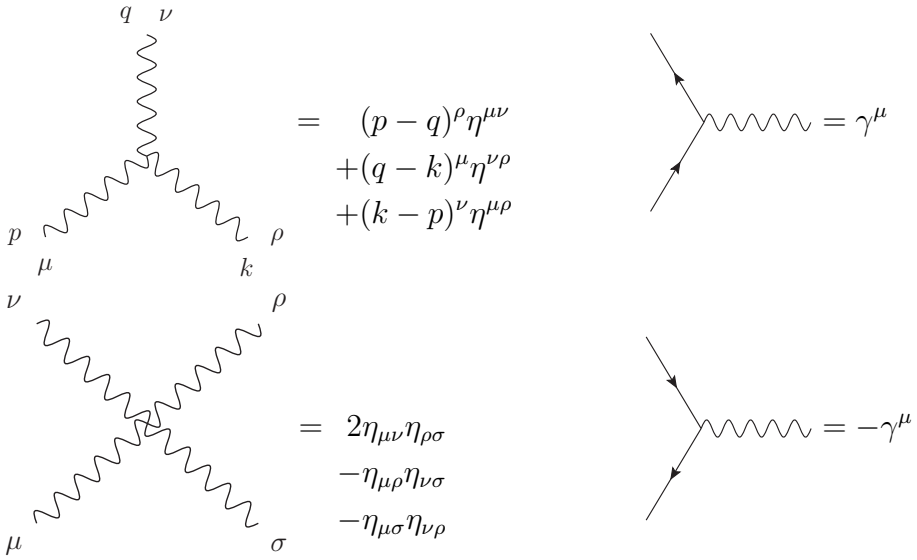

Figure 2.1.: Color ordered Feynman rules for pure gluon and gluon-fermion vertices.

pose partial amplitudes into linear combinations of color ordered amplitudes. However, relating the partial amplitudes to color ordered amplitudes is in general a nontrivial task. In the case of QCD we are going to show, that it is indeed possible to construct an integer valued matrix M^{tree} that is solving the equations

$$P^{\text{tree}}_{n,k} = \sum_j M^{\text{tree}}_{k\,j}\, A^{\text{tree}}_{n,j}\,. \tag{2.3}$$

Besides the obvious computational advantages, such decompositions into color ordered tree amplitudes open up the possibility to relate different gauge theories. On the level of color ordered amplitudes the differences between gauge theories reduce to the helicities and flavors of the matter fields and the pure matter interactions present in the theories. All interactions with the gauge field A_μ are universal as they are induced by the covariant derivative $D_\mu = \partial_\mu - igA_\mu$. This universality results in a surprisingly large number of equivalent color ordered tree amplitudes between differing gauge theories.

In order to be able to write down similar expressions for all one-loop partial amplitudes of QCD we have to divide the one-loop color ordered QCD amplitudes involving quarks into smaller gauge invariant pieces, the primitive amplitudes. In a primitive amplitude each quark line has a definite orientation with respect to the loop, called the routing of the quark. A particular quark can either turn to the left or to the right of the loop. We specify the primitive amplitudes by assigning a routing label to each of the quarks and anti-quarks.

$$A(q_1,\dots,\bar{q}_1,\dots) = A(q_1^L,\dots,\bar{q}_1^L,\dots) + A(q_1^R,\dots,\bar{q}_1^R,\dots) + \dots \tag{2.4}$$

Speaking in terms of diagrams, eq. (2.4) is a disjoint decomposition of all contributing color ordered Feynman diagrams into gauge invariant subsets of all possible routings of the quarks. The gauge invariance of the primitive amplitudes follows from the observation that they can be interpreted as the partial amplitudes of some special gauge theory [22]. Finally, we have to further divide the primitive amplitudes into

the part containing a pure fermion loop and the part with a pure gluon or mixed quark-gluon loop.

In summary, the goal of a tree-level or one-loop color decomposition of QCD is to give an expression for the amplitude in terms of color structures and color ordered amplitudes or primitive amplitudes. Hence, dropping the one-loop label we will derive expressions of the form

$$\mathcal{A}_n^{\text{tree}} = g^{n-2} \sum_k C_{n,k}^{\text{tree}} \sum_j M_{k\,j}^{\text{tree}}\, A_{n,j}^{\text{tree}}\,, \tag{2.5}$$

and

$$\mathcal{A}_n = g^n \sum_k C_{n,k} \left(\sum_j M_{k\,j}\, A_{n,j} + n_f \sum_j (M_f)_{k\,j}\, (A_f)_{n,j} \right)\,, \tag{2.6}$$

for arbitrary tree and one-loop QCD amplitudes, with $A_{n,j}$ denoting the non-fermion loop part and $(A_f)_{n,j}$ denoting the fermion loop part of primitive amplitudes. As a consequence, an arbitrary leading order or next to leading order QCD calculation reduces to the calculation of color ordered tree amplitudes and primitive amplitudes.

2.1.1. Color Decomposition for Adjoint Particles

Since it is instructive for the preceding derivation of the color decomposition of QCD and will yield further insight into the definition and calculation of color ordered amplitudes, we are going to give a derivation of the known results [20] for the color decomposition of scattering amplitudes containing only adjoint particles. Obviously this includes the pure gluon sector, common to all non Abelian gauge theories.

Tree Level

At tree level there are no subleading color contributions and the color decomposition of an n-parton tree amplitude reads

$$\mathcal{A}_n^{\text{tree}}(\{p_i, h_i, f_i, a_i\}) = g^{n-2} \sum_{\sigma \in S_n/Z_n} \text{Tr}(T^{a_{\sigma(1)}} \dots T^{a_{\sigma(n)}})\, A_n^{\text{tree}}(\sigma(1), \dots, \sigma(n))\,, \tag{2.7}$$

with the argument i of the color ordered amplitude A_n^{tree} denoting an outgoing parton of light-like momentum p_i, helicity h_i and flavor f_i, $i \in [1, n]$. The $su(N)$ traceless Hermitian generator matrices T^{a_i} are in the fundamental representation, and are normalized such that $\text{Tr}(T^a T^b) = \delta^{ab}$.

It is straight forward to deduce this decomposition by determining the color structures that can appear in a Feynman diagram. This can be accomplished making use of the Lie algebra the generator matrices are fulfilling

$$[T^a, T^b] = i f^{abc} T^c\,. \tag{2.8}$$

Given an arbitrary Feynman diagram, we choose one external particle. Its adjoint index a appears in the structure constants of the vertex it is connected to. We replace these structure constants by

$$f^{abc} = -i\, \text{Tr}(T^a [T^b, T^c])\,. \tag{2.9}$$

The other adjoint indices in these traces are either belonging to other external legs or are contracted with a structure constant of another vertex. With the help of eq. (2.8) these contractions can be replaced by commutators $f^{dec}T^c = -i[T^d, T^e]$. Continuing this step we end up with a trace of nested commutators of the n generator matrices associated to the external legs. Expanding the commutators we end up with the desired decomposition of the diagram, thereby proving eq. (2.7).

Color Ordered Diagrams and Color Ordered Feynman Rules

Form the above analysis it follows immediately that there is a one to one correspondence between the kinematical contributions of the Feynman diagrams to the color ordered amplitudes and all the planar diagrams whose external legs follow the ordering specified by the color ordered amplitude. The kinematical contributions associated to these color ordered diagrams can be calculated by applying the color ordered Feynman rules listed in fig. 2.1 to them. In general, the color ordered Feynman rules of a particular gauge theory can be obtained by expressing the contractions of structure constants present in the ordinary Feynman rules of the associated gauge theory with only adjoint fields by sums of traces of generators. The coefficients of these traces are the color ordered Feynman rules for the cyclic ordering specified by the traces. As a consequence, the color ordered fermion-gluon vertex is antisymmetric with respect to the ordering of the legs.

One-Loop Level

At one-loop level there are subleading double trace color structures as well as the leading color single trace color structures we encountered already at tree level. The decomposition of a one-loop amplitude of n adjoint particles into color structures and color ordered amplitudes $A(\sigma(1), \ldots, \sigma(n))$ reads

$$\mathcal{A}_n(\{p_i, h_i, f_i, a_i\}) = g^n \Bigg(\sum_{\sigma \in S_n/Z_n} N \,\mathrm{Tr}(T^{a_{\sigma(1)}} \ldots T^{a_{\sigma(n)}})\, A(\sigma) \tag{2.10}$$

$$+ \sum_{k=2}^{\left[\frac{n}{2}\right]} \sum_{\sigma \in S_{n,k}} C_{n,k}(\sigma)\, P_{n,k}(\sigma) \Bigg) , \tag{2.11}$$

with the subleading color structures $C_{n,k}$ and subleading partial amplitudes $P_{n,k}$ being given by

$$C_{n,k}(\sigma) = \mathrm{Tr}(T^{a_{\sigma(1)}} \ldots T^{a_{\sigma(k)}})\, \mathrm{Tr}(T^{a_{\sigma(k+1)}} \ldots T^{a_{\sigma(n)}}) , \tag{2.12}$$

and

$$P_{n,k}(\sigma) = (-1)^k \sum_{\tau \in \mathrm{COP}_k(\sigma)} A(\tau) . \tag{2.13}$$

The permutations $S_{n,k}$ are defined as the permutation group S_n modulo the symmetry group of the double traces $C_{n,k}$ which is isomorphic to $Z_k \times Z_{n-k}$. Hence, $S_{n,k} \simeq S_n/(Z_k \times Z_{n-k})$. The cyclically ordered permutations $\mathrm{COP}_k(\sigma)$ are defined as

$$\mathrm{COP}_k(\sigma) := \mathrm{COP}\{\sigma(k), \ldots, \sigma(1)\}\{\sigma(k+1), \ldots, \sigma(n)\} , \tag{2.14}$$

where $\mathrm{COP}\{\alpha_1,\ldots,\alpha_a\}\{\beta_1,\ldots,\beta_b\}$ denotes all permutations of the α_i and β_i that preserve their cyclic ordering and start with α_1. For example $\mathrm{COP}\{1,2,3\}\{4,5\}$ is given by the twelve permutations

$$\begin{array}{llll} \{1,2,3,5,4\}, & \{1,2,3,4,5\}, & \{1,2,5,3,4\}, & \{1,2,4,3,5\}, \\ \{1,2,5,4,3\}, & \{1,2,4,5,3\}, & \{1,5,2,3,4\}, & \{1,4,2,3,5\}, \\ \{1,5,2,4,3\}, & \{1,4,2,5,3\}, & \{1,5,4,2,3\}, & \{1,4,5,2,3\}. \end{array} \tag{2.15}$$

In order to prove eq. (2.11) we perform the color decomposition of an arbitrary one-loop diagram. This will yield the color structures for the amplitudes as well as a characterization of the Feynman diagrams contributing to the partial amplitudes. Besides eq. (2.8) we need the Fierz identity of the $su(N)$ generator matrices

$$\sum_{a=1}^{N^2-1} (T^a)_{i_1 j_1} (T^a)_{i_2 j_2} = \delta_{i_1 j_2}\delta_{i_2 j_1} - \frac{1}{N}\delta_{i_1 j_1}\delta_{i_2 j_2}\,. \tag{2.16}$$

The term proportional to N^{-1} is reflecting that the generator matrices are traceless.

We start with the basic observation that all one-loop diagrams can be drawn in planar fashion. Given a particular one-loop diagram we simply cut one of the loop propagators. From the previous section we know, that the color parts of the obtained tree diagram are traces of nested commutators. Making use of eq. (2.16) we can contract the adjoint index of the cut loop propagator. Due to the commutators in the trace the $\frac{1}{N}$ term in eq. (2.16) does not contribute and can be omitted. Expanding the commutators we are left with either a contraction of adjacent or a contraction of non-adjacent generators, leading to a single trace of generators multiplied by N or a product of two traces of generators. Using the double line formalism, it is instructive to analyze the color flows corresponding to both types of color structures. In the case of the single trace we have a closed color loop leading to the prefactor of N and by definition eq. (2.2) the partial amplitude is simply the color ordered amplitude whose external legs are ordered according to the generators in the trace. Up to a factor of $(-1)^k$, the contribution of a Feynman diagram to a double trace color structure eq. (2.12) is given by a color ordered diagram whose external legs are ordered such that the cyclic ordering of the legs $\{\sigma(k),\ldots,\sigma(1)\}$ and $\{\sigma(k+1),\ldots,\sigma(n)\}$ are preserved. Furthermore, each tree attached to the loop contain only legs of one of the traces. The reason the order of the legs $\{\sigma(k),\ldots,\sigma(1)\}$ is reversed with respect to the trace is that the color is flowing counter clockwise around the loop opposed to clockwise color flow connecting the legs $\{\sigma(k+1),\ldots,\sigma(n)\}$. The remaining task is to express this set of color ordered diagrams as a linear combination of color ordered amplitudes. Obviously the linear combination in eq. (2.13) contains all contributing color ordered diagrams. Within the sum over the permutations $\mathrm{COP}_{n,k}(\sigma)$ all diagrams containing trees that mix the traces cancel out due to the symmetry properties of the color ordered Feynman rules fig. 2.1.

2.2. Color Decomposition of QCD Amplitudes

The decomposition of an arbitrary QCD tree or one-loop amplitude with k quark anti-quark pairs $\{q_i,\bar{q}_i\}$ of distinct flavors and n gluons into color structures and color ordered or primitive amplitudes has a much richer structure than in the case of only adjoint particles. The reason being the large number of different subleading color

structures that are present already at tree level.

Note that we exploit the fact that the number of flavors n_f is a free parameter of QCD. Hence, unequal flavor amplitudes with $k > 6$ are well defined. The color decomposition of QCD amplitudes containing equally flavored quark–anti-quark pairs can be straightforwardly obtained by summing up the appropriate single flavor amplitudes. Furthermore, we keep the number of colors N of the $SU(N)$ gauge symmetry a free parameter as well.

2.2.1. Tree Level

Let now $i_1, \ldots, i_k$ and $\bar{j}_1, \ldots, \bar{j}_k$ be the color indices of the quarks and anti-quarks. We introduce the short hand notation

$$(n_m)_{i\,\bar{j}} = \left(\prod_{l=n_{m-1}+1}^{n_m} T^{a_{\sigma(l)}} \right)_{i\,\bar{j}} \tag{2.17}$$

where $\sigma \in S_n$ is some arbitrary permutation of the gluons and $0 = n_0 \leq n_1 \leq n_2 \leq \ldots \leq n_k = n$ is some arbitrary partition. As we are going to prove in the following, all color structures are given by

$$\left(\frac{-1}{N}\right)^p \left(\prod_{\alpha=1}^{k} (n_\alpha)_{i_\alpha\,\bar{j}_{\tau(\alpha)}} \right) , \tag{2.18}$$

where $\tau \in S_k$ is some permutation of the anti-quarks, and

$$p = p(\tau) = c(\tau) - 1 \,, \tag{2.19}$$

with $c(\tau)$ being the number of cycles of the permutation τ. Hence, modulo permutations of the gluons we have $k!\binom{n+k-1}{k-1}$ different color structures leading to a total of $k \cdot (n+k-1)!$ terms in the color decomposition of an arbitrary quark-gluon tree amplitude. We recall that a permutation is uniquely determined by its cycles and that a cycle of length l of a permutation τ can be represented by a sequence of the form $\{i, \tau(i), \tau^2(i), \ldots, \tau^{l-1}(i)\}$, with all elements being distinct and $i = \tau^l(i)$. Since we have l choices for i, there are l such representatives, all related by cyclic permutations $\pi \in Z_l$.

Similar to the case of only adjoint particles we are going to prove eq. (2.18) by determining the color structures appearing in an arbitrary Feynman diagram. With regard to the structure of the partial amplitudes it is convenient to include the gluons into the definition of a cycle. Hence, without any reference to a permutation of anti-quarks, we define a cycle to be a sequence that

- starts with a quark and ends with its anti-quark,
- contains additional quarks only as the successors of their anti-quarks, and
- contains gluons only between successive quarks and anti-quarks of different flavor.

Cycles related by a cyclic permutation are considered equal. Disjoint cycles have neither common quarks nor common gluons. An example of a cycle with three quarks and four gluons is $c_1 = \{q_1, 1, 2, \bar{q}_2, q_2, \bar{q}_3, q_3, 3, 4, \bar{q}_1\}$. The integers in the definition of a cycle

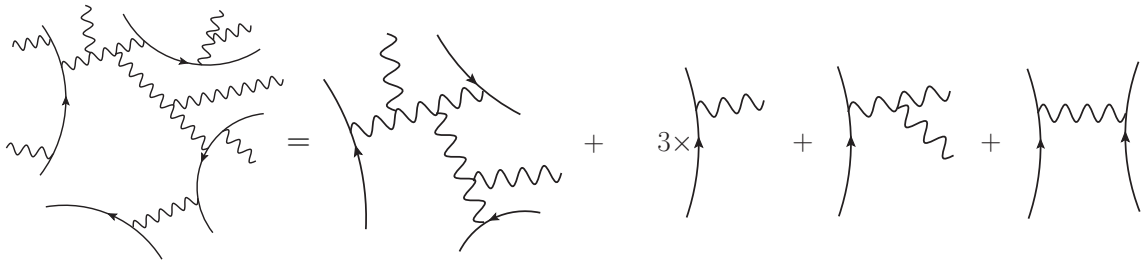

Figure 2.2.: Unique partition of a Feynman diagram into cropped diagrams obtained by cutting quark lines between quark-gluon vertices.

represent the gluons. It is obvious that there is a one to one correspondence between the sets of $p+1$ disjoint cycles with a total of k quarks and n gluons and τ, σ and the gluon partition $\{n_i\}$ in (2.18), e. g. the color structure corresponding to the example cycle c_1 above is just $C_1 = (T^{a_1}T^{a_2})_{i_1\bar{j}_2}\delta_{i_2\bar{j}_3}(T^{a_3}T^{a_4})_{i_3\bar{j}_1}$. The importance of the concept of cycles becomes evident when analyzing the partial amplitude multiplying a color structure corresponding to a single cycle, such as our example C_1. Each Feynman diagram contributing to such a partial amplitude can be drawn in planar fashion such that the external legs are ordered as in the cycle. In other words, the partial amplitude is given by the color ordered amplitude whose external legs are ordered as in the cycle. This observation is crucial for the succeeding analysis of the color decomposition of QCD at tree and one-loop level and a basic fact following from the color flow of a Feynman diagram.

We remark that eq. (2.18) differs from the color structures given in ref. [97] by the power of $\frac{-1}{N}$ associated with the permutation of the anti-quark indices. According to ref. [97] the power p should be equal to $k-1$ for the identity permutation and equal to the number of fixed points of the permutation else. However, this is only valid for up to three quark lines. As will be shown in the following, eq. (2.19) is the correct generalization to an arbitrary number of quark lines.

In order to determine all possible color structures we make use of the simple fact that a given Feynman diagram can be uniquely divided into sub diagrams by cutting the quark lines between quark-gluon vertices. We refer to these sub diagrams as cropped diagrams. An example can be found in fig. 2.2. It is obvious that the color structures of a Feynman diagram are obtained by contracting the color structures of its cropped diagrams. Consequently, it is sufficient to know the color structures of an arbitrary cropped Feynman diagram. To determine the color structure of a cropped Feynman diagram we start in one of its quark lines and contract the adjoint indices along the quark-gluon tree attached to it. As shown in fig. 2.3 the gluon connected to the quark line can be either external (case 1.1), connected to a non-Abelian vertex (cases 1.2a and 1.2b) or directly connected to another quark line (case 1.3). If the gluon is external, the color structure of the cropped diagram is

$$(T^{a_\alpha})_{i_1\bar{j}_1}\,. \tag{2.20}$$

Note that the color indices i_1, $\bar{j}_1$ in general do not belong to external quarks but are contracted along the chosen quark line. If the gluon is connected to a three-vertex we get a sum of two color structures

$$if^{abc}(T^c)_{i_1\bar{j}_1} = [T^a, T^b]_{i_1\bar{j}_1} = (T^a, T^b)_{i_1\bar{j}_1} - (T^b, T^a)_{i_1\bar{j}_1} \tag{2.21}$$

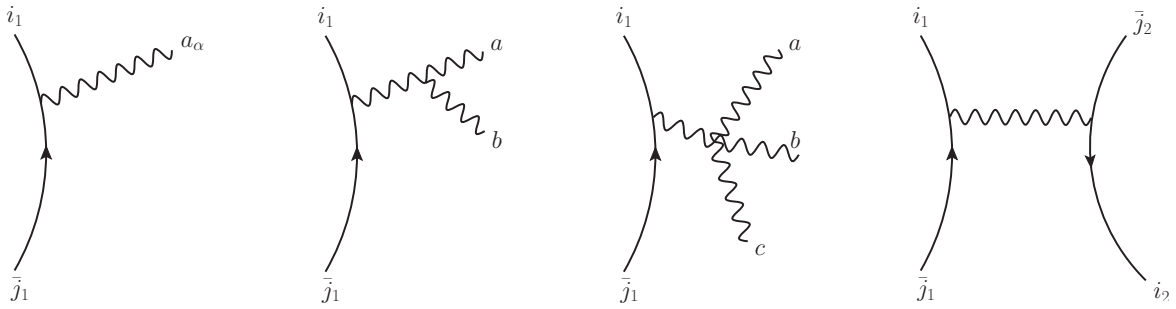

(a) Case 1.1 (b) Case 1.2a (c) Case 1.2b (d) Case 1.3

Figure 2.3.: Determination of the color structure of a cropped quark-gluon Feynman diagram.

and in the case of a four gluon vertex we get a sum of three terms whose color parts read

$$\begin{aligned}(T^d)_{i_1\bar{j}_1} f^{abe} f^{cde} &= [T^c,[T^a,T^b]]_{i_1\bar{j}_1}\,,\\ (T^d)_{i_1\bar{j}_1} f^{ace} f^{bde} &= [T^b,[T^a,T^c]]_{i_1\bar{j}_1}\,,\\ (T^d)_{i_1\bar{j}_1} f^{ade} f^{cbe} &= [T^a,[T^c,T^b]]_{i_1\bar{j}_1}\,.\end{aligned} \tag{2.22}$$

Of course these three terms are not independent due to the Jacobi identity

$$[T^a,[T^b,T^c]] + [T^b,[T^c,T^a]] + [T^c,[T^a,T^b]] = 0\,. \tag{2.23}$$

Since in the end we will expand all commutators, we do not need to care about that. Finally, if the gluon is connected to another quark line we apply eq. (2.16) and get a sum of two color structures for our sub diagram

$$\delta_{i_1\bar{j}_2}\delta_{i_2\bar{j}_1}\,, \tag{2.24}$$

$$\frac{-1}{N}\delta_{i_1\bar{j}_1}\delta_{i_2\bar{j}_2}\,. \tag{2.25}$$

Here (2.25) is a contribution without any color flow between the two quark lines. Hence, it leads to color structures of the whole diagram which are the product of the color structures of the two diagrams we get by removing the gluon connecting the two quarks. In general, if a color structure of a diagram is proportional to $\left(\frac{-1}{N}\right)^p$, than it is a product of $p+1$ terms without color flow between them. As we are going to show now, this QED type gluon exchange between quarks is the only origin of powers of $\frac{-1}{N}$ in the color structures. To further determine the color structure of the cropped diagram we contract all internal gluons of the three- and four-vertex by using eq. (2.21) or eq. (2.22) if the gluon is connected to another three gluon or another four gluon vertex. Proceeding like this we are eventually left with internal gluons contracted with other fermion lines. In fig. 2.4 all possible cases are listed how a three gluon and a four gluon vertex can connect to other fermion lines. The blobs represent sub diagrams and the hatted generators $\widehat{T}^a$ denote the nested commutators belonging to them. In case 2.1a we have a sum of two sub color structures

$$(T^b)_{i_2\bar{j}_2}[\widehat{T}^a,T^b]_{i\bar{j}} = (\widehat{T}^a)_{i\bar{j}_2}\delta_{i_2\bar{j}} - \delta_{i\bar{j}_2}(\widehat{T}^a)_{i_2\bar{j}}\,. \tag{2.26}$$

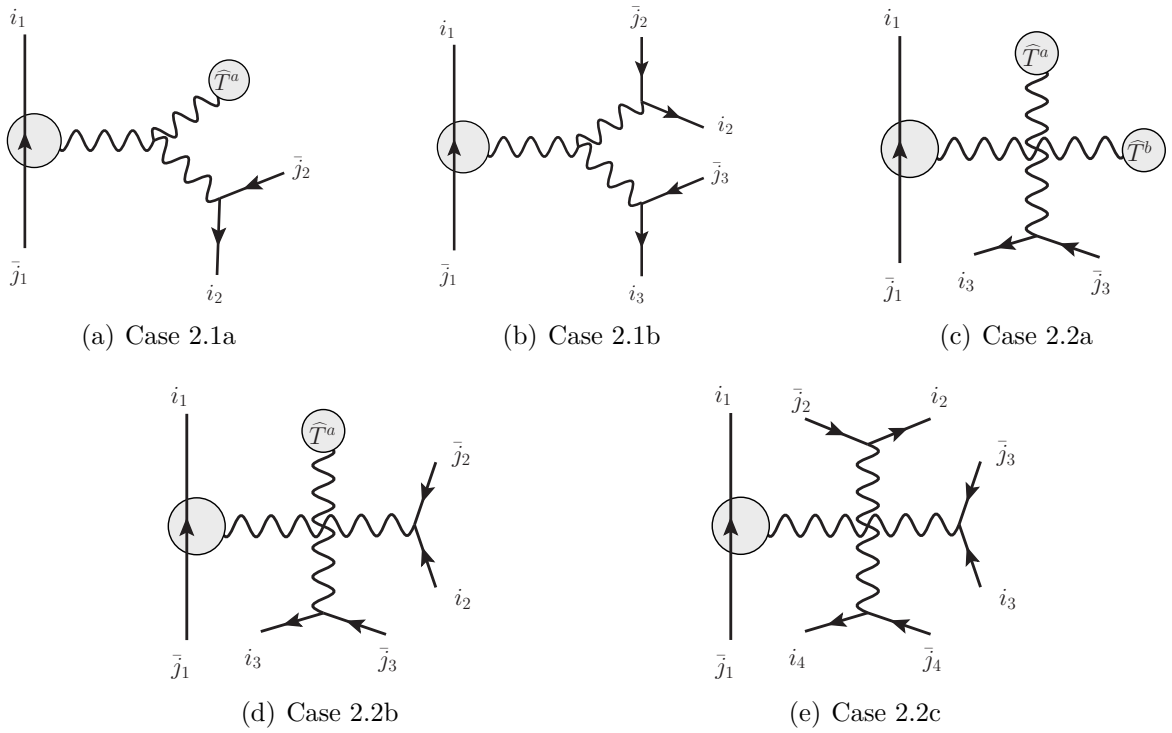

(a) Case 2.1a (b) Case 2.1b (c) Case 2.2a

(d) Case 2.2b (e) Case 2.2c

Figure 2.4.: Determination of the color structure of a quark-gluon Feynman diagram.

The N^{-1} term has vanished due to the commutator and the color indices i, $\bar{j}$ are contracted inside the nested commutators belonging to the blobs in fig. 2.4. If two fermion lines couple to a three gluon vertex we get a sum of two sub color structures as well

$$\begin{aligned}(T^a)_{i_2\,\bar{j}_2}(T^b)_{i_3\,\bar{j}_3}[T^a,T^b]_{i\,\bar{j}} &= (T^a)_{i_2\,\bar{j}_2}\left((\widehat{T}^a)_{i\,\bar{j}_3}\delta_{i_3\,\bar{j}} - \delta_{i\,\bar{j}_3}(\widehat{T}^a)_{i_3\,\bar{j}}\right) \\ &= \delta_{i\,\bar{j}_2}\delta_{i_2\,\bar{j}_3}\delta_{i_3\,\bar{j}} - \delta_{i\,\bar{j}_3}\delta_{i_3\,\bar{j}_2}\delta_{i_2\,\bar{j}}\,.\end{aligned} \tag{2.27}$$

A four gluon vertex can be connected to one, two or three other quark lines. In the case of one additional quark line there are two types of contractions

$$\begin{aligned}(T^c)_{i_2\,\bar{j}_2}[\widehat{T}^a,[\widehat{T}^b,T^c]]_{i\,\bar{j}} &= (\widehat{T}^a\widehat{T}^b)_{i\,\bar{j}_2}\delta_{i_2\,\bar{j}} - (\widehat{T}^a)_{i\,\bar{j}_2}(\widehat{T}^b)_{i_2\,\bar{j}} \\ &\quad + \delta_{i\,\bar{j}_2}(\widehat{T}^b\widehat{T}^a)_{i_2\,\bar{j}} - (\widehat{T}^b)_{i\,\bar{j}_2}(\widehat{T}^a)_{i_2\,\bar{j}}\end{aligned} \tag{2.28}$$

and

$$(T^c)_{i_2\,\bar{j}_2}[T^c,[\widehat{T}^b,\widehat{T}^a]]_{i\,\bar{j}} = [\widehat{T}^a,\widehat{T}^b]_{i\,\bar{j}_2}\delta_{i_2\,\bar{j}} - \delta_{i\,\bar{j}_2}[\widehat{T}^a,\widehat{T}^b]_{i_2\,\bar{j}}\,, \tag{2.29}$$

leading to the following six sub color structures

$$\begin{aligned}&(\widehat{T}^{\pi(a)}\widehat{T}^{\pi(b)})_{i\,\bar{j}_2}\delta_{i_2\,\bar{j}}\,,\\ &(\widehat{T}^{\pi(a)})_{i\,\bar{j}_2}(\widehat{T}^{\pi(b)})_{i_2\,\bar{j}}\,,\\ &\delta_{i\,\bar{j}_2}(\widehat{T}^{\pi(a)}\widehat{T}^{\pi(b)})_{i_2\,\bar{j}}\,,\end{aligned} \tag{2.30}$$

where π is some permutation. Connecting two additional quark lines to the four gluon

vertex, the six encountered sub color structures read

$$\begin{aligned}&(\widehat{T}^a)_{i\,\bar{j}_{\pi(2)}}\delta_{i_{\pi(2)}\,\bar{j}_{\pi(3)}}\delta_{i_{\pi(3)}\,\bar{j}}\,,\\&\delta_{i\,\bar{j}_{\pi(2)}}(\widehat{T}^a)_{i_{\pi(2)}\,\bar{j}_{\pi(3)}}\delta_{i_{\pi(3)}\,\bar{j}}\,,\\&\delta_{i\,\bar{j}_{\pi(2)}}\delta_{i_{\pi(2)}\,\bar{j}_{\pi(3)}}(\widehat{T}^a)_{i_{\pi(3)}\,\bar{j}}\,,\end{aligned}\tag{2.31}$$

and originate from the contractions

$$\begin{aligned}(T^b)_{i_3\,\bar{j}_3}(T^c)_{i_2\,\bar{j}_2}[\widehat{T}^a,[T^b,T^c]]_{i\,\bar{j}} = {}&(\widehat{T}^a)_{i\,\bar{j}_3}\delta_{i_3\,\bar{j}_2}\delta_{i_2\,\bar{j}} - (\widehat{T}^a)_{i\,\bar{j}_2}\delta_{i_2\,\bar{j}_3}\delta_{i_3\,\bar{j}}\\&+\delta_{i\,\bar{j}_2}(\widehat{T}^a)_{i_2\,\bar{j}_3}\delta_{i_3\,\bar{j}} - \delta_{i\,\bar{j}_3}\delta_{i_3\,\bar{j}_2}(\widehat{T}^a)_{i_2\,\bar{j}}\end{aligned}\tag{2.32}$$

and

$$\begin{aligned}(T^b)_{i_3\,\bar{j}_3}(T^c)_{i_2\,\bar{j}_2}[T^c,[T^b,\widehat{T}^a]]_{i\,\bar{j}} = {}&(\widehat{T}^a)_{i\,\bar{j}_3}\delta_{i_3\,\bar{j}_2}\delta_{i_2\,\bar{j}} - \delta_{i\,\bar{j}_3}(\widehat{T}^a)_{i_3\,\bar{j}_2}\delta_{i_2\,\bar{j}}\\&-\delta_{i\,\bar{j}_2}(\widehat{T}^a)_{i_2\,\bar{j}_3}\delta_{i_3\,\bar{j}} + \delta_{i\,\bar{j}_2}\delta_{i_2\,\bar{j}_3}(\widehat{T}^a)_{i_3\,\bar{j}}\,.\end{aligned}\tag{2.33}$$

Finally, if there are three additional quarks we are faced with contractions of the form

$$\begin{aligned}(T^a)_{i_4\,\bar{j}_4}(T^b)_{i_3\,\bar{j}_3}(T^c)_{i_2\,\bar{j}_2}[T^a,[T^b,T^c]]_{i\,\bar{j}} = {}&\delta_{i\,\bar{j}_4}\delta_{i_4\,\bar{j}_3}\delta_{i_3\,\bar{j}_2}\delta_{i_2\,\bar{j}} - \delta_{i\,\bar{j}_4}\delta_{i_4\,\bar{j}_2}\delta_{i_2\,\bar{j}_3}\delta_{i_3\,\bar{j}}\\&+\delta_{i\,\bar{j}_2}\delta_{i_2\,\bar{j}_4}\delta_{i_4\,\bar{j}_3}\delta_{i_3\,\bar{j}} - \delta_{i\,\bar{j}_3}\delta_{i_3\,\bar{j}_2}\delta_{i_2\,\bar{j}_4}\delta_{i_4\,\bar{j}}\,.\end{aligned}\tag{2.34}$$

Hence, the six encountered sub color structures are

$$\delta_{i\,\bar{j}_{\pi(2)}}\delta_{i_{\pi(2)}\,\bar{j}_{\pi(3)}}\delta_{i_{\pi(3)}\,\bar{j}_{\pi(4)}}\delta_{i_{\pi(4)}\,\bar{j}}\tag{2.35}$$

where π is again some permutation. Expanding all remaining commutators we end up with the color decomposition of the cropped Feynman diagram. Except the color structure $\frac{-1}{N}\delta_{i_1\bar{j}_1}\delta_{i_2\bar{j}_2}$ in the case with $k=2$ quark lines and $n=0$ gluons all color structures of a cropped Feynman diagram are cyclic color structures of the general form

$$\begin{aligned}&(T^{\sigma(a_1)}\dots T^{\sigma(a_{n_1})})_{i_1\,\bar{j}_{\pi(2)}}(T^{\sigma(a_{n_1+1})}\dots T^{\sigma(a_{n_2})})_{i_{\pi(2)}\,\bar{j}_{\pi(3)}}\times\dots\\&\qquad\times(T^{\sigma(a_{n_{k-2}+1})}\dots T^{\sigma(a_{n_{k-1}})})_{i_{\pi(k-1)}\,\bar{j}_{\pi(k)}}(T^{\sigma(a_{n_{k-1}+1})}\dots T^{\sigma(a_n)})_{i_{\pi(k)}\,\bar{j}_1}\,.\end{aligned}\tag{2.36}$$

Here $0\le n_1\le n_2\le\dots\le n_{k-1}\le n$ is some partition of the gluons and σ, π are some permutations. As their name indicates, a cyclic color structure corresponds to a cycle. Since contracting a quark and an anti-quark color index between two cyclic color structures (2.36) yields again a cyclic color structure, we have proven that all color structures proportional to $(\frac{-1}{N})^0$ of a quark gluon amplitude have the form (2.36). Contracting a cyclic color structure with $\frac{-1}{N}\delta_{i_1\bar{j}_1}\delta_{i_2\bar{j}_2}$ we get a product of two cyclic color structures. Hence, within a quark-gluon amplitude the color structures proportional to $(\frac{-1}{N})^p$ are a product of $p+1$ cyclic color structures. This concludes the proof of eq. (2.18), as each of the $p+1$ cycles in the permutation τ corresponds to one of the $p+1$ cyclic color structures.

The remaining task is to express the partial amplitudes in terms of color ordered amplitudes. Although the general structure of the color decomposition has in principle been known for a long time, explicit expressions for the partial amplitudes in terms of color ordered amplitudes can be found in the literature only for a small and fixed

number of quarks like e. g. in [97] or more recently in [25]. Given the above derivation of the color structures appearing in an arbitrary quark-gluon Feynman diagram, it is easy to come up with the color decomposition of a QCD tree amplitude with k quark anti-quark pairs $\{q_i, \bar{q}_i\}$ of distinct flavors and n gluons,

$$\mathcal{A}^{\text{tree}}_{(q\bar{q})^k} = g^{n+2k-2} \sum_{\substack{\sigma\in S_n \\ \tau\in S_k}} \sum_{\{n_i\}} \left(\tfrac{-1}{N}\right)^p \left(\prod_{\alpha=1}^{k} (n_\alpha)_{i_\alpha \bar{j}_{\tau(\alpha)}}\right) \sum_{\kappa\in\Gamma(\tau,\sigma,\{n_i\})} A(\kappa)\,. \tag{2.37}$$

The sum over all color structures involves a sum over all permutations σ of the n gluons, over all permutations τ of the k anti-quarks and a sum over all partitions $0 = n_0 < 1 \leq n_1 \leq n_2 \leq \ldots \leq n_k = n$ of the gluons. A given color structure is a product of $p+1$ cyclic color structures and its partial amplitude is given by a sum over all photon exchange permutations $\Gamma(\tau, \sigma, \{n_i\})$, i. e. all possibilities photons can be exchanged between the quarks of different cycles. The number of color ordered amplitudes constituting a partial amplitude only depends on the number of quark lines present, and how the quarks are distributed among the cycles. We have implemented eq. (2.37) in the `Mathematica` package `QCDcolor` described in appendix D.

Before properly defining the photon exchange permutations $\Gamma(\tau, \sigma, \{n_i\})$ and thereby proving the general expression for the partial amplitudes, we give the instructive example of the partial amplitude multiplying the color structure

$$\left(\frac{-1}{N}\right)^2 (T^{a_1}T^{a_2})_{i_1\bar{j}_2} \delta_{i_2\bar{j}_1} \, (T^{a_3}T^{a_4}T^{a_5})_{i_3\bar{j}_3} \, (T^{a_6})_{i_4\bar{j}_4} \tag{2.38}$$

in a four quark line, six gluon amplitude. This color structure contains the three cycles $c_1 = \{q_1, 1, 2, \bar{q}_2, q_2, \bar{q}_1\}$, $c_2 = \{q_3, 3, 4, 5, \bar{q}_3\}$ and $c_3 = \{q_4, 6, \bar{q}_4\}$. According to the derivation of the color structures we have to sum over all possible cyclic subdiagrams whose external legs are ordered according to the three cycles and over all possibilities of exchanging two photons between them. There are four different ways the two photons can be exchanged between the four quark lines in the three cycles. Each of these four contributions is straight forward to express by color ordered amplitudes and the partial amplitude to the color structure eq. (2.38) is given by

$$\left.\begin{aligned} &A(q_1, 1, 2, \bar{q}_2, q_2, \bar{q}_1, q_3, 3, 4, 5, \bar{q}_3, q_4, 6, \bar{q}_4) \\ &+ A(q_1, 1, 2, \bar{q}_2, q_2, \bar{q}_1, q_4, 6, \bar{q}_4, q_3, 3, 4, 5, \bar{q}_3) \end{aligned}\right\} \text{ photons between } q_1,\, q_3,\, q_4$$

$$\left.\begin{aligned} &+ A(q_1, 1, 2, \bar{q}_2, q_3, 3, 4, 5, \bar{q}_3, q_4, 6, \bar{q}_4, q_2, \bar{q}_1) \\ &+ A(q_1, 1, 2, \bar{q}_2, q_4, 6, \bar{q}_4, q_3, 3, 4, 5, \bar{q}_3, q_2, \bar{q}_1) \end{aligned}\right\} \text{ photons between } q_2,\, q_3,\, q_4$$

$$\left.\begin{aligned} &+ A(q_1, 1, 2, \bar{q}_2, q_3, 3, 4, 5, \bar{q}_3, q_2, \bar{q}_1, q_4, 6, \bar{q}_4) \end{aligned}\right\} \begin{array}{l}\text{photon between } q_2,\, q_3 \\ \text{and between } q_1,\, q_4\end{array}$$

$$\left.\begin{aligned} &+ A(q_1, 1, 2, \bar{q}_2, q_4, 6, \bar{q}_4, q_2, \bar{q}_1, q_3, 3, 4, 5, \bar{q}_3) \end{aligned}\right\} \begin{array}{l}\text{photon between } q_2,\, q_4 \\ \text{and between } q_1,\, q_3\end{array}, \tag{2.39}$$

where the helicities h_i of the gluons have been suppressed. Note that the first two color ordered amplitudes in eq. (2.39) each contain contributions from diagrams with a non-Abelian vertex between q_1, q_3, q_4. These contribution cancel in the sum of the amplitudes due to the anti-symmetry of the three gluon vertex. Similar cancellations

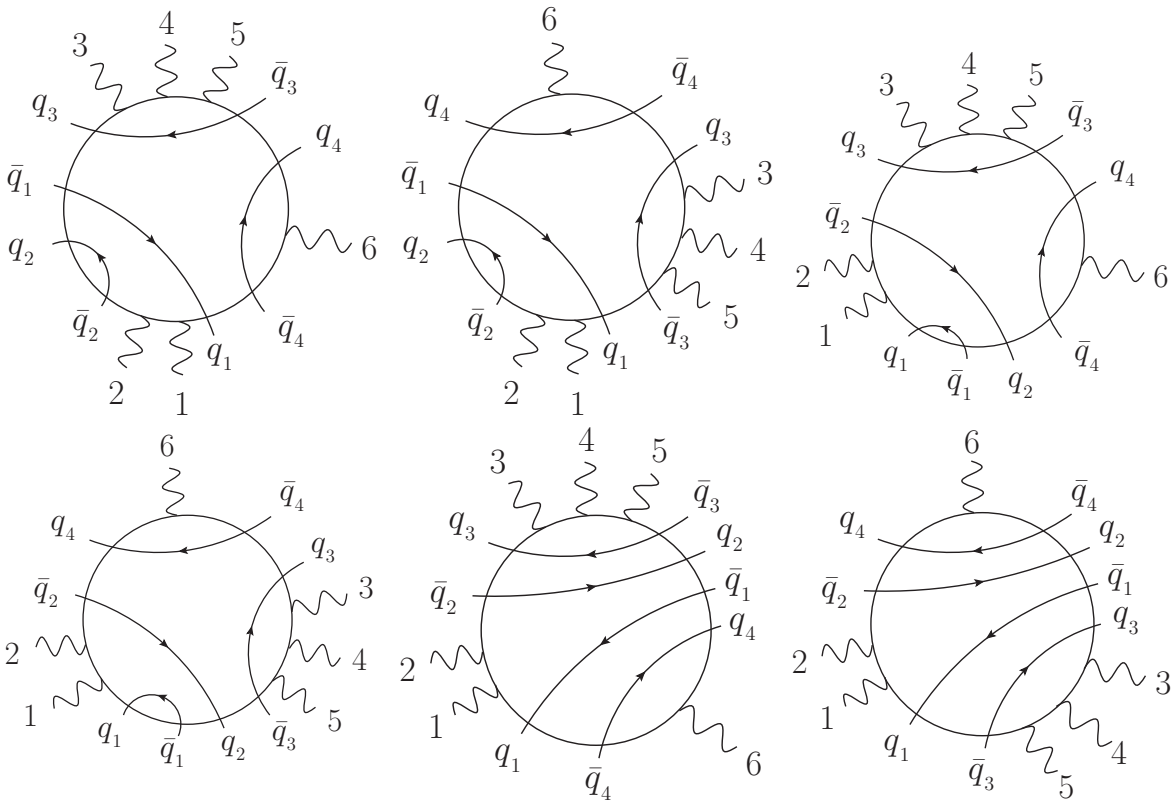

Figure 2.5.: Pictorial representation of the six color ordered amplitudes in eq. (2.39).

appear between the third and fourth amplitude in eq. (2.39). A more intuitive pictorial representation of these color ordered amplitudes can be found in fig. 2.5.

We start the proof of eq. (2.37) by investigating the partial amplitudes multiplying the cyclic color structures of the form eq. (2.36), as these are the simplest ones. As already stated before, given a particular Feynman diagram contributing to the cyclic color structure eq. (2.36), it is a simple fact that it can be drawn in planar fashion such that the external legs follow the ordering of the cycle corresponding to the cyclic color structure

$$q_1,\, \sigma(1),\, \ldots\, \sigma(n_1), \bar{q}_{\pi(2)},\, q_{\pi(2)},\, \sigma(n_1{+}1), \ldots, \sigma(n_2),\, \bar{q}_{\pi(3)},\, q_{\pi(3)},\, \sigma(n_2{+}1), \ldots, \bar{q}_1 \quad (2.40)$$

if we go clockwise around the diagram. Its contribution to the partial amplitude is straightforwardly obtained by applying the color ordered Feynman rules of fig. 2.1 to this planar diagram. Hence, summing up the contributions from all possible Feynman diagrams is equivalent to summing over all possible color ordered Feynman diagrams contributing to the color ordered amplitude

$$A(q_1,\, \sigma(1),\, \ldots\, \sigma(n_1), \bar{q}_{\pi(2)},\, q_{\pi(2)},\, \sigma(n_1+1), \ldots, \sigma(n_2),\, \bar{q}_{\pi(3)},\, q_{\pi(3)},\, \sigma(n_2+1), \ldots, \bar{q}_1)\,. \quad (2.41)$$

In general the color structure (2.18) is a product of $p+1$ cyclic color structures. From the derivation of the color structures we know that each diagram contributing to the color structure (2.18) can be composed of $p+1$ planar sub-diagrams whose external legs are ordered according to the cycles in the color structure. These cyclic sub-diagrams are connected only via QED type gluon exchange between various of the quark lines. To get

the whole partial amplitude we have to sum over all possible cyclic sub-diagrams as well as over all possibilities of photon exchange between them. Again the contribution of such diagrams to the partial amplitude can be obtained by applying the color ordered Feynman rules of fig. 2.1 to it. However, there is a small sign subtlety. The color ordered quark gluon vertex is anti-symmetric whereas the ordinary quark gluon vertex always comes with a plus sign irrespective of the ordering of its legs. Fortunately, the $q\bar{q}g$ vertex appears an even number of times as it is only present in the photon exchange between the cyclic sub-amplitudes.

In order to be able to write down expressions for the partial amplitudes in terms of color ordered amplitudes we need to have control over the photon exchange. In fact, it is straight forward to construct a linear combination of color ordered amplitudes containing the photon exchange between a given number of quark lines. The idea is to let the considered quark lines face against each other and to sum over all non-cyclic permutations of the quarks in order to sum up all possibilities of photon exchange between the quark lines. To be more precise, the photon exchange between k quark lines is given by the linear combination

$$\sum_{\kappa\in S_k/Z_k} A(q_{\kappa(1)}, R_{\kappa(1)}, \bar{q}_{\kappa(1)}, q_{\kappa(2)}, R_{\kappa(2)}, \bar{q}_{\kappa(2)}, \ldots, q_{\kappa(k)}, R_{\kappa(k)}, \bar{q}_{\kappa(k)}) \,, \tag{2.42}$$

where R_i can be any additional partons connected to the right of the quark line of flavor i. The only thing we have to worry about is whether the diagrams containing gluon trees connecting cyclic sub-diagrams cancel within the sum over non-cyclic permutations $\kappa \in S_k/Z_k$. However, this cancellation is a direct consequence of the symmetry properties of the color ordered gluon vertices. As can be easily checked using the color ordered Feynman rules of fig. 2.1, the three gluon vertex is anti-symmetric and the four gluon vertex gives zero when symmetrized over more than two of its legs. For the one-loop amplitudes we need to slightly generalize eq. (2.42) to the case where k quark lines couple via photons to one side of the quark line m and additional legs are connected to the same side of the quark line without sharing any subtree with the other legs on this side of the quark line

$$\sum_{\kappa\in S_k} \sum_{\sigma\in \mathrm{OP}\{L_m\}\{q_{\kappa(1)},R_{\kappa(1)},\bar{q}_{\kappa(1)},\ldots,q_{\kappa(k)},R_{\kappa(k)},\bar{q}_{\kappa(k)}\}} A(q_m, R_m, \bar{q}_m, \sigma) \,, \tag{2.43}$$

$$\sum_{\kappa\in S_k} \sum_{\sigma\in \mathrm{OP}\{R_m\}\{\mathrm{rev}(q_{\kappa(1)},R_{\kappa(1)},\bar{q}_{\kappa(1)},\ldots,q_{\kappa(k)},R_{\kappa(k)},\bar{q}_{\kappa(k)})\}} A(\bar{q}_m, L_m, q_m, \sigma) \,. \tag{2.44}$$

Here L_i and R_i denote arbitrary sets of external legs and $\mathrm{OP}\{\alpha_1\}\{\alpha_2\}$ denotes all permutations preserving the order of each of the α_i. The reason to reverse the order of the legs $q_{\kappa(1)}, R_{\kappa(1)}, \bar{q}_{\kappa(1)}, \ldots, q_{\kappa(k)}, R_{\kappa(k)}, \bar{q}_{\kappa(k)}$ in eq. (2.44) is the anti-symmetry of the quark gluon vertex in color ordered diagrams. Since the quark gluon vertex of QCD is symmetric, not reversing these legs would lead to a non uniform relative sign between the color ordered diagrams and the corresponding contributions of Feynman diagrams to the partial amplitudes of QCD.

Now we can immediately write down the following contribution to the partial am-

plitude of the general color structure eq. (2.18) with $p+1$ cycles of length l_i

$$\sum_{\substack{\pi_i \in Z_{l_i} \\ \kappa \in S_{p+1}/Z_{p+1}}}$$

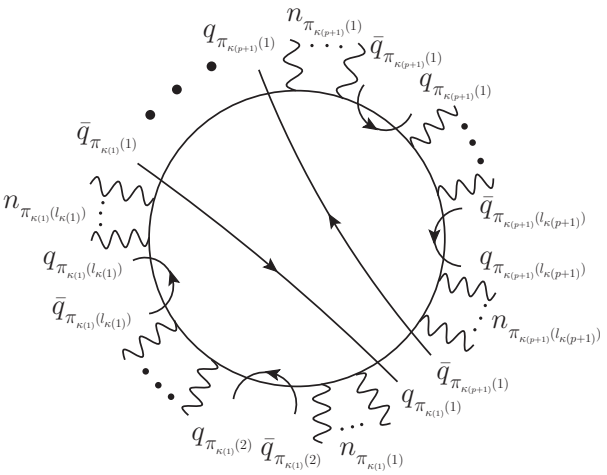

(2.45)

Obviously this sum contains all contributions to the partial amplitude where p photons are exchanged between $p+1$ quark lines. The cyclic permutations $\pi_i \in Z_{l_i}$ fix the quark lines involved in the QED type gluon exchange between the cycles and the non-cyclic permutation $\kappa \in S_{p+1}/Z_{p+1}$ ensures that we get all possibilities p photons can be exchange between these quark lines. Note that the sum of the first four amplitudes in the partial amplitude eq. (2.39) are given by eq. (2.45).

Whenever the number of quarks in the amplitude exceeds the number of cycles in the color structure, there are additional contributions where p photons are exchanged between up to $2p$ quark lines. A characterization of all these contribution leads to a proper definition of the photon exchange permutations $\Gamma(\tau, \sigma, \{n_i\})$ and will conclude the proof of eq. (2.37).

It is convenient to represent the topologically nonequivalent possibilities of photon exchange between cycles by connected planar diagrams. These photon exchange diagrams are assembled from convex polygons, with each pair of polygons sharing at most one vertex. The vertices are indistinguishable and represent cycles. Diagrams which can be related by exchanging subgraphs attached to a polygon are considered equivalent. A convex k-gon represents the photon exchange between k quark lines of k cycles. If a vertex is part of m polygons than m of the quarks of a cycle are involved in photon exchange with other cycles. Alternatively, the photon exchange topologies between k cycles can be represented by the set of connected graphs on k unlabeled vertices where every block is a complete graph. The complete graphs, i. e. graphs where every pair of vertices is connected by an edge, take the role of the convex polygons and incorporate the equivalence relation defined above. Graphically, both representations differ only by attaching or removing some edges inside the polygons or inside the complete graphs.

In fig. 2.6 the photon exchange topologies for up to six cycles are listed. Within a photon exchange diagram consisting of $p+1$ cycles and m polygons there are $p+m$ quark lines involved in the photon exchange. Given a certain color structure which may be represented by a set of cycles or by permutations τ, σ of quarks, gluons and a partition $\{n_i\}$ of the gluons, the photon exchange topologies are straight forward to translate into disjoint subsets of the photon exchange permutations $\Gamma(\tau, \sigma, \{n_i\}) = \Gamma(C_1, \ldots, C_{p+1})$.

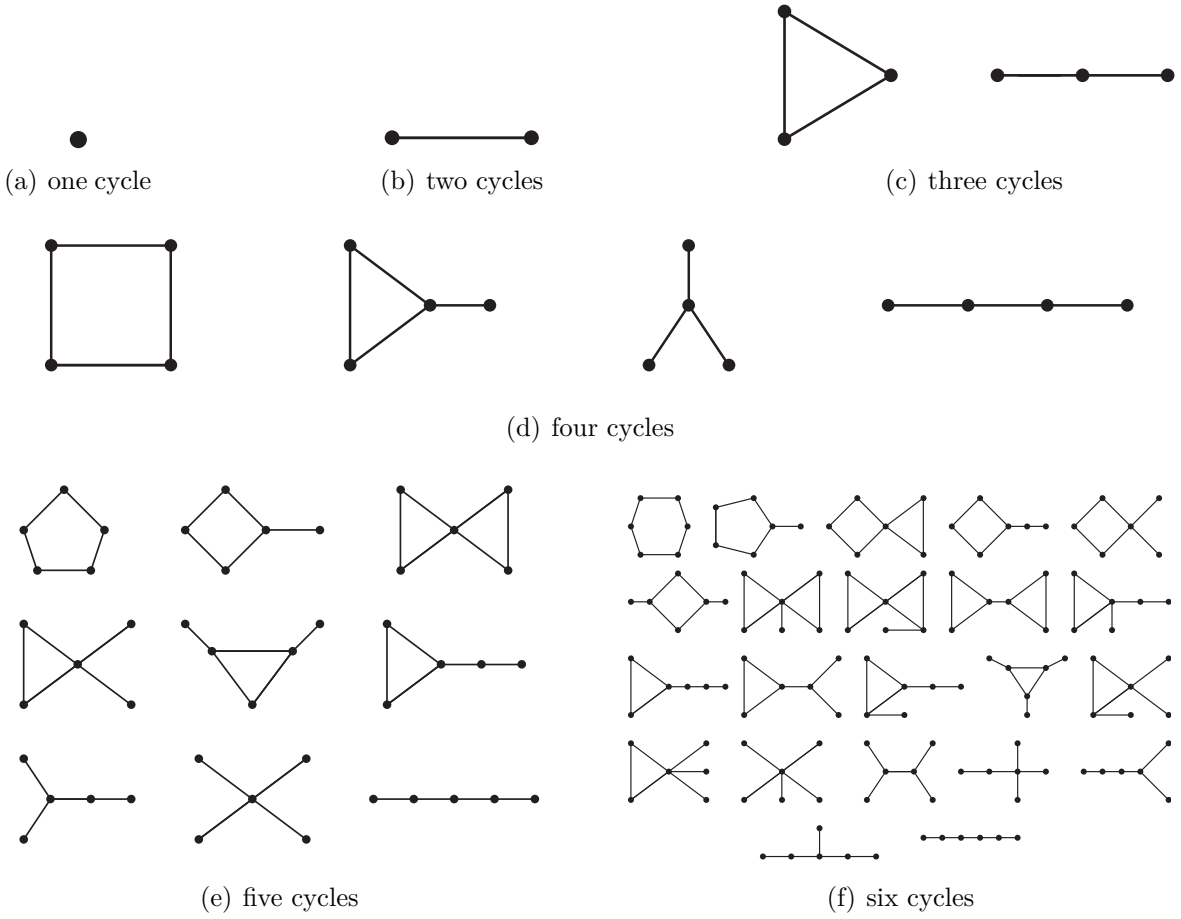

(a) one cycle (b) two cycles (c) three cycles

(d) four cycles

(e) five cycles (f) six cycles

Figure 2.6.: Photon exchange topologies for up to six cycles.

We define $\Gamma(\alpha_1, \ldots, \alpha_{p+1})$ to be the set of permutations obtained by applying the following rules to each photon exchange topology:

1. sum over all possibilities the α_i can be inserted into the topology,

2. for each of these insertions sum over all possible choices of quark lines involved in the photon exchange,

3. enforce the photon exchange between the chosen quarks according to eqs. (2.42) to (2.44).

At tree level the α_i are simply the cycles C_i, hence only eq. (2.42) is necessary to enforce the photons connecting the choice of quarks lines. Apparently, the rules given above yield eq. (2.45) when applied to a $(p+1)$-gon. It is instructive to recall our initial example given in eq. (2.39). The first four amplitudes in eq. (2.39) correspond to the triangle photon exchange diagram in fig. 2.6. Since the amplitudes involves four quark lines, only one of the cycles has two quarks and the second photon exchange topology corresponds to the last two of the color ordered amplitudes in eq. (2.39). The sum over photon exchange permutations is straight forward to implement into a computer algebra system. For details on the `Mathematica` implementation `QCDcolor` as well as some more examples of partial amplitudes we refer to appendix D.

2.2.2. One-Loop Level

At one-loop level the color decomposition is more involved. Despite its increased complexity compared to the tree-level case, it is still possible to directly construct a decomposition of a general QCD one-loop amplitude into color structures and primitive amplitudes. The general idea is again

- identify all color structures,

- characterize all color ordered diagrams contributing to a particular partial amplitude, and

- construct a linear combination of primitive amplitudes that equals the sum of all those diagrams.

Given an arbitrary one-loop Feynman diagram we cut one loop propagator leading to a tree diagram whose color decomposition we already know. Cutting a pure fermion loop we end up with a tree diagram with one additional quark line. From the previous section we know that a color structure in the color decomposition of this tree diagram contains in general up to $k+1$ cycles, where k is the number of quark–anti-quark pairs present in the one-loop amplitude. Depending on the additional partons in the cycle containing the loop quark line we get three different types of color structures when contracting the color indices of the loop quark–anti-quark pair.

If there are additional quarks in the loop cycle we get the tree level color structures up to a factor of n_f

$$n_f \left(\frac{-1}{N}\right)^p \left(\prod_{\alpha=1}^{k} (n_\alpha)_{i_\alpha \bar{j}_{\tau(\alpha)}}\right), \tag{2.46}$$

and all color ordered diagrams contributing to its partial amplitude are composed of $p+1$ cyclic subdiagrams connected by p photons, with one cyclic subdiagram containing the fermion loop.

If the loop cycle contains only gluons and the loop quark, the one-loop color structures are

$$n_f \,\mathrm{Tr}(n_0) \left(\frac{-1}{N}\right)^{p+1} \left(\prod_{\alpha=1}^{k} (n_\alpha)_{i_\alpha \bar{j}_{\tau(\alpha)}}\right) , \tag{2.47}$$

with $\mathrm{Tr}(n_0) = \mathrm{Tr}(T^{\sigma(1)} \dots T^{\sigma(n_0)})$. The corresponding partial amplitude gets contributions from color ordered diagrams composed of $p+1$ cyclic diagrams and a subdiagram containing the fermion loop and the cyclically ordered gluons $\{\sigma(1), \dots, \sigma(n_0)\}$ of the trace. These subdiagrams are connected by $p+1$ photons.

The last possibility is a loop cycle without additional quarks or gluons, leading to the color structure

$$-n_f \left(\frac{-1}{N}\right)^{p} \left(\prod_{\alpha=1}^{k} (n_\alpha)_{i_\alpha \bar{j}_{\tau(\alpha)}}\right) , \tag{2.48}$$

which is equal to the tree level color structures up to a factor of $\frac{-1}{N}\delta_{ii} n_f = -n_f$. The color ordered diagrams contributing to the corresponding partial amplitude are composed of p cyclic subdiagrams and a fermion loop, all connected by $p+1$ photons.

In order to identify all color structures in the non fermion loop part of the amplitude it is convenient to start with the case of at least one photon in the loop. Since there is no color flowing along the photon line, the color structures are equal to the ones in the tree diagram obtained by removing the photon

$$\left(\frac{-1}{N}\right)^{p+1} \left(\prod_{\alpha=1}^{k} (n_\alpha)_{i_\alpha \bar{j}_{\tau(\alpha)}}\right) , \tag{2.49}$$

with an additional factor of $\frac{-1}{N}$ originating from the loop photon. The derivation of the remaining color structures is now simplified as we can neglect the $\frac{-1}{N}$ part in the Fierz identity eq. (2.16) when contracting the loop gluons, since it is either not contributing or leads to the case of at least one photon in the loop.

Contracting the adjoint indices of two gluons in the tree level color structures eq. (2.18) leads to three different color structures at one-loop level. Contracting adjacent gluons leads to the leading order color structures

$$N \left(\frac{-1}{N}\right)^{p} \left(\prod_{\alpha=1}^{k} (n_\alpha)_{i_\alpha \bar{j}_{\tau(\alpha)}}\right) . \tag{2.50}$$

A color ordered diagram contributing to the leading order partial amplitude P_0 is given by $p+1$ cyclic subdiagrams connected by p photons with one of the cyclic subdiagrams containing the loop.

The leading order color structures are up to the sign equal to the cycle split color structures

$$\left(\frac{-1}{N}\right)^{p-1} \left(\prod_{\alpha=1}^{k} (n_\alpha)_{i_\alpha \bar{j}_{\tau(\alpha)}}\right) \tag{2.51}$$

obtained by contracting two non adjacent gluons $n+1$, $n+2$ separated by quarks of one of the tree level cycles $C_{\text{split}} = \{C_i, n+1, C_j, n+2\}$, thereby splitting it into two cycles C_i, C_j of the one-loop color structure. Speaking of diagrams, contracting these

gluons in the tree diagram leads to an unconventionally drawn one-loop diagram, since the external legs of one of the split cycles, e. g. C_j, and of all the cycles being connected to it by photons, face towards the inside of the loop. Flipping all these subtrees facing inside the loop to the outside of the loop leads to the desired planar way of drawing the Feynman diagram.

Contracting two non adjacent gluons emitted between a quark and the successive anti-quark leads to the color structures

$$\mathrm{Tr}(n_0)\left(\frac{-1}{N}\right)^p\left(\prod_{\alpha=1}^{k}(n_\alpha)_{i_\alpha\bar{j}_{\tau(\alpha)}}\right) \tag{2.52}$$

with $n_0 > 1$. A color ordered diagram contributing to the trace partial amplitude P_3 constitutes of $p+1$ cyclic subdiagrams, one of them containing the loop, and the n_0 gluons of the trace being connected to the loop in reversed cyclic ordering with respect to the trace, without sharing a subtree with the remaining external legs. Note that contracting gluons of different cycles of the tree color structure will just fuse them to one larger cycle and leads to a photon loop color structure.

In summary, the decomposition of an arbitrary one-loop QCD amplitude with k quark–anti-quark pairs and n gluons into color structures and partial amplitudes reads

$$\begin{aligned}\mathcal{A}^{\text{1-loop}}_{(q\bar{q})^k} = g^{n+2k}\sum_{\substack{\sigma\in S_n\\ \tau\in S_k}}\Bigg[&\sum_{\{n_i\}}\left(\tfrac{-1}{N}\right)^p\left(\prod_{\alpha=1}^{k}(n_\alpha)_{i_\alpha\bar{j}_{\tau(\alpha)}}\right)\Big(N(P_0-P_1)-\tfrac{1}{N}P_2+n_f(P_0^f-P_1^f)\Big)\\ &+{\sum_{\{n_i\}}}'\left(\tfrac{-1}{N}\right)^p\mathrm{Tr}(n_0)\left(\prod_{\alpha=1}^{k}(n_\alpha)_{i_\alpha\bar{j}_{\tau(\alpha)}}\right)\Big(P_3-\tfrac{n_f}{N}P_2^f\Big)\Bigg].\end{aligned} \tag{2.53}$$

The partial amplitudes P_i and P_i^f depend on the permutation τ of the anti-quarks as well as on the partition $\{n_i\}$ and permutation σ of the gluons. The integer $p(\tau)$ has been defined in eq. (2.19), and the prime on the sum over gluon partitions $\{n_i\}$ in the trace part indicates a sum over $2 \le n_0 \le n_1 \le \cdots \le n_k = n$, compared to the sum over $0 = n_0 \le n_1 \le \cdots \le n_k = n$ in the non-trace part.

In the remainder of this section we present a case by case constructions of all the partial amplitudes in eq. (2.53) as linear combination of primitive amplitudes. Each of the partial amplitudes is equal to the gauge invariant sum over a well defined set of color ordered diagrams. In all cases these sets can be further decomposed into gauge invariant subsets of color ordered diagrams. The construction of the linear combination of primitive amplitudes equaling a certain gauge invariant set of color ordered diagrams is solely based on the symmetries of the color ordered vertices fig. 2.1 and the fact that the position of the loop can be fixed using the routing of the quarks.

The Leading Order Partial Amplitudes P_0 and P_0^f

The partial amplitudes P_0 and P_0^f are the only ones contributing to the leading order in a large N expansion with P_0^f being suppressed by a relative factor of $\frac{n_f}{N}$.

The non fermion loop partial amplitude P_0 has the most similarities with the tree

level partial amplitudes and is given by

$$P_0(\tau,\sigma,\{n_i\}) = \sum_{i=1}^{p+1} \sum_{\kappa\in\Gamma(\tau,\sigma,\{n_i\})} A(\mathcal{R}_i\circ\kappa)\,. \tag{2.54}$$

It involves two ingredients. First of all, we have to sum over all $p+1$ possibilities which cycle is containing the loop by appropriately choosing the routings $r=\{r_1,\ldots,r_k\}\in\{L,R\}^{p+1}$ of the quarks, i. e. $\mathcal{R}_i\circ\kappa$ denotes setting $r_j=L$ for the quarks of the loop cycle C_i and remaining routings are fixed accordingly. Second, we have to sum over all possibilities to connect the cycles by p photons by summing over the photon exchange permutations $\Gamma(\tau,\sigma,\{n_i\})$ which have been defined at the end of the previous section.

The leading order fermion loop partial amplitude is more involved. The idea is to split all contributing color ordered diagrams into the $(p+1)2^p$ gauge invariant subsets with one cycle C_i containing the loop, part of the cycles connecting to the fermion loop via photons and all remaining cycles being connected to the quarks of the loop cycle C_i by photons. Let $\mathcal{C}_i := \{\,\{\alpha,\beta\}\mid \alpha\cup\beta=C\ \wedge\ \alpha\cap\beta=\{\}\ \wedge\ C_i\in\alpha\}$ denote all possibilities to split the set of cycles $C=\{C_1,\ldots,C_{p+1}\}$ into two disjoint subsets α, β with α containing the loop cycle C_i. We have to sum over all possibilities photons can be exchanged between the cycles α as well as over all possibilities the cycles β can be connected to the fermion loop by photons. Similar to the tree level case and eq. (2.54), the photon exchange between the cycles α is given by a sum over the photon exchange permutations $\Gamma(\alpha)$. The permutations of the external legs of the cycles β are given by the set $\Gamma_\star(\beta) := f_q(\Gamma(\{q,\bar{q}\},\beta))$. The additional cycle $\{q,\bar{q}\}$ represents the fermion loop and the function f_q simply removes it from the permutations $\Gamma(\{q,\bar{q}\},\beta)$ such that the remaining permutations start with the quark that succeeded $\bar{q}$, i. e. $f_q(\{\bar{q},\gamma_1,q\})=\{\gamma_1\}$ and $f_q(\{\gamma_1,q,\bar{q},\gamma_2\})=\{\gamma_2,\gamma_1\}$. If $\kappa_1\in\Gamma(\alpha)$ and $\kappa_2\in\Gamma_\star(\beta)$ are two such permutations of the external legs in α and β we need to ensure that the external legs in κ_2 only connect directly to the fermion loop without sharing any subtrees with κ_1. Similar to eq. (2.13) this can be accomplished by summing over cyclic ordered permutations of the two sets of external legs. Hence, the partial amplitude is given by

$$P_0^f(\tau,\sigma,\{n_i\}) = \sum_{i=1}^{p+1} \sum_{\{\alpha,\beta\}\in\mathcal{C}_i} \sum_{\substack{\kappa_1\in\Gamma(\alpha)\\ \kappa_2\in\Gamma_\star(\beta)}} \sum_{\rho\in\mathrm{COP}\{\mathcal{R}_i\circ\kappa_1\}\{\mathcal{R}_\star\circ\mathrm{rev}(\kappa_2)\}} (-1)^{|\kappa_2|} A_f(\rho)\,. \tag{2.55}$$

The order of the external legs κ_2 has been reversed in order to ensure a uniform relative sign of $(-1)^{|\kappa_2|}$ between the color ordered diagrams of the amplitudes and the contributions to the partial amplitude. The routing $\mathcal{R}_\star$ is defined as $\mathcal{R}_\star\circ\{\ldots,q_l,\ldots,\bar{q}_l,\ldots\} = \{\ldots,q_l^R,\ldots,\bar{q}_l^R,\ldots\}$, $\mathcal{R}_\star\circ\{\ldots,\bar{q}_l,\ldots,q_l,\ldots\}=\{\ldots,\bar{q}_l^L,\ldots,q_l^L,\ldots\}$ and the routing $\mathcal{R}_i$ has been defined below eq. (2.54).

The Fermion Loop Partial Amplitude P_1^f

All diagrams where the fermion loop connects via photons to more than one cycle are contributing to the partial amplitude P_1^f. It is straightforward to construct a linear combination of primitive amplitudes that equals all these diagrams. Starting point are the photon exchange permutations $\Gamma(\tau,\sigma,\{n_i\})$ ensuring all possible types of photon exchange between the cycles. For each of these permutations we have to sum over all possibilities to put the fermion loop between quark lines that are involved into photon

exchange between cycles by appropriately choosing the quark routings. The quarks enclosing the fermion loop all get $r_i = R$ and the routings of the remaining quark are fixed by their orientation with respect to the loop. Denoting the set of all such routings by $\overline{\mathcal{R}}(\kappa)$, the partial amplitude reads

$$P_1^f(\tau,\sigma,\{n_i\}) = \sum_{\kappa\in\Gamma(\tau,\sigma,\{n_i\})} \sum_{r\in\overline{\mathcal{R}}(\kappa)} A_f(r\circ\kappa)\,. \tag{2.56}$$

The Trace Partial Amplitudes P_3 and P_2^f

Building on the construction of the tree level partial amplitudes in eq. (2.37) and the double trace color structures eq. (2.13) the non fermion loop partial amplitude can be written down immediately

$$P_3(\tau,\sigma,\{n_i\}) = (-1)^{n_0}\sum_{i=1}^{p+1} \sum_{\kappa\in\Gamma(\tau,\sigma,\{n_i\})} \sum_{\rho\in\mathrm{COP}\{\sigma(n_0),\ldots,\sigma(1)\}\{\kappa\}} A(\mathcal{R}_i\circ\rho)\,. \tag{2.57}$$

It involves a sum over all possibilities which cycle is containing the loop and over all possibilities of photon exchange between the cycles. Furthermore, we have to sum over all cyclic permutations $\mathrm{COP}\{\sigma(n_0),\ldots,\sigma(1)\}\{\kappa\}\}$ between the reversed gluons of the trace and each photon exchange permutation $\kappa\in\Gamma(\tau,\sigma,\{n_i\})$. The prefactor of $(-1)^{n_0}$ compensates the relative sign between the color ordered diagrams in the primitive amplitudes and the contributions to the partial amplitude. The routing $\mathcal{R}_i$ has been defined below eq. (2.54) and fixes the loop to lie inside the cycle C_i.

The trace partial amplitude with a fermion loop has a similar structure

$$P_2^f(\tau,\sigma,\{n_i\}) = (-1)^{n_0} \sum_{\kappa\in\Gamma(\tau,\sigma,\{n_i\})} \sum_{\rho\in\mathrm{COP}\{\sigma(n_0),\ldots,\sigma(1)\}\{\kappa\}} \sum_{r\in\overline{\mathcal{R}}(\kappa)\cup\widetilde{\mathcal{R}}(\kappa)} A_f(r\circ\rho)\,, \tag{2.58}$$

differs however by the set of routings we have to sum over. The fermion loop couples via photons to one or several cycles. Hence, for each photon exchange permutation $\kappa\in\Gamma(\tau,\sigma,\{n_i\})$ we have to sum over the routings $\widetilde{\mathcal{R}}(\kappa)$, locating the loop to the left of a quark line not involved into photon exchange between cycles, as well as over the routings $\overline{\mathcal{R}}(\kappa)$, fixing the fermion loop to be located between cycles.

The Cycle Split Partial Amplitude P_1

A diagram contributing to the cycle split partial amplitude can be categorized according to which cycles C_i, C_j are the split cycles and furthermore according to which sets of cycles $\mathcal{C}_{i,j} := \{\,\{\alpha,\beta\}\mid \alpha\cup\beta = C \;\wedge\; \alpha\cap\beta = \{\} \;\wedge\; C_i\in\alpha \;\wedge\; C_j\in\beta\}$ are connected by photons to either C_i or C_j. Let $\{\alpha_i,\alpha_j\}\in\mathcal{C}_{i,j}$ denote one such possibility to split the cycles $C = \{C_1,\ldots,C_{p+1}\}$ into two subsets. Summing over cyclic permutations of each pair of photon exchange permutations $\kappa_i\in\Gamma(\alpha_i)$, $\kappa_j\in\Gamma(\alpha_j)$ we obtain the partial amplitude

$$P_1(\tau,\sigma,\{n_i\}) = \sum_{1\le i<j\le p+1} \sum_{\{\alpha_i,\alpha_j\}\in\mathcal{C}_{i,j}} \sum_{\substack{\kappa_i\in\Gamma(\alpha_i)\\ \kappa_j\in\Gamma(\alpha_j)}} \sum_{\rho\in\mathrm{COP}\{\mathcal{R}_i\circ\kappa_i\}\{\overline{\mathcal{R}}_j\circ\mathrm{rev}(\kappa_j)\}} (-1)^{|\kappa_j|}A(\rho)\,, \tag{2.59}$$

where the photon exchange permutations of α_j have been reversed in order to match the set of color ordered diagrams described below eq. (2.51). The factor of $(-1)^{|\kappa_j|}$ compensates the relative sign between the color ordered diagrams and the contributions to the partial amplitude. The routings of the quarks are fixed such that the quarks of C_i and C_j enclose the loop, i. e. $\overline{\mathcal{R}}_j \circ \mathrm{rev}(\kappa_j)$ sets $r_m = R$ for all quarks in C_j and fixes the routings of the remaining quarks accordingly. The routing $\mathcal{R}_i$ has been defined below eq. (2.54).

The Loop Photon Partial Amplitude P_2

The partial amplitudes with a photon in the loop are the most intricate. Gaining control over photons in the loop is simply more involved than managing photons in subtrees of loop diagrams. It is reasonable to split the partial amplitude into three gauge invariant pieces

$$P_2 = P_{2,1} + P_{2,2} + P_{2,3}\,, \tag{2.60}$$

with $P_{2,1}$ corresponding to the set of color ordered diagrams where the loop photon in attached to one of the quark lines, $P_{2,2}$ corresponding to the set of color ordered diagrams where the loop photon connects two quark lines of one of the cycles, and $P_{2,3}$ corresponding to the color ordered diagrams where the loop photon connects quark lines of different cycles.

The easiest of the three parts is

$$P_{2,1}(\tau,\sigma,\{n_i\}) = \sum_{i=1}^{k} \sum_{\alpha\in\Gamma(\tau,\sigma,\{n_i\})} \sum_{\rho\in\mathrm{Flip}_i(\alpha)} (-1)^{|L_i(\alpha)|} A(\mathcal{R}_{q_i}\circ\rho)\,. \tag{2.61}$$

Whenever there are external legs $L_i(\alpha)$ to the left of the quark line i in the photon exchange permutation $\alpha \in \Gamma(\tau,\sigma,\{n_i\})$, i. e. $\alpha = \{q_i, R_i(\alpha), \bar{q}_i, L_i(\alpha)\}$ or $\alpha = \{L_i(\alpha), q_i, R_i(\alpha), \bar{q}_i\}$, than we flip these legs to the right side of the fermion line i by summing over the flip permutations $\mathrm{Flip}_i(\alpha) := \{\{q_i,\kappa,\bar{q}_i\} \mid \kappa \in \mathrm{OP}\{R_i(\alpha)\}\{\mathrm{rev}(L_i(\alpha))\}$. Here $R_i(\alpha)$ denotes the legs to the right of the quark line i and $\mathrm{OP}\{\alpha_1\}\{\alpha_2\}$ is the set of permutations that preserve the order of α_1 and α_2 respectively. $\mathcal{R}_{q_i}$ simply sets $r_i = R$ and fixes the other routings accordingly.

Slightly more complicated are the contributions of diagrams with a loop photon connecting two quark lines of one cycle

$$P_{2,2}(\tau,\sigma,\{n_i\}) = \sum_{i=1}^{p+1} \sum_{\{s,t\}\in\mathcal{P}_2(Q_i)} \sum_{\alpha\in\mathrm{COP}_{s,t}(C_i)} \sum_{\rho\in\Gamma(\alpha,C\setminus C_i)} (-1)^{f_{i,s,t}(C,\rho)}\, A(\mathcal{R}_{i,s,t}\circ\rho). \tag{2.62}$$

The construction of the linear combination of primitive amplitudes starts with the loop cycle C_i and one possible choice of quarks $\{s,t\} \in \mathcal{P}_2(Q_i)$ of C_i that are connected by the loop photon, with $Q_i = Q(C_i)$ denoting the set of all quark flavors in the cycle C_i and $\mathcal{P}_k(S) := \{\alpha \mid \alpha \subset S \ \wedge |\alpha| = k\ \}$ denoting all subsets of cardinality k of the set S. The loop cycle gets split into two parts $C_i = \{C_{i,s,t}, C_{i,t,s}\}$, where $C_{i,s,t}$ starts with q_s and ends with $\bar{q}_t$ and $C_{i,t,s}$ starts with q_t and ends with $\bar{q}_s$. Taking into account all cyclic permutations of $C_{i,s,t}$ and $\mathrm{rev}(C_{i,t,s})$ ensures that both quark lines are part of the loop and connected by the loop photon. The set of all cyclic permutations is defined as

$$\mathrm{COP}_{s,t}(C_i) = \mathrm{cyc}_{s,t}(\mathrm{COP}\{C_{i,s,t}\}\{\mathrm{rev}(C_{i,t,s})\}) \tag{2.63}$$

with $\mathrm{cyc}_{s,t}$ denoting the cyclic rotation of each of the permutations such that they start in q_s or $\bar{q}_s$ and end in q_t or $\bar{q}_t$. What remains is to sum over all possibilities the loop cycle can be connected by photons to the other cycles. Hence, for each permutation $\alpha \in \mathrm{COP}_{s,t}(C_i)$, we have to sum over the photon exchange permutations $\Gamma(\alpha, C \setminus C_i)$. The factor $(-1)^{f_{i,s,t}(C,\rho)}$ compensates the relative sign of the color ordered diagrams and the contributions to the partial amplitude, with

$$f_{i,s,t}(C,\rho) = |C_{i,t,s}| + \sum_{\text{reversed cycles in } \rho} |C_j| \tag{2.64}$$

simply counting the number of legs whose order has been reversed due to the presence of the loop or due to eq. (2.44). The routing of the loop quarks is fixed according to

$$\begin{aligned}
\mathcal{R}_{i,s,t} \circ \{q_s, \ldots, \bar{q}_s, \ldots, q_t, \ldots, \bar{q}_t\} &= \{q_s^R, \ldots, \bar{q}_s^R, \ldots, q_t^R, \ldots, \bar{q}_t^R\} \\
\mathcal{R}_{i,s,t} \circ \{q_s, \ldots, \bar{q}_s, \ldots, \bar{q}_t, \ldots, q_t\} &= \{q_s^R, \ldots, \bar{q}_s^R, \ldots, \bar{q}_t^L, \ldots, q_t^L\} \\
\mathcal{R}_{i,s,t} \circ \{\bar{q}_s, \ldots, q_s, \ldots, q_t, \ldots, \bar{q}_t\} &= \{\bar{q}_s^L, \ldots, q_s^L, \ldots, q_t^R, \ldots, \bar{q}_t^R\} \\
\mathcal{R}_{i,s,t} \circ \{\bar{q}_s, \ldots, q_s, \ldots, \bar{q}_t, \ldots, q_t\} &= \{\bar{q}_s^L, \ldots, q_s^L, \ldots, \bar{q}_t^L, \ldots, q_t^L\}
\end{aligned} \tag{2.65}$$

The other quarks in $C_{i,s,t}$ and $C_{i,t,s}$ get $r_j = R$ and $r_j = L$ respectively, and the routings of the quarks of the non-loop cycles are fixed accordingly.

Finally we present the contribution of color ordered diagrams with a loop photon connecting quark lines of different cycles. Adding a photon connecting two of the $p+1$ cycles of a tree diagram yields a one-loop diagram with a loop containing $2 \leq i \leq p+1$ photons. These i loop photons connect i of the cycles with each cycle having either one or two quark lines that are connected via loop photons to other cycles. For each choice of loop cycles $\alpha = \{C_{\alpha_1}, \ldots, C_{\alpha_i}\} \in \mathcal{P}_i(C)$, each choice of loop cycles $\beta = \{C_{\beta_1}, \ldots, C_{\beta_j}\} \in \mathcal{P}_j(\alpha)$ with two loop quarks and each choice of loop quarks $\pi = \{\pi_1, \ldots, \pi_{i-j}\}$ for the cycles $\bar{\beta} = \alpha \setminus \beta = \{C_{\bar{\beta}_1}, \ldots, C_{\bar{\beta}_{i-j}}\}$ and $\kappa = \{\{\kappa_{1,1}, \kappa_{1,2}\}, \ldots, \{\kappa_{j,1}, \kappa_{j,2}\}\}$ for the cycles β, we get a gauge invariant subset of color ordered diagrams whose sum we denote by $p_{2,3}(C, \bar{\beta}, \beta, \pi, \ kappa)$. Hence, the contribution $P_{2,3}$ to the partial amplitude P_2 is given by

$$P_{2,3}(\tau, \sigma, \{n_i\}) = \sum_{i=2}^{p+1} \sum_{j=0}^{i} \sum_{\alpha \in \mathcal{P}_i(C)} \sum_{\substack{\beta \in \mathcal{P}_j(\alpha) \\ \bar{\beta} = \alpha \setminus \beta}} \sum_{\substack{\pi_s \in Q(\bar{\beta}_s) \\ 1 \leq s \leq i-j}} \sum_{\substack{\{\kappa_{t,1}, \kappa_{t,2}\} \in \mathcal{P}_2(Q(\beta_t)) \\ 1 \leq t \leq j}} p_{2,3}(C, \bar{\beta}, \beta, \pi, \kappa)\,. \tag{2.66}$$

In order to write down an expression for $p_{2,3}(C, \bar{\beta}, \beta, \pi, \kappa)$ we need to be able to construct linear combinations of primitive amplitudes that single out diagrams with a loop containing a predefined number of photons connecting a predefined set of quarks. As a first step we consider the special case of photon loop, i. e. a loop containing only quark gluon vertices. The sum over all possible photon loops between $m+1$ quark lines $l_i = \{q_i, R_i, \bar{q}_i\}$ is given by

$$\sum_{f \in \{0,1\}^m} \sum_{\tau \in S_m} (-1)^{\sum_{k=1}^{m} f_k |l_{\tau(k)}|} A(\mathrm{rev}(f_1, \mathcal{R}_{q_{\tau(1)}} \circ l_{\tau(1)}), \ldots, \mathrm{rev}(f_m, \mathcal{R}_{q_{\tau(m)}} \circ l_{\tau(m)}), \mathcal{R}_{q_{m+1}} \circ l_{m+1}), \tag{2.67}$$

where

$$\mathrm{rev}(\theta,\alpha) = \begin{cases} \alpha & \text{if} \quad \theta = 0 \\ \mathrm{rev}(\alpha) & \text{if} \quad \theta = 1\,, \end{cases} \tag{2.68}$$

and the reversal of α is meant to include an inversion of the routings of the quarks, if present. Obviously this linear combination contains all possible photon loop diagrams. All diagrams without a photon loop, that are contributing to individual primitive amplitudes, cancel out. For a fixed f all diagrams with several quark lines connecting to the loop via a gluon tree cancel in the sum over τ due to the symmetries of the color ordered vertices. On the other hand, for a fixed τ all diagrams with some of the quarks connecting to the loop by a gluon cancel in the sum over f due to the anti symmetry of the color ordered quark gluon vertex if we compensate the signs introduced by reversing individual quark lines. Equation (2.67) covers the special case $\kappa = \{\}$ of all loop cycles α only contributing one loop quark, and has to be generalized in order to cover the case of cycles with two loop quarks as well. First of all we define the loop permutations of some set $\omega = \{\omega_1, \ldots, \omega_{m+1}\}$ of sequences ω_i of external legs

$$\mathrm{LP}(\omega) := \left\{ \sigma \in S(\omega) \;\middle|\; \begin{array}{l} \exists\, \tau \in S_m,\ f \in \{0,1\}^m \,: \\ \qquad \sigma = \{\mathrm{rev}(f_1, \omega_{\tau(1)}), \ldots, \mathrm{rev}(f_m, \omega_{\tau(m)}), \omega_{m+1}\} \end{array} \right\}. \tag{2.69}$$

For the loop cycles $\bar{\beta}$ with one loop quark we know from eq. (2.67) that the sequences of external legs entering the loop permutations are given by $\pi \circ \bar{\beta}$, where the action of π on $\bar{\beta}$ indicates a rotation of the cycles such that they start with their loop quark. In case of a cycle C_{β_i} with two loop quarks $q_{\kappa_{i,1}}$, $q_{\kappa_{i,2}}$ the permutations $\delta_i \in \mathrm{COP}_{\kappa_{i,1},\kappa_{i,2}}(C_{\beta_i})$ ensure that both quarks are part of the loop. Hence, we have to take loop permutations of each possible set of sequences $\delta = \{\delta_1, \ldots, \delta_j\}$ and the sequences $\pi \circ \bar{\beta}$. What remains is to connect the loop part via photons to the non-loop cycles $C \setminus (\beta \cup \bar{\beta})$ by summing over all photon exchange permutations, as well as to fix the routings and signs according to eqs. (2.64), (2.65) and (2.67). Consequently, the missing piece in eq. (2.66) is given by

$$p_{2,3}(C, \bar{\beta}, \beta, \pi, \kappa) = \sum_{\substack{\delta_i \in \mathrm{COP}_{\kappa_{i,1},\kappa_{i,2}}(C_{\beta_i}) \\ 1 \le i \le j}} \sum_{\gamma \in \mathrm{LP}(\delta, \pi \circ \bar{\beta})} \sum_{\rho \in \Gamma(\gamma, C \setminus (\beta \cup \bar{\beta}))} (-1)^{f(C,\beta,\kappa,\rho)} A(\mathcal{R}(\beta,\pi,\kappa) \circ \rho), \tag{2.70}$$

with

$$f(C,\beta,\kappa,\rho) = \sum_{i=1}^{j} (\theta(\rho, C_{\beta_j,\kappa_{j,1},\kappa_{j,2}}) + \theta(\rho, C_{\beta_j,\kappa_{j,2},\kappa_{j,1}})) + \sum_{\alpha \in C \setminus \beta} \theta(\rho, \alpha) \tag{2.71}$$

and

$$\theta(\alpha,\beta) = \begin{cases} |\beta| & \text{if } \mathrm{rev}(\beta) \text{ is a sub sequence of } \alpha \\ 0 & \text{else}\,. \end{cases} \tag{2.72}$$

The routing function $\mathcal{R}(\beta,\pi,\kappa)$ acts as follows on the permutation ρ. The routings of the loop quarks π are set to $r_{\pi_i} = L$ if their cycle got reversed and $r_{\pi_i} = R$ if not. For each cycle C_{β_i} in β the quark routings are fixed as described in and below eq. (2.65) whenever $\mathrm{rev}(C_{\beta_i,\kappa_{i,2},\kappa_{i,1}})$ is a sub sequence of ρ. If $C_{\beta_i,\kappa_{i,2},\kappa_{i,1}}$ is a sub sequence of ρ instead, a reversed version of eq. (2.65) applies. The routings of quarks in the non-loop cycles $C \setminus (\beta \cup \bar{\beta})$ are fixed according to their orientations with respect to the loop.

2.3. Identities Among Primitive Amplitudes

Primitive amplitudes fulfill a large number of identities. A detailed understanding of these identities can be used to significantly speed up the numerical evaluation of a scattering amplitude, as the number of primitive amplitudes constituting the QCD amplitude can be reduced. Besides the obvious symmetry under cyclic permutations $\tau \in Z_n$ of the external legs

$$A(1,\ldots,n) = A(\tau(1),\ldots,\tau(n)) \tag{2.73}$$

and the reflection symmetry

$$A(1,\ldots,n) = (-1)^n A(n,\ldots,1)\,, \tag{2.74}$$

there are additional identities that can be easily understood on the level of color ordered Feynman diagrams and color ordered vertices.

All of these additional identities of the primitive amplitudes that rely on symmetries of the color ordered Feynman diagrams can be written as linear combinations of fermion flip identities, which are basically tree level identities relying on the symmetries of the color ordered vertices fig. 2.1 and the resulting reversion properties of the color ordered diagrams. Fermion flip identities have been first observed in [25], however without stating their general form. In general, fermion flip identities allow to flip one quark line with respect to another one by taking a well defined linear combination of amplitudes. Depending on the position of the loop with respect to the two quark lines, there are two different types of flip identities. At first we are going to present the general fermion flip identity for the case of a quark line l_2, on the non-loop side of the loop quark line l_1, gets flipped. We are going to present the identity for the non-fermion loop part of the primitive amplitudes, but emphasize that due to its tree level nature the flip identity equally holds for the fermion loop part and for the tree level color ordered amplitudes. Let l_1 be a quark line with legs α_1 on its loop side and l_2 be a quark line with legs α_2 on its non-loop side, i. e. $l_1 = \{q_1^L, \alpha_1, \bar{q}_1^L\}$ or $l_1 = \{\bar{q}_1^R, \alpha_1, q_1^R\}$, and $l_2 = \{q_2^R, \alpha_2, \bar{q}_2^R\}$ or $l_2 = \{\bar{q}_2^L, \alpha_2, q_2^R\}$. Let further β_1, β_2 denote two sequences of external legs. The general fermion flip identity is given by

$$A(l_1,\beta_1,l_2,\beta_2) = (-1)^{|l_2|+1} \sum_{\sigma\in \mathrm{FOP}\{\beta_1\}\{\mathrm{rev}(\overline{l_2})\}\{\beta_2\}} A(l_1,\sigma)\,, \tag{2.75}$$

where $\overline{l_2}$ indicates the inversion of the quark routings in l_2 and the flip ordered permutations $\mathrm{FOP}\{\gamma_1\}\{\gamma_2\}\{\gamma_3\} \subset \mathrm{OP}\{\gamma_1\}\{\gamma_2\}\{\gamma_3\}$ of three sequences γ_i are the subset of ordered permutations where the last entry of γ_1 is always before the last entry of γ_2 and the first entry of γ_3 is always after the first entry of γ_2. Obviously eq. (2.75) generalizes the examples of flip identities given in [25]. In fact, there are no diagram based identities among the non-fermion loop parts of primitive amplitudes that cannot be written as linear combinations of the fermion flip identities eq. (2.75). The reasoning behind the flip ordered permutations is quite simple. The diagrams contributing to the right side of eq. (2.75) can be categorized according to which parts $L_2(\beta_i)$, $R_2(\beta_i)$ of β_1 and β_2 are to the left and the right of the fermion line l_2. Within each of the diagrams there is a quark gluon vertex connecting the quark line l_2 to the loop part of the diagram. To simplify the discussion we specify the orientation of the quark

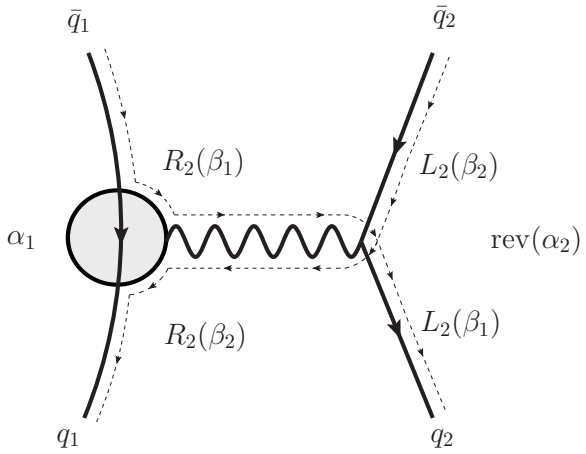

Figure 2.7.: Schematic form of the diagrams contributing to the right side of the fermion flip identity eq. (2.75). All external legs except q_1, q_2, $\bar{q}_1$, $\bar{q}_2$ are omitted. The dotted lines indicate to which part of the diagram the legs β_1 and β_2 can be attached. $R_2(\beta_i)$ and $L_2(\beta_i)$ denote the legs of β_i to the right or to the left of the quark line $\{\bar{q}_2^L, q_2^L\}$.

lines to be $l_1 = \{q_1^L, \alpha_1, \bar{q}_1^L\}$ and $l_2 = \{q_2^R, \alpha_2, \bar{q}_2^R\}$. The schematic form of a diagram contributing to the sum over flip permutations is depicted in fig. 2.7, with all external legs except q_1, q_2, $\bar{q}_1$, $\bar{q}_2$ being omitted. As indicated by the dotted lines, the legs β_i can not be attached to every part of the diagram, e. g. diagrams where part of the legs $R_2(\beta_1)$ connect to the left of the connection vertex cancel within the permutations against diagrams where part of the legs $L_2(\beta_1)$ are attached to the right of the connection vertex. Furthermore, the flip permutations assure that there are no shared trees between the legs $L_2(\beta_i)$ and α_2. Consequently each diagram contributing to the sum over flip permutations is up to a factor of $(-1)^{|l_2|+1}$ equal to a diagram contributing to $A(l_1, \beta_1, l_2, \beta_2)$.

The simplest of the fermion flip identities eq. (2.75) are the ones with $\beta_i = \{\}$

$$A(l_1, l_2) + (-1)^{|l_2|} A(l_1, \mathrm{rev}(l_2)) = 0\,, \tag{2.76}$$

as they involve only two amplitudes. The three term flip identities have the form

$$A(l_1, \beta_1, q_2^R, \bar{q}_2^R) + A(l_1, \beta_1, \bar{q}_2^L, q_2^L) + A(l_1, \bar{q}_2^L, \beta_1, q_2^L) = 0\,, \tag{2.77}$$

with β_1 either being a single gluon or a quark line of the form $\beta_1 = \{\bar{q}_3^L, \ldots, q_3^L\}$ or $\beta_1 = \{q_3^R, \ldots, \bar{q}_3^R\}$. An example of eq. (2.75) with $\beta_1 \neq \{\}$ and $\beta_2 \neq \{\}$ is

$$\begin{aligned} A(q_1^L, \bar{q}_1^L, 1, q_2^R, \bar{q}_2^R, q_3^R, \bar{q}_3^R) = & - A(q_1^L, \bar{q}_1^L, 1, \bar{q}_2^L, q_2^L, q_3^R, \bar{q}_3^R) - A(q_1^L, \bar{q}_1^L, \bar{q}_2^L, 1, q_2^L, q_3^R, \bar{q}_3^R) \\ & - A(q_1^L, \bar{q}_1^L, 1, \bar{q}_2^L, q_3^R, \bar{q}_3^R, q_2^L) - A(q_1^L, \bar{q}_1^L, \bar{q}_2^L, 1, q_3^R, \bar{q}_3^R, q_2^L) \\ & - A(q_1^L, \bar{q}_1^L, \bar{q}_2^L, q_3^R, 1, \bar{q}_3^R, q_2^L) - A(q_1^L, \bar{q}_1^L, \bar{q}_2^L, q_3^R, \bar{q}_3^R, 1, q_2^L)\,. \end{aligned} \tag{2.78}$$

The fermion flip identities eq. (2.75) are implemented in the `Mathematica` package `QCDcolor` described in appendix D.

We remark, that eq. (2.75) holds even in the case of β_1 and β_2 being connected by

one or several quark lines. In this case the routings of the quarks in each of the flip permutations $\sigma \in \mathrm{FOP}\{\beta_1\}\{\mathrm{rev}(l_2)\}\{\beta_2\}$ need to be fixed relative to the loop quark line l_1. This special set of flip identities is reducible. It can be written as a sum of a flip identity eq. (2.75) with β_1 and β_2 not being connected by a quark line and identities of the form

$$\sum_{\sigma \in \mathrm{OP}\{\beta\}\{\gamma\}} A(l_1, \sigma) = 0 \tag{2.79}$$

where β and γ are connected by at least one quark line. In general, the sum over $\mathrm{OP}\{\beta\}\{\gamma\}$ implies that all diagrams with subtrees containing legs of β and of γ cancel. Since β and γ are connected by a quark line, the sum over $\mathrm{OP}\{\beta\}\{\gamma\}$ gives zero.

In the case of the fermion loop part of the primitive amplitudes, there are additional identities that are not captured by eq. (2.75). The reason being the simpler structure of the diagrams with a fermion loop, the furry identity and the fact that massless tadpoles as well as loop corrections to massless external legs vanish

$$A_f(q_1^L, \bar{q}_1^L, \dots) = 0 \tag{2.80}$$

$$A_f(q_1^L, 1, \bar{q}_1^L, \dots) = 0 \tag{2.81}$$

In fact it is straight forward to write down additional non-trivial identities for the fermion loop part of the primitive amplitudes. As a first example we consider the class of color ordered diagrams with a quark line $\{q_1^R, \alpha_1, \bar{q}_1^R\}$ coupling by a photon to the fermion loop and the remaining external legs having a fixed cyclic ordering β. Reversing this quark line in one such diagram leads to a relative factor of $(-1)^{|\alpha_1|+1}$. Hence, the following identity holds

$$\sum_{\sigma \in \mathrm{COP}\{q_1^R, \alpha_1, \bar{q}_1^R\}\{\beta\}} A_f(\sigma) = (-1)^{|\alpha_1|+1} \sum_{\sigma \in \mathrm{COP}\{\bar{q}_1^L, \mathrm{rev}(\overline{\alpha_1}), q_1^L\}\{\beta\}} A_f(\sigma)\,, \tag{2.82}$$

where the cyclic permutations ensure that the quark q_1 couples via a photon to the fermion loop. Again $\overline{\alpha_1}$ indicates the inversion of the quark routings in α_1. Apparently the flip identity eq. (2.82) cannot span the whole null space due to the special nature of the involved diagrams. However, it is possible to perform a flip of a quark line similar to the one in eq. (2.75) in the cases where the loop is between the quark lines l_1 and l_2. In order to simplify the notation we exploit the reflection symmetry to fix the flipped quark line to the form $l_2 = \{q_2^R, \alpha_2, \bar{q}_2^R\}$ whereas the fixed quark line l_1 can be either of the form $l_1 = \{q_1^R, \alpha_1, \bar{q}_1^R\}$ or $l_1 = \{\bar{q}_1^L, \alpha_1, q_1^L\}$. If $\beta = \{\beta_1, \dots, \beta_s\}$ and $\gamma = \{\gamma_1, \dots, \gamma_t\}$ denote sequences of external legs than

$$\begin{aligned} A_f(l_1, \beta, l_2, \gamma) = (-1)^{|\alpha_2|+1} & \sum_{\sigma \in \mathrm{FOP}\{\beta\}\{\mathrm{rev}(\overline{l_2})\}\{\gamma\}} A_f(l_1, \sigma) \\ & + \sum_{i=0}^{|\beta|} \sum_{j=0}^{|\gamma|} (-1)^{j+1} \sum_{\sigma \in \mathrm{OP}\{\alpha_1\}\{\mathrm{rev}(\overline{\gamma_{1,j}})\}\{\gamma_{j+1,t}, l_1, \beta_{1,i}\}} A_f(\sigma, \bar{q}_2^R, \beta_{i+1,s}, q_2^R) \\ & + \sum_{i=0}^{|\beta|} \sum_{j=0}^{|\gamma|} (-1)^{|\beta|-i+1} \sum_{\sigma \in \mathrm{OP}\{\alpha_1\}\{\mathrm{rev}(\overline{\beta_{i+1,s}})\}\{\gamma_{j+1,t}, l_1, \beta_{1,i}\}} A_f(\sigma, \bar{q}_2^R, \gamma_{1,j}, q_2^R)\,, \end{aligned} \tag{2.83}$$

where $\beta_{i,j} = \{\beta_i, \dots, \beta_j\}$ denotes the sub sequence of β starting with β_i and ending in

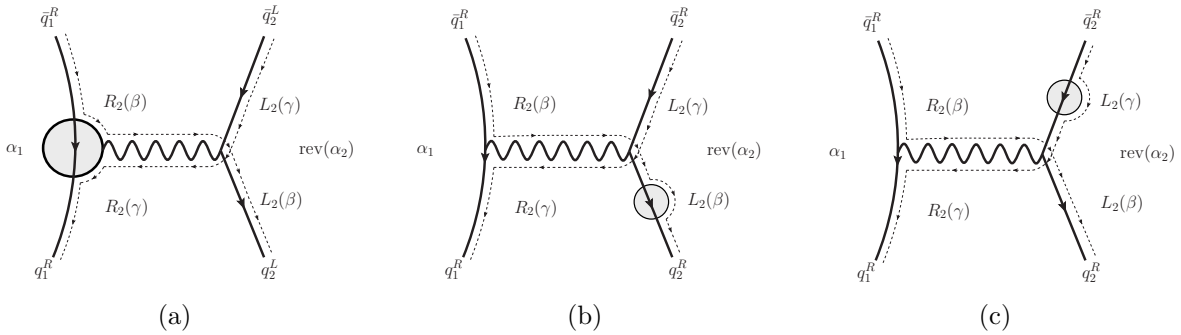

Figure 2.8.: Schematic representations of flipped versions of the diagrams contributing to $A_f(q_1^R, \alpha_1, \bar{q}_1^R, \beta, q_2^R, \alpha_2, \bar{q}_2^R, \gamma)$. All external legs except q_1, q_2, $\bar{q}_1$, $\bar{q}_2$ are omitted. The circle indicates the position of the loop. The dotted lines indicate to which part of the diagram the legs β and γ can be attached. $R_2(\beta)$, $R_2(\gamma)$ and $L_2(\beta)$, $L_2(\gamma)$ denote the legs of β, γ to the right or to the left of the flipped quark line $\{\bar{q}_2, q_2\}$.

β_j. The reasoning behind eq. (2.83) is similar to the one that led to the fermion flip identity eq. (2.75). Depending on the position of the fermion loop, the color ordered diagrams contributing to $A_f(l_1, \beta, l_2, \gamma)$ can be divided into three categories, as depicted in fig. 2.8 for the case $l_1 = \{q_1^R, \alpha_1, \bar{q}_1^R\}$. By summing over the flip permutations $\mathrm{FOP}\{\beta\}\{\mathrm{rev}(l_2)\}\{\gamma\}$, we sum over all flipped diagrams where the fermion loop is to the left of the flipped quark line $\{\bar{q}_2, q_2\}$, which corresponds to fig. 2.8 (a). The relative sign between flipped and non-flipped diagrams is $(-1)^{|\alpha_2|+1}$. All flipped diagrams where the fermion loop is to the right of the flipped quark line $\{\bar{q}_2, q_2\}$ can be further divided into diagrams where either legs of β or legs of γ are connected to the fermion loop, depicted in fig. 2.8 (b) and fig. 2.8 (c). In order to express these diagrams by a linear combination of primitive amplitudes, we need to flip the legs that are not allowed to be connected to the fermion loop, i. e. $\mathrm{rev}(\alpha_2)$ as well as either $L_2(\beta)$ or $L_2(\gamma)$, to the non loop-side of the flipped quark line. This is straight forward to accomplish by summing over ordered permutations $\sigma \in \mathrm{OP}\{\alpha_1\}\{\mathrm{rev}(L_2(\beta))\}\{R_2(\gamma), l_1, R_2(\beta)\}$ or $\sigma \in \mathrm{OP}\{\alpha_1\}\{\mathrm{rev}(L_2(\gamma))\}\{R_2(\gamma), l_1, R_2(\beta)\}$ of the legs on the non-loop side of the flipped quark line $\{\bar{q}_2, q_2\}$. The relative sign between flipped and non-flipped diagrams is $(-1)^{|L_2(\beta)|+1}$ or $(-1)^{|L_2(\gamma)|+1}$.

We emphasize that in the special case of either β or γ containing a quark line $l_3 = \{q_3^L, \alpha_3, \bar{q}_3^L\}$ or $l_3 = \{\bar{q}_3^R, \alpha_3, q_3^R\}$ that separates l_1 and l_2 from the loop, eq. (2.83) holds for the mixed loop part of the primitives as well.

Beside the identities eqs. (2.75) and (2.83) that are solely based on the symmetries of the color ordered Feynman rules fig. 2.1, there are additional identities relying on the Furry identity as well. On the level of Feynman diagrams the Furry identity is the simple observation that a fermion loop with n off-shell gluons connecting to it and a fermion loop with the same n off-shell gluons connecting to it in reversed cyclic ordering are equal up to a relative sign of $(-1)^n$. These properties of the fermion loop allow to reverse the ordering of the legs in every color ordered sub-diagram by properly adjusting the overall sign of the diagram. Before showing how this translates into identities of the primitive amplitudes we present a more straight forward application of the furry identity. Let α_i be either a single gluon or a fermion line of the form

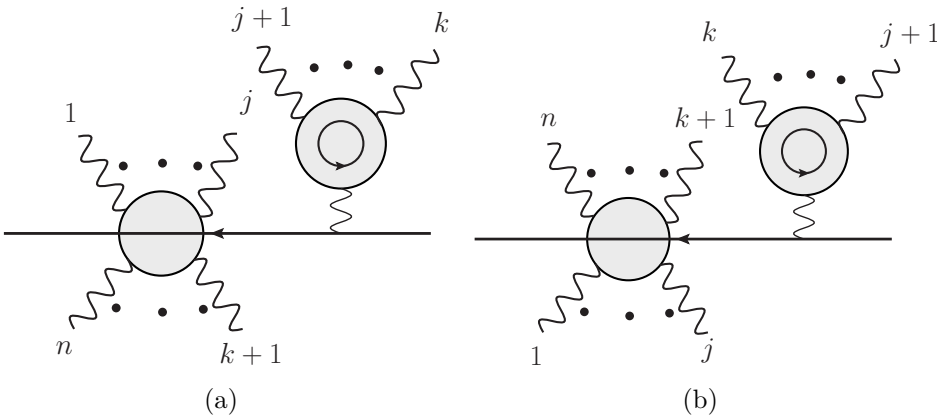

Figure 2.9.: Pictorial representation of the diagrams contributing to the first (a) and second term (b) in eq. (2.85) for $\beta = \{1, \ldots, n\}$ containing only gluons. The external legs α_1 are omitted as they are not relevant for the pairwise cancellation between (a) and (b), which are equal up to a sign of $(-1)^{n+1}$.

$\{q_j^R, \ldots, \bar{q}_j^R\}$ or $\{\bar{q}_j^L, \ldots, q_j^L\}$, than the following identity holds

$$\sum_{\sigma \in \mathrm{COP}\{\alpha_1\}\ldots\{\alpha_{2k+1}\}} A_f(\sigma) = 0\,. \tag{2.84}$$

The cyclically ordered permutations of the α_i ensure that only diagrams with each of the α_i coupling directly to the fermion loop survive in the sum. Since the number of α's is odd all these diagrams cancel pairwise.

Out of all the identities derived so far, only eq. (2.82) and eq. (2.84) apply to the fermion loop part of primitive amplitudes with only one quark line. However, both identities do not span the whole null space of the two quark primitive amplitudes implying that there are additional identities between them. The missing piece is the general reversion identity. Let β, and α_1 be some arbitrary sequences of external legs than

$$\sum_{\sigma \in \mathrm{OP}\{\beta\}\{\bar{q}_1^L, \alpha_1\}} A_f(q_1^L, \sigma) + (-1)^{|\beta|} \sum_{\sigma \in \mathrm{OP}\{\mathrm{rev}(\beta)\}\{\bar{q}_1^L, \alpha_1\}} A_f(q_1^L, \sigma) = 0\,. \tag{2.85}$$

In fig. 2.9 we present a pictorial representation of the diagrams contributing to the first and second term in eq. (2.85) in the case of $\beta = \{1, \ldots, n\}$ containing only gluons. The shaded circles represent some color ordered subdiagrams. Obviously, there is a one to one correspondence between the diagrams (a) and (b). Reversing the order of the legs $j+1, \ldots, k$ in the diagrams of fig. 2.9 (a), by exploiting the symmetries of the color ordered vertices and the Furry identity, leads to a relative sign of $(-1)^{k-j+1}$. Additionally flipping the legs $1, \ldots, j$ and $k+1, \ldots, n$ to the other side of the quark line, as well as reversing the legs on each flipped subtree, we end up in the diagrams (b) with a relative sign of $(-1)^{k-j+1}(-1)^{j+n-k} = (-1)^{n+1}$. The inclusion of quarks in β does not alter the logic presented above. In case of β containing a quark line $l_2 = \{q_2^L, \alpha_2, \bar{q}_2^L\}$ or $l_2 = \{\bar{q}_2^R, \alpha_2, q_2^R\}$ separating $l_1 = \{\bar{q}_1^L, \alpha_1, q_1^L\}$ from the loop, eq. (2.85) is true even for the mixed loop part of the primitive amplitudes. Indeed, eq. (2.85) spans the null space of the mixed loop as well as the fermion loop part of the primitive amplitudes and all

the identities eqs. (2.75), (2.79), (2.82) and (2.83) can be written as linear combinations of reversion identities. In fact, we checked that the null space of the mixed loop part of the primitive amplitudes is spanned by either the fermion flip identity eq. (2.75), the identity eq. (2.79) or the reversion identity eq. (2.85), whereas the null space of the mixed loop part of the primitive amplitudes is spanned by the reversion identity eq. (2.85). Hence, the general reversion identity eq. (2.85) provides full analytical control over expressions containing primitive amplitudes.

2.4. Checks, Remarks and Prospects

Since the primitive amplitudes are not all linear independent, the color decomposition of a QCD amplitude is not unique. However, given the reversion identities eq. (2.85) it is very easy to analytically check the equivalence of two different decompositions of a particular amplitude. Indeed, we analytically checked that our formulas for the partial amplitudes eq. (2.53) agree with all the QCD partial amplitudes presented in the ancillary files of reference [25]. If the diagram based algorithm for the determination of the partial amplitudes incorporates the Furry identities among the color ordered diagrams, as described in [26], the obtained representations of the amplitudes contain only linear independent primitive amplitudes. This is not the case for the representation of the QCD amplitudes obtained from eq. (2.53). However, given a particular QCD one-loop amplitude, it is straightforward to reduce the number of primitive amplitudes in eq. (2.53) to the number of linear independent primitive amplitudes by applying the reversion identities eq. (2.85). Consequently, both approaches can provide the same answer. Exploiting the identities we were able to determine the number $N(k,n)$ of independent mixed loop parts of primitive amplitudes with up to $k=4$ quark lines, as well as the ratio $\kappa(k) = \frac{N(k,n)}{\mathcal{N}(k,n)}$ of the number of independent and the overall number $\mathcal{N}(k,n)$ of mixed loop parts of primitive amplitudes.

$$\begin{aligned} N(1,n) &= (n+1)! & \kappa(1) &= 1 \\ N(2,n) &= \frac{2}{3}(n+3)! & \kappa(2) &= \frac{2}{3} \\ N(3,n) &= \frac{4}{15}(n+5)! & \kappa(3) &= \frac{2}{5} \\ N(4,n) &= \frac{8}{105}(n+7)! & \kappa(4) &= \frac{8}{35} \end{aligned} \tag{2.86}$$

In general the number of independent primitive amplitudes with a mixed loop seems to be

$$N(k,n) = \frac{2^{k-1}}{(2k-1)!!}(n+2k-1)!\,, \tag{2.87}$$

Given the reversion identity eq. (2.85) it is straightforward to determine the number $N_f(k,n)$ of independent fermion loop parts of primitive amplitudes with a particular number of quarks and gluons, like e. g. $N_f(1,n) = \frac{1}{2}(n-1)n!$. In contrast to the mixed loop part, it is however possible to find minimal representations of the $(q\bar{q})^k(g)^n$ QCD amplitude containing less than $N_f(k,n)$ fermion loop primitive amplitudes. Despite the fact that finding such minimal representations is not straightforward, this diminishes the relevance of the numbers $N_f(k,n)$. For up to seven external legs the number $\bar{N}_f(k,n)$ of fermion loop primitive amplitudes in such a minimal representation are

n	$N_f(1,n)$	$\bar{N}_f(1,n)$
2	1	1
3	6	6
4	36	33
5	240	230

n	$N_f(2,n)$	$\bar{N}_f(2,n)$
0	1	1
1	3	3
2	15	13
3	96	75

n	$N_f(3,n)$	$\bar{N}_f(3,n)$
0	7	4
1	36	20

and agree with the numbers presented in [26]. Considering the rapid growth of the number of primitive amplitudes constituting the amplitudes it is tempting to apply a leading color approximation keeping only the terms in eq. (2.53), which are proportional to either N or n_f, which reduces the number of primitives to $2 \cdot (n+k-1)!$. While a leading color approximation for $N = 3$ at a strong coupling of $\alpha_s \approx 0.1$ seems very questionable in theory, keeping in mind that $N = 3$ is not a large number and $N^2\alpha_s = \mathcal{O}(1)$ is of order one, it seems to work quite well in practice [25].

3

All Tree Level Amplitudes in QCD

Based on the color decomposition of QCD tree amplitudes eq. (2.37) and the fermion flip identities eq. (2.75) we prove that every color ordered tree amplitude of massless QCD can be written as a linear combination of gluon-gluino amplitudes of $\mathcal{N} = 4$ super Yang-Mills theory. The proof includes a general construction of these linear combinations. For all color ordered QCD amplitudes with up to four quark-anti-quark pairs and an arbitrary number of gluons, we determine representations containing a minimal number of gluon-gluino amplitudes. Furthermore, we derive analytical formulae for all gluon-gluino amplitudes relevant for QCD by projecting the previously-found expressions for the super-amplitudes of $\mathcal{N} = 4$ SYM [46] onto the relevant components. Explicit expressions are displayed for the NMHV and NNMHV gluon gluino amplitudes. All obtained analytical formulae are implemented in the public `Mathematica` package `GGT`, and in turn yield all QCD tree amplitudes as well as the cut constructable part of all QCD loop amplitudes.

3.1. Introduction

The main purpose of this chapter is to illustrate how the more recent formal developments in understanding scattering amplitudes in gauge theories can reap benefits for phenomenological applications in QCD. In particular, we will evaluate the solution to the supersymmetric BCFW recursion in ref. [46] by carrying out the integrations over Grassmann parameters that are needed to select particular external states. In addition, we will show how to extract tree-level QCD amplitudes from the amplitudes of $\mathcal{N} = 4$ SYM theory. While this extraction is simple for pure-gluon amplitudes, and those with a single massless quark line, it becomes a bit more intricate for amplitudes with multiple quark lines of different flavors, because of the need to forbid the exchange of internal scalar particles, which are present in $\mathcal{N} = 4$ SYM theory but not in QCD.

Although, as mentioned in section 1.1, there are currently many numerical programs available for computing tree amplitudes efficiently, the existence of analytic expressions may provide a yet more efficient approach in some contexts. In fact, the formulae provided in this chapter have already served a practical purpose: They were used to evaluate contributions from real emission in the NLO corrections to the cross section for producing a W boson in association with four jets at the LHC [98]. This process forms an important background to searches for various kinds of new physics, including supersymmetry. The real-emission corrections require evaluating nine-point tree amplitudes at a large number of different phase space points (on the order of 10^8), in order to get good statistical accuracy for the Monte Carlo integration over phase space.

In principle, QCD tree amplitudes can also be used to speed up the evaluation of one-loop amplitudes, when the latter are constructed from tree amplitudes using a numerical implementation of generalized unitarity. Many different generalized unitarity cuts, and hence many different tree amplitudes, are involved in the construction of a single one-loop amplitude. The tree amplitudes described here enter directly into the construction of the cut-constructable part [29] of one-loop amplitudes in current programs such as CutTools [99–101], Rocket [102–104] and BlackHat [105]. On the other hand, the computation-time bottleneck in these programs often comes from the so-called "rational" terms. When these terms are computed using only unitarity, it is via unitarity in D dimensions [103, 104, 106–110], not four dimensions. The amplitudes presented here are four-dimensional ones, so they cannot be used directly to alleviate this bottleneck for the D-dimensional unitarity method. However, in the numerical implementation of loop-level on-shell recursion relations [111, 112] for the rational part in BlackHat [105], or in the OPP method used in CutTools [99–101], there are no D-dimensional trees, so this is not an issue.

The remainder of this chapter is organized as follows. After some preliminary definitions and examples, we explain the strategies of how to extract QCD tree amplitudes with massless quarks from $\mathcal{N} = 4$ SYM in section 3.3. We also discuss how to convert these amplitudes into trees with one electroweak vector boson. Sections 3.4 to 3.6 are devoted to stating the general analytical formulae for gluon-gluino n-parton amplitudes in $\mathcal{N} = 4$ SYM, which are proven in section 3.7. In appendix E.1 we provide a collection of explicit results for pure-gluon trees. Explicit formulae for trees involving up to six fermions are displayed in appendix E.2. Finally, appendix E.3 is devoted to a documentation of the freely available `Mathematica` package `GGT`[1] which implements all of the results of this chapter and yields the analytical expressions for all gluon gluino

[1]The package may be downloaded from `http://qft.physik.hu-berlin.de`.

tree amplitudes of $\mathcal{N}=4$ SYM which are relevant for QCD.

3.2. Preliminaries

Color-ordered amplitudes of massless particles can be compactly expressed in the spinor-helicity formalism introduced in section 1.2.1. Instead of the parton momenta p_i the general tree-level scattering formula will depend on the differences $x_{ij} = x_i - x_j$ of the dual or region momenta $x_i^{\alpha\dot{\alpha}}$ via

$$x_{ij}^{\alpha\dot{\alpha}} \;:=\; (\not{p}_i + \not{p}_{i+1} + \cdots + \not{p}_{j-1})^{\alpha\dot{\alpha}} = \sum_{k=i}^{j-1} \lambda_k^{\alpha}\tilde{\lambda}_k^{\dot{\alpha}}\,, \qquad\qquad i<j\,, \tag{3.1}$$

$x_{ii} = 0$, and $x_{ij} = -x_{ji}$ for $i > j$, compare eq. (1.75). We then define the scalar quantities

$$\langle a_1 a_2 \ldots a_{2k+1}|a\rangle := \langle a_1|x_{a_1a_2}x_{a_2a_3}\ldots x_{a_{2k}a_{2k+1}}|a\rangle\,, \tag{3.2}$$

which we will use frequently in the following. In fact, all QCD amplitudes will be expressed in terms of the quantities $\langle a_1 a_2 \ldots a_{2k+1}|a\rangle$, x_{ij}^2 and the spinor products $\langle i\ j\rangle$.

As an example of the notation and in order to give a flavor of the kinds of results we obtain, we present a compact formula for the n-point NMHV pure gluon amplitude in QCD

$$\begin{aligned} A_n^{\text{NMHV}}(i_1^-, i_2^-, n^-) &= \frac{\delta^{(4)}(p)}{\langle 1\ 2\rangle\ldots\langle n\ 1\rangle}\times \\ &\Bigg[\sum_{i_1<s\le i_2<t\le n-1}\tilde{R}_{n;st}\Big(\langle n\ i_1\rangle\langle nts|i_2\ \rangle\Big)^4 + \sum_{i_1<s<t\le i_2}\tilde{R}_{n;st}\Big(\langle i_2\ n\rangle\langle n\ i_1\rangle x_{st}^2\Big)^4 \\ &+ \sum_{2\le s\le i_1<i_2<t\le n-1}\tilde{R}_{n;st}\Big(\langle i_2\ i_1\rangle\langle nts|n\ \rangle\Big)^4 + \sum_{2\le s\le i_1<t\le i_2}\tilde{R}_{n;st}\Big(\langle n\ i_2\rangle\langle nst|i_1\ \rangle\Big)^4\Bigg]\,. \end{aligned} \tag{3.3}$$

Here i_1, i_2 and n correspond to the positions of the three negative-helicity gluons. Using cyclic symmetry, we have put one of them at position n without loss of generality. The quantities $\tilde{R}_{n;st}$ are simply given by

$$\tilde{R}_{n;st} := \frac{1}{x_{st}^2}\,\frac{\langle s\ s-1\rangle}{\langle nts|s\rangle\,\langle nts|s-1\rangle}\,\frac{\langle t\ t-1\rangle}{\langle nst|t\rangle\,\langle nst|t-1\rangle}\,. \tag{3.4}$$

with $\tilde{R}_{n;st} := 0$ for $t = s+1$ or $s = t+1$. Note that the above formula is given for an arbitrary number of gluons n. In realistic cases this number is usually small, say of the order of 9, in which case relatively few terms are produced by the nested sums in eq. (3.3).

3.3. From $\mathcal{N}=4$ SYM to QCD Tree Amplitudes

In this section we discuss how to assign quantum numbers for external states in $\mathcal{N}=4$ SYM in order to generate tree amplitudes for QCD with massless quarks. We then

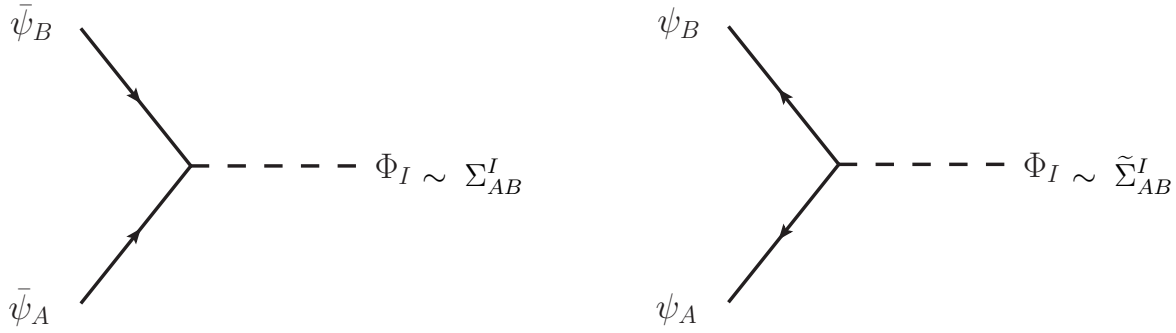

Figure 3.1.: The gluino-scalar vertices in $\mathcal{N} = 4$ SYM are proportional to the antisymmetric six-dimensional euclidean Pauli-matrices.

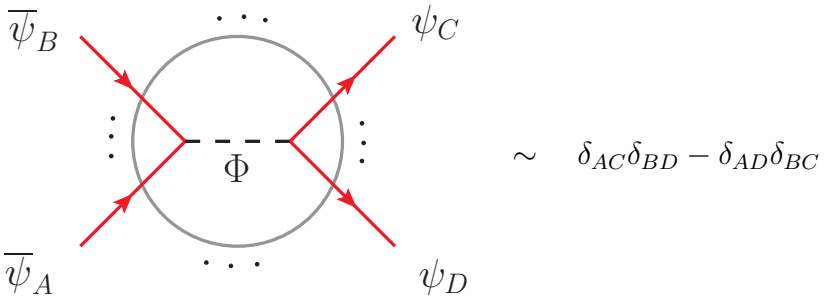

Figure 3.2.: Schematic representation of the simplest contributions from internal scalars in color ordered SYM amplitudes.

discuss the generation of tree amplitudes including an electroweak vector boson (W, Z or virtual photon).

3.3.1. The General Case

From the point of view of tree amplitudes, there are two principal differences between $\mathcal{N} = 4$ SYM and massless QCD. First of all, the fermions in $\mathcal{N} = 4$ SYM, the gluinos, are in the adjoint representation of $su(N_c)$, rather than the fundamental representation, and come in four flavors. Secondly, the $\mathcal{N} = 4$ SYM theory contains six massless scalars in the adjoint representation. As discussed in 2, decomposing gauge theory amplitudes into color structures and color ordered amplitudes, the first difference is fairly unimportant. At the level of color ordered amplitudes there is no difference between gluinos and quarks apart from the differing number of flavors. However, a generic color ordered gluon-gluino SYM amplitude contains contributions from internal scalars, as depicted in 3.3.1. Whilst making the transition to QCD, these internal scalars have to be either avoided or subtracted. In any gauge theory, tree amplitudes that contain only external gluons are independent of the matter states in the theory [35, 36]; hence they are identical between $\mathcal{N} = 4$ SYM and QCD. The reason is simply that the vertices that couple gluons to the other states in the theory always produce the fermions and scalars in pairs. There are no vertices that can destroy all the fermions and scalars, once they have been produced. If a fermion or scalar were produced at

any point in a tree diagram, it would have to emerge from the diagram, which would no longer have only external gluons. In other words, the pure-gluon theory forms a closed subsector of $\mathcal{N} = 4$ SYM.

Another closed subsector of $\mathcal{N} = 4$ SYM is $\mathcal{N} = 1$ SYM, which contains a gluon and a single gluino. Let g denote the gluon, ψ_A, $A = 1, 2, 3, 4$, denote the four gluinos, and Φ_I denote the six real scalars of $\mathcal{N} = 4$ SYM. Then the $\mathcal{N} = 1$ SYM subsector is formed by (g, ψ_1). The reason it is closed is similar to the pure-gluon case just discussed: There are vertices that produce states other than (g, ψ_1), but they always do so in pairs. For example, the Yukawa coupling $\Phi_I \Sigma^{I\,AB} \psi_A \psi_B$, $A \neq B$, can convert ψ_1 into a scalar and a gluino each carrying an index $B \neq 1$. However, this index cannot be destroyed by further interactions. The fact that $\mathcal{N} = 1$ SYM forms a closed subsector of $\mathcal{N} = 4$ SYM, in addition to color ordering, immediately implies that any color-ordered QCD tree amplitude for gluons, plus arbitrarily many quarks of a single flavor, is given directly by the corresponding amplitude (with ψ_1 replacing the single quark flavor) evaluated in $\mathcal{N} = 4$ SYM.

The less trivial QCD amplitudes to extract are those for multiple fermion flavors, primarily because of the potential for intermediate scalar exchange induced by the Yukawa coupling. Looking at the master formula for the color decomposition of QCD at tree level eq. (2.37), it contains only color ordered amplitudes where the quark helicities are alternating. The subset of color ordered SYM amplitudes with alternating gluino helicities is special as these amplitudes do not contain internal scalars. The reason being that any two gluinos of equal helicity and unequal flavor that could potentially be connected to a gluino-scalar vertex, divide the remaining gluinos into two odd sets. However there is no way to connect an odd number of gluinos by a diagram. This immediately proves that all QCD amplitudes with up to four quark lines can be directly obtained from SYM amplitudes by substituting quarks by gluinos in the color ordered amplitudes in eq. (2.37). Increasing the number of quark lines beyond four we run into the problem that in contrast to the number of quark flavors, the number of gluino flavors is not a free parameter. In general, a color ordered amplitude with several quarks of equal flavor is given by a sum over all fermion line configurations compatible with the color ordering and the choice of flavors. Each of these fermion line configurations is equal to a color ordered amplitudes with distinct flavors. These relations can be inverted, making it is possible to express an arbitrary fermion line configuration by a linear combination of color ordered amplitudes containing only four different quark flavors. Indeed, as we checked for up to 10 quark lines, even two different flavors would be sufficient. For a given amplitude with more than four quark lines it is straightforward to transform eq. (2.37) into a representation using only four flavors. Consequently, all QCD tree amplitudes can be obtained from color ordered SYM amplitudes.

When calculating the cut constructable part of QCD loop amplitudes using a maximal number of cuts, color ordered tree amplitudes with non-alternating quark helicities are necessary as well. However, the corresponding gluon gluino amplitudes are not free of internal scalars. Since every color ordered QCD amplitude can be written as a linear combination of color ordered QCD amplitudes with alternating quark helicities, it is possible to obtain all color ordered QCD amplitudes from color ordered SYM amplitudes. In order to prove this statement we will explain how such a linear combination can be obtained by repeated application of the fermion flip identity eq. (2.75). Exploiting the cyclic symmetry, an arbitrary color ordered amplitude has the form

$A(\bar{q}_1, \alpha_1, q_1, \alpha_2)$, where α_1 and α_2 denote the external legs to the left and to the right of the quark line $\{\bar{q}_1, q_1\}$. Repeatedly flipping quark lines with respect to $\{\bar{q}_1, q_1\}$, the amplitude $A(\bar{q}_1, \alpha_1, q_1, \alpha_2)$ is given by a linear combination of amplitudes of the form

$$A(\bar{q}_1, \beta_{i_1}, q_{i_1}, \gamma_{i_1}, \bar{q}_{i_1}, \beta_{i_2}, \dots, q_1, \beta_{j_1}, \bar{q}_{j_1}, \gamma_{j_1}, q_{j_1}, \beta_{j_2}, \dots) \tag{3.5}$$

where the β's contain only gluons. Successively performing analogous flips with respect to each of the other quark lines $\{\bar{q}_i, q_i\}$, yields a representation in terms of color ordered amplitudes with alternating quark helicities, i. e. a representation in terms of SYM amplitudes. Despite being straightforward to implement the described construction of color ordered QCD tree amplitudes is of limited practical relevance. The obtained representations are far from being minimal as, due to the permutations in the flip identity eq. (2.75), the number of SYM amplitudes constituting the color ordered QCD amplitude depends on the number of gluons in the amplitude. For practical applications it is more convenient to construct minimal representations of color ordered QCD amplitudes by summing over different gluino flavor assignments to a fixed helicity configuration.

3.3.2. Constructing Minimal Representations of QCD Amplitudes

The goal of this section is to explain how representations of the form

$$A^{\mathrm{QCD}} = \sum_i^p \alpha_i \, A_i^{\mathrm{SYM}} \tag{3.6}$$

where the A_i^{SYM} are all p different possibilities to assign gluino flavors to the helicity configuration of A^{QCD}. Since the A_i^{SYM} are not all linear independent there is no unique solution to eq. (3.6). The ultimate goal would be to find a minimal solution to eq. (3.6), i. e. a solution containing a minimal number of SYM amplitudes.

The main ideas behind the choice of the gluino flavors are

1. to suppress or subtract the internal exchange of massless scalars, and
2. allow all fermion lines present to have distinct flavors.

In some cases one may want amplitudes with (partially) identical fermions; these can always be constructed from the distinct-flavor case by summing over the relevant exchange-terms, although it may be more efficient to compute the identical-fermion case directly. We will accomplish this goal for amplitudes containing up to four separate fermion lines, that is, eight external fermion states.

The key to avoiding such unwanted scalar exchange is provided by fig. 3.3, which shows four types of vertices that could potentially couple fermion pairs to scalars and gluons. However, all four types of vertices vanish. We recall that helicities are labeled in an all-outgoing convention. Case (a) vanishes because the Yukawa interaction only couples gluinos of different flavors, $A \neq B$. Cases (b) and (c) vanish because of fermion helicity conservation for the gauge interactions, and a helicity flip for the Yukawa coupling. Case (d) vanishes because gluon interactions do not change flavor.

Because the emission of gluons from fermions does not change their helicity or flavor, the α_i are independent of the gluons in A^{QCD}, hence it is sufficient to consider the pure quark case. For example, fig. 3.4 shows the possible cases for amplitudes with one or

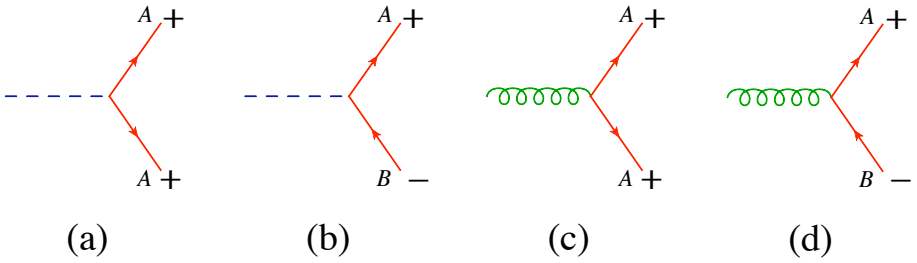

Figure 3.3.: These vertices all vanish, as explained in the text. This fact allows us to avoid scalar exchange and control the flow of fermion flavor.

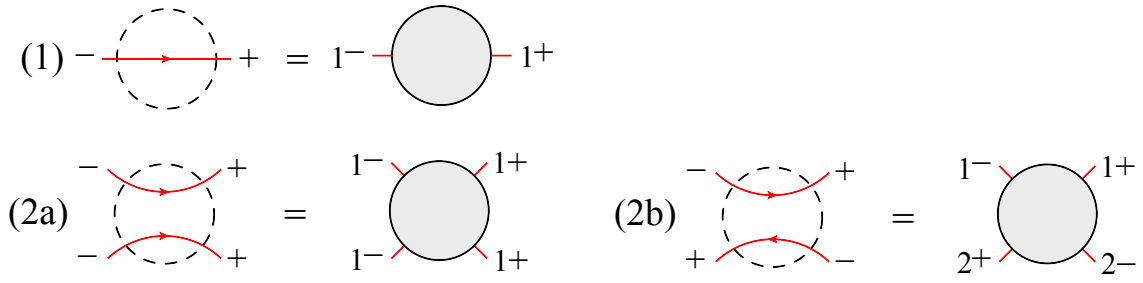

Figure 3.4.: The possible fermion-line configurations for amplitudes with one fermion line, case (1), or two fermion lines, cases (2a) and (2b).

two fermion lines. The left-hand side of the equality shows the desired (color-ordered) fermion-line flow and helicity assignment for a QCD tree amplitude. All gluons have been omitted, and all fermion lines on the left-hand side are assumed to have distinct flavors. The right-hand side of the equality displays a choice of gluino flavor that leads to the desired amplitude. All other one- and two-fermion-line cases are related to the ones shown by parity or cyclic or reflection symmetries.

The Yukawa coupling between the gluinos and the scalars is antisymmetric in the gluino flavors. This opens up two possibilities to project out potential scalar exchange. We can either set gluino flavors equal or symmetrize over pairs of unequal flavor. The one-fermion line, case (1), is trivial because $\mathcal{N} = 1$ SYM forms a closed subsector of $\mathcal{N} = 4$ SYM. In case (2a) we must choose all gluinos to have the same flavor; otherwise the SYM amplitude would contain a scalar exchange in the horizontal direction. Here, helicity conservation prevents the exchange of an unwanted gluon in this direction, keeping the two flavors distinct as desired. In case (2b), we must use two different gluino flavors, as shown; otherwise helicity conservation would allow gluon exchange in the wrong channel, corresponding to identical rather than distinct quarks.

More generally, in order to avoid scalar exchange, if two color-adjacent gluinos have the same helicity, then we should choose them to have the same flavor. In other words, we should forbid all configurations of the form $(\ldots, A^+, B^+, \ldots)$ and $(\ldots, A^-, B^-, \ldots)$ for $A \neq B$, where $A^\pm$ stands for the gluino state $\tilde{g}_A^\pm$. While this is necessary, it is not sufficient. For example, we also need to forbid configurations such as $(\ldots, A^+, C^\pm, C^\mp, B^+, \ldots)$, because the pair $(C^\pm, C^\mp)$ could be produced by a gluon splitting into this pair, which also connects to the (A^+, B^+) fermion line. As a secondary consideration, if two color-adjacent gluinos have opposite helicity, then we

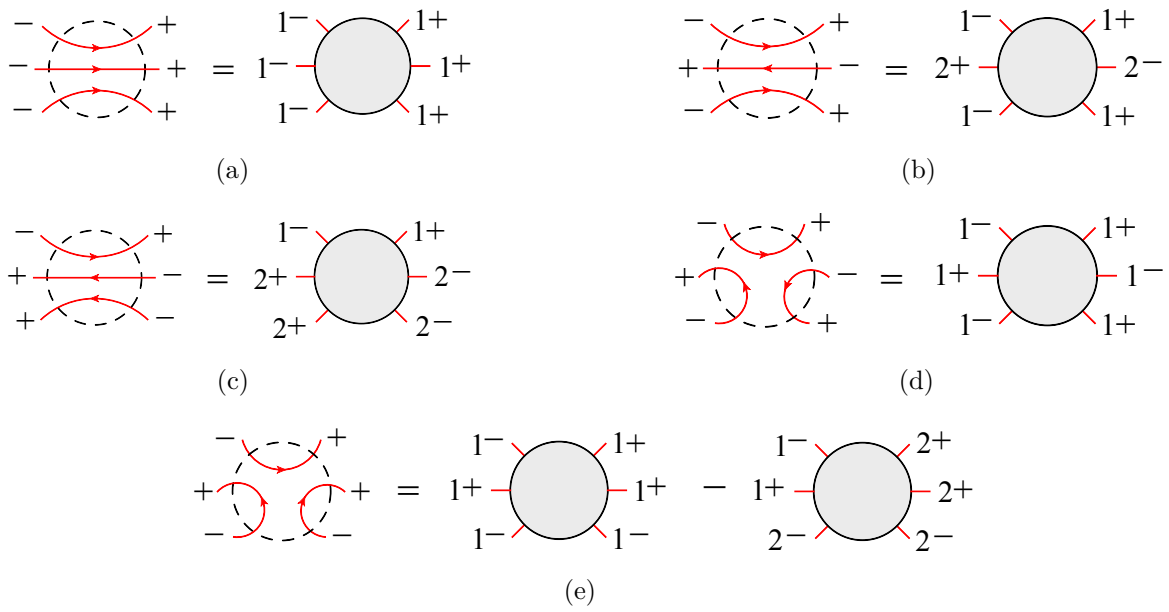

Figure 3.5.: The possible fermion-line configurations for amplitudes with three fermion lines.

should choose them to have the same flavor or different flavor according to the desired quark flavor flow on the left-hand side. However, it will not always be possible to choose them to have a different flavor.

With these properties in mind, we can now examine fig. 3.5, which shows solutions for the three-fermion-line cases. Again, all other three-fermion-line cases are related to the ones shown by parity or cyclic or reflection symmetries. Using the properties of the vanishing vertices in fig. 3.3, it is straightforward to show that only the desired QCD tree amplitudes on the left are produced by the gluino assignments on the right. The most subtle case is 3.5 (e). The two pairs of adjacent identical-helicity quarks force all the gluino flavors to be the same. However, this choice does not result in three distinct fermion lines in the pattern desired. There is a "wrong" fermion-line configuration which, fortunately, coincides with a permutation of case 3.5 (c). Hence we can subtract off this solution, as the second term on the right-hand side of 3.5 (e). Alternatively, case 3.5 (e) can be obtained by a symmetrization over gluino flavors

$$\begin{aligned} A^{QCD}(\bar{q_1}^-, q_1^+, \bar{q_2}^-, q_2^+, q_3^+, \bar{q_3}^-) = A^{\mathrm{SYM}}(2^-, 2^+, 1^-, 1^+, 1^+, 1^-) \\ + A^{\mathrm{SYM}}(1^-, 2^+, 1^-, 1^+, 1^+, 2^-)\,, \end{aligned} \tag{3.7}$$

where $A^{\mathrm{SYM}}(1^-, 2^+, 1^-, 1^+, 1^+, 2^-)$ subtracts the scalar exchange.

We have also examined all different configurations of four distinct fermion lines. Modulo cyclic symmetry, reflection symmetry and parity, there are 16 cases, shown in fig. 3.6, and we determined minimal solutions for each of them. Four of the cases, (g), (k), (l) and (n), require two SYM amplitudes, analogous to case 3.5 (e). Only cases (m), (o) and (p) require three SYM amplitudes. The cases (h), (o), and (m) are special in the sense that completely suppressing the scalar exchange by setting gluino flavors equal does not lead to a minimal representation. Indeed, in the case (h) this does not lead to a representation at all. Suppressing the scalar exchange, case (o) can be written

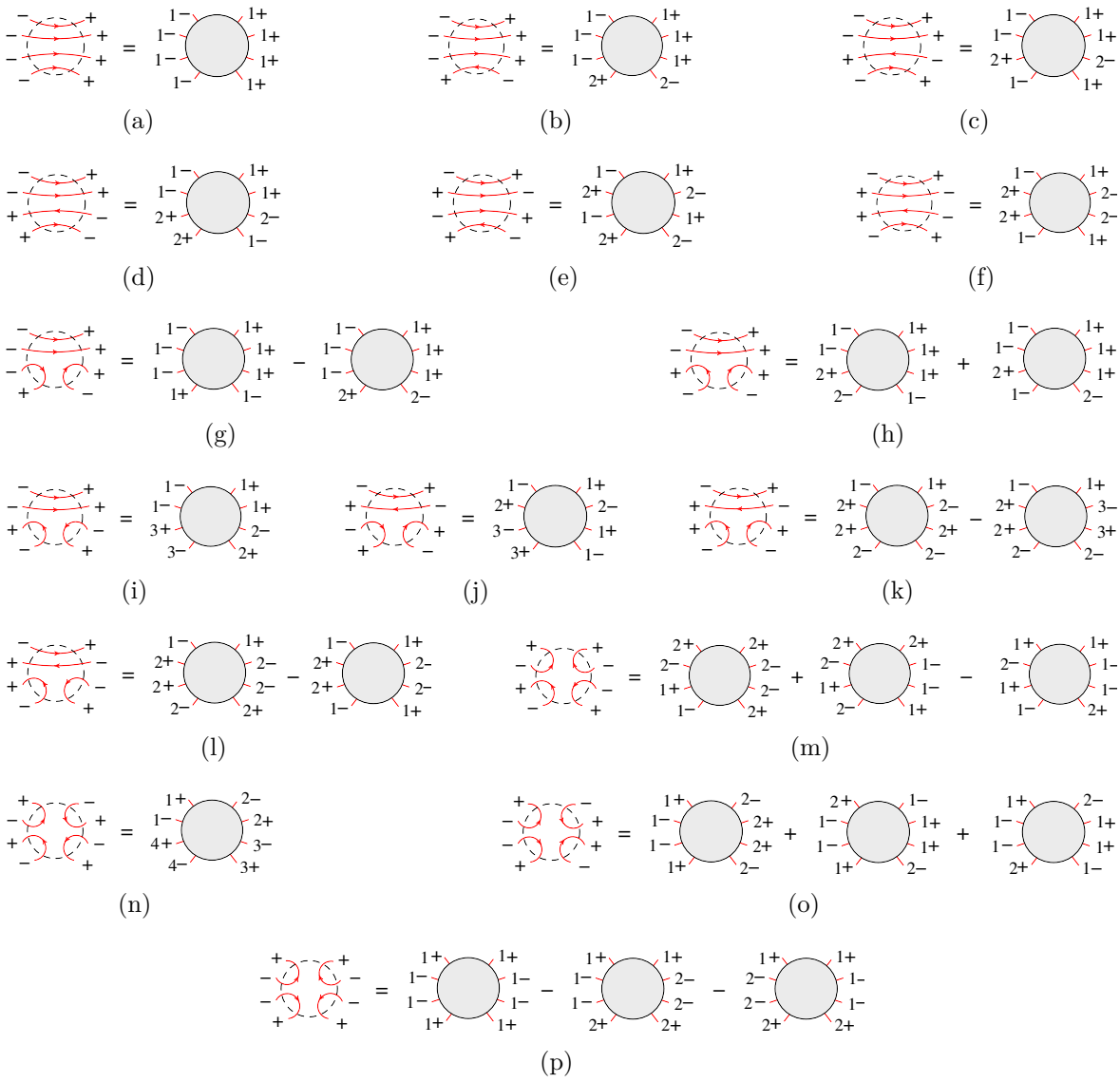

Figure 3.6.: The possible fermion-line configurations for amplitudes with four fermion lines.

as

$$
\begin{aligned}
A^{QCD}(\bar{q}_1^-, q_1^+, \bar{q}_2^-, q_2^+, q_3^+, \bar{q}_3^-, q_4^+, \bar{q}_4^-) &= A^{\mathrm{SYM}}(1^-, 1^+, 1^-, 1^+, 1^+, 1^-, 1^+, 1^-) \\
&\quad - [A^{\mathrm{SYM}}(2^-, 1^+, 1^-, 2^+, 2^+, 2^-, 2^+, 2^-) - A^{\mathrm{SYM}}(2^-, 1^+, 1^-, 2^+, 2^+, 1^-, 1^+, 2^-)] \\
&\quad - [A^{\mathrm{SYM}}(2^-, 2^+, 2^-, 2^+, 2^+, 1^-, 1^+, 2^-) - A^{\mathrm{SYM}}(2^-, 1^+, 1^-, 2^+, 2^+, 1^-, 1^+, 2^-)] \\
&\quad - A^{\mathrm{SYM}}(2^-, 1^+, 1^-, 2^+, 2^+, 1^-, 1^+, 2^-) \qquad (3.8) \\
&= A^{\mathrm{SYM}}(1^-, 1^+, 1^-, 1^+, 1^+, 1^-, 1^+, 1^-) - A^{\mathrm{SYM}}(2^-, 1^+, 1^-, 2^+, 2^+, 2^-, 2^+, 2^-) \\
&\quad - A^{\mathrm{SYM}}(2^-, 2^+, 2^-, 2^+, 2^+, 1^-, 1^+, 2^-) + A^{\mathrm{SYM}}(2^-, 1^+, 1^-, 2^+, 2^+, 1^-, 1^+, 2^-). \qquad (3.9)
\end{aligned}
$$

The first form of this equation indicates that three different wrong-fermion-line configurations have to be removed. However, all removals can be accomplished with the

help of different permutations of two other cases, (4f) and (4l) respectively,

$$A^{\mathrm{QCD}}(\bar{q}_1^-, q_1^+, \bar{q}_2^-, \bar{q}_3^-, q_4^+, \bar{q}_4^-, q_3^+, q_2^+) = A^{\mathrm{SYM}}(1^-, 1^+, 2^-, 2^-, 1^+, 1^-, 2^+, 2^+)\,, \tag{3.10}$$

$$\begin{aligned} &A^{\mathrm{QCD}}(\bar{q}_1^-, q_1^+, \bar{q}_2^-, \bar{q}_3^-, q_3^+, \bar{q}_4^-, q_4^+, q_2^+) \\ &\quad = A^{\mathrm{SYM}}(1^-, 1^+, 2^-, 2^-, 2^+, 2^-, 2^+, 2^+) - A^{\mathrm{SYM}}(1^-, 1^+, 2^-, 2^-, 1^+, 1^-, 2^+, 2^+). \end{aligned} \tag{3.11}$$

Case (4l) itself requires a wrong-fermion-line subtraction. However, the representation eq. (3.9) is not minimal. Subtracting the two possibilities of scalar exchange from $A^{\mathrm{SYM}}(2^-, 1^+, 1^-, 1^-, 1^+, 2^-, 2^+, 2^+)$ requires only three SYM amplitudes.

$$\begin{aligned} &A^{\mathrm{QCD}}(\bar{q}_1^-, q_1^+, \bar{q}_2^-, q_2^+, q_3^+, \bar{q}_3^-, q_4^+, \bar{q}_4^-) = A^{\mathrm{SYM}}(2^-, 1^+, 1^-, 1^-, 1^+, 2^-, 2^+, 2^+) \\ &+ A^{\mathrm{SYM}}(2^-, 1^+, 1^-, 1^-, 2^+, 1^-, 1^+, 1^+) + A^{\mathrm{SYM}}(1^-, 2^+, 1^-, 1^-, 1^+, 2^-, 1^+, 1^+). \end{aligned} \tag{3.12}$$

Instead of five SYM amplitudes without any scalar exchange, case (m) can be obtained by removing one scalar exchange and one wrong fermion line configuration from $A^{\mathrm{SYM}}(1^-, 1^+, 2^-, 2^+, 2^+, 2^-, 2^-, 2^+)$.

$$\begin{aligned} &A^{\mathrm{QCD}}(\bar{q}_1^-, q_1^+, \bar{q}_2^-, q_2^+, q_3^+, \bar{q}_3^-, \bar{q}_4^-, q_4^+) = A^{\mathrm{SYM}}(1^-, 1^+, 2^-, 2^+, 2^+, 2^-, 2^-, 2^+) \\ &+ A^{\mathrm{SYM}}(2^-, 1^+, 2^-, 2^+, 2^+, 1^-, 1^-, 1^+) - A^{\mathrm{SYM}}(1^-, 1^+, 2^-, 1^+, 1^+, 1^-, 1^-, 2^+). \end{aligned} \tag{3.13}$$

Going beyond four fermion lines we are faced with a rapidly increasing number of fermion line configurations. As an automatized implementation of the described flavor construction would be quite involved it is convenient to look for a more straightforward way to construct solutions to eq. (3.6). The idea is to evaluate eq. (3.6) on different infinite precision phase space points. Solving the obtained linear equations will yield an exact solution to eq. (3.6). To be more precisely the algorithm looks as follows:

1. Construct a representation of the desired color ordered QCD amplitude in terms of color ordered QCD amplitudes with alternating helicities (as described in section 3.3.1),
2. map the amplitudes to C^p by evaluating them on p random rational phase space points (generated using momentum twistors): $A^{QCD} \to a$ and $A_i^{SYM} \to v_i$,
3. solve the linear equation $a = \sum_i \alpha_i v_i$.

It should be noted that the solutions obtained in this way are not minimal, albeit containing only linear independent SYM amplitudes. The only way to guarantee that a particular solution is minimal, is to explicitly check that there exists no solution containing less SYM amplitudes. Furthermore, in general the minimal solutions are not unique, e. g. besides eq. (3.13) there are two additional ways to express the four fermion line case (m) by three SYM amplitudes.

3.3.3. Amplitudes with a Single Electroweak Vector Boson

Finally, we remark on the conversion of pure-QCD tree amplitudes, that is amplitudes for quarks and gluons, into amplitudes that contain in addition a single electroweak vector boson, namely a W, Z or virtual photon. It is sufficient to compute the amplitude including the decay of the boson to a fermion-anti-fermion pair.

Consider first the case of a virtual photon which is emitted from a quark q and decays to a charged lepton (Drell-Yan) pair $\ell^+\ell^-$. We can extract this amplitude from a color-ordered amplitude with four consecutive fermions, as follows:

$$A^{\gamma^*}(\ldots, q^+, \ell^-, \ell^+, \bar{q}^-, \ldots) = A^{\rm QCD}(\ldots, q_1^+, \bar{q}_2^-, q_2^+, \bar{q}_1^-, \ldots)\,. \tag{3.14}$$

The color-ordering prevents gluons from being emitted from the quark line q_2, or from the virtual gluon connecting q_1 and q_2. Hence this virtual gluon is functionally identical to a virtual photon. The only other modification comes when dressing A^{γ^*} with couplings. There is a relative factor of $2(-Q^q)e^2/g^2$ when doing so, where the "2" is related to the standard normalizations of the QED interaction with coupling e, versus the QCD interaction with coupling g, and Q^q is the electric charge of the quark q. (The lepton has charge -1.)

It is possible to extract the amplitude (3.14) a second way, using one quark flavor instead of two,

$$A^{\gamma^*}(\ldots, q^+, \ell^-, \ell^+, \bar{q}^-, \ldots) = -A^{\rm QCD}(\ldots, q_1^+, q_1^+, \bar{q}_1^-, \bar{q}_1^-, \ldots)\,. \tag{3.15}$$

This alternative works because the color-ordered interaction for $g^* \to q^+\bar{q}^-$ is anti-symmetric under exchange of q and $\bar{q}$, and because the exchange of a gluon between identical-flavor quarks in the wrong channel is prevented by helicity conservation.

If the virtual photon decays to other charged massless fermions, *i.e.* to a quark-anti-quark pair $q'\bar{q}'$, the only difference is of course to use the appropriate quark charge, $-Q^q e^2 \to Q^q Q^{q'} e^2$. Because helicity amplitudes are used, it is also trivial to convert the virtual-photon amplitudes to ones for (parity-violating) electroweak boson production. For the case of combined exchange of virtual photon and Z boson, with decay to a charged lepton pair, the electric charge factor has to be replaced by

$$2e^2\Big(-Q^q + v^\ell_{L,R} v^q_{L,R} \mathcal{P}_Z(s_{\ell\bar{\ell}})\Big)\,, \tag{3.16}$$

where $v^\ell_{L,R}$ are the left- and right-handed couplings of the lepton to the Z boson, $v^q_{L,R}$ are the corresponding quantities for the quark,

$$\mathcal{P}_Z(s) = \frac{s}{s - M_Z^2 + i\,\Gamma_Z\,M_Z} \tag{3.17}$$

is the ratio of Z to γ^* propagators, and M_Z and Γ_Z are the mass and width of the Z.

Whether v_L or v_R is to be used in eq. (3.16) depends on the helicity assignment, *i.e.* on whether the Z couples to a left- or right-handed outgoing fermion (as opposed to anti-fermion); see ref. [113] for further details. The case of a $W^\pm$ boson is even simpler, because there is no coupling to right-handed fermions (and no interference with another boson).

The relevant MHV and NMHV amplitudes for four external fermions and the rest gluons, and for six external fermions and the rest gluons, have been converted in the above manner into tree amplitudes for $Vq\bar{q}g\ldots g$ and $Vq\bar{q}Q\bar{Q}g\ldots g$, where V stands for W, Z or γ^*. These NMHV amplitudes have been incorporated into the BlackHat library [105] and used there in conjunction with a numerical implementation [114] of the BCFW (on-shell) recursion relations [27, 28] in order to obtain amplitudes at the NNMHV level and beyond. Including the MHV and NMHV formulae speeds up the

numerical recursive algorithm by a factor of about four, in the present implementation. This approach was used to compute the real-radiative corrections entering the recent evaluation of $pp \to W + 4$ jets at NLO [98], in particular the tree amplitudes for $Wq\bar{q}'gggg$ and $Wq\bar{q}'Q\bar{Q}ggg$. These amplitudes have nine external legs, after decaying the W boson to a lepton pair, so there are MHV, NMHV and NNMHV configurations, but no further. All seven-point configurations are either MHV or NMHV, so at most two recursive steps were required to hit an explicit formula (for example, in a schematic notation $A_9 \to A_8 \times A_3 \to A_7 \times A_3 \times A_3$).

We remark that the tree-level color-ordered amplitudes entering subleading-color loop amplitudes can have a more general color ordering from that required for purely tree-level applications. For example, in the pure QCD amplitudes with a single $q\bar{q}$ pair, only the color-ordered amplitudes in which the two fermions are adjacent are needed in 2.37. However, the subleading-color terms in the one-loop amplitudes for $q\bar{q}g\ldots g$ include many cases in which the two fermions are not color-adjacent, and the tree-level $q\bar{q}g\ldots g$ amplitudes that enter their unitarity cuts have the same property. These color-ordered amplitudes are all available in $\mathcal{N} = 4$ super Yang-Mills theory, of course.

Similarly, for computing subleading-color one-loop terms for single-vector boson production processes like $Vq\bar{q}g\ldots g$, one needs tree amplitudes such as for example $A^{\gamma^*}(\ldots, q^+, g, \ell^-, \ell^+, \bar{q}^-, \ldots)$, in which the gluon g is color-ordered with respect to the quark pair, but not the lepton pair. These amplitudes are not equal to any particular color-ordered amplitude in $\mathcal{N} = 4$ SYM, but one can generate them by summing over appropriate color orderings. For example, we have

$$\begin{aligned} A^{\gamma^*}(\ldots, q^+, g, \ell^-, \ell^+, \bar{q}^-, \ldots) &= A^{\mathrm{QCD}}(\ldots, q_1^+, g, \bar{q}_2^-, q_2^+, \bar{q}_1^-, \ldots) \\ &+ A^{\mathrm{QCD}}(\ldots, q_1^+, \bar{q}_2^-, g, q_2^+, \bar{q}_1^-, \ldots) + A^{\mathrm{QCD}}(\ldots, q_1^+, \bar{q}_2^-, q_2^+, g, \bar{q}_1^-, \ldots)\,. \end{aligned} \tag{3.18}$$

The sum over the three permutations properly cancels out the unwanted poles as g becomes collinear with either ℓ^- or ℓ^+.

3.4. All Gluon Tree Amplitudes

In this section we present the general expression for an n-gluon tree amplitude, which we derive in section 3.7 from the solution of ref. [46] for a general $\mathcal{N} = 4$ SYM superamplitude.

Amplitudes for n-gluon scattering are classified by the number of negative-helicity gluons occurring in them. Tree-amplitudes with fewer than two negative-helicity gluons vanish. In our conventions the gluon at position n is always of negative helicity, which does not present a restriction due to cyclicity of the color-ordered amplitude. The Parke-Taylor formula [39] for a maximally-helicity-violating (MHV) gluon amplitude, with the two negative-helicity gluons sitting at positions $c_0 \in [1, n-1]$ and n, then reads

$$A_n(1^+, \ldots, c_0^-, \ldots, , n^-) := A_n^{\mathrm{MHV}}(c_0, n) = \frac{\delta^{(4)}(p)\,\langle c_0\; n\rangle^4}{\langle 1\;2\rangle\langle 2\;3\rangle\ldots\langle n\;1\rangle}\,, \tag{3.19}$$

with the total conserved momentum $p = \sum_{i=1}^n p_i$.

Next-to-maximally-helicity-violating amplitudes of degree p (N^{p}MHV) then consist of $(p+2)$ negative-helicity gluons embedded in $(n-p-2)$ positive-helicity states. We

parametrize the positions of the negative-helicity gluons in the ordered set $(c_0, \ldots, c_p, n)$ with $c_i \in [1, n-1]$.

The general N$^{\rm p}$MHV tree-amplitude then takes the form

$$A_n^{\rm N^pMHV}(c_0^-, c_1^-, \ldots, c_p^-, n^-) = \frac{\delta^{(4)}(p)}{\langle 1\,2\rangle\langle 2\,3\rangle \ldots \langle n\,1\rangle} \times \sum_{\substack{\text{all paths}\\ \text{of length } p}} \left(\prod_{i=1}^{p} \tilde{R}^{\{L_i\};\{U_i\}}_{n;\{I_i\};a_ib_i}\right) \left(\det \Xi_n^{\rm path}(c_0, \ldots, c_p)\right)^4 \quad (3.20)$$

Let us now explain in turn the ingredients of this result, *i.e.* the sum over paths, the $\tilde{R}$-functions, and the path-matrix $\Xi_n^{\rm path}$.

The sum over all paths refers to the rooted tree depicted in fig. 3.7, introduced in ref. [46]. A path of length 0 consists of the initial node "1". A path of length p leads to a sequence of $p+1$ nodes visited starting with node "1". To clarify this all possible paths up to length $p = 3$ are listed in fig. 3.7. In general there are $(2p)!/(p!(p+1)!)$ different paths of length p, which is equal to the number of nodes appearing at level p in the rooted tree, since each final node unambiguously determines a path through the rooted tree.

The $\tilde{R}$-functions are generalizations of eq. (3.4) and may be written rather compactly with the help of eq. (3.2) as

$$\tilde{R}_{n;\{I\};ab} := \frac{1}{x_{ab}^2} \frac{\langle a\,(a-1)\rangle}{\langle n\,\{I\}\,ba|a\rangle\,\langle n\,\{I\}\,ba|a-1\rangle} \frac{\langle b\,(b-1)\rangle}{\langle n\,\{I\}\,ab|b\rangle\,\langle n\,\{I\}\,ab|b-1\rangle}\,; \quad (3.21)$$

they derive from the dual superconformal R-invariants introduced in ref. [46]. In the above and in eq. (3.20), $\{I\}$ is a multi-index deriving from the node in the associated path with the last pair of indices stripped off, *e.g.* $\{I_3\} = \{b_1, a_1, b_2, a_2\}$ for the last node of the first path of length $p = 3$.

In eq. (3.20) we used a further piece of notation, namely $\tilde{R}$-functions with upper indices, which start to appear at the NNMHV level, and which we now define. Generally the $\tilde{R}$-functions appear in the amplitude with an ordered summation over the last pair of indices,

$$\sum_{L \le a < b \le U} \tilde{R}_{n;\{I\};ab}\ . \quad (3.22)$$

$\tilde{R}$-functions with upper indices indicate a special behavior for the boundary terms in this sum when $a = L$ or $b = U$. Specifically if one has

$$\sum_{L \le a < b \le U} \tilde{R}^{l_1,\ldots,l_p;u_1,\ldots,u_q}_{n;\{I\};ab}\,, \quad (3.23)$$

and the boundary of a summation is reached, then the occurrence of the spinor $|a-1\rangle$ or $|b\rangle$ in the $\tilde{R}$-function without upper indices (3.21) is replaced by a novel spinor depending on the upper indices as follows

$$\begin{aligned} \langle L-1| \longrightarrow \langle \xi_L| &:= \langle n|x_{nl_1}x_{l_1l_2}\ldots x_{l_{p-1}l_p} && \text{for } a = L,\\ \langle U| \longrightarrow \langle \xi_U| &:= \langle n|x_{nu_1}x_{u_1u_2}\ldots x_{u_{q-1}u_q} && \text{for } b = U. \end{aligned} \quad (3.24)$$

Effectively this amounts to the following formula for the upper-indexed $\tilde{R}$-functions of

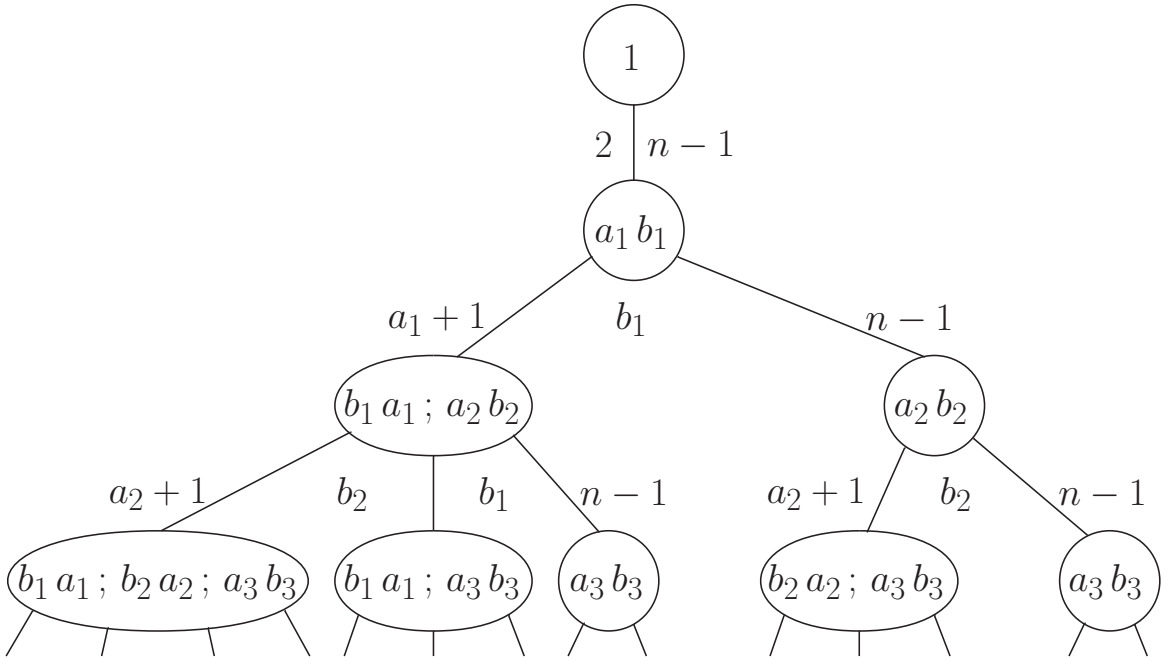

Length p	Paths
0	$[1]$
1	$[1]\cdot[a_1,b_1]$
2	$[1]\cdot[a_1,b_1]\cdot[b_1,a_1;a_2,b_2]$ $[1]\cdot[a_1,b_1]\cdot[a_2,b_2]$
3	$[1]\cdot[a_1,b_1]\cdot[b_1,a_1;a_2,b_2]\cdot[b_1,a_1,b_2,a_2;a_3,b_3]$ $[1]\cdot[a_1,b_1]\cdot[b_1,a_1;a_2,b_2]\cdot[b_1,a_1;a_3,b_3]$ $[1]\cdot[a_1,b_1]\cdot[b_1,a_1;a_2,b_2]\cdot[a_3,b_3]$ $[1]\cdot[a_1,b_1]\cdot[a_2,b_2]\cdot[b_2,a_2;a_3,b_3]$ $[1]\cdot[a_1,b_1]\cdot[a_2,b_2]\cdot[a_3,b_3]$

Figure 3.7.: The rooted tree encoding the sum over paths occurring in eq. (3.20). The table shows all paths up to length 3.

eq. (3.23),

$$\tilde{R}^{l_1,\ldots,l_p;u_1,\ldots,u_q}_{n;\{I\};ab} = \begin{cases} \tilde{R}_{n;\{I\};ab}\cdot\frac{\langle a\ \xi_L\rangle}{\langle n\{I\}ba|\xi_L\rangle}\frac{\langle n\{I\}ba|a-1\rangle}{\langle a\ (a-1)\rangle} & \text{for } a=L,\\ \tilde{R}_{n;\{I\};ab}\cdot\frac{\langle \xi_U\ (b-1)\rangle}{\langle n\{I\}ab|\xi_U\rangle}\frac{\langle n\{I\}ab|b\rangle}{\langle b\ (b-1)\rangle} & \text{for } b=U,\\ \tilde{R}_{n;\{I\};ab}\cdot\frac{\langle a\ \xi_L\rangle}{\langle n\{I\}ba|\xi_L\rangle}\frac{\langle n\{I\}ba|a-1\rangle}{\langle a\ (a-1)\rangle}\frac{\langle \xi_U\ (b-1)\rangle}{\langle n\{I\}ab|\xi_U\rangle}\frac{\langle n\{I\}ab|b\rangle}{\langle b\ (b-1)\rangle} & \text{for } a=L \text{ and } b=U,\\ \tilde{R}_{n;\{I\};ab} & \text{else.}\end{cases} \tag{3.25}$$

In particular there is a term in the double sum where both $a=L$ and $b=U$ are reached and both replacements are to be made. The rules for constructing the sets of upper indices $l_1,\ldots,l_p;u_1,\ldots,u_q$ in eq. (3.23) from the rooted tree are given in ref. [46].

To write down the path-matrix Ξ_n^{path} we furthermore need to define the quantities

$$(\Xi_n)_0^{c_i} := \langle n\ c_i\rangle\,, \tag{3.26}$$

$$(\Xi_n)_{ab}^{c_i} := \langle nba|c_i\rangle\,\chi_{[a,b-1]}(c_i) - x_{ab}^2\,\langle n\ c_i\rangle\,\chi_{[b,n-1]}(c_i)\,, \tag{3.27}$$

$$(\Xi_n)^{c_i}_{\{b_1,a_1,\ldots,b_r,a_r\};ab} := \langle n b_1 a_1 \ldots b_r a_r\, ab | c_i\rangle\, \chi_{[a,b-1]}(c_i) \\ -x^2_{ab}\, \langle n b_1 a_1 \ldots b_r a_r | c_i\rangle\, \chi_{[a_r,a-1]}(c_i)\,, \qquad (3.28)$$

with the support functions

$$\chi_{[a,b]}(i) = \begin{cases} 1 & \text{if} \quad i \in [a,b], \\ 0 & \text{else.} \end{cases} \qquad (3.29)$$

Now to every node $[\{I\}; ab]$ along a given path and to every negative-helicity leg c_i we associate the entry of the path-matrix $(\Xi_n)^{c_i}_{\{I\};ab}$. The entries $(\Xi_n)^A{}_B$ form a $(p+1)\times(p+1)$ matrix. Explicitly one has

$$\Xi^{\text{path}}_n(c_0,\ldots,c_p) := \begin{pmatrix} \langle n\, c_0\rangle & \langle n\, c_1\rangle & \ldots & \langle n\, c_p\rangle \\ (\Xi_n)^{c_0}_{a_1b_1} & (\Xi_n)^{c_1}_{a_1b_1} & \ldots & (\Xi_n)^{c_p}_{a_1b_1} \\ (\Xi_n)^{c_0}_{\{I_2\};a_2b_2} & (\Xi_n)^{c_1}_{\{I_2\};a_2b_2} & \ldots & (\Xi_n)^{c_p}_{\{I_2\};a_2b_2} \\ \vdots & \vdots & & \vdots \\ (\Xi_n)^{c_0}_{\{I_p\};a_pb_p} & (\Xi_n)^{c_1}_{\{I_p\};a_pb_p} & \ldots & (\Xi_n)^{c_p}_{\{I_p\};a_pb_p} \end{pmatrix}. \qquad (3.30)$$

Although $\tilde{R}$ and Ξ^{path}_n look rather involved at first sight, they are determined entirely through the external spinors λ_i and $\tilde{\lambda}_i$.

To clarify the construction principle let us write down the first three amplitudes in the N$^{\text{p}}$MHV series explicitly:

$$A^{\text{MHV}}_n(c_0,n) = \frac{\delta^{(4)}(p)}{\langle 1\,2\rangle\langle 2\,3\rangle\ldots\langle n\,1\rangle}\cdot\langle n\, c_0\rangle^4\,, \qquad (3.31)$$

$$A^{\text{NMHV}}_n(c_0,c_1,n) = \frac{\delta^{(4)}(p)}{\langle 1\,2\rangle\langle 2\,3\rangle\ldots\langle n\,1\rangle}\sum_{2\le a_1<b_1\le n-1}\tilde{R}_{n;a_1b_1}\cdot\begin{vmatrix} \langle n\, c_0\rangle & \langle n\, c_1\rangle \\ (\Xi_n)^{c_0}_{a_1b_1} & (\Xi_n)^{c_1}_{a_1b_1}\end{vmatrix}^4, \qquad (3.32)$$

$$A^{\text{N}^2\text{MHV}}_n(c_0,c_1,c_2,n) = \frac{\delta^{(4)}(p)}{\langle 1\,2\rangle\langle 2\,3\rangle\ldots\langle n\,1\rangle}\sum_{2\le a_1<b_1<n}\tilde{R}_{n;a_1b_1}\cdot \\ \Bigg[\sum_{a_1+1\le a_2<b_2\le b_1}\tilde{R}^{0;a_1b_1}_{n;b_1a_1;a_2b_2}\cdot\begin{vmatrix} \langle n\, c_0\rangle & \langle n\, c_1\rangle & \langle n\, c_2\rangle \\ (\Xi_n)^{c_0}_{a_1b_1} & (\Xi_n)^{c_1}_{a_1b_1} & (\Xi_n)^{c_2}_{a_1b_1} \\ (\Xi_n)^{c_0}_{b_1,a_1;a_2b_2} & (\Xi_n)^{c_1}_{b_1,a_1;a_2b_2} & (\Xi_n)^{c_2}_{b_1,a_1;a_2b_2}\end{vmatrix}^4 \\ +\sum_{b_1\le a_2,b_2<n}\tilde{R}^{a_1b_1;0}_{n;a_2b_2}\cdot\begin{vmatrix} \langle n\, c_0\rangle & \langle n\, c_1\rangle & \langle n\, c_2\rangle \\ (\Xi_n)^{c_0}_{a_1b_1} & (\Xi_n)^{c_1}_{a_1b_1} & (\Xi_n)^{c_2}_{a_1b_1} \\ (\Xi_n)^{c_0}_{a_2b_2} & (\Xi_n)^{c_1}_{a_2b_2} & (\Xi_n)^{c_2}_{a_2b_2}\end{vmatrix}^4\Bigg]. \qquad (3.33)$$

In appendix E.1 we spell out the NMHV and N^{2}MHV amplitudes explicitly. We provide a `Mathematica` package `GGT` with the `arXiv.org` submission of this article, which expands the master formula (3.20) explicitly for any choice of p, positions c_i and momenta $\lambda_i\tilde{\lambda}_i$. See appendix E.3 for documentation. The formula (3.20) is implemented by the function `GGTgluon`.

It should be mentioned that in practice the number of terms arising from the determinants of the path-matrix Ξ^{path}_n is often quite small, see *e.g.* eq. (3.3). Moreover, for

small n the number of non-zero terms in the nested sums can be relatively small.

3.5. All Single-Flavor Quark–Anti-Quark–Gluon Trees

Turning to the gauge-theory amplitudes involving massless single-flavor quark-anti-quark pairs we can write down a similarly general formula based on paths along the rooted tree of fig. 3.7. In an abuse of notation, we refer here to a helicity $+\frac{1}{2}$ fermion as a quark, and a helicity $-\frac{1}{2}$ fermion as an anti-quark. Looking at a color-ordered n-parton amplitude involving gluons and k quark-anti-quark pairs, $g^{n-2k}(q\bar{q})^k$, it is again classified as a N^{p}MHV amplitude by the number $(2+p-k)$ of negative-helicity gluons. In such a color-ordered amplitude we furthermore consider an arbitrary ordering of the fermions. We then have $2+p+k$ 'special' legs (negative-helicity gluon, quark or anti-quark) in such an amplitude, whose position amongst the n legs we parametrize by the set

$$(c_0, \ldots, c_{\alpha_1}, \ldots, c_{\bar{\beta}_1} \ldots, c_{\alpha_k}, \ldots, c_{\bar{\beta}_k}, \ldots, c_{p+k}, n)\,. \tag{3.34}$$

Here c_i denotes the position of a negative-helicity gluon, c_{α_j} a quark and $c_{\bar{\beta}_j}$ an anti-quark location. Note that while the quark and anti-quark locations c_{α_i} and $c_{\bar{\beta}_i}$ are considered as ordered sets, *i.e.* $c_{\alpha_i} < c_{\alpha_j}$ and $c_{\bar{\beta}_i} < c_{\bar{\beta}_j}$ for $i < j$, there is no such ordering in the total set $\{c_{\alpha_i}, c_{\bar{\beta}_i}\}$ reflecting an arbitrary sequence of quarks and anti-quarks in the color-ordered amplitude. Again in our convention one negative-helicity gluon is always located on leg n[2].

The general N^{p}MHV tree-amplitude for such a configuration then reads

$$\begin{aligned} A^{\text{N}^p\text{MHV}}_{(q\bar{q})^k,n} = {} & \frac{\delta^{(4)}(p)}{\langle 1\,2\rangle\langle 2\,3\rangle\ldots\langle n\,1\rangle} \times \\ & \times \text{sign}(\tau) \sum_{\substack{\text{all paths} \\ \text{of length } p}} \left(\prod_{i=1}^{p} \tilde{R}^{\{L_i\};\{U_i\}}_{n;\{I_i\};a_ib_i}\right) \det\Big(\Xi^{\text{path}}_n\Big|_q\Big)^3 \det\Big(\Xi^{\text{path}}_n(\bar{q}\leftrightarrow q)\Big|_{\bar{q}}\Big). \end{aligned} \tag{3.35}$$

Here $\text{sign}(\tau)$ is the sign produced by permuting the quark and anti-quark legs from color ordering into the alternating order $\{c_{\alpha_1}, c_{\bar{\beta}_1}, c_{\alpha_2}, c_{\bar{\beta}_2}, \ldots, c_{\alpha_k}, c_{\bar{\beta}_k}\}$.

Remarkably, the only difference from the pure gluon amplitudes is a change in the determinant factors of the path-matrix Ξ^{path}_n. With $2+p+k$ 'special' legs the path-matrix associated to eq. (3.34) is now a $(p+1)\times(p+1+k)$ matrix of the form

$$\Xi^{\text{path}}_n := \begin{pmatrix} \langle n\,c_0\rangle & \ldots & \langle n\,c_{\alpha_i}\rangle & \ldots & \langle n\,c_{\bar{\beta}_i}\rangle & \ldots & \langle n\,c_{p+k}\rangle \\ (\Xi_n)^{c_0}_{a_1b_1} & \ldots & (\Xi_n)^{c_{\alpha_i}}_{a_1b_1} & \ldots & (\Xi_n)^{c_{\bar{\beta}_i}}_{a_1b_1} & \ldots & (\Xi_n)^{c_p}_{a_1b_1} \\ (\Xi_n)^{c_0}_{\{I_2\};a_2b_2} & \ldots & (\Xi_n)^{c_{\alpha_i}}_{\{I_2\};a_2b_2} & \ldots & (\Xi_n)^{c_{\bar{\beta}_i}}_{\{I_2\};a_2b_2} & \ldots & (\Xi_n)^{c_p}_{\{I_2\};a_2b_2} \\ \vdots & & \vdots & & \vdots & & \vdots \\ (\Xi_n)^{c_0}_{\{I_p\};a_pb_p} & \ldots & (\Xi_n)^{c_{\alpha_i}}_{\{I_p\};a_pb_p} & \ldots & (\Xi_n)^{c_{\bar{\beta}_i}}_{\{I_p\};a_pb_p} & \ldots & (\Xi_n)^{c_p}_{\{I_p\};a_pb_p} \end{pmatrix} \tag{3.36}$$

[2]We comment in section 3.7 on how to circumvent this problem for the case without a single negative-helicity gluon.

The notation $\Xi_n^{\text{path}}|_q$ in eq. (3.35) now refers to the elimination of all the quark columns (the c_{α_i}'s) in the path-matrix and $\Xi_n^{\text{path}}(\bar{q} \leftrightarrow q)|_{\bar{q}}$ denotes the matrix with all the anti-quark columns removed (the $c_{\bar{\beta}_i}$'s) after quark and anti-quark columns have been interchanged, *i.e.* $c_{\bar{\beta}_i} \leftrightarrow c_{\alpha_i}$. The removal of k columns is of course necessary in order to turn the $(p+1+k) \times (p+1)$ matrix Ξ_n^{path} into square form, so that the determinant is defined.

Let us again spell out some of the lower p amplitudes explicitly to clarify the formula (3.35):

$$A^{\text{MHV}}_{q\bar{q},n}((a_q, b_{\bar{q}}, n) = \frac{\delta^{(4)}(p)}{\langle 1\ 2\rangle\langle 2\ 3\rangle \ldots \langle n\ 1\rangle} \cdot \langle n\ b\rangle^3 \cdot \langle n\ a\rangle \tag{3.37}$$

$$A^{\text{NMHV}}_{q\bar{q},n}(a, b_q, c_{\bar{q}}, n) = \frac{\delta^{(4)}(p)}{\langle 1\ 2\rangle\langle 2\ 3\rangle \ldots \langle n\ 1\rangle} \sum_{2\le a_1<b_1\le n-1} \tilde{R}_{n;a_1b_1} \cdot \begin{vmatrix} \langle n\ a\rangle & \langle n\ c\rangle \\ (\Xi_n)^a_{a_1b_1} & (\Xi_n)^c_{a_1b_1} \end{vmatrix}^3 \cdot \begin{vmatrix} \langle n\ a\rangle & \langle n\ b\rangle \\ (\Xi_n)^a_{a_1b_1} & (\Xi_n)^b_{a_1b_1} \end{vmatrix} \tag{3.38}$$

$$A^{\text{NMHV}}_{(q\bar{q})^2,n}(a_q, b_{\bar{q}}, c_q, d_{\bar{q}}, n) = \frac{\delta^{(4)}(p)}{\langle 1\ 2\rangle\langle 2\ 3\rangle \ldots \langle n\ 1\rangle} \sum_{2\le a_1<b_1\le n-1} \tilde{R}_{n;a_1b_1} \cdot \begin{vmatrix} \langle n\ b\rangle & \langle n\ d\rangle \\ (\Xi_n)^b_{a_1b_1} & (\Xi_n)^d_{a_1b_1} \end{vmatrix}^3 \cdot \begin{vmatrix} \langle n\ a\rangle & \langle n\ c\rangle \\ (\Xi_n)^a_{a_1b_1} & (\Xi_n)^c_{a_1b_1} \end{vmatrix} \tag{3.39}$$

$$\begin{aligned} A^{\text{N}^2\text{MHV}}_{q\bar{q},n}(a_q, b, c_{\bar{q}}, d, n) = {} & \frac{\delta^{(4)}(p)}{\langle 1\ 2\rangle\langle 2\ 3\rangle \ldots \langle n\ 1\rangle} \sum_{2\le a_1<b_1<n} \tilde{R}_{n;a_1b_1} \cdot \\ & \Bigg[\sum_{a_1+1\le a_2<b_2\le b_1} \tilde{R}^{0;a_1b_1}_{n;b_1a_1;a_2b_2} \cdot \begin{vmatrix} \langle n\ b\rangle & \langle n\ c\rangle & \langle n\ d\rangle \\ (\Xi_n)^b_{a_1b_1} & (\Xi_n)^c_{a_1b_1} & (\Xi_n)^d_{a_1b_1} \\ (\Xi_n)^b_{b_1,a_1;a_2b_2} & (\Xi_n)^c_{b_1,a_1;a_2b_2} & (\Xi_n)^d_{b_1,a_1;a_2b_2} \end{vmatrix}^3 \cdot \\ & \qquad \begin{vmatrix} \langle n\ b\rangle & \langle n\ a\rangle & \langle n\ d\rangle \\ (\Xi_n)^b_{a_1b_1} & (\Xi_n)^a_{a_1b_1} & (\Xi_n)^d_{a_1b_1} \\ (\Xi_n)^b_{b_1,a_1;a_2b_2} & (\Xi_n)^a_{b_1,a_1;a_2b_2} & (\Xi_n)^d_{b_1,a_1;a_2b_2} \end{vmatrix} \\ & + \sum_{b_1\le a_2,b_2<n} \tilde{R}^{a_1b_1;0}_{n;a_2b_2} \cdot \begin{vmatrix} \langle n\ b\rangle & \langle n\ c\rangle & \langle n\ d\rangle \\ (\Xi_n)^b_{a_1b_1} & (\Xi_n)^c_{a_1b_1} & (\Xi_n)^d_{a_1b_1} \\ (\Xi_n)^b_{a_2b_2} & (\Xi_n)^c_{a_2b_2} & (\Xi_n)^d_{a_2b_2} \end{vmatrix}^3 \begin{vmatrix} \langle n\ b\rangle & \langle n\ a\rangle & \langle n\ d\rangle \\ (\Xi_n)^b_{a_1b_1} & (\Xi_n)^a_{a_1b_1} & (\Xi_n)^d_{a_1b_1} \\ (\Xi_n)^b_{a_2b_2} & (\Xi_n)^a_{a_2b_2} & (\Xi_n)^d_{a_2b_2} \end{vmatrix} \Bigg] \end{aligned} \tag{3.40}$$

$$A^{\text{N}^2\text{MHV}}_{(q\bar{q})^2,n}(a_q, b, c_{\bar{q}}, d_q, e_{\bar{q}}, n) = \frac{\delta^{(4)}(p)}{\langle 1\ 2\rangle\langle 2\ 3\rangle \ldots \langle n\ 1\rangle} \sum_{2\le a_1<b_1<n} \tilde{R}_{n;a_1b_1} \cdot$$

$$\Bigg[\sum_{a_1+1\leq a_2<b_2\leq b_1} \tilde{R}^{0;a_1b_1}_{n;b_1a_1;a_2b_2} \cdot \begin{vmatrix} \langle n\ b\rangle & \langle n\ c\rangle & \langle n\ e\rangle \\ (\Xi_n)^b_{a_1b_1} & (\Xi_n)^c_{a_1b_1} & (\Xi_n)^e_{a_1b_1} \\ (\Xi_n)^b_{b_1,a_1;a_2b_2} & (\Xi_n)^c_{b_1,a_1;a_2b_2} & (\Xi_n)^e_{b_1,a_1;a_2b_2} \end{vmatrix}^3 \cdot \begin{vmatrix} \langle n\ b\rangle & \langle n\ a\rangle & \langle n\ d\rangle \\ (\Xi_n)^b_{a_1b_1} & (\Xi_n)^a_{a_1b_1} & (\Xi_n)^d_{a_1b_1} \\ (\Xi_n)^b_{b_1,a_1;a_2b_2} & (\Xi_n)^a_{b_1,a_1;a_2b_2} & (\Xi_n)^d_{b_1,a_1;a_2b_2} \end{vmatrix}$$
$$+ \sum_{b_1\leq a_2<b_2<n} \tilde{R}^{a_1b_1;0}_{n;a_2b_2} \cdot \begin{vmatrix} \langle n\ b\rangle & \langle n\ c\rangle & \langle n\ e\rangle \\ (\Xi_n)^b_{a_1b_1} & (\Xi_n)^c_{a_1b_1} & (\Xi_n)^e_{a_1b_1} \\ (\Xi_n)^b_{a_2b_2} & (\Xi_n)^c_{a_2b_2} & (\Xi_n)^e_{a_2b_2} \end{vmatrix}^3 \begin{vmatrix} \langle n\ b\rangle & \langle n\ a\rangle & \langle n\ d\rangle \\ (\Xi_n)^b_{a_1b_1} & (\Xi_n)^a_{a_1b_1} & (\Xi_n)^d_{a_1b_1} \\ (\Xi_n)^b_{a_2b_2} & (\Xi_n)^a_{a_2b_2} & (\Xi_n)^d_{a_2b_2} \end{vmatrix} \Bigg] \tag{3.41}$$

This completes our examples. Some explicit formulae with the determinants expanded out may be found in appendix E.2. The formula (3.35) is implemented in `GGT` by the function `GGTfermionS`. See appendix E.3 for the documentation.

Note that the master formula (3.20) reduces as it should to the pure-gluon scattering result (3.20) for a zero number of quark-anti-quark pairs, $k \to 0$. In that case no column removals are to be performed and the determinants combine to the power four.

3.6. All $g^{n-2k}(\psi\bar{\psi})^k$ Tree Amplitudes in $\mathcal{N} = 4$ SYM

The color-ordered tree amplitudes with fermions presented above were special in the sense that they apply both to massless QCD as well as $\mathcal{N} = 4$ super Yang-Mills, due to the single-flavor choice which suppresses intermediate scalar exchange as argued in section 3.3. We now state the master formula for general gluino and gluon tree amplitudes in the $\mathcal{N} = 4$ super Yang-Mills theory from which the above expressions arise. Through specific choices of external flavor configurations, however, this master formula may be used to produce color-ordered gluon and quark trees in massless QCD, as was discussed in section 3.3.

Similar to the notation in section 3.5, for a general $g^{n-2k}(\psi\bar{\psi})^k$ amplitude with arbitrary flavor assignments to the gluinos we have $2 + p + k$ 'special' legs (negative-helicity gluon, gluino or anti-gluino), whose position amongst the n legs we parametrize by the set

$$(c_0, \ldots, c^{A_1}_{\alpha_1}, \ldots, c^{B_1}_{\bar{\beta}_1} \ldots, c^{A_k}_{\alpha_k}, \ldots, c^{B_k}_{\bar{\beta}_k}, \ldots, c_{p+k}, n)\,. \tag{3.42}$$

Again the configuration of gluinos and anti-gluinos inside the gluon background may be arbitrary while the sets $\{\alpha_i\}$ and $\{\bar{\beta}_i\}$ are ordered. The general $g^{n-2k}(\psi\bar{\psi})^k$ amplitude with $(2 + p - k)$ negative-helicity gluons is then expressed in terms of the $\tilde{R}$-functions and the path-matrix Ξ^{path} defined above. It reads

$$A^{\text{N}^p\text{MHV}}_{(\psi\bar{\psi})^k,n}(c^-_0, \ldots, (c_{\alpha_i})_{\psi_{A_i}}, \ldots, (c_{\bar{\beta}_j})_{\bar{\psi}_{B_j}} \ldots, c^-_{p+k}, n^-) = \frac{\delta^{(4)}(p)\,\text{sign}(\tau)}{\langle 1\ 2\rangle\langle 2\ 3\rangle \ldots \langle n\ 1\rangle} \times$$
$$\times \sum_{\substack{\text{all paths} \\ \text{of length } p}} \left(\prod_{i=1}^{p} \tilde{R}^{\{L_i\};\{U_i\}}_{n;\{I_i\};a_ib_i} \right) \prod_{A=1}^{4} \det\left(\Xi^{\text{path}}_n\Big|_{\psi}(\bar{\psi}_A \to \psi_A) \right)\,. \tag{3.43}$$

Here the notation $\Xi^{\text{path}}_n|_{\psi}$ refers to the path-matrix (3.36) with all gluino columns $\{c_{\alpha_i}\}$ removed, whereas $\Xi^{\text{path}}_n\Big|_{\psi}(\bar{\psi}_A \to \psi_A)$ denotes the same path-matrix where the

columns of all anti-gluinos of flavor A are replaced by the previously-removed columns of the gluinos with flavor A, i. e. $c_{\bar{\beta}_i} \to c_{\alpha_i}$ for $A_i = B_i = A$. Also $\mathrm{sign}(\tau)$ is the sign of the permutation for bringing the initial color-ordering of the fermionic legs into the canonical alternating helicity order $\{c_{\alpha_1}, c_{\bar{\beta}_1}, c_{\alpha_2}, c_{\bar{\beta}_2}, \ldots, c_{\alpha_k}, c_{\bar{\beta}_k}\}$. This formula is implemented in `GGT` by the function `GGTfermion`. Obviously eq. (3.43) produces both eq. (3.35) and eq. (3.20) in the single flavor or gluon case. Several explicit examples can be found in appendix E.

3.7. Proof of the Master Formula

In this section we prove the master formula (3.43) for a general $\mathcal{N} = 4$ super Yang-Mills tree amplitude with external gluons and gluinos of arbitrary flavor, as well as the more compact single-flavor expression (3.35) and the pure gluon expression (3.20) as sub-cases.

The general solution for tree super-amplitudes of J. Drummond and J. Henn [46] takes the compact form

$$\mathcal{A}_n^{\mathrm{N}^p\mathrm{MHV}} = \frac{\delta^{(4)}(p)\,\delta^{(8)}(q)}{\langle 1\,2\rangle\langle 2\,3\rangle\ldots\langle n\,1\rangle} \sum_{\substack{\text{all paths}\\ \text{of length } p}} \prod_{i=1}^{p} R_{n;\{I_i\};a_ib_i}^{\{L_i\};\{U_i\}}\,, \tag{3.44}$$

where $q^{\alpha\,A} = \sum_{i=1}^n \lambda_i^\alpha\,\eta_i^A$ is the total conserved fermionic momentum, and the dual superconformal R-invariant is

$$R_{n;\{I\};ab} = \tilde{R}_{n;\{I\};ab}\,\delta^{(4)}\left(\sum_{i=1}^{n}\Xi_{n;\{I\};ab}(i)\,\eta_i\right)\,, \tag{3.45}$$

in the notation of the previous sections. We now wish to project this result in on-shell superspace onto the relevant components for a general $g^{n-2k}(\psi\bar{\psi})^k$ amplitude. For this purpose we set all of the η_i associated to positive-helicity gluon states to zero. This leaves us with the $p+2+k$ remaining Grassmann numbers η_{c_i} associated to the 'special' legs of helicities -1 and $\pm\frac{1}{2}$. To project onto a negative-gluon state at position i one simply has to integrate eq. (3.44) against $\int d^4\eta_i$. Similarly, to project to a gluino or anti-gluino state at position i of flavor A_i one integrates eq. (3.44) against $\int d\eta_i^{A_i}$ or $-\int d^4\eta_i\,\eta_i^{A_i}$. All integrations have to be in color order.

In accord with our convention above the leg n is chosen to be a negative-helicity gluon state, or an anti-gluino if there are no negative-helicity gluons. This is a convenient choice because the only dependence of the super-amplitude on η_n is through the total fermionic momentum conserving delta function, which can be written as

$$\delta^{(8)}(q) = \delta^{(8)}\left(\sum_{i=0}^{p+k}\lambda_{c_i}\,\eta_{c_i} + \lambda_n\,\eta_n\right) = \delta^{(4)}\left(\sum_{i=1}^{p+k}\frac{\langle c_0\;c_i\rangle}{\langle c_0\;n\rangle}\,\eta_{c_i} + \eta_n\right)\,\delta^{(4)}\left(\sum_{i=0}^{p+k}\langle n\;c_i\rangle\,\eta_{c_i}\right)\,. \tag{3.46}$$

For each path in eq. (3.44) the four-dimensional Grassmann delta functions in eq. (3.46), together with the p delta functions arising from the R-invariants (3.45), may be written as

$$\prod_{i=0}^{p+1} \delta^{(4)}\left(\sum_{j=0}^{p+k}\left(\Xi_n^{\text{path}}\right)_{ij}\eta_{c_j}\right) :=$$
$$\delta^{(4)}\left(\sum_{i=1}^{p+k}\frac{\langle c_0\ c_i\rangle}{\langle c_0\ n\rangle}\eta_{c_i}+\eta_n\right)\delta^{(4)}\left(\sum_{i=0}^{p+k}\langle n\ c_i\rangle\,\eta_{c_i}\right)\prod_{i=1}^{p}\delta^{(4)}\left(\sum_{j=0}^{p+k}\Xi_{n;\{I_i\};a_ib_i}(c_j)\,\eta_{c_j}\right), \quad (3.47)$$

with the $(p+2)\times(p+k+2)$ path-matrix Ξ_n^{path}. If we have a negative-helicity gluon at position n, the η_n integration is trivial and we can drop the trial η_n column and the row determined by the first delta function in eq. (3.47), ending up with the $(p+1)\times(p+k+1)$ path-matrix given in eq. (3.36). For the sake of readability we will drop the labels on the path-matrix in what follows, just denoting it by Ξ, and assume a negative-helicity gluon at position n. The projection to the general $g^{n-2k}(\psi\bar{\psi})^k$ amplitude of eq. (3.20), with quarks of flavor A_i at positions c_{α_i} and anti-quarks of flavor B_j at positions $c_{\bar{\beta}_j}$,

$$A^{\text{N}^p\text{MHV}}_{(q\bar{q})^k,n}(c_0,\ldots,c^{A_i}_{\alpha_i},\ldots,c^{B_j}_{\bar{\beta}_j},\ldots,c_{p+k},n)\,,$$

is then performed via the Grassmann integrals

$$(-1)^k\,\text{sign}(\tau)\left(\prod_{\substack{j=0\\ j\notin\{\alpha_1,\ldots,\alpha_k\}}}^{p+k}\int d^4\eta_{c_j}\right)\left(\prod_{l=1}^{k}\int d\eta^{A_l}_{c_{\alpha_l}}\,\eta^{B_l}_{c_{\bar{\beta}_l}}\right)\prod_{i=0}^{p+1}\delta^{(4)}\left(\sum_{j=0}^{p+k}\Xi_{i\,j}\eta_{c_j}\right). \quad (3.48)$$

Here $\text{sign}(\tau)$ compensates the minus signs we encountered by permuting the quark and anti-quark Grassmann variables from color order to the canonical order $\prod_{l=1}^{k}\int d\eta^{A_l}_{c_{\alpha_l}}\,\eta^{B_l}_{c_{\bar{\beta}_l}}$.

Let us first consider the pure gluon case, *i. e.* $k=0$. Performing the change of variables $\eta_{c_i}\to\Xi^{-1}_{ij}\eta_{c_j}$ immediately gives

$$\left(\prod_{j=0}^{p}\int d^4\eta_{c_j}\right)\prod_{i=0}^{p+1}\delta^{(4)}\left(\sum_{j=0}^{p}\Xi_{i\,j}\eta_{c_j}\right)=(\det\Xi)^4\,, \quad (3.49)$$

thereby proving eq. (3.20). To evaluate the general integral (3.48) we first perform the $(p+1)$ four-dimensional integrations with respect to the η's of the anti-gluinos and gluons by making a change of variables similar to the pure-gluon case, leading to

$$\text{sign}(\tau)\left(\det\Xi\Big|_\psi\right)^4\prod_{l=1}^{k}\int d\eta^{A_l}_{c_{\alpha_l}}\sum_{\substack{i=0\\ i\notin\{\alpha_1,\ldots,\alpha_k\}}}^{p+k}\left(\Xi\Big|^{-1}_{\psi}\right)_{\bar{\beta}_l\,i}\sum_{j=1}^{k}\Xi_{i\,\alpha_j}\eta^{B_l}_{c_{\alpha_j}}. \quad (3.50)$$

Here $\Xi\Big|_\psi$ refers to the elimination of all gluino columns in the path-matrix. We can simplify the sum over i by making use of some basic facts of linear algebra. Namely, given a square matrix $M=(m_{ij})$ with minors M_{ij}, its determinant and inverse can be written as

$$\det M=\sum_i(-1)^{i+j}m_{ij}\det M_{ij}\qquad\text{and}\qquad\left(M^{-1}\right)_{ij}=(-1)^{i+j}\frac{\det M_{ji}}{\det M}\,. \quad (3.51)$$

Hence, eq. (3.50) simplifies to

$$\mathrm{sign}(\tau)\left(\det\Xi\Big|_{\psi}\right)^{4-k}\prod_{l=1}^{k}\int d\eta_{c_{\alpha_l}}^{A_l}\sum_{j=1}^{k}\det\left(\Xi\Big|_{\psi}(\bar{\beta}_l\to\alpha_j)\right)\eta_{c_{\alpha_j}}^{B_l}\,, \tag{3.52}$$

where $\Xi\Big|_{\psi}(\bar{\beta}_l\to\alpha_j)$ denotes the replacement of an anti-gluino column by a gluino column. The remaining integrations are straightforward and give

$$\mathrm{sign}(\tau)\left(\det\Xi\Big|_{\psi}\right)^{4-k}\sum_{\sigma\in S_k}\mathrm{sign}(\sigma)\prod_{i=1}^{k}\delta^{A_iB_{\sigma(i)}}\det\left(\Xi\Big|_{\psi}(\bar{\beta}_{\sigma(i)}\to\alpha_i)\right)= \\ \mathrm{sign}(\tau)\prod_{A=1}^{4}\det\left(\Xi\Big|_{\psi}(\bar{\psi}_A\to\psi_A)\right)\,. \tag{3.53}$$

By $\Xi\Big|_{\psi}(\bar{\psi}_A\to\psi_A)$ we denote replacing all columns of anti-gluinos with flavor A by the columns of the gluinos of the same flavor. If no gluinos of flavor A are present the corresponding factor should be $\det\left(\Xi\Big|_{\psi}\right)$. The general $\mathcal{N}=4$ super Yang-Mills $g^{n-2k}(\psi\bar{\psi})^k$ amplitude is therefore

$$A^{\mathrm{N^pMHV}}_{(\psi\bar{\psi})^k,n}(c_0,\ldots,c^{A_i}_{\alpha_i},\ldots,c^{B_j}_{\bar{\beta}_j}\ldots,c_{p+k},n)=\frac{\delta^{(4)}(p)\,\mathrm{sign}(\tau)}{\langle 1\;2\rangle\langle 2\;3\rangle\ldots\langle n\;1\rangle}\times \\ \sum_{\substack{\text{all paths}\\ \text{of length } p}}\left(\prod_{i=1}^{p}\tilde{R}^{L_i;R_i}_{n;\{I_i\};a_ib_i}\right)\prod_{A=1}^{4}\det\left(\Xi\Big|_{\psi}(\bar{\psi}_A\to\psi_A)\right)\,. \tag{3.54}$$

Note that during the derivation of this formula we assumed that there is at least one negative-helicity gluon. The only change in the case $k=p+2$ is that the η_n integration is no longer trivial and we put a gluino at position n. Hence, the path matrix has the size $(p+2)\times(2p+4)$ and eq. (3.54) still holds as its derivation did not depend on the matrix dimensions. Using (3.47) the path matrix (3.30) then generalizes to the form

$$\Xi:=\begin{pmatrix}
0 & \frac{\langle c_0\;c_1\rangle}{\langle c_0\;n\rangle} & \frac{\langle c_0\;c_2\rangle}{\langle c_0\;n\rangle} & \ldots & \frac{\langle c_0\;c_{p+k}\rangle}{\langle c_0\;n\rangle} & 1\\
\langle n\;c_0\rangle & \langle n\;c_1\rangle & \langle n\;c_2\rangle & \ldots & \langle n\;c_{p+k}\rangle & 0\\
(\Xi_n)^{c_0}_{a_1b_1} & (\Xi_n)^{c_1}_{a_1b_1} & (\Xi_n)^{c_2}_{a_1b_1} & \ldots & (\Xi_n)^{c_{p+k}}_{a_1b_1} & 0\\
(\Xi_n)^{c_0}_{\{I_2\};a_2b_2} & (\Xi_n)^{c_1}_{\{I_2\};a_2b_2} & (\Xi_n)^{c_2}_{\{I_2\};a_2b_2} & \ldots & (\Xi_n)^{c_{p+k}}_{\{I_2\};a_2b_2} & 0\\
\vdots & \vdots & & & \vdots & \vdots\\
(\Xi_n)^{c_0}_{\{I_p\};a_pb_p} & (\Xi_n)^{c_1}_{\{I_p\};a_pb_p} & (\Xi_n)^{c_2}_{\{I_p\};a_pb_p} & \ldots & (\Xi_n)^{c_{p+k}}_{\{I_p\};a_pb_p} & 0
\end{pmatrix}\,. \tag{3.55}$$

Generally the amplitudes take a more compact form if the gluino at position n is taken to be of helicity $-1/2$. Several explicit formulas for the MHV and NMHV cases can be found in Appendix E.2. In particular Appendix E.2.2 discusses a case without a negative helicity gluon at position n.

As we are interested in QCD tree amplitudes, we need to decouple possible intermediate scalar states arising from the Yukawa couplings fig. 3.1 in the $\mathcal{N}=4$ super

Yang-Mills Lagrangian eq. (B.25). As discussed in section 3.3, one case in which this can be achieved is when the external fermion states all have the same flavor, due to the anti-symmetry of $\phi^{AB} = \frac{1}{2}\epsilon^{ABCD}\,\phi_{CD}$. For this case, we specialize to $A_i = B_i = A$ for all external fermion in our master formula (3.54), which reproduces eq. (3.35). If no fermions are present eq. (3.54) reduces to the pure gluon formula eq. (3.20).

4

Numerical Evaluation of Tree-Level QCD Amplitudes: Closed Analytic Formulae versus Berends-Giele Recursion

As described in chapter 3, analytical formulae for all color ordered QCD tree amplitudes can be constructed from color ordered tree amplitudes of $\mathcal{N} = 4$ SYM theory. In this chapter we compare the numerical efficiency of evaluating these closed analytic formulae to a numerically efficient implementation of the Berends-Giele recursion. We compare calculation times for tree-amplitudes with parton numbers ranging from 4 to 25 with no, one, two and three external quark lines. It turns out that the exact results are generally faster in the case of MHV and NMHV amplitudes. Starting with the NNMHV amplitudes the Berends-Giele recursion becomes more efficient. In addition to the runtime we also compared the numerical accuracy. The analytic formulae are on average more accurate than the off-shell recursion relations though both are well suited for complicated phenomenological applications. In both cases we observe a reduction in the average accuracy when phase space configurations close to singular regions are evaluated. We believe that the above findings provide valuable information to select the right method for phenomenological applications.

4.1. Introduction

Numerically fast and accurate computation methods for multi-parton tree-level amplitudes in QCD are of great importance from many points of view. They crucially enter the theoretical prediction for cross sections of multi-jet processes at leading order (LO) in the QCD coupling α_s as they occur at present particle colliders such as the Large Hadron Collider (LHC). Here a variety of computer programs based on the numerical evaluation of Feynman diagrams have been developed in the past see for example [6, 9, 11]. With the LHC data from the year 2011 jet multiplicities of up to 9 jets in the final state are probed. With the data of the year 2012, LHC will be able to investigate jet multiplicities of up to 12 jets. However, for high multiplicities, the conventional Feynman diagram based approach quickly reaches its limit, for example 8 jets in the final state would require already the evaluation of more than 10^7 Feynman diagrams! Hence more efficient methods are needed. Moreover, QCD tree-amplitudes are crucially needed for the computation of one-loop corrections, when these are constructed using a numerical implementation of generalized unitarity, for recent reviews see refs. [24, 31, 115, 116]. Recently rapid progress has been made in developing and automating the generalized unitarity and integrand reduction approaches to computation of loop amplitudes [104, 105, 117–124]. These techniques have made NLO predictions for multi-jet final states at hadron colliders feasible for up to $2 \to 5$ processes (for recent results see for example [32, 98, 125–142]).

As shown in chapter 3 all color ordered tree level amplitudes of QCD can be obtained from linear combination of color ordered gluon-gluino amplitudes of $\mathcal{N} = 4$ SYM. The analytical formulae for all gluon-gluino amplitudes relevant for QCD[1] are provided by the publicly available MATHEMATICA package `GGT`, described in appendix E.3. In its current version, GGT directly provides all QCD tree amplitudes with up to six quarks. The obtained analytic formulae are very compact at the maximally-helicity-violating (MHV) and next-to-maximally helicity violating (NMHV) levels but do grow considerably in complexity with growing k for N^kMHV amplitudes. Hence, the "$\mathcal{N} = 4$ SUSY method" of chapter 3, for the evaluation of massless QCD trees based on exact formulae displays a complementary situation to the conventional Berends-Giele recursive approach for the efficient numerical evaluation of trees in that its evaluation time scales mildly with the parton number n but strongly depends on the number of helicity flips k of the amplitude considered. In contrast the Berends-Giele recursion evaluation time is independent of k but strongly depends on the number of partons n.

The purpose of this chapter is a detailed analysis of the computation times for these two approaches as well as a test of their numerical accuracy. The outcome of our analysis may serve as a guideline on which implementation should be used in order to maximally speed up the numerical implementation of massless QCD trees in future numerical calculations. The ability to calculate tree amplitudes numerically in a fast and accurate manner even for high multiplicity opens up a variety of new applications beyond the current uses in fixed order calculations. Given the recent progress in the refinement of matching and parton-shower algorithms together with extended reach of the LHC searches it is very likely that amplitudes involving ten or even more external partons will enter phenomenological studies in the future.

A similar analysis as presented in this chapter has been performed in Refs. [114, 144]. In difference to Refs. [114, 144] we focus on the comparison of a purely numerical

[1] A MATHEMATICA package for all tree-level amplitudes in N=4 SYM appeared in [143].

approach with the usage of analytic formulae for color ordered amplitudes with varying numbers of quarks, since this has not been studied in detail before.

4.2. Description of Used Methods

As explained in detail in chapter 2, a general tree-level QCD amplitude for k quark–anti-quark pairs and $(n-2k)$ gluons may be conveniently separated into a sum of terms, each composed of a simple prefactor containing the color indices, multiplied by a kinematical factor known as a partial amplitude. The partial amplitudes are constructed from suitable linear combinations of the color-ordered amplitudes for $2k$ external quarks and $(n-2k)$ external gluons, which in turn can be constructed from suitable linear combination of color ordered SYM amplitudes for $2k$ external gluinos and $(n-2k)$ external gluons, as explained in chapter 3.

4.2.1. Closed Analytic Formulae

The complexity of the analytic formulae derived in chapter 3 can be classified by the amount of helicity violation. The simplest class is the MHV one. Here either two negative helicity gluons, one negative helicity gluon and one quark-anti-quark pair or two quark-anti-quark pairs sit at arbitrary positions within positive helicity gluon states of the color-ordered amplitude. In general the N^{p}MHV class includes all QCD amplitudes where the sum of the number n^- of negative helicity gluons and the number k of quark anti-quark pairs exceeds the helicity degree by two, $n^- + k = p + 2$.

It is straightforward to deduce the asymptotic scaling of the evaluation times from the structure of the formulae. The MHV amplitudes, e. g. eq. (3.31), are given by a single term consisting of approximately n spinor products. Hence, we expect an n^1 scaling of the evaluation time of all MHV amplitudes. An estimate for the scaling of the evaluation time of the other closed formulae is the number of terms the expression has. For large multiplicities n the number of terms in the formulae for the NMHV amplitudes, e. g. eq. (3.32), grows as n^2. Excluding the MHV prefactor the complexity of each of the terms is independent of the parton number, hence the asymptotic scaling in evaluation time is n^2. This is competitive with the Berends-Giele recursion method which grows independent on the helicity distributions of the partons as n^4, discussed in the next subsection. The NNMHV formulae, e. g. eq. (3.32), display a growth in the number of terms as n^4. Due to the same arguments as in the NMHV case we thus expect a similar performance of the NNMHV formulae as the Berends-Giele recursion and a detailed comparison is needed to see which method wins. Going beyond the NNMHV level with the analytic formulae of chapter 3 for the amplitudes appears to be disfavored as in general the number of terms in an N^{k}MHV formula grows as n^{2k} for large parton numbers.

In order to compare their evaluation time and numerical accuracy to the Berends-Giele recursion, the closed analytic formulae of appendix E for the MHV, NMHV and NNMHV amplitudes with zero to three quark-anti-quark lines have been directly implemented in a `C++` program `cGGT.cpp`, which can be provided upon request. `cGGT.cpp` contains the straightforwardly hard-coded analytic formulae and a natural amount of caching is performed in order to speed up the numerical evaluation of the amplitudes for a given phase space point. As such all the region momenta are evaluated and stored during initialization, similarly all spinor brackets are evaluated with the reduced spinors

in eq. (1.7) without the square root dependent pre-factor, which is only evaluated at the very end, as typically even powers of the pre-factor arise.

4.2.2. Berends-Giele Recursion

In this subsection we briefly comment on a purely numerical implementation of leading-order scattering amplitudes in massless QCD. Since an extensive literature exists on the subject we limit ourselves to the basic ingredients. More details can be found in Ref. [10]. In difference to on-shell recurrence relations developed more recently [27,28], the Berends-Giele recursion uses off-shell currents as basic building blocks. In pure gauge theory the off-shell currents $J_\mu(1^{h_1}, 2^{h_2} \ldots, n^{h_n})$ correspond to the amplitudes for the production of n gluons with helicities h_i and one off-shell gluon with the corresponding polarization vector stripped off. The on-shell scattering amplitude is thus obtained by taking the on-shell limit and contracting with the polarization vector of the additional gluon. As explained in detail in chapter 2, it is convenient to split the scattering amplitude into a color part and the remaining Lorentz structure. In practice this can be done for example by using color-ordered Feynman rules (for details we refer to Ref.). The full amplitude will in general contain different color structures. However since not all of these structures are independent it is usually sufficient to calculate only a few of them and reconstruct the remaining ones by permuting the external gluons. The key observation leading to the Berends-Giele recurrence relation is the fact that any off-shell current can be written as a sum of simpler off-shell currents connected via the appropriate three- (V_{3g}) and four-gluon (V_{4g}) vertices:

$$J_\mu(1,...,n) = \frac{-i}{P_{i,n}^2}\left[\sum_{i=1}^{n-1} V_{3g}^{\mu\nu\rho}(P_{1,i}, P_{i+1,n})\, J_\nu(1,...,i)\, J_\rho(i+1,...,n) + \sum_{j=i+1}^{n-1}\sum_{i=1}^{n-2} V_{4g}^{\mu\nu\rho\sigma}\, J_\nu(1,...,i) J_\rho(i+1,...,j)\, J_\sigma(j+1,...,n)\right] \quad (4.1)$$

where we have suppressed the helicity index and the gauge coupling is set to one. In addition the definition

$$P_{i,j} = \sum_{k=i}^{j} p_k \qquad \text{for} \quad j \geq i \quad (4.2)$$

is used, we note $P_{i,j} = x_{i,j+1}$. The color-ordered vertices are given by

$$V_{3g}^{\mu\nu\rho}(P_1, P_2) = \frac{i}{\sqrt{2}}\left(g^{\nu\rho}(P_1 - P_2)^\mu + 2g^{\rho\mu}P_2^\nu - 2g^{\mu\nu}P_1^\rho\right),$$
$$V_{4g}^{\mu\nu\rho\sigma} = \frac{i}{2}(2g^{\mu\rho}g^{\nu\sigma} - g^{\mu\nu}g^{\rho\sigma} - g^{\mu\sigma}g^{\nu\rho}). \quad (4.3)$$

Since the right hand side of eq. (4.1) is formally simpler—only off-shell currents with a lower number of gluons are involved—eq. (4.1) can be used to calculate off-shell currents recursively. The end-point of the recursion is given by

$$J_\mu(i^{h_i}) = \left(\varepsilon_\mu^{(h_i)}(p_i)\right)^* \quad (4.4)$$

where $\varepsilon_\mu^{(h_i)}(p_i)$ denotes the polarization vector of a gluon with momentum p_i and polarization h_i. We take all the partons as outgoing, that is the on-shell limit of the

scattering amplitudes correspond to the transition $0 \to g(1^{h_1}) \cdots g(n^{h_n}) g((n+1)^{h_{n+1}})$. Scattering amplitudes for physical processes are obtained as usual by crossing. Using the explicit form of the three- and four-point vertices as given above, the implementation of eq. (4.1) in a computer program is straight forward. As can be seen from eq. (4.1) the same sub-current may appear at different depths of the recursion. To speed up the numerical evaluation it is thus important to cache the sub-currents and evaluate them only once. We note that the possibility to reuse sub-currents during the calculation is a major advantage of off-shell recurrence relations compared to on-shell methods. Since recursive implementations tend to be sub-optimal to get high computing performance eq. (4.1) is implemented as a bottom–up approach. The program uses the one-point currents specified by the user in terms of particular polarization states together with the respective momenta to calculate the two-gluon off-shell currents $J_\mu(i^{h_i}, (i+1)^{h_{i+1}})$. The two-point currents together with the one-point currents are then used in the subsequent step to calculate the three-point currents. This procedure is repeated until the current of maximal length is obtained. Owing to our restriction to specific color structures only a fixed cyclic ordering needs to be considered. One can show that if sub-currents are cached the computational effort for the evaluation of an n-point current scales as n^4. Whereas without caching the scaling would be 4^n. We will come back to this point when we discuss the numerical performance. As a technical detail we remark that in the implementation presented here [117] no specific basis for the polarization vectors has been used. In particular no helicity methods have been applied. Since in (almost) all phenomenological applications the gluon polarization is not observed, only matrix elements squared summed over all polarization states will occur. As a consequence an arbitrary basis can be used as long as the sum over all possible polarization states is complete. Using real polarization vectors could thus yield a significant speed up since the entire calculation can be done using real numbers instead of complex arithmetic.

The extension to include also quarks—massive as well as massless ones—is straight forward. The main difference, namely that some sub-currents do not exist since there is no direct coupling between quarks, is merely a matter of bookkeeping. We stress that the quark currents calculated in the way described above in general do not correspond to partial amplitudes. However partial amplitudes can be constructed from the aforementioned currents. The reconstruction of the full matrix elements—not subject of this article—has been checked for a variety of different processes [145].

4.3. Performance and Numerical Accuracy

The scattering amplitudes described in the previous section find their application in leading-order phenomenology at hadron colliders. However, this is not the only application. With the development of unitarity inspired techniques, leading-order amplitudes represent an important input to the evaluation of one-loop amplitudes. In both cases the amplitudes need to be evaluated for millions of phase space points. The required computation time is thus an important factor in choosing the optimal approach. We compare the evaluation time in detail in section 4.3.1.

In particular when using leading-order amplitudes in the evaluation of one-loop amplitudes, not only the speed but also the numerical accuracy matters. In the unitarity method the one-loop amplitude is reconstructed from a large number of different cuts requiring the evaluation of the corresponding tree amplitudes. It is thus important to

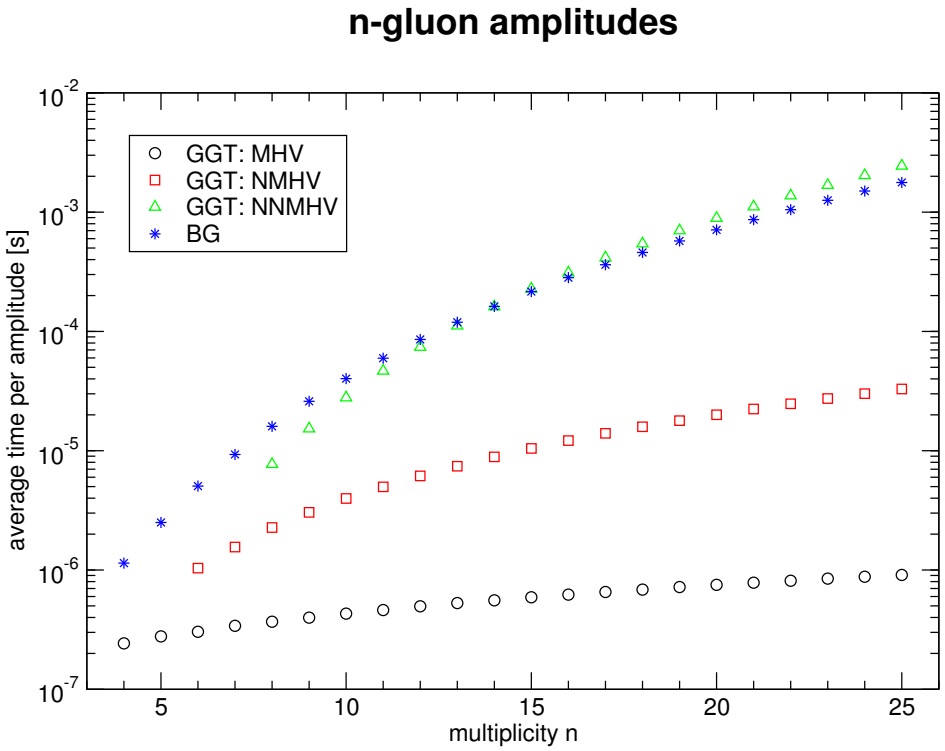

Figure 4.1.: Average time required per phase space point for the evaluation of pure gluon amplitudes as a function of the parton multiplicity.

assure a good accuracy of the individual contributions. Even in the case that analytic formulae are available one should keep in mind that when it comes to the numerical evaluation usually only a finite floating point precision is employed — unless special libraries to allow for extended precision are used. As a consequence, numerical cancellations between individual contributions may result in a loss of accuracy of the final result. Since a detailed understanding of the numerical uncertainties is also important when results from different methods are compared we investigate the numerical uncertainties of the two approaches discussed in the previous Section in section 4.3.2.

4.3.1. Evaluation Time

Before discussing the results in detail we briefly describe how the runtime is analyzed. To investigate the performance we used a computer with 16 GByte main memory and Intel(R) Core(TM) i5 3.33GHz cpu running under Debian 6.04. To reduce context switches as much as possible we payed attention to the fact that the computer was used exclusively for the performance measurements. Furthermore we used the POSIX function `getrusage` for the measurement of the used cpu time, which is to some great extent context independent. The function returns the time spent in user mode split into seconds and micro seconds. It is not documented whether the underlying clock provides a real time accuracy at the level of micro seconds. One can assume however that a precision at the level of milli seconds should be feasible which is sufficient for our purpose using the procedure described in the following.

The key observation is that both the evaluation time of the analytical formulae

and of the Berends-Giele recursion depend on the positions of the fermions. In the case of the analytical formulae we additionally have a dependence on the position of the negative helicity gluons. Hence, we chose to average over all configurations to which the analytical formulae directly apply without exploiting the cyclic symmetry of the amplitudes, e.g. all configurations with a negative helicity gluon at position n for amplitudes with at least one gluon of negative helicity. To obtain reproducible results and to reduce the computational effort to a minimum we took the following approach: Per measurement a minimum cpu time of at least one second is required to obtain reliable results. Using empirical knowledge together with the known scaling of the runtime as a function of the multiplicity we estimated the number of phase space evaluations for each sub-process/multiplicity. We then generated one phase space point and evaluated all matrix elements corresponding to our desired average the required number of times. While in the determination of the accuracy it is important that on-shell condition and four momentum conservation are respected as precisely as possible, the runtime measurement is insensitive to the "quality" of the phase space point—as long as no floating exceptions are encountered. (Floating point exceptions would lead to exception handling and the execution of different code.) In fig. 4.1 the cpu time per phase space point for pure gluon amplitudes is shown. We compare analytic formulae for three different helicity configurations (MHV, NMHV, NNMHV) with the purely numerical approach using the Berends-Giele recursion. Since in the implementation of the Berends-Giele recursion no helicity methods are used the runtime is the same for different helicity configurations. Fitting the last five data points with $f(n) = A\,n^B$, where n is the gluon multiplicity, we obtain $B \approx 4.12$ which is already quite close to the predicted asymptotic $\mathcal{O}(n^4)$ behavior. We stress that this is a property of the algorithm and cannot be changed by a different implementation. The implementation can only affect the normalization factor in front of the n^4 behavior. Let us now compare with the runtime required for the evaluation of the analytic formulae. In case of the MHV amplitude the evaluation is more than three orders of magnitude faster for 25 gluons—as one would have expected given the compactness of the analytic results. We have checked that the timings shown for the MHV amplitudes perfectly agree with the predicted n^1 scaling. Indeed all MHV amplitudes with k quark lines scale as $Bn + C_k$ where C_k increases with k, as one would expect from the structure of the MHV formulae. We emphasize that no time consuming square roots (contained in the spinor products) have to be evaluated in all gluon amplitudes since each spinor appears an even number of times. This is no longer true for amplitudes involving fermions as their associated spinors appear an odd number of times. Hence, for each fermion one square root is required. The predicted large n behavior of n^2 for the NMHV amplitudes is in good agreement with the $n^{2.2}$ fit from the last five data points in fig. 4.1. This is still much better than the n^4 of the Berends-Giele approach. As a consequence for large multiplicities the analytic results are almost two orders of magnitude faster than Berends-Giele. The situation changes when it comes to the NNMHV amplitudes. From the number of terms in the analytic expression we expect an asymptotic behavior of the form n^4 leading to a similar rise of the runtime as a function of the gluon multiplicity as observed in the Berends-Giele case. However, fitting the last five data points reveals that, with a scaling of $n^{4.5}$ the analytic formulae are still farther away from the asymptotic behavior than Berends-Giele. Consequently for 15 gluons and more the Berends-Giele recursion starts to become more efficient. As mentioned already, the asymptotic behavior is a property of the underlying algorithm

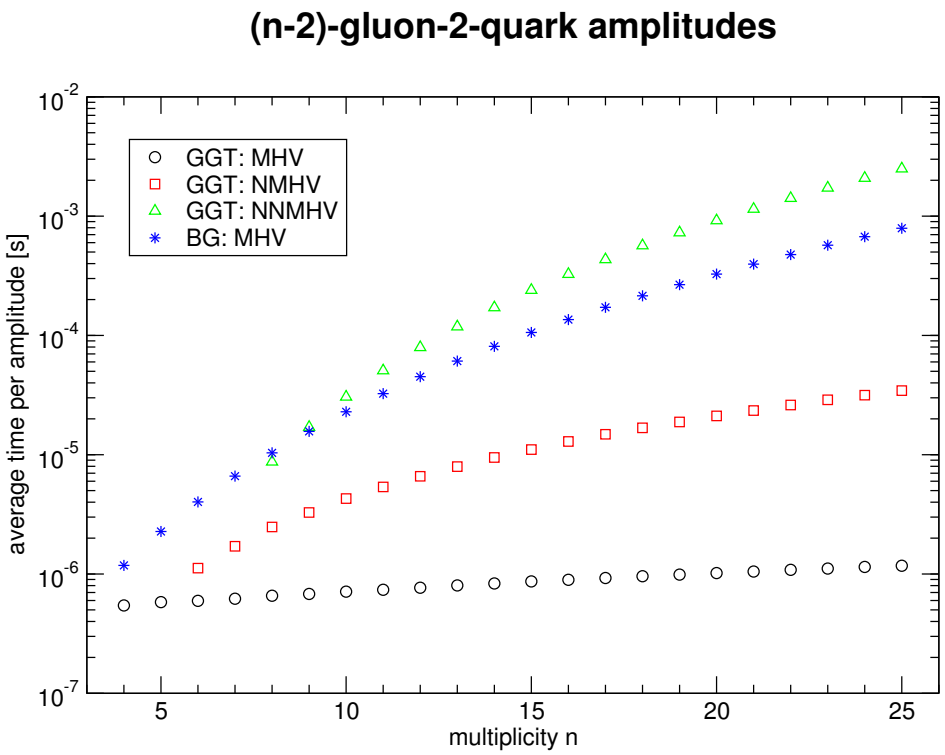

Figure 4.2.: Evaluation time per phase space point for amplitudes with a quark–anti-quark pair and $n-2$ gluons.

and cannot be changed by a 'more clever' implementation.

Let us add at that point a remark concerning the absolute timings: For low multiplicities the evaluation time is of the order of micro seconds while for $n = 25$ order milli seconds are required. For practical applications one should keep in mind, that the timings are for specific color and spin configurations. While for low multiplicities the number of color and spin configurations is still small (i.e. for $n \leq 5$ only MHV amplitudes exist) one can expect that color and spin summed squared amplitudes can be evaluated in less than one milli second per phase space point. However for large multiplicities the number of color and spin configurations grows rapidly. A naive sum over color and spin would thus give an additional factor which would render a brute force evaluation impossible given today's computing resources. In such cases refined methods like for example Monte Carlo sums over spins and colors would be required.

In fig. 4.2, fig. 4.3 and fig. 4.4 we show the results of a similar analysis, now for amplitudes involving up to three quark–anti-quark pairs. Again the Berends-Giele recursion method is presented only for a fixed number of negative helicity gluons since our implementation is independent of the gluon helicities. However, to take into account that the runtime depends on the position of the quarks in the primitive amplitude we took the same configuration average as for the corresponding analytic formula of smallest MHV degree. Overall we observe a picture similar to the pure gluon case: for MHV and NMHV amplitudes the analytic results are much faster than the evaluation based on the Berends-Giele recursion. Comparing the performance of the Berends-Giele recursion for 0, 2, 4, 6 quarks we find a decreasing dependence on the parton multiplicity. This is simply due to the fact that for a fixed multiplicity the number

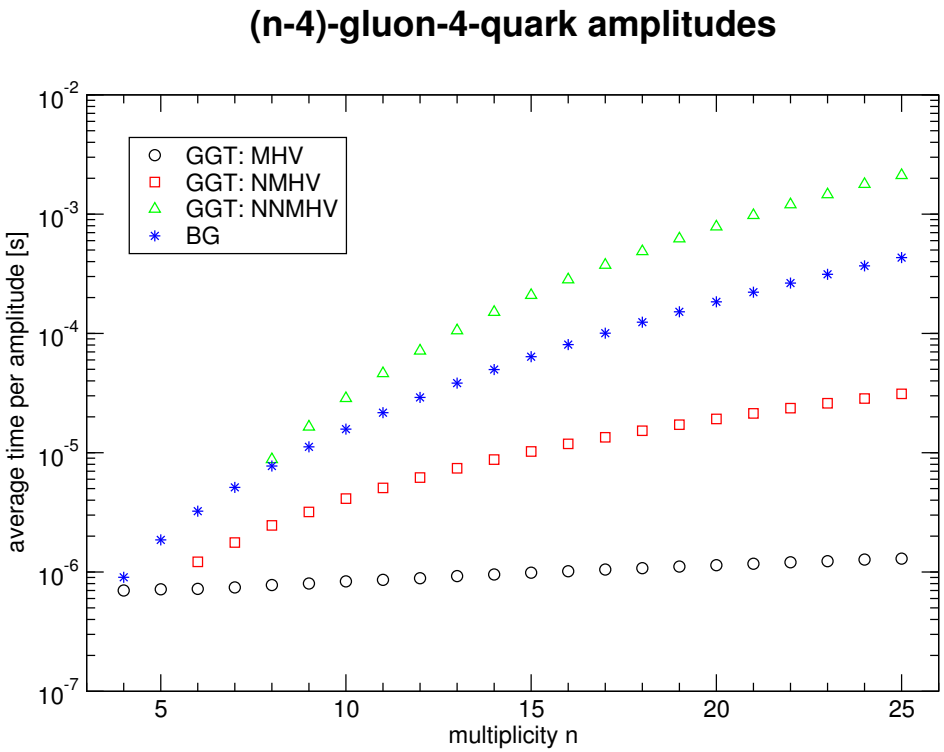

Figure 4.3.: Evaluation time per phase space point for amplitudes with two quark–anti-quark pairs (different flavors) and $n-4$ gluons.

of currents which have to be evaluated decreases if more fermions are involved. Since the n^4 asymptotic of the recursion is due to the four gluon vertex, we expect that the asymptotic scaling will be approached from below. Indeed, for two, four, six quarks we get $n^{3.96}$, $n^{3.83}$, $n^{3.64}$ from the last five data points, compared to $n^{3.77}$, $n^{3.43}$, $n^{3.19}$ for all data points up to $n = 15$ partons. The timings of the analytical formulae show only a small dependence on the number of quarks. As a consequence the Berends-Giele recursion is more efficient for the NNMHV amplitudes involving quarks. In case of all MHV amplitudes it is remarkable that the analytic formulae for MHV amplitudes show a very weak dependence on the parton multiplicity. The evaluation of an MHV amplitude for $n = 25$ takes only $6 \times 10^{-7} s$ longer than the evaluation of the four point amplitude. This is easily understood from the structure of formulae since increasing the multiplicity by one results only in the additional evaluation of two reduced spinor products and one squared spinor normalization factor.

In our analysis we have refrained from comparing the evaluation times for amplitudes involving 4 quark-anti-quark pairs, although closed analytical formulae exist also for this case [2]. The reason is that these will necessarily be in the NNMHV regime, which is not competitive against Berends-Giele as we discussed in the above. In addition, the complexity of the formulae grows at the 4 quark-anti-quark level as up to four gluon-gluino amplitudes need to be combined in order to represent quark-gluon amplitudes in massless QCD.

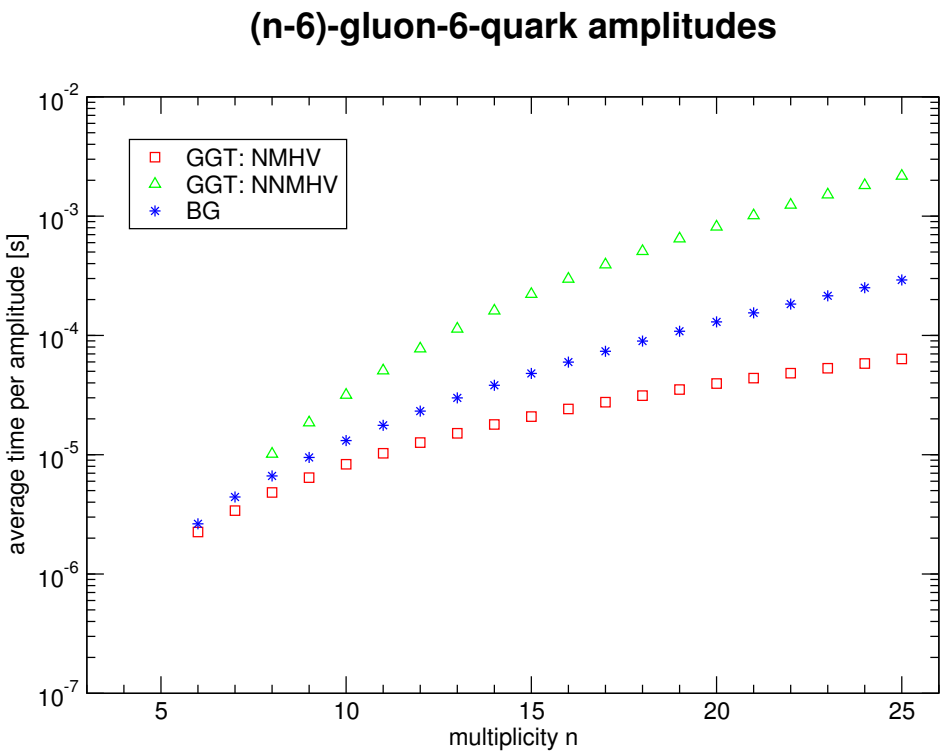

Figure 4.4.: Evaluation time per phase space point for amplitudes with three quark–anti-quark pairs (different flavors) and $n-6$ gluons.

4.3.2. Numerical Accuracy

Understanding the numerical accuracy is crucial for numerical cross section evaluations. In cases where analytic results are available it is possible to assess the accuracy of purely numerical approaches by comparing with analytic results. However the numerical evaluation of analytic formulae may also be affected by numerical instabilities. Furthermore a reliable method is also required for situations where no analytic results are available. In [117] the so-called scaling test was proposed. When applying the scaling test the scattering amplitudes are calculated twice for a given phase space point: for each phase space point the scattering amplitudes are calculated for the given momentum configuration. The evaluation is then repeated for a re-scaled set of momenta. Since the corresponding effective operators are not renormalized no anomalous dimension appears. The two evaluations are thus related by their naive mass dimension:

$$A_n(p_1, p_2, \ldots, p_n) = x^{n-4} A_n(xp_1, xp_2, \ldots, xp_n). \tag{4.5}$$

As was pointed out in [117] using a value for x which is not a power of 2 will lead to a different mantissa in the floating point representation and thus to different numerics. The method thus allows to assess the size of rounding errors. To estimate the numerical uncertainties we have applied the scaling test for a large number of phase space points. As a measure for the uncertainty we have evaluated for each phase space point the quantity δ:

$$\delta = \log_{10}\left(2\left|\frac{A_1 - A_2}{A_1 + A_2}\right|\right), \tag{4.6}$$

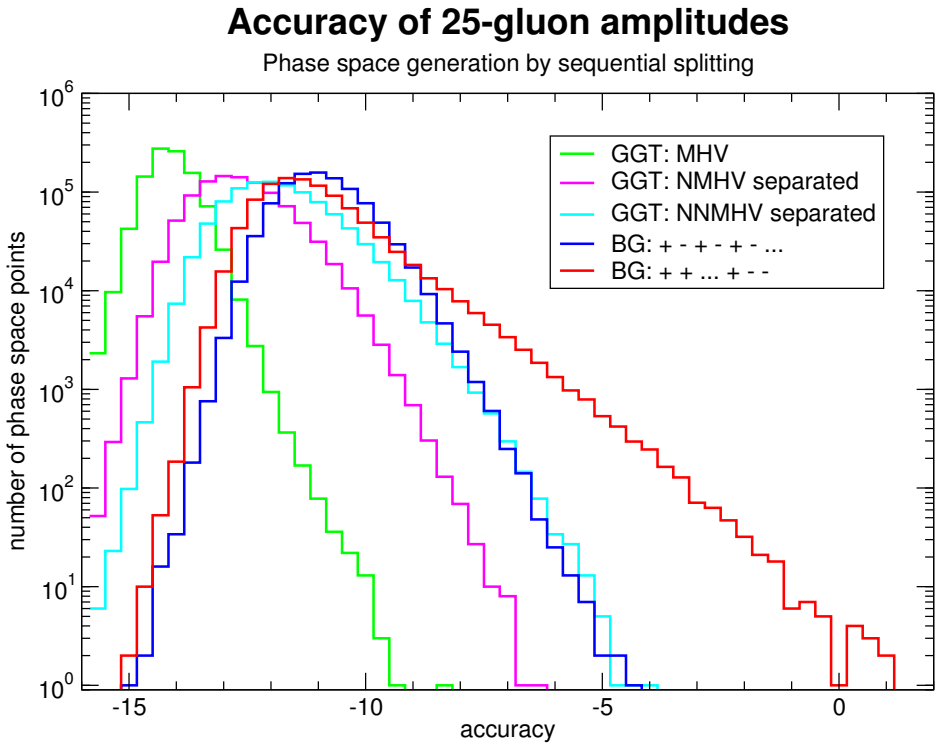

Figure 4.5.: Accuracy δ for 25 gluon amplitude for purely numerical evaluation based on the Berends-Giele recursion (BG) and for analytic formulae (GGT) as described in Section 4.2.1. Phase space generation by sequential splitting.

where A_1 denotes the result of the amplitude evaluation for unscaled momenta while A_2 is calculated from eq. (4.5). The quantity δ gives a measure for the valid digits in the evaluation, i.e. a value of $\delta = -3$ would mean that we expect ~ 3 digits to be correct and $\delta \geq 0$ corresponds to no valid digits. In all of the following accuracy plots we evaluated one million phase space points with a center of mass energy of $s = 1$. The kinematics is such that all momenta are outgoing, with the momenta in the first and second position having negative energy and opposite spatial components. The scaling factor is chosen to be $x = 7$. We emphasize that both the choice of s and the choice of x are irrelevant for the outcome of the accuracy analysis.

In fig. 4.5 we present results for the 25 gluon amplitude. The first three histograms show results using analytic formulae for MHV, NMHV, and NNMHV amplitudes. As expected $\langle\delta\rangle$ as well as the width of the distribution increase with N^kMHV degree. In case of the Berends-Giele recursion the situation is more intricate. We show the $\mathrm{N}^{\lfloor n/2 \rfloor - 2}$MHV alternating helicity configuration $+-+-\ldots$ and the MHV configuration $+\ldots+--$. Although their mean accuracy is almost equal, the width of the distributions indicates that this particular MHV configuration is numerically less stable. The phase space points are generated using a sequential splitting algorithm as described in [146]. This algorithm does not produce a flat distribution in phase space. In fact collinear configurations are preferred. We note that we always use a default cut based on the JADE jet algorithm to avoid singular regions in the phase space. In

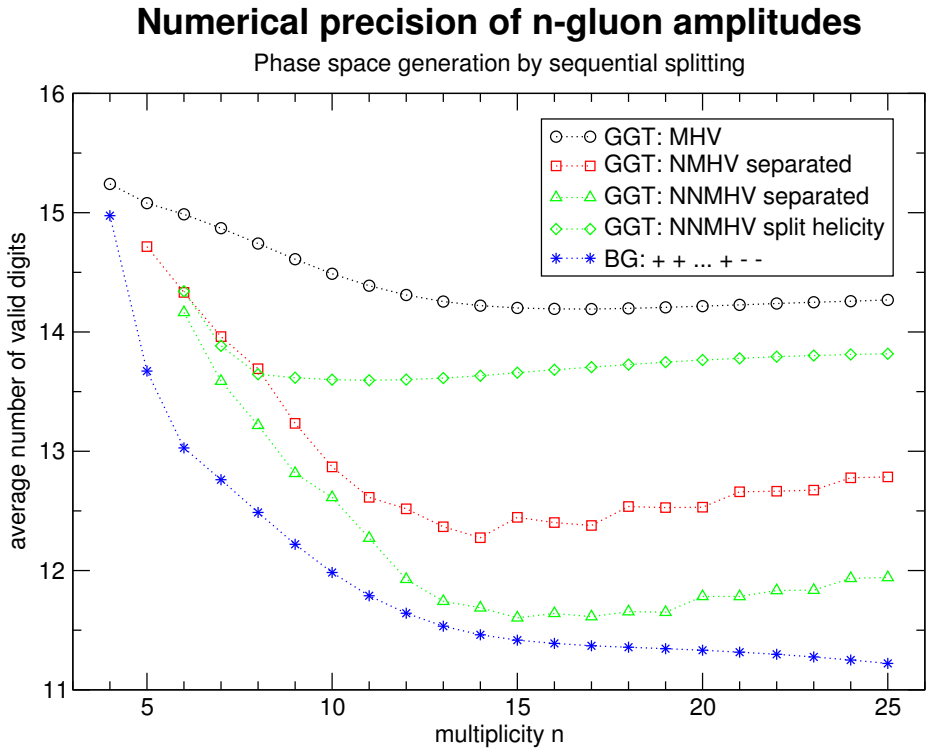

Figure 4.6.: Average accuracy $|\delta|$ for pure gluon amplitudes as a function of the gluon multiplicity (GGT analytic formulae, BG Berends-Giele). Phase space generation by sequential splitting.

particular we require $(2p_i \cdot p_j)/s > 10^{-10}$. We emphasize that as a consequence of the sequential splitting algorithm collinear configurations will dominate for multiplicities greater than 15, e.g. for $N = 20$ almost all phase space points have a collinearity of order 10^{-10}. A detailed analysis of the collinearity of the phase space points can be found in appendix F. It follows from fig. 4.5 that most of the phase space points are evaluated with a precision better than 5 valid digits — largely sufficient for any practical application at hadron colliders. Since we are mainly interested in a comparison between the purely numerical approach and the usage of analytic formulae for different parton multiplicities we have calculated an average accuracy for different parton multiplicities and different helicity configurations. For the analytical formulae we investigated the two extreme helicity configurations, leading to the smallest and largest number of terms. These are the split helicity configurations where all positive helicity gluons form a block, and the separated helicity configurations where all quarks and negative helicity gluons are equidistantly distributed in the sea of positive helicity gluons. The results are shown in fig. 4.6, together with the average accuracy of the Berends-Giele recursion for the MHV configuration of fig. 4.5. First of all we observe that in general the analytic formulae perform better as far as the accuracy is concerned. Furthermore it can be seen that for the analytic formulae the accuracy degrades when we move to the more complex configurations as for example the NNMHV amplitudes. This has two reasons. First of all the corresponding formulae are more involved and are thus more

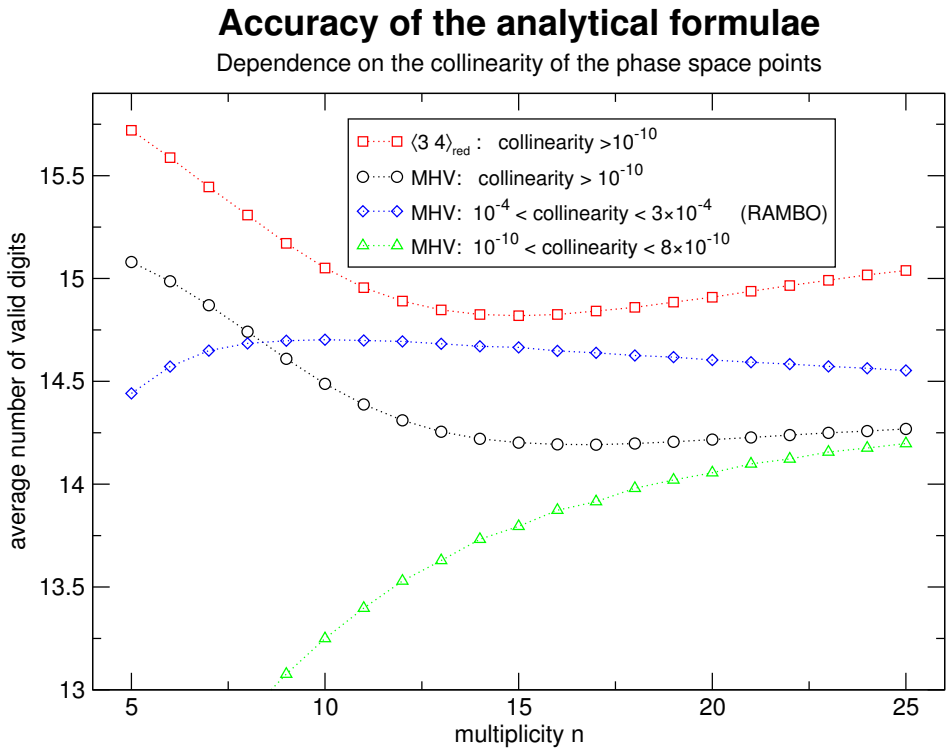

Figure 4.7.: Average accuracy of the reduced spinor product $\langle 3\ 4\rangle_{\mathrm{red}}$, and the MHV formula for different collinearity cuts. If not stated otherwise sequential splitting has been used.

difficult to evaluate numerically. The second reason is due to numerical cancellations between individual terms which leads to a loss of accuracy. This is supported by the observation that the NNMHV split helicity where no cancellation occurs is almost as accurate as the MHV formula. In the worst case the accuracy is only marginally better than what we observe in the purely numerical case.

A very interesting feature of the analytical formulae is that, starting from approximately $n = 15$, their accuracy increases. As illustrated in fig. 4.7 for the spinor product $\langle 3|4\rangle$, all building blocks of the amplitudes — being $\langle i|j\rangle$, $\langle i|x_{kl}x_{mn}|j\rangle$ and x_{ij}^2 — show the same counter intuitive behavior. Since the number of building blocks in each formula increases with the multiplicity n, the origin of this effect has to be the phase space generator and the applied collinearity cut. Let us have a closer look at the accuracy of a spinor product $\langle i|j\rangle$. Let us set $s = 1$ and assume that the components of the momenta are on average of order $\langle\mathcal{O}(p_i)\rangle = 10^{a_i}$, implying $\langle\mathcal{O}(|\lambda_i|)\rangle = 10^{a_i/2}$ for the spinor components. Due to the collinearity cut we have $\langle\mathcal{O}\left(|\langle i|j\rangle|\right)\rangle = 10^{a_{ij}} > 10^{-5}$. Hence, the average number of digits one loses when calculating $\lambda_i^1\lambda_j^1 - \lambda_i^2\lambda_j^2$ is approximately $\frac{a_i+a_j}{2} - a_{ij}$ and cannot be bigger than $5 + \frac{a_i+a_j}{2}$. It is clear that a_i and a_{ij} depend on the phase space generator as well as on the collinearity cut. It is also clear that the momenta become softer and more collinear with increasing multiplicity. Consequently, once a_{ij} has become close enough to the cut off, the average number

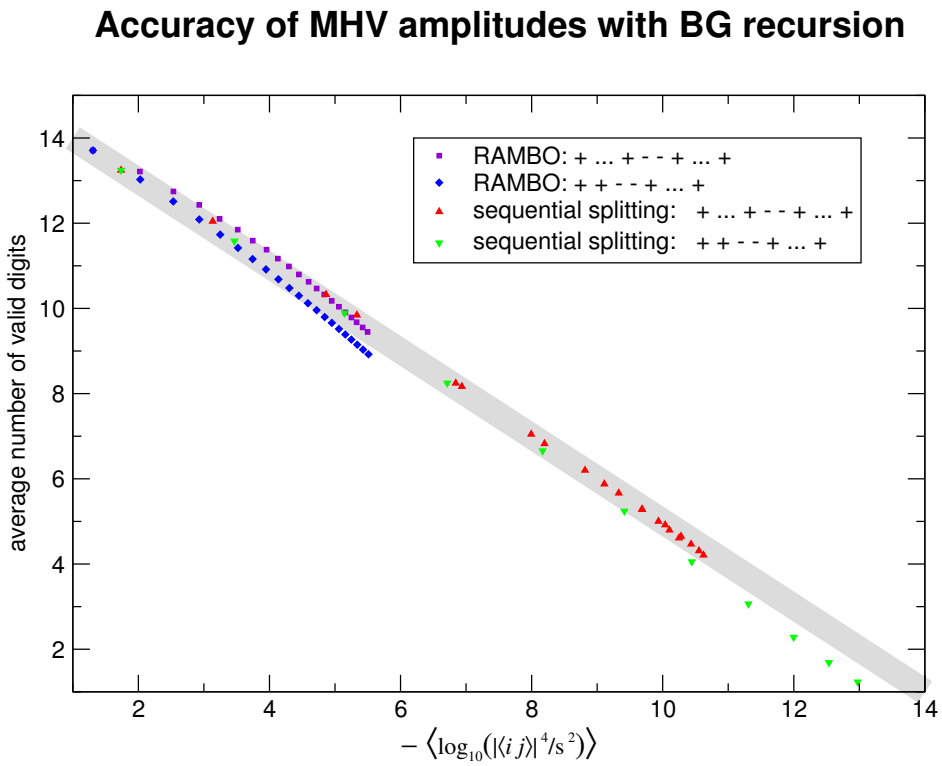

Figure 4.8.: The average accuracy of different MHV amplitudes is plotted against $\langle \log_{10}(|\langle i\ j\rangle|^4/s^2)\rangle$, where i and j are the positions of the negative helicity gluons. The data points have been determined using RAMBO and sequential splitting for multiplicities from $n = 5$ to $n = 25$. The thick gray line is the theoretical prediction of equation (4.8).

of digits one loses will decrease. With regard to the accuracy of the whole formulae besides the collinearity of the phase space points also the total number of terms leads to a loss of accuracy. Of course, if a collinearity cut is applied there will be a multiplicity from which on the accuracy will no longer be dominated by the collinearities in a small number of building blocks but by the overall number of terms in the formula. In fig. 4.7 we have plotted the accuracy of the MHV gluon amplitude for phase space points of fixed collinearity. If the collinearity is approximately 10^{-10}, the accuracy is still increasing at $n = 25$ gluon level, whereas for a collinearity of approximately 10^{-4} the accuracy starts decreasing at about $n = 10$ partons.

Since the helicity of the gluons enters the Berends-Giele recursion only via the polarization four-vectors, the naive expectation would be that all helicity configurations should perform similar. As already anticipated in fig. 4.5, this is not the case. Actually, the helicity dependence of the accuracy is much stronger for the Berends-Giele recursion than for the analytical formulae. For a phase space point describing $2 \to n-2$ scattering we have $2p_ip_j/s < 1$ for all outgoing particles. Hence, $A^{\mathrm{MHV}}(1^-, 2^-)$ is the

largest of all MHV amplitudes

$$Q_{ij} := \left| \frac{A^{\mathrm{MHV}}(i^-, j^-)}{A^{\mathrm{MHV}}(1^-, 2^-)} \right| = \left| \frac{\langle i\ j \rangle^4}{s^2} \right| < 1\,. \tag{4.7}$$

The size of Q_{ij} depends on the collinearity of legs i and j, but even if we apply a collinearity cut of 10^{-3}, Q can be of order 10^{-6}. The fact that the MHV amplitudes differ largely in their order of magnitude is completely irrelevant for the accuracy of the analytical formulae, but has a crucial impact on the accuracy of the Berends-Giele recursion. Independent of the position of the two negative helicities there are diagrams of order $\mathcal{O}(A^{\mathrm{MHV}}(1^-, 2^-))$ within the Berends-Giele recursion. These leading order contributions have to cancel, which obviously leads to a loss of accuracy. Indeed, it is actually simple to quantify this loss of accuracy:

$$\delta\mathrm{BG}^{\mathrm{MHV}}(i^-, j^-) = 15 + \langle \log_{10}(Q_{ij}) \rangle\ , \tag{4.8}$$

where $\delta\mathrm{BG}^{\mathrm{MHV}}(i^-, j^-)$ is the average number of valid digits of the Berends-Giele recursion for this particular MHV amplitude. As fig. 4.8 impressively demonstrates, equation (4.8) is a very precise description of the accuracy of the MHV amplitudes. Since the plotted data points are for different phase space generators, different positions of the negative helicities, as well as for different multiplicities ranging from $n = 5$ to $n = 25$, it is obvious that the cancellation of leading order contributions is the main source of loss of accuracy. The slight bending of the data points towards the abscissa is due to the multiplicity increasing from left to right. Depending on the phase space generator there will be a MHV amplitude which performs worst. Flipping the helicity of one additional gluon the relative order of magnitude of the leading order contribution in the recursion and the amplitudes decreases. Hence, the average accuracy increases. On the other hand, if we flip the helicity of one additional gluon in the most accurate MHV amplitude $\mathrm{BG}^{\mathrm{MHV}}(1^-, 2^-)$, than the accuracy will decrease. Due to the fact that the accuracy of the Berends-Giele recursion is parity invariant, it follows that the average accuracy of an arbitrary $\mathrm{N}^k\mathrm{MHV}$ amplitude is bound from above and below by the best and worst performing MHV amplitudes. In general the numerical accuracy increases with k until its maximum at $\mathrm{N}^{\lfloor n/2 \rfloor - 2}\mathrm{MHV}$ level.

To assess the dependence of accuracy results on the phase space generation we show in fig. 4.9 and fig. 4.10 the average accuracy for sequential splitting and a flat phase space generation obtained by using the algorithm RAMBO described in [147]. For the used implementation of sequential splitting the collinearity of the legs i and $i+1$ decreases clockwise starting from its maximum at $i = 3$ to its minimum at $i = 1$. As a consequence of equation (4.8), $\mathrm{BG}^{\mathrm{MHV}}(3^-, 4^-)$ and $\mathrm{BG}^{\mathrm{MHV}}(1^-, 2^-)$ are the lower and upper bound for the average accuracy. For the accuracy of $\mathrm{BG}^{\mathrm{MHV}}(1^-, 2^-)$ we observe a similar behavior as the analytic formulae because there is no cancellation of leading order contributions. Hence, the accuracy is dominated by the collinearities in a small subset of the propagators and scalar products. As fig. 4.9 shows, $\mathrm{BG}^{\mathrm{MHV}}(3^-, 4^-)$ has on average only one valid digit for $n = 15$ gluons. However, having a look at the distribution of the collinearity of the phase space points for sequential splitting, reveals that the situation is even worse. With the help of fig. F.2 and equation (4.8) it is possible to determine the average accuracy of the worst performing amplitude per phase space point $\delta_{\mathrm{low}} = \langle \min(\delta\mathrm{Amp}) \rangle$, which will be lower than $\min(\langle \delta\mathrm{Amp} \rangle)$. For $n = 10$ we have only $\delta_{\mathrm{low}} \approx 3$ valid digits, but with a standard deviation of

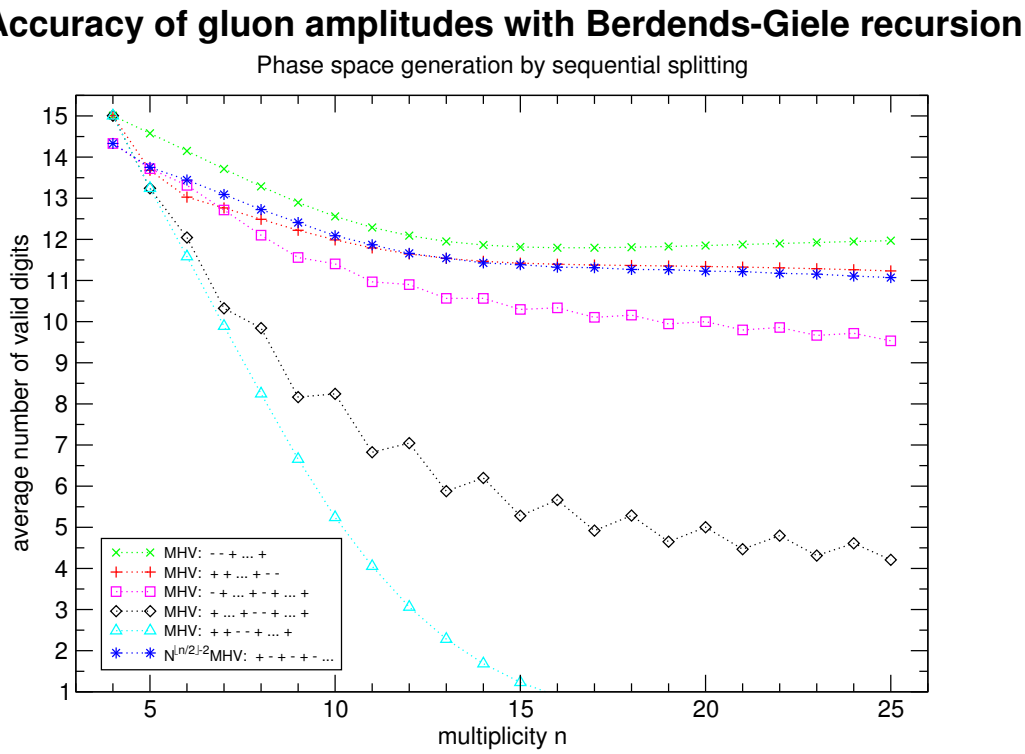

Figure 4.9.: Average accuracy of the amplitude evaluation using Berends-Giele recursion for phase space generation with sequential splitting.

$\sigma \approx 4$. Considering the asymmetry of the distribution, it is pretty likely to get no valid digits at all. Comparing fig. 4.9 and fig. 4.10 we observe that the dependence of the average accuracy on the helicity configuration is less pronounced for flat phase space points, because they are less collinear. In the particular case $\mathrm{BG}^{\mathrm{MHV}}(1^-, 2^-)$ and its parity conjugate the accuracy can compete with the numerical evaluation using analytic formulae. The lower bound for the accuracy is given by all $\mathrm{BG}^{\mathrm{MHV}}(i^-, j^-)$ with $i, j > 2$, which due to the flatness of the phase space generator perform all almost equal. Using fig. F.1 and (4.8) to determine the average accuracy of the worst performing amplitude per phase space point we get $\delta_{\mathrm{low}} \approx 8.4$ valid digits, with a standard deviation of $\sigma \approx 1.2$. This is significantly below the lower bound of approximately 11.5 digits for the average accuracy of an arbitrary helicity amplitude. However, one should keep in mind at this point that for all practical applications in collider phenomenology 5 significant digits are largely sufficient.

As far as the analytic formulae are concerned we observe no particular cancellations in case of a flat phase space generation. As a consequence the average accuracy is close to the maximum of about 15 digits as one would have expected, e.g. even for the most complicated NNMHV formulae the average accuracy is more than 13 digits.

One could argue that a flat phase space generation would be more appropriate to investigate the average accuracy. However we believe that for practical applications the average accuracy evaluated in that way would be less meaningful. In phenomenological applications the cross sections will get important contributions from collinear

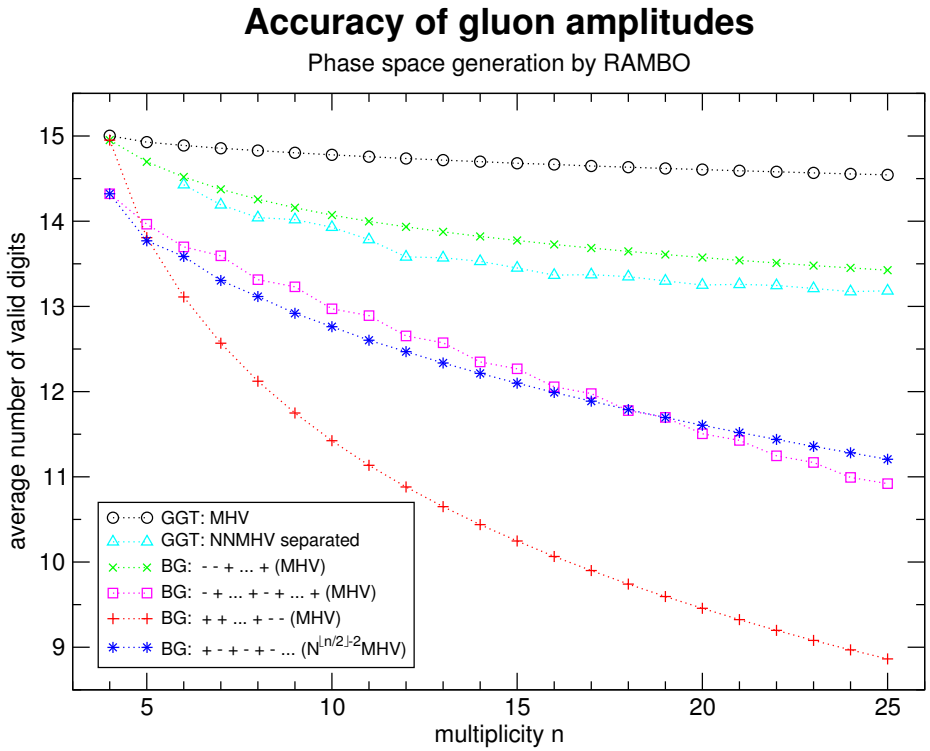

Figure 4.10.: Average accuracy of the amplitude evaluation using Berends-Giele recursion for flat phase space generation.

configurations. Using Monte Carlo methods for the cross section evaluation collinear events will thus dominate the total result. In an ideal situation this would be taken into account through the phase space integrator by preferring collinear configurations. This reasoning is also supported by the empirical observation that using RAMBO for the cross section evaluation usually leads to a poor performance of the Monte Carlo phase space integration in terms of computational effort and achieved integration accuracy.

For completeness we analyzed also the average accuracy for different separate helicity amplitudes involving two, four and six quarks. The result is shown in fig. 4.11. Again we have used a phase space generation preferring collinear events. As far as the numerical approach is concerned the result looks similar to the pure gluon case. This is just a consequence of the basic fact that the recurrence relation is very similar apart from the spin dependence. Since some vertices do not exist in the quark case the mixed amplitudes contain less terms and are slightly more precise. Concerning the analytic formulae we observe that the accuracy is not as good as in the pure gluon case. Our naive understanding is again that the corresponding formulae are more involved requiring more floating point evaluations and leaving more room for (unwanted) cancellations in the case of collinear phase space configurations.

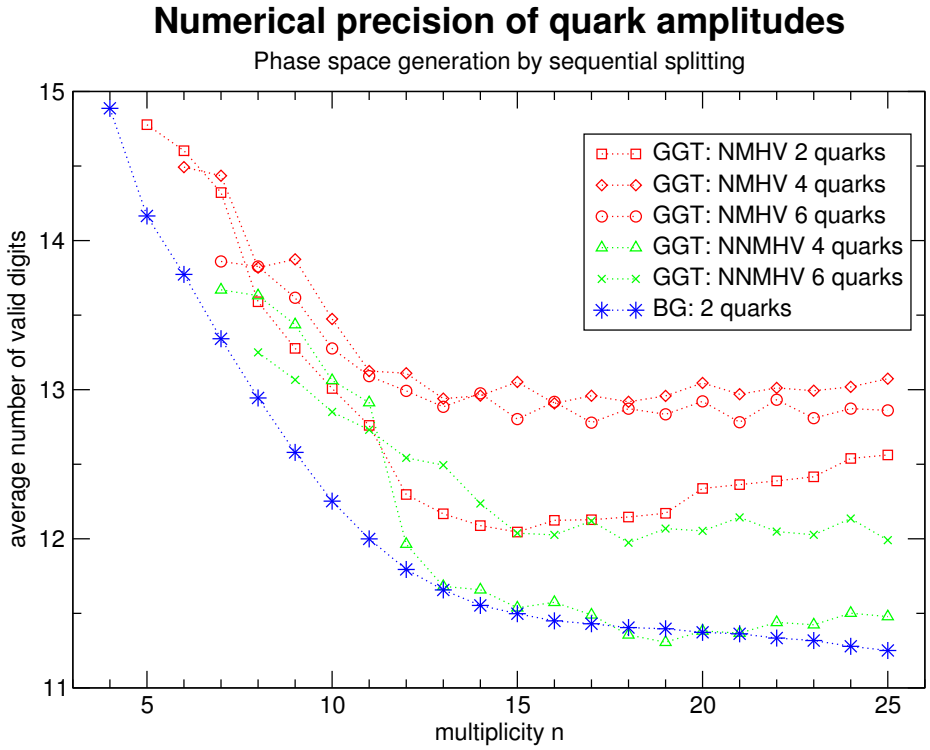

Figure 4.11.: Average accuracy for separate helicity amplitudes involving quarks. Phase space generation by sequential splitting.

5

Massive Trees in $\mathcal{N} = 4$ Super Yang-Mills Theory

Massive tree amplitudes on the Coulomb branch of $\mathcal{N} = 4$ SYM theory can be obtained by dimensionally reducing the massless tree amplitudes of the six-dimensional $\mathcal{N} = (1, 1)$ SYM theory. We exploit this correspondence to derive the symmetries of massive tree amplitudes in $\mathcal{N} = 4$ SYM theory. Furthermore, we investigate the tree amplitudes of $\mathcal{N} = (1, 1)$ SYM and explain how analytical formulae can be obtained from a numerical implementation of the BCFW recursion relation. We derive compact, manifest dual conformal covariant representations of the five- and six-point superamplitudes as well as arbitrary multiplicity formulae valid for large classes of component amplitudes with two consecutive massive legs. In [85] it has been claimed that all superamplitudes of $\mathcal{N} = (1, 1)$ SYM can be obtained by uplifting massless tree amplitudes of $\mathcal{N} = 4$ SYM. We confirm the uplift for multiplicities up to eight by performing numerical checks but prove that uplifting $\mathcal{N} = 4$ SYM amplitudes is non-trivial for multiplicities larger than five.

5.1. Introduction

Of all four dimensional gauge theories $\mathcal{N} = 4$ SYM is the most symmetric, compare section 1.4.2. Mainly due to the dual conformal properties of its massless tree amplitudes it has been possible to obtain analytical formulae for chiral superamplitudes of arbitrary multiplicity. As demonstrated in chapter 3 these results carry over to amplitudes with less supersymmetry, like e. g. all massless tree amplitudes of QCD. While massless QCD provides a reasonable approximation for energies well above the quark masses it fails for energies approaching the top mass. Since processes that produce top quarks in association with additional jets can form important backgrounds to new physics at the LHC, massive quark amplitudes are of particular interest.

The general aim of this chapter is to try to generalize the results presented in chapter 3 to QCD amplitudes containing massive quarks, or other massive colored states. Judging from the massless case, it should be possible to obtain at least part of the tree amplitudes with massive quarks, or other massive states, from linear combinations of massive amplitudes on the Coulomb branch of $\mathcal{N} = 4$ SYM.

Coulomb branch amplitudes under consideration here can be either obtained by giving mass to the on-shell states of $\mathcal{N} = 4$ SYM through a super-Higgs mechanism, or by dimensional reduction of the massless six-dimensional superamplitudes of $\mathcal{N} = (1, 1)$ SYM. While we opt for the latter in this chapter, a detailed description of the super-Higgs mechanism can be found in chapter 6.

We study how the symmetries of the $\mathcal{N} = (1, 1)$ SYM amplitudes translate to the Coulomb branch of $\mathcal{N} = 4$ SYM. In particular it was shown by Dennen and Huang in reference [52] that $\mathcal{N} = (1, 1)$ SYM, despite not being conformal, has a *dual conformal* symmetry at tree-level. Moreover, this symmetry remains intact also at loop-level iff one restricts the loop-momentum integrations to a four-dimensional subspace - under the assumption of cut-constructability of the theory. This prescription is *equivalent* to the Higgs regularization proposed in chapter 6, where such an extended dual conformal invariance was conjectured and tested at the one-loop four-particle level.

In analogy to the massless case, the guiding principle for obtaining analytical formulae for tree-level superamplitudes of $\mathcal{N} = (1, 1)$ SYM should be their dual conformal properties. Since, as explained in section 1.6.2, the six-dimensional BCFW recursion is ill-suited to obtain reasonable analytical formulae, new methods are needed. With regard to the difficulties in obtaining $\mathcal{N} = (1, 1)$ SYM amplitudes it would be nice to have a decomposition similar to the MHV decomposition of the massless four-dimensional superamplitudes, that allows to separate parts of the superamplitudes with varying complexity.

As a very tempting third option to obtain Coulomb branch amplitudes, it has been claimed in [85] that it is indeed possible to invert the dimensional reduction by uplifting the massless non-chiral superamplitudes of $\mathcal{N} = 4$ SYM to six-dimensional superamplitudes of $\mathcal{N} = (1, 1)$ SYM. Non-chiral superamplitudes of $\mathcal{N} = 4$ SYM are straightforward to obtain using the non-chiral BCFW recursion 1.6.1, resulting in an eminent practical relevance of a potential uplift. Furthermore it is very surprising that in fact the massive Coulomb branch amplitudes or equivalently the six-dimensional amplitudes might not contain any more information than the massless four-dimensional amplitudes of $\mathcal{N} = 4$ SYM.

5.2. From Massless 6d to Massive 4d

In section 1.5.2 we dimensionally reduced the massless six-dimensional amplitudes to massless four-dimensional ones. In analogy, we now want to perform the dimensional reduction of the superamplitudes of $\mathcal{N} = (1,1)$ SYM to the massive Coulomb branch amplitudes of $\mathcal{N} = 4$ SYM. When performing the dimensional reduction we need to choose an appropriate set of massive four-dimensional on-shell variables. For the bosonic part of the on-shell variables we choose *two* sets of helicity spinors $\{\lambda_\alpha, \tilde{\lambda}_{\dot{\alpha}}\}$ and $\{\mu_\alpha, \tilde{\mu}_{\dot{\alpha}}\}$ which allow for the following bispinor representation of a four dimensional massive momentum

$$p_\mu \sigma^\mu_{\alpha\dot{\alpha}} = p_{\alpha\dot{\alpha}} = \lambda_\alpha \tilde{\lambda}_{\dot{\alpha}} + \mu_\alpha \tilde{\mu}_{\dot{\alpha}} \,. \tag{5.1}$$

We introduce abbreviations for the spinor contractions

$$\langle \lambda\, \mu \rangle = m \,, \qquad [\tilde{\mu}\, \tilde{\lambda}] = \bar{m} \,, \tag{5.2}$$

where the mass parameters m and $\bar{m}$ are in general complex numbers, related to the physical mass by $p^2 = m\bar{m}$.

For the particular representation of the six-dimensional Pauli matrices listed in appendix A, the six-dimensional spinors can be expressed using the two sets of four dimensional spinors introduced above

$$\lambda^{A\,a} = \begin{pmatrix} -\mu_\alpha & \lambda_\alpha \\ \tilde{\lambda}^{\dot{\alpha}} & \tilde{\mu}^{\dot{\alpha}} \end{pmatrix} \quad \text{and} \quad \tilde{\lambda}_{A\,\dot{a}} = \begin{pmatrix} \bar{\rho}\mu^\alpha & \lambda^\alpha \\ -\tilde{\lambda}_{\dot{\alpha}} & \rho\tilde{\mu}_{\dot{\alpha}} \end{pmatrix} \quad \text{with} \quad \rho = \bar{\rho}^{-1} = \frac{m}{\bar{m}} \,, \tag{5.3}$$

and the six-dimensional momenta and dual momenta are given by

$$p_{AB} = \begin{pmatrix} -\bar{m}\,\epsilon^{\alpha\beta} & -p^\alpha{}_{\dot{\beta}} \\ p_{\dot{\alpha}}{}^\beta & m\,\epsilon_{\dot{\alpha}\dot{\beta}} \end{pmatrix} \qquad p^{AB} = \begin{pmatrix} m\,\epsilon_{\alpha\beta} & -p_\alpha{}^{\dot{\beta}} \\ p^{\dot{\alpha}}{}_\beta & -\bar{m}\,\epsilon^{\dot{\alpha}\dot{\beta}} \end{pmatrix} \tag{5.4}$$

and

$$x_{AB} = \begin{pmatrix} -\bar{n}\,\epsilon^{\alpha\beta} & -x^\alpha{}_{\dot{\beta}} \\ x_{\dot{\alpha}}{}^\beta & n\,\epsilon_{\dot{\alpha}\dot{\beta}} \end{pmatrix} \qquad x^{AB} = \begin{pmatrix} n\,\epsilon_{\alpha\beta} & -x_\alpha{}^{\dot{\beta}} \\ x^{\dot{\alpha}}{}_\beta & -\bar{n}\,\epsilon^{\dot{\alpha}\dot{\beta}} \end{pmatrix} . \tag{5.5}$$

Here $p_{\alpha\dot{\alpha}} = p_\mu \sigma^\mu_{\alpha\dot{\alpha}}$, $x_{\alpha\dot{\alpha}} = x_\mu \sigma^\mu_{\alpha\dot{\alpha}}$ are the contractions of the first four components of the six-dimensional vectors with the four-dimensional Pauli matrices and $m = p_5 - ip_4$, $n = x_5 - ix_4$. Our conventions for four dimensional spinors can be found in appendix A.

Since we are interested in massive four dimensional amplitudes we, from now on, set the fourth component of all six-dimensional vectors to zero, thereby effectively performing the dimensional reduction from a massless five-dimensional to a massive four dimensional theory. This is equivalent to setting $n = \bar{n} = x_5$ and imposing the constraint $m = \bar{m}$ on the spinor variables, which together with the reality condition for the momenta $\lambda^* = \pm\tilde{\lambda}$, $\mu^* = \pm\tilde{\mu}$ results in the 5 real degrees of freedom of a massive four dimensional momentum and a spin quantization axis[1].

Inserting the dimensional reduction of the spinors into the definition of the super-

[1] Each helicity spinor starts out with 4 real degrees of freedom, the reality condition $\lambda^* = \pm\tilde{\lambda}$ and the $U(1)$ helicity scaling $\lambda \to \exp[i\alpha]\lambda$ cuts this down to 3 real degrees of freedom. The further condition $\langle \lambda\, \mu \rangle = \langle \tilde{\mu} | \tilde{\lambda} \rangle$ brings us to 5=3+3-1 degrees of freedom.

momenta we obtain

$$q^A = \lambda^{Aa}\xi_a = \begin{pmatrix} -\mu_\alpha\xi_1 + \lambda_\alpha\xi_2 \\ \tilde{\lambda}^{\dot{\alpha}}\xi_1 + \tilde{\mu}^{\dot{\alpha}}\xi_2 \end{pmatrix}, \quad \tilde{q}_A = \tilde{\lambda}_{A\dot{a}}\tilde{\xi}^{\dot{a}} = \begin{pmatrix} \mu^\alpha\tilde{\xi}^{\dot{1}} + \lambda^\alpha\tilde{\xi}^{\dot{2}} & -\tilde{\lambda}_{\dot{\alpha}}\tilde{\xi}_{\dot{1}} + \tilde{\mu}_{\dot{\alpha}}\tilde{\xi}_{\dot{2}} \end{pmatrix}, \tag{5.6}$$

making it convenient to define the Grassmann part of our four-dimensional on-shell variables to be

$$\zeta^a = \begin{pmatrix} \xi_1 \\ -\tilde{\xi}^{\dot{1}} \end{pmatrix}, \qquad \bar{\zeta}^a = \begin{pmatrix} \xi_2 \\ \tilde{\xi}^{\dot{2}} \end{pmatrix}, \tag{5.7}$$

leading to the four-dimensional supermomenta

$$q^a_\alpha = \lambda_\alpha\bar{\zeta}^a - \mu_\alpha\zeta^a \qquad \tilde{q}^a_{\dot{\alpha}} = \tilde{\lambda}_{\dot{\alpha}}\zeta^a + \tilde{\mu}_{\dot{\alpha}}\bar{\zeta}^a \tag{5.8}$$

related to the six-dimensional ones by

$$q^A = \begin{pmatrix} q^1_\alpha \\ \tilde{q}^{\dot{\alpha}\,1} \end{pmatrix}, \qquad \tilde{q}_A = \begin{pmatrix} q^{\alpha\,2} & \tilde{q}^2_{\dot{\alpha}} \end{pmatrix}. \tag{5.9}$$

The dual fermionic momenta $\theta^a_{i\,\alpha}$, $\tilde{\theta}^a_{i\,\dot{\alpha}}$ are defined by

$$(\theta_i - \theta_{i+1})^a_\alpha = q^a_{i\,\alpha} \tag{5.10}$$

$$(\tilde{\theta}_i - \tilde{\theta}_{i+1})^a_{\dot{\alpha}} = \tilde{q}^a_{i\,\dot{\alpha}}\,, \tag{5.11}$$

and are related to the six-dimensional dual fermionic momenta by

$$\theta^A = \begin{pmatrix} \theta^1_\alpha \\ \tilde{\theta}^{\dot{\alpha}\,1} \end{pmatrix}, \qquad \tilde{\theta}_A = \begin{pmatrix} \theta^{\alpha\,2} & \tilde{\theta}^2_{\dot{\alpha}} \end{pmatrix}. \tag{5.12}$$

In conclusion the massive Coulomb branch amplitudes may be expressed either by the on-shell variables

$$\{\lambda^\alpha_i, \mu^\alpha_i, \zeta^a_i, \bar{\zeta}^a_i\} \tag{5.13}$$

or the dual variables

$$\{x^{\dot{\alpha}\beta}_i, n_i, \theta^a_{i\,\alpha}, \tilde{\theta}^a_{i\,\dot{\alpha}}\}\,. \tag{5.14}$$

in the associated full superspace the constraints on the variables read

$$(x_i - x_{i+1})_{\alpha\dot{\alpha}} = p_{i\,\alpha\dot{\alpha}}\,, \tag{5.15}$$

$$n_i - n_{i+1} = m_i\,, \tag{5.16}$$

$$m_i = \bar{m}_i\,, \tag{5.17}$$

$$(\theta_i - \theta_{i+1})^a_\alpha = q^a_{i\,\alpha} \tag{5.18}$$

$$(\tilde{\theta}_i - \tilde{\theta}_{i+1})^a_{\dot{\alpha}} = \tilde{q}^a_{i\,\dot{\alpha}}\,. \tag{5.19}$$

With the help of the maps eqs. (5.3) to (5.5), (5.7), (5.9) and (5.12) it is straightforward to translate any representation of a six-dimensional superamplitude into our four-dimensional variables. From the general form of the six-dimensional superampli-

tudes we can deduce the general form of the massive amplitudes to be

$$\mathcal{A}_n = \delta^{(1)}(n_{1\,n+1})\delta^{(4)}(x_{1\,n+1})\delta^{(4)}(\theta^{\alpha\,a}_{1\,n+1})\delta^{(4)}(\tilde{\theta}^{\dot{\alpha}\,a}_{1\,n+1}) f_n(\{x_{ij}, n_{ij}, \theta_{ij}, \tilde{\theta}_{ij}\})\,. \tag{5.20}$$

5.3. Symmetries of Massive Tree Amplitudes

We now want to investigate the symmetries of the massive amplitudes using the on-shell variables eq. (5.13) introduced in the last section. To be more precise, we are interested in the symmetries of f_n, defined in eq. (5.20), on the support of the delta functions. Similar to the massless four-dimensional case we define shorthand notations for derivatives with respect to spinors

$$\partial_{i\,\alpha} = \frac{\partial}{\partial\lambda_i^\alpha}\,, \qquad \partial_{i\,\dot{\alpha}} = \frac{\partial}{\partial\tilde{\lambda}_i^{\dot{\alpha}}}\,, \qquad \delta_{i\,\alpha} = \frac{\partial}{\partial\mu_i^\alpha}\,, \qquad \delta_{i\,\dot{\alpha}} = \frac{\partial}{\partial\tilde{\mu}_i^{\dot{\alpha}}}\,, \tag{5.21}$$

Judging from the symmetries of the six-dimensional superamplitudes, presented in section 1.5.1, and the imposed constraint $m = \bar{m}$, we expect a five-dimensional super Poincaré symmetry. It remains to show how this symmetry is realized on the on-shell variables eq. (5.13).

Obviously we have translation invariance

$$p^{\alpha\dot{\alpha}} = \sum_i \lambda_i^\alpha\tilde{\lambda}_i^{\dot{\alpha}} + \mu_i^\alpha\tilde{\mu}_i^{\dot{\alpha}}\,, \qquad m = \sum_i \langle\lambda_i\;\mu_i\rangle = \sum_i [\tilde{\mu}_i\;\tilde{\lambda}_i]\,. \tag{5.22}$$

as well as the Lorentz generators

$$l_{\alpha\beta} = \sum_i \lambda_{i\,(\alpha}\partial_{i\,\beta)} + \mu_{i\,(\alpha}\delta_{i\,\beta)}\,, \qquad \bar{l}_{\dot{\alpha}\dot{\beta}} = \sum_i \tilde{\lambda}_{i\,(\dot{\alpha}}\partial_{i\,\dot{\beta})} + \tilde{\mu}_{i\,(\dot{\alpha}}\delta_{i\,\dot{\beta})}\,, \tag{5.23}$$

associated to rotations in the first four spatial directions. Lorentz rotations $l^{\mu 5}$ involving the fifth spatial dimension correspond to the generator

$$w_{\alpha\dot{\alpha}} = \sum_i \tilde{\mu}_{i\,\dot{\alpha}}\partial_{i\,\alpha} - \tilde{\lambda}_{i\,\dot{\alpha}}\delta_{i\,\alpha} + \mu_{i\,\alpha}\partial_{i\,\dot{\alpha}} - \lambda_{i\,\alpha}\delta_{i\,\dot{\alpha}}\,. \tag{5.24}$$

Supersymmetry is realized as

$$q^a_\alpha = \sum_i \lambda_{i\,\alpha}\bar{\zeta}_i^a - \mu_{i\,\alpha}\zeta_i^a\,, \qquad \tilde{q}^a_{\dot{\alpha}} = \sum_i \tilde{\lambda}_{i\,\dot{\alpha}}\zeta_i^a + \tilde{\mu}_{i\,\dot{\alpha}}\bar{\zeta}_i^a\,, \tag{5.25}$$

$$\bar{q}_{\dot{\alpha}\,a} = \sum_i \tilde{\lambda}_{i\,\dot{\alpha}}\frac{\partial}{\partial\bar{\zeta}_i^a} - \tilde{\mu}_{i\,\dot{\alpha}}\frac{\partial}{\partial\zeta_i^a}\,, \qquad \bar{\tilde{q}}_{\alpha\,a} = \sum_i \lambda_{i\,\alpha}\frac{\partial}{\partial\zeta_i^a} + \mu_{i\,\alpha}\frac{\partial}{\partial\bar{\zeta}_i^a}\,. \tag{5.26}$$

Trivially we have a dilatation symmetry with the generator

$$d = \tfrac{1}{2}\sum_i (\lambda_i^\alpha\partial_{i\,\alpha} + \tilde{\lambda}_i^{\dot{\alpha}}\partial_{i\,\dot{\alpha}} + \mu_i^\alpha\delta_{i\,\alpha} + \tilde{\mu}_i^{\dot{\alpha}}\delta_{i\,\dot{\alpha}} + 2)\,. \tag{5.27}$$

Performing the dimensional reduction of the spinors, eq. (5.3), the independence of λ_A and $\tilde{\lambda}^A$ gets lost. As a consequence only one $SU(2)$ factor of the $SU(2) \times SU(2)$ little group symmetry survives the dimensional reduction. Indeed we have the $SU(2)$

helicity generators

$$h_+ = \frac{1}{\sqrt{2}}\sum_i \left(\lambda_i^\alpha \delta_{i\,\alpha} - \tilde{\mu}_i^{\dot\alpha}\partial_{i\,\dot\alpha} + \zeta_i^a \frac{\partial}{\partial \bar\zeta_i^a}\right), \qquad h_- = \frac{1}{\sqrt{2}}\sum_i \left(\mu_i^\alpha \partial_{i\,\alpha} - \tilde\lambda_i^{\dot\alpha}\delta_{i\,\dot\alpha} + \bar\zeta_i^a \frac{\partial}{\partial \zeta_i^a}\right),$$
$$h = \frac{1}{2}\sum_i \left(\lambda_i^\alpha \partial_{i\,\alpha} + \tilde\mu_i^{\dot\alpha}\delta_{i\,\dot\alpha} - \mu_i^\alpha \delta_{i\,\alpha} - \tilde\lambda_i^{\dot\alpha}\partial_{i\,\dot\alpha} + \zeta_i^a \frac{\partial}{\partial \zeta_i^a} - \bar\zeta_i^a \frac{\partial}{\partial \bar\zeta_i^a}\right). \tag{5.28}$$

They fulfill the following closing algebra

$$\begin{aligned}
[h_+, h_-] &= h & [h, h_\pm] &= \pm h_\pm \\
[l_{\alpha\beta}, l_{\gamma\delta}] &= 2\epsilon_{\gamma(\alpha} l_{\beta)\delta} + 2\epsilon_{\delta(\alpha} l_{\beta)\gamma} & [\bar l_{\dot\alpha\dot\beta}, \bar l_{\dot\gamma\dot\delta}] &= 2\epsilon_{\dot\gamma(\dot\alpha}\bar l_{\dot\beta)\dot\delta} + 2\epsilon_{\dot\delta(\dot\alpha}\bar l_{\dot\beta)\dot\gamma} \\
[w_{\alpha\dot\alpha}, w_{\beta\dot\beta}] &= 2\epsilon_{\alpha\beta}\bar l_{\dot\alpha\dot\beta} + 2\epsilon_{\dot\alpha\dot\beta} l_{\alpha\beta} & & \\
[\, l_{\beta\gamma}, w_{\alpha\dot\alpha}\,] &= \epsilon_{\alpha(\beta}\, w_{\gamma)\dot\alpha} & [\,\bar l_{\dot\beta\dot\gamma}, w_{\alpha\dot\alpha}\,] &= -w_{\alpha(\dot\beta}\,\epsilon_{\dot\gamma)\dot\alpha} \\
[\, l_{\beta\gamma}, p_{\alpha\dot\alpha}\,] &= \epsilon_{\alpha(\beta}\, p_{\gamma)\dot\alpha} & [\,\bar l_{\dot\beta\dot\gamma}, p_{\alpha\dot\alpha}\,] &= -p_{\alpha(\dot\beta}\,\epsilon_{\dot\gamma)\dot\alpha} \\
[w_{\alpha\dot\alpha}, m] &= p_{\alpha\dot\alpha} & [w_{\alpha\dot\alpha}, p_{\beta\dot\beta}] &= 2\epsilon_{\alpha\beta}\epsilon_{\dot\alpha\dot\beta} m \\
[\, l_{\beta\gamma}, q_\alpha^a\,] &= \epsilon_{\alpha(\beta}\, q_{\gamma)}^a & [\, l_{\beta\gamma}, \bar{\tilde q}_{\alpha\, a}\,] &= \epsilon_{\alpha(\beta}\,\bar{\tilde q}_{\gamma)\, a} \\
[\,\bar l_{\dot\beta\dot\gamma}, \tilde q_{\dot\alpha}^a\,] &= \epsilon_{\dot\alpha(\dot\beta}\,\tilde q_{\dot\gamma)}^a & [\,\bar l_{\dot\beta\dot\gamma}, \bar q_{\dot\alpha\, a}\,] &= \epsilon_{\dot\alpha(\dot\beta}\,\bar q_{\dot\gamma)\, a} \\
[w_{\alpha\dot\alpha}, q_\beta^a] &= -\epsilon_{\alpha\beta}\tilde q_{\dot\alpha}^a & [w_{\alpha\dot\alpha}, \tilde q_{\dot\beta}^a] &= \epsilon_{\dot\alpha\dot\beta} q_\alpha^a \\
[w_{\alpha\dot\alpha}, \bar{\tilde q}_{\beta\, a}] &= \epsilon_{\alpha\beta}\bar q_{\dot\alpha\, a} & [w_{\alpha\dot\alpha}, \bar q_{\dot\beta\, a}] &= -\epsilon_{\dot\alpha\dot\beta}\bar{\tilde q}_{\alpha\, a} \\
\{q_\alpha^a, \bar q_{\dot\alpha\, b}\} &= p_{\alpha\dot\alpha}\,\delta_b^a & \{\tilde q_{\dot\alpha}^a, \bar{\tilde q}_{\alpha\, b}\} &= p_{\alpha\dot\alpha}\,\delta_b^a \\
\{q_\alpha^a, \bar{\tilde q}_{\beta\, b}\} &= m\,\epsilon_{\alpha\beta}\,\delta_b^a & \{\tilde q_{\dot\alpha}^a, \bar q_{\dot\beta\, b}\} &= -m\,\epsilon_{\dot\alpha\dot\beta}\,\delta_b^a
\end{aligned} \tag{5.29}$$

along with the generic $[d, j] = \dim(j)\, j$ for any generator j, all other commutators vanishing. A necessary condition for the generators to be well defined on the massive amplitudes under consideration is that they commute with the constraint $m = \bar m$. One indeed shows that this is the case, e.g.

$$[\, w_{\alpha\dot\alpha}, \langle\lambda_i\, \mu_i\rangle - [\tilde\mu_i\, \tilde\lambda_i]\,] = 0\,. \tag{5.30}$$

Clearly the nice form of the algebra is suggesting the existence of a $SU(2)$ symmetry with respect to the Grassmann label a, introduced in eq. (5.7). However, at this point we see no indication that such a symmetry is realized on the massive superamplitudes (5.20) for multiplicities larger than four and the introduction of the Grassmann variables ζ^a, $\bar\zeta^a$ and their dual partners θ^a, $\tilde\theta^a$ should be regarded as a very convenient way to compactly write down the algebra. Indeed, the $SU(2)$ symmetry of the algebra will be explicitly broken if we include the generators r_1, r_2 of $U(1) \times U(1)$ R-symmetry realized on the massive superamplitudes (5.20)

$$r_1 = \sum_i \left(\zeta_i^1 \frac{\partial}{\partial \zeta_i^1} + \bar\zeta_i^1 \frac{\partial}{\partial \bar\zeta_i^1}\right) - n + 4 \qquad r_2 = \sum_i \left(\zeta_i^2 \frac{\partial}{\partial \zeta_i^2} + \bar\zeta_i^2 \frac{\partial}{\partial \bar\zeta_i^2}\right) - n + 4\,. \tag{5.31}$$

Invariance under r_a follows from the R-symmetry charges b, $\tilde b$ (1.163) of the six-dimensional superamplitudes. We have

$$[r_a, q_\alpha^b] = \delta_a^b q_\alpha^b\,, \quad [r_a, \tilde q_{\dot\alpha}^b] = \delta_a^b \tilde q_{\dot\alpha}^b\,, \quad [r_a, \bar q_{\dot\alpha\, b}] = -\delta_a^b \bar q_{\dot\alpha\, b}\,, \quad [r_a, \bar{\tilde q}_{\alpha\, b}] = -\delta_a^b \bar{\tilde q}_{\alpha\, b}\,. \tag{5.32}$$

We now want to investigate the symmetries in the dual superspace (5.14). Similar to the on-shell case we already know from the six-dimensional amplitudes that we will have an extended dual conformal symmetry. Obviously the massive amplitudes have an extended Poincaré symmetry with generators

$$\{P_{\alpha\dot\alpha},\, M,\, L_{\alpha\beta},\, \bar L_{\dot\alpha\dot\beta},\, W_{\alpha\dot\alpha}\}\,. \tag{5.33}$$

Translation invariance in the dual variables implies the symmetries

$$P_{\alpha\dot\alpha} = \sum_i \frac{\partial}{\partial x_i^{\dot\alpha\alpha}}\,, \qquad\qquad M = \sum_i \frac{\partial}{\partial n_i}\,. \tag{5.34}$$

and

$$Q_{\alpha\, a} = \sum_i \frac{\partial}{\partial \theta_i^{\alpha\, a}}\,, \qquad\qquad \tilde Q_{\dot\alpha\, a} = \sum_i \frac{\partial}{\partial \theta_i^{\dot\alpha\, a}}\,. \tag{5.35}$$

The Lorentz generators $L_{\alpha\beta}$, $\bar L_{\dot\alpha\dot\beta}$, $W_{\alpha\dot\alpha}$ are simply given by the action of the on-shell Lorentz generators $l_{\alpha\beta}$, $\bar l_{\dot\alpha\dot\beta}$, $w_{\alpha\dot\alpha}$ in dual superspace

$$L_{\alpha\beta} = \sum_i \left(x_{i(\alpha}^{\dot\alpha}\partial_{i\beta)\dot\alpha} + \theta_{i(\alpha}^{a}\frac{\partial}{\partial\theta_i^{\beta)a}}\right)\,, \qquad \bar L_{\dot\alpha\dot\beta} = \sum_i \left(x_{i(\dot\alpha}^{\alpha}\partial_{i\dot\beta)\alpha} + \tilde\theta_{i(\dot\alpha}^{a}\frac{\partial}{\partial\tilde\theta_i^{\dot\beta)a}}\right)\,, \tag{5.36}$$

and

$$W_{\alpha\dot\alpha} = \sum_i \left(x_{\alpha\dot\alpha}\frac{\partial}{\partial n} + 2\,n\frac{\partial}{\partial x_i^{\dot\alpha\alpha}} + \tilde\theta_{i\,\dot\alpha}^{a}\frac{\partial}{\partial\theta_i^{\alpha a}} - \theta_{i\,\alpha}^{a}\frac{\partial}{\partial\tilde\theta_i^{\dot\alpha a}}\right) \tag{5.37}$$

making the relation of $W_{\alpha\dot\alpha}$ to the Lorentz rotations $l_{\mu 5}$ more obvious than in on-shell superspace. The dual dilatation is given by

$$D = -\tfrac{1}{2}\sum_i \Big[2x_i^{\dot\alpha\alpha}\partial_{i\,\alpha\dot\alpha} + 2n\frac{\partial}{\partial n} + \theta_i^{\alpha\, a}\frac{\partial}{\partial\theta_i^{\alpha a}} + \tilde\theta_i^{\dot\alpha\, a}\frac{\partial}{\partial\tilde\theta_i^{\dot\alpha a}}\Big] \tag{5.38}$$

and acts covariantly on the amplitude

$$D f_n = n\, f_n\,. \tag{5.39}$$

From the six-dimensional superamplitude we know that the massive tree amplitudes are covariant under dual conformal inversion

$$I[f_n] = \left(\prod_i (x_i^2 - n_i^2)\right) f_n\,, \tag{5.40}$$

and we only need to find the representation of the dual conformal boost generator in the dual variables eq. (5.14). We emphasize that in order to obtain the correct expression for the $\mu = 0,1,2,3$ components of the dual conformal boost generator we cannot simply plug the $4d$ variables into the expression for K^{AB} given in eq. (1.182) since this leads to the wrong result. The four-dimensional spinor variables solve the constraint (1.21) on the six-dimensional spinors and thus spoil the assumed independence of chiral and anti-chiral spinors $\frac{\partial\tilde\lambda_A}{\partial\lambda^B} = 0$ in the six-dimensional representation of the dual conformal boost generator K^{AB}.

Since there is no obstacle in translating the inversion rules of the six-dimensional dual momenta (1.172), one possibility to obtain the action of the dual conformal boost generator $K_{\alpha\dot\beta} = IP_{\beta\dot\alpha}I$ in the full superspace is to start with the inversion rules for the bosonic dual variables

$$I[x_{\alpha\dot\beta}] = -\frac{x_{\beta\dot\alpha}}{x^2-n^2}\,, \qquad\qquad I[n] = \frac{n}{x^2-n^2}\,, \tag{5.41}$$

and extend the corresponding part of the dual conformal boost generator $K_{\alpha\dot\alpha}$ acting only on the bosonic dual variables

$$K_{\alpha\dot\alpha}\Big|_{x,n} = \sum_i \left(x_{i\,\alpha\dot\gamma}\, x_{i\,\dot\alpha\gamma}\, \frac{\partial}{\partial x_{i\,\gamma\dot\gamma}} + x_{i\,\alpha\dot\alpha}\, n_i \frac{\partial}{\partial n_i} + n_i^2\, \frac{\partial}{\partial x_i^{\dot\alpha\alpha}} \right) \tag{5.42}$$

such that it commutes with the constraints (5.15) to (5.19). Note that the additional minus sign in the inversion rules for n originates from the six-dimensional mostly minus metric $\eta_{55} = -1$.

Requiring that the dual conformal generator $K_{\alpha\dot\alpha}\Big|_{x,n}$ commutes with the bosonic constraints (5.15) to (5.17) leads to

$$\begin{aligned} K^{\text{boson}}_{\alpha\dot\alpha} = K_{\alpha\dot\alpha}\Big|_{x,n} + \tfrac{1}{2}\sum_i \Big[&(x_i + x_{i+1})^{\beta}{}_{\dot\alpha}\; l_{i\,\alpha\beta} + (x_i + x_{i+1})_{\alpha}{}^{\dot\beta}\; \bar l_{i\,\dot\alpha\dot\beta} \\ &+ (x_i + x_{i+1})_{\alpha\dot\alpha}\,(d_i - 1) + (n_i + n_{i+1})\, w_{i\,\alpha\dot\alpha} \Big] \end{aligned} \tag{5.43}$$

Since $K^{\text{boson}}_{\alpha\dot\alpha}$ has a non-vanishing commutator with the right hand side of the fermionic constraints (5.18) and (5.19), we have to introduce the following fermionic terms:

$$\begin{aligned} K^{\text{fermion}}_{\alpha\dot\alpha} = \sum_i \Big[&\theta^a_{i\,\alpha}\, x_{i\,\beta\dot\alpha}\, \frac{\partial}{\partial\theta^a_{i\,\beta}} + \tilde\theta^a_{i\,\dot\alpha}\, x_{i\,\alpha\dot\beta}\, \frac{\partial}{\partial\tilde\theta^a_{i\,\dot\beta}} + n_i\, \tilde\theta^a_{i\,\dot\alpha}\, \frac{\partial}{\partial\theta^{\alpha\,a}_i} + n_i\, \theta^a_{i\,\alpha}\, \frac{\partial}{\partial\tilde\theta^{\dot\alpha\,a}_i} \\ &+ \tfrac{1}{2}(\theta_i + \theta_{i+1})^a_{\alpha}\, \bar q_{i\,\dot\alpha\,a} + \tfrac{1}{2}(\theta_i + \theta_{i+1})^a_{\dot\alpha}\, \bar{\tilde q}_{i\,\alpha\,a} \Big] \end{aligned} \tag{5.44}$$

Their sum $K_{\alpha\dot\alpha} = K^{\text{boson}}_{\alpha\dot\alpha} + K^{\text{fermion}}_{\alpha\dot\alpha}$ commutes with all constraints. The part of $K_{\alpha\dot\alpha}$ acting on the on-shell variables is given by

$$\begin{aligned} K_{\alpha\dot\alpha}\Big|_{\text{on-shell}} = \tfrac{1}{2}\sum_i \Big[&(x_i + x_{i+1})^{\beta}{}_{\dot\alpha}\; l_{i\,\alpha\beta} + (x_i + x_{i+1})_{\alpha}{}^{\dot\beta}\; \bar l_{i\,\dot\alpha\dot\beta} + (n_i + n_{i+1})\, w_{i\,\alpha\dot\alpha} \\ &+ (x_i + x_{i+1})_{\alpha\dot\alpha}\,(d_i - 1) + (\theta_i + \theta_{i+1})^a_{\alpha}\, \bar q_{i\,\dot\alpha\,a} + (\theta_i + \theta_{i+1})^a_{\dot\alpha}\, \bar{\tilde q}_{i\,\alpha\,a} \Big]\,. \end{aligned} \tag{5.45}$$

The representation of $K_5 = IMI$ in the our four-dimensional variables can be obtained in a similar way or by Lorentz rotation $[W_{\alpha\dot\alpha}, K_{\beta\dot\beta}] = \epsilon_{\alpha\beta}\epsilon_{\dot\alpha\dot\beta}K_5$ of $K_{\alpha\dot\alpha}$. The representations of $K_{\alpha\dot\alpha}$ and K_5 in dual superspace are

$$\begin{aligned} K_{\alpha\dot\alpha} = \sum_i \Big[&x_{i\,\alpha\dot\gamma}\, x_{i\,\dot\alpha\gamma}\, \frac{\partial}{\partial x_{i\,\gamma\dot\gamma}} + x_{i\,\alpha\dot\alpha}\, n_i \frac{\partial}{\partial n_i} + n_i^2\, \frac{\partial}{\partial x_i^{\dot\alpha\alpha}} \\ &+ \theta^a_{i\,\alpha}\, x_{i\,\beta\dot\alpha}\, \frac{\partial}{\partial\theta^a_{i\,\beta}} + \tilde\theta^a_{i\,\dot\alpha}\, x_{i\,\alpha\dot\beta}\, \frac{\partial}{\partial\tilde\theta^a_{i\,\dot\beta}} + n_i\, \tilde\theta^a_{i\,\dot\alpha}\, \frac{\partial}{\partial\theta^{\alpha\,a}_i} - n_i\, \theta^a_{i\,\alpha}\, \frac{\partial}{\partial\tilde\theta^{\dot\alpha\,a}_i} \Big]\,, \end{aligned} \tag{5.46}$$

$$K_5 = \sum_i \Big[n_i^2 \frac{\partial}{\partial n_i} + 2\, n_i\, x_i^{\dot\alpha\alpha} \frac{\partial}{\partial x_i^{\dot\alpha\alpha}} + x_i^2 \frac{\partial}{\partial n_i} + \theta_i^{\alpha\, a}\, x_{i\,\alpha\dot\beta} \frac{\partial}{\partial \tilde\theta^a_{i\,\dot\beta}} + \tilde\theta^a_{i\,\dot\alpha}\, x_i^{\dot\alpha\beta} \frac{\partial}{\partial \theta_i^{\beta a}} + n_i\, \theta_i^{\alpha\, a} \frac{\partial}{\partial \theta_i^{\alpha\, a}} + n_i\, \tilde\theta_i^{a\,\dot\alpha} \frac{\partial}{\partial \tilde\theta_i^{\dot\alpha\, a}} \Big]. \tag{5.47}$$

and the action of K_5 on the on-shell variables is given by

$$K_5\Big|_{\text{on-shell}} = \tfrac{1}{2} \sum_i \Big[w_{i\,\alpha\dot\alpha} (x_i + x_{i+1})^{\dot\alpha\alpha} + 2(d_i - 1)(n_i + n_{i+1}) - (\tilde\theta_i - \tilde\theta_{i+1})^{\dot\alpha\, a} \bar q_{\dot\alpha\, a} + (\theta_i - \theta_{i+1})^{\alpha\, a} \bar{\tilde q}_{\alpha\, a} \Big] \tag{5.48}$$

The dual superconformal generators

$$\bar S_{\dot\alpha\, a} = \sum_i x_{i\,\alpha\dot\alpha} \frac{\partial}{\partial \theta^a_{i\,\alpha}} - n_i \frac{\partial}{\partial \theta_i^{\dot\alpha\, a}}\,, \qquad \bar{\tilde S}_{\alpha\, a} = \sum_i x_{i\,\alpha\dot\alpha} \frac{\partial}{\partial \tilde\theta^a_{i\,\dot\alpha}} + n_i \frac{\partial}{\partial \theta_i^{\alpha\, a}}\,. \tag{5.49}$$

can be obtained from the commutators of $K_{\alpha\dot\alpha}$ with the dual supermomenta Q_a^β and $\tilde Q_a^{\dot\beta}$. In full superspace they coincide with the supersymmetry generators $\bar q_{\dot\alpha\, a}$, $\bar{\tilde q}_{\alpha\, a}$

$$\bar S_{\dot\alpha\, a} = \bar q_{\dot\alpha\, a}\,, \qquad \bar{\tilde S}_{\dot\alpha\, a} = \bar{\tilde q}_{\alpha\, a}\,, \tag{5.50}$$

similar to the massless case. The dual conformal algebra reads

$$\begin{aligned}
[M, K_{\alpha\dot\alpha}] &= W_{\alpha\dot\alpha} & [M, K_5] &= -2\, D \\
[W_{\alpha\dot\alpha}, K_{\beta\dot\beta}] &= \epsilon_{\alpha\beta}\epsilon_{\dot\alpha\dot\beta} K_5 & [W_{\alpha\dot\alpha}, K_5] &= 2 K_{\alpha\dot\alpha} \\
[K_{\alpha\dot\alpha}, Q_a^\beta] &= \delta_\alpha^\beta \bar S_{\dot\alpha\, a} & [K_{\alpha\dot\alpha}, \tilde Q_a^{\dot\beta}] &= \delta_{\dot\alpha}^{\dot\beta} \bar{\tilde S}_{\alpha\, a} \\
[K_5, Q_a^\alpha] &= -\bar{\tilde S}_{\alpha\, a} & [K_5, \tilde Q_a^{\dot\alpha}] &= \bar S_{\dot\alpha\, a} \\
[K_{\alpha\dot\alpha}, P^{\dot\beta\beta}] &= \delta_\alpha^\beta \delta_{\dot\alpha}^{\dot\beta} D + \delta_\alpha^\beta \bar L_{\dot\alpha}{}^{\dot\beta} + \delta_{\dot\alpha}^{\dot\beta} L_\alpha{}^\beta
\end{aligned} \tag{5.51}$$

along with the generic $[D, J] = \dim(J) J$ for all generators J. We omitted all commutators that are either vanishing or equal to the corresponding commutators in the on-shell algebra eq. (5.29). The action of the R-symmetry charges r_a in dual superspace are given by

$$R_1 = \sum_i \left(\theta^1_{i\alpha} \frac{\partial}{\partial \theta_i^{\alpha\, 1}} + \tilde\theta^1_{i\dot\alpha} \frac{\partial}{\partial \tilde\theta_i^{\dot\alpha\, 1}} \right) - n + 4 \quad R_2 = \sum_i \left(\theta^2_{i\alpha} \frac{\partial}{\partial \theta_i^{\alpha\, 2}} + \tilde\theta^2_{i\dot\alpha} \frac{\partial}{\partial \tilde\theta_i^{\dot\alpha\, 2}} \right) - n + 4\,, \tag{5.52}$$

with the non-vanishing commutators

$$[R_a, Q_b] = -\delta_a^b Q_b\,, \quad [R_a, \tilde Q_b] = -\delta_a^b \tilde Q_b\,, \quad [R_a, \bar S_b] = -\delta_a^b \bar S_b\,, \quad [R_a, \bar{\tilde S}_b] = -\delta_a^b \bar{\tilde S}_b\,. \tag{5.53}$$

Some further Remarks are in order here. as we already mentioned, the generator $w_{\alpha\dot\alpha}$ arises from the Lorentz-generators $l^{\mu 5}$, just as m is related to the momentum in the extra dimensional direction p^5. As has been shown in [52], if the loop momentum is restricted to be four-dimensional, which is equivalent to the Higgs regularization

described in chapter 6, the cut constructable parts of the loop amplitudes invert as

$$I\left[\int\left(\prod_i^L d^4x_{l_i}\right)\mathcal{I}_n^L\right]=\left(\prod_i^n x_i^2\right)\int\left(\prod_i^L d^4x_{l_i}\right)\mathcal{I}_n^L\,. \tag{5.54}$$

Due to the four dimensional loop momenta, the five dimensional Lorentz invariance as well as the dual translation invariance in the x^5 direction are lost. Hence, $w_{\alpha\dot\alpha}$ is a manifest symmetry of the tree-superamplitudes but no symmetry of the Higgs regularized loop amplitudes. Since the dual conformal boost generator is given by $K^\mu = IP_\mu I$, the inversion properties (5.54) only imply that $(K^\mu + 2\sum_i x_i^\mu)$ is a symmetry of the regularized loop amplitudes for $\mu = 0,1,2,3$, whereas the tree-amplitudes have the full five-dimensional dual conformal symmetry.

5.3.1. Synergy and Yangian/Non-Local Symmetry

We want to ask the questions: Can one reinterpret the dual conformal operator in six dimensions as a non-local generator in a four dimensional massive theory? And what local densities of symmetry generators does it give rise to?

For this we proceed in great analogy to the work [49] where a Yangian symmetry of tree superamplitudes was established for $\mathcal{N}=4$ SYM, compare section 1.4.2. We continue by translating the expression for $K_{\alpha\dot\alpha}+\sum_i x_{i\,\alpha\dot\alpha}$ to four dimensional on-shell variables. Inserting

$$x_i^{\dot\alpha\alpha}=x_1^{\dot\alpha\alpha}-\sum_{j=1}^{i-1}p_j^{\dot\alpha\alpha} \qquad\qquad n_i=n_1-\sum_{j=1}^{i-1}m_j \tag{5.55}$$

$$\theta_{i\,\alpha}^a=\theta_{1\,\alpha}^a-\sum_{j=1}^{i-1}q_{i\,\alpha}^a \qquad\qquad \theta_{i\,\dot\alpha}^a=\theta_{1\,\dot\alpha}^a-\sum_{j=1}^{i-1}\tilde q_{i\,\dot\alpha}^a \tag{5.56}$$

into the part of the dual conformal boost generator acting on the on-shell variables eq. (5.45), one finds the interesting bi-spinorial result

$$\begin{aligned}K_{\alpha\dot\alpha}+\sum_i x_{i\,\alpha\dot\alpha}=&-\sum_{j<i}\Big[p_j^{\ \beta}{}_{\dot\alpha}\,l_{i\,\alpha\beta}+p_{j\,\alpha}{}^{\dot\beta}\bar l_{i\,\dot\alpha\dot\beta}+p_{j\,\alpha\dot\alpha}d_i+m_j w_{i\,\alpha\dot\alpha}+q_{j\,\dot\alpha}^a\bar{\tilde q}_{i\,\alpha\,a}+q_{j\,\alpha}^a\bar q_{i\,\dot\alpha\,a}\Big]\\&-\tfrac12\sum_{i=1}^n\Big[p_i^{\ \beta}{}_{\dot\alpha}\,l_{i\,\alpha\beta}+p_{i\,\alpha}{}^{\dot\beta}\bar l_{i\,\dot\alpha\dot\beta}+p_{i\,\alpha\dot\alpha}d_i+m_i w_{i\,\alpha\dot\alpha}+q_{i\,\dot\alpha}^a\bar{\tilde q}_{i\,\alpha\,a}+q_{i\,\alpha}^a\bar q_{i\,\dot\alpha\,a}\Big]\end{aligned} \tag{5.57}$$

Here we dropped the terms

$$+(x_1)_{\dot\alpha}{}^{\beta}l_{\alpha\beta}+(x_1)_{\alpha}{}^{\dot\beta}\bar l_{\dot\alpha\dot\beta}+(x_1)_{\alpha\dot\alpha}\,d+\,n_1\,w_{\alpha\dot\alpha}+(\theta_1)_\alpha^a\,\bar q_{\dot\alpha\,a}+(\theta_1)_{\dot\alpha}^a\,\bar{\tilde q}_{\alpha\,a}+\tfrac12 p_{\alpha\dot\alpha} \tag{5.58}$$

which annihilate the tree amplitudes on their own because they are each proportional to symmetry generators. Since the tree superamplitude is independent of x_1, θ_1, n_1 and $K_{\alpha\dot\alpha}+\sum_i x_{i\,\alpha\dot\alpha}$ annihilates it, one could also apply the reverse logic by concluding from (5.58) that $d, l_{\alpha\beta}, \bar l_{\dot\alpha\dot\beta}, w_{\alpha\dot\alpha}, \bar q_{\dot\alpha\,a}, \bar{\tilde q}_{\alpha\,a}$ are symmetries of the tree amplitudes. The Higgs regularized loop amplitudes explicitly depend on n_1 and are not invariant under $w_{\alpha\dot\alpha}$. Consequently, the term $n_1\,w_{\alpha\dot\alpha}$ cannot be dropped at loop level.

Let us proceed by investigating the structure of the dual conformal boost generator

in on-shell variables a bit further. Upon adding to $(K_{\alpha\dot\alpha} + \sum_i x_{i\,\alpha\dot\alpha})$ of eq. (5.57) the quantity

$$\Delta K_{\alpha\dot\alpha} = \tfrac{1}{2}\Big[p^{\beta}_{\dot\alpha}\, l_{\alpha\beta} + p^{\dot\beta}_{\alpha}\, \bar l_{\dot\alpha\dot\beta} + p_{\alpha\dot\alpha}\, d + m\, \bar w_{\alpha\dot\alpha} + q^{a}{}_{\dot\alpha}\, \bar q_{\alpha a} + q^{a}{}_{\alpha}\, \bar q_{\dot\alpha a}\Big]\,, \tag{5.59}$$

which is a manifest symmetry of the super-amplitudes, as $\{p_{\alpha\dot\alpha}, m, l_{\alpha\beta}, \bar l_{\dot\alpha\dot\beta}\}$ annihilate it, we find the bi-local representation of the level-one $p^{(1)}_{\alpha\dot\alpha}$ generator,

$$\begin{aligned} p^{(1)}_{\alpha\dot\alpha} &= K_{\alpha\dot\alpha} + \Delta K_{\alpha\dot\alpha} + \sum_i x_{i\,\alpha\dot\alpha} \\ &= -\tfrac{1}{2}\sum_{j<i}\Big[p_j^{\beta\dot\beta}\,(\epsilon_{\dot\alpha\dot\beta}\, l_{i\,\alpha\beta} + \epsilon_{\alpha\beta}\, \bar l_{i\,\dot\alpha\dot\beta} + \epsilon_{\alpha\beta}\,\epsilon_{\dot\alpha\dot\beta}\, d_i\,) + m_j\, w_{i\,\alpha\dot\alpha} \\ &\qquad + q^{a}_{j\,\dot\alpha}\, \bar q_{i\,\alpha a} + q^{a}_{j\,\alpha}\, \bar q_{i\,\dot\alpha a} - (i \leftrightarrow j)\Big]\,. \end{aligned} \tag{5.60}$$

which indeed obeys a level-one Yangian like relation, eq. (1.137),

$$[\, w_{\alpha\dot\alpha}, p^{(1)}_{\beta\dot\beta}\,] = 2\,\epsilon_{\alpha\beta}\,\epsilon_{\dot\alpha\dot\beta}\, m^{(1)}\,, \tag{5.61}$$

giving rise to the novel level one generator

$$m^{(1)} = -\tfrac{1}{4}\sum_{j<i}\Big[p_j^{\gamma\dot\gamma}\, w_{i\,\gamma\dot\gamma} + 2m_j\, d_i + q_j^{a\gamma}\, \bar q_{i\,\gamma a} + q^{a}_{j\,\dot\gamma}\, \bar q_i^{\dot\gamma}{}_{a} - (i \leftrightarrow j)\Big]\,. \tag{5.62}$$

One checks that it indeed obeys the commutation relation

$$[\, w_{\alpha\dot\alpha}, m^{(1)}\,] = p^{(1)}_{\alpha\dot\alpha}\,. \tag{5.63}$$

We note that $m^{(1)}$ can also be obtained from the action of K_5 on the on-shell variables (5.48) in the same way as $p^{(1)}$ has been obtained from $K_{\alpha\dot\alpha}$ in (5.42).

A natural question to be addressed in future work is whether or not there exist the level-one fermionic generators $q^{(1)}_{a\,\alpha}$, $q^{(1)}_{a\,\dot\alpha}$. However, already at this point it is clear that the non-local symmetry generators found will not lift to the complete super Poincaré algebra but rather stay confined to the super-translational piece. In particular there will be no level-one $w^{(1)}_{\alpha\dot\alpha}$ symmetry generator.

5.4. Tree Amplitudes of $\mathcal{N} = (1,1)$ SYM

Now that the symmetries of the massive amplitudes have been investigated in detail, we want to exploit these symmetries to calculate them. The most reasonable way of calculating the four-dimensional massive amplitudes on the Coulomb branch of $\mathcal{N} = 4$ SYM is by calculating the massless superamplitude of $\mathcal{N} = (1,1)$ SYM in six dimensions, which then can be dimensionally reduced as described in section 5.2.

In four dimensions the supersymmetric BCFW recursion, section 1.6.1, together with the dual conformal invariance, section 1.4.2, led to analytical formulae for all superamplitudes of $\mathcal{N} = 4$ SYM theory [46]. Key for this remarkable result were

the use of dual conformal invariant functions for the construction of a manifest dual conformal covariant solution to the BCFW recursion. Of similar importance was the MHV decomposition (1.61) of the superamplitudes, allowing to successively solve the recursion for the increasingly complex N^{p}MHV superamplitudes. Albeit the non-chiral superamplitudes of $\mathcal{N} = (1,1)$ SYM do not possess a decomposition according to the violation of the R-symmetry, they still have a dual conformal symmetry and obey a supersymmetric BCFW recursion relation. Hence, it is natural to try to find dual conformal invariant functions suitable to construct a solution to the BCFW recursion. Unfortunately, the six-dimensional BCFW recursion, as presented in section 1.6.2, is ill suited to produce reasonable analytical expressions. In contrast to four dimensions the shift (1.247) is not uniquely fixed and contains auxiliary spinor variables x_a, $x_{\dot{a}}$. Although the amplitudes are independent of these variables, their removal is non-trivial. The main obstacle is that the individual BCFW diagrams are in general not independent of x_a, $x_{\dot{a}}$ but only their sum, denying any straight forward removal of the auxiliary variables. In spite of its limitations the six-dimensional BCFW recursion is a powerful tool to obtain numerical values for arbitrary tree amplitudes of $\mathcal{N} = (1,1)$ SYM theory. As we will explain in what follows, this can be exploited to determine manifest dual conformal covariant representations of superamplitudes.

5.4.1. Analytical Formulae from Numerical BCFW

The general idea is to fix a sufficiently large set of dual conformal covariant functions $\Omega_{n,i}$ which are invariant under the dual symmetries $\{P_{AB}, M^A{}_B, Q_A, \tilde{Q}^A, B, \tilde{B}\}$, covariant under the dual dilatation D, and are symmetric under chiral conjugation. In other words the $\Omega_{n,i}$ are Lorentz invariant functions of differences of dual variables, have Grassmann degree $\Omega_{n,i} = \mathcal{O}(\theta^{n-4}\tilde{\theta}^{n-4})$, are of dimension $-n$, and invert in the same way as f_n

$$I[\Omega_{n,j}] = \left(\prod_i x_i^2\right) \Omega_{n,j} \,. \tag{5.64}$$

On the support of the momentum and supermomentum conserving delta functions, the $\Omega_{n,i}$ possess all continuous symmetries of f_n. Note that the invariance under the supersymmetry generators $\overline{q}^A$ and $\overline{\tilde{q}}_A$ follows from the invariance under Q_A, $\tilde{Q}^A$ and the covariance under dual conformal boosts K_{AB}, compare eqs. (1.183) and (1.186). Besides chiral symmetry, we could equally enforce the other discrete symmetries, which are cyclic invariance and the reflection symmetry. As will become clear in what follows, only enforcing symmetry under chiral conjugation is essential.

Given a set of functions $\{\Omega_{n,j}\}$, we can make the ansatz

$$f_n = \sum_i \alpha_i \Omega_{n,i} \,, \tag{5.65}$$

By construction, the coefficients are dimensionless, dual conformal invariant functions of differences x_{ij} of the region momenta x_i. The only dual conformal covariant objects that can be built from the x_{ij} are the traces

$$\widetilde{\mathrm{Tr}}(i_1 \dots i_{2k}) := (x_{i_1 i_2})_{A_1 A_2} (x_{i_2 i_3})^{A_2 A_3} \dots \left(x_{i_{2k-1} i_{2k}}\right)_{A_{2k-1} A_{2k}} (x_{i_{2k} i_1})^{A_{2k} A_1} \,. \tag{5.66}$$

However, these traces contain six-dimensional Levi-Civita tensors if six linear independent momenta are present, i. e. if $k > 3$ and $n > 6$. Since $\mathcal{N} = (1,1)$ SYM is a

non-chiral theory, all of its component amplitudes should be free of Levi-Civita tensors. Consequently, all Levi-Civita tensors present in the coefficients α_i have to cancel out if we project the ansatz eq. (5.65) onto any component amplitude. The functions $\Omega_{n,i}$ are symmetric under chiral conjugation and therefore cannot produce Levi-Civita tensors. Hence, we conclude that only the chiral symmetric traces

$$\mathrm{Tr}(i_1 \dots i_{2k}) = \tfrac{1}{2}\left(\widetilde{\mathrm{Tr}}(i_1 \dots i_{2k}) + \widetilde{\mathrm{Tr}}(i_2 \dots i_{2k} i_1)\right) \tag{5.67}$$

can appear in the coefficients. These traces are given by

$$\begin{aligned} \mathrm{Tr}(i\,j\,k\,l) &= 2(x_{ij}^2 x_{kl}^2 - x_{ik}^2 x_{jl}^2 + x_{il}^2 x_{jk}^2) \\ \mathrm{Tr}(i_1\,\dots\,i_{2k}) &= -\tfrac{1}{2}\sum_{\alpha=2}^{2k}(-1)^\alpha x_{i_1 i_\alpha}^2\,\mathrm{Tr}(i_2\,\dots\,i_{\alpha-1}\,i_{\alpha+1}\,\dots\,i_{2k})\,, \end{aligned} \tag{5.68}$$

and we can draw the important conclusion that the coefficients α_i are rational functions of dual conformal invariant cross ratios

$$u_{ijkl} = \frac{x_{ij}^2 x_{kl}^2}{x_{il}^2 x_{kj}^2}\,, \qquad \text{with} \qquad x_{ij}^2 \neq 0\,,\ x_{kl}^2 \neq 0\,,\ x_{il}^2 \neq 0\,,\ x_{kj}^2 \neq 0\,. \tag{5.69}$$

At multiplicity n, only $\nu_n = \frac{1}{2}n(n-5)$ of these cross ratios are independent. Since there are no cross ratios at four and five points, the α_i will be rational numbers in these cases. Unless the choice of the $\Omega_{n,i}$ has been extremely good, the α_i will depend on the phase space points for multiplicities greater than five. Nevertheless, it is straightforward to determine them using a numerical implementation of the BCFW recursion relation. Evaluating both sides of eq. (5.65) for a given phase space point π_j on a sufficiently large number of component amplitudes, the resulting linear equations can be solved for $\alpha_i(\pi_j)$. Numbering the cross ratios $\{u_1, u_2, \dots, u_{\nu_n}\}$ we make an ansatz for each of the coefficients

$$\alpha_i = \frac{a_0 + \sum_{i=1}^{k}\sum_{\{n_j\}_k} a_{n_1 \dots n_{\nu_n}} \prod_{\sigma=1}^{\nu_n} u_\sigma^{n_\sigma}}{b_0 + \sum_{i=1}^{k}\sum_{\{n_j\}_k} b_{n_1 \dots n_{\nu_n}} \prod_{\sigma=1}^{\nu_n} u_\sigma^{n_\sigma}}\,, \tag{5.70}$$

where $\{n_j\}_k$ are all different distributions of k powers among the cross ratios. Inserting the values of the cross ratios and the calculated values of the coefficients $\alpha_i(\pi_j)$ for a sufficiently large number of phase space points, the resulting linear equations can be solved for $\{a_I, b_I\}$.

Some remarks are in order here. It is very important to randomly choose the set of component amplitudes used to calculate the $\alpha_i(\pi_j)$. As will be demonstrated later, picking only amplitudes of a particular sector, like e. g. only gluon amplitudes, can lead to dual conformal extensions of this particular sector that are not equal to the full superamplitude. In practice one will successively increase the rank k of the polynomials in eq. (5.70) until a solution is found. In order to not have to worry about numerical uncertainties or instabilities, we chose to use rational phase space points. Using momentum twistors it is straightforward to generate four-dimensional rational phase space points which can be used to obtain rational six-dimensional phase space points of the form $p_i^\mu = \{p_i^0, 0, p_i^2, p_i^3, 0, p_i^5\}$. Although these phase space points only

have four non-zero components, they are sufficiently complex to yield non-zero results for all massive amplitudes. The only flaw in using them would have been the ruled out six-dimensional Levi-Civita tensors. The obvious benefit of the rational phase space points is that all found solutions to the ansatz eq. (5.65) are exact. An important property of the described method for the determination of the superamplitudes is that the obtained representations will contain only linear independent subsets of the basis functions $\Omega_{n,i}$. This may become an obstacle when looking for nice solutions with very simple coefficients α_i or ultimately for master formulae valid for arbitrary multiplicities since these do not necessarily consist only of linear independent $\Omega_{n,i}$.

Essential for making the ansatz, eq. (5.65), is knowledge of the possible dual conformal covariant objects involving dual fermionic momenta θ_i, $\tilde{\theta}_i$. Therefore we recall the inversion of the dual coordinates, compare (1.172)-(1.178),

$$I[x_{ij}^{AB}] = -(x_i^{-1}x_{ij}x_j^{-1})_{AB}\,, \qquad I[(x_{ij})_{AB}] = -(x_i^{-1}x_{ij}x_j^{-1})^{AB}\,, \tag{5.71}$$

$$I[\theta_i^A] = \theta_i^B(x_i^{-1})_{BA}\,, \qquad I[\tilde{\theta}_{i\,A}] = (x_i^{-1})^{AB}\tilde{\theta}_{i\,B}\,. \tag{5.72}$$

Clearly the objects

$$\begin{gathered}\langle\theta_{i_1}|x_{i_1i_2}\dots x_{i_{2k-1}i_{2k}}|\theta_{i_{2k}}\rangle \qquad [\tilde{\theta}_{i_1}|x_{i_1i_2}\dots x_{i_{2k-1}i_{2k}}|\tilde{\theta}_{i_{2k}}] \\ \langle\theta_{i_1}|x_{i_1i_2}\dots x_{i_{2k}i_{2k+1}}|\tilde{\theta}_{i_{2k+1}}]\end{gathered} \tag{5.73}$$

have inversion weight minus one on each of the appearing dual points but lack a translation invariance in θ and $\tilde{\theta}$. Fortunately there is a unique way to obtain manifest dual translation invariant objects from the dual conformal covariants eq. (5.73). We define the dual translation invariant objects

$$\langle B_{ijk}| = \langle\theta_{ij}|x_{jk}x_{ki}| + \langle\theta_{ik}|x_{kj}x_{ji}|\,, \qquad [\widetilde{B}_{ijk}| = [\tilde{\theta}_{ij}|x_{jk}x_{ki}| + [\tilde{\theta}_{ik}|x_{kj}x_{ji}|\,. \tag{5.74}$$

Because of $\langle B_{ijk}| = -|x_{ij}x_{jk}|\theta_{ki}\rangle - |x_{ik}x_{kj}|\theta_{ji}\rangle$ we define $|B_{ijk}\rangle = -\langle B_{ijk}|$ and similar for the chiral conjugate. The dual conformal inversion properties become obvious if we expand them in θ and $\tilde{\theta}$, leading to

$$\langle B_{ijk}| = -x_{jk}^2\langle\theta_i| + \langle\theta_j|x_{jk}x_{ki}| + \langle\theta_k|x_{kj}x_{ji}|\,. \tag{5.75}$$

Hence, the dual conformal covariant, dual translation invariant building blocks for the superamplitudes are

$$\langle B_{i_1i_2i_3}|m_1\,\dots\,m_{2k}|B_{j_1j_2j_3}\rangle = \langle B_{i_1i_2i_3}|x_{i_1m_1}x_{m_1m_2}\dots x_{m_{2k}j_1}|B_{j_1j_2j_3}\rangle\,, \tag{5.76}$$

$$[\widetilde{B}_{i_1i_2i_3}|m_1\,\dots\,m_{2k}|\widetilde{B}_{j_1j_2j_3}] = [\widetilde{B}_{i_1i_2i_3}|x_{i_1m_1}x_{m_1m_2}\dots x_{m_{2k}j_1}|\widetilde{B}_{j_1j_2j_3}]\,, \tag{5.77}$$

and

$$\langle B_{i_1i_2i_3}|m_1\,\dots\,m_{2k+1}|\widetilde{B}_{j_1j_2j_3}] = \langle B_{i_1i_2i_3}|x_{i_1m_1}x_{m_1m_2}\dots x_{m_{2k+1}j_1}|\widetilde{B}_{j_1j_2j_3}]\,. \tag{5.78}$$

They all have inversion weight minus one on every appearing dual point, e. g.

$$I\left(\,\langle B_{i_1i_2i_3}|m_1\,\dots\,m_{2k+1}|\widetilde{B}_{j_1j_2j_3}]\,\right) = \frac{\langle B_{i_1i_2i_3}|m_1\,\dots\,m_{2k+1}|\widetilde{B}_{j_1j_2j_3}]}{x_{i_1}^2x_{i_2}^2x_{i_3}^2x_{m_1}^2\dots x_{m_{2k+1}}^2x_{j_1}^2x_{j_2}^2x_{j_3}^2} \tag{5.79}$$

Keeping in mind that the degree in both θ and $\tilde{\theta}$ always increases by one if we successively increase the multiplicity, the last of the building blocks appears most natural. The first two building blocks necessarily appear in pairs and lead to a partial decoupling of the chiral and anti-chiral supermomenta. Consequently the building blocks eqs. (5.76) and (5.77) alone cannot be sufficient to construct an even multiplicity amplitude. Furthermore they are very unfavorable from the four-dimensional perspective as the massless projection of amplitudes containing them has an obscured R symmetry, for details we refer to section 5.5. Although we found solutions to eq. (5.65) containing all three types of building blocks, we will neglect the building blocks eqs. (5.76) and (5.77) in what follows.

To be more precise we will try to find representations of the superamplitudes with the general form

$$f_n = \sum_{I\,J\,K} \beta_{IJK} \prod_{i=1}^{n-4} \langle B_{I_i} | J_i | \widetilde{B}_{K_i}] \,, \tag{5.80}$$

where the coefficients β_{IJK} are functions of the dual conformal covariants x_{ij}^2 with the correct mass dimension and the correct inversion weights on each of the dual points in the multi-indices I, J, K. Manifest symmetry under chiral conjugation implies $\beta_{IJK} = (-1)^{n-4}\beta_{KJI}$.

Clearly not all of the building blocks (5.78) are independent. All simple relations follow from

$$\begin{aligned} \langle B_{i\,j\,k}| &= \langle B_{i\,k\,j}| \,, & \langle B_{i\,i+1\,k}| &= -\langle B_{i+1\,i\,k}| \,, \\ \langle B_{i\,j\,j+1}| &= 0 \,, & \langle B_{i\,i+1\,j}| x_{i\,i+1} &= 0 \,, \end{aligned} \tag{5.81}$$

and

$$\langle B_I| \dots i\,j\,k\,j\,l \dots |\widetilde{B}_J] = -x_{jk}^2 \langle B_I| \dots i\,l \dots |\widetilde{B}_J] \,. \tag{5.82}$$

5.4.2. The Four and Five Point Amplitudes

As an instructive illustration of the severe restrictions the dual conformal covariance, eq. (1.170), puts on the functional form of the superamplitudes, we consider the four point amplitude. Indeed, dual conformal covariance fixes the four point amplitude up to a constant and the only possible ansatz is

$$f_4 = \frac{\alpha}{x_{13}^2 x_{24}^2} \,. \tag{5.83}$$

The constant can be fixed by performing the dimensional reduction onto any massless four-dimensional amplitude. For the MHV gluon amplitude with negative helicity gluons at positions three and four we obtain

$$\begin{aligned} A_4(1^1{}_{\dot{1}}, 2^1{}_{\dot{1}}, 3^2{}_{\dot{2}}, 4^2{}_{\dot{2}}) &= \frac{\alpha}{x_{13}^2 x_{24}^2} \langle 1^1 2^1 3^2 4^2 \rangle \, [1_{\dot{1}} 2_{\dot{1}} 3_{\dot{2}} 4_{\dot{2}}] \\ &= \frac{\alpha}{x_{13}^2 x_{24}^2} \det \begin{pmatrix} 0 & 0 & \lambda_{3\alpha} & \lambda_{4\alpha} \\ \tilde{\lambda}_1^{\dot{\alpha}} & \tilde{\lambda}_2^{\dot{\alpha}} & 0 & 0 \end{pmatrix} \det \begin{pmatrix} 0 & 0 & \lambda_3^{\alpha} & \lambda_4^{\alpha} \\ -\tilde{\lambda}_{1\dot{\alpha}} & -\tilde{\lambda}_{2\dot{\alpha}} & 0 & 0 \end{pmatrix} \\ &= \frac{\alpha \, \langle 34 \rangle^2 \, [12]^2}{\langle 12 \rangle \, [21] \, \langle 23 \rangle \, [32]} = -\alpha \frac{\langle 34 \rangle^4}{\langle 12 \rangle \, \langle 23 \rangle \, \langle 34 \rangle \, \langle 41 \rangle} \,. \end{aligned} \tag{5.84}$$

Comparison with the well known Parke-Taylor formula yields $\alpha = -i$. This trivial calculation should be compared to the comparably complicated calculation using the BCFW recursion in references [54, 89].

Recalling the known result for the five point amplitude, eq. (1.148), we want to find the most simple representation of f_5 that is manifest dual conformal covariant. Hence we are searching for dual translation invariant functions of mass dimension minus five, that are of degree one in both θ and $\tilde{\theta}$ and invert as

$$I[f_5] = x_1^2 x_2^2 x_3^2 x_4^2 x_5^2 f_5 \,. \tag{5.85}$$

The most simple dual conformal covariant building blocks invariant under chiral conjugation are given by

$$\Omega_{i\,j\,k\,l\,m} := \tfrac{1}{2}\left(\langle B_{ijl}|\widetilde{B}_{ikm}] - \langle B_{ikm}|\widetilde{B}_{ijl}]\right) , \quad \text{with} \quad I[\Omega_{i\,j\,k\,l\,m}] = \frac{\Omega_{i\,j\,k\,l\,m}}{x_i^2 x_j^2 x_k^2 x_l^2 x_m^2} \,. \tag{5.86}$$

Obviously Ω_{ijklm} is zero if less than three of its indices are distinct. From the properties of $\langle B_{ijk}|$, eq. (5.81), and its definition above follow the properties

$$\begin{aligned} &\Omega_{i\,j\,k\,l\,m} = \Omega_{i\,l\,k\,j\,m} \,, && \Omega_{i\,j\,k\,l\,m} = -\Omega_{i\,k\,j\,m\,l} \,, && \Omega_{i\,i+1\,k\,l\,m} = -\Omega_{i+1\,i\,k\,l\,m} \,, \\ &\Omega_{i\,j\,k\,j+1\,m} = 0 \,. && \Omega_{i\,j\,k\,j\,m} = 0 && \Omega_{i\,i\,k\,j\,m} = 0 \,. \end{aligned} \tag{5.87}$$

At five point level the indices of $\Omega_{i\,j\,k\,l\,m}$ need to be a permutation of $\{1, 2, 3, 4, 5\}$. Applying the symmetry properties (5.87) to all these permutations of the indices reveal that they are either zero or up to a sign equal to $\Omega_{1\,2\,3\,4\,5}$. Furthermore $\Omega_{1\,2\,3\,4\,5}$ is cyclically symmetric

$$\Omega_{1\,2\,3\,4\,5} = \Omega_{2\,3\,4\,5\,1} = \Omega_{3\,4\,5\,1\,2} = \Omega_{4\,5\,1\,2\,3} = \Omega_{5\,1\,2\,3\,4} \,, \tag{5.88}$$

and has the reflection symmetry

$$\Omega_{1\,2\,3\,4\,5} = -\Omega_{5\,4\,3\,2\,1} \,. \tag{5.89}$$

Therefore the simplest possible structure for the five point amplitude is

$$\frac{\Omega_{1\,2\,3\,4\,5}}{x_{13}^2 x_{24}^2 x_{35}^2 x_{41}^2 x_{52}^2} \quad \text{with} \quad I\left[\frac{\Omega_{1\,2\,3\,4\,5}}{x_{13}^2 x_{24}^2 x_{35}^2 x_{41}^2 x_{52}^2}\right] = x_1^2 x_2^2 x_3^2 x_4^2 x_5^2 \frac{\Omega_{1\,2\,3\,4\,5}}{x_{13}^2 x_{24}^2 x_{35}^2 x_{41}^2 x_{52}^2} \,. \tag{5.90}$$

Since there are no dual conformal invariant cross ratios at five point level, we know that eq. (5.90) is either up to a constant equal to f_5 or we need to make a more complicated ansatz including the building blocks $\langle B_{ijk}|x_{il}x_{lk}|\widetilde{B}_{kmn}]$. Comparing this ansatz with the numerical BCFW recursion we indeed find the beautiful result

$$f_5 = -i\frac{\Omega_{1\,2\,3\,4\,5}}{x_{13}^2 x_{24}^2 x_{35}^2 x_{41}^2 x_{52}^2} \,. \tag{5.91}$$

This remarkably compact representation of the five point amplitude makes all continuous and discrete symmetries of the superamplitude manifest. Interestingly it can be simplified even more if we do not require manifest symmetry under chiral conjugation. On the support of the momentum and supermomentum conserving delta functions

$\langle B_{124}|\widetilde{B}_{135}]$ is symmetric under chiral conjugation

$$\langle B_{124}|\widetilde{B}_{135}] = -\langle B_{135}|\widetilde{B}_{124}] \tag{5.92}$$

and the five point amplitude is given by

$$\mathcal{A}_5 = -i\delta^{(4)}(q)\delta^{(4)}(\tilde{q})\frac{\langle B_{124}|\widetilde{B}_{135}]}{x_{13}^2 x_{24}^2 x_{35}^2 x_{41}^2 x_{52}^2}\,. \tag{5.93}$$

This is the most compact dual conformal covariant representation of the five point amplitude and should be compared to the representation (1.148). Making the dual conformal properties manifest led to a significant simplification. After (5.93) has been found another manifest dual conformal covariant representation appeared in reference [85] by uplifting the four-dimensional five point amplitude of non-chiral superspace. We will discuss the potential uplift of massless four-dimensional amplitudes in section 5.5.

5.4.3. The Six Point Amplitude

As it turned out, the four and also the five point amplitudes were trivial examples of our general ansatz eq. (5.65), since the coefficients α_i were constants. At six points they will in general no longer be constant but rational functions of the three dual conformal invariant cross ratios

$$u_1 = \frac{x_{13}^2 x_{46}^2}{x_{14}^2 x_{36}^2}\,, \qquad u_2 = \frac{x_{15}^2 x_{24}^2}{x_{14}^2 x_{25}^2}\,, \qquad u_3 = \frac{x_{26}^2 x_{35}^2}{x_{25}^2 x_{36}^2}\,. \tag{5.94}$$

Similar to the five point case we try to find a representation of the six point amplitude using only the simplest of the building blocks of eq. (5.78). To further reduce the resulting basis, we require chiral symmetry of the building blocks. Hence we only use the Ω_{ijklm} defined in eq. (5.86). In contrast to five points the objects Ω_{ijjlm} are not all zero at multiplicity six. Nevertheless, we neglect them and stick to the Ω_{ijklm} with distinct indices. What we are left with are the six building blocks

$$\begin{aligned}
\Omega_1 &:= \Omega_{12345}\,,\\
\Omega_2 &:= \Omega_{23456}\\
\Omega_3 &:= \Omega_{34561}\,,\\
\Omega_4 &:= \Omega_{45612}\,,\\
\Omega_5 &:= \Omega_{56123}\,,\\
\Omega_6 &:= \Omega_{61234}
\end{aligned} \tag{5.95}$$

The basis of fifteen terms that we built from the Ω_i is

$$\Omega_{ij} = \frac{\beta_{ij}\Omega_i\Omega_j}{x_{13}^2 x_{24}^2 x_{35}^2 x_{46}^2 x_{51}^2 x_{62}^2} \tag{5.96}$$

where the β_{ij} cancel out the inversion weights of the four overlapping indices present in $\Omega_i\Omega_j$. Because of the existence of the three cross ratios, β_{ij} are not uniquely fixed.

One possible choice is

$$\beta_{ij} = \begin{pmatrix} 0 & (x_{24}^2 x_{35}^2)^{-1} & (x_{14}^2 x_{35}^2)^{-1} & (x_{15}^2 x_{24}^2)^{-1} & (x_{13}^2 x_{25}^2)^{-1} & (x_{13}^2 x_{24}^2)^{-1} \\ 0 & 0 & (x_{35}^2 x_{46}^2)^{-1} & (x_{25}^2 x_{46}^2)^{-1} & (x_{26}^2 x_{35}^2)^{-1} & (x_{24}^2 x_{36}^2)^{-1} \\ 0 & 0 & 0 & (x_{15}^2 x_{46}^2)^{-1} & (x_{35}^2 x_{46}^2)^{-1} & (x_{13}^2 x_{46}^2)^{-1} \\ 0 & 0 & 0 & 0 & (x_{15}^2 x_{26}^2)^{-1} & (x_{14}^2 x_{26}^2)^{-1} \\ 0 & 0 & 0 & 0 & 0 & (x_{13}^2 x_{26}^2)^{-1} \\ 0 & 0 & 0 & 0 & 0 & 0 \end{pmatrix} \tag{5.97}$$

We exclude terms of the form $(\Omega_i)^2$ and make the following ansatz for the five point amplitude

$$f_6 = \sum_{i<j} \alpha_{ij} \Omega_{i\,j}\,. \tag{5.98}$$

with $\alpha_{ij} = \alpha_{ij}(u_1, u_2, u_3)$ being a rational function of the cross ratios. Making an ansatz of the form eq. (5.70) it is straightforward to determine the α_{ij}. The first observation is that out of our fifteen basis elements only eleven are linearly independent, leading to a large number of different representations of the form (5.98). The highly nontrivial linear relations between the $\Omega_{i\,j}$ are only valid on the support of the momentum and supermomentum conserving delta functions and can be determined in the same way as the amplitude. The two ten-term and two eleven-term identities involving complicated functions of the cross ratios can be used to transform a particular solution to eq. (5.98) to any other solution of this form. The complexity of the coefficients α_{ij} varies largely with the choice of linear independent $\Omega_{i\,j}$ in the solution, e. g. some solutions involve rational functions of degree twelve in the cross rations u_i. The three simplest of the solutions involve nine $\Omega_{i\,j}$ and rational functions of degrees less than three. One particular of these simple solutions is

$$(\alpha_{ij}) = \frac{1}{1+u_1-u_2-u_3} \begin{pmatrix} 0 & u_2 u_3 & -u_3 & u_2\,(u_3-u_1) & 0 & 0 \\ 0 & 0 & 0 & 0 & u_3\,(u_2-u_1) & -u_2 \\ 0 & 0 & 0 & 0 & -u_2 & u_1\,(u_2+u_3) \\ 0 & 0 & 0 & 0 & u_2 u_3 & -u_3 \\ 0 & 0 & 0 & 0 & 0 & 0 \\ 0 & 0 & 0 & 0 & 0 & 0 \end{pmatrix}. \tag{5.99}$$

Inserting the coefficients, the definitions of Ω_{ij} and the cross rations u_i, as well as the identity

$$\mathrm{Tr}\,(1\,2\,3\,5\,6\,4) = x_{14}^2 x_{25}^2 x_{36}^2\,(1+u_1-u_2-u_3)\,, \tag{5.100}$$

into the ansatz eq. (5.98), the six point amplitude reads

$$\begin{aligned} f_6 = \frac{1}{x_{13}^2 x_{24}^2 x_{35}^2 x_{46}^2 x_{51}^2 x_{62}^2} \frac{i}{\mathrm{Tr}\,(1\,2\,3\,5\,6\,4)} \Bigg(& -x_{26}^2 \Omega_1 \Omega_3 - x_{15}^2 \Omega_2 \Omega_6 - x_{24}^2 \Omega_3 \Omega_5 - x_{35}^2 \Omega_4 \Omega_6 \\ & + \frac{x_{26}^2 x_{15}^2}{x_{25}^2} \Omega_1 \Omega_2 + \frac{x_{24}^2 x_{35}^2}{x_{25}^2} \Omega_4 \Omega_5 + \left(\frac{x_{15}^2 x_{24}^2}{x_{25}^2} - \frac{x_{13}^2 x_{46}^2}{x_{36}^2} \right) \Omega_2 \Omega_5 \\ & + \left(\frac{x_{26}^2 x_{35}^2}{x_{25}^2} - \frac{x_{13}^2 x_{46}^2}{x_{14}^2} \right) \Omega_1 \Omega_4 + \left(\frac{x_{15}^2 x_{24}^2}{x_{14}^2} + \frac{x_{26}^2 x_{35}^2}{x_{36}^2} \right) \Omega_3 \Omega_6 \Bigg). \end{aligned} \tag{5.101}$$

Note that this representation of the six point amplitude has an unphysical pole $u_2 + u_3 - u_1 = 1$, contained in the trace. From the analysis of the solutions to eq. (5.98) we conclude that unphysical poles are a general feature for representations in terms of the Ω_{ij}. Of course, all the unphysical poles are only spurious and cancel out if we project onto any component amplitude. The other two nine term solutions can be obtained by cyclic permutations of eq. (5.101).

Albeit all continuous symmetries and the symmetry under chiral conjugation of the six point amplitude are manifest in the solutions to eq. (5.98), the cyclic[2] and reflection symmetry are not obvious. However, there is no obstacle in finding manifest cyclically symmetric representations by constructing manifest cyclically symmetric basis elements from the Ω_i. As a consequence of the manifest cyclic invariance of the basis, the coefficients in the general ansatz eq. (5.65) are cyclically symmetric as well, i. e. are rational functions of symmetric polynomials of the cross ratios.

There are three types of such manifest cyclically symmetric basis elements

$$\begin{aligned} &g_1(u_1,u_2,u_3)\Omega_{12} + \text{five cyclic rotations} \\ &g_2(u_1,u_2,u_3)\Omega_{13} + \text{five cyclic rotations} \\ &g_3(u_1,u_2,u_3)\Omega_{14} + f_3(u_2,u_3,u_1)\Omega_{24} + f_3(u_3,u_1,u_2)\Omega_{36} \end{aligned} \tag{5.102}$$

The functions g_i are arbitrary rational functions of the cross ratios leaving a lot of freedom to define a cyclic basis. Looking at the solution eq. (5.99), reasonable choices are $g_1 \in \{u_1u_2, u_1u_3, u_2u_3\}$, $g_2 \in \{u_1, u_2, u_3\}$, and $g_3 \in \{u_1(u_2 \pm u_3), u_2(u_3 \pm u_1), u_3(u_1 \pm u_2)\}$. Indeed, this leads to a solution involving only three cyclically symmetric basis elements. Choosing $g_1 = u_2u_3$, $g_2 = u_3$, and $g_3 = u_2(u_1 + u_3)$ we find

$$(\alpha_i) = \frac{1}{3 - u_1 - u_2 - u_3}\begin{pmatrix} 1 & -2 & 1 \end{pmatrix} \tag{5.103}$$

or equivalently

$$\begin{aligned} f_6 = \frac{1}{x_{13}^2x_{24}^2x_{35}^2x_{46}^2x_{51}^2x_{62}^2}\frac{i}{x_{14}^2x_{25}^2x_{36}^2(3-u_1-u_2-u_3)}\Bigg(&\frac{x_{15}^2x_{26}^2}{x_{25}^2}\,\Omega_1\Omega_2 - 2\,x_{26}^2\,\Omega_1\Omega_3 + \\ &+ \left(\frac{x_{13}^2x_{46}^2}{x_{14}^2} + \frac{x_{26}^2x_{35}^2}{x_{25}^2}\right)\Omega_1\Omega_4 + \text{cyclic permutations}\Bigg)\,. \end{aligned} \tag{5.104}$$

Clearly this representation is not minimal as it consists of all fifteen Ω_{ij}. The contained unphysical pole at $u_1 + u_2 + u_3 = 3$, might be expressed by the traces

$$x_{14}^2x_{25}^2x_{36}^2\,(3-u_1-u_2-u_3) = \tfrac{1}{2}\,(\ \mathrm{Tr}\,(1\,2\,3\,5\,6\,4) + \text{cyclic permutations}\ )\,. \tag{5.105}$$

As emphasized in section 5.4.1 it is very important to randomly choose the component amplitudes which are used to calculate the coefficients α_i in the general ansatz eq. (5.65). Since we are dealing with a maximally supersymmetric theory one might wonder if it would not be sufficient to consider e. g. only gluon amplitudes and let supersymmetry care for all other amplitudes. Indeed this is a widespread claim within the literature which can be easily disproved. In fact, only eight of the fifteen Ω_{ij} are linear independent on gluon amplitudes compared to eleven on all component amplitudes. Consequently, supersymetrizing gluon amplitudes as has been done in reference [89]

[2]Equation (5.101) is manifest invariant under the cyclic permutation $i \to i + 3$.

for the three, four and five point amplitudes will not yield the correct superamplitude for multiplicities greater than five. Having said that, it is nevertheless interesting to investigate how such a supersymmetrization of the gluon amplitudes looks like. Therefore we try to find a dual conformal invariant extension of the gluon amplitudes, that is a solution to eq. (5.65) valid on all gluon amplitudes. At six points we do not have to worry about six-dimensional Levi-Civita tensors and it is not necessary to use chiral self-conjugate building blocks. Instead of the Ω_i we use the building blocks

$$\Omega^u_{i,j} = \langle B_{i\,i+1\,i+3}|\widetilde{B}_{i\,i+2\,i+4}]\,, \qquad \Omega^d_{i,n} = \langle B_{i\,i-1\,i-3}|\widetilde{B}_{i\,i-2\,i-4}] \tag{5.106}$$

where the label j indicates that the indices $\{i, i\pm1, i\pm2, \pm3, i\pm4\}$ in $\Omega^{u/d}_{i,n}$ have to be taken modulo j. Whenever the label j is equal to the multiplicity n, we will usually drop it. The $\Omega^{u/d}_i$ are related to the chiral self-conjugate Ω_i by

$$\Omega_i = \tfrac{1}{2}\left(\Omega^u_i - \Omega^d_{i+4}\right)\,. \tag{5.107}$$

The resulting ansatz for the dual conformal extension of the gluon sector is

$$\begin{aligned} f_6\big|_{\text{gluons}} = \frac{i}{x^2_{13}x^2_{24}x^2_{35}x^2_{46}x^2_{51}x^2_{62}x^2_{14}x^2_{25}x^2_{36}}\Big(\sum_{i,j}\ & \alpha_{ij}x^2_{i-1\,j-1}\Omega^u_i\Omega^u_j \\ & + \beta_{ij}x^2_{i-1\,j+1}\Omega^u_i\Omega^d_j \\ & + \gamma_{ij}x^2_{i+1\,j+1}\Omega^d_i\Omega^d_j\Big) \end{aligned} \tag{5.108}$$

Since the gluon sector is not closed under dual conformal symmetry, the massless coefficients α_{ij}, β_{ij}, γ_{ij} are in general rational functions of the Lorentz invariants x^2_{kl}. As expected not all of the $\Omega^{u/d}_i\Omega^{u/d}_j$ are linear independent on the gluon amplitudes. A good indication that we will find dual conformal covariant solutions to eq. (5.108) is the fact that all two term identities that the $\Omega^{u/d}_i\Omega^{u/d}_j$ fulfill on the gluon amplitudes are in fact dual conformal covariant. On the support of the momentum and supermomentum conserving delta functions we have for example the six identities

$$\begin{aligned} x^2_{i-1\,i+1}\Omega^u_i\Omega^d_i\big|_{\text{gluons}} &= x^2_{i+2\,i+4}\Omega^u_{i+3}\Omega^d_{i+3}\big|_{\text{gluons}}\,, \\ x^2_{i-1\,i+3}\Omega^u_i\Omega^d_{i+2}\big|_{\text{gluons}} &= x^2_{i+2\,i}\Omega^u_{i+3}\Omega^d_{i+5}\big|_{\text{gluons}}\,. \end{aligned} \tag{5.109}$$

Indeed there are 24 nice three term solutions to eq. (5.108) that are all dual conformal covariant. One of these solutions is

$$f_6\big|_{\text{gluons}} = \frac{i}{x^2_{13}x^2_{24}x^2_{35}x^2_{46}x^2_{51}x^2_{62}x^2_{14}x^2_{25}x^2_{36}}\left(x^2_{24}\Omega^d_3\Omega^u_3 - x^2_{13}\Omega^d_2\Omega^d_6 - x^2_{26}\Omega^u_1\Omega^u_3\right)\,. \tag{5.110}$$

Unfortunately, none of the found dual conformal extensions of the gluon sector were equal to the superamplitude. However, they all gave the correct ultra helicity violating (UHV) amplitudes.

5.4.4. Towards Higher Multiplicities

Inspired by the compact representations eqs. (5.91), (5.101) and (5.104) the next logical step is to try to find a nice representation of the seven point amplitude with the

ultimate goal of a master formula valid for arbitrary multiplicities. The main difficulty at higher multiplicities is to make a good choice for the basis $\Omega_{n,i}$ used to express the amplitude, compare eq. (5.65). Going from five to six partons the number of terms in the amplitudes increased roughly by a factor of ten. Hence, the number of terms in the seven point amplitude is expected to be of order 100, making systematic studies of the solutions to eq. (5.65) impossible for multiplicities $n > 6$. Furthermore, the generic solution α_i to eq. (5.65) contains complicated rational functions of the $\nu_n = \frac{1}{2}n(n-5)$ cross ratios which require a huge calculational effort to be obtained from the BCFW recursion using eq. (5.70).

At seven points, a natural starting point is to use a basis constructed from products of the chiral self-conjugate $\Omega_{i\,j\,k\,l\,m}$ defined in eq. (5.86). Hence, the ansatz for the seven point amplitude reads

$$f_7 = \sum_{I,J,K} \alpha_{IJK}\beta_{IJK}\Omega_I\Omega_J\Omega_K \tag{5.111}$$

where the coefficient β_{IJK} are functions of the covariants x_{ij}^2 compensating the negative inversion weights in the dual points present in $\{I, J, K\}$. The β_{IJK} have mass dimension -22 and are straightforward to obtain by counting the inversion weights in $\{I, J, K\}$, compare eq. (5.97). The dimensionless α_{IJK} are rational functions of the seven cross ratios

$$u_i = \frac{x_{i\,i+2}^2 x_{i+3\,i+6}^2}{x_{i\,i+3}^2 x_{i+2\,i+6}^2}\,. \tag{5.112}$$

Even if we restrict the basis to products of distinct Ω_I and only consider $\Omega_I = \Omega_{i_1\,i_2\,i_3\,i_4\,i_5}$ with distinct indices we end up with more than 10^4 basis elements. Solving for $\alpha_{IJK}(\pi_i)$ at different phase space points reveals that approximately 70 basis elements are required to obtain a representation of the seven point amplitude. Analyzing different choices of a linear independent subset of basis elements, for none of them the complexity of the coefficients α_{IJK} turned out to be sufficiently low to justify the computational effort necessary to determine their analytical form. Due to the astronomical number of different solutions to eq. (5.111) it is impossible to decide whether or not simple solutions to it exist or if the restriction to use only the building blocks Ω_{ijklm} needs to be relaxed.

Looking at the representations eqs. (5.91), (5.101) and (5.104) found for the five and six point amplitude we observe the prefactor

$$\frac{1}{\prod x_{ij}^2}\,, \qquad \text{with} \qquad I\left[\frac{1}{\prod x_{ij}^2}\right] = \frac{(\prod x_i^2)^{n-3}}{\prod x_{ij}^2}\,, \tag{5.113}$$

containing the product of all $\frac{1}{2}n(n-3)$ physical poles. It seems natural to expect this prefactor in a potential master formula for arbitrary multiplicities. With the definition

$$\Omega_{I;J;K} = \tfrac{1}{2}\left(\langle B_I|J|\widetilde{B}_K] - \langle B_K|J|\widetilde{B}_I]\right) \tag{5.114}$$

of the chiral self-conjugate building blocks $\Omega_{I;J;K}$ we can easily write down a nice ansatz valid for arbitrary multiplicities

$$f_n = \frac{1}{\prod x_{ij}^2} \sum_{I,J,K,L} \alpha_{I,J,K,L}\,\Omega_I \prod_{i=1}^{n-5} \Omega_{J_i;K_i;L_i}\,. \tag{5.115}$$

Here the sum goes over all multi-indices $I = \{i_1, i_2, i_3, i_4, i_5\}$, $J = \{J_1, \ldots, J_{n-5}\}$,

$K = \{K_1, \ldots, K_{n-5}\}$, $L = \{L_1, \ldots, L_{n-5}\}$ with $|J_i| = |L_i| = 3$, $|K_i| = 2i - 1$, where $\{I, J, K, L\}$ is a permutation of $\{\{1\}^{n-4}, \ldots, \{n\}^{n-4}\}$. By construction the $\alpha_{I,J,K,L}$ are dimensionless and dual conformal invariant. Clearly the representation of the five point amplitude eq. (5.91) is a solution to eq. (5.115) whereas the representations of the six point amplitude eqs. (5.101) and (5.104) are not a solution to it. We leave it to future work to investigate whether there exist nice solutions to the master ansatz eq. (5.115) for multiplicities greater than five.

5.4.5. The Little Group Decomposition of the Superamplitudes

With regard to the MHV decomposition of the massless amplitudes of $\mathcal{N} = 4$ SYM it would be nice to have a similar decomposition of the massless six-dimensional amplitudes of $\mathcal{N} = (1, 1)$ into sectors of varying complexity. Here we propose a decomposition of the amplitudes according to the violation of the $SU(2) \times SU(2)$ little group which is the six-dimensional analog of the MHV-band decomposition introduced by N. Craig, H. Elvang, M. Kiermaier, T. Slatyer in reference [51].

The starting point is the decomposition of the six-dimensional superamplitude into the component amplitudes A_n

$$\mathcal{A}_n = \sum_{I,J} \xi_{i_1 a_1} \xi_{i_2 a_2} \ldots \xi_{i_n a_n} \tilde{\xi}^{\dot{b}_1}_{j_1} \tilde{\xi}^{\dot{b}_2}_{j_2} \ldots \tilde{\xi}^{\dot{b}_n}_{j_n} A_n \left(i_1^{a_1}, i_2^{a_2}, \ldots, i_n^{a_n}, j_{1\dot{b}_1}, j_{2\dot{b}_2}, \ldots, j_{n\dot{b}_n} \right) , \quad (5.116)$$

with neither possible values of the little group indices $a_i = 1$ or $a_i = 2$ as well as $\dot{b}_i = 1$ or $\dot{b}_i = 2$ being singlet out. With regard to the particular choice of six-dimensional Pauli matrices eqs. (A.13) and (A.24) and the resulting map of the six-dimensional supermomenta

$$q^A = \begin{pmatrix} q^1_\alpha \\ \tilde{q}^{\dot{\alpha}}_3 \end{pmatrix} , \qquad \tilde{q}_A = \begin{pmatrix} -q^{\alpha\,4} & -\tilde{q}_{\dot{\alpha}\,2} \end{pmatrix} . \quad (5.117)$$

and Grassmann variables

$$\xi_a = \left(\tilde{\eta}_3, \eta^1 \right) , \qquad \tilde{\xi}^{\dot{a}} = \left(\tilde{\eta}_2, -\eta^4 \right) , \quad (5.118)$$

derived in section 1.5.2, this is no longer true if we project to four dimensions where e. g. $\xi_1, \tilde{\xi}^{\dot{1}}$, or $\xi_2, \tilde{\xi}^{\dot{2}}$ correspond to a positive, or a negative helicity gluon.

It is instructive to translate the MHV decomposition of the massless four-dimensional superamplitudes into six-dimensional language. Because of the $SU(4)_R$ symmetry the N^{p}MHV superamplitude in chiral superspace has the Grassmann dependence

$$\text{4d chiral superspace:} \qquad \mathcal{A}_n^{\text{N}^p\text{MHV}} = \mathcal{O}\left((\eta^1)^{p+2} (\eta^2)^{p+2} (\eta^3)^{p+2} (\eta^4)^{p+2} \right) \quad (5.119)$$

According to eq. (1.70), the chiral super field $\mathcal{A}_n(\Phi_1, \ldots, \Phi_1)$ is related to the non-chiral superfield $\mathcal{A}_n(\Upsilon_1, \ldots, \Upsilon_n)$ by the half Fourier transformation

$$\mathcal{A}_n(\Upsilon_1, \ldots, \Upsilon_n) = \prod_i \int d\eta_i^3 d\eta_i^2 \; e^{\eta_i^2 \tilde{\eta}_{i\,2} + \eta_i^3 \tilde{\eta}_{i\,3}} \mathcal{A}_n(\Phi_1, \ldots, \Phi_1) . \quad (5.120)$$

Consequently, the N^{p}MHV superamplitude in non-chiral superspace has the Grassmann

dependence

$$\text{4d non-chiral superspace:} \qquad \mathcal{A}_n^{\mathrm{N}^p\mathrm{MHV}} = \mathcal{O}\left((\eta^1)^{p+2}(\tilde{\eta}_2)^{n-p-2}(\tilde{\eta}_3)^{n-p-2}(\eta^4)^{p+2}\right) . \tag{5.121}$$

With the help of the map eq. (5.118) between the four-dimensional and six-dimensional Grassmann variables we can deduce which of the six-dimensional component amplitudes $A_n\left(i_1^{a_1}, \ldots, i_n^{a_n}, j_{1\dot{b}_1}, \ldots, j_{n\dot{b}_n}\right)$, defined in eq. (5.116), correspond to massless four-dimensional N^{p}MHV amplitudes

$$\text{6d non-chiral superspace:} \qquad \mathcal{A}_n\Big|_{\mathrm{N}^p\mathrm{MHV}} = \mathcal{O}\left((\xi_1)^{n-p-2}(\xi_2)^{p+2}(\tilde{\xi}^{\dot{1}})^{n-p-2}(\tilde{\xi}^{\dot{2}})^{p+2}\right) . \tag{5.122}$$

Hence, the $SU(4)_R$ symmetry of the massless chiral superamplitudes in four dimensions leads to a Grassmann dependence of the form $(\xi_1)^{n-a}(\xi_2)^a(\tilde{\xi}^{\dot{1}})^{n-a}(\tilde{\xi}^{\dot{2}})^a$ in six dimensions. From the six-dimensional perspective the Grassmann dependence of the superamplitudes in the massless four-dimensional limit is a consequence of breaking the $SU(2) \times SU(2)$ little group to a $U(1)$ little group in four dimensions because on the four-dimensional subspace the chiral and anti-chiral spinors λ^A and $\tilde{\lambda}_A$ are equal.

In the case of the massive four dimensional amplitudes the $SU(4)_R$ symmetry is broken and the Grassmann dependence of the corresponding six-dimensional superamplitude is no longer restricted, i. e. all terms of the form $(\xi_1)^{n-a}(\xi_2)^a(\tilde{\xi}^{\dot{1}})^{n-b}(\tilde{\xi}^{\dot{2}})^b$ are appearing except the ones with $a,\, b \in \{0, n\}$, and we propose the following little group decomposition of the superamplitudes of $\mathcal{N} = (1,1)$ SYM

$$\mathcal{A}_n = \sum_{a=1}^{n-1}\sum_{b=1}^{n-1} \mathcal{A}_n^{a\times b}, \qquad \text{with} \qquad \mathcal{A}_n^{a\times b} = \mathcal{O}\left((\xi_1)^{n-a}(\xi_2)^a(\tilde{\xi}^{\dot{1}})^{n-b}(\tilde{\xi}^{\dot{2}})^b\right) . \tag{5.123}$$

This decomposition can be further motivated by translating the Grassmann dependence of $\mathcal{A}_n^{a\times b}$ back to chiral superspace using eqs. (5.118) and (5.120)

$$\text{6d:} \qquad \mathcal{A}_n^{a\times b} \qquad \longrightarrow \qquad \text{4d:} \qquad \mathcal{O}\left((\eta^1)^a(\eta^3)^a(\eta^2)^b(\eta^4)^b\right) \tag{5.124}$$

Hence the little group decomposition in six dimensions corresponds to breaking the four-dimensional $SU(4)_R$ symmetry to a $SU(2)_R \times SU(2)_R$ symmetry.

For the little group decomposition to be of any use, the complexity of the $\mathcal{A}_n^{a\times b}$ should vary with the values of a and b. In the massless four-dimensional theory the simplest amplitudes are the MHV amplitudes. In the massive case, gluon amplitudes with helicity configurations of the form $+ - \ldots -$ or $- + \ldots +$ are no longer zero and belong to the ultra helicity violating (UHV) amplitudes. The UHV amplitudes are the simplest of the massive amplitudes and vanish in the massless limit. Within the little group decomposition of the six-dimensional superamplitudes the UHV amplitudes are given by

$$\text{UHV amplitudes:} \qquad \mathcal{A}_n^{1\times 1}, \qquad \mathcal{A}_n^{(n-1)\times 1}, \qquad \mathcal{A}_n^{1\times(n-1)}, \qquad \mathcal{A}_n^{(n-1)\times(n-1)} . \tag{5.125}$$

Now that the simplest parts of the superamplitude are identified, the numerical BCFW recursion relation can be used to investigate their analytical form.

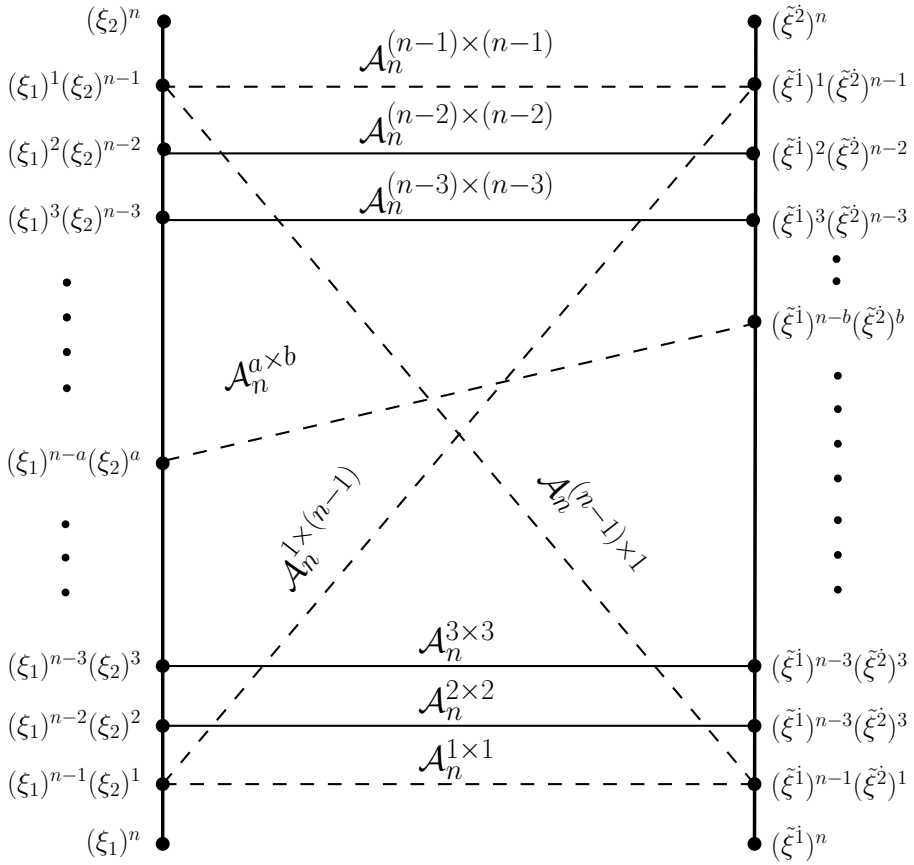

Figure 5.1.: Little group decomposition of the $\mathcal{N} = (1,1)$ SYM amplitudes. The general amplitude $\mathcal{A}_n^{a\times b}$ has the Grassmann dependence $(\xi_1)^{n-a}(\xi_2)^a(\tilde{\xi}^{\dot{1}})^{n-b}(\tilde{\xi}^{\dot{2}})^b$. In the massless four-dimensional limit only $\mathcal{A}_n^{(p+2)\times(p+2)}$ with $p = 0, 1, \ldots, n-4$ are non-zero and give the N^{p}MHV amplitudes (continuous horizontal lines). Some examples of amplitudes that are vanishing in the massless limit to four dimensions are represented by dashed lines.

5.4.6. The UHV Amplitudes in $\mathcal{N} = (1,1)$ SYM

Since the UHV amplitudes are not closed under the dual conformal symmetry, we cannot expect the coefficients α_i in our general ansatz eq. (5.65) to be dual conformal invariant. In general the coefficients α_i will be rational functions of the $\rho_n = \frac{1}{2}n(n-3)$ Lorentz invariants $\{x_{13}^2, x_{24}^2, \ldots\} =: \{s_1, s_2, \ldots, s_{\rho_n}\}$ and similar to eq. (5.70) they can be obtained by solving the linear equations derived from the ansatz

$$\alpha_i = \frac{\sum\limits_{\{n_i\}_k} a_{n_1 \ldots n_{\rho_n}} \prod\limits_{\sigma=1}^{\rho_n} s_\sigma^{n_\sigma}}{\sum\limits_{\{n_i\}_k} b_{n_1 \ldots n_{\rho_n}} \prod\limits_{\sigma=1}^{\rho_n} s_\sigma^{n_\sigma}}, \tag{5.126}$$

where $\{n_j\}_k$ are all different distributions of k powers among the Lorentz invariants. In contrast to the dual conformal invariant case, eq. (5.70), numerator and denominator need to be homogeneous polynomials of equal degree k.

To get an idea of the complexity of the UHV amplitudes we turn to the six point

case and make the same ansatz as in eq. (5.108) for the gluon sector

$$f_6^{\text{UHV}} = \frac{i}{x_{13}^2 x_{24}^2 x_{35}^2 x_{46}^2 x_{51}^2 x_{62}^2 x_{14}^2 x_{25}^2 x_{36}^2} \Big(\sum_{i,j} \alpha_{ij} x_{i-1\,j-1}^2 \Omega_i^u \Omega_j^u + \beta_{ij} x_{i-1\,j+1}^2 \Omega_i^u \Omega_j^d + \gamma_{ij} x_{i+1\,j+1}^2 \Omega_i^d \Omega_j^d \Big) . \tag{5.127}$$

Looking for solutions to eq. (5.127), the first observation is that only two of the $\Omega_i^{u/d}\Omega_j^{u/d}$ are linear independent. Further restricting to either the little group sectors $1 \times 1 \cup (n-1) \times (n-1)$ or $1 \times (n-1) \cup (n-1) \times 1$ every single term in eq. (5.127) gives a solution. This is an impressive display of the simplicity of the Grassmann dependence of the UHV amplitudes as well as belated justification of the use of the dual conformal covariant building blocks $\Omega_j^{u/d}$. Unfortunately, all the two term solutions to eq. (5.127) have very complicated coefficients. In order to cure this fact we try to find non-minimal and ideally dual conformal covariant solutions with simple coefficients. Due to eq. (5.107) we already know four dual conformal covariant solutions to eq. (5.127), namely eq. (5.101) and its cyclic rotations and eq. (5.104). A key observation towards simple dual conformal covariant representations of the UHV amplitudes is that on the UHV amplitudes the basis elements $\Omega_i^{u/d}\Omega_j^{u/d}$ obey the same dual conformal covariant two term identities (5.109) as on the gluon amplitudes. Hence it is natural to look for nice three term solutions similar to ones obtained for the gluon sector. A very basic way to to find three term solutions to eq. (5.127) is fix one of the coefficients to some simple function of the cross ratios, e. g. $\alpha_{13} = g(u_1, u_2, u_3)$ and solve for the remaining coefficients. With regard to the nice representations found for the gluons (5.110), we start with the most simple choices possible $g = \pm 1$. Indeed for $\alpha_{13} = -1$ we find four simple dual conformal covariant solutions

$$\begin{aligned} -i \left(x_{13}^2 x_{24}^2 x_{35}^2 x_{46}^2 x_{51}^2 x_{62}^2 x_{14}^2 x_{25}^2 x_{36}^2 \right) f_6^{\text{UHV}} &= x_{24}^2 \Omega_3^d \Omega_3^u - x_{13}^2 \Omega_2^d \Omega_6^d - x_{26}^2 \Omega_1^u \Omega_3^u \\ &= x_{46}^2 \Omega_3^d \Omega_1^u - x_{15}^2 \Omega_4^d \Omega_6^d - x_{26}^2 \Omega_1^u \Omega_3^u \\ &= x_{13}^2 \Omega_6^d \Omega_4^u - x_{15}^2 \Omega_4^d \Omega_6^d - x_{26}^2 \Omega_1^u \Omega_3^u \\ &= x_{24}^2 \Omega_6^d \Omega_6^u - x_{13}^2 \Omega_2^d \Omega_6^d - x_{26}^2 \Omega_1^u \Omega_3^u . \end{aligned} \tag{5.128}$$

As it turns out, the 24 three-term solutions that can be obtained in this way exactly match the 24 gluon representations found in section 5.4.3, i. e. the dual conformal extension of the UHV sector includes the gluon sector. This observation is highly nontrivial. At this point it is not clear whether this is a special feature of the six point amplitude or a multiplicity independent statement.

UHV Amplitudes with Two Massive Legs

Motivated by compact formulae obtained by Henriette Elvang et al. in reference [51] for SYM amplitudes with two neighboring massive legs we investigate the UHV sector in the special kinematics where only the first two legs are massive from the four-dimensional point of view. By cyclic permutations of the indices this is straightforward to translate to the case where another pair of consecutive legs is massive. In six-dimensional language this is equivalent to the restriction to phase space points of the

form

$$p_1^5 = -p_2^5\,, \qquad p_1^6 = -p_2^6 \qquad \text{and} \qquad p_i^5 = p_i^6 = 0 \qquad \text{for} \qquad i = 3, \ldots, n\,. \tag{5.129}$$

Similar to the four-dimensional calculation in reference [51] we are searching for a formula valid for all multiplicities. Therefore we make the recursive ansatz

$$f_n = f_{n-1}\left(\sum_i \alpha_i \Omega^u_{i,n} + \beta_i \Omega^d_{i,n}\right)\,, \tag{5.130}$$

where at each recursion step we only use the $2n$ dual conformal covariant building blocks $\Omega^u_{i,n}$ defined in eq. (5.106). Due to the special kinematics eq. (5.129) we do not have to worry about the six-dimensional Levi-Civita tensors for multiplicities larger than six, hence there is no need for chiral self-conjugate building blocks. The coefficients α_i, β_i have mass dimension minus six and their functional dependence on the Lorentz invariants x_{ij}^2 can be obtained by modifying the ansatz eq. (5.126) accordingly. We successively determine the solutions to eq. (5.130) and at each multiplicity we keep all one term solutions and feed them back into the recursive ansatz eq. (5.130). As initial data we take the ten representations of the full five point amplitude

$$f_5 = -\frac{i}{x_{13}^2 x_{24}^2 x_{35}^2 x_{41}^2 x_{52}^2}\Omega^u_{i,5}\,, \qquad\qquad f_5 = \frac{i}{x_{13}^2 x_{24}^2 x_{35}^2 x_{41}^2 x_{52}^2}\Omega^d_{i,5}\,, \tag{5.131}$$

obtained in section 5.4.2. Only the two of them containing $\Omega^u_{1,5}$ or $\Omega^d_{5,5}$ yield one term solutions for f_6 and out of the four one term solutions they produce again only two, namely

$$f_6^{\text{UHV}} = -\frac{i}{x_{13}^2 x_{24}^2 x_{35}^2 x_{46}^2 x_{51}^2 x_{62}^2}\frac{\Omega^u_{1,5}\Omega^u_{4,6}}{x_{14}^2 x_{25}^2} \tag{5.132}$$

and

$$f_6^{\text{UHV}} = \frac{i}{x_{13}^2 x_{24}^2 x_{35}^2 x_{46}^2 x_{51}^2 x_{62}^2}\frac{\Omega^d_{5,5}\Omega^u_{5,6}}{x_{13}^2 x_{25}^2}\,. \tag{5.133}$$

lead to one term solutions for f_7. Interestingly both solutions are dual conformal covariant with inversion weight one on each dual point just like the full amplitude. Both solutions for f_6^{UHV} nicely evolve through all subsequent recursion steps. Looking at the two representations they yield for the UHV amplitudes of multiplicity seven

$$f_7^{\text{UHV}} = -\frac{i}{x_{13}^2 x_{24}^2 x_{35}^2 x_{46}^2 x_{57}^2 x_{61}^2 x_{72}^2}\Omega^u_{1,5}\frac{\Omega^u_{4,6}}{x_{14}^2 x_{25}^2}\frac{\Omega^u_{5,7}}{x_{15}^2 x_{26}^2} \tag{5.134}$$

and

$$f_7^{\text{UHV}} = \frac{i}{x_{13}^2 x_{24}^2 x_{35}^2 x_{46}^2 x_{57}^2 x_{61}^2 x_{72}^2}\Omega^d_{5,5}\frac{\Omega^u_{5,6}}{x_{13}^2 x_{25}^2}\frac{\Omega^u_{6,7}}{x_{13}^2 x_{26}^2}\,, \tag{5.135}$$

it is straightforward to generalize them to arbitrary multiplicities. We conjecture the formulae

$$f_n^{\text{UHV}} = -\frac{i}{\prod x_{i\,i+2}} \Omega^u_{1,5} \prod_{i=6}^{n} \frac{\Omega^u_{i-2,i}}{x^2_{1\,i-2} x^2_{2\,i-1}} \tag{5.136}$$

and

$$f_n^{\text{UHV}} = \frac{i}{\prod x_{i\,i+2}} \Omega^d_{5,5} \prod_{i=6}^{n} \frac{\Omega^u_{i-1,i}}{x^2_{13} x^2_{2\,i-1}}\,, \tag{5.137}$$

to be valid for multiplicities greater than four. Up to multiplicity $n = 13$ both formulae have been checked by determining the solutions to the recursive ansatz eq. (5.130) which seems sufficient to us to consider eqs. (5.136) and (5.137) to be proven.

With regard to the three term solutions (5.128) for all gluon and UHV amplitudes on general kinematics, we expect the formulae eqs. (5.136) and (5.137) to be valid for other sectors as well. The natural guess is of course that the dual conformal extensions of the UHV amplitudes on the special kinematics eq. (5.129) produce the correct gluon amplitudes. However, this is not the case. The reason might be that the gluon sector does not undergo the same significant simplifications as the UHV sector if we specialize the kinematics. Fortunately the found dual conformal extensions of eqs. (5.136) and (5.137) yield an even bigger class of amplitudes. We find the remarkable results that eq. (5.136) is equal to the superamplitude on all little group sectors of the form $1 \times a$, $(n-1) \times a$, whereas eq. (5.137) is correct for the chiral conjugate little group sectors $a \times 1$, $a \times (n-1)$. We indicate this by writing

$$f_n^{1\times a\,(n-1)\times a} = -\frac{i}{\prod x_{i\,i+2}} \Omega^u_{1,5} \prod_{i=6}^{n} \frac{\Omega^u_{i-2,i}}{x^2_{1\,i-2} x^2_{2\,i-1}} \tag{5.138}$$

and

$$f_n^{a\times 1\,a\times(n-1)} = \frac{i}{\prod x_{i\,i+2}} \Omega^d_{5,5} \prod_{i=6}^{n} \frac{\Omega^u_{i-1,i}}{x^2_{13} x^2_{2\,i-1}}\,. \tag{5.139}$$

Clearly the chiral conjugate of the formula for $f_n^{1\times a\,(n-1)\times a}$ is an alternative representation of $f_n^{a\times 1\,a\times(n-1)}$ and vice versa.

5.5. The Uplift from Four Dimensions

A very exciting question, first discussed by Yu-tin Huang in reference [85], is whether or not it is possible to obtain the massless tree-level superamplitudes of the six-dimensional $\mathcal{N} = (1,1)$ SYM by uplifting the massless non-chiral superamplitudes of the four-dimensional $\mathcal{N} = 4$ SYM. If so, as claimed by Yu-tin Huang, this implies that the massive four-dimensional amplitudes of $\mathcal{N} = 4$ SYM can be obtained from the massless ones. Since the non-chiral superamplitudes of $\mathcal{N} = 4$ are straightforward to obtain using the well behaved non-chiral BCFW recursion, described in section 1.6.1, such a correspondence could provide an easy way to obtain the tree amplitudes of $\mathcal{N} = (1,1)$ SYM.

In this section we want to thoroughly investigate the potential uplift of the massless

four-dimensional amplitudes and thereby clarify some mistakes made in [85].

5.5.1. Dimensional Reduction of $\mathcal{N} = (1,1)$ SYM Revisited

As explained in detail in section 1.5.2 performing the dimensional reduction of the superamplitudes of $\mathcal{N} = (1,1)$ to massless four dimensions yields the non-chiral superamplitudes of $\mathcal{N} = (1,1)$. The symmetries of the six-dimensional and four-dimensional superamplitudes have been discussed in detail in sections 1.4.2 and 1.5.1. The most relevant in this discussion are the discrete symmetry under chiral conjugation and the R-symmetry of the four-dimensional superamplitudes. In particular the invariance under the R-symmetry generators m_{nm} and $\widetilde{m}_{n'm'}$ implies that all R-symmetry indices within a superamplitude are contracted.

With the help of the maps between the six-dimensional on-shell variables $\{\lambda_i^A,\ \tilde{\lambda}_{i\,A},\ \xi_i^a,\ \tilde{\xi}_i^{\dot{a}}\}$ and the massless four-dimensional on-shell variables $\{\lambda_i^\alpha,\ \tilde{\lambda}_i^{\dot{\alpha}},\ \eta_i^m,\ \tilde{\eta}_i^{m'}\}$ eqs. (1.191) and (1.194) it is straightforward to obtain the projection of every six-dimensional object. Since there is a one-to-one map between the supermomentum conserving delta functions (1.196) we neglect them straight away and investigate the correspondence

$$f_n^{\text{6d}} \qquad \underset{\text{uplift?}}{\overset{\text{projection}}{\longrightarrow}} \qquad f_n^{\text{4d}}\,. \tag{5.140}$$

The tree-level amplitudes of $\mathcal{N} = (1,1)$ SYM theory consist of Lorentz invariant contractions of momenta p_i and supermomenta q_i, $\tilde{q}_i$. The only purely bosonic Lorentz invariants are traces of an even number of momenta $(k_i)_{AB}$, $(k_i)^{AB}$. However chiral conjugate traces project to the same four-dimensional traces

$$\begin{aligned} \mathrm{Tr}^{6d}(\Gamma_+ \not{k}_1 \not{k}_2 \dots \not{k}_{2n}) &= (k_1)_{A_1A_2} \dots (k_{2n})^{A_{2n}A_1} \\ \mathrm{Tr}^{6d}(\Gamma_- \not{k}_1 \not{k}_2 \dots \not{k}_{2n}) &= (k_1)^{A_1A_2} \dots (k_{2n})_{A_{2n}A_1} \end{aligned} \quad \longrightarrow \quad \mathrm{Tr}^{\,4d}\,(\not{k}_1 \not{k}_2 \dots \not{k}_{2n}) \tag{5.141}$$

where $\not{k}_i$ denotes the contraction of the momentum k_i with either the six-dimensional or the four-dimensional gamma matrices and $\Gamma_\pm = \frac{1}{2}(1 \pm \gamma^7)$. Hence, the presence of traces in f_n^{6d} that are not chiral self-conjugate would already spoil the uplift. The chiral conjugate traces differ by terms containing the six-dimensional Levi-Civita tensor. Since $\mathcal{N} = (1,1)$ SYM is a non-chiral theory it is symmetric under chiral conjugation $(p_i)_{AB} \leftrightarrow (p_i)^{AB}$, $q_i \leftrightarrow \tilde{q}_i$ and therefore free of the six-dimensional Levi-Civita tensor. In conclusion, the only purely bosonic invariants in f_n^{6d} are chiral self-conjugate traces whose projections can be uniquely uplifted from four dimensions

$$\tfrac{1}{2}\,\mathrm{Tr}^{\,6d}\,(\not{k}_1 \not{k}_2 \dots \not{k}_{2n}) \qquad \underset{\longleftarrow}{\longrightarrow} \qquad \mathrm{Tr}^{\,4d}\,(\not{k}_1 \not{k}_2 \dots \not{k}_{2n}) \tag{5.142}$$

Inserting the definition of the gamma matrices, the four-dimensional trace may be written as the sum of two chiral conjugate traces of four-dimensional Pauli matrices

$$\mathrm{Tr}^{\,4d}\,(\not{k}_1 \not{k}_2 \dots \not{k}_{2n}) = (k_1)_{\alpha_1\dot{\alpha}_2} \dots (k_{2n})^{\dot{\alpha}_{2n}\alpha_1} + (k_1)^{\dot{\alpha}_1\alpha_2} \dots (k_{2n})_{\alpha_{2n}\dot{\alpha}_1} \tag{5.143}$$

There are three possible Lorentz invariants containing supermomenta. All of them

have a unique projection to four dimensions

$$\langle q_i|k_1\dots k_{2n}|\tilde{q}_j] \quad\longrightarrow\quad \langle q_i^1|k_1\dots k_{2n}|q_j^4\rangle + [\tilde{q}_{i3}|k_1\dots k_{2n}|\tilde{q}_{j2}] \tag{5.144}$$

$$\langle q_i|k_1\dots k_{2n+1}|q_j\rangle \quad\longrightarrow\quad \langle q_i^1|k_1\dots k_{2n+1}|\tilde{q}_{j3}] - [\tilde{q}_{i3}|k_1\dots k_{2n+1}|q_j^1\rangle \tag{5.145}$$

$$[\tilde{q}_i|k_1\dots k_{2n+1}|\tilde{q}_j] \quad\longrightarrow\quad \langle q_i^4|k_1\dots k_{2n+1}|\tilde{q}_{j2}] - [\tilde{q}_{i2}|k_1\dots k_{2n+1}|q_j^4\rangle \tag{5.146}$$

Non-chirality of the four-dimensional superamplitudes implies their invariance under the exchanges $q_i^1 \leftrightarrow \tilde{q}_{i3}$ and $q_i^4 \leftrightarrow \tilde{q}_{i2}$. Since Lorentz invariants of the last two types, eqs. (5.145) and (5.146), can only occur pairwise in a six-dimensional superamplitude, it follows that the projection of a six-dimensional superamplitude has always a manifest chiral symmetry in four dimensions. Apparently none of these three six-dimensional Lorentz invariants leads to a manifest R-symmetry in four dimensions. However, any reasonable representation of $f_n^{4\text{d}}$ has a manifest R-symmetry. In conclusion, a potential uplift of $f_n^{4\text{d}}$ to six-dimensions can only consist of building blocks whose projection to four dimensions is R-symmetric. From the investigation of the three types of six-dimensional Lorentz invariants and their projections, eqs. (5.144) to (5.146), it immediately follows that there is only one such object

$$\langle q_i|k_1\dots k_{2n}|\tilde{q}_j] + [\tilde{q}_i|k_1\dots k_{2n}|q_j\rangle \quad\overrightarrow{\longleftarrow}\quad \langle q_i^m|k_1\dots k_{2n}|q_{j\,m}\rangle + [\tilde{q}_{im'}|k_1\dots k_{2n}|\tilde{q}_j^{m'}] \tag{5.147}$$

Unlike the claim in [85] there is no combination of six-dimensional Lorentz invariants of the second and third type, eqs. (5.145) and (5.146), that has a R invariant projection to four dimensions. We conclude that if a correspondence of the form eq. (5.140) exists, then the involved representations of $f_n^{6\text{d}}$ and $f_n^{4\text{d}}$ only contain the building blocks eq. (5.147). As will be explained in the next section, for multiplicities larger than five this is a severe constraint on the representations of $f_n^{6\text{d}/4\text{d}}$.

5.5.2. Uplifting Superamplitudes

We want to discuss the implications of eq. (5.147). At four point level $f_4^{4\text{d}}$ is purely bosonic and the uplift is trivial

$$f_4^{4\text{d}} = -\frac{i}{x_{13}^2 x_{24}^2} \qquad\Longrightarrow\qquad f_4^{6\text{d}} = -\frac{i}{x_{13}^2 x_{24}^2}\,. \tag{5.148}$$

At five points, any representation of $f_5^{4\text{d}}$ that has a manifest R-symmetry and a manifest symmetry under chiral conjugation automatically only consists of the building blocks eq. (5.147). Since any reasonable representation of $f_5^{4\text{d}}$ has a manifest R-symmetry and the chiral symmetry can be made manifest by replacing e. g. the MHV part by the chiral conjugate of the $\overline{\text{MHV}}$ part, any representation of $f_5^{4\text{d}}$ can be uplifted to six dimensions. By uplifting the representation, eq. (1.244),

$$f_5^{4\text{d}} = \frac{i}{x_{13}^2 x_{24}^4 x_{25}^4 x_{35}^2 x_{41}^2}\left(\langle B_{542}|\,1\,2\,3\,|B_{542}\rangle + [\tilde{B}_{542}|\,1\,2\,3\,|\tilde{B}_{542}]\right) \tag{5.149}$$

obtained from the BCFW recursion yields the following representation of the six-dimensional amplitude

$$f_5^{6\mathrm{d}} = \frac{i}{x_{13}^2 x_{24}^4 x_{25}^4 x_{35}^2 x_{41}^2} \tfrac{1}{2} \left(\langle B_{542}| \, 1\,2\,3 \, |\tilde{B}_{542}] + [\tilde{B}_{542}| \, 1\,2\,3 \, |B_{542}\rangle \right) \tag{5.150}$$

$$= i \frac{\Omega_{542;123;542}}{x_{13}^2 x_{24}^4 x_{25}^4 x_{35}^2 x_{41}^2} \,, \tag{5.151}$$

where the factor of $\frac{1}{2}$ originates from the definition (1.243) and we inserted the definition of $\Omega_{I;J;K}$, eq. (5.114). We checked numerically that eq. (5.150) is indeed equal to the six-point amplitude in six dimensions.

Unfortunately the uplift starts to be non-trivial already at multiplicity six. Let $\{\Omega_i\}$ denote a set of the chiral self-conjugate building blocks (5.147) for the six-dimensional superamplitudes

$$\Omega_i \qquad \begin{array}{c} \longrightarrow \\ \longleftarrow \end{array} \qquad \omega_i + \tilde{\omega}_i \tag{5.152}$$

where $\omega_i = \mathcal{O}(q^2)$ and $\tilde{\omega}_i = \mathcal{O}(\tilde{q}^2)$ are the chiral conjugates in the projection of Ω_i. As a consequence of eq. (5.147) an upliftable representation of the six-point amplitudes has the form

$$f_6^{4\mathrm{d}} = \sum_{i,j} \alpha_{ij} (\omega_i + \tilde{\omega}_i)(\omega_j + \tilde{\omega}_j) \tag{5.153}$$

and uplifts to

$$f_6^{6\mathrm{d}} = \sum_{i,j} \alpha_{ij} \Omega_i \Omega_j \,. \tag{5.154}$$

From eq. (5.153) it follows

$$\left(f_6^{4\mathrm{d}}\right)^{\mathrm{MHV}} = \sum_{i,j} \alpha_{ij} \tilde{\omega}_i \tilde{\omega}_j \,, \quad \left(f_6^{4\mathrm{d}}\right)^{\mathrm{NMHV}} = \sum_{i,j} \alpha_{ij} (\omega_i \tilde{\omega}_j + \tilde{\omega}_i \omega_j) \,, \quad \left(f_6^{4\mathrm{d}}\right)^{\overline{\mathrm{MHV}}} = \sum_{i,j} \alpha_{ij} \omega_i \omega_j \,. \tag{5.155}$$

Comparing this with the representation eq. (1.245) obtained for $f_6^{4\mathrm{d}}$ from the BCFW recursion it is apparent that a generic representation of $f_6^{4\mathrm{d}}$ does not have the form eq. (5.153) required for an uplift. In contrast to the five point case, making the chiral symmetry manifest does not solve the problem because the minimal helicity violating (minHV) NMHV amplitudes are independent of the MHV and $\overline{\mathrm{MHV}}$ amplitudes. As a consequence, it is straightforward to turn a generic representation into the form

$$f_6^{4\mathrm{d}} = \sum_{i,j} \beta_{ij} \omega_i \omega_j + \gamma_{ij} (\omega_i \tilde{\omega}_j + \tilde{\omega}_i \omega_j) + \beta_{ij} \tilde{\omega}_i \tilde{\omega}_j \,, \tag{5.156}$$

but in general the coefficients β_{ij} and γ_{ij} are unrelated. This is the key issue, that has been overlooked in reference [85]. As a result, finding any representation of $f_n^{4\mathrm{d}}$ is not sufficient to obtain the six-dimensional amplitude. In fact, under the assumption that the uplift works, obtaining $f_n^{6\mathrm{d}}$ is equivalent to finding a representation of the form

$$f_n^{4\mathrm{d}} = \sum_{|I|=n-4} \alpha_I \prod_{k=1}^{n-4} (\omega_{i_k} + \tilde{\omega}_{i_k}) \,, \tag{5.157}$$

for the four-dimensional amplitude. While such a representation trivially uplifts to

$$f_n^{\text{6d}} = \sum_{|I|=n-4} \alpha_I \prod_{k=1}^{n-4} \Omega_{i_k} \,, \tag{5.158}$$

obtaining it is non-trivial and a rigorous proof that eq. (5.158) is always a valid representation of the six-dimensional superamplitude is still missing. Of course we could use a numerical implementation of the non-chiral BCFW recursion relation to determine a solution to an ansatz of the form eq. (5.157) but this is not easier than determining f_n^{6d} directly, using the methods described in section 5.4.1.

Albeit it seems save to say that the uplift is of no practical relevance for the determination of the six-dimensional superamplitudes, it is still very fascinating from the theoretical point of view. It is intriguing that the correct representation of the MHV superamplitude

$$(f_n^{\text{4d}})^{\text{MHV}} = \sum_{|I|=n-4} \alpha_I \prod_{k=1}^{n-4} \tilde{\omega}_{i_k} \,, \tag{5.159}$$

might be sufficient to get the whole six-dimensional superamplitude, or equivalently all massive four-dimensional amplitudes.

One thing that would immediately invalidate the uplift are identities of the $\omega_i + \tilde{\omega}_i$ that do not uplift to identities of the Ω_i. Though we do not have a concrete counterexample for the uplift, there are indeed four-dimensional identities of strings of momenta k_i that do not have a six-dimensional counterpart, i. e.

$$\text{4d:} \quad (p_i k_1 \dots k_{2n} p_i)_\alpha^{\ \beta} = (\, |i\rangle[i|k_1 \dots k_{2n}|i]\langle i|\,)_\alpha^{\ \beta} = -(p_i k_{2n} \dots k_1 p_i)_\alpha^{\ \beta} \tag{5.160}$$

but

$$\text{6d:} \quad (p_i k_1 \dots k_{2n} p_i)_A^{\ B} = \Big(\, |i_{\dot{a}}][i^{\dot{a}}|k_1 \dots k_{2n}|i^b\rangle\langle i_b|\,\Big)_A^{\ B} \neq -(p_i k_{2n} \dots k_1 p_i)_A^{\ B} \tag{5.161}$$

At this point we do not see how such identities could not spoil the uplift without restricting the allowed four-dimensional building blocks.

Using the numerical implementation of the six-dimensional BCFW recursion it is possible to numerically check the uplift. The easiest way to do so is to make an ansatz (5.65) for f_n^{6d} using only the minimal building blocks Ω_{ijkl} defined in eq. (5.78) and determine a solution $\alpha_i(\pi)$ for a massless phase space point with momenta of the form $\{p_i^1, p_i^2, p_i^3, p_i^4, 0, 0\}$. Since the coefficients are functions of the Lorentz invariants x_{ij}^2 they have identical numerical values on the 'massive' phase space point $\{p_i^1, 0, p_i^3, p_i^4, 0, p_i^2\}$ and we can check whether the obtained coefficients $\alpha_i(\pi)$ provide a solution to the massive amplitudes as well. In fact, we checked that up to multiplicity eight that representation of the massless non-chiral amplitudes containing only the minimal building blocks $\langle B_{ijk}|B_{ilm}\rangle + [\tilde{B}_{ijk}|\tilde{B}_{ilm}]$ did always uplift to six dimensions. Since the eight-point amplitude is already very complicated, there is no reason to believe that the uplift of a representation containing only the minimal building blocks will fail beyond eight points. In case of more complicated building blocks the identities (5.160) might become an issue even at multiplicities lower than eight.

6

Infrared Regularization of $\mathcal{N} = 4$ Super Yang-Mills Theory

We study an alternative to dimensional regularization of planar scattering amplitudes in $\mathcal{N} = 4$ super Yang-Mills theory by going to the Coulomb branch of the theory. The infrared divergences are regulated by masses obtained from a Higgs mechanism, allowing us to work in four dimensions. The corresponding string theory set-up suggests that the amplitudes have an exact dual conformal symmetry. The latter acts on the kinematical variables of the amplitudes as well as on the Higgs masses in an effectively five dimensional space. We confirm this expectation by an explicit calculation in the gauge theory. A consequence of this exact dual conformal symmetry is a significantly reduced set of scalar basis integrals that are allowed to appear in an amplitude. For example, triangle sub-graphs are ruled out. We argue that the study of exponentiation of amplitudes is simpler in the Higgsed theory because evanescent terms in the mass regulator can be consistently dropped. We illustrate this by showing the exponentiation of a four-point amplitude to two loops. Finally, we also analytically compute the small mass expansion of a two-loop master integral with an internal mass.

6.1. Introduction

Based on an iterative structure [30] found at lower loop levels, Bern, Dixon and Smirnov (BDS) [148] conjectured an all-loop form of the maximally helicity violating (MHV) amplitudes. By now, this ansatz is believed to be correct for four and five gluon amplitudes (but known to fail for more than five particles [149], see also [77, 150–152]). The correctness of the BDS ansatz for four and five gluons stems from a novel hidden symmetry of the planar theory, dual conformal symmetry.

The dual conformal symmetry is anomalous at loop level due to ultraviolet divergences associated with cusps of the Wilson loops. These UV divergences are related to the infrared divergences of the scattering amplitudes [153]. However, the breaking of dual conformal symmetry is under full control and can be written in terms of all-order anomalous Ward identities derived in [75, 76] (see also [79–81, 154]). In particular, the latter determine the finite part of the Wilson loops for four and five cusps to be of the form of the BDS ansatz, to all orders in the coupling constant. The dual conformal anomaly is proportional to the anomalous dimension of a light-like Wilson loop cusp [155–157], a universal function in turn conjectured to be exactly known as a key outcome of the above mentioned AdS/CFT integrability investigations [158]. The existence of two copies of the superconformal symmetry algebra is a hallmark of integrability [82, 83, 159], as their closure results in an infinite dimensional symmetry algebra of Yangian structure under which the tree-level amplitudes are invariant [49]. At the loop-level the status of the Yangian symmetry is unclear at present: The IR divergences destroy both the standard and dual superconformal symmetries. However, while the breaking of the dual conformal symmetry can be controlled, similar control does not (yet) exist for the standard conformal symmetry. A key issue here, and one of the motivations for this work, is clearly the regularization prescription and its behavior under the conformal symmetry transformations.

The most widespread regularization is certainly dimensional regularization, or rather dimensional reduction in order to preserve supersymmetry. This method is very well developed. An inconvenience of this regularization is that when computing for example the logarithm of an amplitude, as suggested by the form of infrared divergences and the BDS ansatz, there is an interference between poles in the dimensional regulator ϵ and evanescent terms in ϵ coming from lower-loop amplitudes. As a result, one has to compute these higher order ϵ terms in the lower-loop amplitudes.

An idea to circumvent this problem was proposed in [74], where an off-shell regulator was used. Divergences in this regulator would take the form of logarithms, and therefore, the above interference could not take place, at least to a given order in the coupling constant. Also, one could have hoped that this regulator is more suited to expose dual conformal symmetry. Unfortunately, the use of an off-shell regulator leads to other problems such as the lack of manifest gauge invariance.

However, there is another regularization motivated naturally by the dual string picture that is somewhat similar in spirit but different from the off-shell regularization, which we shall employ. This regularization was discussed in [73, 82, 160–162] and consists in turning on a vacuum expectation value for one of the scalars in $\mathcal{N} = 4$ SYM. Specifically, one takes a $U(N + M)$ theory and applies the Higgs mechanism to break the symmetry to $U(N) \times U(M)$. Then, one considers the scattering of the $U(M)$ fields, which lead to massive propagators in the loops. Note that we do not set $M = 1$ because we want to be able to define a color ordering for the outer legs. In the $N \gg M$ limit,

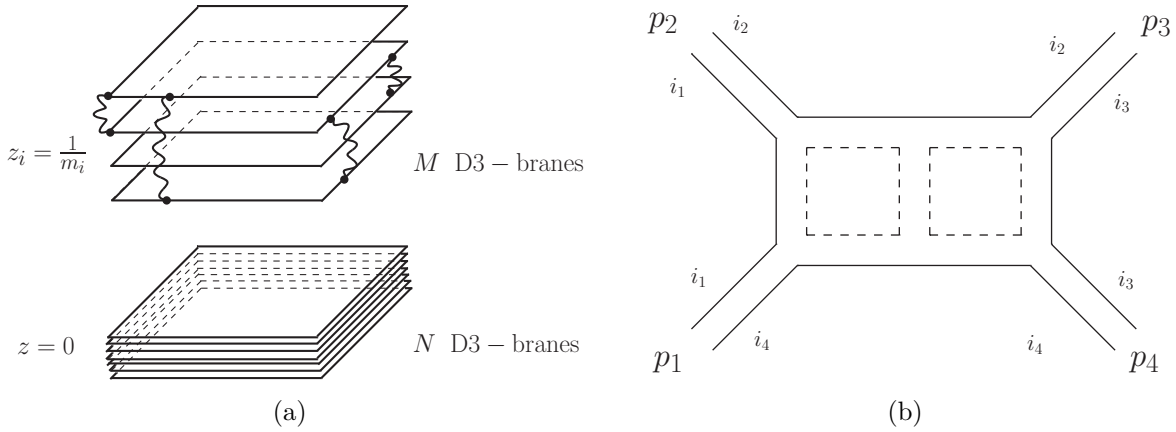

Figure 6.1.: (a) String theory description for the scattering of M gluons in the large N limit. Putting the M D3-branes at different positions $z_i \neq 0$ serves as a regulator and also allows us to exhibit dual conformal symmetry. (b) Gauge theory analogue of (a): a generic scattering amplitude at large N (here: a sample two-loop diagram).

the following picture emerges: If we use a double-line notation, then the $U(M)$ lines will be on the outside of the diagram, while in the interior we will have $U(N)$ lines only. Hence the massive particles will flow around the outer line of the diagram, and thereby regulate the infrared divergences. Hence in the planar, large N limit, one can consider scattering processes in the Higgsed theory that are regulated by the Higgs mass and therefore can be defined in four dimensions. We expect this regularization to work to all orders in the coupling constant.

Importantly, we can improve this set-up by allowing for different Higgs masses, breaking the $U(N+M)$ gauge symmetry down to $U(N) \times U(1)^M$. In the dual string picture this amounts to moving M D3-branes away from the N parallel D3-branes and also separating these M distinct branes from one another. One then has "light" gauge fields corresponding to strings stretching between the M separated D3-branes, which are our external scattering states. Then there are the "heavy" gauge fields corresponding to the strings stretching between the coincident N D3-branes and one of the M branes. These are the massive particles running on the outer line of the diagrams, see section 6.1. In doing so, we argue that dual conformal symmetry, suitably extended to act on the Higgs masses as well, is an exact, i.e. unbroken, symmetry of the scattering amplitudes.

This exact symmetry has very profound consequences. It was already noticed in [72] that the integrals contributing to loop amplitudes in $\mathcal{N} = 4$ SYM have very special properties under dual conformal transformations, but this observation was somewhat obscured by the infrared regulator. With our infrared regularization, the dual conformal symmetry is exact and hence so is the symmetry of the integrals. Therefore, the loop integrals appearing in our regularization will have an exact dual conformal symmetry. This observation severely restricts the class of integrals allowed to appear in an amplitude. As a simple application, triangle sub-graphs are immediately excluded.

The alert reader might wonder whether computing a scattering amplitude with several, distinct Higgs masses might not be hopelessly complicated. In fact, this is not the case. The different masses are crucial for the exact dual conformal symmetry to work. However, once we have used this symmetry in order to restrict the number of basis

loop integrals, we can set all Higgs masses equal and think about the common mass as a regulator. As we will show in several examples, computing the small mass expansion in this regulator is particularly simple. In fact, to two loops, only very simple (two-) and (one-)fold Mellin-Barnes integrals are needed.

The reader may be worried that the infrared regulator we propose is not complete, i.e. that one might still find infrared divergences at some higher loop order from massless subgraphs. Infrared divergences come from regions of the integration space where the loop momentum is soft and/or collinear to some external momentum. At low loop level, we will see explicitly that the massive particles flowing around the outer line of the diagrams regulate these potential divergences. At higher loop order diagrams with massless subgraphs may occur, and while we do not have a formal proof, we do expect that also such diagrams are finite in our setup [1]. An argument in favor of this is that from the strong coupling string perspective there is no divergence.

This chapter is organized as follows. In section 6.2 we describe scattering amplitudes from the string theory perspective in the above mentioned regularization and argue, in agreement with [82], that the amplitudes are expected to possess dual conformal invariance. In section 6.3 we consider the analogous regularization in perturbation theory. In particular, we consider the case of the four point amplitude up to two loops and show that the expectations from the strong coupling side are indeed fulfilled. Furthermore, we show that exponentiation holds for this case. Finally, we present an overview about the more recent results that appeared after the work presented in this chapter has been completed. Especially we make contact to the more recent results concerning the by now proven dual conformal properties of massive amplitudes on the coulomb branch of $\mathcal{N} = 4$ SYM theory presented in chapter 5. Many technical details relevant to the body of the chapter have been referred to appendix G.

In contrast to the other chapters we will use a mostly plus metric here.

6.2. The String Theory Perspective

In this section we analyze the above mentioned scattering amplitudes from the string theory picture, which is the appropriate description around the regime of strong coupling. If one focuses on planar amplitudes, the appropriate world-sheet has the topology of a disk, with vertex operator insertions at the boundary corresponding to the external states undergoing the scattering.

On the string side, the regularization to be considered here is quite natural and corresponds to introducing M $D3-$branes in the background $AdS_5 \times S^5$. To be more precise, if we write the AdS_5 metric in Poincaré coordinates $ds^2 = \frac{1}{z^2}(dy_{3,1}^2 + dz^2)$, then the M branes are sitting at the positions $z_i = 1/m_i$ $(i = 1, \ldots, M)$ and extend along the $y_{3,1}$ directions. The asymptotic states to be scattered are the open strings between a pair of consecutive $D3-$branes, for instance at z_i and z_{i+1}. These open strings represent the gluons.

As argued in [73, 82], to which we refer the reader for more details, it is convenient to perform four T-dualities in the y_{3+1} directions, followed by a change of coordinates $r = \frac{1}{z}$ (we are setting the AdS radius to one for convenience). After this, we end up with a dual AdS metric

$$ds^2 = \frac{dx_{3,1}^2 + dr^2}{r^2} \,. \tag{6.1}$$

[1] We are grateful to G. Korchemsky and L. Dixon for discussions of this point.

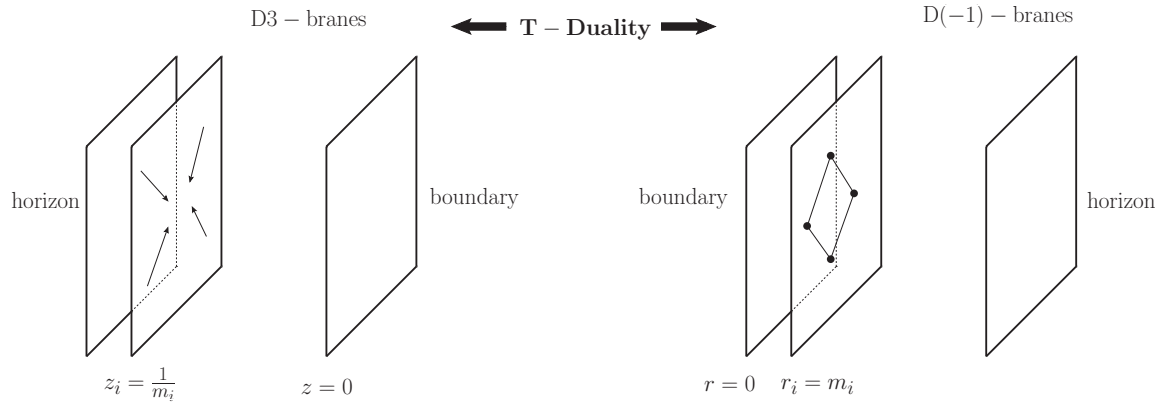

Figure 6.2.: Original (left) and dual (right) pictures of a scattering amplitude. On the original picture the open strings end at $D3-$branes located at $z_i = \frac{1}{m_i}$. In the dual picture we have open strings stretched between $D-$instantons separated by a light-like distance.

As T-duality interchanges Dirichlet and Neumann boundary conditions, the $D3$-branes become $D(-1)$-branes, or D-instantons. Each of these instantons is located at a fixed position in the $x_{3,1}$ coordinates and sits at $r_i = m_i$. The open strings are then stretching between consecutive D-instantons and the rules of T-duality fix the distance between these instantons to be proportional to the momentum of the original external state that the open string represented, see fig. 6.2.

If the D-instantons are away from the boundary, namely, $m_i > 0$, the amplitude is finite. On the other hand, it can only depend on the covariant AdS distances between the D-instantons (furthermore, at strong coupling, or when considering Wilson loops, the amplitude does not depend on the details of the inserted states). On the other hand, on dimensional grounds, we can only have dependence on ratios of these distances.

The dual conformal symmetry, being the conformal symmetry in the T-dual space, now acts in the above system by changing the location of the $D-$instantons $(r, x_{3,1}) \to (r', x'_{3,1})$. For instance, one can consider special conformal transformations, in which case one has

$$\begin{aligned} r' &= \frac{r}{1 + 2\, x \cdot \beta + \beta^2 \left(r^2 + x^2\right)}, \\ (x')^\mu &= \frac{x^\mu + \left(r^2 + x^2\right) \beta^\mu}{1 + 2\, x \cdot \beta + \beta^2 (r^2 + x^2)} \end{aligned} \tag{6.2}$$

Since the amplitude is regularized, hence finite, and since the system possesses dual conformal symmetry, the amplitude should be invariant under these transformations, at least when not taking into account the contribution from the polarization of the external states. [2]

This symmetry can be easily checked at strong coupling. In such a regime the amplitude does not depend on the details of the external states and is dominated by a saddle point of the classical action, whose Lagrangian, in conformal gauge, reads

$$\mathcal{L} = \frac{\partial_i r \partial_i r + \eta_{\mu\nu} \partial_i x^\mu \partial_i x^\nu}{r^2}\,. \tag{6.3}$$

[2] In other words, when considering the "Wilson loop" computation.

One can check that eq. (6.2) maps solutions of the equations of motion into solutions, keeping the Lagrangian invariant. Furthermore, the transformations are such that the boundary conditions are still the boundary conditions of a scattering problem, see discussion below. Hence the amplitude is invariant.

Unfortunately, it is hard to find classical solutions with boundary conditions at $r > 0$ even for the four cusp situation. However, the single cusp solution can be found in terms of a perturbation series, which we derive in appendix G.4. This is the conformal gauge version of the Nambu-Goto solution found in [82] and should describe the limiting form of a generic scattering string world-sheet when approaching any of the cusps.

Even though the full solution is not known, the single cusp solution allows one to extract the form of the cusp anomalous dimension at strong coupling in this regularization. We indeed find

$$\lim_{\lambda\to\infty} \Gamma_{\text{cusp}} = \frac{\sqrt{\lambda}}{\pi}\,, \qquad \text{where} \qquad \lambda = g_{\text{YM}}^2 N\,, \tag{6.4}$$

in agreement with the well known result.

The statement of invariance of the amplitudes under $SO(2,4)$ transformations can also be written in an infinitesimal form (see appendix G.6 for a derivation of the infinitesimal generators from the AdS_5 isometries). The relevant dual dilatation and special conformal generators take the form

$$\hat{D} = r\partial_r + x^\mu \partial_\mu\,, \tag{6.5}$$

$$\hat{K}_\mu = 2\,x_\mu(x_\nu\partial^\nu + r\partial_r) - (x^2 + r^2)\partial_\mu\,. \tag{6.6}$$

Now, we are interested in computing the classical string action S for a world-sheet with suitable boundary conditions. The action will be invariant under these transformations, but the boundary conditions might change, see below. We do not need to worry about a regulator as long as the world-sheet does not end on the boundary at $r = 0$. However, we should have boundary conditions that transform nicely under eq. (6.5). For $r = 0$, the appropriate boundary contour on which the world-sheet should end is a polygon with $(x_i - x_{i+1})^2 = 0$. Importantly, such a light-like polygon is mapped into another light-like polygon. For $r \neq 0$, we see that the conditions $(x_i - x_{i+1})^2 + (r_i - r_{i+1})^2 = 0$ are similarly preserved by eq. (6.5). Let us denote the contour formed by the M points $\{x_i^\mu, r_i\}$ by C. Then, doing infinitesimal transformations we find that indeed

$$\hat{K}_\mu S(C) = 0\,. \tag{6.7}$$

Where $K = \sum K_i$ and K_i acts on the coordinates of the ith $D-$instanton. We stress that in order to write eq. (6.7) we need to consider the amplitude for the case in which the $D-$instantons are at different radial distances r_i. On the other hand, even if we started with a configuration in which all the radial distances are the same, then a general dual conformal transformation would make them different.

The argument above only depends on using classical string theory, so it should be valid for the planar theory at large $\sqrt{\lambda}$. If we are interested in computing the Wilson loop expectation value, considering quantum fluctuations about such a minimal surface will not change the boundary conditions of the fields. Hence, we expect the dual conformal symmetry to prevail to all orders in a $1/\sqrt{\lambda}$ expansion in the planar theory, as argued by [82].

In order to find the same constraint on scattering amplitudes, one should understand how to introduce the dependence on the helicity of the external states. However, it seems reasonable to assume that a formula very similar to eq. (6.7) holds for scattering amplitudes as well. In the next section we will indeed identify a class of scalar amplitudes which for four particle scattering exhibit a parallel expression to eq. (6.7), see eq. (6.28) and eq. (6.48) at one-loop order. We take this as an indication that this exact dual conformal symmetry is present from weak to strong coupling.

6.3. The Gauge Theory Perspective

6.3.1. Higgsing $\mathcal{N} = 4$ super Yang Mills

Let us now work out the spontaneous symmetry breaking of $\mathcal{N} = 4$ SYM in more detail. We consider the breaking of $U(N+M) \to U(N) \times U(1)^M$. The component field spectrum consists of the vectors A_μ, the six scalars Φ_I and the ten dimensional Majorana-Weyl spinors Ψ governed by the action

$$\hat{S}^{U(N+M)}_{\mathcal{N}=4} = \int d^4x \ \mathrm{Tr}\Big(-\tfrac{1}{4}\,\hat{F}^2_{\mu\nu} - \tfrac{1}{2}(D_\mu\hat{\Phi}_I)^2 + \tfrac{g^2}{4}\,[\hat{\Phi}_I,\hat{\Phi}_J]^2 + \tfrac{i}{2}\,\hat{\overline{\Psi}}\,\Gamma^\mu\,D_\mu\hat{\Psi} + \tfrac{g}{2}\hat{\overline{\Psi}}\,\Gamma^I[\hat{\Phi}_I,\hat{\Psi}]\Big)\,, \tag{6.8}$$

where $D_\mu = \partial_\mu - ig[A_\mu,\ ]$. All fields are hermitian matrices, which we decompose into blocks as

$$\hat{A}_\mu = \begin{pmatrix} (A_\mu)_{ab} & (A_\mu)_{aj} \\ (A_\mu)_{ia} & (A_\mu)_{ij} \end{pmatrix}, \quad \hat{\Phi}_I = \begin{pmatrix} (\Phi_I)_{ab} & (\Phi_I)_{aj} \\ (\Phi_I)_{ia} & \delta_{I9}\,\frac{m_i}{g}\,\delta_{ij} + (\Phi_I)_{ij} \end{pmatrix}, \quad \hat{\Psi} = \begin{pmatrix} (\Psi)_{ab} & (\Psi)_{aj} \\ (\Psi)_{ia} & (\Psi)_{ij} \end{pmatrix},$$
$$a,b = 1,\ldots,N\,,\, i,j = N+1,\ldots,N+M\,, \tag{6.9}$$

thereby turning on a vacuum expectation value (VEV) for the scalars $\hat{\Phi}_I = \delta_{I9}\,\langle\Phi_9\rangle + \Phi_I$ in the $I = 9$ direction. This shift introduces terms of linear and quadratic order in m_i

$$\hat{S}_{\mathcal{N}=4} = S_{\mathcal{N}=4} + \int d^4x \ \mathrm{Tr}\Big(ig\,D_\mu\Phi_9\,[A_\mu,\langle\Phi_9\rangle] + \tfrac{g^2}{2}[A_\mu,\langle\Phi_9\rangle\,]^2 + \tfrac{g^2}{2}[\Phi_{I'},\langle\Phi_9\rangle\,]^2$$
$$+ g^2\,[\langle\Phi_9\rangle,\Phi_{J'}]\,[\Phi_9,\Phi_{J'}] + \tfrac{g}{2}\overline{\Psi}\Gamma^9\,[\langle\Phi_9\rangle,\Psi]\Big)\,, \tag{6.10}$$

where $I', J' = 4,\ldots,8$. We proceed by adding a R_ξ gauge fixing term $-\frac{1}{2}\,\mathrm{Tr}(G^2)$ with

$$G = \frac{1}{\sqrt{\xi}}\Big[\partial_\mu A^\mu - ig\,\xi\,[\langle\Phi_9\rangle,\Phi_9]\Big]\,, \tag{6.11}$$

and the appropriate ghost term

$$\mathcal{L}_{\mathrm{ghost}} = \mathrm{Tr}\left\{\bar{c}(\partial^\mu D_\mu c - g^2\xi[\langle\Phi_9\rangle,[\Phi_9+\langle\Phi_9\rangle,c]])\right\}\,. \tag{6.12}$$

The gauge fixing term $-\frac{1}{2}\,\mathrm{Tr}(G^2)$ cancels the unwanted scalar-vector mixing first term in eq. (6.10) and gives a gauge parameter ξ dependent mass term for Φ_9 and c. We specialize to the choice $\xi = 1$ to obtain identical propagators for vectors and scalars.

The Higgsing adds mass terms and novel cubic interaction terms for the bosonic fields coupling to Φ_9, explicitly $\hat{S}_{\mathcal{N}=4}$ of eq. (6.10) now contains the quadratic terms

$(A_M := (A_\mu, \Phi_I))$

$$\begin{aligned}\hat{S}_{\mathcal{N}=4}\Big|_{\text{quad.}} = \int d^4x \Big\{ &-\tfrac{1}{2}\,\mathrm{Tr}(\partial_\mu A_M\,\partial^\mu A^M) + \tfrac{i}{2}\,\mathrm{Tr}(\overline{\Psi}\,\Gamma^\mu\,\partial_\mu\Psi) \\ &-\tfrac{1}{2}(m_i-m_j)^2\,(A_M)_{ij}\,(A^M)_{ji} - m_i^2\,(A_M)_{ia}\,(A^M)_{ai} \\ &-\tfrac{1}{2}(m_i-m_j)\,\overline{\Psi}_{ij}\Gamma^9\Psi_{ji} + \tfrac{1}{2}m_i\,(\overline{\Psi}_{ai}\Gamma^9\Psi_{ia} - \overline{\Psi}_{ia}\Gamma^9\Psi_{ai})\Big\}, \quad (6.13)\end{aligned}$$

i.e. we have the 'light' fields $\mathcal{O}_{ij}$ $(i \neq j)$ with masses $(m_i - m_j)$, where $\mathcal{O}$ denotes a generic parton $\{A_\mu, \Phi_I, \Psi\}$, and the heavy fields $\mathcal{O}_{ia}$ of mass m_i. The $\mathcal{O}_{ab}$ and $\mathcal{O}_{ii}$ remain massless. Furthermore we pick up new cubic bosonic interaction terms proportional to m_i

$$\begin{aligned}\hat{S}_{\mathcal{N}=4}\Big|_{\mathcal{O}(g\,m_i)} = g\int d^4x \Big\{ &m_i\,([\Phi_9, A^\mu]\,A_\mu\,)_{ii} - m_i(A_\mu\,[\Phi_9, A^\mu]\,)_{ii} \\ &+ m_i\,([\Phi_9, \Phi_{I'}]\,\Phi_{I'}\,)_{ii} - \,m_i\,(\Phi_{I'}\,[\Phi_9, \Phi_{I'}]\,)_{ii}\Big\}, \quad (6.14)\end{aligned}$$

where the not-spelled out matrix index sums run over the full $N+M$ range. Furthermore the ghosts c and $\bar{c}$ will also receive a mass term and a new $\bar{c}\,c\,\Phi_9$ interaction term.

Given this we note the following: If we use the VEVs m_i as an IR regulator and consider the scattering of color ordered light gluons $(A_\mu)_{ij}$ (or scalars $(\Phi_I)_{ij}$) with $i \neq j$ along with the large N 't Hooft limit, a one-loop computation of an n-particle scattering process will involve precisely the same Feynman diagrams as in the $m_i = 0$ case but with massive $\mathcal{O}_{ia}$ propagators. In particular the box integral will be that of fig. 6.3 (a). In addition we will have new Feynman graphs involving the new $\mathcal{O}(m_i)$ 3-point vertices eq. (6.14). We will see in the next subsections that the new vertices are engineered in precisely such a way that the amplitudes respect the dual conformal symmetry.

6.3.2. One Loop Test of Dual Conformal Symmetry

Here we want to investigate whether a perturbative calculation in the Higgsed version of $\mathcal{N}=4$ SYM has the dual conformal symmetry discussed in section 6.2. We choose a scattering amplitude of four scalars and compute it to one-loop level. Specifically, we consider the color-ordered amplitude

$$A_4 = \langle \Phi_4(p_1)\,\Phi_5(p_2)\,\Phi_4(p_3)\,\Phi_5(p_4)\rangle\,, \quad (6.15)$$

which is related to the leading color contribution of the four scalar scattering amplitude by

$$\mathcal{A}_4 = \sum_{\sigma\in S_4/Z_4} \delta^{j_{\sigma(1)}}_{i_{\sigma(1)}}\delta^{j_{\sigma(2)}}_{i_{\sigma(2)}}\delta^{j_{\sigma(3)}}_{i_{\sigma(3)}}\delta^{j_{\sigma(4)}}_{i_{\sigma(4)}} A_4(\sigma(1),\sigma(2),\sigma(3),\sigma(4))\,. \quad (6.16)$$

Here $(i_1, j_1), \ldots, (i_4, j_4)$ are the $U(M)$ matrix indices of the four scattered scalars, and σ stands for non-cyclic permutations of the set $\{1,\ldots,4\}$. The flavor choice of the scalars in eq. (6.15) was made in such a way that a proliferation of Feynman graphs is avoided. For example, at tree-level, we need to compute only one Feynman diagram

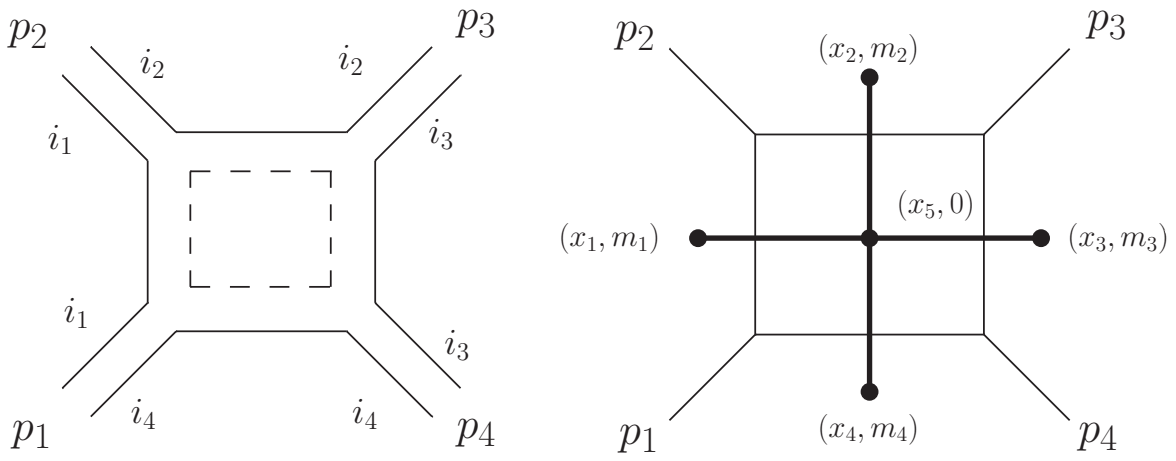

Figure 6.3.: (a) Double line notation of the gauge factor corresponding to a one-loop box integral. The $U(M)$ indices i_n determine the masses of the different propagators. (b) Dual diagram (thick black lines) and dual coordinates. The fifth component of the dual coordinates corresponds to the radial AdS_5 direction.

and we obtain [3]

$$A_4^{tree} = ig_{\rm YM}^2 \,. \tag{6.17}$$

The corresponding one-loop calculation is carried out in appendix G.2. Introducing the notation

$$A_4 = A_4^{tree} M_4 \,, \tag{6.18}$$

and using the result eq. (G.27) we obtain

$$M_4 = 1 - \frac{a}{2} I^{(1)}(s,t,m_i) + O(a^2) \,, \tag{6.19}$$

where $s = (p_1+p_2)^2$, $t = (p_2+p_3)^2$ are the usual Mandelstam variables, m_i are the Higgs masses introduced in the previous section, and $a = g_{\rm YM}^2 N/(8\pi^2)$, with $g_{\rm YM}$ being the Yang-Mills coupling constant.

The integral $I^{(1)}$ is a box integral, depicted in fig. 6.3. In contrast to dimensional regularization, it is defined in four dimensions and depends on several masses coming from the Higgs mechanism. The integral is given by

$$I^{(1)}(s,t,m_i) = c_0 \int d^4k \frac{(s+(m_1-m_3)^2)(t+(m_2-m_4)^2)}{(k^2+m_1^2)((k+p_1)^2+m_2^2)((k+p_1+p_2)^2+m_3^2)(k-p_4)^2+m_4^2)} \,. \tag{6.20}$$

Here $c_0 = -i/\pi^2$. From section 6.3.1 and appendix G.1, we see that the external masses are

$$p_i^2 = -(m_i - m_{i+1})^2 \,. \tag{6.21}$$

As was explained in section 6.2, in the string theory picture the m_i correspond to the distances between the branes in the stack of M branes and the N branes. The scattering amplitude (say, of M gluons) corresponds to strings stretched between the different M

[3] We redefine the coupling constant $g = g_{YM}/\sqrt{2}$ in order to compare to results in the conventions of [30,148]. Also, we omit writing the momentum conservation delta function $\delta^{(4)}(p_1+p_2+p_3+p_4)$.

branes, with i numbering the consecutive gluons. Since two branes i and $i+1$ are separated by $m_i - m_{i+1}$, the string connecting them should have mass $|m_i - m_{i+1}|$ (in appropriate string units) [160]. This situation corresponds precisely to the breaking of $U(N+M)$ to $U(N) \times U(1)^{(M-1)}$. Later, we will take all masses equal, and the external momenta will become light-like in this limit (and we restore $U(N) \times U(M)$). However keeping the masses distinct will allow us to make an interesting observation, as we will see presently.

In [72] it was observed that the analogue of the above box integral in dimensional regularization has a broken dual conformal symmetry. This symmetry was made manifest by introducing dual coordinates whose differences are the momenta of the scattered particles,

$$k = x_5 - x_1 =: x_{51}\,, \qquad p_1 = x_{12}\,, \qquad p_2 = x_{23}\,, \qquad p_3 = x_{34}\,, \quad p_4 = x_{41}\,. \tag{6.22}$$

Carrying out this change of variables in $I^{(1)}$ we obtain

$$I^{(1)}(s,t,m_i) = c_0 \int d^4x_5 \frac{(x_{13}^2 + (m_1 - m_3)^2)(x_{24}^2 + (m_2 - m_4)^2)}{(x_{15}^2 + m_1^2)(x_{25}^2 + m_2^2)(x_{35}^2 + m_3^2)(x_{45}^2 + m_4^2)}\,. \tag{6.23}$$

From the discussion in 6.2, it is natural to think of the masses as the fifth components of the coordinates in the T-dual AdS_5 space. Therefore, let us define five-dimensional vectors $\hat{x}^M$, with $M = 0 \ldots 4$, and denote the usual four-dimensional vectors by x^μ, with $\mu = 0 \ldots 3$. Then, we define

$$\hat{x}_i^\mu := x_i^\mu\,, \qquad\qquad \hat{x}_i^4 := m_i\,, \qquad\qquad i = 1 \ldots 4\,, \tag{6.24}$$

which allows us to rewrite $I^{(1)}$ as

$$I^{(1)}(s,t,m_i) = c_0\, \hat{x}_{13}^2 \hat{x}_{24}^2 \int d^5\hat{x}_5 \frac{\delta(\hat{x}_5^{M=4})}{\hat{x}_{15}^2 \hat{x}_{25}^2 \hat{x}_{35}^2 \hat{x}_{45}^2}\,. \tag{6.25}$$

Here, the one-dimensional delta function was introduced for convenience. It enables us to write the denominator of the integral in terms of five-dimensional, 'hatted', quantities only. Notice that, importantly, due to eq. (6.21) we have that

$$\hat{x}_{12}^2 = \hat{x}_{23}^2 = \hat{x}_{34}^2 = \hat{x}_{41}^2 = 0\,. \tag{6.26}$$

We note that these conditions are invariant under inversions in the five-dimensional space,

$$\hat{x}_i \to \frac{\hat{x}_i}{\hat{x}_i^2}\,. \tag{6.27}$$

Note that eq. (6.27) implies that $m_i \to m_i/\hat{x}_i^2$. Moreover, in the form eq. (6.25) it is also obvious that $I^{(1)}$ is invariant under the inversions eq. (6.27). Indeed, in order to see the invariance of the integral in eq. (6.25) it suffices to count the conformal weight of the various terms in eq. (6.25). Importantly, as for the integrals discussed in [72], the conformal weight of the integration point is zero. Moreover, the integral is normalized in such a way that the conformal weight at the external points is also zero, and hence the integral is invariant under eq. (6.27). By the same reasoning, one can see that e.g. triangle integrals would not be invariant. Indeed, in the calculation leading to eq. (6.19), all triangle integrals canceled out. This confirms that the symmetry

expected from the string theory argument is present in the four-point amplitude we computed.

In addition to invariance under inversions, we have invariance under dilatations, and *four-dimensional* translation and rotation symmetry [4]. The statement of the invariance of the integral under dual conformal transformations can of course also be written in terms of differential equations. The infinitesimal form of the dual conformal transformations is given in appendix G.5. In particular we have

$$\hat{K}_\mu I^{(1)}(s,t,m_i) := \sum_{i=1}^{4} \left[2x_{i\mu} \left(x_i^\nu \frac{\partial}{\partial x_i^\nu} + m_i \frac{\partial}{\partial m_i} \right) - (x_i^2 + m_i^2) \frac{\partial}{\partial x_i^\mu} \right] I^{(1)}(s,t,m_i) = 0\,. \tag{6.28}$$

Let us stress that this is an *exact* symmetry, i.e. there is no anomaly term on the r.h.s. of eq. (6.28). Three remarks are in order here. Firstly, imagine expanding an arbitrary function $f(s,t,m_i = m\,\alpha_i)$ for small m, and truncating this expansion at some order. Then, looking at the explicit form of $\hat{K}_\mu$, we see that if $\hat{K}_\mu f = 0$ then the truncated expansion will have the same property, up to higher order terms in the expansion parameter. Secondly, we remark that although the dual conformal symmetry is valid for genuine values of the Higgs masses m_i, restricting the amplitude to the equal mass case $m_i = m$ will break the dual conformal symmetry. Indeed, for dual conformal symmetry to work, it is important that $\hat{K}_\mu$ in *eq.* (6.28) can act on the different masses m_i. [5] We will come back to this point in section 6.3.4 (see also the first reference in [79–81]). Thirdly, in the conventional sense this exact dual conformal symmetry of the scattering amplitude is not really a symmetry, as it acts on the masses m_i and hence maps $\mathcal{N} = 4$ super Yang-Mills theories at different points of moduli space into each other. While unconventional from the field theory point of view, this mapping is nothing but an isometry in the dual string theory, where the masses m_i are coordinates in the fifth dimension of the dual space, as was discussed in section two.

From the string theory argument given in section 6.2, we expect this dual conformal symmetry to be a generic property of scattering amplitudes in the Higgsed version of $\mathcal{N} = 4$ SYM, independently of the coupling constant and the number of external legs, see also sections 6.3.3 and 6.3.5.

This symmetry immediately allows us to make the observations of [72] more precise and useful. As was already discussed, triangle (sub-)diagrams are excluded and only the restricted set of dual conformal integrals (with the mass assignments as explained in section 6.3.1 are allowed in the final answer for a scattering amplitude. In practice, once one has identified those integrals for the scattering amplitude under consideration, e.g. eq. (6.25) in the one-loop and eq. (6.33) in the two-loop case, one can set $m_i = m$ in order to simplify the calculation of the integrals. Moreover, one can consider the small m expansion and neglect any terms evanescent in m^2.

We write down invariants of this five-dimensional dual conformal symmetry. In the generic n-point case, we can start from the four-dimensional Lorentz invariants x_{ij}^2. It is easy to see that they can be turned into dual conformal invariants by defining

$$u_{ij} := \frac{m_i m_j}{\hat{x}_{ij}^2}\,. \tag{6.29}$$

[4] Note that because we have four-dimensional Lorentz symmetry only it would be mistaken to conclude that the only allowed conformal invariants are five-dimensional cross-ratios.

[5] Phrased differently, the equal mass configuration is not stable under dual conformal transformations, as the latter would lead to a configuration with different masses.

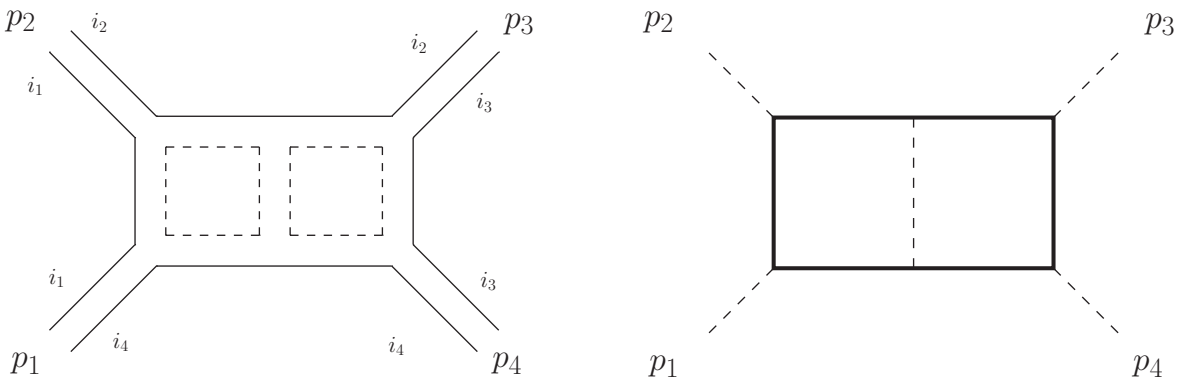

Figure 6.4.: (a) Double line notation of the gauge factor corresponding to the two-loop box integral in the Higgsed theory. The integral is dual conformally invariant. (b) Diagram for the same integral in the equal mass case $m_i = m$. Dashed thin lines denote massless propagators, thick black lines denote massive propagators.

Note that $u_{i,i+1}$ is ill defined in view of the light-likeness conditions eq. (6.26). Therefore, we can have the following two conformal invariants in the four-point case,

$$u := u_{13} = \frac{m_1 m_3}{\hat{x}_{13}^2}\,, \qquad\qquad v := u_{24} = \frac{m_2 m_4}{\hat{x}_{24}^2}\,. \tag{6.30}$$

Hence we arrive at the non-trivial statement that

$$I^{(1)}(x_{13}^2, x_{24}^2, m_i) = f\left(\frac{m_1 m_3}{\hat{x}_{13}^2}, \frac{m_2 m_4}{\hat{x}_{24}^2}\right)\,. \tag{6.31}$$

As a consequence of dual conformal symmetry, the integral with four different masses is reduced to a two-variable function. The relevant four-point integral is given in [163], and it can be checked that the known answer for $I^{(1)}$ is in agreement with eq. (6.31).

If we think about the masses m_i as regulating the amplitude, then it is interesting to know the integral $I^{(1)}$ for the equal mass case $m_i = m$ and m small compared to the kinematical variables s and t. If we did not know the result of [163], we could carry out a simpler calculation for $m_i = m$ and obtain

$$I^{(1)}(x_{13}^2, x_{24}^2, m) = 2\ln\left(\frac{m^2}{x_{13}^2}\right)\,\ln\left(\frac{m^2}{x_{24}^2}\right) - \pi^2 + O(m^2)\,. \tag{6.32}$$

We remark that from eq. (6.32) it follows that the function f in eq. (6.31) is given by $f(u,v) = 2\ln(u)\ln(v) - \pi^2 + O(m^2)$.

6.3.3. Higher Loops and Four-Point Exponentiation

If the inversion symmetry found in section 6.3.2 is present at any loop order then it dramatically restricts the set of scalar integrals that can appear. We would basically find the integrals considered in [72], with the difference that the outer loop carries masses, with the mass assignments as explained in section 6.3.1. E.g. at two loops we

expect to find the following integral only (cf. section 6.3.3),

$$I^{(2)}(s,t,m_i) = (c_0)^2\,(\hat{x}_{13}^2)^2(\hat{x}_{24}^2)\int d^5\hat{x}_5 \int d^5\hat{x}_6 \frac{\delta(\hat{x}_5^{M=4})\delta(\hat{x}_6^{M=4})}{\hat{x}_{15}^2\hat{x}_{25}^2\hat{x}_{35}^2\hat{x}_{56}^2\hat{x}_{36}^2\hat{x}_{46}^2\hat{x}_{16}^2}\,, \tag{6.33}$$

where $\hat{x}_{i,i+1}^2 = 0$ as in the one-loop case. The momentum space notation may be more familiar to some readers, which in the equal mass case is given by

$$\begin{aligned} I^{(2)}(s,t,m) = (c_0)^2\,s^2t \int d^4k_1 \int d^4k_2 \Big[& P(k_1,m^2)P(k_1+p_1,m^2)P(k_1+p_1+p_2,m^2) \\ & \times P(k_1-k_2,0)P(k_2,m^2)P(k_2-p_4,m^2)P(k_2-p_3-p_4,m^2)\Big]\,, \end{aligned} \tag{6.34}$$

where $P(k,m^2) = (k^2+m^2)^{-1}$ and the external momenta are light-like, $p_i^2 = 0$. The double box integral may also appear in a different orientation obtained by replacing $\hat{x}_1 \to \hat{x}_2\,,\ldots,\hat{x}_4 \to \hat{x}_1$, which amounts to interchanging s and t in eq. (6.34). We argue that the coefficients of the box integrals must be the same as those obtained in dimensional regularization [30,148]. The reason is that the leading infrared divergence cannot depend on the regularization. Therefore, based on dual conformal symmetry we expect [6]

$$M_4 = 1 - \frac{a}{2}I^{(1)}(s,t,m) + \frac{a^2}{4}\Big[I^{(2)}(s,t,m) + I^{(2)}(t,s,m)\Big] + O(a^3)\,, \tag{6.35}$$

with $a = g_{\rm YM}^2 N/(8\pi^2)$. Following [30,148], we compute

$$\ln M_4 = a\,w^{(1)} + a^2\,w^{(2)} + O(a^3)\,, \tag{6.36}$$

in order to see whether we find exponentiation in our Higgs regularization. It is convenient to write all quantities that appear in a small m^2 expansion in the following form,

$$f(s,t,m^2) = \sum_{i=1}^{i_{max}} \Big[\ln^i(m^2/s) + \ln^i(m^2/t)\Big]\ f_i(s/t) + f_0(s/t) + O(m^2)\,. \tag{6.37}$$

At one loop, we find, using eq. (6.32),

$$w^{(1)} = -\frac{1}{2}\Big[\ln^2(m^2/s) + \ln^2(m^2/t)\Big] + \frac{1}{2}\ln^2(s/t) + \frac{1}{2}\pi^2 + O(m^2)\,. \tag{6.38}$$

At two loops, using equations eq. (G.34) and eq. (G.35) of appendix C we obtain

$$w^{(2)} = -\frac{1}{8}(I^{(1)}(s,t,m))^2 + \frac{1}{4}I^{(2)}(s,t,m) + \frac{1}{4}I^{(2)}(t,s,m) \tag{6.39}$$

$$\begin{aligned} &= \frac{1}{2}\zeta_2\Big[\ln^2(m^2/s) + \ln^2(m^2/t)\Big] - \zeta_3\Big[\ln(m^2/s) + \ln(m^2/t)\Big] \\ &\quad + \Big[-\frac{1}{2}\zeta_2\ln^2(s/t) - \frac{3}{40}\pi^4\Big] + O(m^2)\,, \end{aligned} \tag{6.40}$$

[6] For convenience, we write the following formulae in the equal mass case $m_i = m$. Note that one can always restore the full dependence on the m_i by substituting $m^2/s \to m_1m_3/\hat{x}_{13}^2$ and similarly $m^2/t \to m_2m_4/\hat{x}_{24}^2$, thanks to dual conformal symmetry.

where various terms canceled when taking the logarithm. Let us now discuss these results.

To begin with, in analogy with dimensional regularization, we define the cusp anomalous dimension by (see [74] and references therein)

$$\left(\frac{\partial}{\partial \ln(m^2)}\right)^2 \ln M_4 = -\Gamma_{cusp}(a) + O(m^2)\,. \tag{6.41}$$

Plugging in the explicit results eq. (6.38) and eq. (6.39) into eq. (6.41) we find

$$\Gamma_{cusp}(a) = 2a - 2\zeta_2 a^2 + O(a^3)\,, \tag{6.42}$$

in agreement with the expression in dimensional regularization. Next, we check whether the finite part of the two-loop result can be thought of as the exponentiation of the finite part of the one-loop result, as in dimensional regularization. Indeed, let us define a finite part F_4 of $\ln M_4$ according to

$$\ln M_4 = D_4 + F_4 + O(m^2)\,. \tag{6.43}$$

Here D_4 contains the terms associated to the infrared divergences,

$$D_4 = -\frac{1}{4}\Gamma_{cusp}(a)\,\left[\ln^2(m^2/s) + \ln^2(m^2/t)\right] + G(a)\,\left[\ln(m^2/s) + \ln(m^2/t)\right]\,, \tag{6.44}$$

where we have introduced the 'collinear anomalous dimension' $G(a) = -\zeta_3 a^2 + O(a^3)$. Note that F_4 is a function of s/t (and of the coupling a) and that it is defined up to an additive (coupling-dependent) constant. The value of this constant and that of $G(a)$ in eq. (6.44) are scheme dependent and can be modified by a redefinition

$$m^2 \to m^2\, e^{h(a)}\,, \tag{6.45}$$

where $h(a)$ is an arbitrary function.

Let us now expand eq. (6.43) in the coupling constant. Writing $F_4 = a\,F_4^{(1)} + a^2\,F_4^{(2)} + O(a^3)$, we obtain (cf. eq. (6.38) and eq. (6.39))

$$F_4^{(1)} = \frac{1}{2}\ln^2(s/t) + \frac{1}{2}\pi^2\,, \qquad F_4^{(2)} = -\frac{1}{2}\zeta_2 \ln^2(s/t) - \frac{3}{40}\pi^4\,. \tag{6.46}$$

Combining these results we see that, up to two loops,

$$F_4 = \frac{1}{2}\Gamma_{cusp}(a) F_4^{(1)} + C(a)\,, \tag{6.47}$$

just as in dimensional regularization, and in agreement with the anomalous dual conformal Ward identity derived in [47, 76]. We will comment on the relation between the exact dual conformal symmetry in the Higgs regularization and that anomalous Ward identity in section 6.3.4. We find that $C(a) = \frac{1}{120}\pi^4\,a^2 + O(a^3)$.

To summarize, we see that taking only the integrals allowed by dual conformal symmetry at two loops agrees with all features discovered for the corresponding amplitudes computed in dimensional regularization.

One can extend the analysis presented here to higher loops and more external legs. Interestingly, it was technically quite simple to evaluate the small mass expansion of

the double box integral (see appendix G.3. It is desirable to automatize the method used to compute that integral and to apply it to more complicated cases.

6.3.4. Anomalous Dual Conformal Ward Identity vs. Exact Dual Conformal Symmetry

We argued that the scalar four-point scattering amplitudes in the Higgsed version of $\mathcal{N} = 4$ SYM eq. (6.15) should have an exact dual conformal symmetry, i.e. they should satisfy the equation

$$\hat{K}_\mu M_4 := \sum_{i=1}^{4} \left[2x_{i\mu} \left(x_i^\nu \frac{\partial}{\partial x_i^\nu} + m_i \frac{\partial}{\partial m_i} \right) - (x_i^2 + m_i^2) \frac{\partial}{\partial x_i^\mu} \right] M_4 = 0 \,, \tag{6.48}$$

where we recall that $A_4 = A_4^{tree} M_4$. Notice that an equation very similar to eq. (6.48) has already appeared at strong coupling in the first reference of [79–81]. It seems natural to ask what the relation between eq. (6.48) and the anomalous dual conformal Ward identity of [47, 76] is, namely

$$K_\mu F_n := \sum_{i=1}^{n} \left[2x_{i\mu} x_i^\nu \frac{\partial}{\partial x_i^\nu} - x_i^2 \frac{\partial}{\partial x_i^\mu} \right] F_n = \frac{1}{2} \Gamma_{cusp}(a) \sum_{i=1}^{n} \left[x_{i,i+1}^\mu \, \ln \frac{x_{i,i+2}^2}{x_{i-1,i+1}^2} \right] F_n \,, \tag{6.49}$$

where F_n is defined as the finite part of $\ln M_n$, i. e. with the logarithm terms e. g. $\ln^2 m^2$, $\ln m^2$, removed. Equation (6.49) was initially derived in [76] for certain light-like Wilson loops dual to maximally-helicity-violating amplitudes by analyzing the structure of divergences of the latter, which leads to the appearance of the anomalous term on the r.h.s. of eq. (6.49).

Now, notice that in eq. (6.48) we could replace M_4 by $\ln M_4$. Then, splitting up $\ln M_4 = D_4 + F_4 + O(m_i^2)$ into a divergent and a finite part, it is clear that the action of the differential operator on the l.h.s. of eq. (6.48) on D_4 will produce an anomalous term [7]. Although this is not obvious, we expect the quantity F_4 to be independent of the regularization method that was used to calculate it (up to a scheme-dependent additive constant, as was discussed in the previous section). Therefore, we expect that F_4 computed in the Higgsed theory should satisfy the same anomalous Ward identity eq. (6.49) as when computed in dimensional regularization. We indeed see that this is the case in the two-loop example considered in section 6.3.3, as one can easily check. There is little doubt that one can prove that eq. (6.49) follows from eq. (6.48) by studying the structure of divergences of scattering amplitudes in the Higgsed theory (with different masses).

6.3.5. More External Legs

Turning to the generic n-point case, we would like to argue that at one loop the only effect of the new regularization is to replace the dimensionally regulated box integrals appearing in dimensional regularization by our mass regulated box integrals, with the specific mass assignment explained earlier [8]. See fig. 6.5, which illustrates the only five-

[7] Note that acting on F_n, which by definition is independent of the regulator m_i, we have $\hat{K}_\mu F_n = K_\mu F_n + O(m_i^2)$, and we can simply replace $\hat{K}_\mu$ by K_μ.

[8] When scattering particles with helicity, there will also be a slight change in the spinor helicity formalism since in the distinct mass case the external states are massive with masses squared

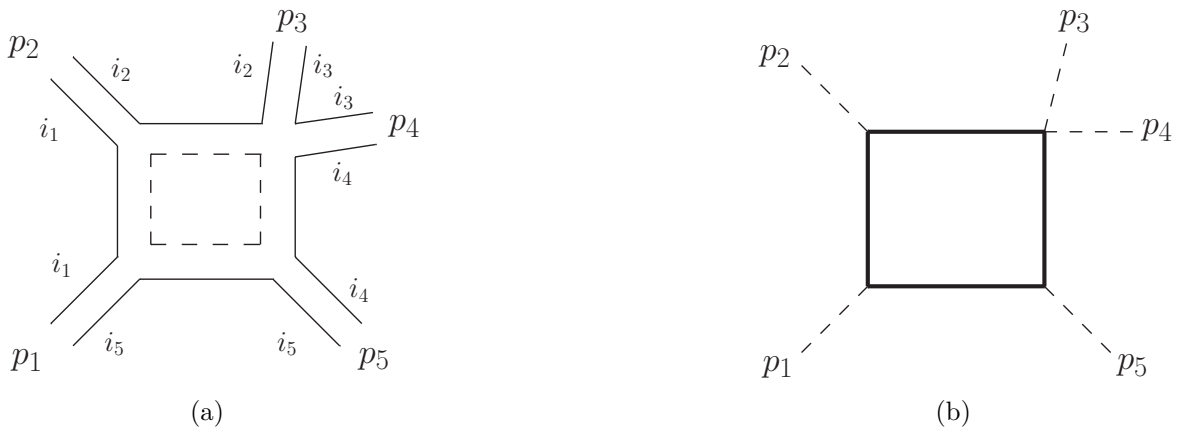

Figure 6.5.: (a) An example of a higher-point dual conformal integral. The picture corresponds to a '1-mass' integral, since the sum p_3+p_4 is in general not light-like. As in the four-point case, there are the masses of the Higgsed particles circulating in the outer loops. (b) In the equal mass case $m_i = m$, all outer legs become massless (dashed lines), while the internal propagators (full black lines) have uniform mass m, making the integral infrared finite.

point dual conformal scalar integral at one loop. The generalization to an arbitrary number of external legs is straightforward (see also appendix G.3).

For this it is desirable to have a suitable n-leg generalization of the four scalar amplitude eq. (6.15) considered above at hand, which has the virtue of coming from a single planar tree-diagram. We propose the non-MHV amplitude of $2n$ external scalar fields,

$$A_{2n} = \langle \Phi_4 \underbrace{\Phi_5 \Phi_6 \Phi_7 \Phi_5 \Phi_6 \Phi_7 \ldots}_{n-1} \Phi_4 \underbrace{\ldots \Phi_7 \Phi_6 \Phi_5 \Phi_7 \Phi_6 \Phi_5}_{n-1} \rangle \,. \tag{6.50}$$

Note that A_{2n} is an N^{k}MHV amplitude where $k = n-2$, with $n \geq 2$. For $n = 2$ it is equivalent to the four-scalar amplitude considered in equation eq. (6.15). In eq. (6.50) we suppressed the dependence on the scattering momenta $p_1, \ldots p_n$, and the flavor choice of the scalars was made in a way such that there is only one tree-level diagram (compare fig. 6.6), which can be readily evaluated,

$$A_{2n}^{tree} = i g_{\mathrm{YM}}^{(2n-2)} \frac{1}{\hat{x}_{2n,3}^2 \, \hat{x}_{2n-1,4}^2 \ldots \hat{x}_{n+3,n}^2} = i g_{\mathrm{YM}}^{(2n-2)} \prod_{i=0}^{n-3} \frac{1}{\hat{x}_{2n-i,i+3}^2} \,. \tag{6.51}$$

At one-loop level, the calculation of A_{2n}^{1-loop} would be very similar to that done for A_4^{1-loop} in appendix G.2. As a result, we expect that A_{2n}^{1-loop} will be given by a linear combination of the dual conformal integrals given in appendix G.3, with certain coefficients.

We remark that eq. (6.50) may be very interesting in its own right[9]. It appears to be a new example of an amplitude that is dual conformal on its own, without having to consider superamplitudes. In this sense, eq. (6.50) is very similar to split helicity amplitudes. Moreover, it is given by a single term. This may suggest using an

$(m_i - m_{i+1})^2$. We could argue that this effect is irrelevant since we could consider a situation where $(m_i - m_{i+1})^2 \ll m_j^2$.

[9]We thank J. Drummond for discussions on this point.

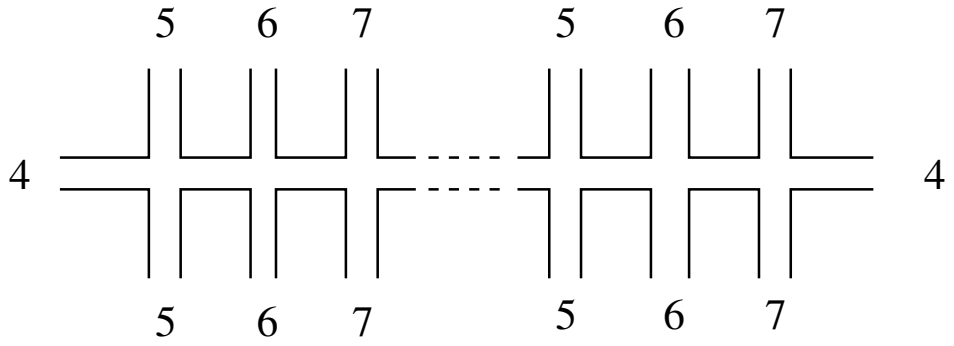

Figure 6.6.: The unique planar tree-level diagram contributing to the family of multi-leg amplitudes A_{2n} of eq. (6.50). Note that the flavor sequence $567\ldots567$ does not need to end on the 7.

alternative formulation of tree-level amplitudes (as compared to the one given in [46]), where eq. (6.50) plays the role of the starting point.

6.3.6. Dual Conformal Symmetry vs. Dual Superconformal Symmetry

The four-point amplitude we considered in the previous sections is special in the sense that it is very similar to the so-called 'split-helicity' case. This refers to the scattering of gluons where the gluons with negative helicity sit on one side of the color ordered amplitude and all gluons with positive helicity sit on the other side. In [47] it was shown that these amplitudes are dual conformal on their own. For generic helicity configurations, this is not true and one needs to consider certain super-amplitudes which are dual conformal [47]. In particular, the dual conformal generator then receives additional terms depending on Grassmann variables that parametrize the on-shell states of the $\mathcal{N} = 4$ on-shell supermultiplet. Here we want to argue that the observation that the integrals appearing in loop calculations have the exact conformal symmetry discussed earlier applies to all amplitudes, not just to the split helicity case. Indeed, the reason for the non-covariance of generic amplitudes under dual conformal symmetry is that different amplitudes can transform into each other under this symmetry. When one considers super-amplitudes as in [47], the latter transform covariantly. However, knowing that a generic amplitude can be expressed as a sum over scalar integrals multiplied by certain coefficients, it is clear that the non-covariance under the dual conformal transformations can affect the coefficients only. The integrals, on the other hand, should have the exact dual conformal symmetry.

6.4. Making Contact to More Recent Results

In this final section we want to mention a few more recent results that have been motivated by the work presented in this chapter. In particular we want to make contact to the results presented in chapter 5.

In references [164,165] the massive regulator presented here has been successfully applied at up to four loops at four points and up to two loops at five points and has been shown to be consistent with the results from dimensional regularization. The suggested

interpretation of the regulator masses m_i as components of higher-dimensional momenta motivated several groups to investigate the dual conformal symmetry in higher dimensions. It was shown that at tree-level superamplitudes of the six-dimensional $\mathcal{N} = (1,1)$ SYM theory [52], compare section 1.5.1, and the ten-dimensional $\mathcal{N} = 1$ SYM theory [166] have a dual con- formal symmetry. As explained in section 5.2, this proves the dual conformal covariance (5.40) of the massive tree-level superamplitudes (5.20) on the Coulomb branch of $\mathcal{N} = 4$ SYM theory.

Whereas the dual conformal symmetry of the Higgs regularized loop amplitudes has been first conjectured in the work presented in this chapter it has by now been essentially proven in [52]. Previous evidence in support of this had come from [90, 164, 165, 167]. As already mentioned in eq. (5.54), it was shown in [52] that the cut constructable part of the six-dimensional superamplitudes of $\mathcal{N} = (1,1)$ SYM theory is covariant under dual conformal inversions if the loop momentum is restricted to four dimensions. However, this prescription is equivalent to the massive regularization of the four-dimensional amplitudes described here. Hence, this proves the dual conformal symmetry of the Higgs-regularized loop amplitudes in $\mathcal{N} = 4$ SYM theory, up to potential terms not determined by unitarity cuts.

In section 5.3 we derived the symmetries of the coulomb branch, tree-level superamplitudes (5.20). Most notably they invert covariantly (5.40) and consequently exhibit a five-dimensional dual conformal symmetry, eqs. (5.46) and (5.47). Due to the four-dimensional loop momenta in the Higgs regularized loop amplitudes the translation invariance in the 'extra dimensional' directions is lost and consequently only the four-dimensional $\mu = 0, 1, 2, 3$ components of the six-dimensional dual conformal boost generator $K_\mu = IP^\mu I$ remain symmetries. The action of the extended dual conformal generator $\hat{K}_{\alpha\dot{\alpha}} = \frac{1}{2}\sigma^\mu_{\alpha\dot{\alpha}}\hat{K}_\mu$ (G.52) in the dual superspace (5.14) is given by eq. (5.46)

$$\begin{aligned}\hat{K}_{\alpha\dot{\alpha}} = \sum_i \Bigg[& x_{i\,\alpha\dot{\gamma}}\, x_{i\,\dot{\alpha}\gamma}\, \frac{\partial}{\partial x_{i\,\gamma\dot{\gamma}}} + x_{i\,\alpha\dot{\alpha}}\, n_i \frac{\partial}{\partial n_i} + n_i^2\, \frac{\partial}{\partial x_i^{\dot{\alpha}\alpha}} \\ & + \theta^a_{i\,\alpha}\, x_{i\,\beta\dot{\alpha}}\, \frac{\partial}{\partial \theta^a_{i\,\beta}} + \tilde{\theta}^a_{i\,\dot{\alpha}}\, x_{i\,\alpha\dot{\beta}}\, \frac{\partial}{\partial \tilde{\theta}^a_{i\,\dot{\beta}}} + n_i\, \tilde{\theta}^a_{i\,\dot{\alpha}}\, \frac{\partial}{\partial \theta^{\alpha\,a}_i} - n_i\, \theta^a_{i\,\alpha}\, \frac{\partial}{\partial \tilde{\theta}^{\dot{\alpha}\,a}_i} \Bigg],\end{aligned} \tag{6.52}$$

where we, in contrast to the rest of this chapter, used mostly minus metric and made the change of variables $n_i = m_i$, in order to match the conventions of chapter 5.

7

Conclusion and Outlook

QCD tree amplitudes are of great phenomenological and theoretical interest. The detailed analysis of their analytic structure may lead to a more profound understanding of $SU(N)$ gauge theories exposing further symmetries undiscovered so far. Concerning phenomenological applications tree amplitudes represent an important input for cross section evaluations in Born approximation and beyond. In sections 2.2.1, 2.2.2 and 2.3 we derived the color decomposition of an arbitrary QCD amplitude at tree- and one-loop level necessary for efficient leading and next-to leading order calculations. Furthermore we derived general fermion flip and reversion identities, spanning the null space among the primitive one-loop amplitudes. The obtained results are implemented in the freely available `Mathematica` package `QCDcolor` described in appendix D and shall provide an alternative to the diagram based algorithm for the determination of the color decomposition of a particular QCD amplitude [23–26]. The identities among the primitive amplitudes can be used to reduce the number of primitives constituting the amplitude to a minimum, as well as to analytically compare different color decompositions of a particular QCD amplitude.

Exploiting the fermion flip identities derived in section 2.3 we were able to prove in chapter 3 that all color ordered tree amplitudes of massless QCD can be written as linear combinations of color ordered tree amplitudes of $\mathcal{N} = 4$ SYM theory. We also discussed how to convert these amplitudes into trees with one electroweak vector boson. We explained how representations of QCD amplitudes containing a minimal number of gluon-gluino amplitudes can be obtained and derived minimal representations for all QCD amplitudes with up to four quark lines. Furthermore, we derived closed analytical formulae for all gluon gluino amplitudes relevant for QCD and implemented them in the freely available `Mathematica` package `GGT`. Together with the color decomposition derived in chapter 2 this leads to the remarkable consequence that all tree amplitudes as well as the cut constructable part of all QCD loop amplitudes can be obtained from $\mathcal{N} = 4$ SYM theory. Furthermore, any future progress on tree-level amplitudes of $\mathcal{N} = 4$ SYM automatically carries over to QCD.

Despite the indisputable powers of the color ordered approach to calculating QCD

scattering amplitudes it has obvious limitations. The number of primitive amplitudes constituting the one-loop QCD amplitude with n gluons and k quarks–anti-quark pairs grows as $(n + 2k - 1)!$, which results in some hard cut off for the multiplicities that allow for a numerical evaluation of a one-loop QCD amplitude on a particular computer. Since the factorial growth in complexity seems to be intrinsic to the one loop corrections, the goal should be to either dampen it by refining the computational methods or by using approximations like e. g. monte carlo methods or a leading color approximation.

In an independent work published recently in reference [168], C. Reuschle and S. Weinzierl found a tree-level and a one-loop color decomposition of QCD similar to our results by using shuffle relations. A detailed comparison to our results would be an interesting future project. In reference [169], which appeared shortly after the publication of our results in [4], T. Melia presents an alternative to the general construction of QCD amplitudes using fermion flip identities, presented in section 3.3.1, by recursively construction single flavor representations of multi-flavor color ordered tree amplitudes. Similar to our general fermion flip construction the single flavor representations are of limited practical relevance since they are not minimal and the number of necessary gluon-gluino amplitudes strongly depends on the number of involved gluons. Hence, despite their relevance for formal considerations, for practical applications it is much more convenient to use the minimal representations of QCD amplitudes derived in section 3.3.2, i. e. maximally three gluon-gluino tree amplitudes are necessary to give a particular color ordered QCD amplitude with up to eight quarks and an arbitrary number of gluons.

In chapter 4 we have analyzed two different approaches to evaluate color ordered tree amplitudes. We have compared the numerical performance of a purely numerical approach based on the Berends-Giele recursion with the numerical evaluation of the analytic formulae derived in chapter 3. In detail we find that MHV and NMHV amplitudes are most efficiently calculated using the analytic formulae. For NNMHV amplitudes and beyond we find the purely numerical approach more efficient. We have also investigated the numerical accuracy. In general the numerical accuracy of the analytic formulae (evaluated numerically) is superior compared to the purely numerical approach. However we find that close to exceptional phase space configuration, such as soft/collinear configurations, analytic formulae suffer also from rounding errors. In both approaches we find even for large multiplicities an average accuracy of at least 9 digits — sufficient for phenomenological applications.

As an interesting avenue we took a first step towards a generalization of the results from massless QCD amplitudes to amplitudes containing massive quarks, or other massive colored states by investigating massive amplitudes on the Coulomb branch of $\mathcal{N} = 4$ SYM in chapter 5. We derived all symmetries of the massless six-dimensional superamplitudes of $\mathcal{N} = (1, 1)$ SYM theory in sections 1.5.1 and 1.6.2 thereby correcting small mistakes in the proof of the dual conformal symmetry given in [52]. We exploited the symmetries of the six-dimensional amplitudes to derive the symmetries of massive tree amplitudes in $\mathcal{N} = 4$ SYM theory and showed that the five dimensional dual conformal symmetry of the massive amplitudes leads to the presence of non-local Yangian-like generators $m^{(1)}$, $p^{(1)}$ associated to the masses and momenta in on-shell superspace. An interesting open question is whether or not there exist level-one supermomenta as well.

Furthermore, we explained how analytical formulae for tree-level superamplitudes of

$\mathcal{N} = (1,1)$ SYM can be obtained from a numerical implementation of the BCFW recursion relation. The developed method is very general and can be easily applied to other theories as well. We used it to derive compact, manifest dual conformal covariant representations of the five- and six-point superamplitudes. To facilitate the investigation of the six-dimensional superamplitudes we proposed a little group decomposition of them. The little group decomposition is the six-dimensional analog of the MHV-band decomposition introduced in [51] and allows to separate parts of varying complexity as well as to clearly specify the parts of the superamplitude that survive in the massless limit to four-dimensions. We exploited the little group decomposition to study UHV amplitudes in section 5.4.6, leading to arbitrary multiplicity formulae valid for large classes of component amplitudes with two consecutive massive legs.

We disproved the widespread claim within the literature that within a maximally supersymmetric theory it is sufficient to consider e. g. only gluon amplitudes and the remaining amplitudes by supersymmetry. Indeed, the supersymetrization of the six-dimensional gluon amplitudes, as has been done in reference [89] for the three, four and five point amplitudes, will not necessarily yield the correct superamplitude for multiplicities greater than five. We derived examples of supersymmetric, dual conformal covariant representations of the gluon sector which do not coincide with the superamplitude. Nevertheless, we observed that dual conformal extensions and consequently supersymetrizations of subsets of amplitudes reproduce at least part of the other component amplitudes. It would be interesting to investigate this in more detail in the future since finding dual conformal extensions of subsets of amplitudes is much simpler than finding the whole superamplitude.

In [85] it has been claimed that all superamplitudes of $\mathcal{N} = (1,1)$ SYM can be obtained by uplifting massless tree-level superamplitudes of $\mathcal{N} = 4$ SYM in non-chiral superspace. We derived the superconformal and dual superconformal symmetries of the non-chiral superamplitudes in section 1.4.2 and used the non-chiral BCFW recursion to prove the dual conformal symmetry as well as to derive the five and six-point superamplitude. We thoroughly investigated the implications of a potential uplift by identifying the correct four- and six-dimensional Lorentz invariants that should appear in such a correspondence. By performing numerical checks we confirmed the uplift of representations containing only a restricted set of dual conformal covariant and chiral self-conjugate building blocks up to a multiplicity of eight. However, we proved that finding a representation of the massless non-chiral superamplitudes of $\mathcal{N} = 4$ SYM that can be uplifted is non-trivial for multiplicities larger than five. One possible flaw of the uplift are identities of the four-dimensional building blocks that do not uplift to identities of the corresponding six-dimensional building blocks. We gave examples of such identities that need to be avoided by restricting the allowed building blocks in order to not spoil the uplift. Despite being of no practical relevance for the determination of the six-dimensional superamplitudes or the massive four-dimensional amplitudes, it is still very fascinating from the theoretical point of view, that the correct representation of the non-chiral MHV superamplitude in four dimensions might be sufficient to get the whole six-dimensional superamplitude, or equivalently all massive four-dimensional amplitudes on the coulomb branch of $\mathcal{N} = 4$ SYM theory.

In the last chapter we investigated a dual conformal covariant regularization of (planar) scattering amplitudes in $\mathcal{N} = 4$ SYM that is an alternative to the commonly used dimensional regularization/reduction which breaks the dual conformal symmetry. This regularization was motivated by the string theory side of the AdS/CFT correspondence

and, as for instance mentioned in [82] and argued in chapter 6, it also suggests that the previously discovered broken dual conformal symmetry [72, 73, 75, 76] of scattering amplitudes can be turned into an exact symmetry when considering scattering amplitudes in the Higgsed theory. Indeed the dual conformal symmetry of the Higgs-regularized loop amplitudes has been proven in reference [52] after the investigation presented in chapter 6 has been completed.

We worked out the gauge theory analogue of this regularization and argued that the scattering amplitudes on the gauge theory side should possess the aforementioned exact dual conformal symmetry. The latter severely restricts the number and type of loop integrals that can appear in the calculation of the amplitudes. In dimensional regularization, the observation that the integrals appearing in the four-gluon amplitude of [30, 148] all have dual conformal properties was made in [72]. However, since the dimensional regularization breaks this symmetry, other integrals could also appear in principle. In contrast, in the case of the mass regularization considered here, the dual conformal symmetry is exact and hence so is the restriction on the possible integrals appearing in the amplitude. In particular, dual conformal symmetry forbids all triangle sub-graphs. Furthermore, there are simple rules for determining whether an integral is dual conformal, see [72]. Hence, the dual conformal symmetry is a very helpful tool for establishing the set of scalar integrals that are allowed to appear in an amplitude and therefore simplifies the determination of the loop integrand through the generalized unitarity method.

Recently, it was realized that the idea of constructing tree-level amplitudes from their factorization channels, as exploited in the BCFW recursion, can be equally applied to the planar loop integrand of $\mathcal{N} = 4$ SYM theory [170–172]. Therefore the four-dimensional loop integrand of a given amplitude can be easily obtained in an iterative way. However, the integrand leads to infrared divergences, requiring the d-dimensional loop integrand if dimensional regularization is used, or the integrand on the Coulomb branch in order to be safely integrated. Given the four-dimensional integrand, the extended dual conformal symmetry can be exploited to translate the four-dimensional integrand to the coulomb branch, up to corrections of order $\mathcal{O}(m^2)$ [171]. Consequently, solving $\mathcal{N} = 4$ SYM theory boils down to the evaluation of the dual conformal loop integrals.

An important question we hope to address in the future is whether the conventional conformal symmetry of $\mathcal{N} = 4$ SYM can be used to constrain scattering amplitudes at loop level. It may be that it is easier to understand that symmetry in our regularization.

Finally, as the suggestion for studying scattering amplitudes in the Higgsed theory came from the AdS/CFT correspondence, one may wonder whether it is also useful to carry out computations on the string theory side of the correspondence. On the string theory side, while this regularization is conceptually very appealing, it seems difficult to carry out actual computations. On the other hand, this regularization may be more amendable to systematically computing sub-leading corrections [1] in $1/\sqrt{\lambda}$ and in order to answer questions related to the symmetries of the scattering amplitudes where finding the classical solutions may not be necessary.

[1] See for instance [173] regarding difficulties when using dimensional regularization.

Acknowledgment

First of all I would like to thank my supervisor Prof. Jan Plefka for his time, helpful advises and encouragement, as well as for giving me the opportunity to freely choose the research topics of this thesis. Furthermore, I am grateful for the many opportunities to take part in international summer schools and conferences that were given to me and my fellow PhD students. The atmosphere was very collaborative and I will remember the time in this research group as a very pleasant one.

I am very thankful to Luis Fernando Alday, Simon Badger, Benedikt Biedermann, Lance Dixon, Johannes Henn, Jan Plefka, Peter Uwer and Valentin Verschinin for the fruitful collaboration on great parts of the results presented here.

Furthermore, I am especially grateful to Prof. Dietmar Ebert for being a valuable constant throughout my time at the Humboldt-Universität.

I have profited from discussions and correspondence with Simon Badger, Zvi Bern, Jake Bourjaily, James Drummond, Henriette Elvang, Martin Heinze, Harald Ita, Thomas Klose, Gregory Korchemsky, Juan Maldacena, Sven Moch, Stephen Naculich, Kemal Ozeren, Andreas Rodigast, Ralf Sattler, Pedro Vieira, Konstantin Wiegandt, Sebastian Wuttke, Valeri Yundin.

Finally, I would like to thank my family for there constant love and support over the last years. I am particularly thankful to my wonderful wife Susanne Schuster for her enormous support in the final phase of this work.

The Appendix

Additional material

In the appendix we present further details of the investigations presented in the main part in order to make the presentation of our results as comprehensive as possible while not spoiling the readability of the main part.

Appendix A

Spinor Conventions

In this appendix we summarize our convention for the four- and six-dimensional spinors and provide the identities relevant for calculations within the spinor helicity formalism. Additionally we derive the general Fierz identity in even dimensions and discuss the properties of the charge conjugation matrix since both of them are relevant for the derivation of the $\mathcal{N} = 4$ SYM Lagrangian in appendix B.

A.1. Four-Dimensional Spinors

Raising and lowering of spinor indices is defined by left multiplication with the ϵ symbol and its inverse:

$$\lambda_\alpha = \epsilon_{\alpha\beta}\lambda^\beta\,, \qquad \lambda^\alpha = \epsilon^{\alpha\beta}\lambda_\beta\,, \tag{A.1}$$

$$\tilde{\lambda}_{\dot\alpha} = \epsilon_{\dot\alpha\dot\beta}\tilde{\lambda}^{\dot\beta}\,, \qquad \tilde{\lambda}^{\dot\alpha} = \epsilon^{\dot\alpha\dot\beta}\tilde{\lambda}_{\dot\beta}\,, \tag{A.2}$$

where the antisymmetric ϵ symbol is defined as

$$\epsilon = i\sigma_2 \qquad \epsilon_{12} = \epsilon_{\dot1\dot2} = -\epsilon^{12} = -\epsilon^{\dot1\dot2} = 1 \tag{A.3}$$

and is obeying the equations

$$\begin{aligned} \epsilon_{\alpha\beta}\epsilon^{\beta\gamma} &= \delta_\alpha^\gamma\,, & \epsilon_{\dot\alpha\dot\beta}\epsilon^{\dot\beta\dot\gamma} &= \delta_{\dot\alpha}^{\dot\gamma}\,, \\ \epsilon_{\beta\gamma}\delta_\delta^\alpha + \epsilon_{\gamma\delta}\delta_\beta^\alpha + \epsilon_{\delta\beta}\delta_\gamma^\alpha &= 0 & \epsilon^{\dot\beta\dot\gamma}\delta_{\dot\alpha}^{\dot\delta} + \epsilon^{\dot\gamma\dot\delta}\delta_{\dot\alpha}^{\dot\beta} + \epsilon^{\dot\delta\dot\beta}\delta_{\dot\alpha}^{\dot\gamma} &= 0 \end{aligned} \tag{A.4}$$

For the spinor products we choose the conventions

$$\langle\lambda\,\mu\rangle = \lambda^\alpha\mu_\alpha \qquad \text{and} \qquad [\tilde\lambda\,\tilde\mu] = \tilde\lambda_{\dot\alpha}\tilde\mu^{\dot\alpha}\,, \tag{A.5}$$

which implies

$$\lambda_\alpha \mu_\beta - \lambda_\beta \mu_\alpha = \epsilon_{\alpha\beta} \langle \lambda\, \mu \rangle \qquad \tilde{\lambda}_{\dot\alpha} \tilde{\mu}_{\dot\beta} - \tilde{\lambda}_{\dot\beta} \tilde{\mu}_{\dot\alpha} = -\epsilon_{\dot\alpha\dot\beta} [\tilde{\lambda}\, \tilde{\mu}] \tag{A.6}$$

The four-dimensional sigma matrices are defined as

$$\sigma^\mu{}_{\alpha\dot\alpha} = (1, \vec{\sigma})_{\alpha\dot\alpha} \qquad \text{and} \qquad \bar{\sigma}^{\mu\,\dot\alpha\alpha} = (1, -\vec{\sigma})^{\dot\alpha\alpha} \tag{A.7}$$

and have the properties

$$\sigma^\mu \bar{\sigma}^\nu + \sigma^\nu \bar{\sigma}^\mu = 2\eta^{\mu\nu}\,, \qquad \bar{\sigma}^\mu \sigma^\nu + \bar{\sigma}^\nu \sigma^\mu = 2\eta^{\mu\nu}\,, \tag{A.8}$$

$$\sigma^\mu_{\alpha\dot\alpha} \bar{\sigma}^{\dot\beta\beta}_\mu = 2\delta^\beta_\alpha \delta^{\dot\beta}_{\dot\alpha}\,, \qquad \sigma^{\mu\,\alpha\dot\beta} = \bar{\sigma}^{\mu\,\dot\beta\alpha}\,, \tag{A.9}$$

which are consequences of the properties of the ordinary three-dimensional Pauli matrices $\vec{\sigma} = \begin{pmatrix}\sigma_1 & \sigma_2 & \sigma_3\end{pmatrix}$

$$\sigma_1 = \begin{pmatrix} 0 & 1 \\ 1 & 0 \end{pmatrix}, \qquad \sigma_2 = \begin{pmatrix} 0 & -i \\ i & 0 \end{pmatrix}, \qquad \sigma_3 = \begin{pmatrix} 1 & 0 \\ 0 & -1 \end{pmatrix}. \tag{A.10}$$

Raising and lowering of spinor indices on derivatives with respect to a spinor leads to an additional minus sign

$$\frac{\partial}{\partial \lambda_\alpha} = \frac{\partial \lambda^\beta}{\partial \lambda_\alpha} \frac{\partial}{\partial \lambda^\beta} = -\epsilon_{\alpha\beta} \frac{\partial}{\partial \lambda^\beta}\,, \tag{A.11}$$

which is a general feature of derivatives carrying $su(2)$ indices.

A.2. Six dimensional Spinors

The six-dimensional Pauli matrices fulfill the algebra

$$\Sigma^\mu \widetilde{\Sigma}^\nu + \Sigma^\nu \widetilde{\Sigma}^\mu = 2\eta^{\mu\nu}\,. \tag{A.12}$$

We choose the antisymmetric representation

$$\Sigma^0 = i\sigma_1 \otimes \sigma_2\,, \qquad \widetilde{\Sigma}^0 = -\Sigma^0\,, \tag{A.13}$$

$$\Sigma^1 = i\sigma_2 \otimes \sigma_3\,, \qquad \widetilde{\Sigma}^1 = \Sigma^1\,, \tag{A.14}$$

$$\Sigma^2 = -\sigma_2 \otimes \sigma_0\,, \qquad \widetilde{\Sigma}^2 = -\Sigma^2\,, \tag{A.15}$$

$$\Sigma^3 = -i\sigma_2 \otimes \sigma_1\,, \qquad \widetilde{\Sigma}^3 = \Sigma^3\,, \tag{A.16}$$

$$\Sigma^4 = -\sigma_3 \otimes \sigma_2\,, \qquad \widetilde{\Sigma}^4 = -\Sigma^4\,, \tag{A.17}$$

$$\Sigma^5 = i\sigma_0 \otimes \sigma_2\,, \qquad \widetilde{\Sigma}^5 = \Sigma^5\,. \tag{A.18}$$

They satisfy the following identities

$$\Sigma^\mu_{AB} = \tfrac{1}{2}\epsilon_{ABCD} \widetilde{\Sigma}^{CD}_\mu\,, \qquad \widetilde{\Sigma}^{AB}_\mu = \tfrac{1}{2}\epsilon^{ABCD} \Sigma^\mu_{CD} \tag{A.19}$$

$$\Sigma^\mu_{AB} \Sigma_{\mu\, CD} = -2\epsilon_{ABCD}\,, \qquad \widetilde{\Sigma}^{\mu\, AB} \widetilde{\Sigma}^{CD}_\mu = -2\epsilon^{ABCD}\,, \tag{A.20}$$

$$\widetilde{\Sigma}^{AB}_\mu \Sigma^\mu_{CD} = -2(\delta^A_C \delta^B_D - \delta^B_C \delta^A_D)\,, \qquad \mathrm{Tr}(\widetilde{\Sigma}^\mu \Sigma^\nu) = 4\eta^{\mu\nu}\,. \tag{A.21}$$

The six dimensional Shouten identity reads

$$\delta_A^F\epsilon_{BCDE} + \delta_B^F\epsilon_{CDEA} + \delta_C^F\epsilon_{DEAB} + \delta_D^F\epsilon_{EABC} + \delta_E^F\epsilon_{ABCD} = 0\,, \tag{A.22}$$

and contractions of epsilon tensors may be deduced from

$$\epsilon_{ABCD}\epsilon^{EFGD} = \delta_A^E\delta_B^F\delta_C^G + \delta_A^F\delta_B^G\delta_C^E + \delta_A^G\delta_B^E\delta_C^F - \delta_C^E\delta_B^F\delta_A^G - \delta_C^F\delta_B^G\delta_A^E - \delta_C^G\delta_B^E\delta_A^F \tag{A.23}$$

The first four of the six dimensional sigma matrices are simply related to the Weyl representation of the four dimensional gamma matrices

$$\Sigma^\mu = 1\otimes\epsilon\cdot\gamma^\mu = \begin{pmatrix} 0 & -\sigma^{\mu\,\alpha}{}_{\dot\beta} \\ \bar\sigma^\mu{}_{\dot\alpha}{}^\beta & 0 \end{pmatrix}\,,\quad \widetilde\Sigma^\mu = \gamma^\mu\cdot 1\otimes\epsilon^{-1} = \begin{pmatrix} 0 & -\sigma^\mu{}_\alpha{}^{\dot\beta} \\ \bar\sigma^{\mu\,\dot\alpha}{}_\beta & 0 \end{pmatrix}\,. \tag{A.24}$$

A.2.1. Three-Point Kinematics

The three-point kinematics

$$p_1 + p_2 + p_3 = 0\,, \qquad\qquad p_i^2 = 0 \tag{A.25}$$

imply the vanishing of all invariants

$$p_1\cdot p_2 = p_1\cdot p_3 = p_2\cdot p_3 = 0\,. \tag{A.26}$$

As a consequence of eq. (1.24), the spinor products $\langle i|j]$ have rank one and posses a bispinor representation. A consistent set of spinors $\{u_i, \tilde u_i\}$ associated to the external legs has been introduced by C. Cheung and D. O'Connell in [54] and reads

$$\langle i_a|j_{\dot a}] = u_{i\,a}\tilde u_{j\,\dot a}\,, \qquad \langle j_a|i_{\dot a}] = -u_{j\,a}\tilde u_{i\,\dot a}\,, \qquad \text{for } \{i,j\} \text{ cyclic.} \tag{A.27}$$

Due to momentum conservation, these spinors are subject to the constraints

$$u_1^a\langle 1_a| = u_2^a\langle 2_a| = u_3^a\langle 3_a|\,, \tilde u_1^{\dot a}[1_{\dot a}| = \tilde u_1^{\dot a}[1_{\dot a}| = \tilde u_1^{\dot a}[1_{\dot a}|\,. \tag{A.28}$$

Furthermore pseudoinverses of the spinors can be introduced

$$u_a w_b - u_b w_a = \epsilon_{ab}\,, \qquad\qquad \tilde u_{\dot a}\tilde w_{\dot b} - \tilde u_{\dot b}\tilde w_{\dot a} = \epsilon_{\dot a\dot b}\,. \tag{A.29}$$

In order to reduce the redundancy in the definition of the spinors w_i and $\tilde w_i$ it is convenient to impose the constraints

$$w_1^a\langle 1_a| + w_2^a\langle 2_a| + w_3^a\langle 3_a| = 0\,, \qquad \tilde w_1^{\dot a}[1_{\dot a}| + \tilde w_2^{\dot a}[2_{\dot a}| + \tilde w_3^{\dot a}[3_{\dot a}| = 0\,. \tag{A.30}$$

A.3. Fierz Identities in even Dimensions

The aim of this section is to derive the general Fierz identity in an even dimensional space. Starting point are the $2^{\frac{d}{2}}$ dimensional Gamma matrices

$$\{\gamma^\mu, \gamma^\nu\} = 2\eta^{\mu\nu} \qquad\qquad \gamma^{d+1} = i^{-1-\frac{d}{2}}\gamma^0\ldots\gamma^{d-1} \tag{A.31}$$

with $\eta^{\mu\nu} = \mathrm{diag}(+,-,\dots,-)$. The normalization of γ^{d+1} is chosen in such a way that

$$\left(\gamma^{d+1}\right)^2 = (-1)^{-1-\frac{d}{2}}\gamma^0\dots\gamma^{d-1}\gamma^0\dots\gamma^{d-1} = (-1)^{-1-\frac{d}{2}}(-1)^{d-1}(-1)^{\frac{d(d-1)}{2}} = (-1)^{\frac{d^2}{2}} = 1 \tag{A.32}$$

It is easy to verify that the matrices

$$\{\mathbb{1}\,, \gamma^{\mu_1\dots\mu_k}\} \qquad \text{with} \qquad \gamma^{\mu_1\dots\mu_k} = \gamma^{[\mu_1}\dots\gamma^{\mu_k]} \tag{A.33}$$

form a bases of $\mathrm{Gl}(2^{\frac{d}{2}},\mathbb{C})$. This basis is orthogonal with respect to taking the trace. Hence we have

$$\mathrm{Tr}\{\gamma^{\mu_1\dots\mu_k}\} = 0 \qquad \text{and for } k\neq l \qquad \mathrm{Tr}\{\gamma^{\mu_1\dots\mu_k}\gamma^{\nu_1\dots\nu_l}\} = 0\,. \tag{A.34}$$

A bit more involved is the case $k = l$

$$\begin{aligned}\mathrm{Tr}\{\gamma^{\mu_1\dots\mu_k}\gamma_{\nu_1\dots\nu_k}\} &= \mathrm{Tr}\{\gamma^{[\mu_1}\dots\gamma^{\mu_k]}\gamma_{[\nu_1}\dots\gamma_{\nu_k]}\}\\ &= 2^{\frac{d}{2}}(-1)^{\frac{k(k-1)}{2}}\sum_{\sigma\in S_k}\mathrm{sign}(\sigma)\delta^{[\mu_1}_{[\nu_{\sigma(1)}}\delta^{\mu_2}_{\nu_{\sigma(2)}}\dots\delta^{\mu_k]}_{\nu_{\sigma(k)}]}\\ &= k!\,2^{\frac{d}{2}}(-1)^{\frac{k(k-1)}{2}}\delta^{[\mu_1}_{\nu_1}\dots\delta^{\mu_k]}_{\nu_k}\end{aligned} \tag{A.35}$$

Note that $\delta^{[\mu_1}_{\nu_1}\dots\delta^{\mu_k]}_{\nu_k} = \delta^{\mu_1}_{[\nu_1}\dots\delta^{\mu_k}_{\nu_k]}$. The general Fierz identity in even dimension thus reads

$$M = \frac{1}{2^{\frac{d}{2}}}\sum_{k=0}^{d}\frac{(-1)^{\frac{k(k-1)}{2}}}{k!}\gamma_{\mu_1\dots\mu_k}\,\mathrm{Tr}\{\gamma^{\mu_1\dots\mu_k}M\} \tag{A.36}$$

The following identity

$$\begin{aligned}\gamma_{\mu_1\dots\mu_k}\gamma^{\mu_k} &= \frac{1}{k}\sum_{l=0}^{k-1}(-1)^{k-l-1}\gamma_{[\mu_1}\dots\gamma_{\mu_l}\gamma^{\mu_k}\gamma_{\mu_{l+1}}\dots\gamma_{\mu_{k-1}]}\gamma_{\mu_k}\\ &= \frac{1}{k}\sum_{l=0}^{k-1}\Big(d\,\gamma_{\mu_1\dots\mu_{k-1}}\\ &\qquad + 2(-1)^{k-l-1}\sum_{j=1}^{k-l-1}(-1)^{j+1}\gamma_{[\mu_1}\dots\gamma_{\mu_l}\gamma_{\mu_{k-j}}\gamma_{\mu_{l+1}}\dots\widehat{\gamma_{\mu_{k-j}}}\dots\gamma_{\mu_{k-1}]}\Big)\\ &= d\,\gamma_{\mu_1\dots\mu_{k-1}} - \frac{2}{k}\gamma_{\mu_1\dots\mu_{k-1}}\sum_{l=0}^{k-1}\sum_{j=1}^{k-l-1} = (d-k+1)\gamma_{\mu_1\dots\mu_{k-1}}\end{aligned} \tag{A.37}$$

can be used to inductively proof that the $\gamma_{\mu_1\dots\mu_k}$ obey the relation

$$\gamma_{\mu_1\dots\mu_k} = i^{\frac{d}{2}-1}\frac{1}{(d-k)!}\varepsilon_{\mu_1\dots\mu_d}\gamma^{d+1}\gamma^{\mu_d\dots\mu_{k+1}}\,. \tag{A.38}$$

Therefore the Fierz identity for $\psi\bar\chi$ in four dimensions reads

$$4\,\psi\bar\chi = -\bar\chi\psi - \gamma_\mu\,\bar\chi\gamma^\mu\psi + \tfrac{1}{2}\gamma_{\mu\nu}\,\bar\chi\gamma^{\mu\nu}\psi + \gamma^5\gamma_\mu\,\bar\chi\gamma^5\gamma^\mu\psi - \gamma^5\,\bar\chi\gamma^5\psi\,. \tag{A.39}$$

In ten dimensions the Fierz identity for $\Psi\bar{\chi}$ is given by

$$\begin{aligned}32\Psi\bar{\chi} = &-\bar{\chi}\Psi - \Gamma_{M}\,\bar{\chi}\Gamma^{M}\Psi + \frac{1}{2!}\Gamma_{MN}\,\bar{\chi}\Gamma^{MN}\Psi + \frac{1}{3!}\Gamma_{MNO}\,\bar{\chi}\Gamma^{MNO}\Psi - \frac{1}{4!}\Gamma_{MNOP}\,\bar{\chi}\Gamma^{MNOP}\Psi \\ &-\frac{1}{5!}\Gamma_{MNOPQ}\,\bar{\chi}\Gamma^{MNOPQ}\Psi - \frac{1}{4!}\Gamma^{11}\Gamma_{MNOP}\,\bar{\chi}\Gamma^{11}\Gamma^{MNOP}\Psi \\ &-\frac{1}{3!}\Gamma^{11}\Gamma_{MNO}\,\bar{\chi}\Gamma^{11}\Gamma^{MNO}\Psi + \frac{1}{2!}\Gamma^{11}\Gamma_{MN}\,\bar{\chi}\Gamma^{11}\Gamma^{MN}\Psi \\ &+\Gamma^{11}\Gamma_{M}\,\bar{\chi}\Gamma^{11}\Gamma^{M}\Psi - \Gamma^{11}\,\bar{\chi}\Gamma^{11}\Psi\,. \end{aligned} \tag{A.40}$$

To derive these Fierz identities we have used that

$$\epsilon_{\mu_1\dots\mu_d}\epsilon^{\mu_1\dots\mu_k\nu_{k+1}\dots\nu_d} = (-1)^{d-1}k!(d-k)!\,\delta^{\nu_{k+1}}_{[\mu_{k+1}}\dots\delta^{\nu_d}_{\mu_d]} \tag{A.41}$$

The above relation can be obtained by noting that

$$\epsilon_{\mu_1\dots\mu_d} = d!\,\delta^{0}_{[\mu_1}\delta^{1}_{\mu_2}\dots\delta^{d-1}_{\mu_d]} \quad \text{and therefore} \quad \epsilon_{\mu_1\dots\mu_d}\epsilon^{\nu_1\dots\nu_d} = (-1)^{d-1}d!\,\delta^{\nu_1}_{[\mu_1}\delta^{\nu_2}_{\mu_2}\dots\delta^{\nu_d}_{\mu_d]}\,. \tag{A.42}$$

Using the Laplace rule to expand the determinant it is easy to calculate the contractions eq. (A.41).

A.4. The Charge Conjugation Matrix

We search for a unitary matrix C such that the charge conjugate spinor

$$\psi_c = C\overline{\psi}^{\mathrm{T}} \tag{A.43}$$

fulfills the dirac equation with the opposite charge:

$$i\gamma^{\mu}(\partial_\mu - ieA_\mu)\psi = 0 \qquad \Rightarrow \qquad i\gamma^{\mu}(\partial_\mu + ieA_\mu)\psi_c = 0 \tag{A.44}$$

This implies that the charge conjugation matrix has to satisfy

$$C\gamma_{\mu}^{\mathrm{T}}C^{-1} = \eta\,\gamma_\mu \tag{A.45}$$

with η being an arbitrary complex number. However, the unitarity of the charge conjugation matrix implies $\eta = \pm 1$. This is a consequence of the consistency of the Majorana condition. Suppose we have a Majorana spinor satisfying

$$\psi = C\overline{\psi}^{\mathrm{T}} \tag{A.46}$$

This implies

$$\psi^* = (C\gamma_0)^*C\gamma_0\psi^* \quad \Rightarrow \quad (C\gamma_0)^*C\gamma_0 = \mathbb{1} \quad \Rightarrow \quad C^*C\eta = CC^*\eta^* = \mathbb{1} \tag{A.47}$$

As a consequence $\eta = \eta^*$ has to be a real number and the charge conjugation matrix has to obey $C^{-1} = \eta C^*$ or equivalently $C^{\mathrm{T}} = \eta C$, which implies $\eta = \pm 1$.

Note that in the presence of massive fermions one would want $\eta = -1$ in order to

have

$$i\gamma^\mu(\partial_\mu - ieA_\mu)\psi - m\psi = 0 \qquad \Rightarrow \qquad i\gamma^\mu(\partial_\mu + ieA_\mu)\psi_c - m\psi_c = 0 \tag{A.48}$$

But there are also massless theories where we want $\eta = -1$. For example we need $\eta = -1$ in the four dimensional $\mathcal{N} = 1$ super Yang-Mills theory in order to have invariance under susy transformations.

Appendix B

The Lagrangian of $\mathcal{N} = 4$ SYM

In this appendix we present a derivation of the Lagrangian of $\mathcal{N} = 4$ SYM theory by dimensional reduction of the ten dimensional $\mathcal{N} = 1$ SYM theory. Furthermore, we explicitly check the supersymmetry of the theory.

B.1. Derivation of the Lagrangian

Starting point is $\mathcal{N} = 1$ super Yang Mills theory in ten dimensions. Denoting the ten dimensional spacetime indices by M, N, its action is given by

$$S_{\mathcal{N}=1} = \int d^{10}x \ \mathrm{Tr}\left\{-\tfrac{1}{4}\, F_{MN}^2 + \tfrac{i}{2}\, \overline{\Psi}\, \not{D} \Psi\right\}. \tag{B.1}$$

and is invariant under the on-shell supersymmetry transformations

$$\delta_\alpha A_M = i\bar{\alpha}\Gamma_M \Psi \qquad \delta_\alpha \Psi = iF^{MN}\Sigma_{MN}\alpha \qquad \delta_\alpha \overline{\Psi} = -iF^{MN}\bar{\alpha}\Sigma_{MN} \tag{B.2}$$

Here Ψ and α are Majorana-Weyl Spinors and $\Sigma_{MN} = \frac{1}{2i}\Gamma_{MN}$. The gluinos Ψ take values in the Lie algebra of the Gauge group. We choose mostly minus metric $\eta_{MN} = \mathrm{diag}(+,-,-,\ldots,-)$. A proof of the invariance under the supersymmetry transformations eq. (B.2) can be found in the next section.

Let us now perform the dimensional reduction of the ten-dimensional theory to four dimensions. Therefore we compactify six of the space dimensions and assume that all fields are independent of the compactified space coordinates $\{x_4, \ldots x_9\}$. After a rescaling of the fields and the gauge coupling we obtain the following formulation of $\mathcal{N} = 4$ super Yang Mills theory

$$S_{\mathcal{N}=4} = \int d^4x \ \mathrm{Tr}\Big(-\tfrac{1}{4}\, F_{\mu\nu}^2 + \tfrac{1}{2}(D_\mu \Phi_I)^2 + \tfrac{g^2}{4}\,[\Phi_I, \Phi_J]^2 + \tfrac{i}{2}\,\overline{\Psi}\,\Gamma^\mu\, D_\mu \Psi + \tfrac{g}{2}\overline{\Psi}\,\Gamma^I [\Phi_I, \Psi]\Big), \tag{B.3}$$

in terms of the the gauge field A_μ, the six scalars Φ_I and the ten-dimensional Majorana-

Weyl Spinor Ψ satisfying $\Psi = C_{10}\overline{\Psi}^{\mathrm{T}}$ and $\Gamma^{11}\Psi = \pm\Psi$. The theory is invariant under the supersymmetry transformations

$$\begin{aligned}
\delta_\alpha A_\mu &= i\bar{\alpha}\Gamma_\mu\Psi \\
\delta_\alpha \Phi_I &= -i\bar{\alpha}\Gamma^I\Psi \\
\delta_\alpha \Psi &= iF^{\mu\nu}\Sigma_{\mu\nu}\alpha + g[\Phi_I,\Phi_J]\Sigma^{IJ}\alpha - 2iD_\mu\Phi_I\Sigma^{I\mu}\alpha \\
\delta_\alpha \overline{\Psi} &= -iF^{\mu\nu}\bar{\alpha}\Sigma_{\mu\nu} - g[\Phi_I,\Phi_J]\bar{\alpha}\Sigma^{IJ} + 2iD_\mu\Phi_I\bar{\alpha}\Sigma^{I\mu}
\end{aligned} \tag{B.4}$$

which follows immediately from the invariance of the ten dimensional theory under the supersymmetry transformations eq. (B.2).

By fixing a concrete representation of the ten-dimensional gamma matrices Γ^M, as well as for C_{10}, it is possible to get rid of the ten-dimensional spinor in favor of four dimensional spinors. Let us choose the following representation for the ten-dimensional Gamma matrices:

$$\Gamma^M = \left(\mathbb{1}\otimes\gamma^\mu, \hat{\gamma}^a\otimes\gamma^5\right) \quad \Rightarrow \quad \{\Gamma^M,\Gamma^N\} = 2\eta^{MN}, \quad (\Gamma^M)^\dagger = \Gamma^0\Gamma^M\Gamma^0 \tag{B.5}$$

Here γ^μ are the four-dimensional gamma matrices

$$\gamma^\mu = \begin{pmatrix} 0 & \sigma^\mu \\ \bar{\sigma}^\mu & 0 \end{pmatrix} \qquad \text{obeying} \qquad \{\gamma^\mu,\gamma^\nu\} = 2\eta^{\mu\nu} \quad \text{and} \quad (\gamma^\mu)^\dagger = \gamma^0\gamma^\mu\gamma^0 \tag{B.6}$$

with the usual definitions $\sigma^\mu = (\mathbb{1},\boldsymbol{\sigma})$ and $\bar{\sigma}^\mu = (\mathbb{1},-\boldsymbol{\sigma})$. Introducing $\epsilon = i\sigma^2$, the four dimensional charge conjugation matrix and γ^5 are given by:

$$C_4 = -i\gamma^0\gamma^2 = \begin{pmatrix} -i\sigma^2 & 0 \\ 0 & i\sigma^2 \end{pmatrix} = \sigma^3\otimes\epsilon \qquad \gamma^5 = -i\gamma^0\gamma^1\gamma^2\gamma^3 = \begin{pmatrix} \mathbb{1} & 0 \\ 0 & -\mathbb{1} \end{pmatrix} \tag{B.7}$$

The charge conjugation matrix has the properties $C_4^2 = -\mathbb{1}$, $C_4^{\mathrm{T}} = -C_4$ and $C_4\gamma^\mu = -(\gamma^\mu)^{\mathrm{T}}C_4$. For some general properties of the d-dimensional charge conjugation matrix we refer to appendix A.4. The six-dimensional anti-Hermitian euclidean gamma matrices are given by

$$\hat{\gamma}^a = \begin{pmatrix} 0 & \Sigma^a \\ \bar{\Sigma}^a & 0 \end{pmatrix} \qquad \text{and fulfill the algebra} \qquad \{\hat{\gamma}^a,\hat{\gamma}^b\} = -2\delta^{ab} \tag{B.8}$$

which implies the following properties of the six-dimensional euclidean Pauli matrices

$$\Sigma^a\bar{\Sigma}^b + \Sigma^b\bar{\Sigma}^a = -2\delta^{ab} \qquad\qquad \bar{\Sigma}^a\Sigma^b + \bar{\Sigma}^b\Sigma^a = -2\delta^{ab} \tag{B.9}$$

In terms of the 't Hooft symbols the six-dimensional euclidean Pauli matrices are given by $\Sigma^a = (\eta_k, i\bar{\eta}_k)$ and $\bar{\Sigma}^a = (\eta_k, -i\bar{\eta}_k) = (\Sigma^a)^*$. The real and antisymmetric 't Hooft symbols are defined as

$$\eta_{i\,AB} = \begin{pmatrix} \epsilon_{ijk} & \delta_{ij} \\ -\delta_{ik} & 0 \end{pmatrix} \qquad\qquad \bar{\eta}_{i\,AB} = \begin{pmatrix} \epsilon_{ijk} & -\delta_{ij} \\ \delta_{ik} & 0 \end{pmatrix}. \tag{B.10}$$

They have the self-duality properties

$$\eta_{i\,AB} = \tfrac{1}{2}\epsilon_{ABCD}\eta_{i\,CD}\,, \qquad\qquad \bar{\eta}_{i\,AB} = -\tfrac{1}{2}\epsilon_{ABCD}\bar{\eta}_{i\,CD} \tag{B.11}$$

and fulfill the following algebra

$$\{\eta_k, \eta_l\} = -2\delta^{kl}\,, \qquad \{\bar{\eta}_k, \bar{\eta}_l\} = -2\delta^{kl}\,, \qquad [\eta_k, \bar{\eta}_l] = 0\,, \tag{B.12}$$

which implies additional properties of the six dimensional euclidean Pauli matrices

$$\{\Sigma^a, \Sigma^b\} = -2\delta^{ab} \quad \{\bar{\Sigma}^a, \bar{\Sigma}^b\} = -2\delta^{ab} \quad \text{for} \quad a, b \in \{1,2,3\} \vee a, b \in \{4,5,6\} \tag{B.13}$$

$$[\Sigma^a, \Sigma^b] = 0 \qquad [\bar{\Sigma}^a, \bar{\Sigma}^b] = 0 \qquad \text{for} \quad a \in \{1,2,3\} \wedge b \in \{4,5,6\} \tag{B.14}$$

and

$$\Sigma^a_{AB} = \tfrac{1}{2}\epsilon_{ABCD}\bar{\Sigma}^{a\,CD}\,. \tag{B.15}$$

The six-dimensional charge conjugation matrix and $\hat{\gamma}^7$are given by

$$C_6 = \hat{\gamma}^1\hat{\gamma}^2\hat{\gamma}^3 = \begin{pmatrix} 0 & \mathbb{1} \\ \mathbb{1} & 0 \end{pmatrix} \qquad \hat{\gamma}^7 = i\hat{\gamma}^1\hat{\gamma}^2\hat{\gamma}^3\hat{\gamma}^4\hat{\gamma}^5\hat{\gamma}^6 = \begin{pmatrix} \mathbb{1} & 0 \\ 0 & -\mathbb{1} \end{pmatrix} \tag{B.16}$$

with the properties $C_6^2 = \mathbb{1}$, $C_6^{\mathrm{T}} = C_6$ and $C_6\hat{\gamma}^a = -(\hat{\gamma}^a)^{\mathrm{T}}C_6$. Let us now define the ten-dimensional charge conjugation matrix and the chiral matrix

$$C_{10} = C_6 \otimes C_4 \qquad \Gamma^{11} = \hat{\gamma}^7 \otimes \gamma^5 \tag{B.17}$$

with the properties $C_{10}^{\mathrm{T}} = -C_{10}$, $C_{10}^2 = -\mathbb{1}$ and $C_{10}\Gamma^M = -(\Gamma^M)^{\mathrm{T}}C_{10}$.

A ten-dimensional Majorana-Weyl spinor has to obey $\Psi^{\mathrm{T}}C_{10} = \Psi^\dagger\Gamma^0$ and $\Gamma^{11}\Psi = \Psi$. To find the general solution to both equations we make the ansatz $\Psi = \chi \otimes \rho$ for the Majorana-Weyl spinor. The general solution to the Weyl condition

$$\Gamma^{11}\Psi = \hat{\gamma}^7\chi \otimes \gamma^5\rho = \chi \otimes \rho \tag{B.18}$$

is given by

$$\Psi = \sum_{A=1}^{4} \begin{pmatrix} e_A \\ 0 \end{pmatrix} \otimes \begin{pmatrix} \psi_A \\ 0 \end{pmatrix} + \begin{pmatrix} 0 \\ e_A \end{pmatrix} \otimes \begin{pmatrix} 0 \\ \tilde{\psi}^A \end{pmatrix}\,, \tag{B.19}$$

where $e_A \in R^4$ denotes the unit vector pointing in direction A and ψ_A, $\tilde{\psi}^A$ are arbitrary four dimensional Weyl spinors. The Majorana condition

$$\begin{aligned} \Psi^{\mathrm{T}}C_{10} = & \sum_{A=1}^{4} \begin{pmatrix} 0 & e_A^{\mathrm{T}} \end{pmatrix} \otimes \begin{pmatrix} \psi_A^{\mathrm{T}}\epsilon & 0 \end{pmatrix} + \begin{pmatrix} e_A^{\mathrm{T}} & 0 \end{pmatrix} \otimes \begin{pmatrix} 0 & -(\tilde{\psi}^A)^{\mathrm{T}}\epsilon \end{pmatrix} \\ = & \sum_{A=1}^{4} \begin{pmatrix} 0 & e_A^{\mathrm{T}} \end{pmatrix} \otimes \begin{pmatrix} (\tilde{\psi}^A)^\dagger & 0 \end{pmatrix} + \begin{pmatrix} e_A^{\mathrm{T}} & 0 \end{pmatrix} \otimes \begin{pmatrix} 0 & \psi_A^\dagger \end{pmatrix} \\ = & \Psi^\dagger\Gamma^0 \end{aligned} \tag{B.20}$$

implies $\tilde{\psi}^A = -\epsilon\psi_A^*$. Hence, a ten-dimensional Majorana-Weyl spinor is given by

$$\Psi = \sum_{A=1}^{4} \begin{pmatrix} e_A \\ 0 \end{pmatrix} \otimes \begin{pmatrix} \psi_A \\ 0 \end{pmatrix} + \begin{pmatrix} 0 \\ e_A \end{pmatrix} \otimes \begin{pmatrix} 0 \\ \bar{\psi}^A \end{pmatrix}\,, \tag{B.21}$$

$$\overline{\Psi} = \sum_{A=1}^{4} \begin{pmatrix} e_A^{\mathrm{T}} & 0 \end{pmatrix} \otimes \begin{pmatrix} 0 & -(\bar{\psi}^A)^{\mathrm{T}}\epsilon \end{pmatrix} + \begin{pmatrix} 0 & e_A^{\mathrm{T}} \end{pmatrix} \otimes \begin{pmatrix} \psi_A^{\mathrm{T}}\epsilon & 0 \end{pmatrix}\,, \tag{B.22}$$

with $\psi^* = \epsilon\bar{\psi}$. Now we can plug these expressions into the $\mathcal{N}=4$ super Yang Mills Lagrangian (B.3). Using the identity $(\bar{\sigma}^\mu)^{\mathrm{T}}\epsilon = \epsilon\sigma^\mu$, which is a consequence of $C_4\gamma^\mu = -(\gamma^\mu)^{\mathrm{T}}C_4$, we obtain

$$\mathrm{Tr}\{\overline{\Psi}\,\Gamma^\mu\, D_\mu\Psi\} = \mathrm{Tr}\{-(\bar{\psi}^A)^{\mathrm{T}}\epsilon D_\mu\bar{\sigma}^\mu\psi_A + \psi_A^{\mathrm{T}}\epsilon D_\mu\sigma^\mu\bar{\psi}_A\} = -2\,\mathrm{Tr}\{(\bar{\psi}^A)^{\mathrm{T}}\epsilon D_\mu\bar{\sigma}^\mu\psi_A\} + \text{t.d.} \tag{B.23}$$

For the scalar–fermion interaction term we get

$$\overline{\Psi}\,\Gamma^I[\Phi_I,\Psi] = \psi_A^{\mathrm{T}}\epsilon\bar{\Sigma}^{I\,AB}[\Phi_I,\psi_B] + (\bar{\psi}^A)^{\mathrm{T}}\epsilon\Sigma^I_{AB}[\Phi_I,\bar{\psi}^B] \tag{B.24}$$

Thus we arrive at the following formulation of $\mathcal{N}=4$ super Yang-Mills theory

$$\begin{aligned} S_{\mathcal{N}=4} = \int d^4x\ \mathrm{Tr}\Big(&-\tfrac{1}{4}F_{\mu\nu}^2 + \tfrac{1}{2}(D_\mu\Phi_I)^2 + \tfrac{g^2}{4}[\Phi_I,\Phi_J]^2 - i\,(\bar{\psi}^A)^{\mathrm{T}}_A\epsilon D_\mu\bar{\sigma}^\mu\psi_A \\ &+ \tfrac{g}{2}\psi_A^{\mathrm{T}}\epsilon\bar{\Sigma}^{I\,AB}[\Phi_I,\psi_B] + \tfrac{g}{2}(\bar{\psi}^A)^{\mathrm{T}}\epsilon\Sigma^I_{AB}[\Phi_I,\bar{\psi}^B]\Big) \qquad \text{with} \quad \psi_A^* = \epsilon\bar{\psi}^A \end{aligned} \tag{B.25}$$

The invariance of the ten-dimensional theory (B.1) under the supersymmetry transformations (B.2) implies the invariance of $\mathcal{N}=4$ super Yang-Mills theory under the transformations

$$\delta_\alpha A_\mu = i\alpha_A^{\mathrm{T}}\epsilon\sigma_\mu\bar{\psi}^A - i(\bar{\alpha}^A)^{\mathrm{T}}\epsilon\bar{\sigma}_\mu\psi_A \tag{B.26}$$

$$\delta_\alpha\Phi_I = -i\Sigma^I_{AB}\,(\bar{\alpha}^A)^{\mathrm{T}}\epsilon\bar{\psi}^B - i\bar{\Sigma}^{I\,AB}\,\alpha_A^{\mathrm{T}}\epsilon\psi_B \tag{B.27}$$

$$\delta_\alpha\psi_A = \tfrac{1}{2}F^{\mu\nu}\sigma_\mu\bar{\sigma}_\nu\alpha_A - \tfrac{i}{2}g[\Phi_I,\Phi_J]\Sigma^I_{AB}\bar{\Sigma}^{J\,BC}\alpha_C + 2i\,D_\mu\Phi_I\Sigma^I_{AB}\bar{\alpha}^B \tag{B.28}$$

$$\delta_\alpha\bar{\psi}^A = \tfrac{1}{2}F^{\mu\nu}\bar{\sigma}_\mu\sigma_\nu\bar{\alpha}^A - \tfrac{i}{2}g[\Phi_I,\Phi_J]\bar{\Sigma}^{I\,AB}\Sigma^J_{BC}\bar{\alpha}^C - 2i\,D_\mu\Phi_I\bar{\Sigma}^{I\,AB}\alpha_B \tag{B.29}$$

The Noether current is given by

$$\mathcal{V}^\mu_A = \mathrm{Tr}\{(\star F^{\mu\nu} - iF^{\mu\nu})\bar{\sigma}_\nu\psi_A\} + i\,\mathrm{Tr}\{D_\nu\Phi_I\Sigma^I_{AB}\bar{\sigma}^\mu\sigma^\nu\bar{\psi}_B\} + \tfrac{g}{2}\,\mathrm{Tr}\{[\Phi_I,\Phi_J]\Sigma^I_{AB}\bar{\Sigma}^{J\,BC}\bar{\sigma}^\mu\psi_C\} \tag{B.30}$$

and can be obtained from the ten-dimensional Noether current (B.43).

B.2. Invariance under Supersymmetry Transformations

Let us now check the invariance of the $\mathcal{N}=1$ super Yang-Mills Lagrangian (B.1) under the supersymmetry transformations (B.2). For the Gauge field term we get

$$\delta_\alpha(-\tfrac{1}{4}F_{MN}^2) = -F^{MN}D_M\delta_\alpha A_N = -iF^{MN}\bar{\alpha}\Gamma_N D_M\Psi \tag{B.31}$$

The variation of the Fermion term is given by

$$\delta_\alpha(\tfrac{i}{2}\overline{\Psi}\not{D}\Psi) = \tfrac{1}{2}F^{MN}\bar{\alpha}\Sigma_{MN}\not{D}\Psi - \tfrac{1}{2}\overline{\Psi}\not{D}F^{MN}\Sigma_{MN}\alpha + \tfrac{1}{2}\overline{\Psi}\Gamma^M[\bar{\alpha}\Gamma_M\Psi,\Psi] \tag{B.32}$$

Now we use the identity

$$\gamma_{\mu\nu}\gamma_\rho = -\eta_{\mu\rho}\gamma_\nu + \eta_{\nu\rho}\gamma_\mu + \gamma_{\mu\nu\rho} \tag{B.33}$$

$$\gamma_\rho\gamma_{\mu\nu} = \eta_{\mu\rho}\gamma_\nu - \eta_{\nu\rho}\gamma_\mu + \gamma_{\mu\nu\rho} \tag{B.34}$$

as well as $D_{[\rho}F_{\mu\nu]} = 0$, which both hold in arbitrary dimensions.

$$\begin{aligned}\delta_\alpha \operatorname{Tr}\{\tfrac{i}{2}\overline{\Psi}\not{D}\Psi\} &= \operatorname{Tr}\Big\{\partial_M\left(\tfrac{1}{2}F^{PQ}\bar{\alpha}\Sigma_{PQ}\Gamma^M\Psi\right) - \tfrac{i}{2}(D_M F^{MN})\bar{\alpha}\Gamma_N\Psi \\ &\quad + \tfrac{i}{2}\overline{\Psi}D_M F^{MN}\Gamma_N\alpha + \tfrac{1}{2}\overline{\Psi}\Gamma^M[\bar{\alpha}\Gamma_M\Psi,\Psi]\Big\} \\ &= \operatorname{Tr}\Big\{\partial_M\left(\tfrac{1}{2}F^{PQ}\bar{\alpha}\Sigma_{PQ}\Gamma^M\Psi - iF^{MN}\bar{\alpha}\Gamma_N\Psi\right) + iF^{MN}\bar{\alpha}\Gamma_N D_M\Psi \\ &\quad + \tfrac{1}{2}\overline{\Psi}\Gamma^M[\bar{\alpha}\Gamma_M\Psi,\Psi]\Big\} \end{aligned} \tag{B.35}$$

It remains to show, that the quantity $\operatorname{Tr}\Big\{\overline{\Psi}\Gamma^M[\bar{\alpha}\Gamma_M\Psi,\Psi]\Big\}$ is equal to zero.

$$i\operatorname{Tr}\Big\{\overline{\Psi}\Gamma^M[\bar{\alpha}\Gamma_M\Psi,\Psi]\Big\} = f_{abc}\,\overline{\Psi}^a\Gamma^M\Psi^b\,\bar{\alpha}\Gamma_M\Psi^c = f_{abc}\,\bar{\alpha}\Gamma_M\Psi^c\overline{\Psi}^a\Gamma^M\Psi^b \tag{B.36}$$

To see that this expression is equal to zero we use the Fierz identity (A.40) for $\Psi^c\overline{\Psi}^a$ as well as the Weyl condition $\Gamma^{11}\Psi = \pm\Psi$ and the simple identity

$$\gamma_\alpha\gamma^{\mu_1\cdots\mu_k}\gamma^\alpha = (-1)^k\,(d-2k)\,\gamma^{\mu_1\cdots\mu_k}\,. \tag{B.37}$$

What we obtain is

$$\bar{\alpha}\Gamma_M\Psi^c\overline{\Psi}^a\Gamma^M\Psi^b = \tfrac{1}{2}\,\bar{\alpha}\Gamma_M\Psi^b\,\overline{\Psi}^a\Gamma^M\Psi^c - \tfrac{1}{4!}\bar{\alpha}\Gamma_{MNO}\Psi^b\,\overline{\Psi}^a\Gamma^{MNO}\Psi^c \tag{B.38}$$

For Majorana spinors we have the general symmetry property

$$\overline{\Psi}^a\gamma^{\mu_1\cdots\mu_k}\Psi^b = -(-1)^{\frac{k(k-1)}{2}}\eta^{k+1}\overline{\Psi}^b\gamma^{\mu_1\cdots\mu_k}\Psi^a \tag{B.39}$$

which can be derived using $C\gamma_\mu^{\mathrm{T}}C^{-1} = \eta\,\gamma_\mu$ and $C^{\mathrm{T}} = \eta\,C$. This implies that $\overline{\Psi}^a\Gamma^{MNO}\Psi^c$ is symmetric in a and c. Hence we have derived

$$f_{abc}\,\bar{\alpha}\Gamma_M\Psi^c\overline{\Psi}^a\Gamma^M\Psi^b = -\tfrac{1}{2}f_{abc}\,\bar{\alpha}\Gamma_M\Psi^c\overline{\Psi}^a\Gamma^M\Psi^b = 0 \tag{B.40}$$

What we found is

$$\delta_\alpha\mathcal{L} = \bar{\alpha}\,\partial^M V_M \qquad \text{with} \qquad V_M = -\tfrac{i}{4}\operatorname{Tr}\{F^{PQ}\Gamma_{PQM}\Psi\} - \tfrac{i}{2}\operatorname{Tr}\{F^{MN}\Gamma_N\Psi\} \tag{B.41}$$

Because of

$$\begin{aligned}\frac{\partial\mathcal{L}}{\partial\partial_\mu A_\nu}\delta_\alpha A_\nu + \frac{\partial\mathcal{L}}{\partial\partial_\mu\Psi}\delta_\alpha\Psi &= -i\operatorname{Tr}\{F^{MN}\bar{\alpha}\Gamma_N\Psi\} - \tfrac{1}{2}\operatorname{Tr}\{F^{PQ}\,\overline{\Psi}\Gamma_M\Gamma_{PQ}\alpha\} \\ &= -\tfrac{3}{2}i\operatorname{Tr}\{F^{MN}\bar{\alpha}\Gamma_N\Psi\} + \tfrac{i}{4}\operatorname{Tr}\{F_{PQ}\,\overline{\alpha}\Gamma_{PQM}\Psi\}\end{aligned} \tag{B.42}$$

the Noether current is given by

$$\mathcal{V}^M = \tfrac{i}{2}\operatorname{Tr}\{F_{PQ}\Gamma^{PQM}\Psi\} - i\operatorname{Tr}\{F_{MN}\Gamma^N\Psi\}\,, \tag{B.43}$$

and concludes our investigation of the Lagrangian of $\mathcal{N} = 4$ SYM.

Appendix C

Symmetry Algebras of $\mathcal{N} = 4$ SYM

We present a complete list of the symmetry algebras relevant for the massless $\mathcal{N} = 4$ super Yang-Mills amplitudes in chiral and non-chiral superspace.

C.1. The Superconformal Algebra u(2,2|4)

Before presenting the conventional and the dual representation of the superconformal algebra we list the commutation relations of the algebra $u(2,2|4)$. The $su(2) \times su(2)$ Lorentz-generators $\mathbb{M}_{\alpha\beta}$, $\overline{\mathbb{M}}_{\dot\alpha\dot\beta}$ and the $SU(4)_R$ symmetry generators $\mathbb{R}^A_{\ B}$ of the superconformal algebra $u(2,2|4)$ act canonically on the remaining generators carrying $su(2)$ indices $\alpha, \dot\alpha$ or $su(4)$ indices A, B.

$$
\begin{aligned}
\left[\mathbb{M}_{\alpha\beta}, \mathbb{M}^{\gamma\delta}\right] &= \delta_{(\beta}^{(\gamma}\mathbb{M}_{\alpha)}^{\ \ \delta)} & \left[\overline{\mathbb{M}}_{\dot\alpha\dot\beta}, \overline{\mathbb{M}}^{\dot\gamma\dot\delta}\right] &= \delta_{(\dot\beta}^{(\dot\gamma}\overline{\mathbb{M}}_{\dot\alpha)}^{\ \ \dot\delta)} \\
\left[\mathbb{M}_{\alpha\beta}, \mathbb{P}^{\gamma\dot\delta}\right] &= \delta_{(\beta}^{\gamma}\mathbb{P}_{\alpha)}^{\ \dot\delta} & \left[\overline{\mathbb{M}}_{\dot\alpha\dot\beta}, \mathbb{P}^{\gamma\dot\delta}\right] &= \delta_{(\dot\beta}^{\dot\delta}\mathbb{P}^{\gamma}_{\ \dot\alpha)} \\
\left[\mathbb{M}_{\alpha\beta}, \mathbb{K}^{\gamma\dot\delta}\right] &= -\delta_{(\beta}^{\gamma}\mathbb{K}_{\alpha)}^{\ \dot\delta} & \left[\overline{\mathbb{M}}_{\dot\alpha\dot\beta}, \mathbb{K}^{\gamma\dot\delta}\right] &= -\delta_{(\dot\beta}^{\dot\delta}\mathbb{K}^{\gamma}_{\ \dot\alpha)} \\
\left[\mathbb{M}_{\alpha\beta}, \mathbb{Q}^{\gamma A}\right] &= \delta_{(\beta}^{\gamma}\mathbb{Q}_{\alpha)}^{A} & \left[\overline{\mathbb{M}}_{\dot\alpha\dot\beta}, \overline{\mathbb{Q}}^{\dot\gamma}_{A}\right] &= \delta_{(\dot\beta}^{\dot\gamma}\overline{\mathbb{Q}}_{\dot\alpha)A} \\
\left[\mathbb{M}_{\alpha\beta}, \mathbb{S}^{\gamma}_{A}\right] &= -\delta_{(\beta}^{\gamma}\mathbb{S}_{\alpha)A} & \left[\overline{\mathbb{M}}_{\dot\alpha\dot\beta}, \overline{\mathbb{S}}^{\dot\gamma A}\right] &= -\delta^{\dot\gamma}_{(\dot\beta}\overline{\mathbb{S}}^{A}_{\dot\alpha)} \\
\left[\mathbb{R}^A_{\ B}, \mathbb{R}^C_{\ D}\right] &= \delta^C_{\ B}\mathbb{R}^A_{\ D} - \delta^A_{\ D}\mathbb{R}^C_{\ B} & & \\
\left[\mathbb{R}^A_{\ B}, \mathbb{Q}^C_{\alpha}\right] &= \delta^C_{\ B}\mathbb{Q}^A_{\alpha} - \tfrac{1}{4}\delta^A_{\ B}\mathbb{Q}^C_{\alpha} & \left[\mathbb{R}^A_{\ B}, \overline{\mathbb{Q}}_{C\dot\alpha}\right] &= -\delta^A_{\ C}\overline{\mathbb{Q}}_{B\dot\alpha} + \tfrac{1}{4}\delta^A_{\ B}\overline{\mathbb{Q}}_{C\dot\alpha} \\
\left[\mathbb{R}^A_{\ B}, \mathbb{S}_{C\alpha}\right] &= -\delta^A_{\ C}\mathbb{S}_{B\alpha} + \tfrac{1}{4}\delta^A_{\ B}\mathbb{S}_{C\alpha} & \left[\mathbb{R}^A_{\ B}, \overline{\mathbb{S}}^{C}_{\dot\alpha}\right] &= \delta^C_{\ B}\overline{\mathbb{S}}^{A}_{\dot\alpha} - \tfrac{1}{4}\delta^A_{\ B}\overline{\mathbb{S}}^{C}_{\dot\alpha}
\end{aligned}
\tag{C.1}
$$

The action of the dilatation $\mathbb{D}$ and the hypercharge $\mathbb{B}$ are given by:

$$
[\mathbb{D}, \mathbb{G}] = \dim(\mathbb{G})\,\mathbb{G} \qquad [\mathbb{B}, \mathbb{G}] = \mathrm{hyp}(\mathbb{G})\,\mathbb{G} \tag{C.2}
$$

for all generators $\mathbb{G}$. The non-zero dimensions and hypercharges are:

$$\begin{aligned} &\dim(\mathbb{P})=1 && \dim(\mathbb{Q})=\dim\left(\overline{\mathbb{Q}}\right)=\tfrac{1}{2} && \dim(\mathbb{S})=\dim\left(\overline{\mathbb{S}}\right)=-\tfrac{1}{2} \\ &\dim(\mathbb{K})=-1 && \mathrm{hyp}(\mathbb{Q})=\mathrm{hyp}\left(\overline{\mathbb{S}}\right)=\tfrac{1}{2} && \mathrm{hyp}\left(\overline{\mathbb{Q}}\right)=\mathrm{hyp}(\mathbb{S})=-\tfrac{1}{2} \end{aligned} \tag{C.3}$$

The remaining non-trivial commutation relations are:

$$\begin{aligned} \left\{\mathbb{Q}^A_\alpha,\overline{\mathbb{Q}}_{\dot\alpha B}\right\}&=\delta^A_B\mathbb{P}_{\alpha\dot\alpha} & \left\{\mathbb{S}_{\alpha A},\overline{\mathbb{S}}^B_{\dot\alpha}\right\}&=\delta^B_A\mathbb{K}_{\alpha\dot\alpha} \\ \left[\mathbb{P}_{\alpha\dot\alpha},\mathbb{S}^\beta_A\right]&=\delta^\beta_\alpha\overline{\mathbb{Q}}_{\dot\alpha A} & \left[\mathbb{K}_{\alpha\dot\alpha},\mathbb{Q}^{\beta A}\right]&=\delta^\beta_\alpha\overline{\mathbb{S}}^A_{\dot\alpha} \\ \left[\mathbb{P}_{\alpha\dot\alpha},\overline{\mathbb{S}}^{\dot\beta A}\right]&=\delta^{\dot\beta}_{\dot\alpha}\mathbb{Q}^A_\alpha & \left[\mathbb{K}_{\alpha\dot\alpha},\overline{\mathbb{Q}}^{\dot\beta}_A\right]&=\delta^{\dot\beta}_{\dot\alpha}\mathbb{S}_{\alpha A} \\ \left[\mathbb{K}_{\alpha\dot\alpha},\mathbb{P}^{\beta\dot\beta}\right]&=\delta^\beta_\alpha\delta^{\dot\beta}_{\dot\alpha}\mathbb{D}+\delta^{\dot\beta}_{\dot\alpha}\mathbb{M}^\beta{}_\alpha+\delta^\beta_\alpha\overline{\mathbb{M}}^{\dot\beta}{}_{\dot\alpha} \\ \left\{\mathbb{Q}^{\alpha A},\mathbb{S}_{\beta B}\right\}&=\delta^A_B\mathbb{M}^\alpha{}_\beta-\delta^\alpha_\beta\mathbb{R}^A{}_B+\tfrac{1}{2}\delta^\alpha_\beta\delta^A_B(\mathbb{D}-\mathbb{C}) \\ \left\{\overline{\mathbb{Q}}^{\dot\alpha}_A,\overline{\mathbb{S}}^B_{\dot\beta}\right\}&=\delta^B_A\overline{\mathbb{M}}^{\dot\alpha}{}_{\dot\beta}+\delta^{\dot\alpha}_{\dot\beta}\mathbb{R}^B{}_A+\tfrac{1}{2}\delta^{\dot\alpha}_{\dot\beta}\delta^B_A(\mathbb{D}+\mathbb{C}) \end{aligned} \tag{C.4}$$

Note that we swopped the signs of $\mathbb{C}$ and $\mathbb{R}^A_B$ with respect to the conventions in [49].

C.1.1. The On-Shell Representation

Adapting the conventions of [49] we use the following abbreviations for derivatives:

$$\partial_{i\alpha}=\frac{\partial}{\partial\lambda^\alpha_i}\qquad \partial_{i\dot\alpha}=\frac{\partial}{\partial\tilde\lambda^{\dot\alpha}_i}\qquad \partial_{iA}=\frac{\partial}{\partial\eta^A_i} \tag{C.5}$$

with respect to spinors or Grassmann variables and use lower case letters to denote the generators of the conventional superconformal symmetry.

$$\begin{aligned} p^{\dot\alpha\alpha}&=\sum_i\lambda^\alpha_i\tilde\lambda^{\dot\alpha}_i & k_{\dot\alpha\alpha}&=\sum_i\partial_{i\alpha}\partial_{i\dot\alpha} \\ m_{\alpha\beta}&=\sum_i\lambda_{i(\alpha}\partial_{i\beta)} & \overline{m}_{\dot\alpha\dot\beta}&=\sum_i\tilde\lambda_{i(\dot\alpha}\partial_{i\dot\beta)} \\ d&=\tfrac{1}{2}\sum_i\left(\lambda^\alpha_i\partial_{i\alpha}+\tilde\lambda^{\dot\alpha}_i\partial_{i\dot\alpha}+2\right) & r^A_B&=\sum_i\left(\eta^A_i\partial_{iB}-\tfrac{1}{4}\delta^A_B\eta^C_i\partial_{iC}\right) \\ q^{\alpha A}&=\sum_i\lambda^\alpha_i\eta^A_i & \overline{q}^{\dot\alpha}_A&=\sum_i\tilde\lambda^{\dot\alpha}_i\partial_{iA} \\ s_{\alpha A}&=\sum_i\partial_{i\alpha}\partial_{iA} & \overline{s}^A_{\dot\alpha}&=\sum_i\eta^A_i\partial_{i\dot\alpha} \\ c&=\tfrac{1}{2}\sum_i\left(-\lambda^\alpha_i\partial_{i\alpha}+\tilde\lambda^{\dot\alpha}_i\partial_{i\dot\alpha}+\eta^A_i\partial_{iA}-2\right) & b&=\tfrac{1}{2}\sum_i\eta^A_i\partial_{iA} \end{aligned} \tag{C.6}$$

Note that the generator of the hypercharge b counts the Grassmann degree. Hence, $b-4-2p$ annihilates the N^{p}MHV superamplitudes.

C.1.2. The Dual Representation

The dual representation of the superconformal algebra $u(2,2|4)$ can be obtained by starting with the standard chiral representation and extending the generators such

that they commute with the constraints

$$x_i^{\alpha\dot\alpha} - x_{i+1}^{\alpha\dot\alpha} - \lambda_i^\alpha \tilde\lambda_i^{\dot\alpha} = 0\,, \qquad \theta_i^{\alpha A} - \theta_{i+1}^{\alpha A} - \lambda_i^\alpha \eta_i^A = 0\,. \tag{C.7}$$

We use the following shorthand notations for derivatives

$$\partial_{i\alpha\dot\alpha} = \frac{\partial}{\partial x_i^{\alpha\dot\alpha}}\,, \qquad \partial_{i\alpha A} = \frac{\partial}{\partial \theta_i^{\alpha A}}\,, \tag{C.8}$$

with respect to region momenta and dual fermionic momenta. The dual superconformal generators in full chiral superspace $\{\lambda_i^\alpha, \tilde\lambda_i^{\dot\alpha}, x_i^{\dot\alpha\alpha}, \eta^A, \theta_i^{A\,\alpha}\}$ are:

$$\begin{aligned}
P_{\alpha\dot\alpha} &= \sum_i \partial_{i\alpha\dot\alpha} \qquad Q_{\alpha A} = \sum_i \partial_{i\alpha A} \qquad \overline{Q}^A_{\dot\alpha} = \sum_i (\theta_i^{\alpha A}\partial_{i\alpha\dot\alpha} + \eta_i^A \partial_{i\dot\alpha}) \\
M_{\alpha\beta} &= \sum_i (x_{i(\alpha}{}^{\dot\alpha}\partial_{i\beta)\dot\alpha} + \theta^A_{i(\alpha}\partial_{i\beta)A} + \lambda_{i(\alpha}\partial_{i\beta)}) \qquad \overline{M}_{\dot\alpha\dot\beta} = \sum_i (x_{i(\dot\alpha}{}^{\alpha}\partial_{i\dot\beta)\alpha} + \tilde\lambda_{i(\dot\alpha}\partial_{i\dot\beta)}) \\
R^A_{\ B} &= \sum_i (-\theta_i^{\alpha A}\partial_{i\alpha B} - \eta_i^A \partial_{iB} + \tfrac{1}{4}\delta^A_B \theta_i^{\alpha C}\partial_{i\alpha C} + \tfrac{1}{4}\delta^A_B \eta_i^C \partial_{iC}) \\
D &= \sum_i (-x_i^{\alpha\dot\alpha}\partial_{i\alpha\dot\alpha} - \tfrac{1}{2}\theta_i^{\alpha A}\partial_{i\alpha A} - \tfrac{1}{2}\lambda_i^\alpha \partial_{i\alpha} - \tfrac{1}{2}\tilde\lambda_i^{\dot\alpha}\partial_{i\dot\alpha}) \\
C &= \sum_i (\tfrac{1}{2}\lambda_i^\alpha \partial_{i\alpha} - \tfrac{1}{2}\tilde\lambda_i^{\dot\alpha}\partial_{i\dot\alpha} - \tfrac{1}{2}\eta_i^A \partial_{iA}) \\
S^A_\alpha &= \sum_i (-\theta^B_{i\alpha}\theta_i^{\beta A}\partial_{i\beta B} + x_{i\alpha}{}^{\dot\beta}\theta_i^{\beta A}\partial_{i\beta\dot\beta} + \lambda_{i\alpha}\theta_i^{\gamma A}\partial_{i\gamma} + x_{i+1\alpha}{}^{\dot\beta}\eta_i^A\partial_{i\dot\beta} - \theta^B_{i+1\alpha}\eta_i^A\partial_{iB}) \\
\overline{S}_{\dot\alpha A} &= \sum_i (x_{i\dot\alpha}{}^{\beta}\partial_{i\beta A} + \tilde\lambda_{i\dot\alpha}\partial_{iA}) \\
K_{\alpha\dot\alpha} &= \sum_i (x_{i\alpha}{}^{\dot\beta}x_{i\dot\alpha}{}^{\beta}\partial_{i\beta\dot\beta} + x_{i\dot\alpha}{}^{\beta}\theta^B_{i\alpha}\partial_{i\beta B} + x_{i\dot\alpha}{}^{\beta}\lambda_{i\alpha}\partial_{i\beta} + x_{i+1\alpha}{}^{\dot\beta}\tilde\lambda_{i\dot\alpha}\partial_{i\dot\beta} + \tilde\lambda_{i\dot\alpha}\theta^B_{i+1\alpha}\partial_{iB}) \\
B &= \sum_i \tfrac{1}{2}\left(-\eta_i^A\partial_{iA} - \theta_i^{A\alpha}\partial_{iA\alpha}\right)
\end{aligned} \tag{C.9}$$

The obvious relations between the dual and conventional superconformal generators are

$$\begin{aligned}
m_{\alpha\beta} &= M_{\alpha\beta} & \bar m_{\dot\alpha\dot\beta} &= \overline{M}_{\dot\alpha\dot\beta} \\
\bar q_{\dot\alpha A} &= \overline{S}_{\dot\alpha A} & \bar s^A_{\dot\alpha} &= \overline{Q}^A_{\dot\alpha} \\
d &= -D + n \qquad c = -C - n \qquad b = -B
\end{aligned} \tag{C.10}$$

C.2. The Non-Chiral Superconformal Algebra

The $su(2) \times su(2)$ Lorentz generators $\mathbb{M}_{\alpha\beta}$, $\overline{\mathbb{M}}_{\dot\alpha\dot\beta}$ and the $su(2) \times su(2)$ R-symmetry generators $\mathfrak{M}_{nm}$, $\widetilde{\mathfrak{M}}_{n'm'}$ act canonically on the remaining generators carrying Lorentz and Grassmann indices:

$$\left[\mathbb{M}_{\alpha\beta}, \mathbb{M}^{\gamma\delta}\right] = \delta_{(\beta}^{(\gamma}\mathbb{M}_{\alpha)}^{\ \ \delta)} \qquad [\overline{\mathbb{M}}_{\dot\alpha\dot\beta}, \overline{\mathbb{M}}^{\dot\gamma\dot\delta}] = \delta_{(\dot\beta}^{(\dot\gamma}\overline{\mathbb{M}}_{\dot\alpha)}^{\ \ \dot\delta)} \tag{C.11}$$

$$[\mathbb{M}_{\alpha\beta}, \mathbb{P}^{\gamma\dot\delta}] = \delta_{(\beta}^{\gamma}\mathbb{P}_{\alpha)}^{\ \dot\delta} \qquad [\overline{\mathbb{M}}_{\dot\alpha\dot\beta}, \mathbb{P}^{\gamma\dot\delta}] = \delta_{(\dot\beta}^{\dot\delta}\mathbb{P}^{\gamma}_{\ \dot\alpha)} \tag{C.12}$$

$$[\mathbb{M}_{\alpha\beta}, \mathbb{K}^{\gamma\dot\delta}] = -\delta_{(\beta}^{\gamma}\mathbb{K}_{\alpha)}^{\ \dot\delta} \qquad [\overline{\mathbb{M}}_{\dot\alpha\dot\beta}, \mathbb{K}^{\gamma\dot\delta}] = -\delta_{(\dot\beta}^{\dot\delta}\mathbb{K}^{\gamma}_{\ \dot\alpha)} \tag{C.13}$$

$$[\mathbb{M}_{\alpha\beta}, \mathbb{Q}^{\gamma n}] = \delta_{(\beta}^{\gamma}\mathbb{Q}^{n}_{\alpha)} \qquad [\overline{\mathbb{M}}_{\dot\alpha\dot\beta}, \overline{\mathbb{Q}}^{\dot\gamma}_{n}] = \delta_{(\dot\beta}^{\dot\gamma}\overline{\mathbb{Q}}_{\dot\alpha)n} \tag{C.14}$$

$$[\mathbb{M}_{\alpha\beta},\overline{\widetilde{\mathbb{Q}}}^{\gamma n'}]=\delta^{\gamma}_{(\beta}\overline{\widetilde{\mathbb{Q}}}^{n'}_{\alpha)} \qquad [\overline{\mathbb{M}}_{\dot\alpha\dot\beta},\widetilde{\mathbb{Q}}^{\dot\gamma}_{n'}]=\delta^{\dot\gamma}_{(\dot\beta}\widetilde{\mathbb{Q}}_{\dot\alpha)n'} \tag{C.15}$$

$$[\mathbb{M}_{\alpha\beta},\mathbb{S}^{\gamma}_{n}]=-\delta^{\gamma}_{(\beta}\mathbb{S}_{\alpha)n} \qquad [\overline{\mathbb{M}}_{\dot\alpha\dot\beta},\overline{\mathbb{S}}^{\dot\gamma n}]=-\delta^{\dot\gamma}_{(\dot\beta}\overline{\mathbb{S}}^{n}_{\dot\alpha)} \tag{C.16}$$

$$[\mathbb{M}_{\alpha\beta},\overline{\widetilde{\mathbb{S}}}^{\gamma}_{n'}]=-\delta^{\gamma}_{(\beta}\overline{\widetilde{\mathbb{S}}}_{\alpha)n'} \qquad [\overline{\mathbb{M}}_{\dot\alpha\dot\beta},\widetilde{\mathbb{S}}^{\dot\gamma n'}]=-\delta^{\dot\gamma}_{(\dot\beta}\widetilde{\mathbb{S}}^{n'}_{\dot\alpha)} \tag{C.17}$$

$$\left[\mathfrak{M}_{nm},\mathfrak{M}^{kl}\right]=\delta^{(k}_{(m}\mathfrak{M}^{\,l)}_{n)} \qquad [\widetilde{\mathfrak{M}}_{n'm'},\widetilde{\mathfrak{M}}^{k'l'}]=\delta^{(k'}_{(m'}\widetilde{\mathfrak{M}}^{\,l')}_{n')} \tag{C.18}$$

$$[\mathfrak{M}_{nm},\mathfrak{P}^{kl'}]=\delta^{k}_{(m}\mathfrak{P}^{\,l'}_{n)} \qquad [\widetilde{\mathfrak{M}}_{n'm'},\mathfrak{P}^{kl'}]=\delta^{l'}_{(m'}\mathfrak{P}^{k}_{\,n')} \tag{C.19}$$

$$[\mathfrak{M}_{nm},\mathfrak{K}^{kl'}]=-\delta^{k}_{(m}\mathfrak{K}^{\,l'}_{n)} \qquad [\widetilde{\mathfrak{M}}_{n'm'},\mathfrak{K}^{kl'}]=-\delta^{l'}_{(m'}\mathfrak{K}^{k}_{\,n')} \tag{C.20}$$

$$[\mathfrak{M}_{nm},\mathbb{Q}^{\gamma k}]=\delta^{k}_{(m}\mathbb{Q}^{\gamma}_{n)} \qquad [\widetilde{\mathfrak{M}}_{n'm'},\widetilde{\mathbb{Q}}^{k'}_{\dot\alpha}]=\delta^{k'}_{(n'}\widetilde{\mathbb{Q}}_{\dot\alpha m')} \tag{C.21}$$

$$[\mathfrak{M}_{nm},\overline{\mathbb{S}}^{k}_{\dot\gamma}]=\delta^{k}_{(m}\overline{\mathbb{S}}_{\dot\gamma n)} \qquad [\widetilde{\mathfrak{M}}_{n'm'},\overline{\widetilde{\mathbb{S}}}^{k'}_{\alpha}]=\delta^{k'}_{(n'}\overline{\widetilde{\mathbb{S}}}_{\alpha m')} \tag{C.22}$$

$$[\mathfrak{M}_{nm},\mathbb{S}^{k}_{\alpha}]=-\delta^{k}_{(n}\mathbb{S}_{\alpha m)} \qquad [\mathfrak{M}_{nm},\overline{\mathbb{Q}}^{k}_{\dot\alpha}]=-\delta^{k}_{(n}\overline{\mathbb{Q}}_{\dot\alpha m)} \tag{C.23}$$

$$[\widetilde{\mathfrak{M}}_{n'm'},\widetilde{\mathbb{S}}^{k'}_{\dot\alpha}]=-\delta^{k'}_{(m'}\widetilde{\mathbb{S}}_{\dot\alpha n')} \qquad [\widetilde{\mathfrak{M}}_{n'm'},\overline{\widetilde{\mathbb{Q}}}^{k'}_{\alpha}]=-\delta^{k'}_{(m'}\overline{\widetilde{\mathbb{Q}}}_{\alpha n')} \tag{C.24}$$

The action of the dilatation $\mathbb{D}$ and hypercharge $\mathbb{B}$ on a generator $\mathbb{G}$ is given by:

$$[\mathbb{D},\mathbb{G}]=\dim(\mathbb{G})\,\mathbb{G} \qquad [\mathbb{B},\mathbb{G}]=\mathrm{hyp}(\mathbb{G})\,\mathbb{G} \tag{C.25}$$

The non-zero dimensions and hypercharges of the various generators are

$$\begin{aligned}
&\dim(\mathbb{P})=1\,, && \dim(\mathbb{Q})=\dim\left(\widetilde{\mathbb{Q}}\right)=\dim\left(\overline{\mathbb{Q}}\right)=\dim(\overline{\widetilde{\mathbb{Q}}})=\tfrac{1}{2}\,,\\
&\dim(\mathbb{K})=-1\,, && \dim(\mathbb{S})=\dim(\widetilde{\mathbb{S}})=\dim\left(\overline{\mathbb{S}}\right)=\dim(\overline{\widetilde{\mathbb{S}}})=-\tfrac{1}{2}\,,\\
&&& \mathrm{hyp}(\mathbb{Q})=\mathrm{hyp}(\overline{\widetilde{\mathbb{Q}}})=\mathrm{hyp}\left(\overline{\mathbb{S}}\right)=\mathrm{hyp}(\widetilde{\mathbb{S}})=\tfrac{1}{2}\,,\\
&&& \mathrm{hyp}\left(\overline{\mathbb{Q}}\right)=\mathrm{hyp}(\widetilde{\mathbb{Q}})=\mathrm{hyp}(\mathbb{S})=\mathrm{hyp}(\overline{\widetilde{\mathbb{S}}})=-\tfrac{1}{2}\,.
\end{aligned} \tag{C.26}$$

The action of the fermionic dilatation $\mathfrak{D}$ on some generator $\mathbb{G}$ is given by:

$$[\mathfrak{D},\mathbb{G}]=\mathrm{ferm}(\mathbb{G})\,\mathbb{G}\,. \tag{C.27}$$

The non-zero fermionic dimensions of the superconformal generators are:

$$\begin{aligned}
&\mathrm{ferm}(\mathfrak{P})=1\,, && \mathrm{ferm}(\mathbb{Q})=\mathrm{ferm}(\widetilde{\mathbb{Q}})=\mathrm{ferm}\left(\overline{\mathbb{S}}\right)=\mathrm{ferm}(\overline{\widetilde{\mathbb{S}}})=\tfrac{1}{2}\\
&\mathrm{ferm}(\mathfrak{K})=-1 && \mathrm{ferm}\left(\overline{\mathbb{Q}}\right)=\mathrm{ferm}(\overline{\widetilde{\mathbb{Q}}})=\mathrm{ferm}(\mathbb{S})=\mathrm{ferm}(\widetilde{\mathbb{S}})=-\tfrac{1}{2}\,.
\end{aligned} \tag{C.28}$$

The remaining non-trivial commutation relations are

$$\{\mathbb{Q}^{n}_{\alpha},\overline{\mathbb{Q}}_{\dot\alpha m}\}=\delta^{n}_{m}\mathbb{P}_{\alpha\dot\alpha} \qquad \{\widetilde{\mathbb{Q}}^{n'}_{\dot\alpha},\overline{\widetilde{\mathbb{Q}}}_{\alpha m'}\}=\delta^{n'}_{m'}\mathbb{P}_{\alpha\dot\alpha} \tag{C.29}$$

$$[\mathbb{K}_{\alpha\dot\alpha},\mathbb{Q}^{\beta n}]=\delta^{\beta}_{\alpha}\overline{\mathbb{S}}^{n}_{\dot\alpha} \qquad [\mathbb{K}_{\alpha\dot\alpha},\widetilde{\mathbb{Q}}^{\dot\beta n'}]=\delta^{\dot\beta}_{\dot\alpha}\overline{\widetilde{\mathbb{S}}}^{n'}_{\alpha} \tag{C.30}$$

$$[\mathbb{K}_{\alpha\dot\alpha},\overline{\mathbb{Q}}^{\dot\beta}_{n}]=\delta^{\dot\beta}_{\dot\alpha}\mathbb{S}_{\alpha n} \qquad [\mathbb{K}_{\alpha\dot\alpha},\overline{\widetilde{\mathbb{Q}}}^{\beta}_{n'}]=\delta^{\beta}_{\alpha}\widetilde{\mathbb{S}}_{\dot\alpha n'} \tag{C.31}$$

$$[\mathbb{S}_{\alpha n},\mathbb{P}^{\beta\dot\beta}]=\delta^{\beta}_{\alpha}\overline{\mathbb{Q}}^{\dot\beta}_{n} \qquad [\widetilde{\mathbb{S}}_{\dot\alpha n'},\mathbb{P}^{\beta\dot\beta}]=\delta^{\dot\beta}_{\dot\alpha}\overline{\widetilde{\mathbb{Q}}}^{\beta}_{n'} \tag{C.32}$$

$$[\overline{\mathbb{S}}^{n}_{\dot\alpha},\mathbb{P}^{\beta\dot\beta}]=\delta^{\dot\beta}_{\dot\alpha}\mathbb{Q}^{\beta n} \qquad [\overline{\widetilde{\mathbb{S}}}^{n'}_{\alpha},\mathbb{P}^{\beta\dot\beta}]=\delta^{\beta}_{\alpha}\widetilde{\mathbb{Q}}^{\dot\beta n'} \tag{C.33}$$

$$\{\mathbb{S}_{\alpha n},\overline{\mathbb{S}}^{m}_{\dot\alpha}\}=\delta^{m}_{n}\mathbb{K}_{\alpha\dot\alpha} \qquad \{\widetilde{\mathbb{S}}_{\dot\alpha n'},\overline{\widetilde{\mathbb{S}}}^{m'}_{\alpha}\}=\delta^{m'}_{n'}\mathbb{K}_{\alpha\dot\alpha} \tag{C.34}$$

$$\{\mathbb{S}_{\alpha n},\overline{\widetilde{\mathbb{Q}}}^{\beta}_{n'}\}=\delta^{\beta}_{\alpha}\mathfrak{K}_{nn'} \qquad \{\widetilde{\mathbb{S}}_{\dot\alpha n'},\overline{\mathbb{Q}}^{\dot\beta}_{n}\}=-\delta^{\dot\beta}_{\dot\alpha}\mathfrak{K}_{nn'} \tag{C.35}$$

$$\{\overline{\mathbb{S}}^{n}_{\dot\alpha},\widetilde{\mathbb{Q}}^{\dot\beta n'}\}=\delta^{\dot\beta}_{\dot\alpha}\mathfrak{P}^{nn'} \qquad \{\overline{\widetilde{\mathbb{S}}}^{n'}_{\alpha},\mathbb{Q}^{\beta n}\}=-\delta^{\beta}_{\alpha}\mathfrak{P}^{nn'} \tag{C.36}$$

$$[\,\overline{\mathbb{Q}}^{\dot\beta}_{m},\mathfrak{P}^{nn'}\,]=\delta^{n}_{m}\widetilde{\mathbb{Q}}^{\dot\beta n'} \qquad [\overline{\widetilde{\mathbb{Q}}}^{\beta}_{m'},\mathfrak{P}^{nn'}]=-\delta^{n'}_{m'}\mathbb{Q}^{\beta n} \tag{C.37}$$

$$[\mathbb{S}_{\alpha m},\mathfrak{P}^{nn'}]=\delta^{n}_{m}\overline{\widetilde{\mathbb{S}}}^{n'}_{\alpha} \qquad [\widetilde{\mathbb{S}}_{\dot\alpha m'},\mathfrak{P}^{nn'}]=-\delta^{n'}_{m'}\overline{\mathbb{S}}^{n}_{\dot\alpha} \tag{C.38}$$

$$[\mathfrak{K}_{nn'},\mathbb{Q}^{\alpha m}]=-\delta^{m}_{n}\overline{\widetilde{\mathbb{Q}}}^{\alpha}_{n'} \qquad [\mathfrak{K}_{nn'},\widetilde{\mathbb{Q}}^{\dot\alpha m'}]=\delta^{m'}_{n'}\overline{\mathbb{Q}}^{\dot\alpha}_{n} \tag{C.39}$$

$$[\mathfrak{K}_{nn'},\overline{\mathbb{S}}^{m}_{\dot\alpha}]=-\delta^{m}_{n}\widetilde{\mathbb{S}}_{\dot\alpha n'} \qquad [\mathfrak{K}_{nn'},\overline{\widetilde{\mathbb{S}}}^{n'}_{\alpha}]=\delta^{m'}_{n'}\mathbb{S}_{\alpha n} \tag{C.40}$$

as well as

$$\{\mathbb{S}_{\alpha n},\mathbb{Q}^{\beta m}\}=\delta^{m}_{n}\mathbb{M}^{\beta}{}_{\alpha}-\delta^{\beta}_{\alpha}\mathfrak{M}^{m}{}_{n}+\tfrac{1}{2}\delta^{m}_{n}\delta^{\beta}_{\alpha}(\mathbb{D}-\mathbb{C}-\mathfrak{D}) \tag{C.41}$$

$$\{\widetilde{\mathbb{S}}_{\dot\alpha n'},\widetilde{\mathbb{Q}}^{\dot\beta m'}\}=\delta^{m'}_{n'}\overline{\mathbb{M}}^{\dot\beta}{}_{\dot\alpha}-\delta^{\dot\beta}_{\dot\alpha}\widetilde{\mathfrak{M}}^{m'}{}_{n'}+\tfrac{1}{2}\delta^{m'}_{n'}\delta^{\dot\beta}_{\dot\alpha}(\mathbb{D}+\mathbb{C}-\mathfrak{D}) \tag{C.42}$$

$$\{\overline{\mathbb{S}}^{n}_{\dot\alpha},\overline{\mathbb{Q}}^{\dot\beta}_{m}\}=\delta^{n}_{m}\overline{\mathbb{M}}^{\dot\beta}{}_{\dot\alpha}+\delta^{\dot\beta}_{\dot\alpha}\mathfrak{M}^{n}{}_{m}+\tfrac{1}{2}\delta^{n}_{m}\delta^{\dot\beta}_{\dot\alpha}(\mathbb{D}+\mathbb{C}+\mathfrak{D}) \tag{C.43}$$

$$\{\overline{\widetilde{\mathbb{S}}}^{n'}_{\alpha},\overline{\widetilde{\mathbb{Q}}}^{\beta}_{m'}\}=\delta^{n'}_{m'}\mathbb{M}^{\beta}{}_{\alpha}+\delta^{\beta}_{\alpha}\widetilde{\mathfrak{M}}^{n'}{}_{m'}+\tfrac{1}{2}\delta^{n'}_{m'}\delta^{\dot\beta}_{\dot\alpha}(\mathbb{D}-\mathbb{C}+\mathfrak{D}) \tag{C.44}$$

$$[\mathfrak{K}_{mm'},\mathfrak{P}^{nn'}]=\delta^{n'}_{m'}\delta^{n}_{m}\mathfrak{D}+\delta^{n}_{m}\widetilde{\mathfrak{M}}^{m'}{}_{n'}+\delta^{n'}_{m'}\mathfrak{M}^{m}{}_{n} \tag{C.45}$$

$$[\mathbb{K}_{\alpha\dot\alpha},\mathbb{P}^{\beta\dot\beta}]=\delta^{\beta}_{\alpha}\delta^{\dot\beta}_{\dot\alpha}\mathbb{D}+\delta^{\dot\beta}_{\dot\alpha}\mathbb{M}^{\beta}{}_{\alpha}+\delta^{\beta}_{\alpha}\overline{\mathbb{M}}^{\dot\beta}{}_{\dot\alpha} \tag{C.46}$$

C.2.1. The On-Shell Representation

We denote the generators of the on-shell representation of the non-chiral superconformal algebra by small letters a,b,c and $\mathfrak{a},\mathfrak{b},\mathfrak{c}$. We introduce the following abbreviations

$$\partial_{in}=\frac{\partial}{\partial\eta^{n}_{i}} \qquad \partial_{in'}=\frac{\partial}{\partial\tilde\eta^{n'}_{i}} \tag{C.47}$$

for derivatives with respect to the Grassmann variables. The on-shell generators are

$$p^{\dot\alpha\alpha}=\sum_{i}\lambda^{\alpha}_{i}\tilde\lambda^{\dot\alpha}_{i} \qquad k_{\dot\alpha\alpha}=\sum_{i}\partial_{i\alpha}\partial_{i\dot\alpha} \tag{C.48}$$

$$m_{\alpha\beta}=\sum_{i}\lambda_{i(\alpha}\partial_{i\beta)} \qquad \overline{m}_{\dot\alpha\dot\beta}=\sum_{i}\tilde\lambda_{i(\dot\alpha}\partial_{i\dot\beta)} \tag{C.49}$$

$$q^{\alpha n}=\sum_{i}\lambda^{\alpha}_{i}\eta^{n}_{i} \qquad \tilde q^{\dot\alpha n'}=\sum_{i}\tilde\lambda^{\dot\alpha}_{i}\tilde\eta^{n'}_{i} \tag{C.50}$$

$$\bar q^{\dot\alpha}_{n}=\sum_{i}\tilde\lambda^{\dot\alpha}_{i}\partial_{in} \qquad \bar{\tilde q}^{\alpha}_{n'}=\sum_{i}\lambda^{\alpha}_{i}\partial_{in'} \tag{C.51}$$

$$s_{\alpha n}=\sum_{i}\partial_{i\alpha}\partial_{in} \qquad \tilde s_{\dot\alpha n'}=\sum_{i}\partial_{i\dot\alpha}\partial_{in'} \tag{C.52}$$

$$\bar s^{n}_{\dot\alpha}=\sum_{i}\eta^{n}_{i}\partial_{i\dot\alpha} \qquad \bar{\tilde s}^{n'}_{\alpha}=\sum_{i}\tilde\eta^{n'}_{i}\partial_{i\alpha} \tag{C.53}$$

$$d=\tfrac{1}{2}\sum_{i}\left(\lambda^{\alpha}_{i}\partial_{i\alpha}+\tilde\lambda^{\dot\alpha}_{i}\partial_{i\dot\alpha}+2\right) \qquad b=\tfrac{1}{2}\sum_{i}\left(\eta^{n}_{i}\partial_{in}-\tilde\eta^{n'}_{i}\partial_{in'}\right) \tag{C.54}$$

$$c=\tfrac{1}{2}\sum_{i}\left(-\lambda^{\alpha}_{i}\partial_{i\alpha}+\tilde\lambda^{\dot\alpha}_{i}\partial_{i\dot\alpha}+\eta^{n}_{i}\partial_{in}-\tilde\eta^{n'}_{i}\partial_{in'}\right) \tag{C.55}$$

$$p^{nn'} = \sum_i \eta_i^n \tilde{\eta}_i^{n'} \qquad \mathcal{k}_{nn'} = \sum_i \partial_{in}\partial_{in'} \tag{C.56}$$

$$\mathcal{m}_{nm} = \sum_i \eta_{i(n}\partial_{im)} \qquad \tilde{\mathcal{m}}_{n'm'} = \sum_i \tilde{\eta}_{i(n'}\partial_{im')} \tag{C.57}$$

$$\mathcal{d} = \tfrac{1}{2}\sum_i \left(\eta_i^n\partial_{in} + \tilde{\eta}_i^{n'}\partial_{in'} - 2\right) \tag{C.58}$$

C.2.2. The Dual Representation

We denote the generators of the dual representation of the non-chiral superconformal algebra by capital letters A, B, C and $\mathcal{A}, \mathcal{B}, \mathcal{C}$. We present the dual representation in dual non-chiral superspace $(x, y, \theta, \tilde{\theta})$ using the following abbreviations

$$\partial_{inn'} = \frac{\partial}{\partial y_i^{nn'}} \qquad \partial_{\alpha n} = \frac{\partial}{\partial \tilde{\theta}_i^{\alpha n}} \qquad \partial_{i\dot{\alpha}n'} = \frac{\partial}{\partial \tilde{\theta}_i^{\dot{\alpha}n'}} \tag{C.59}$$

for derivatives with respect to y, θ and $\tilde{\theta}$. In the dual superspace $\{x_i^{\dot{\alpha}\alpha}, \theta_i^{m\,\alpha}, \tilde{\theta}_i^{m'\,\dot{\alpha}}\}$ the generators of the dual non-chiral superconformal symmetry are given by

$$\begin{aligned}
P_{\alpha\dot{\alpha}} &= \sum_i \partial_{i\alpha\dot{\alpha}} & \mathcal{P}_{nn'} &= -\sum_i \partial_{inn'} \\
Q_{\alpha n} &= -\sum_i \partial_{i\alpha n} & \widetilde{Q}_{\dot{\alpha}n'} &= -\sum_i \partial_{i\dot{\alpha}n'} \\
\overline{Q}^n_{\dot{\alpha}} &= \sum_i (\theta_i^{\alpha n}\partial_{i\alpha\dot{\alpha}} + y_i^{nn'}\partial_{i\dot{\alpha}n'}) & \overline{\widetilde{Q}}^{n'}_{\alpha} &= \sum_i (\tilde{\theta}_i^{\dot{\alpha}n'}\partial_{i\alpha\dot{\alpha}} - y_i^{nn'}\partial_{i\alpha n}) \\
M_{\alpha\beta} &= \sum_i \left(\theta^n_{i(\alpha}\partial_{i\beta)n} + x^{\dot{\alpha}}_{i(\alpha}\partial_{i\beta)\dot{\alpha}}\right) & \overline{M}_{\dot{\alpha}\dot{\beta}} &= \sum_i \left(\tilde{\theta}^{n'}_{i(\dot{\alpha}}\partial_{i\dot{\beta})n'} + x^{\alpha}_{i(\dot{\alpha}}\partial_{i\dot{\beta})\alpha}\right) \\
\mathcal{M}_{nm} &= \sum_i \left(\theta_{i\alpha(n}\partial^{\alpha}_{im)} + y_{i(n}{}^{n'}\partial_{im)n'}\right) & \widetilde{\mathcal{M}}_{n'm'} &= \sum_i \left(\tilde{\theta}_{i\dot{\alpha}(n'}\partial^{\dot{\alpha}}_{im')} + y_{in(n'}\partial^{n}_{im')}\right) \\
\overline{S}^{\dot{\alpha}}_n &= -\sum_i (\tilde{\theta}_i^{\dot{\alpha}n'}\partial_{inn'} + x_i^{\alpha\dot{\alpha}}\partial_{i\alpha n}) & \overline{\widetilde{S}}^{\alpha}_{n'} &= \sum_i (\theta_i^{\alpha n}\partial_{inn'} - x_i^{\alpha\dot{\alpha}}\partial_{i\dot{\alpha}n'}) \\
S^{\alpha n} &= \sum_i \left(-\theta_i^{\alpha m}\theta_i^{\beta n}\partial_{i\beta m} + x_i^{\alpha\dot{\beta}}\theta_i^{\beta n}\partial_{i\beta\dot{\beta}} - \theta_i^{\alpha m}y_i^{nm'}\partial_{imm'} + y_i^{nm'}x_i^{\alpha\dot{\alpha}}\partial_{i\dot{\alpha}m'}\right) \\
\widetilde{S}^{\dot{\alpha}n'} &= \sum_i \left(-\tilde{\theta}_i^{\dot{\alpha}m'}\tilde{\theta}_i^{\dot{\beta}n'}\partial_{i\dot{\beta}m'} + x_i^{\dot{\alpha}\beta}\tilde{\theta}_i^{\dot{\beta}n'}\partial_{i\beta\dot{\beta}} - \tilde{\theta}_i^{\dot{\alpha}m'}y_i^{mn'}\partial_{imm'} - y_i^{mn'}x_i^{\dot{\alpha}\alpha}\partial_{i\alpha m}\right) \\
K_{\alpha\dot{\alpha}} &= \sum_i \left(x_{i\alpha}{}^{\dot{\beta}}x_{i\dot{\alpha}}{}^{\beta}\partial_{i\beta\dot{\beta}} + x_{i\dot{\alpha}}{}^{\beta}\theta^n_{i\alpha}\partial_{in\beta} + x_{i\alpha}{}^{\dot{\beta}}\tilde{\theta}^{n'}_{i\dot{\alpha}}\partial_{in'\dot{\beta}} + \theta^n_{i\alpha}\tilde{\theta}^{n'}_{i\dot{\alpha}}\partial_{inn'}\right) \\
\mathcal{K}^{nn'} &= \sum_i \left(-y_i^{nm'}y_i^{mn'}\partial_{imm'} - \tilde{\theta}_i^{\dot{\alpha}n'}y_i^{nm'}\partial_{i\dot{\alpha}m'} - \theta_i^{\alpha n}y_i^{mn'}\partial_{i\alpha m} + \theta_i^{n\alpha}\tilde{\theta}^{n'\dot{\alpha}}\partial_{\alpha\dot{\alpha}}\right) \\
D &= -\tfrac{1}{2}\sum_i \left(\theta_i^{n\alpha}\partial_{i\alpha n} + \tilde{\theta}_i^{\dot{\alpha}n'}\partial_{i\dot{\alpha}n'} + 2x_i^{\alpha\dot{\alpha}}\partial_{i\alpha\dot{\alpha}}\right) \\
\mathcal{D} &= -\tfrac{1}{2}\sum_i \left(\theta_i^{n\alpha}\partial_{i\alpha n} + \tilde{\theta}_i^{\dot{\alpha}n'}\partial_{i\dot{\alpha}n'} + 2y_i^{nn'}\partial_{inn'}\right) \\
B &= \tfrac{1}{2}\sum_i \left(\tilde{\theta}_i^{\dot{\alpha}n'}\partial_{i\dot{\alpha}n'} - \theta_i^{n\alpha}\partial_{i\alpha n}\right)
\end{aligned} \tag{C.60}$$

We note that there are seven other possibilities to choose the signs of the generators such that they fulfill the non-chiral superconformal algebra listed at the beginning of appendix C.2. It is straightforward to obtain the generators in full non-chiral superspace $\{\lambda_i^{\alpha}, \tilde{\lambda}_i^{\dot{\alpha}}, x_i^{\dot{\alpha}\alpha}, \eta^m, \tilde{\eta}^{m'}\theta_i^{m\,\alpha}, \tilde{\theta}_i^{m'\,\dot{\alpha}}\}$ by extending the action of the generators in dual

non-chiral superspace such that they commute with the constraints eq. (1.88). Alternatively one could derive the action of the conformal and superconformal generators $K_{\alpha\dot{\alpha}}$, $S^{\alpha n}$, $\widetilde{S}^{\dot{\alpha}n'}$, $\overline{S}_n^{\dot{\alpha}}$ and $\overline{\widetilde{S}}_{n'}^{\alpha}$ in full superspace from their definition (1.125) and the inversion rules (1.127) of the onshell variables. The action of all remaining generators on the onshell variables can then be obtained from the non-chiral superconformal algebra.

Appendix D

The Mathematica Package QCDcolor

The Mathematica package QCDcolor provides the color decomposition of QCD at tree (section 2.2.1) and one-loop level (section 2.2.2) as well as implementations of all the identities of primitive amplitudes derived in section 2.3. Accompanying the package is a notebook file QCDcolor.nb demonstrating its usage. Within the package QCDcolor gluons are specified by distinct integers.

Quarks are represented by Q[i,R], Q[i,L], where i is some integer labeling different flavors and the routing label R,L is absent at tree level. Anti-quarks are represented by Qb[i,R], Qb[i,L], where i is some integer labeling different flavors and the routing label R, L is absent at tree level. Integer labels of gluons and quarks can overlap. Color ordered tree amplitudes are represented by the function Atree[...]. The part of the primitive amplitude containing no fermion loop is represented by the function A[...], whereas the fermion loop part is represented by Af[...]. In contrast to the conventions in the rest of this thesis (compare eqs. (2.1), (2.37) and (2.53)) the dependence of the amplitudes on the number of different quark flavors nf and the number of colors Nc is not absorbed into the definition of the color structures, leading to partial amplitudes with explicit nf, Nc dependence. In this way a color structure can be uniquely represented by lists of cycles. A cycle is represented by a list of the form {Q[i],...,Qb[k],Q[k],..., Qb[i]}. A trace in the color structure is represented by a list of integers. Traces have to be in the last entries of the list representing the color structure.

Just type

```
« QCDcolor.m
```

To load the package. A list of all stored in the variable $QCDcolorFunction. The documentations of the functions can be accessed by typing e. g.

```
?QCDnice
```

will return

`Typing: QCDnice (shift+enter), leads to nicely formatted output using the Notation package.`

Evaluating `QCDbasic` it is possible to return to basic input formatting of the output. The functions `ColorS[k,n]` and `ColorSLoop[k,n]` generate all color structures in a tree or a one-loop amplitude with `k` quark lines and `n` gluons. For example evaluation of `ColorS[3,1]` gives the list

$$\begin{aligned}
&\{\{\{Q_1,1,\bar{Q}_1\},\{Q_2,\bar{Q}_2\},\{Q_3,\bar{Q}_3\}\},\{\{Q_1,1,\bar{Q}_1\},\{Q_2,\bar{Q}_3,Q_3,\bar{Q}_2\}\},\\
&\{\{Q_1,1,\bar{Q}_2,Q_2,\bar{Q}_1\},\{Q_3,\bar{Q}_3\}\},\{\{Q_1,1,\bar{Q}_2,Q_2,\bar{Q}_3,Q_3,\bar{Q}_1\}\},\\
&\{\{Q_1,1,\bar{Q}_3,Q_3,\bar{Q}_2,Q_2,\bar{Q}_1\}\},\{\{Q_1,1,\bar{Q}_3,Q_3,\bar{Q}_1\},\{Q_2,\bar{Q}_2\}\},\\
&\{\{Q_1,\bar{Q}_1\},\{Q_2,1,\bar{Q}_2\},\{Q_3,\bar{Q}_3\}\},\{\{Q_1,\bar{Q}_1\},\{Q_2,1,\bar{Q}_3,Q_3,\bar{Q}_2\}\},\\
&\{\{Q_1,\bar{Q}_2,Q_2,1,\bar{Q}_1\},\{Q_3,\bar{Q}_3\}\},\{\{Q_1,\bar{Q}_2,Q_2,1,\bar{Q}_3,Q_3,\bar{Q}_1\}\},\\
&\{\{Q_1,\bar{Q}_3,Q_3,\bar{Q}_2,Q_2,1,\bar{Q}_1\}\},\{\{Q_1,\bar{Q}_3,Q_3,\bar{Q}_1\},\{Q_2,1,\bar{Q}_2\}\},\\
&\{\{Q_1,\bar{Q}_1\},\{Q_2,\bar{Q}_2\},\{Q_3,1,\bar{Q}_3\}\},\{\{Q_1,\bar{Q}_1\},\{Q_2,\bar{Q}_3,Q_3,1,\bar{Q}_2\}\},\\
&\{\{Q_1,\bar{Q}_2,Q_2,\bar{Q}_1\},\{Q_3,1,\bar{Q}_3\}\},\{\{Q_1,\bar{Q}_2,Q_2,\bar{Q}_3,Q_3,1,\bar{Q}_1\}\},\\
&\{\{Q_1,\bar{Q}_2,Q_2,\bar{Q}_1\},\{Q_3,1,\bar{Q}_3\}\},\{\{Q_1,\bar{Q}_2,Q_2,\bar{Q}_3,Q_3,1,\bar{Q}_1\}\}\\
&\{\{Q_1,\bar{Q}_3,Q_3,1,\bar{Q}_2,Q_2,\bar{Q}_1\}\},\{\{Q_1,\bar{Q}_3,Q_3,1,\bar{Q}_1\},\{Q_2,\bar{Q}_2\}\}\},
\end{aligned} \tag{D.1}$$

and evaluation of `ColorS[2,2]` generates

$$\begin{aligned}
&\{\{\{Q_1,1,2,\bar{Q}_1\},\{Q_2,\bar{Q}_2\}\},\{\{Q_1,1,2,\bar{Q}_2,Q_2,\bar{Q}_1\}\},\{\{Q_1,1,\bar{Q}_1\},\{Q_2,2,\bar{Q}_2\}\},\\
&\{\{Q_1,1,\bar{Q}_2,Q_2,2,\bar{Q}_1\}\},\{\{Q_1,\bar{Q}_1\},\{Q_2,1,2,\bar{Q}_2\}\},\{\{Q_1,\bar{Q}_2,Q_2,1,2,\bar{Q}_1\}\},\\
&\{\{Q_1,2,1,\bar{Q}_1\},\{Q_2,\bar{Q}_2\}\},\{\{Q_1,2,1,\bar{Q}_2,Q_2,\bar{Q}_1\}\},\{\{Q_1,2,\bar{Q}_1\},\{Q_2,1,\bar{Q}_2\}\},\\
&\{\{Q_1,2,\bar{Q}_2,Q_2,1,\bar{Q}_1\}\},\{\{Q_1,\bar{Q}_1\},\{Q_2,2,1,\bar{Q}_2\}\},\{\{Q_1,\bar{Q}_2,Q_2,2,1,\bar{Q}_1\}\},\\
&\{\{Q_1,\bar{Q}_1\},\{Q_2,\bar{Q}_2\},\{1,2\}\},\{\{Q_1,\bar{Q}_2,Q_2,\bar{Q}_1\},\{1,2\}\}\}.
\end{aligned} \tag{D.2}$$

The tree-level partial amplitudes multiplying the color structure `C` are implemented in the function `PartialAmplitudeTree[C]`. Make sure `C` is in cycle notation and consistent or simply use the output of `ColorS[k,n]`. Evaluating

```
PartialAmplitudeTree[{{Q[1],1,2,Qb[1]},
                      {Q[2],Qb[2]},{Q[3],Qb[3]},{Q[4],Qb[4]}}]
```

generates the partial amplitude

$$\begin{aligned}
-\frac{1}{N_c^3}\Big(&A_{\text{tree}}\left[Q_1,1,2,\bar{Q}_1,Q_2,\bar{Q}_2,Q_3,\bar{Q}_3,Q_4,\bar{Q}_4\right]\\
&+A_{\text{tree}}\left[Q_1,1,2,\bar{Q}_1,Q_2,\bar{Q}_2,Q_4,\bar{Q}_4,Q_3,\bar{Q}_3\right]\\
&+A_{\text{tree}}\left[Q_1,1,2,\bar{Q}_1,Q_3,\bar{Q}_3,Q_2,\bar{Q}_2,Q_4,\bar{Q}_4\right]\\
&+A_{\text{tree}}\left[Q_1,1,2,\bar{Q}_1,Q_3,\bar{Q}_3,Q_4,\bar{Q}_4,Q_2,\bar{Q}_2\right]\\
&+A_{\text{tree}}\left[Q_1,1,2,\bar{Q}_1,Q_4,\bar{Q}_4,Q_2,\bar{Q}_2,Q_3,\bar{Q}_3\right]\\
&+A_{\text{tree}}\left[Q_1,1,2,\bar{Q}_1,Q_4,\bar{Q}_4,Q_3,\bar{Q}_3,Q_2,\bar{Q}_2\right]\Big),
\end{aligned} \tag{D.3}$$

multiplying the color structure $(T^{a_1}T^{a_2})i_1\bar{j}_1\delta_{i_2\bar{j}_2}\delta_{i_2\bar{j}_2}\delta_{i_3\bar{j}_3}\delta_{i_4\bar{j}_4}$ within the eight quark two gluon amplitude. Evaluation of

```
PartialAmplitudeTree[{{Q[1],1,2,Qb[2],Q[2],Qb[1]},
                                {Q[3],3,4,5,Qb[3]}, {Q[4],6,Qb[4]}}]
```

yields the partial amplitude

$$\begin{aligned}\frac{1}{N_c^2}\Big(&A_{\text{tree}}\left[Q_1,1,2,\bar{Q}_2,Q_2,\bar{Q}_1,Q_3,3,4,5,\bar{Q}_3,Q_4,6,\bar{Q}_4\right]\\&+A_{\text{tree}}\left[Q_1,1,2,\bar{Q}_2,Q_2,\bar{Q}_1,Q_4,6,\bar{Q}_4,Q_3,3,4,5,\bar{Q}_3\right]\\&+A_{\text{tree}}\left[Q_1,1,2,\bar{Q}_2,Q_3,3,4,5,\bar{Q}_3,Q_2,\bar{Q}_1,Q_4,6,\bar{Q}_4\right]\\&+A_{\text{tree}}\left[Q_1,1,2,\bar{Q}_2,Q_3,3,4,5,\bar{Q}_3,Q_4,6,\bar{Q}_4,Q_2,\bar{Q}_1\right]\\&+A_{\text{tree}}\left[Q_1,1,2,\bar{Q}_2,Q_4,6,\bar{Q}_4,Q_2,\bar{Q}_1,Q_3,3,4,5,\bar{Q}_3\right]\\&+A_{\text{tree}}\left[Q_1,1,2,\bar{Q}_2,Q_4,6,\bar{Q}_4,Q_3,3,4,5,\bar{Q}_3,Q_2,\bar{Q}_1\right]\Big),\end{aligned}\tag{D.4}$$

which is multiplying $(T^{a_1}T^{a_2})_{i_1\bar{j}_2}\delta_{i_2\bar{j}_1}(T^{a_3}T^{a_4}T^{a_5})_{i_3\bar{j}_3}(T^{a_6})_{i_4\bar{j}_4}$. The one-loop partial amplitudes are implemented in the function `PartialAmplitudeLoop`, which generates the coefficients of the color structure `C`. As explained at the beginning of this section, `PartialAmplitudeLoop` contains the N and n_f dependence of the amplitude and is related to the N, n_f independent partial amplitude defined in eq. (2.53) by

$$\texttt{PartialAmplitudeLoop[C]} = \begin{cases}\left(\frac{-1}{N}\right)^p\left(P_3 - \frac{n_f}{N}P_2^f\right) & \text{if C contains a trace}\\ \left(\frac{-1}{N}\right)^p\left(N(P_0-P_1) - \frac{1}{N}P_2 + n_f(P_0^f - P_1^f)\right) & \text{else}\end{cases}\tag{D.5}$$

The cyclic symmetry, reversion identity and the two term fermion flip and furry identities eqs. (2.73), (2.74), (2.76), (2.83) and (2.84) are applied in order to canonicalize the arguments of the primitives generated by eqs. (2.54) to (2.60), e. g. the first argument of all primitives is always `Q[1,L]`. Furthermore, tadpoles and loop corrections to massless legs are removed, eq. (2.80). This canonicalization of expressions of primitives is implemented in the function `canonical[...]` and removes the most basic redundancies. Equations (2.54) to (2.60) are all implemented separately, the map of the function names is

$$\begin{aligned}P_0 &\rightarrow \texttt{LOpartial}\\ P_1 &\rightarrow \texttt{CycleSplit}\\ P_2 &\rightarrow \texttt{PhotonLoop}\\ P_3 &\rightarrow \texttt{TracePart}\\ P_0^f &\rightarrow \texttt{FermionLoop}\\ P_1^f &\rightarrow \texttt{FermionLoopPhoton}\\ P_2^f &\rightarrow \texttt{FermionLoopTrace}.\end{aligned}\tag{D.6}$$

Evaluation of

```
PartialAmplitudeLoop[{{Q[1],1,Qb[1]},{Q[2],2,Qb[2]}}]
```

gives the partial amplitude

$$
\begin{aligned}
&- A\left[Q_1^L,1,2,Q_2^R,\bar{Q}_2^R,\bar{Q}_1^L\right] + A\left[Q_1^L,1,2,\bar{Q}_1^L,\bar{Q}_2^L,Q_2^L\right] - A\left[Q_1^L,1,Q_2^R,\bar{Q}_2^R,2,\bar{Q}_1^L\right] \\
&- A\left[Q_1^L,1,Q_2^R,\bar{Q}_2^R,\bar{Q}_1^L,2\right] - A\left[Q_1^L,1,\bar{Q}_1^L,2,Q_2^R,\bar{Q}_2^R\right] - A\left[Q_1^L,1,\bar{Q}_1^L,Q_2^R,\bar{Q}_2^R,2\right] \\
&- A\left[Q_1^L,1,\bar{Q}_1^L,\bar{Q}_2^L,2,Q_2^L\right] - A\left[Q_1^L,1,\bar{Q}_2^R,2,Q_2^R,\bar{Q}_1^L\right] - A\left[Q_1^L,2,1,Q_2^R,\bar{Q}_2^R,\bar{Q}_1^L\right] \\
&+ A\left[Q_1^L,2,1,\bar{Q}_1^L,\bar{Q}_2^L,Q_2^L\right] - A\left[Q_1^L,2,Q_2^R,1,\bar{Q}_2^R,\bar{Q}_1^L\right] - A\left[Q_1^L,2,Q_2^R,\bar{Q}_2^R,1,\bar{Q}_1^L\right] \\
&+ A\left[Q_1^L,Q_2^L,1,2,\bar{Q}_2^L,\bar{Q}_1^L\right] + A\left[Q_1^L,Q_2^L,2,1,\bar{Q}_2^L,\bar{Q}_1^L\right] - A\left[Q_1^L,Q_2^L,2,\bar{Q}_2^L,\bar{Q}_1^L,1\right] \\
&- A\left[Q_1^L,Q_2^R,1,\bar{Q}_2^R,2,\bar{Q}_1^L\right] - A\left[Q_1^L,Q_2^R,1,\bar{Q}_2^R,\bar{Q}_1^L,2\right] - A\left[Q_1^L,Q_2^R,\bar{Q}_2^R,1,2,\bar{Q}_1^L\right] \\
&- A\left[Q_1^L,Q_2^R,\bar{Q}_2^R,1,\bar{Q}_1^L,2\right] - A\left[Q_1^L,Q_2^R,\bar{Q}_2^R,2,1,\bar{Q}_1^L\right] - A\left[Q_1^L,\bar{Q}_2^R,2,Q_2^R,1,\bar{Q}_1^L\right] \\
&+ \frac{1}{N_c^2}\Big(- A\left[Q_1^L,2,\bar{Q}_2^R,Q_2^R,\bar{Q}_1^L,1\right] + A\left[Q_1^L,Q_2^L,\bar{Q}_2^L,\bar{Q}_1^L,1,2\right] \\
&\qquad + A\left[Q_1^L,Q_2^L,\bar{Q}_2^L,\bar{Q}_1^L,2,1\right] - A\left[Q_1^L,Q_2^R,2,\bar{Q}_2^R,\bar{Q}_1^L,1\right] \\
&\qquad - A\left[Q_1^L,\bar{Q}_1^L,1,Q_2^R,2,\bar{Q}_2^R\right] - A\left[Q_1^L,\bar{Q}_1^L,Q_2^R,2,\bar{Q}_2^R,1\right] \\
&\qquad + A\left[Q_1^L,\bar{Q}_1^L,\bar{Q}_2^L,1,2,Q_2^L\right] + A\left[Q_1^L,\bar{Q}_1^L,\bar{Q}_2^L,2,1,Q_2^L\right] \\
&\qquad + A\left[Q_1^L,\bar{Q}_2^L,2,Q_2^L,\bar{Q}_1^L,1\right] - A\left[Q_1^L,\bar{Q}_2^R,Q_2^R,2,\bar{Q}_1^L,1\right]\Big) \\
&- \frac{1}{N_c}n_f\Big(- A_f\left[Q_1^L,1,\bar{Q}_2^L,2,Q_2^L,\bar{Q}_1^L\right] - A_f\left[Q_1^L,2,\bar{Q}_2^L,Q_2^L,\bar{Q}_1^L,1\right] \\
&\qquad - A_f\left[Q_1^L,\bar{Q}_2^L,1,2,Q_2^L,\bar{Q}_1^L\right] - A_f\left[Q_1^L,\bar{Q}_2^L,2,1,Q_2^L,\bar{Q}_1^L\right] \\
&\qquad - A_f\left[Q_1^L,\bar{Q}_2^L,2,Q_2^L,1,\bar{Q}_1^L\right] - A_f\left[Q_1^L,\bar{Q}_2^L,2,Q_2^L,\bar{Q}_1^L,1\right] \\
&\qquad - A_f\left[Q_1^L,\bar{Q}_2^L,Q_2^L,2,\bar{Q}_1^L,1\right] - A_f\left[Q_1^L,\bar{Q}_2^L,Q_2^L,\bar{Q}_1^L,1,2\right] \\
&\qquad - A_f\left[Q_1^L,\bar{Q}_2^L,Q_2^L,\bar{Q}_1^L,2,1\right]\Big),
\end{aligned}
\tag{D.7}
$$

which multiplies the color structure $(T^{a_1})_{i_1\bar{j}_1}(T^{a_2})_{i_2\bar{j}_2}$ within the four quark two gluon one-loop QCD amplitude.

The identities among the primitive amplitudes are implemented in the package `QCDcolor` as well. The general reversion identity eq. (2.85) for the mixed loop primitives `A[...]` and the fermion loop primitives `Af[...]` is implemented as `RevID[l1,a1,A or Af]`. Modulo cyclic and reflection symmetry all other identities are linear combinations of reversion identities. `l1` is a list of the form `{Q[1,L],Qb[i,L],...}` or `{Qb[1,R],Q[i,R],...}` and `a1` is a list of external legs. In the case of the mixed loop primitives `A[...]`, `a1` has to be of the form `{...,Q[i,L],...,Qb[i,L],...}` or `{...,Qb[i,R],...,Q[i,R],...}`. The output is canonicalized. Two examples are

```
RevID[Q[1,L],Qb[1,L],1,2,3,4,Af]
```

returning the identity

$$
\begin{aligned}
&A_f\left[Q_1^L,2,3,4,\bar{Q}_1^L,1\right] + A_f\left[Q_1^L,2,3,\bar{Q}_1^L,1,4\right] + A_f\left[Q_1^L,2,3,\bar{Q}_1^L,4,1\right] \\
&+ A_f\left[Q_1^L,3,4,\bar{Q}_1^L,1,2\right] + A_f\left[Q_1^L,3,4,\bar{Q}_1^L,2,1\right] - A_f\left[Q_1^L,4,3,2,\bar{Q}_1^L,1\right]
\end{aligned}
\tag{D.8}
$$

and

```
RevID[Q[1,L],Qb[1,L],1,2,Q[2,L],3,4,Qb[2,L],A]
```

returning the identity

$$\begin{aligned} &A\left[Q_1^L,2,Q_2^L,3,4,\bar{Q}_2^L,\bar{Q}_1^L,1\right]+A\left[Q_1^L,Q_2^L,3,4,\bar{Q}_2^L,\bar{Q}_1^L,1,2\right]\\ &+A\left[Q_1^L,Q_2^L,3,4,\bar{Q}_2^L,\bar{Q}_1^L,2,1\right]-A\left[Q_1^L,\bar{Q}_2^R,4,3,Q_2^R,2,\bar{Q}_1^L,1\right]. \end{aligned} \tag{D.9}$$

`FFId[Amplitude,flip quark,loop quark]` gives the fermion flip identity eq. (2.75) for the one loop amplitude `Amplitude` where the flip quark gets flipped with respect to the loop quark. For example

```
FFId[A[Q[1,L],Qb[1,L],2,Q[2,R],Qb[2,R],1,Q[3,R],Qb[3, R]],Q[2,R],Q[1,
L]]
```

returns the linear combination

$$\begin{aligned} &A\left[Q_1^L,\bar{Q}_1^L,2,Q_2^R,1,Q_3^R,\bar{Q}_3^R,\bar{Q}_2^R\right]+A\left[Q_1^L,\bar{Q}_1^L,2,Q_2^R,1,\bar{Q}_2^R,Q_3^R,\bar{Q}_3^R\right]\\ &+A\left[Q_1^L,\bar{Q}_1^L,2,Q_2^R,\bar{Q}_2^R,1,Q_3^R,\bar{Q}_3^R\right]+A\left[Q_1^L,\bar{Q}_1^L,2,\bar{Q}_2^L,Q_2^L,1,Q_3^R,\bar{Q}_3^R\right]\\ &+A\left[Q_1^L,\bar{Q}_1^L,Q_2^R,1,2,Q_3^R,\bar{Q}_3^R,\bar{Q}_2^R\right]+A\left[Q_1^L,\bar{Q}_1^L,Q_2^R,1,2,\bar{Q}_2^R,Q_3^R,\bar{Q}_3^R\right]\\ &+A\left[Q_1^L,\bar{Q}_1^L,Q_2^R,1,Q_3^R,2,\bar{Q}_3^R,\bar{Q}_2^R\right]+A\left[Q_1^L,\bar{Q}_1^L,Q_2^R,1,Q_3^R,\bar{Q}_3^R,2,\bar{Q}_2^R\right]\\ &+A\left[Q_1^L,\bar{Q}_1^L,Q_2^R,2,1,Q_3^R,\bar{Q}_3^R,\bar{Q}_2^R\right]+A\left[Q_1^L,\bar{Q}_1^L,Q_2^R,2,1,\bar{Q}_2^R,Q_3^R,\bar{Q}_3^R\right]\\ &+A\left[Q_1^L,\bar{Q}_1^L,Q_2^R,2,\bar{Q}_2^R,1,Q_3^R,\bar{Q}_3^R\right], \end{aligned} \tag{D.10}$$

which equals zero. An alternative implementation of the fermion flip identity (2.75) is given by `FFId1[l1,a1,l2,a2]`, where `l1` is the loop quark line `l2` the flipped quark line and `a1`, `a2` lists of external legs, e. g. `FFId1[Q[1,L],Qb[1,L],2,Qb[2,L],Q[2,L],1,Q[3,R],Qb[3,R]]` reproduces the flip identity given above. `FFId2[l1,b1]` is an implementation of eq. (2.82). `l1` is the flipped fermion line and `b1` is a list of external legs. The output is canonicalized.

```
FFId2[{Q[1,L],Qb[1,L]},{2,Qb[2,L],Q[2,L]}]
```

will return the identity

$$\begin{aligned} &-A_f\left[Q_1^L,2,Q_2^R,\bar{Q}_2^R,\bar{Q}_1^L\right]+A_f\left[Q_1^L,2,\bar{Q}_2^L,Q_2^L,\bar{Q}_1^L\right]-A_f\left[Q_1^L,Q_2^R,\bar{Q}_2^R,2,\bar{Q}_1^L\right]\\ &+A_f\left[Q_1^L,\bar{Q}_2^L,Q_2^L,2,\bar{Q}_1^L\right]+2A_f\left[Q_1^L,\bar{Q}_2^L,Q_2^L,\bar{Q}_1^L,2\right] \end{aligned} \tag{D.11}$$

`FFId3[l1,a1,l2,a2]` is an implementation of a fermion flip identity eq. (2.83) that applies to the fermion loop primitives. The fermion line `l2` is flipped with respect to the fermion line `l1`. `a1` and `a2` are lists of external legs. The quark routing have to be such that the loop in `Af[l1,a1,l2,a2]` is in between `l1` and `l2`. The output is canonicalized.

```
FFId3[{Q[1,R],Qb[1,R]},{2},{Qb[2,L],Q[2,L]},{1,Q[3,R],Qb[3,R]}]
```

will return the identity

$$\begin{aligned}
&- A_f\left[Q_1^L, Q_2^L, 1, Q_3^R, \bar{Q}_3^R, \bar{Q}_2^L, \bar{Q}_1^L\right] - A_f\left[Q_1^L, \bar{Q}_2^L, \bar{Q}_3^L, Q_3^L, 1, Q_2^L, \bar{Q}_1^L\right] \\
&- A_f\left[Q_1^L, \bar{Q}_3^L, Q_3^L, 1, Q_2^R, \bar{Q}_2^R, \bar{Q}_1^L\right] - A_f\left[Q_1^L, \bar{Q}_3^L, Q_3^L, 1, \bar{Q}_2^L, Q_2^L, \bar{Q}_1^L\right] \\
&- A_f\left[Q_1^L, \bar{Q}_3^L, Q_3^L, \bar{Q}_2^L, 1, Q_2^L, \bar{Q}_1^L\right] .
\end{aligned} \tag{D.12}$$

`Furry[list]` gives the furry identity for a list of gluons and quark-lines. Gluons are specified by `{integer}`, and a quark line by lists of the form `{Q[i,R],...,Qb[i,R]}`, or `{Qb[i,L],...,Q[i,L]}`. The output is canonicalized.

```
Furry[{{Qb[1,L],Q[1,L]},{Q[2,R],2,Qb[2,R]},{1}}]
```

returns the identity

$$\begin{aligned}
&A_f\left[Q_1^L, 1, Q_2^R, 2, \bar{Q}_2^R, \bar{Q}_1^L\right] + A_f\left[Q_1^L, Q_2^R, 2, \bar{Q}_2^R, 1, \bar{Q}_1^L\right] - A_f\left[Q_1^L, \bar{Q}_2^L, 1, 2, Q_2^L, \bar{Q}_1^L\right] \\
&- A_f\left[Q_1^L, \bar{Q}_2^L, 2, 1, Q_2^L, \bar{Q}_1^L\right] + A_f\left[Q_1^L, \bar{Q}_2^L, 2, Q_2^L, \bar{Q}_1^L, 1\right] .
\end{aligned} \tag{D.13}$$

Appendix E

Explicit Gluon-Gluino Amplitudes

We present explicit expressions for color ordered gluon-gluino amplitudes of up to NNMHV degree and with up to six fermions which for a suitable choice of the gluino flavors ether directly give the QCD amplitudes or have to be linearly combined to give them in a special case with 6 quarks. The details of the map between amplitudes in $\mathcal{N} = 4$ SYM and QCD are described in section 3.3. We also introduce the `Mathematica` package GGT, which can generate analytical expressions for all color ordered QCD amplitudes with up to six quarks as well as analytical expressions for all SYM amplitudes relevant for QCD.

E.1. Explicit Formulae for Gluon Trees

Here we explicitly apply our formula (3.20) to the NMHV and NNMHV cases.

E.1.1. NMHV Amplitudes

Without loss of generality, we take the negative-helicity gluons to be at positions c_0, c_1, n with $c_0 < c_1$. In the NMHV case only one path in fig. 3.7 contributes and the path-matrix is a 2×2 matrix whose determinant we denote by $D^{c_0 c_1}_{n;a_1 b_1}$. Hence, the NMHV gluon amplitude is given by

$$A_n^{\text{NMHV}}(c_0^-, c_1^-, n^-) = \frac{\delta^{(4)}(p)}{\langle 1\ 2\rangle \dots \langle n\ 1\rangle} \sum_{2 \le a_1 < b_1 \le n-1} \tilde{R}_{n;a_1 b_1} \cdot \left(D^{c_0 c_1}_{n,a_1 b_1}\right)^4 \tag{E.1}$$

where the determinant of the path-matrix is given explicitly by

$$D^{ab}_{n,st} := \begin{vmatrix} \langle n\ a\rangle & \langle n\ b\rangle \\ (\Xi_n)^a_{st} & (\Xi_n)^b_{st} \end{vmatrix} \overset{a\le b}{=} \begin{cases} \langle n\ a\rangle\langle nts|b\rangle & a < s \le b < t\,, \\ \langle n\ a\rangle\langle b\ n\rangle x^2_{st} & a < s < t \le b\,, \\ \langle b\ a\rangle\langle nts|n\rangle & s \le a, b < t\,, \\ \langle n\ b\rangle\langle nst|a\rangle & s \le a < t \le b\,. \end{cases} \tag{E.2}$$

For $a > b$ one can use the antisymmetry of the determinant, $D^{ab}_{n,st} = -D^{ba}_{n,st}$. Equation (E.2) is exactly the result we already stated in eq. (3.3). This formula is implemented in `GGT` by `GGTnmhvgluon`.

E.1.2. N^{2}MHV Amplitudes

The negative-helicity gluons are taken to be a^-, b^-, c^-, n^- with $a < b < c$, without loss of generality. According to fig. 3.7 there are two contributing paths. Denoting the determinants of their corresponding path-matrices by D_1^{abc} and D_2^{abc}, the NNMHV gluon amplitude is given by

$$A_n^{\text{N}^2\text{MHV}}(a^-, b^-, c^-, n^-) = \frac{\delta^{(4)}(p)}{\langle 1\ 2\rangle \dots \langle n\ 1\rangle} \sum_{2 \le a_1 < b_1 < n} \tilde{R}_{n;a_1 b_1} \cdot \Bigg[\sum_{a_1+1 \le a_2 < b_2 \le b_1} \tilde{R}^{0;a_1 b_1}_{n;b_1 a_1;a_2 b_2} \cdot \left(D_1^{abc}\right)^4 + \sum_{b_1 \le a_2 < b_2 < n} \tilde{R}^{a_1 b_1;0}_{n;a_2 b_2} \cdot \left(D_2^{abc}\right)^4 \Bigg]. \tag{E.3}$$

The explicit forms of the determinants of the path-matrices

$$D_1^{abc}(n, a_1, b_1, a_2, b_2) := \begin{vmatrix} \langle n\ a\rangle & \langle n\ b\rangle & \langle n\ c\rangle \\ (\Xi_n)^a_{a_1 b_1} & (\Xi_n)^b_{a_1 b_1} & (\Xi_n)^c_{a_1 b_1} \\ (\Xi_n)^a_{b_1,a_1;a_2 b_2} & (\Xi_n)^b_{b_1,a_1;a_2 b_2} & (\Xi_n)^c_{b_1,a_1;a_2 b_2} \end{vmatrix} \tag{E.4}$$

and

$$D_2^{abc}(n, a_1, b_1, a_2, b_2) := \begin{vmatrix} \langle n\ a\rangle & \langle n\ b\rangle & \langle n\ c\rangle \\ (\Xi_n)^a_{a_1 b_1} & (\Xi_n)^b_{a_1 b_1} & (\Xi_n)^c_{a_1 b_1} \\ (\Xi_n)^a_{a_2 b_2} & (\Xi_n)^b_{a_2 b_2} & (\Xi_n)^c_{a_2 b_2} \end{vmatrix} \tag{E.5}$$

are given by

$$D_1^{abc} = \begin{cases} \langle a\ n\rangle\langle nb_1a_1|b\rangle\langle nb_1a_1b_2a_2|c\rangle & a<a_1\le b,c<b_1 \quad b<a_2\le c<b_2 \\ \langle n\ a\rangle\langle nb_1a_1|b\rangle\langle nb_1a_1|c\rangle x_{a_2b_2}^2 & a<a_1\le b,c<b_1 \quad b<a_2,b_2\le c \\ \langle a\ n\rangle\langle b\ c\rangle\langle nb_1a_1a_2b_2|nb_1a_1\rangle & a<a_1\le b,c<b_1 \quad a_2\le b,c<b_2 \\ \langle a\ n\rangle\langle nb_1a_1|c\rangle\langle nb_1a_1a_2b_2|b\rangle & a<a_1\le b,c<b_1 \quad a_2\le b<b_2\le c \\ \langle n\ a\rangle\langle c\ n\rangle\langle nb_1a_1|b\rangle x_{a_1b_1}^2 x_{a_2b_2}^2 & a<a_1\le b<b_1\le c \quad b<a_2,b_2\le c \\ \langle n\ a\rangle\langle n\ c\rangle x_{a_1b_1}^2\langle nb_1a_1a_2b_2|b\rangle & a<a_1\le b<b_1\le c \quad a_2\le b<b_2 \\ \langle a\ b\rangle\langle nb_1a_1|n\rangle\langle nb_1a_1b_2a_2|c\rangle & a_1\le a,b,c<b_1 \quad b<a_2\le c<b_2 \\ \langle c\ b\rangle\langle nb_1a_1|n\rangle\langle nb_1a_1b_2a_2|a\rangle & a_1\le a,b,c<b_1 \quad a<a_2\le b,c<b_2 \\ \langle b\ a\rangle\langle nb_1a_1|n\rangle\langle nb_1a_1|c\rangle x_{a_2b_2}^2 & a_1\le a,b,c<b_1 \quad b<a_2,b_2\le c \\ \langle nb_1a_1|n\rangle\,(x_{a_2b_2}^2\langle nb_1a_1|a\rangle\langle b\ c\rangle & a_1\le a,b,c<b_1 \quad a<a_2\le b<b_2\le c \\ \qquad +\langle nb_1a_1a_2b_2|b\rangle\langle a\ c\rangle) & \\ \langle a\ b\rangle\langle nb_1a_1|n\rangle\langle nb_1a_1a_2b_2|c\rangle & a_1\le a,b,c<b_1 \quad a_2\le a,b<b_2\le c \\ \langle c\ b\rangle\langle nb_1a_1|n\rangle\langle nb_1a_1a_2b_2|a\rangle & a_1\le a,b,c<b_1 \quad a_2\le a<b_2\le b \\ \langle b\ c\rangle\langle nb_1a_1|a\rangle\langle nb_1a_1|n\rangle x_{a_2b_2} & a_1\le a,b,c<b_1 \quad a_2\le a<b_2\le b \\ \langle c\ n\rangle\langle a\ b\rangle\langle na_1|nb_1\rangle x_{a_1b_1}^2 x_{a_2b_2}^2 & a_1\le a,b<b_1\le c \quad b<a_2,b_2\le b_1 \\ \langle c\ n\rangle\,(x_{a_2b_2}^2\langle nb_1a_1|a\rangle\langle na_1b_1|b\rangle & a_1\le a,b<b_1\le c \quad a<a_2\le b<b_2 \\ \qquad +\langle na_1b_1|a\rangle\langle nb_1a_1a_2b_2|b\rangle) & \\ \langle n\ c\rangle\langle a\ b\rangle\langle nb_1a_1a_2b_2|na_1b_1\rangle & a_1\le a,b<b_1\le c \quad a_2\le a,b<b_2 \\ \langle c\ n\rangle\langle nb_1a_1|a\rangle\langle na_1b_1|b\rangle x_{a_2b_2}^2 & a_1\le a,b<b_1\le c \quad a<a_2,b_2\le b \\ \langle n\ c\rangle\langle na_1b_1|b\rangle\langle nb_1a_1a_2b_2|a\rangle & a_1\le a,b<b_1\le c \quad a_2\le a<b_2\le b \end{cases} \tag{E.6}$$

for $1<a_1<a_2<b_2\le b_1<n$ and

$$D_2^{abc} = \begin{cases} \langle n\ a\rangle\langle nb_1a_1|b\rangle\langle nb_2a_2|c\rangle & a<a_1\le b<b_1\le c \quad a_2\le c<b_2 \\ \langle n\ a\rangle\langle c\ n\rangle\langle nb_1a_1|b\rangle x_{a_2b_2}^2 & a<a_1\le b<b_1\le c \quad b_2\le c \\ \langle n\ a\rangle\langle b\ n\rangle\langle nb_2a_2|c\rangle x_{a_1b_1}^2 & a<a_1,b_1\le b \quad b<a_2\le c<b_2 \\ \langle n\ a\rangle\langle b\ n\rangle\langle n\ c\rangle x_{a_1b_1}^2 x_{a_2b_2}^2 & a<a_1,b_1\le b \quad b<a_2,b_2\le c \\ \langle n\ a\rangle\langle b\ c\rangle\langle nb_2a_2|n\rangle x_{a_1b_1}^2 & a<a_1,b_1\le b \quad a_2\le b,c<b_2 \\ \langle n\ a\rangle\langle c\ n\rangle\langle nb_2a_2|b\rangle x_{a_1b_1}^2 & a<a_1,b_1\le b \quad a_2\le b<b_2\le c \\ \langle a\ b\rangle\langle na_1b_1|n\rangle\langle nb_2a_2|c\rangle & a_1\le a,b<b_1\le c \quad a_2\le c<b_2 \\ \langle c\ n\rangle\langle a\ b\rangle\langle na_1b_1|n\rangle x_{a_2b_2}^2 & a_1\le a,b<b_1\le c \quad b_2\le c \\ \langle n\ b\rangle\langle na_1b_1|a\rangle\langle nb_2a_2|c\rangle & a_1\le a<b_1\le b \quad b<a_2\le c<b_2 \\ \langle n\ b\rangle\langle c\ n\rangle\langle na_1b_1|a\rangle x_{a_2b_2}^2 & a_1\le a<b_1\le b \quad b<a_2,b_2\le c \\ \langle c\ b\rangle\langle na_1b_1|a\rangle\langle nb_2a_2|n\rangle & a_1\le a<b_1\le b \quad a_2\le b,c<b_2 \\ \langle n\ c\rangle\langle na_1b_1|a\rangle\langle na_2b_2|b\rangle & a_1\le a<b_1\le b \quad a_2\le b<b_2\le c \end{cases} \tag{E.7}$$

for $1<a_1<b_1\le a_2<b_2<n$. For other orderings of a,b,c one can use the total antisymmetry of D_1^{abc} and D_2^{abc} under permutations of a,b,c. It is quite astonishing that in 28 out of 30 cases these determinants are given by a single term. This formula is implemented in `GGT` by `GGTnnmhvgluon`.

E.2. Explicit Formulae for Trees with Fermions

Here we explicitly write out our formulas (3.35) and (3.43) for the MHV, NMHV and NNMHV cases with up to six fermions.

E.2.1. MHV Amplitudes

The simplest amplitudes involving fermions are the MHV amplitudes. The amplitudes with one negative-helicity gluon at position a and two fermions of opposite helicity and the same flavor, are given by

$$A_n(a^-, b_q, c_{\bar{q}}) = \delta^{(4)}(p)\frac{\langle a\ c\rangle^3\langle a\ b\rangle}{\langle 1\ 2\rangle\dots\langle n\ 1\rangle}\,, \tag{E.8}$$

$$A_n(a^-, b_{\bar{q}}, c_q) = -\delta^{(4)}(p)\frac{\langle a\ b\rangle^3\langle a\ c\rangle}{\langle 1\ 2\rangle\dots\langle n\ 1\rangle}\,. \tag{E.9}$$

These formulae correspond to case (1) in fig. 3.4. We note that the latter formula is related to the former one by a reflection symmetry, under which the cyclic ordering is reversed and there is a relabeling $b \leftrightarrow c$. In the NMHV case we will omit formulae that can be obtained from the presented formulae by a reflection symmetry.

An equally compact formula can be obtained for the MHV amplitudes with four fermions and only positive-helicity gluons:

$$A_n(a_{q_A}, b_{\bar{q}_B}, c_{q_C}, d_{\bar{q}_D}) = \frac{\delta^{(4)}(p)\langle b\ d\rangle^2}{\langle 1\ 2\rangle\dots\langle n\ 1\rangle}\left(\delta^{AB}\delta^{CD}\langle d\ a\rangle\langle c\ b\rangle - \delta^{AD}\delta^{BC}\langle d\ c\rangle\langle a\ b\rangle\right)\,, \tag{E.10}$$

$$A_n(a_{q_A}, b_{q_B}, c_{\bar{q}_C}, d_{\bar{q}_D}) = \frac{\delta^{(4)}(p)\langle c\ d\rangle^2}{\langle 1\ 2\rangle\dots\langle n\ 1\rangle}\left(\delta^{AD}\delta^{BC}\langle d\ b\rangle\langle a\ c\rangle - \delta^{AC}\delta^{BD}\langle d\ a\rangle\langle b\ c\rangle\right)\,, \tag{E.11}$$

which in the single-flavor case simplifies to

$$A_n(a_q, b_{\bar{q}}, c_q, d_{\bar{q}}) = \frac{\delta^{(4)}(p)\langle b\ d\rangle^3\langle a\ c\rangle}{\langle 1\ 2\rangle\dots\langle n\ 1\rangle}\,, \tag{E.12}$$

$$A_n(a_q, b_q, c_{\bar{q}}, d_{\bar{q}}) = -\frac{\delta^{(4)}(p)\langle c\ d\rangle^3\langle a\ b\rangle}{\langle 1\ 2\rangle\dots\langle n\ 1\rangle}\,. \tag{E.13}$$

Equation (E.13) corresponds to case (2a) in fig. 3.4, whereas eq. (E.10) for $A = B \neq C = D$ corresponds to case (2b).

To complete the list of MHV amplitudes with up to four fermions we also give the MHV amplitude with four positive-helicity fermions and one negative-helicity gluon:

$$\begin{aligned} A_n(a_{\psi_A}, b_{\psi_B}, c_{\psi_C}, d_{\psi_D}, n^-) &= \int d\eta_a^A \int d\eta_b^B \int d\eta_c^C \int d\eta_d^D \int d^4\eta_n\, \mathcal{A}_n^{\mathrm{MHV}} \\ &= \frac{\delta^{(4)}(p)\epsilon^{ABCD}}{\langle 1\ 2\rangle\dots\langle n\ 1\rangle}\langle n\ a\rangle\langle n\ b\rangle\langle n\ c\rangle\langle n\ d\rangle\,. \end{aligned} \tag{E.14}$$

This amplitude is not needed for QCD.

E.2.2. NMHV Amplitudes

Two Fermions

To illustrate the use of our master formula (3.35) we compute the NMHV amplitude with two opposite-helicity fermions at positions a, $\bar{b}$ and two negative-helicity gluons at positions c and n. At this stage we leave the color order arbitrary. Starting with the path-matrix

$$\Xi^{\text{path}} = \begin{pmatrix} \langle n\ c\rangle & \langle n\ a\rangle & \langle n\ \bar{b}\rangle \\ (\Xi_n)^c_{st} & (\Xi_n)^a_{st} & (\Xi_n)^{\bar{b}}_{st} \end{pmatrix} \tag{E.15}$$

we can immediately write down the amplitude

$$(A_n)^{\text{NMHV}}_{q\bar{q}} = \frac{\delta^{(4)}(p)\,\text{sign}(\tau)}{\langle 1\ 2\rangle \ldots \langle n\ 1\rangle} \sum_{1<s<t<n} \tilde{R}_{n;st} D^{ca}_{n;st} \left(D^{c\bar{b}}_{n;st}\right)^3 , \tag{E.16}$$

where the 2×2 determinant $D^{ab}_{n;st}$ has been defined in eq. (E.2). As already stated, the last equation holds for an arbitrary color ordering. In the following we take $a<b<c$ and specify the color ordering:

$$\begin{aligned} A_n(a_q, b^-, c_{\bar{q}}, n^-) = \frac{\delta^{(4)}(p)}{\langle 1\ 2\rangle \ldots \langle n\ 1\rangle} \Bigg[& - \langle a\ b\rangle \langle b\ c\rangle^3 \sum_{1<s\le a,b,c<t<n} \langle nts|n\rangle^4 \tilde{R}_{n,st} \\ & - \langle b\ c\rangle^3 \langle a\ n\rangle \sum_{a<s\le b,c<t<n} \langle nts|b\rangle \langle nts|n\rangle^3 \tilde{R}_{n,st} \\ & - \langle c\ n\rangle^3 \langle a\ n\rangle \sum_{a<s\le b<t\le c} \langle nst|b\rangle^3 \langle nts|b\rangle \tilde{R}_{n,st} \\ & - \langle c\ n\rangle^3 \langle a\ b\rangle \sum_{1<s\le a,b<t\le c} \langle nst|b\rangle^3 \langle nts|n\rangle \tilde{R}_{n,st} \Bigg] , \end{aligned} \tag{E.17}$$

$$\begin{aligned} A_n(a_q, b_{\bar{q}}, c^-, n^-) = \frac{\delta^{(4)}(p)}{\langle 1\ 2\rangle \ldots \langle n\ 1\rangle} \Bigg[& + \langle a\ c\rangle \langle b\ c\rangle^3 \sum_{1<s\le a,b,c<t<n} \langle nts|n\rangle^4 \tilde{R}_{n,st} \\ & + \langle a\ n\rangle \langle b\ n\rangle^3 \sum_{b<s\le c<t<n} \langle nts|c\rangle^4 \tilde{R}_{n,st} \\ & + \langle n\ c\rangle^4 \langle a\ n\rangle \langle b\ n\rangle^3 \sum_{b<s<t\le c} (x^2_{st})^4 \tilde{R}_{n,st} \\ & + \langle c\ n\rangle^4 \sum_{1<s\le a,b<t\le c} \langle nst|b\rangle^3 \langle nst|a\rangle \tilde{R}_{n,st} \\ & + \langle b\ c\rangle^3 \langle a\ n\rangle \sum_{a<s\le b,c<t<n} \langle nts|c\rangle \langle nts|n\rangle^3 \tilde{R}_{n,st} \\ & + \langle c\ n\rangle^4 \langle a\ n\rangle \sum_{a<s\le b<t\le c} x^2_{st} \langle nst|b\rangle^3 \tilde{R}_{n,st} \Bigg] . \end{aligned} \tag{E.18}$$

These simplified expressions are implemented in `GGT` by `GGTnmhv2ferm` (see appendix E.3).

Four Fermions

We proceed with the NMHV amplitude with four fermions at positions $a_1^{A_1}, a_2^{A_2}, \bar{b}_1^{B_1}, \bar{b}_2^{B_2}$ and one negative-helicity gluon. Without loss of generality we put the negative-helicity gluon at position n. Again we leave the color ordering arbitrary. A straightforward application of our formulas (3.43) and (3.35) yields

$$(A_n)^{\text{NMHV}}_{(\psi\bar{\psi})^2} = \frac{\delta^{(4)}(p)\,\text{sign}(\tau)}{\langle 1\,2\rangle \ldots \langle n\,1\rangle} \sum_{1<s<t<n} \tilde{R}_{n;st} \left(D^{\bar{b}_1\bar{b}_2}_{n;st}\right)^2 \left(\begin{array}{r} \delta^{A_1B_1}\delta^{A_2B_2} D^{a_1\bar{b}_2}_{n;st} D^{\bar{b}_1 a_2}_{n;st} \\ - \delta^{A_1B_2}\delta^{A_2B_1} D^{a_2\bar{b}_2}_{n;st} D^{\bar{b}_1 a_1}_{n;st} \end{array} \right) \tag{E.19}$$

in the $\mathcal{N}=4$ super Yang-Mills case, and

$$(A_n)^{\text{NMHV}}_{(q\bar{q})^2} = \frac{\delta^{(4)}(p)\,\text{sign}(\tau)}{\langle 1\,2\rangle \ldots \langle n\,1\rangle} \sum_{1<s<t<n} \tilde{R}_{n;st} \left(D^{\bar{b}_1\bar{b}_2}_{n;st}\right)^3 D^{a_1 a_2}_{n;st} \tag{E.20}$$

for single-flavor QCD, with $D^{ab}_{n;st}$ defined in equation (E.2). Taking $a<b<c<d$ we now specify the color ordering,

$$\begin{aligned} A_n(a_{\psi_A}, b_{\psi_B}, c_{\bar{\psi}_C}, d_{\bar{\psi}_D}, n^-) &= \frac{\delta^{(4)}(p)}{\langle 1\,2\rangle \ldots \langle n\,1\rangle} \times \\ \times \Bigg[&+ \delta^{AC}\delta^{BD}\langle a\,n\rangle\langle b\,c\rangle\langle c\,d\rangle^2 \sum_{a<s\le b, d<t<n} \langle nts|d\rangle\langle nts|n\rangle^3 \tilde{R}_{n,st} - (c \leftrightarrow d) \\ &+ \delta^{AC}\delta^{BD}\langle a\,d\rangle\langle b\,c\rangle\langle d\,c\rangle^2 \sum_{1<s\le a, d<t<n} \langle nts|n\rangle^4 \tilde{R}_{n,st} - (a \leftrightarrow b) \\ &+ \delta^{AC}\delta^{BD}\langle n\,a\rangle\langle b\,c\rangle\langle d\,n\rangle^3 \sum_{a<s\le b, c<t\le d} x_{st}^2 \langle nst|n\rangle\langle nst|c\rangle^2 \tilde{R}_{n,st} \\ &- \delta^{AD}\delta^{BC}\langle a\,n\rangle\langle d\,n\rangle^3 \sum_{a<s\le b, c<t\le d} \langle nts|c\rangle\langle nst|b\rangle\langle nst|c\rangle^2 \tilde{R}_{n,st} \\ &+ \delta^{AC}\delta^{BD}\langle b\,c\rangle\langle d\,n\rangle^3 \sum_{1<s\le a, c<t\le d} \langle nst|a\rangle\langle nts|n\rangle\langle nst|c\rangle^2 \tilde{R}_{n,st} - (a \leftrightarrow b) \Bigg], \end{aligned} \tag{E.21}$$

where "$(c \leftrightarrow d)$" implies the substitution $c \leftrightarrow d$ in the arguments of the spinor strings, as well as the corresponding substitution $C \leftrightarrow D$ in the arguments of the δ functions, but *no* change in the summation range. The other inequivalent orderings of quarks and anti-quarks are,

$$\begin{aligned} A_n(a_{q_A}, b_{\bar{q}_B}, c_{q_C}, d_{\bar{q}_D}, n^-) &= \frac{\delta^{(4)}(p)}{\langle 1\,2\rangle \ldots \langle n\,1\rangle} \times \\ \times \Bigg[&+ \delta^{AB}\delta^{CD}\langle a\,n\rangle\langle b\,n\rangle^3 \sum_{b<s\le c, d<t<n} \langle nts|c\rangle\langle nts|d\rangle^3 \tilde{R}_{n,st} \\ &+ \delta^{AB}\delta^{CD}\langle n\,a\rangle\langle c\,b\rangle\langle b\,d\rangle^2 \sum_{a<s\le b, d<t<n} \langle nts|d\rangle\langle nts|n\rangle^3 \tilde{R}_{n,st} - (b \leftrightarrow d) \end{aligned}$$

$$
\begin{aligned}
&+ \delta^{AB}\delta^{CD}\langle a\ d\rangle\langle b\ c\rangle\langle d\ b\rangle^2 \sum_{1<s\le a,d<t<n} \langle nts|n\rangle^4 \tilde{R}_{n,st} - (a \leftrightarrow c) \\
&+ \delta^{AB}\delta^{CD}\langle n\ a\rangle\langle d\ n\rangle^3\langle n\ b\rangle^3 \sum_{b<s\le c<t\le d} \langle nts|c\rangle (x_{st}^2)^3 \tilde{R}_{n,st} \\
&+ \delta^{AB}\delta^{CD}\langle n\ a\rangle\langle n\ c\rangle\langle n\ b\rangle^3\langle n\ d\rangle^3 \sum_{b<s<t\le c} (x_{st}^2)^4 \tilde{R}_{n,st} \\
&+ \delta^{AB}\delta^{CD}\langle n\ a\rangle\langle b\ c\rangle\langle d\ n\rangle^3 \sum_{a<s\le b,c<t\le d} x_{st}^2 \langle nst|n\rangle\langle nst|b\rangle^2 \tilde{R}_{n,st} \\
&\quad - \delta^{AD}\delta^{CB}\langle n\ a\rangle\langle d\ n\rangle^3 \sum_{a<s\le b,c<t\le d} \langle nts|b\rangle\langle nst|c\rangle\langle nst|b\rangle^2 \tilde{R}_{n,st} \\
&+ \delta^{AB}\delta^{CD}\langle n\ a\rangle\langle n\ c\rangle\langle d\ n\rangle^3 \sum_{a<s\le b<t\le c} x_{st}^2 \langle nst|b\rangle^3 \tilde{R}_{n,st} \\
&+ \delta^{AB}\delta^{CD}\langle b\ c\rangle\langle d\ n\rangle^3 \sum_{1<s\le a,c<t\le d} \langle nst|a\rangle\langle nts|n\rangle\langle nst|b\rangle^2 \tilde{R}_{n,st} - (a\ \leftrightarrow c) \\
&+ \delta^{AB}\delta^{CD}\langle n\ c\rangle\langle n\ d\rangle^3 \sum_{1<s\le a,b<t\le c} \langle nst|a\rangle\langle nst|b\rangle^3 \tilde{R}_{n,st} \Bigg],
\end{aligned}
\tag{E.22}
$$

$$
\begin{aligned}
A_n(a_{\psi_A}, b_{\bar{\psi}_B}, c_{\bar{\psi}_C}, d_{\psi_D}, n^-) = &-\frac{\delta^{(4)}(p)}{\langle 1\ 2\rangle \dots \langle n\ 1\rangle} \times \\
\times \Bigg[&+ \delta^{AB}\delta^{CD}\langle a\ n\rangle\langle b\ n\rangle^3 \sum_{b<s\le c,d<t<n} \langle nts|d\rangle\langle nts|c\rangle^3 \tilde{R}_{n,st} \\
&+ \delta^{AB}\delta^{CD}\langle n\ a\rangle\langle n\ d\rangle\langle b\ n\rangle^3 \sum_{b<s\le c<t\le d} x_{st}^2 \langle nts|c\rangle^3 \tilde{R}_{n,st} \\
&+ \delta^{AB}\delta^{CD}\langle n\ a\rangle\langle d\ b\rangle\langle b\ c\rangle^2 \sum_{a<s\le b,d<t<n} \langle nts|c\rangle\langle nts|n\rangle^3 \tilde{R}_{n,st} - (b \leftrightarrow c) \\
&+ \delta^{AB}\delta^{CD}\langle n\ a\rangle\langle n\ d\rangle\langle b\ c\rangle^2 \sum_{a<s\le b,c<t\le d} \langle nts|c\rangle\langle nst|b\rangle\langle nts|n\rangle^2 \tilde{R}_{n,st} - (b \leftrightarrow c) \\
&+ \delta^{AB}\delta^{CD}\langle a\ c\rangle\langle b\ d\rangle\langle c\ b\rangle^2 \sum_{1<s\le a,d<t<n} \langle nts|n\rangle^4 \tilde{R}_{n,st} - (a \leftrightarrow d) \\
&+ \delta^{AB}\delta^{CD}\langle a\ c\rangle\langle n\ d\rangle\langle c\ b\rangle^2 \sum_{1<s\le a,c<t\le d} \langle nst|b\rangle\langle nst|n\rangle^3 \tilde{R}_{n,st} - (b \leftrightarrow c) \\
&+ \delta^{AB}\delta^{CD}\langle n\ a\rangle\langle n\ d\rangle\langle n\ b\rangle^3\langle n\ c\rangle^3 \sum_{b<s<t\le c} (x_{st}^2)^4 \tilde{R}_{n,st} \\
&+ \delta^{AB}\delta^{CD}\langle n\ a\rangle\langle n\ d\rangle\langle c\ n\rangle^3 \sum_{a<s\le b<t\le c} x_{st}^2 \langle nst|b\rangle^3 \tilde{R}_{n,st} \\
&+ \delta^{AB}\delta^{CD}\langle n\ d\rangle\langle n\ c\rangle^3 \sum_{1<s\le a,b<t\le c} \langle nst|a\rangle\langle nst|b\rangle^3 \tilde{R}_{n,st} \Bigg],
\end{aligned}
\tag{E.23}
$$

$$
\begin{aligned}
A_n(a_{\bar\psi_A}, b_{\psi_B}, c_{\psi_C}, d_{\bar\psi_D}, n^-) = &-\frac{\delta^{(4)}(p)}{\langle 1\,2\rangle\ldots\langle n\,1\rangle}\times \\
\times\Bigg[&+\delta^{AB}\delta^{CD}\langle b\,n\rangle\langle a\,n\rangle^3 \sum_{b<s\le c,d<t<n} \langle nts|c\rangle\langle nts|d\rangle^3 \tilde R_{n,st} \\
&+\delta^{AB}\delta^{CD}\langle b\,d\rangle\langle a\,n\rangle^3 \sum_{a<s\le b,d<t<n} \langle nts|n\rangle\langle nts|c\rangle\langle nts|d\rangle^2 \tilde R_{n,st} - (b\leftrightarrow c) \\
&+\delta^{AB}\delta^{CD}\langle b\,d\rangle\langle a\,c\rangle\langle d\,a\rangle^2 \sum_{1<s\le a,d<t<n} \langle nts|n\rangle^4 \tilde R_{n,st} - (b\leftrightarrow c) \\
&+\delta^{AB}\delta^{CD}\langle n\,b\rangle\langle d\,n\rangle^3\langle n\,a\rangle^3 \sum_{b<s\le c<t\le d} \langle nts|c\rangle (x_{st}^2)^3 \tilde R_{n,st} \\
&+\delta^{AB}\delta^{CD}\langle n\,b\rangle\langle n\,c\rangle\langle n\,a\rangle^3\langle n\,d\rangle^3 \sum_{b<s<t\le c} (x_{st}^2)^4 \tilde R_{n,st} \\
&+\delta^{AB}\delta^{CD}\langle n\,a\rangle^3\langle n\,d\rangle^3 \sum_{a<s\le b,c<t\le d} \langle nst|b\rangle\langle nts|c\rangle (x_{st}^2)^2 \tilde R_{n,st} - (b\ \leftrightarrow c) \\
&+\delta^{AB}\delta^{CD}\langle n\,c\rangle\langle d\,n\rangle^3\langle n\,a\rangle^3 \sum_{a<s\le b<t\le c} \langle nst|b\rangle (x_{st}^2)^3 \tilde R_{n,st} \\
&+\delta^{AB}\delta^{CD}\langle a\,c\rangle\langle d\,n\rangle^3 \sum_{1<s\le a,c<t\le d} \langle nst|b\rangle\langle nts|n\rangle\langle nst|a\rangle^2 \tilde R_{n,st} - (b\ \leftrightarrow c) \\
&+\delta^{AB}\delta^{CD}\langle n\,c\rangle\langle n\,d\rangle^3 \sum_{1<s\le a,b<t\le c} \langle nst|b\rangle\langle nst|a\rangle^3 \tilde R_{n,st}\Bigg].
\end{aligned}
\tag{E.24}
$$

For $A \neq B$, and all fermions cyclically adjacent we have

$$
\begin{aligned}
A_n(a_{q_A}, (a{+}1)_{\bar q_B}, (a{+}2)_{q_B}, (a{+}3)_{\bar q_A}, n^-) = &\frac{\delta^{(4)}(p)}{\langle 1\,2\rangle\ldots\langle n\,1\rangle}\times \\
\Bigg[&\langle a\,n\rangle\langle a{+}2\ a{+}3\rangle\langle a{+}1\ a{+}3\rangle^2 \sum_{a+3<t<n} \langle nta{+}2|a{+}1\rangle\langle nta{+}1|n\rangle^3 \tilde R_{n,a+1t} \\
&+\langle a{+}2\ a{+}3\rangle\langle a\ a{+}1\rangle\langle a{+}1\ a{+}3\rangle^2 \sum_{1<s\le a,a+3<t<n} \langle nts|n\rangle^4 \tilde R_{n,st} \\
&+\langle a\,n\rangle\langle a{+}3\,n\rangle^3\langle a{+}1\ a{+}2\rangle^4 \langle n|x_{n\,a+3}|a{+}2]\langle n|x_{n\,a+1}|a{+}1]\langle n|x_{n\,a+1}|a{+}2]^2 \tilde R_{n,a+1a+3} \\
&-\langle a\ a{+}1\rangle\langle a{+}3\,n\rangle^3 \sum_{1<s\le a} \langle nsa{+}3|a{+}2\rangle\langle nsa{+}3|n\rangle\langle nsa{+}3|a{+}1\rangle^2 \tilde R_{n,sa+3}\Bigg].
\end{aligned}
\tag{E.25}
$$

This amplitude may be used to generate the NMHV amplitudes for $Vq\bar qg\ldots g$, as discussed in section 3.

In the single-flavor case we obtain

$$
\begin{aligned}
A_n(a_q, b_q, c_{\bar q}, d_{\bar q}, n^-) = \frac{\delta^{(4)}(p)}{\langle 1\,2\rangle\ldots\langle n\,1\rangle}\Bigg[&+\langle n\,a\rangle\langle c\,d\rangle^3 \sum_{a<s\le b,d<t<n} \langle nts|b\rangle\langle nts|n\rangle^3 \tilde R_{n,st} \\
&+\langle a\,b\rangle\langle d\,c\rangle^3 \sum_{1<s\le a,d<t<n} \langle nts|n\rangle^4 \tilde R_{n,st}
\end{aligned}
$$

$$
\begin{aligned}
&+ \langle n\ a\rangle\langle d\ n\rangle^3 \sum_{a<s\leq b,c<t\leq d} \langle nts|b\rangle\langle nst|c\rangle^3 \tilde{R}_{n,st} \\
&+ \langle b\ a\rangle\langle d\ n\rangle^3 \sum_{1<s\leq a,c<t\leq d} \langle nts|n\rangle\langle nst|c\rangle^3 \tilde{R}_{n,st}\Bigg],
\end{aligned}
\tag{E.26}
$$

$$
\begin{aligned}
A_n(a_q, b_{\bar{q}}, c_q, d_{\bar{q}}, n^-) = \frac{\delta^{(4)}(p)}{\langle 1\ 2\rangle \dots \langle n\ 1\rangle}\Bigg[&+ \langle a\ n\rangle\langle b\ n\rangle^3 \sum_{b<s\leq c,d<t<n} \langle nts|c\rangle\langle nts|d\rangle^3 \tilde{R}_{n,st} \\
&+ \langle n\ a\rangle\langle d\ b\rangle^3 \sum_{a<s\leq b,d<t<n} \langle nts|c\rangle\langle nts|n\rangle^3 \tilde{R}_{n,st} \\
&+ \langle a\ c\rangle\langle b\ d\rangle^3 \sum_{1<s\leq a,d<t<n} \langle nts|n\rangle^4 \tilde{R}_{n,st} \\
&+ \langle n\ a\rangle\langle d\ n\rangle^3\langle n\ b\rangle^3 \sum_{b<s\leq c<t\leq d} \langle nts|c\rangle (x_{st}^2)^3 \tilde{R}_{n,st} \\
&+ \langle n\ a\rangle\langle n\ c\rangle\langle n\ b\rangle^3\langle n\ d\rangle^3 \sum_{b<s<t\leq c} (x_{st}^2)^4 \tilde{R}_{n,st} \\
&+ \langle n\ a\rangle\langle n\ d\rangle^3 \sum_{a<s\leq b,c<t\leq d} \langle nts|c\rangle\langle nst|b\rangle^3 \tilde{R}_{n,st} \\
&+ \langle n\ a\rangle\langle n\ c\rangle\langle d\ n\rangle^3 \sum_{a<s\leq b<t\leq c} x_{st}^2 \langle nst|b\rangle^3 \tilde{R}_{n,st} \\
&+ \langle a\ c\rangle\langle d\ n\rangle^3 \sum_{1<s\leq a,c<t\leq d} \langle nts|n\rangle\langle nst|b\rangle^3 \tilde{R}_{n,st} \\
&+ \langle n\ c\rangle\langle n\ d\rangle^3 \sum_{1<s\leq a,b<t\leq c} \langle nst|a\rangle\langle nst|b\rangle^3 \tilde{R}_{n,st}\Bigg],
\end{aligned}
\tag{E.27}
$$

$$
\begin{aligned}
A_n(a_q, b_{\bar{q}}, c_{\bar{q}}, d_q, n^-) = -\frac{\delta^{(4)}(p)}{\langle 1\ 2\rangle \dots \langle n\ 1\rangle}\Bigg[&+ \langle a\ n\rangle\langle b\ n\rangle^3 \sum_{b<s\leq c,d<t<n} \langle nts|d\rangle\langle nts|c\rangle^3 \tilde{R}_{n,st} \\
&+ \langle n\ a\rangle\langle n\ d\rangle\langle b\ n\rangle^3 \sum_{b<s\leq c<t\leq d} x_{st}^2 \langle nts|c\rangle^3 \tilde{R}_{n,st} \\
&+ \langle n\ a\rangle\langle c\ b\rangle^3 \sum_{a<s\leq b,d<t<n} \langle nts|d\rangle\langle nts|n\rangle^3 \tilde{R}_{n,st} \\
&+ \langle n\ a\rangle\langle n\ d\rangle\langle b\ c\rangle^3 \sum_{a<s\leq b,c<t\leq d} x_{st}^2 \langle nts|n\rangle^3 \tilde{R}_{n,st} \\
&+ \langle a\ d\rangle\langle b\ c\rangle^3 \sum_{1<s\leq a,d<t<n} \langle nts|n\rangle^4 \tilde{R}_{n,st} \\
&+ \langle b\ c\rangle^3\langle n\ d\rangle \sum_{1<s\leq a,c<t\leq d} \langle nst|a\rangle\langle nst|n\rangle^3 \tilde{R}_{n,st}
\end{aligned}
$$

$$
\begin{aligned}
&+ \langle n\ a\rangle\langle n\ d\rangle\langle n\ b\rangle^3\langle n\ c\rangle^3 \sum_{b<s<t\le c} (x_{st}^2)^4 \tilde{R}_{n,st} \\
&+ \langle n\ a\rangle\langle n\ d\rangle\langle c\ n\rangle^3 \sum_{a<s\le b<t\le c} x_{st}^2 \langle nst|b\rangle^3 \tilde{R}_{n,st} \\
&+ \langle n\ d\rangle\langle n\ c\rangle^3 \sum_{1<s\le a,b<t\le c} \langle nst|a\rangle\langle nst|b\rangle^3 \tilde{R}_{n,st} \Bigg],
\end{aligned}
\tag{E.28}
$$

$$
\begin{aligned}
A_n(a_{\bar{q}}, b_q, c_q, d_{\bar{q}}, n^-) = \frac{-\delta^{(4)}(p)}{\langle 1\ 2\rangle \ldots \langle n\ 1\rangle} \Bigg[&+ \langle b\ n\rangle\langle a\ n\rangle^3 \sum_{b<s\le c,d<t<n} \langle nts|c\rangle\langle nts|d\rangle^3 \tilde{R}_{n,st} \\
&+ \langle b\ c\rangle\langle a\ n\rangle^3 \sum_{a<s\le b,d<t<n} \langle nts|n\rangle\langle nts|d\rangle^3 \tilde{R}_{n,st} \\
&+ \langle b\ c\rangle\langle a\ d\rangle^3 \sum_{1<s\le a,d<t<n} \langle nts|n\rangle^4 \tilde{R}_{n,st} \\
&+ \langle n\ b\rangle\langle d\ n\rangle^3\langle n\ a\rangle^3 \sum_{b<s\le c<t\le d} \langle nts|c\rangle (x_{st}^2)^3 \tilde{R}_{n,st} \\
&+ \langle n\ b\rangle\langle n\ c\rangle\langle n\ a\rangle^3\langle n\ d\rangle^3 \sum_{b<s<t\le c} (x_{st}^2)^4 \tilde{R}_{n,st} \\
&+ \langle n\ a\rangle^3\langle n\ d\rangle^3\langle b\ c\rangle \sum_{a<s\le b,c<t\le d} \langle nts|n\rangle (x_{st}^2)^3 \tilde{R}_{n,st} \\
&+ \langle n\ c\rangle\langle d\ n\rangle^3\langle n\ a\rangle^3 \sum_{a<s\le b<t\le c} \langle nst|b\rangle (x_{st}^2)^3 \tilde{R}_{n,st} \\
&+ \langle b\ c\rangle\langle d\ n\rangle^3 \sum_{1<s\le a,c<t\le d} \langle nts|n\rangle\langle nst|a\rangle^3 \tilde{R}_{n,st} \\
&+ \langle n\ c\rangle\langle n\ d\rangle^3 \sum_{1<s\le a,b<t\le c} \langle nst|b\rangle\langle nst|a\rangle^3 \tilde{R}_{n,st} \Bigg].
\end{aligned}
\tag{E.29}
$$

These simplified expressions are implemented in `GGT` by `GGTnmhv4fermS` for the single-flavor case, and by `GGTnmhv4ferm` for the general-flavor case. See appendix E.3 for the documentation.

Six Fermions

In the case of the six-fermion NMHV amplitude there is no negative-helicity gluon for us to put at position n as we did in the previous examples. The fermions are at positions $a_1^{A_1}, a_2^{A_2}, a_3^{A_3}, \bar{b}_1^{B_1}, \bar{b}_2^{B_2}$ and $\bar{n}^{B_3}$. This time the path-matrix (3.55) is given by

$$
\Xi^{\text{path}} = \begin{pmatrix}
\frac{\langle \bar{b}_2\ \bar{b}_1\rangle}{\langle \bar{b}_2\ n\rangle} & 0 & 1 & \frac{\langle \bar{b}_2\ a_1\rangle}{\langle \bar{b}_2\ n\rangle} & \frac{\langle \bar{b}_2\ a_2\rangle}{\langle \bar{b}_2\ n\rangle} & \frac{\langle \bar{b}_2\ a_3\rangle}{\langle \bar{b}_2\ n\rangle} \\
\langle n\ \bar{b}_1\rangle & \langle n\ \bar{b}_2\rangle & 0 & \langle n\ a_1\rangle & \langle n\ a_2\rangle & \langle n\ a_3\rangle \\
(\Xi_n)_{st}^{\bar{b}_1} & (\Xi_n)_{st}^{\bar{b}_2} & 0 & (\Xi_n)_{st}^{a_1} & (\Xi_n)_{st}^{a_2} & (\Xi_n)_{st}^{a_3}
\end{pmatrix}.
\tag{E.30}
$$

As ingredients of formula (3.43) we need the determinants

$$\det\left(\Xi^{\text{path}}|_q\right) = D^{\bar{b}_1\bar{b}_2}_{n;st}\,, \qquad \det\left(\Xi^{\text{path}}|_q(\bar{b}_1 \to a_i)\right) = D^{a_i\bar{b}_2}_{n;st}\,, \tag{E.31}$$

$$\det\left(\Xi^{\text{path}}|_q(\bar{b}_2 \to a_i)\right) = D^{\bar{b}_1 a_i}_{n;st}\,, \qquad \det\left(\Xi^{\text{path}}|_q(\bar{n} \to a_i)\right) = D^{\bar{b}_1\bar{b}_2 a_i}_{n;st}\,. \tag{E.32}$$

We recall that $D^{ab}_{n;st}$ has been defined in eq. (E.2) and the 3×3 determinant $D^{abc}_{n;st}$ reads

$$D^{abc}_{n;st} := \begin{vmatrix} \frac{\langle b\,a\rangle}{\langle b\,n\rangle} & 0 & \frac{\langle b\,c\rangle}{\langle b\,n\rangle} \\ \langle n\,a\rangle & \langle n\,b\rangle & \langle n\,c\rangle \\ (\Xi_n)^a_{st} & (\Xi_n)^b_{st} & (\Xi_n)^c_{st} \end{vmatrix} = \langle a\,b\rangle(\Xi_n)^c_{st} + \langle b\,c\rangle(\Xi_n)^a_{st} + \langle c\,a\rangle(\Xi_n)^b_{st}\,. \tag{E.33}$$

For $a<b<c$ we have

$$D^{abc}_{n;st} = \begin{cases} \langle a\,b\rangle\langle nts|c\rangle & b<s\le c<t \\ \langle a\,b\rangle\langle c\,n\rangle x^2_{st} & b<s<t\le c \\ \langle nts|a\rangle\langle c\,b\rangle & a<s\le b, c<t \\ \langle n\,a\rangle\langle b\,c\rangle x^2_{st} & a<s<t\le b \\ \langle a\,b\rangle\langle c\,n\rangle x^2_{st} - \langle a\,c\rangle\langle nts|b\rangle & a<s\le b<t\le c \\ \langle a\,b\rangle\langle nst|c\rangle & s\le a,b<t\le c \\ \langle c\,b\rangle\langle nst|a\rangle & s\le a<t\le b\,, \end{cases} \tag{E.34}$$

and $D^{abc}_{n;st}$ is totally antisymmetric in a,b,c. Thus, the $\mathcal{N}=4$ super Yang-Mills NMHV six-fermion amplitude is

$$\begin{aligned}(A_n)^{\text{NMHV}}_{(q\bar{q})^3} = \frac{\delta^{(4)}(p)\,\text{sign}(\tau)}{\langle 1\,2\rangle\ldots\langle n\,1\rangle}\sum_{1<s<t<n}\tilde{R}_{n;st}D^{\bar{b}_1\bar{b}_2}_{n;st}\Big(&+\delta^{A_1B_1}\delta^{A_2B_2}\delta^{A_3B_3}D^{a_1\bar{b}_2}_{n;st}D^{\bar{b}_1a_2}_{n;st}D^{\bar{b}_1\bar{b}_2a_3}_{n;st} \\ &-\delta^{A_1B_2}\delta^{A_2B_1}\delta^{A_3B_3}D^{a_2\bar{b}_2}_{n;st}D^{\bar{b}_1a_1}_{n;st}D^{\bar{b}_1\bar{b}_2a_3}_{n;st} \\ &-\delta^{A_1B_3}\delta^{A_2B_2}\delta^{A_3B_1}D^{a_3\bar{b}_2}_{n;st}D^{\bar{b}_1a_2}_{n;st}D^{\bar{b}_1\bar{b}_2a_1}_{n;st} \\ &-\delta^{A_1B_1}\delta^{A_2B_3}\delta^{A_3B_2}D^{a_1\bar{b}_2}_{n;st}D^{\bar{b}_1a_3}_{n;st}D^{\bar{b}_1\bar{b}_2a_2}_{n;st} \\ &+\delta^{A_1B_2}\delta^{A_2B_3}\delta\ ^{scriptscriptstyle A_3B_1}D^{a_3\bar{b}_2}_{n;st}D^{\bar{b}_1a_1}_{n;st}D^{\bar{b}_1\bar{b}_2a_2}_{n;st} \\ &+\delta^{A_1B_3}\delta^{A_2B_1}\delta^{A_3B_2}D^{a_2\bar{b}_2}_{n;st}D^{\bar{b}_1a_3}_{n;st}D^{\bar{b}_1\bar{b}_2a_1}_{n;st}\Big)\end{aligned} \tag{E.35}$$

which in the single-flavor case (3.35) reduces to

$$(A_n)^{\text{NMHV}}_{(q\bar{q})^3} = \frac{\delta^{(4)}(p)\,\text{sign}(\tau)}{\langle 1\,2\rangle\ldots\langle n\,1\rangle}\sum_{1<s<t<n}\tilde{R}_{n;st}\left(D^{\bar{b}_1\bar{b}_2}_{n;st}\right)^3 D^{a_1a_2a_3}_{n;st}\,. \tag{E.36}$$

In the two flavor case two out of the six permutations in eq. (E.42) contribute. Due to the basic identities

$$D^{a_1\bar{b}_2}_{n;st}D^{\bar{b}_1a_2}_{n;st} - D^{a_2\bar{b}_2}_{n;st}D^{\bar{b}_1a_1}_{n;st} = D^{\bar{b}_1\bar{b}_2}_{n;st}D^{a_1a_2}_{n;st} \tag{E.37}$$

$$D^{\bar{b}_1a_1}_{n;st}D^{\bar{b}_1\bar{b}_2a_2}_{n;st} - D^{\bar{b}_1a_2}_{n;st}D^{\bar{b}_1\bar{b}_2a_1}_{n;st} = D^{\bar{b}_1\bar{b}_2}_{n;st}D^{\bar{b}_1a_1a_2}_{n;st}\,, \tag{E.38}$$

it is possible to combine these contributions. These simplified expressions are implemented in the `Mathematica` package `GGT` by the functions `GGTnmhv6fermS` for the single-flavor case and `GGTnmhv6ferm` for the general-flavor case. See appendix E.3 for the documentation.

E.2.3. N^{2}MHV Amplitudes

Two Fermions

We continue the list of quark-gluon amplitudes by applying the master formulas (3.35) and (3.43) in the N^{2}MHV case with up to six fermions. The amplitude with three negative-helicity gluons at positions c_1, c_2, n, a quark at position a and an anti-quark at position $\bar{b}$, is

$$\begin{aligned}(A_n)^{\mathrm{N^2MHV}}_{(q\bar{q})} = \frac{\delta^{(4)}(p)\,\mathrm{sign}(\tau)}{\langle 1\ 2\rangle \ldots \langle n\ 1\rangle} \times \\ \sum_{2\le a_1<b_1<n} \tilde{R}_{n;a_1b_1} \Bigg[\sum_{a_1+1\le a_2<b_2\le b_1} \tilde{R}^{0;a_1b_1}_{n;b_1a_1;a_2b_2} \cdot D_1^{c_1c_2a} \left(D_1^{c_1c_2\bar{b}}\right)^3 \\ + \sum_{b_1\le a_2<b_2<n} \tilde{R}^{a_1b_1;0}_{n;a_2b_2} \cdot D_2^{c_1c_2a} \left(D_2^{c_1c_2\bar{b}}\right)^3 \Bigg],\end{aligned} \tag{E.39}$$

with the 3×3 determinants D_1^{abc} and D_2^{abc} from eqs. (E.6) and (E.7).

Four Fermions

For the amplitude with two negative-helicity gluons at positions c, n, as well as gluinos and anti-gluinos at positions $\alpha_1^{A_1}$, $\alpha_2^{A_2}$ and $\bar{\beta}_1^{B_1}$, $\bar{\beta}_2^{B_2}$, we obtain

$$\begin{aligned}(A_n)^{\mathrm{N^2MHV}}_{(\psi\bar{\psi})^2} = \frac{\delta^{(4)}(p)\,\mathrm{sign}(\tau)}{\langle 1\ 2\rangle \ldots \langle n\ 1\rangle} \sum_{2\le a_1<b_1<n} \tilde{R}_{n;a_1b_1} \times \\ \times \Bigg[\sum_{a_1<a_2<b_2\le b_1} \tilde{R}^{0;a_1b_1}_{n;b_1a_1;a_2b_2} \left(D_1^{c\bar{\beta}_1\bar{\beta}_2}\right)^2 \left(\delta^{B_1}_{A_1}\delta^{B_2}_{A_2} D_1^{c\alpha_1\bar{\beta}_2} D_1^{c\bar{\beta}_1\alpha_2} - \delta^{B_2}_{A_1}\delta^{B_1}_{A_2} D_1^{c\alpha_2\bar{\beta}_2} D_1^{c\bar{\beta}_1\alpha_1}\right) \\ + \sum_{b_1\le a_2<b_2<n} \tilde{R}^{a_1b_1;0}_{n;a_2b_2} \left(D_2^{c\bar{\beta}_1\bar{\beta}_2}\right)^2 \left(\delta^{B_1}_{A_1}\delta^{B_2}_{A_2} D_2^{c\alpha_1\bar{\beta}_2} D_2^{c\bar{\beta}_1\alpha_2} - \delta^{B_2}_{A_1}\delta^{B_1}_{A_2} D_2^{c\alpha_2\bar{\beta}_2} D_2^{c\bar{\beta}_1\alpha_1}\right) \Bigg]\end{aligned} \tag{E.40}$$

in the $\mathcal{N}=4$ super Yang-Mills case, and

$$\begin{aligned}(A_n)^{\mathrm{N^2MHV}}_{(q\bar{q})^2} = \frac{\delta^{(4)}(p)\,\mathrm{sign}(\tau)}{\langle 1\ 2\rangle \ldots \langle n\ 1\rangle} \sum_{2\le a_1<b_1<n} \tilde{R}_{n;a_1b_1} \cdot \Bigg[\sum_{a_1<a_2<b_2\le b_1} \tilde{R}^{0;a_1b_1}_{n;b_1a_1;a_2b_2} \cdot D_1^{c\alpha_1\alpha_2} \left(D_1^{c\bar{\beta}_1\bar{\beta}_2}\right)^3 \\ + \sum_{b_1\le a_2<b_2<n} \tilde{R}^{a_1b_1;0}_{n;a_2b_2} \cdot D_2^{c\alpha_1\alpha_2} \left(D_2^{c\bar{\beta}_1\bar{\beta}_2}\right)^3 \Bigg]\end{aligned} \tag{E.41}$$

for single-flavor QCD.

Six Fermions

For the $\mathcal{N}=4$ super Yang-Mills amplitude with one negative-helicity gluon at position n, gluinos and anti-gluinos at positions $\alpha_1^{A_1}$, $\alpha_2^{A_2}$, $\alpha_3^{A_3}$ and $\bar{\beta}_1^{B_1}$, $\bar{\beta}_2^{B_2}$, $\bar{\beta}_3^{B_3}$, our master formula yields

$$
\begin{aligned}
(A_n)^{\mathrm{N^2MHV}}_{(\psi\bar{p}si)^3} = \frac{\delta^{(4)}(p)\,\mathrm{sign}(\tau)}{\langle 1\,2\rangle\ldots\langle n\,1\rangle} \sum_{2\le a_1<b_1<n} \tilde{R}_{n;a_1b_1}\times \\
\times\Bigg[\sum_{a_1<a_2<b_2\le b_1} \tilde{R}^{0;a_1b_1}_{n;b_1a_1;a_2b_2}\, D_1^{\bar{\beta}_1\bar{\beta}_2\bar{\beta}_3}\left(\begin{array}{r}\delta^{B_1}_{A_1}\delta^{B_2}_{A_2}\delta^{B_3}_{A_3} D_1^{\alpha_1\bar{\beta}_2\bar{\beta}_3} D_1^{\bar{\beta}_1\alpha_2\bar{\beta}_3} D_1^{\bar{\beta}_1\bar{\beta}_2\alpha_3} \\ \pm \text{ permutations of } \left\{\begin{matrix}A_i\\ \alpha_i\end{matrix}\right\}\end{array}\right) \\
+\sum_{b_1\le a_2<b_2<n} \tilde{R}^{a_1b_1;0}_{n;a_2b_2}\, D_2^{\bar{\beta}_1\bar{\beta}_2\bar{\beta}_3}\left(\begin{array}{r}\delta^{B_1}_{A_1}\delta^{B_2}_{A_2}\delta^{B_3}_{A_3} D_2^{\alpha_1\bar{\beta}_2\bar{\beta}_3} D_2^{\bar{\beta}_1\alpha_2\bar{\beta}_3} D_2^{\bar{\beta}_1\bar{\beta}_2\alpha_3} \\ \pm \text{ permutations of } \left\{\begin{matrix}A_i\\ \alpha_i\end{matrix}\right\}\end{array}\right)\Bigg],
\end{aligned}
\tag{E.42}
$$

which in the single-flavor case simplifies to

$$
\begin{aligned}
(A_n)^{\mathrm{N^2MHV}}_{(q\bar{q})^3} = \frac{\delta^{(4)}(p)\,\mathrm{sign}(\tau)}{\langle 1\,2\rangle\ldots\langle n\,1\rangle}\times \qquad\qquad (\text{E.43})\\
\sum_{2\le a_1<b_1<n} \tilde{R}_{n;a_1b_1}\cdot\Bigg[\sum_{a_1<a_2<b_2\le b_1} \tilde{R}^{0;a_1b_1}_{n;b_1a_1;a_2b_2}\, D_1^{\alpha_1\alpha_2\alpha_3}\left(D_1^{\bar{\beta}_1\bar{\beta}_2\bar{\beta}_3}\right)^3 \\
+\sum_{b_1\le a_2<b_2<n} \tilde{R}^{a_1b_1;0}_{n;a_2b_2}\, D_2^{\alpha_1\alpha_2\alpha_3}\left(D_2^{\bar{\beta}_1\bar{\beta}_2\bar{\beta}_3}\right)^3\Bigg].
\end{aligned}
$$

We recall that these formulas hold for arbitrary color-orderings of the n partons. Similar to the NMHV six fermion amplitudes, the two flavor case can be simplified as well. In this case two out of the six permutations in eq. (E.42) contribute. The basic identity

$$
D_i^{\alpha_1\bar{\beta}_2\bar{\beta}_3} D_i^{\bar{\beta}_1\alpha_2\bar{\beta}_3} - D_i^{\alpha_2\bar{\beta}_2\bar{\beta}_3} D_2^{\bar{\beta}_1\alpha_1\bar{\beta}_3} = D_i^{\bar{\beta}_1\bar{\beta}_2\bar{\beta}_3} D_i^{\alpha_1\alpha_2\bar{\beta}_3} \tag{E.44}
$$

allows to combine both contributions.

We have implemented all of the above simplified expressions for NNMHV amplitudes with up to six fermions in the functions `GGTnnmhv2ferm`, `GGTnnmhv4ferm`, and `GGTnnmhv6ferm` in the `GGT` package.

E.3. The `Mathematica` Package `GGT`

Here we describe the `Mathematica` package `GGT` (gluon-gluino trees) provided with the `arXiv.org` submissions of references [2, 3] and also accessible on the web page `http://qft.physik.hu-berlin.de`.

The idea is to provide the formulas derived in chapter 3 and appendices E.1 and E.2 in computer-readable form, such that the interested reader can use them without having to type them in. We have also included a simple numerical evaluation routine for given phase space points in the `GGT` package, as well as an interface to the spinor-helicity package `S@M` [174]. The issue of computer speed optimization will be commented upon

below.

Let us now describe the different functions in `GGT` and then give a specific example. The following functions are provided in `GGT`

- `GGTgluon[n,H]`
  gives the n-gluon amplitude (3.20), with the positions of the negative-helicity gluons given by the list `H`.

- `GGTfermionS[n, gluonlist, fermlist, afermlist]`
  gives the n-parton amplitude (3.35) of an arbitrary number of gluons and single-flavor fermion/antifermions. The positions of the negative-helicity gluons, helicity $+\frac{1}{2}$ fermions, and helicity $-\frac{1}{2}$ anti-fermions are given by the lists `gluonlist`, `fermlist`, and `afermlist`, respectively.

- `GGTfermion[n, gluonlist, fermlist, afermlist]`
  is the generalization of `GGTfermionS` to multiple fermion flavors, eq. (3.43). The positions of the negative-helicity gluons are given by the list `gluonlist`. The positions $q_i, \bar{q}_i$ and flavors A_i, B_i of the helicity $+\frac{1}{2}$ fermions and helicity $-\frac{1}{2}$ anti-fermions are given by the lists `fermlist`$= \{\{q_i, A_i\}, \ldots\}$, and `afermlist`$= \{\{\bar{q}_i, A_i\}, \ldots\}$, respectively.

- `GGTsuperamp[`n, k`]`
  is the N^{k}MHV superamplitude of n superfields, with the MHV superamplitude factored out, in terms of the R invariants.

Let us give an example. We can load the `GGT` package using

```
« GGT.m
```

Suppose we want to evaluate a gluon amplitude. Typing

```
GGTgluon[6,{3,5,6}]
```

prints the 6-gluon NMHV amplitude with helicity configuration $++-+--$,

$$\frac{1}{\langle 1|2\rangle\langle 2|3\rangle\langle 3|4\rangle\langle 4|5\rangle\langle 5|6\rangle\langle 6|1\rangle}$$
$$\Bigg(\frac{\langle 2|1\rangle\langle 4|3\rangle\left(s_{2,4}\langle 6|3\rangle\langle 6|5\rangle + \langle 6|x_{6,4}|x_{4,2}|3\rangle\langle 6|5\rangle\right)^4}{s_{2,4}\langle 6|x_{6,2}|x_{2,4}|3\rangle\langle 6|x_{6,2}|x_{2,4}|4\rangle\langle 6|x_{6,4}|x_{4,2}|1\rangle\langle 6|x_{6,4}|x_{4,2}|2\rangle}$$
$$+\frac{\langle 2|1\rangle\langle 5|4\rangle\left(s_{2,5}\langle 6|3\rangle\langle 6|5\rangle\langle 6|x_{6,5}|x_{5,2}|3\rangle\langle 6|5\rangle\right)^4}{s_{2,5}\langle 6|x_{6,2}|x_{2,5}|4\rangle\langle 6|x_{6,2}|x_{2,5}|5\rangle\langle 6|x_{6,5}|x_{5,2}|1\rangle\langle 6|x_{6,5}|x_{5,2}|2\rangle}$$
$$+\frac{\langle 3|2\rangle\langle 5|4\rangle\left(s_{3,5}\langle 6|3\rangle\langle 6|5\rangle + \langle 6|x_{6,5}|x_{5,3}|3\rangle\langle 6|5\rangle\right)^4}{s_{3,5}\langle 6|x_{6,3}|x_{3,5}|4\rangle\langle 6|x_{6,3}|x_{3,5}|5\rangle\langle 6|x_{6,5}|x_{5,3}|2\rangle\langle 6|x_{6,5}|x_{5,3}|3\rangle}\Bigg)$$

`GGT` formatted the output for better readability. The underlying formula, which can be accessed explicitly, *e.g.* by using `Inputform[...]`, depends on the following quantities: The spinor products $\langle ij\rangle$ are denoted by `GGTspaa[i,j]`. Differences between dual coordinates $x_{i,j} = p_i + p_{i+1} + \ldots + p_{j-1}$ are denoted by `GGTx[i,j]` . Finally, the abbreviation $x_{ij}^2 = s_{i,j-1}$ is used and denoted by `GGTs[i,j-1]`.

In order to obtain numerical values, we can use the spinor-helicity package `S@M` [174]. The function `GGTtoSpinors` converts the expression into one that can be evaluated by the latter package. In our example, the commands

```
« Spinors.m
GenMomenta[1,2,3,4,5,6]
```

load the S@M package and use one of its functions to generate arbitrary momenta for a six-particle scattering process. Finally, numerical values of the amplitude at that phase space point can be obtained by the command

```
GGTtoSpinors[GGTgluon[6,{3,5,6}]] //N
```

A faster implementation for the numerical evaluation of the GGT formulas is provided by the function GGTgenvar[P] which generates the spinors and region momenta for a numerical evaluation of an amplitude at a desired phase space point $P = \{p_1, p_2, \ldots, p_n\}$. For example, for the kinematic point given in eq. (4.6) of ref. [175] (which to save space we give here to only three significant digits), one would use

```
GGTgenvar[{{−3.0, 2.12, 1.06, 1.84}, {−3.0, −2.12, −1.06, −1.84},
{2.0, 2.0, 0.0, 0.0}, {0.857, −0.316, 0.797, 0.0}, {1.0, −0.184, 0.465, 0.866},
{2.14, −1.5, −1.26, −0.866}}]
```

One can then evaluate an amplitude numerically by the command

```
GGTnumeric[GGTfermionS[6, {1, 6}, {2, 4}, {3, 5}]]
- 0.496838 + 0.0714737 i
```

This approach is considerably faster than the GGTtoSpinors[...]//N function discussed above.

Let us comment about the evaluation time needed using our approach. It is clear that for any serious applications or for comparisons with other methods, one should implement our analytical formulas using a low-level programming language, such as C, C++ or FORTRAN. For example, an implementation of the NMHV formulas in C++ results in a speedup of orders of magnitude over a similar implementation in Mathematica. Moreover, it is important to efficiently cache (store the numerical values of) quantities that are used repeatedly. In this spirit, the Mathematica demonstration package GGT provides a computer-readable version of the formulas needed for such an approach, so that the user does not have to type them in manually.

Our analytical formulas are very similar, and in some cases identical, to the ones obtained in a very recent paper [143]. The latter also correspond to solutions of the BCFW recursion relations, based on refs. [176, 177], but may differ in form since they can correspond to different factorization channels. Another difference is that they are written using momentum-twistor variables [178, 179]. Ref. [143] contains a numerical Mathematica implementation of these formulas. When the formulas presented here and that of ref. [143] are both implemented with appropriate caching in C++, for the NMHV tree amplitudes for $Vq\bar{q}gggggg$ and $Vq\bar{q}Q\bar{Q}ggg$, their evaluation time is similar [180].

We remark that in approaches based on BCFW recursion relations, the asymptotic number of terms in $\mathrm{N}^k\mathrm{MHV}_n$ amplitudes as n becomes large is quadratic in n for NMHV, quartic for NNMHV and worse for higher k. This is the reason we especially simplified the NMHV and NNMHV formulas presented here, since we expect that they will be the most useful for practical applications, especially for small n. For $k > 2$ and large n there are at least two efficient numerical strategies making use of these formulae. First, one could use our formulae as initial conditions for a numerical implementation

of the BCFW recursion relations, as described in section 3. Alternatively, one could use the Berends-Giele approach for $k > 2$, implemented using an efficient caching, in combination with our formulas for $k \leq 2$ [181].

We also included further functions that evaluate directly the simplified amplitudes of Appendix E.1 and E.2. They can be accessed via the following functions.

- `GGTnmhvgluon`$[n, a, b]$
  is the simplified n-parton NMHV gluon amplitude with negative-helicity gluons at positions a, b and n.

- `GGTnnmhvgluon`$[n, a, b, c]$
  is the simplified n-parton NNMHV gluon amplitude with negative-helicity gluons at positions a, b, c and n.

- `GGTnmhv2ferm`$[n, c, a, \bar{b}]$
  is the simplified n-parton NMHV two-fermion amplitude with negative-helicity gluons at positions c, n and a fermion/anti-fermion at positions a and $\bar{b}$.

- `GGTnnmhv2ferm`$[n, c_1, c_2, a, \bar{b}]$
  is the simplified n-parton NNMHV two-fermion amplitude with negative-helicity gluons at positions c_1, c_2 and n and a fermion/anti-fermion at position a and $\bar{b}$.

- `GGTnmhv4ferm`$[n, \{\{a_1, A_1\}, \{a_2, A_2\}\}, \{\{\bar{b}_1, B_1\}, \{\bar{b}_2, B_2\}\}]$
  is the simplified n-parton NMHV four-fermion amplitude with a negative-helicity gluon at position n, two gluinos of flavors A_i at positions a_i and two anti-gluinos of flavors B_i at positions $\bar{b}_i$.

- `GGTnmhv4fermS`$[n, \{a_1, a_2\}, \{\bar{b}_1, \bar{b}_2\}]$
  is the simplified n-parton NMHV four-fermion amplitude with a negative-helicity gluon at position n and equally flavored gluinos/anti-gluinos at positions a_i and $\bar{b}_i$, respectively.

- `GGTnnmhv4ferm`$[n, c, \{\{a_1, A_1\}, \{a_2, A_2\}\}, \{\{\bar{b}_1, B_1\}, \{\bar{b}_2, B_2\}\}]$
  is the simplified n-parton NNMHV four-fermion amplitude with two negative-helicity gluons at position c, n, two gluinos of flavors A_i at positions a_i and two anti-gluinos of flavors B_i at positions $\bar{b}_i$.

- `GGTnnmhv4fermS`$[n, c, \{a_1, a_2\}, \{\bar{b}_1, \bar{b}_2\}]$
  is the simplified n-parton NNMHV four-fermion amplitude with negative-helicity gluons at positions c, n and equally flavored gluinos/anti-gluinos at positions a_i and $\bar{b}_i$, respectively.

- `GGTnmhv6ferm`$[n, B_3, \{\{a_1, A_1\}, \{a_2, A_2\}, \{a_3, A_3\}\}, \{\{\bar{b}_1, B_1\}, \{\bar{b}_2, B_2\}\}]$
  is the simplified n-parton NMHV six-fermion amplitude with three gluinos of flavors A_i at positions a_i and three anti-gluinos of flavors B_i at positions $\bar{b}_i$. Note that $\bar{b}_3 = n$.

- `GGTnmhv6fermS`$[n, \{a_1, a_2, a_3\}, \{\bar{b}_1, \bar{b}_2\}]$
  is the simplified n-parton NMHV six-fermion amplitude with equally flavored gluinos/anti-gluinos at positions a_i and $\bar{b}_i$, respectively. Note that $\bar{b}_3 = n$.

- `GGTnnmhv6ferm[`$n, \{\{a_1, A_1\}, \{a_2, A_2\}, \{a_3, A_3\}\}, \{\{\bar{b}_1, B_1\}, \{\bar{b}_2, B_2\}, \{\bar{b}_3, B_3\}\}$`]`
  is the simplified n-parton NNMHV six-fermion amplitude with a negative helicity gluon at position n and three gluinos of flavors A_i at positions a_i and three anti-gluinos of flavors B_i at positions $\bar{b}_i$.

- `GGTnnmhv6fermS[`$n, \{a_1, a_2, a_3\}, \{\bar{b}_1, \bar{b}_2, \bar{b}_3\}$`]`
  is the simplified n-parton NNMHV six-fermion amplitude with a negative helicity gluon at position n and equally flavored gluinos/anti-gluinos at positions a_i and $\bar{b}_i$, respectively.

The full list of functions available in `GGT` can be obtained by typing

```
$GGTfunctions
```

along with the documentation of each implemented function that can be accessed via the command

```
?GGTgluon
```

for example.

Appendix F

Phase Space Generators

As we have shown in section 4.3.2 the collinearity of the phase space points has a crucial impact on the accuracy of the amplitudes. How collinear the phase space points are depends on the phase space generator and on the applied collinearity cut. We define the collinearity $\mathcal{C}$ of a phase space point to be $\mathcal{C} = \min\left(\log_{10}(2p_i p_j/s)\right)$. In fig. F.1 and fig. F.2 we show the probability density of the collinearity for RAMBO and sequential splitting. For RAMBO the average collinearity decreases slowly from $\langle\mathcal{C}\rangle \approx -1.5$ for $n = 5$ to $\langle\mathcal{C}\rangle \approx -5.3$ for $n = 25$, with an almost constant width of $2\sigma \approx 1.1$. In contrast, for sequential splitting the phase space points are much more collinear, going from $\langle\mathcal{C}\rangle \approx -1.7$ for $n = 5$ down to $\langle\mathcal{C}\rangle \approx -19.1$ for $n = 25$. Additionally, the width of the distribution increases from $2\sigma \approx 1.4$ to $2\sigma \approx 7.8$.

In practice, one has to take care that the collinearity cut is compatible with the phase space generator, e. g. for $\mathcal{C} > 10^{-3}$ and RAMBO it will be impossible to obtain phase space points for multiplicities larger than 15. On the other hand, using sequential splitting without a collinearity cut one has to take care of the accuracy if one wants to go beyond $n = 8$, because quantities like x^2_{ii+2} become numerically unstable and have to be replaced by $2p_i p_{i+1}$ or even by $\langle i\, i+1\rangle[i\, i+1]$.

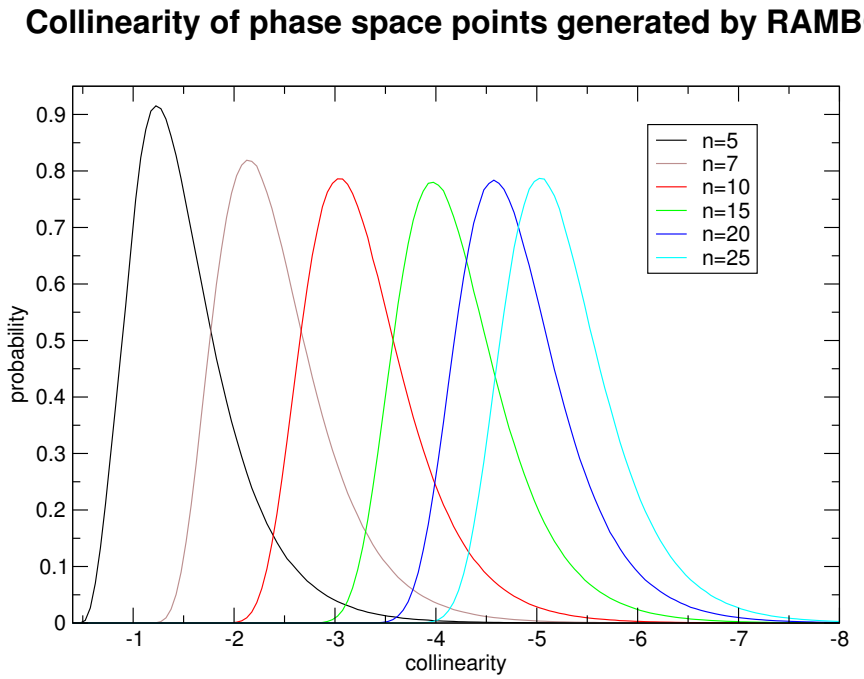

Figure F.1.: Probability density of the collinearity of phase space points generated by Rambo.

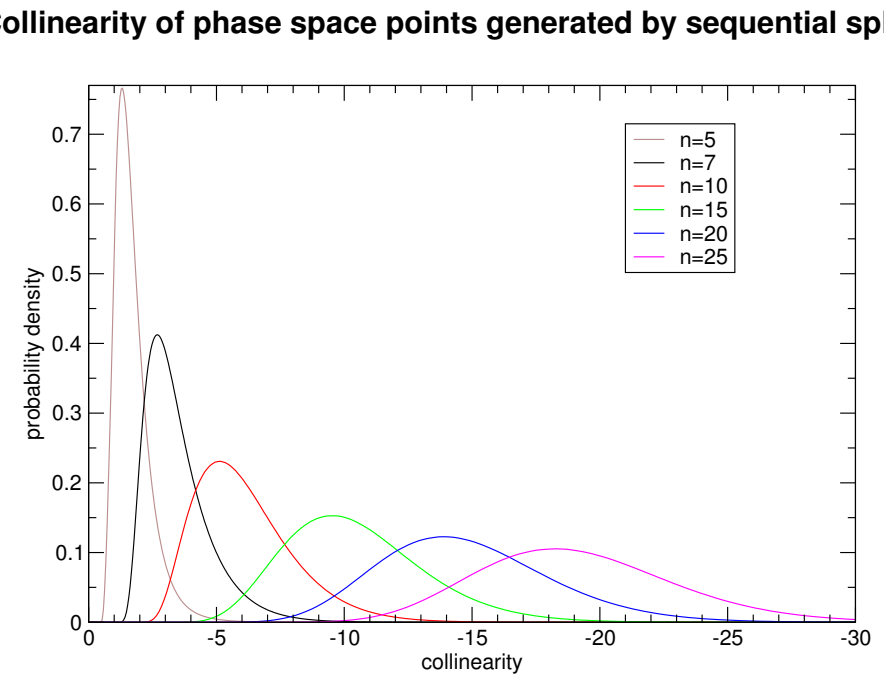

Figure F.2.: Probability density of the collinearity of phase space points generated by sequential splitting.

Appendix G

Higgs Regularization

In this appendix we provide supplemental material to chapter 6. We present the Feynman rules of the Higgsed theory and apply them in appendix G.2 to calculate the one-loop correction to the four-point function. Furthermore we illustrate the use of the Mellin-Barnes method for calculating the Higgs-regularized loop integrals. In appendix G.4 we derive the Berkovits-Maldacena solution in conformal gauge and we consider the infinitesimal form of the dual conformal generator in appendices G.5 and G.6.

G.1. Feynman Rules for Higgsed $\mathcal{N} = 4$ SYM

G.1.1. Ten-Dimensional Formulation

Here we give a short list of the Feynman rules necessary for the computation in appendix G.2. Keeping the ten dimensional notation for the spinors we have to impose both the Majorana and the Weyl condition. This leads to the appearance of the ten dimensional charge conjugation matrix C and the projection matrix $L = \frac{1}{2}(1 + \Gamma^{11})$ in the Feynman rules.

Gluon Propagators

$$\mu \quad \begin{matrix} b_1 \\ a_1 \end{matrix} \sim\sim\sim \begin{matrix} a_2 \\ b_2 \end{matrix} \quad \nu = \frac{-i\eta^{\mu\nu}}{q^2}\delta^{b_1}_{a_2}\delta^{b_2}_{a_1} \tag{G.1}$$

$$\mu \quad \begin{matrix} b_1 \\ i_1 \end{matrix} \sim\sim\sim \begin{matrix} a_2 \\ j_2 \end{matrix} \quad \nu = \frac{-i\eta^{\mu\nu}}{q^2 + m^2_{i_1}}\delta^{b_1}_{a_2}\delta^{j_2}_{i_1} \tag{G.2}$$

$$\mu \quad \begin{matrix} j_1 \\ i_1 \end{matrix} \sim\sim\sim \begin{matrix} i_2 \\ j_2 \end{matrix} \quad \nu = \frac{-i\eta^{\mu\nu}}{q^2 + (m_{i_2} - m_{i_1})^2}\delta^{j_1}_{i_2}\delta^{j_2}_{i_1} \tag{G.3}$$

Scalar Propagators

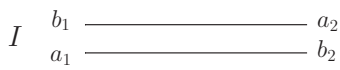

$$J = \frac{-i\delta^{IJ}}{q^2}\delta^{b_1}_{a_2}\delta^{b_2}_{a_1} \tag{G.4}$$

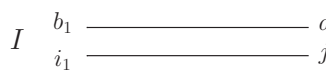

$$J = \frac{-i\delta^{IJ}}{q^2+m_{i_1}^2}\delta^{b_1}_{a_2}\delta^{j_2}_{i_1} \tag{G.5}$$

$$J = \frac{-i\delta^{IJ}}{q^2+(m_{i_2}-m_{i_1})^2}\delta^{j_1}_{i_2}\delta^{j_2}_{i_1} \tag{G.6}$$

We use dotted double lines to denote the field Φ_9.

Fermion Propagators

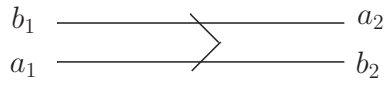

$$= \frac{iL\not{q}C^{-1}}{q^2}\delta^{b_1}_{a_2}\delta^{b_2}_{a_1} \tag{G.7}$$

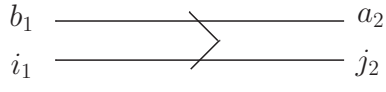

$$= \frac{iL(\not{q}+m_{i_1}\Gamma^9)C^{-1}}{q^2+m_{i_1}^2}\delta^{b_1}_{a_2}\delta^{j_2}_{i_1} \tag{G.8}$$

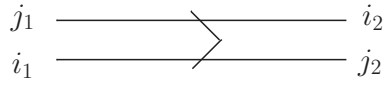

$$= \frac{iL(\not{q}+(m_{i_2}-m_{i_1})\Gamma^9)C^{-1}}{q^2+(m_{i_2}-m_{i_1})^2}\delta^{j_1}_{i_2}\delta^{j_2}_{i_1} \tag{G.9}$$

Vertices

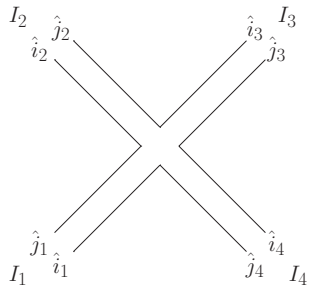

$$\begin{aligned} = ig^2\Big(&2\delta^{I_1I_3}\delta^{I_2I_4} \\ &- \delta^{I_1I_2}\delta^{I_3I_4} \\ &- \delta^{I_1I_4}\delta^{I_2I_3}\Big)\delta^{\hat{j}_1}_{\hat{i}_2}\delta^{\hat{j}_2}_{\hat{i}_3}\delta^{\hat{j}_3}_{\hat{i}_4}\delta^{\hat{j}_4}_{\hat{i}_1} \end{aligned} \tag{G.10}$$

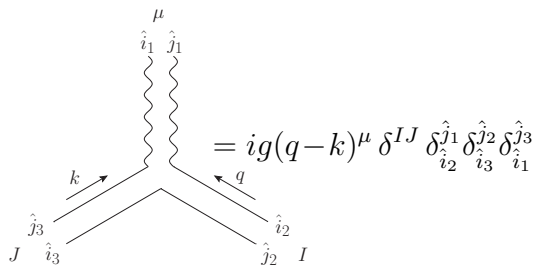

$$= ig(q-k)^\mu\,\delta^{IJ}\,\delta^{\hat{j}_1}_{\hat{i}_2}\delta^{\hat{j}_2}_{\hat{i}_3}\delta^{\hat{j}_3}_{\hat{i}_1} \qquad = ig\delta^{I'J'}\,(2m_{i_3}-m_{i_2})\,\delta^{j_1}_{i_2}\delta^{j_2}_{i_3}\delta^{b_3}_{a_1} \tag{G.11}$$

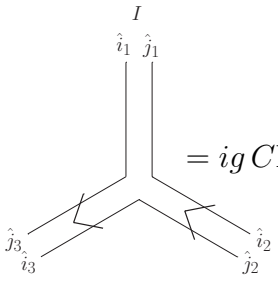

$$= ig\, C\Gamma^I L\, \delta^{\hat{j}_1}_{\hat{i}_2}\delta^{\hat{j}_2}_{\hat{i}_3}\delta^{\hat{j}_3}_{\hat{i}_1}$$

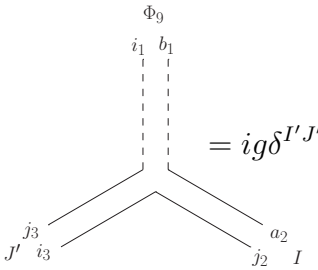

$$= ig\delta^{I'J'}\,(2m_{i_3}-m_{i_1})\,\delta^{b_1}_{a_2}\delta^{j_2}_{i_3}\delta^{j_3}_{i_1} \tag{G.12}$$

Hatted indices $\hat{i}$ mean that $\hat{i} \in \{1, 2, ..., N+M\}$.

G.1.2. Four-Dimensional Formulation

If we decompose the ten-dimensional Majorana-Weyl spinor in terms of two-component spinors λ_A, $\bar{\lambda}_A$ we have an increased number of Feynman rules involving fermions. They can be obtained from the Feynman rules with the ten-dimensional fermions or directly from the Lagrangian.

Fermion Propagators

$$\langle \lambda_{ia} \bar{\lambda}^{\mathrm{T}}_{ai} \rangle = \frac{i\bar{\sigma}_\mu p^\mu \epsilon}{p^2 + m_i^2} \tag{G.13}$$

$$\langle \bar{\lambda}_{ia} \lambda^{\mathrm{T}}_{ai} \rangle = \frac{-i\sigma_\mu p^\mu \epsilon}{p^2 + m_i^2} \tag{G.14}$$

$$\langle \lambda_{ia} \lambda^{\mathrm{T}}_{ai} \rangle = \frac{i\epsilon m_i \Sigma_9}{p^2 + m_i^2} \tag{G.15}$$

$$\langle \bar{\lambda}_{ia} \bar{\lambda}^{\mathrm{T}}_{ai} \rangle = \frac{i\epsilon m_i \bar{\Sigma}_9}{p^2 + m_i^2} \tag{G.16}$$

Vertices

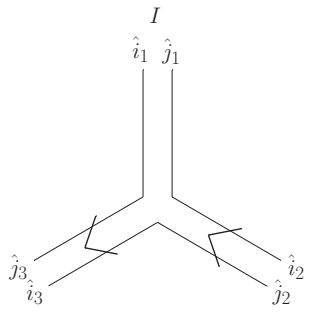

$$= ig\epsilon\Sigma^I\, \delta^{\hat{j}_1}_{\hat{i}_2}\delta^{\hat{j}_2}_{\hat{i}_3}\delta^{\hat{j}_3}_{\hat{i}_1}$$

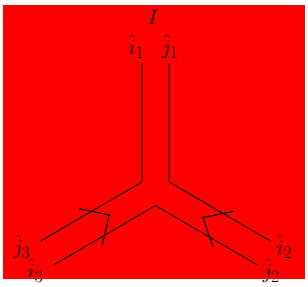

$$= ig\epsilon\bar{\Sigma}^I\, \delta^{\hat{j}_1}_{\hat{i}_2}\delta^{\hat{j}_2}_{\hat{i}_3}\delta^{\hat{j}_3}_{\hat{i}_1} \tag{G.17}$$

G.2. One-Loop Gauge Theory Computation

We want to calculate the one-loop contribution to the color ordered amplitude

$$A_4 = \langle \Phi_{I'}(p_1)\, \Phi_{J'}(p_2)\, \Phi_{I'}(p_3)\, \Phi_{J'}(p_4) \rangle\,, \tag{G.18}$$

where we recall that $I', J' \in \{4, \ldots, 8\}$, and here we take $I' \neq J'$ with no sum on either index. We know that the amplitude is UV finite. Hence all bubble and tadpole integrals have to cancel and we can drop all bubble and tadpole diagrams from the beginning. What we are left with are the 8 triangle diagrams and the one box diagram listed in fig. G.1. However we only need to calculate the following two triangle diagrams and obtain the others by cyclically permuting the indices. Using the Feynman rules of appendix G.1 we obtain:

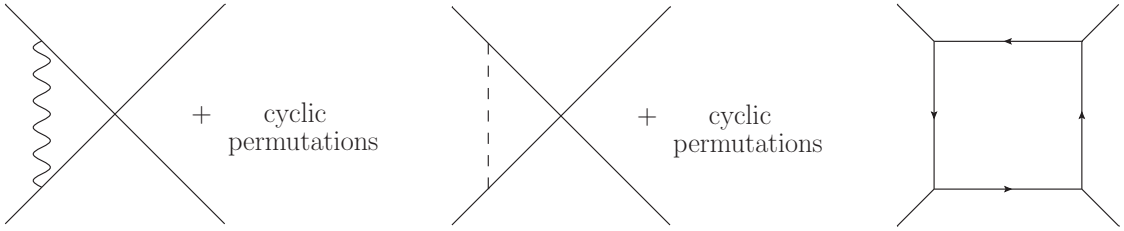

Figure G.1.: Relevant one-loop diagrams.

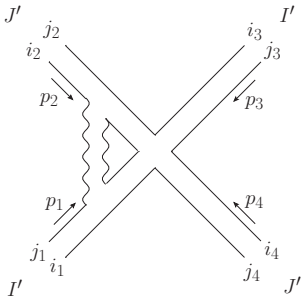

$$= 2Ng^4 \delta_{i_2}^{j_1} \delta_{i_3}^{j_2} \delta_{i_4}^{j_3} \delta_{i_1}^{j_4} \int \frac{d^4 l}{(2\pi)^4} \frac{(l_1 + p_1) \cdot (l_3 - p_2)}{(l_1^2 + m_{i_1}^2)(l_2^2 + m_{i_2}^2)(l_3^2 + m_{i_3}^2)} \,, \tag{G.19}$$

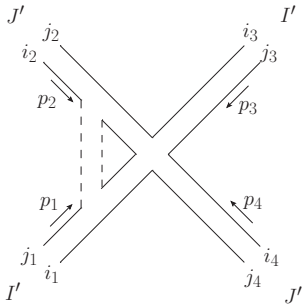

$$= 2Ng^4 \delta_{i_2}^{j_1} \delta_{i_3}^{j_2} \delta_{i_4}^{j_3} \delta_{i_1}^{j_4} \int \frac{d^4 l}{(2\pi)^4} \frac{(2m_{i_1} - m_{i_2})(2m_{i_3} - m_{i_2})}{(l_1^2 + m_{i_1}^2)(l_2^2 + m_{i_2}^2)(l_3^2 + m_{i_3}^2)} \,. \tag{G.20}$$

Both diagrams can be combined using the five dimensional momenta

$$\hat{p}_k = (p_k, m_{i_k} - m_{i_{k+1}}) \qquad\qquad \hat{l}_k = (l_k, m_{i_k}) \,, \tag{G.21}$$

leading to

$$\text{(G.19)} + \text{(G.20)} = 2Ng^4 \delta_{i_2}^{j_1} \delta_{i_3}^{j_2} \delta_{i_4}^{j_3} \delta_{i_1}^{j_4} \int \frac{d^4 l}{(2\pi)^4} \frac{(\hat{l}_2 + 2\hat{p}_1) \cdot (\hat{l}_2 - 2\hat{p}_2)}{\hat{l}_1^2 \, \hat{l}_2^2 \, \hat{l}_3^2} \tag{G.22}$$

Because of the two identities

$$2\hat{l}_2 \cdot \hat{p}_2 = \hat{l}_2^2 - \hat{l}_3^2 \qquad \text{and} \qquad 2\hat{l}_2 \cdot \hat{p}_2 = \hat{l}_1^2 - \hat{l}_2^2 \tag{G.23}$$

the triangle coefficient is simply $-8Ng^4\hat{p}_1\cdot\hat{p}_2$. Summing up all triangle diagrams we obtain

$$-8Ng^4\delta^{j_1}_{i_2}\delta^{j_2}_{i_3}\delta^{j_3}_{i_4}\delta^{j_4}_{i_1}\int\frac{d^4l}{(2\pi)^4}\left(\frac{\hat{p}_1\cdot\hat{p}_2}{\hat{l}_1^2\,\hat{l}_2^2\,\hat{l}_3^2}+\frac{\hat{p}_2\cdot\hat{p}_3}{\hat{l}_2^2\,\hat{l}_3^2\,\hat{l}_4^2}+\frac{\hat{p}_1\cdot\hat{p}_2}{\hat{l}_3^2\,\hat{l}_4^2\,\hat{l}_1^2}+\frac{\hat{p}_2\cdot\hat{p}_3}{\hat{l}_4^2\,\hat{l}_1^2\,\hat{l}_2^2}\right)\quad+\text{bubbles}\,. \tag{G.24}$$

The box diagram is given by

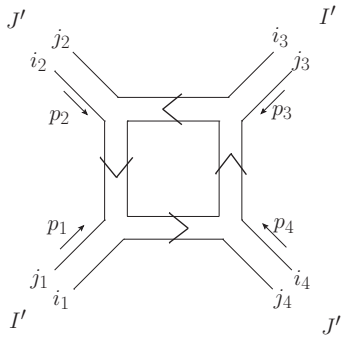

$$\begin{aligned}&=-Ng^4\delta^{j_1}_{i_2}\delta^{j_2}_{i_3}\delta^{j_3}_{i_4}\delta^{j_4}_{i_1}\int\frac{d^4l}{(2\pi)^4}\frac{\mathrm{Tr}\left[\Gamma^{I'}L\hat{l}_1\Gamma^{J'}L\hat{l}_4\Gamma^{I'}L\hat{l}_3\Gamma^{J'}L\hat{l}_2\right]}{\hat{l}_1^2\,\hat{l}_2^2\,\hat{l}_3^2\,\hat{l}_4^2}\\&=Ng^4\delta^{j_1}_{i_2}\delta^{j_2}_{i_3}\delta^{j_3}_{i_4}\delta^{j_4}_{i_1}\int\frac{d^4l}{(2\pi)^4}\frac{\mathrm{Tr}\left[L\hat{l}_1\,\hat{l}_4\,\hat{l}_3\,\hat{l}_2\right]}{\hat{l}_1^2\,\hat{l}_2^2\,\hat{l}_3^2\,\hat{l}_4^2}\end{aligned}$$

$$=16Ng^4\delta^{j_1}_{i_2}\delta^{j_2}_{i_3}\delta^{j_3}_{i_4}\delta^{j_4}_{i_1}\int\frac{d^4l}{(2\pi)^4}\frac{(\hat{l}_1\cdot\hat{l}_4)(\hat{l}_3\cdot\hat{l}_2)-(\hat{l}_1\cdot\hat{l}_3)(\hat{l}_2\cdot\hat{l}_4)+(\hat{l}_1\cdot\hat{l}_2)(\hat{l}_4\cdot\hat{l}_3)}{\hat{l}_1^2\,\hat{l}_2^2\,\hat{l}_3^2\,\hat{l}_4^2}\,. \tag{G.25}$$

Only the term $(\hat{l}_1\cdot\hat{l}_3)(\hat{l}_2\cdot\hat{l}_4)$ contributes to the box and triangle integrals. Making use of the simple identity

$$(\hat{l}_1\cdot\hat{l}_3)(\hat{l}_2\cdot\hat{l}_4)=\left(\tfrac{1}{2}\hat{l}_1^2+\tfrac{1}{2}\hat{l}_3^2-\hat{p}_1\cdot\hat{p}_2\right)\left(\tfrac{1}{2}\hat{l}_2^2+\tfrac{1}{2}\hat{l}_4^2-\hat{p}_2\cdot\hat{p}_3\right)\,, \tag{G.26}$$

we can read off the box and triangle coefficients and see that the triangle integrals indeed cancel:

$$(\text{G.25})+(\text{G.24})=-16Ng^4\delta^{j_1}_{i_2}\delta^{j_2}_{i_3}\delta^{j_3}_{i_4}\delta^{j_4}_{i_1}\int\frac{d^4l}{(2\pi)^4}\frac{(\hat{p}_1\cdot\hat{p}_2)(\hat{p}_2\cdot\hat{p}_3)}{\hat{l}_1^2\,\hat{l}_2^2\,\hat{l}_3^2\,\hat{l}_4^2}\quad+\text{bubbles}\,. \tag{G.27}$$

G.3. Results for Integrals in the Higgsed Theory

G.3.1. The One-loop Box Integral by Mellin-Barnes Method

We illustrate the use of the Mellin-Barnes (MB) representation for computing loop integrals (for further reading see [182]). Consider the one-loop box integral of eq. (6.20) with massless external lines and a uniform mass $m_i=m$ circulating in the loop. Using the Mathematica package *AMBRE* [183], a two-fold MB representation is automatically generated. It reads

$$\begin{aligned}I^{(1)}(s,t,m)=\int d\tilde{z}_1 d\tilde{z}_2(m^2)^{z_1}s^{(1+z_2)}t^{(-1-z_1-z_2)}\times\\\Gamma(-z_1)\Gamma^2(-1-z_1-z_2)\Gamma(-z_2)\Gamma^2(1+z_2)\Gamma(2+z_1+z_2)\frac{1}{\Gamma(-2z_1)}\,,\end{aligned} \tag{G.28}$$

where $d\tilde{z}=dz/(2\pi i)$ and the real part of z_1,z_2 can be taken to be -1 and $-1/2$, respectively. In order to take the small m limit, we want to deform the integration contour for z_1 such that its real part is positive. In doing so, we pick up a pole at

$z_1 = -1 - z_2$ originating from $\Gamma^2(-1 - z_1 - z_2)$. Note that the pole at $z_1 = 0$ is spurious. The deformed integral with $Re(z_1) > 0$ vanishes as $m^2 \to 0$, therefore, taking the residue at $z_1 = -1 - z_2$ we obtain

$$I^{(1)}(s,t,m) = -\int d\tilde{z}_2 (m^2)^{(-1-z_2)} s^{(1+z_2)} \frac{\Gamma(-z_2)\Gamma^3(1+z_2)}{\Gamma(2+2z_2)} \times \Big[-h(z_2) + 2h(1+2z_2) + \ln(m^2/t)\Big] + O(m^2)\,, \tag{G.29}$$

where $Re(z_2) = -1/2$ and $h(z) = \Psi(1+z) - \gamma$. We can reiterate the above procedure and deform the integration contour for z_2. We want to take it from $Re(z_2) = -1/2$ to $Re(z_2) < -1$. In doing so, we pick up a pole at $Re(z_2) = -1$. Taking the residue, we obtain the final result

$$I^{(1)}(s,t,m) = 2\ln(m^2/s)\ln(m^2/t) - \pi^2 + O(m^2)\,. \tag{G.30}$$

Note that in this simple example we were able to find the answer without doing any integrations, just by using Cauchy's theorem.

G.3.2. The Two-Loop Box Integral by Mellin-Barnes Method

The Mathematica package *AMBRE* [183] automatically produces the following five-fold MB representation for the two-loop box integral of eq. (6.34),

$$\begin{aligned} I^{(2)}(s,t,m) = \int d\tilde{z}_1\, d\tilde{z}_2\, d\tilde{z}_3\, d\tilde{z}_7\, d\tilde{z}_8\, (m^2)^{(z_1+z_7)}\, s^{(1-z_1+z_8)}\, t^{(-1-z_7-z_8)} \\ \times\Gamma(-z_1)\Gamma(1+z_1)\Gamma(-z_2)\Gamma(-z_1+z_2)\Gamma(-z_2-z_3)\Gamma(-z_3)\Gamma(-z_1+z_3) \\ \times\Gamma(-z_7)\Gamma(-1-z_7-z_8)\Gamma(-1+z_2+z_3-z_7-z_8)\Gamma(-z_8) \\ \times\frac{\Gamma(1-z_2+z_8)\Gamma(1-z_3+z_8)\Gamma(2+z_7+z_8)}{\Gamma(-2z_1)\Gamma(1-z_2)\Gamma(1-z_3)\Gamma(-2z_7)}\,. \end{aligned} \tag{G.31}$$

Here all integrations go from $-i\infty$ to $+i\infty$ and the real part of the integration variables z_1, z_2, z_3, z_7, z_8 is taken to be $-21/32, -1/8, -1/4, -7/8, -9/16$, respectively. Although this formula may appear somewhat complicated at first glance, it is very easy to extract the small m^2 expansion from it, just as in the one-loop example of the previous subsection. One obtains a few constant two- and one-fold MB integrals, and only one simple one-fold MB integral that depends on $x = s/t$, namely

$$\begin{aligned} f(x) &:= \frac{1}{2\pi i}\int_{1/2-i\infty}^{1/2+i\infty} x^z \Gamma^3(-z)\Gamma^2(z)\Gamma(1+z)dz \\ &= \frac{1}{2}\Big[\pi^2 \mathrm{Li}_2(-x) + \ln^2(x)\mathrm{Li}_2(-x) - 4\ln(x)\mathrm{Li}_3(-x) + 6\mathrm{Li}_4(-x)\Big]\,. \end{aligned} \tag{G.32}$$

All other contributions are obtained via Cauchy's theorem without doing any integrations. The result is

$$\begin{aligned} I^{(2)}(s,t,m) = \frac{1}{3}\ln^4(u) - \frac{4}{3}\ln^3(u)\ln(v) + 2\ln^2(u)\ln^2(v) + 2\pi^2\ln^2(u) - \frac{8}{3}\pi^2\ln(u)\ln(v) \\ -4\zeta_3\ln(v) + 8f(v/u) + \frac{2}{3}\pi^4 + O(m^2)\,, \end{aligned} \tag{G.33}$$

where $u = m^2/s$ and $v = m^2/t$. A short calculation gives

$$\frac{1}{4}I^{(2)}(s,t,m)+\frac{1}{4}I^{(2)}(t,s,m) = \frac{1}{4}\left[\ln^4(u)+\ln^4(v)\right]+\left[-\frac{1}{2}\ln^2(v/u)-\zeta_2\right]\left[\ln^2(u)+\ln^2(v)\right] - \zeta_3\left[\ln(u)+\ln(v)\right]+\left[\frac{1}{4}\ln^4(v/u)+\zeta_2\ln^2(v/u)+\frac{1}{20}\pi^4\right]+O(m^2)\,. \quad \text{(G.34)}$$

Finally, we also compute the square of the one-loop result that is needed in order to check the exponentiation at two loops, see equation eq. (6.39),

$$-\frac{1}{8}(I^{(1)}(s,t,m))^2 = -\frac{1}{4}\left[\ln^4(u)+\ln^4(v)\right]+\left[\frac{1}{2}\ln^2(v/u)+\frac{1}{4}\pi^2\right]\left[\ln^2(u)+\ln^2(v)\right] -\frac{1}{4}\ln^4(v/u)-\frac{1}{4}\pi^2\ln^2(v/u)-\frac{1}{8}\pi^4+O(m^2)\,. \quad \text{(G.35)}$$

G.3.3. Generic Dual Conformal One-Loop Box Integrals

Here we give the one-loop scalar dual conformal box integrals that appear in the Higgsed theory. A generic one-loop dual conformal integral is given by

$$J^{(1)}(\hat{x}_r,\hat{x}_s,\hat{x}_t,\hat{x}_u) = c_0\,\hat{x}_{rt}^2\hat{x}_{su}^2\int d^5\hat{x}_0\frac{\delta(\hat{x}_0^{M=4})}{\hat{x}_{r0}^2\hat{x}_{s0}^2\hat{x}_{t0}^2\hat{x}_{u0}^2}\,, \quad \text{(G.36)}$$

in dual notation. This integral generalises the 4-point dual conformal integral given in 6.3.2 to an arbitrary number of points. Equivalently, in momentum notation (setting with $m_i = m$ for convenience) we have

$$J^{(1)}(K_1,K_2,K_3,K_4,m) = c_0\,P^{-1}(K_1+K_2,m^2)P^{-1}(K_2+K_3,m^2) \times\int d^4k\,P(k,m^2)P(k+K_1,m^2)P(k+K_1+K_2,m^2)P(k-K_4,m^2)\,,$$

where $P(k,m^2) = (k^2+m^2)^{-1}$ and $K_1 = p_r+\ldots+p_{s-1}, K_2 = p_s+\ldots+p_{t-1}, K_3 = p_t+\ldots+p_{u-1}, K_4 = p_u+\ldots+p_{r-1}$, and $p_i^2 = 0$. The K_i can be light-like if they are built from one momentum only. If q is the number of non-light-like K_i, we call the integral in eq. (G.37) q-mass with uniform internal mass m, in analogy with the nomenclature for the corresponding integrals in dimensional regularization. The explicit expressions for $J^{(1)}$ can be obtained from [163]. See fig. 6.5 for the specific example of the 1-mass integral with uniform internal mass m.

G.4. Berkovits-Maldacena Solution in Conformal Gauge

The world-sheet relevant for the regularized scattering amplitudes considered in chapter 6 ends in a light-like polygon at some finite radial distance r_c from the boundary. Unfortunately, such a solution is very hard to construct. On the other hand, one could consider the simplified problem of a single cusp ending at $z = r_c$. The scattering solution should then be given by this one when approaching any of the cusps.

The solution for a single cusp was given by Berkovits and Maldacena (BM) in the appendix of [82], as a solution of the equations of motion of the Nambu-Goto action.

The solution reads

$$T = e^{\tau}\cosh\sigma, \qquad X = e^{\tau}\sinh\sigma, \qquad Z(\tau,\sigma) = e^{\tau}\omega(\tau) \tag{G.37}$$

with

$$\frac{e^{\tau}}{r_c} = \left(\frac{w+\sqrt{2}}{w-\sqrt{2}}\right)^{\frac{1}{\sqrt{2}}} \frac{1}{1+w} \tag{G.38}$$

The cusp is located at $\tau \to \infty$ and $\omega = r_c e^{-\tau} + 1 + ...$ It is not possible to give a closed form for $\omega(\tau)$, however, it is very easy to solve for it as a power expansion in e^{τ}, close to the cusp. For the first few orders we obtain

$$Z(\tau) = r_c + e^{\tau} + \frac{2}{3r_c^2}e^{3\tau} - \frac{2}{r_c^3}e^{4\tau} + \frac{26}{5r_c^4}e^{5\tau} + \dots \tag{G.39}$$

without following an apparent pattern. Notice that the above gives Z as a function of $e^{\tau} = \sqrt{T^2 - X^2}$.

G.4.1. Conformal gauge

For many purposes, a solution to the equations of motion in conformal gauge is desirable. According to the above analysis, we propose an ansatz of the form

$$T(u,v) = f(v)\cosh u, \qquad X(u,v) = f(v)\sinh u, \qquad Z(u,v) = g(v) \tag{G.40}$$

with boundary conditions $f(v) = 0 + v + ..., g(v) = r_c + ...$, namely, the cusp is located at $v = 0$. The topology of the World-sheet is that of the upper half plane, hence equivalent to the disk. We have checked that with the above ansatz we can write a series expansion for $f(v)$ and $g(v)$ and satisfy both the equations of motion and the Virasoro constraints order by order in the v expansion (this is non trivial, since there are more equations than free parameters). This of course is due to the symmetries of the problem. The Virasoro constraints are particularly simple and imply

$$f(v)^2 + f'(v)^2 - g'(v)^2 = 0 \tag{G.41}$$

As already mentioned, one can solve the above equations order by order in v, obtaining for the first few terms

$$f(v) = kv + \frac{k^2}{r_c}v^2 + \dots, \qquad g(v) = r_c + kv + \frac{k^2}{r_c}v^2 + \dots \tag{G.42}$$

At this point the solution depends on a free parameter k, which is not fixed by the equations of motion or Virasoro constraints. Such coefficient, presumably can be fixed by requiring the correct boundary conditions. In order to compare this solution with the BM solution we can express $Z = g(v)$ in terms of $f(v) = \sqrt{T^2 - X^2}$, we obtain

$$g(v) = r_c + f(v) + \frac{1}{6k^2}f(v)^3 - \frac{1}{2r_c k^2}f(v)^4 + \dots \tag{G.43}$$

We see that the BM solution corresponds to $k = \pm r_c/2$. Setting this value, all the terms in the expansion match the corresponding terms in the BM solution, so the solutions are indeed the same. (presumably the same value for k can be found by requiring the

correct boundary conditions, for instance $g(v) = \sqrt{2}f(v)$ for large v.)

The main lesson is that a solution can be constructed and indeed has the topology of the upper half plane, as expected for a regularized world-sheet.

G.4.2. A Pleasant Surprise

One advantage of writing a solution of strings on AdS_3 in conformal gauge, is that one can perform a Pohlmeyer type reduction as done in [184]. There, it was seen that given a solution of classical strings on AdS_3, one could obtain a holomorphic function $p(z)$ (with $z = u+iv$) plus a field $\alpha(z, \bar{z})$ (or $\hat{\alpha}(w, \bar{w})$) satisfying the generalized Sinh-Gordon equation. In [184] it was found that for the problem relevant to scattering amplitudes, $p(z)$ is simply given by a polynomial and $\hat{\alpha}$ is such that it decays at infinity (with α regular everywhere). The area of the world-sheet is then obtained by expressing the conformal gauge action in terms of the reduced fields and is simply

$$A = \int e^{\hat{\alpha}(w,\bar{w})} dw d\bar{w} \tag{G.44}$$

One natural question is to which field and holomorphic function does the above solution correspond to. Performing the reduction we find (order by order in v)

$$p(z) = i, \qquad e^{\hat{\alpha}} = \frac{v^2}{2} - \frac{v^4}{6} + \frac{17}{360}v^6 + \ldots = \tanh^2\left(\frac{v}{\sqrt{2}}\right) \tag{G.45}$$

Namely, both quantities have a very simple expression and they can be written in a closed form! Notice that $\hat{\alpha}(v)$ satisfies the Sinh-Gordon equation [1] (for the particular case in which α depends only on v), namely

$$\hat{\alpha}''(v) = 2\sinh\hat{\alpha}(v) \tag{G.46}$$

Also, notice that $\hat{\alpha}$ has the correct boundary conditions corresponding to a scattering problem, since it vanishes at $v \to \infty$ (see [184] for the details).

The solution corresponding to a general scattering can then be chosen to live in the upper half plane, such that the cusps are located at $v = 0$ (and each cusp corresponds to a segment). When approaching one of the cusps (and far from the others) the solution should approach the single cusp solution given here.

G.4.3. Computing the Leading Area

Once we have the single cusp solution, we can extract the value of the cusp anomalous dimension at strong coupling by computing the area of the corresponding world-sheet. The single cusp solution possesses both, IR and UV divergences. UV divergences (or IR depending how the solution is interpreted) are regularized by putting boundary conditions at $r = r_c$. On the other hand, we can set a IR cut-off, for instance by considering $T < t_c$. By dimensional analysis the area should then depend on the dimensionless quantity $\frac{t_c}{r_c}$. We are interested in the value of the area for large values of $\frac{t_c}{r_c}$.

[1] Actually, this is nothing but the soliton solution of Sinh-Gordon, see *e.g.* eq. (3.2) of [185]. However, note that the space-time interpretation of this solution (and the topology of the world-sheet) is very different from the one of that paper.

First, notice that the cusp is located at $v = 0$. However, in the regularization we are using, the contribution to the area from the $v \approx 0$ region is small (since it is finite). The biggest contribution comes from large values of v. In order to implement the IR cut-off, we need to understand how $f(v)$ in eq. (G.40) behaves for large values of v. The single cusp solution with boundary conditions at $r = 0$ is

$$T(u,v) = e^v \cosh u, \qquad X(u,v) = e^v \sinh u, Z(u,v) \qquad = \sqrt{2} e^v \tag{G.47}$$

As far from the cusp we expect the two solutions (with boundary conditions at $r = r_c$ and $r = 0$) to look alike, we conclude that $f(v) \approx r_c e^v$ for large values of v. In order to compute the area, we then need to integrate $e^{\hat{\alpha}}$ in the range in which $0 < T(u,v) < t_c$. The second constraint implies $e^v \cosh u < t_c/r_c$, hence

$$A = \int du\, dv\, e^{\hat{\alpha}} = 2 \int_0^{\log t_c} \tanh^2\left(\frac{v}{\sqrt{2}}\right) \operatorname{arcosh}\left(\frac{t_c}{e^v}\right) = \log^2(2t_c) + \dots \tag{G.48}$$

where we have suppressed the r_c, as all depends on the ratio t_c/r_c. In order to compute the leading piece of the above integral, we have set $\tanh^2 \to 1$, which we can do if we assume that the contribution from the region $v \approx 0$ is small.

Expressing the leading contribution to the area as $A = \frac{1}{4} \log^2 \frac{t_c^2}{r_c^2} + \dots$ (we have reinstated r_c) we see that the overall factor is exactly the same as the factor obtained in the first reference in [79–81] , so the value of the cusp anomalous dimension computed with this regularization agrees with the well known result $(\sqrt{\lambda}/\pi)$.

In principle one could compute the collinear anomalous dimension, characterizing sub-leading IR divergences, from this solution. It is not clear whether the result will agree with the one obtained in the first reference in [79–81], since we will have additional contributions that were not taken into account properly there. On the other hand, one expects the argument leading to the dual conformal ward identity presented in the first reference in [79–81] to go through, also when considering the "correct" solution.

G.5. The Infinitesimal Form of the Dual Conformal Generators

The conformal group generators in dimension $d > 2$ are given by [2]

$$D = \sum_i x_i^\mu \partial_{i\mu}\,, \qquad M_{\mu\nu} = \sum_i \left(-x_{i\mu}\partial_{i\nu} + x_{i\nu}\partial_{i\mu}\right)\,, \tag{G.49}$$

$$P_\mu = \sum_i \partial_{i\mu} \qquad K_\mu = \sum_i (2x_{i\mu}x_i^\nu \partial_{i\nu} - x_i^2 \partial_{i\mu})\,, \tag{G.50}$$

where $\partial_\mu := \frac{\partial}{\partial x^\mu}$. We recall that special conformal transformations can be obtained by doing an inversion, followed by a translation, and another inversion. Since our integrals only have four-dimensional translation symmetry, only the corresponding four components of the five-dimensional $\hat{K}^M$ will be symmetries of the integral. Starting with eq. (G.49) in five dimensions and using $\hat{x}^M = (x^\mu, m)$ we find

$$\hat{D} = \sum_i (x_i^\mu \partial_{i\mu} + m_i \partial_{m_i})\,, \tag{G.51}$$

[2] A factor of $(-i)$ was removed from all generators.

$$\hat{K}_\mu = \sum (2x_{i\mu}(x_i^\nu \partial_{i\nu} + m_i \partial_{m_i}) - (x_i^2 + m_i^2)\partial_{i\mu}) \,, \tag{G.52}$$

where $\partial_{m_i} := \frac{\partial}{\partial m_i}$. In four dimensions, $(x_i - x_j)^2$ is covariant under conformal boosts,

$$K^\mu (x_i - x_j)^2 = 2(x_i + x_j)^\mu \, (x_i - x_j)^2 \,. \tag{G.53}$$

In our case, the latter equation generalizes to

$$\hat{K}^\mu (\hat{x}_i - \hat{x}_j)^2 = \hat{K}^\mu \left[(x_i - x_j)^2 + (m_i - m_j)^2 \right] = 2(x_i + x_j)^\mu \, \left[(x_i - x_j)^2 + (m_i - m_j)^2 \right] . \tag{G.54}$$

Similarly, we have

$$\hat{K}^\mu m_i m_j = 2(x_i + x_j)^\mu \, m_i m_j \,. \tag{G.55}$$

From eq. (G.54) and eq. (G.55) we see that

$$\hat{K}^\mu \, \frac{m_i m_j}{\hat{x}_{ij}^2} = 0 \,. \tag{G.56}$$

Note also that we have $\hat{K}^\mu O(m) = O(m)$, so that the small m expansion commutes with $\hat{K}^\mu$.

G.6. AdS_5 Isometries and Dual Conformal Symmetry Generators

Here we explicitly derive the form of the dual conformal symmetry generators acting in the bulk of AdS_5. We can define AdS_5 in embedding coordinates through the equation

$$-Y_{-1}^2 - Y_0^2 + Y_1^2 + Y_2^2 + Y_3^2 + Y_4^2 = -R^2 \,, \tag{G.57}$$

and we will set $R = 1$ for simplicity. We expect the classical string action to have an $SO(2,4)$ symmetry, whose infinitesimal generators are given by

$$J_{MN} = Y_M \frac{\partial}{\partial Y^N} - Y_N \frac{\partial}{\partial Y^M} \,, \tag{G.58}$$

where $\frac{\partial}{\partial Y^M} Y_N = \eta_{MN}$ and $\eta_{MN} = \mathrm{d}iag(-1,-1,1,1,1,1)$. On the other hand, we can define Poincaré coordinates

$$Y^\mu = \frac{x^\mu}{r} \,, \qquad Y_{-1} + Y_4 = \frac{1}{r} \,, \qquad Y_{-1} - Y_4 = \frac{r^2 + x_\mu x^\mu}{r} \,, \tag{G.59}$$

where the $SO(1,3)$ indices $\mu = 0,1,2,3$ are raised and lowered using $\eta_{\mu\nu}$. Now we can act with the generators eq. (G.58) on the equations given in eq. (G.59) and find the action of the symmetry generators when acting on the Poincaré coordinates. We find

$$J_{-1,4} = r\partial_r + x^\mu \partial_\mu = \hat{D} \,, \tag{G.60}$$

$$J_{4,\mu} - J_{-1,\mu} = \partial_\mu = \hat{P}_\mu \,, \tag{G.61}$$

$$J_{4,\mu} + J_{-1,\mu} = 2x_\mu (x_\nu \partial^\nu + r\partial_r) - (x^2 + r^2)\partial_\mu = \hat{K}_\mu \,, \tag{G.62}$$

and $SO(1,3)$ rotations $J^{\mu\nu}$ of course. $\hat{K}_\mu = J_{4,\mu} + J_{-1,\mu}$ is precisely the conformal generator studied in section 2.

Bibliography

[1] L. F. Alday, J. M. Henn, J. Plefka, and T. Schuster, "Scattering into the fifth dimension of N=4 super Yang-Mills", *JHEP* **1001** (2010) 077, arXiv:0908.0684 [hep-th].

[2] L. J. Dixon, J. M. Henn, J. Plefka, and T. Schuster, "All tree-level amplitudes in massless QCD", *JHEP* **1101** (2011) 035, arXiv:1010.3991 [hep-ph].

[3] S. Badger, B. Biedermann, L. Hackl, J. Plefka, T. Schuster, *et al.*, "Comparing efficient computation methods for massless QCD tree amplitudes: Closed analytic formulas versus Berends-Giele recursion", *Phys.Rev.* **D87** (2013) no. 3, 034011, arXiv:1206.2381 [hep-ph].

[4] T. Schuster, "Color ordering in QCD", *Submitted to Phys.Rev.D* (2013) , arXiv:1311.6296 [hep-ph].

[5] J. Plefka, T. Schuster, and V. Verschinin, "From Six to Four and More", *In preparation for submission to JHEP* (2014) .

[6] T. Stelzer and W. Long, "Automatic generation of tree level helicity amplitudes", *Comput.Phys.Commun.* **81** (1994) 357–371, arXiv:hep-ph/9401258 [hep-ph].

[7] J. Alwall *et al.*, "MadGraph/MadEvent v4: The New Web Generation", *JHEP* **0709** (2007) 028, arXiv:arXiv:0706.2334 [hep-ph].

[8] A. Pukhov *et al.*, "CompHEP: A Package for evaluation of Feynman diagrams and integration over multiparticle phase space", arXiv:hep-ph/9908288 [hep-ph]. user's manual for version 33.

[9] F. Krauss, R. Kuhn, and G. Soff, "AMEGIC++ 1.0: A Matrix element generator in C++", *JHEP* **0202** (2002) 044, arXiv:hep-ph/0109036 [hep-ph].

[10] F. A. Berends and W. T. Giele, "Recursive Calculations for Processes with n Gluons", *Nucl. Phys.* **B306** (1988) 759.

[11] T. Gleisberg and S. Höche, "Comix, a new matrix element generator", *JHEP* **0812** (2008) 039, arXiv:arXiv:0808.3674 [hep-ph].

[12] F. Caravaglios and M. Moretti, "An algorithm to compute Born scattering amplitudes without Feynman graphs", *Phys.Lett.* **B358** (1995) 332–338, arXiv:hep-ph/9507237 [hep-ph].

[13] F. Caravaglios, M. L. Mangano, M. Moretti, and R. Pittau, "A New approach to multijet calculations in hadron collisions", *Nucl.Phys.* **B539** (1999) 215–232, arXiv:hep-ph/9807570 [hep-ph].

[14] A. Kanaki and C. G. Papadopoulos, "HELAC: A Package to compute electroweak helicity amplitudes", *Comput.Phys.Commun.* **132** (2000) 306–315, arXiv:hep-ph/0002082 [hep-ph].

[15] A. Cafarella, C. G. Papadopoulos, and M. Worek, "Helac-Phegas: A Generator for all parton level processes", *Comput.Phys.Commun.* **180** (2009) 1941–1955, arXiv:arXiv:0710.2427 [hep-ph].

[16] M. Moretti, T. Ohl, and J. Reuter, "O'Mega: An Optimizing matrix element generator", arXiv:hep-ph/0102195 [hep-ph].

[17] W. Kilian, T. Ohl, and J. Reuter, "WHIZARD: Simulating Multi-Particle Processes at LHC and ILC", arXiv:arXiv:0708.4233 [hep-ph].

[18] F. A. Berends and W. Giele, "The Six Gluon Process as an Example of Weyl-Van Der Waerden Spinor Calculus", *Nucl.Phys.* **B294** (1987) 700.

[19] M. L. Mangano, "The Color Structure of Gluon Emission", *Nucl.Phys.* **B309** (1988) 461.

[20] Z. Bern and D. A. Kosower, "Color decomposition of one loop amplitudes in gauge theories", *Nucl.Phys.* **B362** (1991) 389–448.

[21] Z. Bern, L. J. Dixon, D. C. Dunbar, and D. A. Kosower, "One-Loop n-Point Gauge Theory Amplitudes, Unitarity and Collinear Limits", *Nucl. Phys.* **B425** (1994) 217–260, arXiv:hep-ph/9403226.

[22] Z. Bern, L. J. Dixon, and D. A. Kosower, "One loop corrections to two quark three gluon amplitudes", *Nucl.Phys.* **B437** (1995) 259–304, arXiv:hep-ph/9409393 [hep-ph].

[23] R. K. Ellis, W. Giele, Z. Kunszt, K. Melnikov, and G. Zanderighi, "One-loop amplitudes for W^+ 3 jet production in hadron collisions", *JHEP* **0901** (2009) 012, arXiv:0810.2762 [hep-ph].

[24] R. K. Ellis, Z. Kunszt, K. Melnikov, and G. Zanderighi, "One-loop calculations in quantum field theory: from Feynman diagrams to unitarity cuts", *Phys.Rept.* **518** (2012) 141–250, arXiv:1105.4319 [hep-ph].

[25] H. Ita and K. Ozeren, "Colour Decompositions of Multi-quark One-loop QCD Amplitudes", *JHEP* **1202** (2012) 118, arXiv:1111.4193 [hep-ph].

[26] S. Badger, B. Biedermann, P. Uwer, and V. Yundin, "Numerical evaluation of virtual corrections to multi-jet production in massless QCD", *Comput.Phys.Commun.* **184** (2013) 1981–1998, arXiv:1209.0100 [hep-ph].

[27] R. Britto, F. Cachazo, and B. Feng, "New recursion relations for tree amplitudes of gluons", *Nucl. Phys.* **B715** (2005) 499–522, hep-th/0412308.

[28] R. Britto, F. Cachazo, B. Feng, and E. Witten, "Direct proof of tree-level recursion relation in yang-mills theory", *Phys. Rev. Lett.* **94** (2005) 181602, hep-th/0501052.

[29] Z. Bern, L. J. Dixon, D. C. Dunbar, and D. A. Kosower, "Fusing gauge theory tree amplitudes into loop amplitudes", *Nucl. Phys.* **B435** (1995) 59–101, arXiv:hep-ph/9409265.

[30] C. Anastasiou, Z. Bern, L. J. Dixon, and D. A. Kosower, "Planar amplitudes in maximally supersymmetric Yang-Mills theory", *Phys. Rev. Lett.* **91** (2003) 251602, arXiv:hep-th/0309040.

[31] Z. Bern, L. J. Dixon, and D. A. Kosower, "On-Shell Methods in Perturbative QCD", *Annals Phys.* **322** (2007) 1587–1634, arXiv:0704.2798 [hep-ph].

[32] Z. Bern, G. Diana, L. Dixon, F. Febres Cordero, S. Hoeche, *et al.*, "Four-Jet Production at the Large Hadron Collider at Next-to-Leading Order in QCD", *Phys.Rev.Lett.* **109** (2012) 042001, arXiv:1112.3940 [hep-ph].

[33] S. Badger, B. Biedermann, P. Uwer, and V. Yundin, "NLO QCD corrections to multi-jet production at the LHC with a centre-of-mass energy of $\sqrt{s} = 8$ TeV", *Phys.Lett.* **B718** (2013) 965–978, arXiv:1209.0098 [hep-ph].

[34] S. Badger, B. Biedermann, P. Uwer, and V. Yundin, "Next-to-leading order QCD corrections to five jet production at the LHC", arXiv:1309.6585 [hep-ph].

[35] S. J. Parke and T. R. Taylor, "Perturbative QCD Utilizing Extended Supersymmetry", *Phys. Lett.* **B157** (1985) 81.

[36] Z. Kunszt, "Combined Use of the Calkul Method and N=1 Supersymmetry to Calculate QCD Six Parton Processes", *Nucl. Phys.* **B271** (1986) 333.

[37] M. T. Grisaru, H. Pendleton, and P. van Nieuwenhuizen, "Supergravity and the S Matrix", *Phys.Rev.* **D15** (1977) 996.

[38] M. T. Grisaru and H. Pendleton, "Some Properties of Scattering Amplitudes in Supersymmetric Theories", *Nucl.Phys.* **B124** (1977) 81.

[39] S. J. Parke and T. R. Taylor, "An Amplitude for n Gluon Scattering", *Phys. Rev. Lett.* **56** (1986) 2459.

[40] V. P. Nair, "A current algebra for some gauge theory amplitudes", *Phys. Lett.* **B214** (1988) 215.

[41] E. Witten, "Perturbative gauge theory as a string theory in twistor space", *Commun. Math. Phys.* **252** (2004) 189–258, arXiv:hep-th/0312171.

[42] R. Britto, B. Feng, R. Roiban, M. Spradlin, and A. Volovich, "All split helicity tree-level gluon amplitudes", *Phys. Rev.* **D71** (2005) 105017, hep-th/0503198.

[43] N. Arkani-Hamed, F. Cachazo, C. Cheung, and J. Kaplan, "A Duality For The S Matrix", *JHEP* **03** (2010) 020, arXiv:0907.5418 [hep-th].

[44] A. Brandhuber, P. Heslop, and G. Travaglini, "A note on dual superconformal symmetry of the $\mathcal{N} = 4$ super Yang-Mills S-matrix", *Phys. Rev.* **D78** (2008) 125005, arXiv:0807.4097 [hep-th].

[45] M. Bianchi, H. Elvang, and D. Z. Freedman, "Generating Tree Amplitudes in $\mathcal{N} = 4$ SYM and $\mathcal{N} = 8$ SG", *JHEP* **09** (2008) 063, arXiv:0805.0757 [hep-th].

[46] J. M. Drummond and J. M. Henn, "All tree-level amplitudes in $\mathcal{N} = 4$ SYM", *JHEP* **04** (2009) 018, arXiv:0808.2475 [hep-th].

[47] J. M. Drummond, J. Henn, G. P. Korchemsky, and E. Sokatchev, "Dual superconformal symmetry of scattering amplitudes in $\mathcal{N} = 4$ super-Yang–Mills theory", *Nucl. Phys.* **B828** (2010) 317–374, arXiv:0807.1095 [hep-th].

[48] J. M. Drummond, J. Henn, G. P. Korchemsky, and E. Sokatchev, "Generalized unitarity for $\mathcal{N} = 4$ super-amplitudes", arXiv:0808.0491 [hep-th].

[49] J. M. Drummond, J. M. Henn, and J. Plefka, "Yangian symmetry of scattering amplitudes in $\mathcal{N} = 4$ super Yang-Mills theory", *JHEP* **05** (2009) 046, arXiv:0902.2987 [hep-th].

[50] J. Drummond, "Hidden Simplicity of Gauge Theory Amplitudes", arXiv:arXiv:1010.2418 [hep-th].

[51] N. Craig, H. Elvang, M. Kiermaier, and T. Slatyer, "Massive amplitudes on the Coulomb branch of N=4 SYM", *JHEP* **1112** (2011) 097, arXiv:1104.2050 [hep-th].

[52] T. Dennen and Y.-t. Huang, "Dual Conformal Properties of Six-Dimensional Maximal Super Yang-Mills Amplitudes", *JHEP* **1101** (2011) 140, arXiv:1010.5874 [hep-th].

[53] L. J. Dixon, "Calculating scattering amplitudes efficiently", arXiv:hep-ph/9601359 [hep-ph].

[54] C. Cheung and D. O'Connell, "Amplitudes and Spinor-Helicity in Six Dimensions", *JHEP* **0907** (2009) 075, arXiv:0902.0981 [hep-th].

[55] V. Braun, G. Korchemsky, and D. Mueller, "The Uses of conformal symmetry in QCD", *Prog.Part.Nucl.Phys.* **51** (2003) 311–398, arXiv:hep-ph/0306057 [hep-ph].

[56] J. M. Maldacena, "The large n limit of superconformal field theories and supergravity", *Adv. Theor. Math. Phys.* **2** (1998) 231–252, hep-th/9711200.

[57] S. S. Gubser, I. R. Klebanov, and A. M. Polyakov, "Gauge theory correlators from non-critical string theory", *Phys. Lett.* **B428** (1998) 105–114, hep-th/9802109.

[58] E. Witten, "Anti-de sitter space and holography", *Adv. Theor. Math. Phys.* **2** (1998) 253–291, hep-th/9802150.

[59] J. A. Minahan and K. Zarembo, "The bethe-ansatz for $\mathcal{N} = 4$ super yang-mills", *JHEP* **0303** (2003) 013, hep-th/0212208.

[60] N. Beisert, C. Kristjansen, and M. Staudacher, "The dilatation operator of $\mathcal{N} = 4$ conformal super yang-mills theory", *Nucl. Phys.* **B664** (2003) 131–184, hep-th/0303060.

[61] I. Bena, J. Polchinski, and R. Roiban, "Hidden symmetries of the $AdS_5 \times S^5$ superstring", *Phys. Rev.* **D69** (2004) 046002, hep-th/0305116.

[62] A. A. Tseytlin, "Semiclassical strings in $ads_5 \times s^5$ and scalar operators in $\mathcal{N} = 4$ sym theory", *Comptes Rendus Physique* **5** (2004) 1049–1059, hep-th/0407218.

[63] A. V. Belitsky, V. M. Braun, A. S. Gorsky, and G. P. Korchemsky, "Integrability in qcd and beyond", *Int. J. Mod. Phys.* **A19** (2004) 4715–4788, hep-th/0407232.

[64] N. Beisert, "The dilatation operator of $\mathcal{N} = 4$ super yang-mills theory and integrability", *Phys. Rept.* **405** (2004) 1–202, hep-th/0407277.

[65] J. Plefka, "Spinning strings and integrable spin chains in the ads/cft correspondence", *Living. Rev. Relativity* **8** (2005) 9, hep-th/0507136.

[66] J. A. Minahan, "A brief introduction to the Bethe ansatz in $\mathcal{N} = 4$ super-Yang-Mills", *J. Phys.* **A39** (2006) 12657–12677.

[67] G. Arutyunov and S. Frolov, "Foundations of the $AdS_5 \times S^5$ Superstring. Part I", *J. Phys.* **A42** (2009) 254003, arXiv:0901.4937 [hep-th].

[68] L. Brink, J. H. Schwarz, and J. Scherk, "Supersymmetric Yang-Mills Theories", *Nucl. Phys.* **B121** (1977) 77.

[69] F. Gliozzi, J. Scherk, and D. I. Olive, "Supersymmetry, Supergravity Theories and the Dual Spinor Model", *Nucl. Phys.* **B122** (1977) 253–290.

[70] G. Georgiou, E. W. N. Glover, and V. V. Khoze, "Non-MHV Tree Amplitudes in Gauge Theory", *JHEP* **07** (2004) 048, arXiv:hep-th/0407027.

[71] G. Korchemsky and E. Sokatchev, "Symmetries and analytic properties of scattering amplitudes in N=4 SYM theory", *Nucl.Phys.* **B832** (2010) 1–51, arXiv:0906.1737 [hep-th].

[72] J. M. Drummond, J. Henn, V. A. Smirnov, and E. Sokatchev, "Magic identities for conformal four-point integrals", *JHEP* **01** (2007) 064, arXiv:hep-th/0607160.

[73] L. F. Alday and J. M. Maldacena, "Gluon scattering amplitudes at strong coupling", *JHEP* **06** (2007) 064, arXiv:0705.0303 [hep-th].

[74] J. M. Drummond, G. P. Korchemsky, and E. Sokatchev, "Conformal properties of four-gluon planar amplitudes and Wilson loops", *Nucl. Phys.* **B795** (2008) 385–408, arXiv:0707.0243 [hep-th].

[75] J. M. Drummond, J. Henn, G. P. Korchemsky, and E. Sokatchev, "On planar gluon amplitudes/Wilson loops duality", *Nucl. Phys.* **B795** (2008) 52–68, arXiv:0709.2368 [hep-th].

[76] J. M. Drummond, J. Henn, G. P. Korchemsky, and E. Sokatchev, "Conformal Ward identities for Wilson loops and a test of the duality with gluon amplitudes", *Nucl. Phys.* **B826** (2010) 337–364, arXiv:0712.1223 [hep-th].

[77] L. F. Alday and J. Maldacena, "Comments on gluon scattering amplitudes via AdS/CFT", *JHEP* **11** (2007) 068, arXiv:0710.1060 [hep-th].

[78] A. Brandhuber, P. Heslop, and G. Travaglini, "MHV Amplitudes in $\mathcal{N} = 4$ Super Yang–Mills and Wilson Loops", *Nucl. Phys.* **B794** (2008) 231–243, arXiv:0707.1153 [hep-th].

[79] L. F. Alday, "Lectures on Scattering Amplitudes via AdS/CFT", *Fortsch.Phys.* **56** (2008) 816–823, arXiv:0804.0951 [hep-th].

[80] L. F. Alday and R. Roiban, "Scattering Amplitudes, Wilson Loops and the String/Gauge Theory Correspondence", *Phys. Rept.* **468** (2008) 153–211, arXiv:0807.1889 [hep-th].

[81] J. M. Henn, "Duality between Wilson loops and gluon amplitudes", *Fortschr. Phys.* **57** (2009) 729, arXiv:0903.0522 [hep-th].

[82] N. Berkovits and J. Maldacena, "Fermionic T-Duality, Dual Superconformal Symmetry, and the Amplitude/Wilson Loop Connection", *JHEP* **09** (2008) 062, arXiv:0807.3196 [hep-th].

[83] N. Beisert, R. Ricci, A. A. Tseytlin, and M. Wolf, "Dual Superconformal Symmetry from $AdS_5 \times S^5$ Superstring Integrability", *Phys. Rev.* **D78** (2008) 126004, arXiv:0807.3228 [hep-th].

[84] J. Drummond, "Tree-level amplitudes and dual superconformal symmetry", *J.Phys.* **A44** (2011) 454010, arXiv:1107.4544 [hep-th].

[85] Y.-t. Huang, "Non-Chiral S-Matrix of N=4 Super Yang-Mills", arXiv:1104.2021 [hep-th].

[86] N. Arkani-Hamed, F. Cachazo, and C. Cheung, "The Grassmannian Origin Of Dual Superconformal Invariance", *JHEP* **1003** (2010) 036, arXiv:0909.0483 [hep-th].

[87] N. Arkani-Hamed, J. L. Bourjaily, F. Cachazo, A. B. Goncharov, A. Postnikov, *et al.*, "Scattering Amplitudes and the Positive Grassmannian", arXiv:1212.5605 [hep-th].

[88] N. Arkani-Hamed and J. Trnka, "The Amplituhedron", arXiv:1312.2007 [hep-th].

[89] T. Dennen, Y.-t. Huang, and W. Siegel, "Supertwistor space for 6D maximal super Yang-Mills", *JHEP* **1004** (2010) 127, arXiv:0910.2688 [hep-th].

[90] Z. Bern, J. J. Carrasco, T. Dennen, Y.-t. Huang, and H. Ita, "Generalized Unitarity and Six-Dimensional Helicity", *Phys.Rev.* **D83** (2011) 085022, arXiv:1010.0494 [hep-th].

[91] A. Brandhuber, D. Korres, D. Koschade, and G. Travaglini, "One-loop Amplitudes in Six-Dimensional (1,1) Theories from Generalised Unitarity", *JHEP* **1102** (2011) 077, arXiv:1010.1515 [hep-th].

[92] Y.-t. Huang and A. E. Lipstein, "Amplitudes of 3D and 6D Maximal Superconformal Theories in Supertwistor Space", *JHEP* **1010** (2010) 007, arXiv:1004.4735 [hep-th].

[93] H. Elvang, Y.-t. Huang, and C. Peng, "On-shell superamplitudes in N<4 SYM", *JHEP* **1109** (2011) 031, arXiv:1102.4843 [hep-th].

[94] C. Cheung, "On-Shell Recursion Relations for Generic Theories", *JHEP* **1003** (2010) 098, arXiv:0808.0504 [hep-th].

[95] N. Arkani-Hamed and J. Kaplan, "On Tree Amplitudes in Gauge Theory and Gravity", *JHEP* **0804** (2008) 076, arXiv:0801.2385 [hep-th].

[96] N. Arkani-Hamed, F. Cachazo, and J. Kaplan, "What is the Simplest Quantum Field Theory?", arXiv:0808.1446 [hep-th].

[97] M. L. Mangano and S. J. Parke, "Multi-Parton Amplitudes in Gauge Theories", *Phys. Rept.* **200** (1991) 301–367, arXiv:hep-th/0509223.

[98] C. Berger *et al.*, "Precise Predictions for W + 4 Jet Production at the Large Hadron Collider", arXiv:arXiv:1009.2338 [hep-ph].

[99] G. Ossola, C. G. Papadopoulos, and R. Pittau, "Reducing full one-loop amplitudes to scalar integrals at the integrand level", *Nucl.Phys.* **B763** (2007) 147–169, arXiv:hep-ph/0609007 [hep-ph].

[100] G. Ossola, C. G. Papadopoulos, and R. Pittau, "CutTools: A Program implementing the OPP reduction method to compute one-loop amplitudes", *JHEP* **0803** (2008) 042, arXiv:arXiv:0711.3596 [hep-ph].

[101] G. Ossola, C. G. Papadopoulos, and R. Pittau, "On the Rational Terms of the one-loop amplitudes", *JHEP* **0805** (2008) 004, arXiv:arXiv:0802.1876 [hep-ph].

[102] R. K. Ellis, W. Giele, and Z. Kunszt, "A Numerical Unitarity Formalism for Evaluating One-Loop Amplitudes", *JHEP* **0803** (2008) 003, arXiv:arXiv:0708.2398 [hep-ph].

[103] W. T. Giele, Z. Kunszt, and K. Melnikov, "Full one-loop amplitudes from tree amplitudes", *JHEP* **0804** (2008) 049, arXiv:arXiv:0801.2237 [hep-ph].

[104] W. Giele and G. Zanderighi, "On the Numerical Evaluation of One-Loop Amplitudes: The Gluonic Case", *JHEP* **0806** (2008) 038, arXiv:arXiv:0805.2152 [hep-ph].

[105] C. Berger *et al.*, "An Automated Implementation of On-Shell Methods for One-Loop Amplitudes", *Phys.Rev.* **D78** (2008) 036003, arXiv:arXiv:0803.4180 [hep-ph].

[106] Z. Bern and A. Morgan, "Massive loop amplitudes from unitarity", *Nucl.Phys.* **B467** (1996) 479–509, arXiv:hep-ph/9511336 [hep-ph].

[107] Z. Bern, L. J. Dixon, D. C. Dunbar, and D. A. Kosower, "One loop self-dual and $\mathcal{N} = 4$ super Yang-Mills", *Phys.Lett.* **B394** (1997) 105–115, arXiv:hep-th/9611127 [hep-th].

[108] C. Anastasiou, R. Britto, B. Feng, Z. Kunszt, and P. Mastrolia, "D-dimensional unitarity cut method", *Phys.Lett.* **B645** (2007) 213–216, arXiv:hep-ph/0609191 [hep-ph].

[109] R. Britto and B. Feng, "Integral coefficients for one-loop amplitudes", *JHEP* **0802** (2008) 095, arXiv:arXiv:0711.4284 [hep-ph].

[110] S. Badger, "Direct Extraction Of One Loop Rational Terms", *JHEP* **0901** (2009) 049, arXiv:arXiv:0806.4600 [hep-ph].

[111] Z. Bern, L. J. Dixon, and D. A. Kosower, "Bootstrapping multi-parton loop amplitudes in QCD", *Phys.Rev.* **D73** (2006) 065013, arXiv:hep-ph/0507005 [hep-ph].

[112] C. F. Berger, Z. Bern, L. J. Dixon, D. Forde, and D. A. Kosower, "Bootstrapping One-Loop QCD Amplitudes with General Helicities", *Phys.Rev.* **D74** (2006) 036009, arXiv:hep-ph/0604195 [hep-ph].

[113] Z. Bern, L. J. Dixon, and D. A. Kosower, "One-loop amplitudes for e^+ e^- to four partons", *Nucl. Phys.* **B513** (1998) 3–86, arXiv:hep-ph/9708239.

[114] M. Dinsdale, M. Ternick, and S. Weinzierl, "A Comparison of efficient methods for the computation of Born gluon amplitudes", *JHEP* **0603** (2006) 056, arXiv:hep-ph/0602204 [hep-ph].

[115] C. F. Berger and D. Forde, "Multi-Parton Scattering Amplitudes via On-Shell Methods", *Ann.Rev.Nucl.Part.Sci.* **60** (2010) 181–205, arXiv:0912.3534 [hep-ph].

[116] H. Ita, "Susy Theories and QCD: Numerical Approaches", *J.Phys.A* **A44** (2011) 454005, arXiv:1109.6527 [hep-th].

[117] S. Badger, B. Biedermann, and P. Uwer, "NGluon: A Package to Calculate One-loop Multi-gluon Amplitudes", *Comput.Phys.Commun.* **182** (2011) 1674–1692, arXiv:1011.2900 [hep-ph].

[118] S. Becker, C. Reuschle, and S. Weinzierl, "Numerical NLO QCD calculations", *JHEP* **1012** (2010) 013, arXiv:1010.4187 [hep-ph].

[119] G. Bevilacqua, M. Czakon, M. Garzelli, A. van Hameren, A. Kardos, *et al.*, "HELAC-NLO", arXiv:1110.1499 [hep-ph].

[120] F. Cascioli, P. Maierhofer, and S. Pozzorini, "Scattering Amplitudes with Open Loops", *Phys.Rev.Lett.* **108** (2012) 111601, arXiv:1111.5206 [hep-ph].

[121] G. Cullen, N. Greiner, G. Heinrich, G. Luisoni, P. Mastrolia, *et al.*, "Automated One-Loop Calculations with GoSam", *Eur.Phys.J.* **C72** (2012) 1889, arXiv:1111.2034 [hep-ph].

[122] W. Giele, Z. Kunszt, and J. Winter, "Efficient Color-Dressed Calculation of Virtual Corrections", *Nucl.Phys.* **B840** (2010) 214–270, arXiv:0911.1962 [hep-ph].

[123] V. Hirschi, R. Frederix, S. Frixione, M. V. Garzelli, F. Maltoni, *et al.*, "Automation of one-loop QCD corrections", *JHEP* **1105** (2011) 044, arXiv:1103.0621 [hep-ph].

[124] A. Lazopoulos, "Multi-gluon one-loop amplitudes numerically", arXiv:0812.2998 [hep-ph].

[125] H. Ita, Z. Bern, L. Dixon, F. Febres Cordero, D. Kosower, *et al.*, "Precise Predictions for Z + 4 Jets at Hadron Colliders", *Phys.Rev.* **D85** (2012) 031501, arXiv:1108.2229 [hep-ph].

[126] A. Bredenstein, A. Denner, S. Dittmaier, and S. Pozzorini, "NLO QCD corrections to pp → t anti-t b anti-b + X at the LHC", *Phys.Rev.Lett.* **103** (2009) 012002, arXiv:0905.0110 [hep-ph].

[127] A. Denner, S. Dittmaier, S. Kallweit, and S. Pozzorini, "NLO QCD corrections to WWbb production at hadron colliders", *Phys.Rev.Lett.* **106** (2011) 052001, arXiv:1012.3975 [hep-ph].

[128] R. Frederix, S. Frixione, K. Melnikov, and G. Zanderighi, "NLO QCD corrections to five-jet production at LEP and the extraction of $\alpha_s(M_Z)$", *JHEP* **1011** (2010) 050, arXiv:1008.5313 [hep-ph].

[129] S. Becker, D. Goetz, C. Reuschle, C. Schwan, and S. Weinzierl, "NLO results for five, six and seven jets in electron-positron annihilation", *Phys.Rev.Lett.* **108** (2012) 032005, arXiv:1111.1733 [hep-ph].

[130] N. Greiner, G. Heinrich, P. Mastrolia, G. Ossola, T. Reiter, *et al.*, "NLO QCD corrections to the production of W+ W- plus two jets at the LHC", arXiv:1202.6004 [hep-ph].

[131] N. Greiner, A. Guffanti, T. Reiter, and J. Reuter, "NLO QCD corrections to the production of two bottom-antibottom pairs at the LHC", *Phys.Rev.Lett.* **107** (2011) 102002, arXiv:1105.3624 [hep-ph].

[132] G. Bevilacqua, M. Czakon, C. Papadopoulos, and M. Worek, "Hadronic top-quark pair production in association with two jets at Next-to-Leading Order QCD", *Phys.Rev.* **D84** (2011) 114017, arXiv:1108.2851 [hep-ph].

[133] G. Bevilacqua, M. Czakon, C. Papadopoulos, R. Pittau, and M. Worek, "Assault on the NLO Wishlist: pp → t t anti-t b anti-b", *JHEP* **0909** (2009) 109, arXiv:0907.4723 [hep-ph].

[134] G. Bevilacqua, M. Czakon, A. van Hameren, C. G. Papadopoulos, and M. Worek, "Complete off-shell effects in top quark pair hadroproduction with leptonic decay at next-to-leading order", *JHEP* **1102** (2011) 083, arXiv:1012.4230 [hep-ph].

[135] G. Bozzi, F. Campanario, M. Rauch, and D. Zeppenfeld, "$Z\gamma\gamma$ production with leptonic decays and triple photon production at NLO QCD", *Phys.Rev.* **D84** (2011) 074028, arXiv:1107.3149 [hep-ph].

[136] F. Campanario, C. Englert, M. Rauch, and D. Zeppenfeld, "Precise predictions for $W\gamma\gamma$ +jet production at hadron colliders", *Phys.Lett.* **B704** (2011) 515–519, arXiv:1106.4009 [hep-ph].

[137] K. Arnold, J. Bellm, G. Bozzi, M. Brieg, F. Campanario, *et al.*, "VBFNLO: A parton level Monte Carlo for processes with electroweak bosons – Manual for Version 2.5.0", arXiv:1107.4038 [hep-ph].

[138] S. Becker, C. Reuschle, and S. Weinzierl, "Efficiency improvements for the numerical computation of NLO corrections", arXiv:1205.2096 [hep-ph].

[139] R. K. Ellis, K. Melnikov, and G. Zanderighi, "W+3 jet production at the Tevatron", *Phys.Rev.* **D80** (2009) 094002, arXiv:0906.1445 [hep-ph].

[140] R. Frederix, S. Frixione, V. Hirschi, F. Maltoni, R. Pittau, *et al.*, "aMC@NLO predictions for Wjj production at the Tevatron", *JHEP* **1202** (2012) 048, arXiv:1110.5502 [hep-ph].

[141] T. Melia, K. Melnikov, R. Rontsch, and G. Zanderighi, "Next-to-leading order QCD predictions for W^+W^+jj production at the LHC", *JHEP* **1012** (2010) 053, arXiv:1007.5313 [hep-ph].

[142] T. Melia, K. Melnikov, R. Rontsch, and G. Zanderighi, "NLO QCD corrections for W^+W^- pair production in association with two jets at hadron colliders", *Phys.Rev.* **D83** (2011) 114043, arXiv:1104.2327 [hep-ph].

[143] J. L. Bourjaily, "Efficient Tree-Amplitudes in N=4: Automatic BCFW Recursion in Mathematica", arXiv:1011.2447 [hep-ph].

[144] C. Duhr, S. Hoeche, and F. Maltoni, "Color-dressed recursive relations for multi-parton amplitudes", *JHEP* **0608** (2006) 062, arXiv:hep-ph/0607057 [hep-ph].

[145] S. Badger, B. Biedermann, and P. Uwer, "One-Loop Amplitudes for Multi-Jet Production at Hadron Colliders", arXiv:1201.1187 [hep-ph].

[146] E. Byckling and K. Kajantie, *Particle kinematics*. Wiley, 1973.

[147] R. Kleiss, W. J. Stirling, and S. Ellis, "A new Monte Carlo treatment of multiparticle phase space at high-energies", *Comput.Phys.Commun.* **40** (1986) 359.

[148] Z. Bern, L. J. Dixon, and V. A. Smirnov, "Iteration of planar amplitudes in maximally supersymmetric yang-mills theory at three loops and beyond", *Phys. Rev.* **D72** (2005) 085001, hep-th/0505205.

[149] Z. Bern, L. J. Dixon, D. A. Kosower, R. Roiban, M. Spradlin, C. Vergu, and A. Volovich, "The Two-Loop Six-Gluon MHV Amplitude in Maximally Supersymmetric Yang-Mills Theory", *Phys. Rev.* **D78** (2008) 045007, arXiv:0803.1465 [hep-th].

[150] J. Bartels, L. Lipatov, and A. Sabio Vera, "BFKL Pomeron, Reggeized gluons and Bern-Dixon-Smirnov amplitudes", *Phys.Rev.* **D80** (2009) 045002, arXiv:0802.2065 [hep-th].

[151] J. M. Drummond, J. Henn, G. P. Korchemsky, and E. Sokatchev, "The hexagon Wilson loop and the BDS ansatz for the six-gluon amplitude", *Phys. Lett.* **B662** (2008) 456–460, arXiv:0712.4138 [hep-th].

[152] J. M. Drummond, J. Henn, G. P. Korchemsky, and E. Sokatchev, "Hexagon Wilson loop = six-gluon MHV amplitude", *Nucl. Phys.* **B815** (2009) 142–173, arXiv:0803.1466 [hep-th].

[153] S. Ivanov, G. Korchemsky, and A. Radyushkin, "Infrared Asymptotics of Perturbative QCD: Contour Gauges", *Yad.Fiz.* **44** (1986) 230–240.

[154] Z. Komargodski, "On collinear factorization of Wilson loops and MHV amplitudes in $\mathcal{N} = 4$ SYM", *JHEP* **05** (2008) 019, arXiv:0801.3274 [hep-th].

[155] A. M. Polyakov, "Gauge Fields as Rings of Glue", *Nucl. Phys.* **B164** (1980) 171–188.

[156] G. P. Korchemsky and A. V. Radyushkin, "Renormalization of the Wilson Loops Beyond the Leading Order", *Nucl. Phys.* **B283** (1987) 342–364.

[157] I. A. Korchemskaya and G. P. Korchemsky, "On lightlike Wilson loops", *Phys. Lett.* **B287** (1992) 169–175.

[158] N. Beisert, B. Eden, and M. Staudacher, "Transcendentality and crossing", *J. Stat. Mech.* **07** (2007) P01021, hep-th/0610251.

[159] R. Ricci, A. A. Tseytlin, and M. Wolf, "On T-Duality and Integrability for Strings on AdS Backgrounds", *JHEP* **12** (2007) 082, arXiv:0711.0707 [hep-th].

[160] H. Kawai and T. Suyama, "Some Implications of Perturbative Approach to AdS/CFT Correspondence", *Nucl. Phys.* **B794** (2008) 1–12, arXiv:0708.2463 [hep-th].

[161] R. M. Schabinger, "Scattering on the Moduli Space of $\mathcal{N} = 4$ Super Yang-Mills", arXiv:0801.1542 [hep-th].

[162] J. McGreevy and A. Sever, "Planar scattering amplitudes from Wilson loops", *JHEP* **08** (2008) 078, arXiv:0806.0668 [hep-th].

[163] G. 't Hooft and M. Veltman, "Scalar One Loop Integrals", *Nucl.Phys.* **B153** (1979) 365–401.

[164] J. M. Henn, S. G. Naculich, H. J. Schnitzer, and M. Spradlin, "Higgs-regularized three-loop four-gluon amplitude in N=4 SYM: exponentiation and Regge limits", *JHEP* **1004** (2010) 038, arXiv:1001.1358 [hep-th].

[165] J. M. Henn, S. G. Naculich, H. J. Schnitzer, and M. Spradlin, "More loops and legs in Higgs-regulated N=4 SYM amplitudes", *JHEP* **1008** (2010) 002, arXiv:1004.5381 [hep-th].

[166] S. Caron-Huot and D. O'Connell, "Spinor Helicity and Dual Conformal Symmetry in Ten Dimensions", *JHEP* **1108** (2011) 014, arXiv:1010.5487 [hep-th].

[167] R. H. Boels, "No triangles on the moduli space of maximally supersymmetric gauge theory", *JHEP* **1005** (2010) 046, arXiv:1003.2989 [hep-th].

[168] C. Reuschle and S. Weinzierl, "Decomposition of one-loop QCD amplitudes into primitive amplitudes based on shuffle relations", arXiv:1310.0413 [hep-ph].

[169] T. Melia, "Getting more flavour out of one-flavour QCD", arXiv:1312.0599 [hep-ph].

[170] S. Caron-Huot, "Loops and trees", *JHEP* **1105** (2011) 080, arXiv:1007.3224 [hep-ph].

[171] N. Arkani-Hamed, J. L. Bourjaily, F. Cachazo, S. Caron-Huot, and J. Trnka, "The All-Loop Integrand For Scattering Amplitudes in Planar N=4 SYM", *JHEP* **1101** (2011) 041, arXiv:1008.2958 [hep-th].

[172] R. H. Boels, "On BCFW shifts of integrands and integrals", *JHEP* **1011** (2010) 113, arXiv:1008.3101 [hep-th].

[173] M. Kruczenski, R. Roiban, A. Tirziu, and A. A. Tseytlin, "Strong-coupling expansion of cusp anomaly and gluon amplitudes from quantum open strings in $AdS_5 \times S^5$", *Nucl. Phys.* **B791** (2008) 93–124, arXiv:0707.4254 [hep-th].

[174] D. Maitre and P. Mastrolia, "S@M, a Mathematica Implementation of the Spinor-Helicity Formalism", *Comput. Phys. Commun.* **179** (2008) 501–574, arXiv:0710.5559 [hep-ph].

[175] R. K. Ellis, W. Giele, and G. Zanderighi, "The One-loop amplitude for six-gluon scattering", *JHEP* **0605** (2006) 027, arXiv:hep-ph/0602185 [hep-ph].

[176] N. Arkani-Hamed, F. Cachazo, C. Cheung, and J. Kaplan, "The S-Matrix in Twistor Space", arXiv:0903.2110 [hep-th].

[177] J. L. Bourjaily, J. Trnka, A. Volovich, and C. Wen, "The Grassmannian and the Twistor String: Connecting All Trees in N=4 SYM", arXiv:1006.1899 [hep-th].

[178] A. Hodges, "Eliminating spurious poles from gauge-theoretic amplitudes", arXiv:0905.1473 [hep-th].

[179] L. Mason and D. Skinner, "Dual Superconformal Invariance, Momentum Twistors and Grassmannians", *JHEP* **11** (2009) 045, arXiv:0909.0250 [hep-th].

[180] Z. Bern, H. Ita, and K. Ozeren. private communication.

[181] P. Uwer and B. Biedermann. private communication.

[182] V. A. Smirnov, "Evaluating Feynman integrals", *Springer Tracts Mod.Phys.* **211** (2004) 1–244.

[183] J. Gluza, K. Kajda, and T. Riemann, "AMBRE: A Mathematica package for the construction of Mellin-Barnes representations for Feynman integrals", *Comput.Phys.Commun.* **177** (2007) 879–893, arXiv:0704.2423 [hep-ph].

[184] L. F. Alday and J. Maldacena, "Minimal surfaces in AdS and the eight-gluon scattering amplitude at strong coupling", arXiv:0903.4707 [hep-th].

[185] A. Jevicki, K. Jin, C. Kalousios, and A. Volovich, "Generating AdS String Solutions", *JHEP* **0803** (2008) 032, arXiv:0712.1193 [hep-th].

[186] D. Binosi and L. Theussl, "JaxoDraw: A Graphical user interface for drawing Feynman diagrams", *Comput.Phys.Commun.* **161** (2004) 76–86, arXiv:hep-ph/0309015 [hep-ph].

[187] D. Binosi, J. Collins, C. Kaufhold, and L. Theussl, "JaxoDraw: A Graphical user interface for drawing Feynman diagrams. Version 2.0 release notes", *Comput.Phys.Commun.* **180** (2009) 1709–1715, arXiv:arXiv:0811.4113 [hep-ph].

[188] J. Vermaseren, "Axodraw", *Comput.Phys.Commun.* **83** (1994) 45–58.

Software

- This thesis was typeset in LaTeX.
- Mathematica 9.0 was used for the calculations.
- Several figures in this thesis were made with JaxoDraw [186, 187], based on Axodraw [188].